Precision Frequency Control

Volume 2
Oscillators and Standards

Edited by

EDUARD A. GERBER
ARTHUR BALLATO

U.S. Army Electronics Technology and Devices Laboratory
Fort Monmouth, New Jersey

1985



ACADEMIC PRESS, INC.
(Harcourt Brace Jovanovich, Publishers)
Orlando San Diego New York London
Toronto Montreal Sydney Tokyo



COPYRIGHT © 1985, BY ACADEMIC PRESS, INC.
ALL RIGHTS RESERVED.
NO PART OF THIS PUBLICATION MAY BE REPRODUCED OR TRANSMITTED IN ANY FORM OR BY ANY MEANS, ELECTRONIC OR MECHANICAL, INCLUDING PHOTOCOPY, RECORDING, OR ANY INFORMATION STORAGE AND RETRIEVAL SYSTEM, WITHOUT PERMISSION IN WRITING FROM THE PUBLISHER.

ACADEMIC PRESS, INC.
Orlando, Florida 32887

United Kingdom Edition published by
ACADEMIC PRESS INC. (LONDON) LTD.
24–28 Oval Road, London NW1 7DX

Library of Congress Cataloging in Publication Data

Main entry under title:

Precision frequency control.

Includes bibliographies and indexes.
Contents: v. 1. Acoustic resonators and filters -- v. 2. Oscillators and standards.
1. Piezoelectric devices. 2. Electric resonators. 3. Oscillators, Crystal. 4. Acoustic surface wave devices. I. Gerber, Eduard A. II. Ballato, Arthur.
TK7872.P54P74 1984 621.3815'363 84-14630
ISBN 0-12-280602-6 (v. 2 : alk. paper)

PRINTED IN THE UNITED STATES OF AMERICA

85 86 87 88 9 8 7 6 5 4 3 2 1

Contents

CONTRIBUTORS xi
PREFACE xiii
CONTENTS OF VOLUME 1 xvii
INTRODUCTION xxi

7 Resonator and Device Measurements
by Erich Hafner

List of Symbols 2
7.1 Introduction 2
7.2 The Crystal Unit and Its Equivalent Circuit 4
7.2.1 The Resonator-Equivalent Electrical Circuit 4
7.2.2 Device Properties of the Crystal Unit 6
7.2.3 The Characteristic Parameters of a Crystal Unit 11
7.3 Crystal-Resonator Measurements 16
7.3.1 General 16
7.3.2 Resonator Measurement Instruments 19
7.3.3 Measurement Methods 33
7.4 Summary and Conclusions 38
Appendix I: The Generalized Equivalent Circuit 41
Appendix II: Two-Port Relations for the IEC-444 π Network 43
Appendix III: Two-Port Relations for a Transmission Bridge 44

8 Precision Oscillators

List of Symbols for Section 8.1 46
8.1 Bulk-Acoustic-Wave Oscillators 47
by Warren L. Smith

8.1.1 General Characteristics of Crystal-Controlled Oscillators 47
8.1.2 Circuit Configurations for Crystal-Controlled Oscillators 53
8.1.3 Temperature-Control Techniques for Precision Oscillators 61
8.1.4 Temperature-Compensation Methods for Semiprecision Oscillators 63
8.1.5 Miniature Integrated-Circuit Oscillators 64
List of Symbols for Section 8.2 65
8.2 Surface-Acoustic-Wave Oscillators 66
by Thomas E. Parker
8.2.1 Introduction 66
8.2.2 The Basic SAW Oscillator—A Physical Point of View 67
8.2.3 Frequency Stability 72
8.2.4 Multifrequency Oscillators 76
8.2.5 Electronic Amplifiers and Other External Components 77
8.2.6 Advantages and Disadvantages of SAW Oscillators 78
8.2.7 Conclusion 79
List of Symbols for Section 8.3 79
8.3 Quartz Frequency Standards and Clocks—Frequency Standards in General 79
by Warren L. Smith
8.3.1 Design Considerations 80
8.3.2 Measurement and Specification of Frequency Stability 89

9 Temperature Control and Compensation
by Marvin E. Frerking

List of Symbols 99
9.1 Temperature Control 101
9.1.1 Thermal Loss 105
9.1.2 Warm-Up Considerations 107
9.2 Temperature Compensation 108
9.2.1 Analog Temperature Compensation 109
9.2.2 Digital Temperature Compensation 110
9.2.3 Microprocessor Temperature Compensation 111

10 Microwave Frequency and Time Standards
by Helmut Hellwig

List of Symbols 114
10.1 Concepts, Design, and Performance 115
10.1.1 Historical Perspective 115
10.1.2 Concept of an Atomic Resonator 116
10.1.3 Design Principles 119
10.1.4 Performance Principles 123
10.1.5 Active and Passive Electronic Systems 125
10.1.6 Phase-Lock Servos 128
10.1.7 Frequency-Lock Servos 128
10.1.8 Electronic Systems 133
10.2 Passive Beam Standards 137
10.2.1 Beam Generation 137
10.2.2 Spatial State Selection 138

10.2.3 Microwave Interrogation 139
10.2.4 Detection of Atoms 142
10.2.5 The Cesium-Beam Standard 143
10.2.6 Other Passive Beam Standards 148
10.2.7 New Horizons 149
10.3 Gas-Cell Standards 150
10.3.1 Gas-Cell Principles 150
10.3.2 Optical State Selection 152
10.3.3 The Rubidium Gas-Cell Standard 153
10.3.4 Other Gas-Cell Standards 157
10.3.5 New Horizons 158
10.4 Hydrogen Masers 159
10.4.1 Hydrogen-Maser Principles 159
10.4.2 Active and Passive Masers 161
10.4.3 Frequency Stability and Accuracy 163
10.4.4 Other Masers 165
10.4.5 New Horizons 166
10.5 Other Microwave Frequency Standards 169
10.5.1 The Ammonia Maser 169
10.5.2 Trapped Ions 169
10.6 Comparison of Frequency Standards 171
10.7 Applications 171
10.7.1 Metrology and Science 171
10.7.2 Technology 175

11 Laser Frequency Standards
by Rudolf Buser and Walter Koechner

11.1 Introduction 177
11.2 The Potential Role of Lasers 179
11.3 Basic Laser Configuration 181
11.4 Stabilization of Lasers 182
11.4.1 He–Ne Laser Stabilized with a Ne Cell 184
11.4.2 He–Ne Laser with an I_2 Cell 185
11.4.3 He–Ne Laser and Methane Absorption Cell 185
11.4.4 CO_2 Laser with a CO_2 Absorption Cell 185
11.5 Measurement of Optical Oscillation Frequencies 185
11.6 Future Prospects and Problems 189

12 Frequency and Time—Their Measurement and Characterization
by Samuel R. Stein

List of Symbols 192
12.1 Concepts, Definitions, and Measures of Stability 193
12.1.1 Relationship between the Power Spectrum and the Phase Spectrum 195
12.1.2 The IEEE Recommended Measures of Frequency Stability 195
12.1.3 The Concepts of the Frequency Domain and the Time Domain 203

12.1.4 Translation between the Spectral Density of Frequency and the Allan Variance 203
12.1.5 The Modified Allan Variance 205
12.1.6 Determination of the Mean Frequency and Frequency Drift of an Oscillator 207
12.1.7 Confidence of the Estimate and Overlapping Samples 210
12.1.8 Efficient Use of the Data and Determination of the Degrees of Freedom 213
12.1.9 Separating the Variances of the Oscillator and the Reference 216
12.2 Direct Digital Measurement 217
12.2.1 Time-Interval Measurements 217
12.2.2 Frequency Measurements 219
12.2.3 Period Measurements 219
12.3 Sensitivity-Enhancement Methods 220
12.3.1 Heterodyne Techniques 220
12.3.2 Homodyne Techniques 221
12.3.3 Multiple Conversion Methods 227
12.4 Conclusion 231

13 Frequency and Time Coordination, Comparison, and Dissemination
by David W. Allan

List of Acronyms 233
13.1 Introduction 234
13.1.1 Historical Perspectives and Methods of Comparison 234
13.1.2 Time and Frequency Standards 235
13.2 Terrestrial Time and Frequency Comparison or Dissemination Methods 237
13.2.1 High and Medium Frequency 237
13.2.2 Low- and Very-Low-Frequency Transmissions 237
13.2.3 Other Methods 250
13.3 Extraterrestrial Time and Frequency Comparison or Dissemination Methods 253
13.3.1 Operational-Satellite Techniques 253
13.3.2 Experimental-Satellite Techniques 258
13.3.3 Deep-Space Radio-Source Techniques 268
13.4 Coordinate Time for the Earth 268
13.5 Levels of Sophistication and Accuracies for the Users 270
13.5.1 Typical User Applications 272
13.5.2 Sophisticated and High-Accuracy Techniques 272
13.6 Summary 272

14 Other Means for Precision Frequency Control
by Fred L. Walls

14.1 Introduction 275
14.2 Low-Frequency Devices 276
14.2.1 Quartz Tuning Forks 276
14.2.2 Other Low-Frequency Devices 279

14.3 Microwave Devices 281
14.3.1 Superconducting Cavities 281
14.3.2 Dielectrically Loaded Cavities 284

15 Special Applications
by Fred L. Walls and Jean-Jacques Gagnepain

15.1 Microbalances, Thin-Film Measurement, and Other Mass-Loading Phenomena 288
15.2 Measurements of Force, Pressure, and Acceleration 290
15.2.1 Force 290
15.2.2 Pressure 291
15.2.3 Acceleration 291
15.3 Temperature Measurements 293

16 Specifications and Standards
by Erich Hafner

16.1 Specifications 297
16.2 Standards 299
16.3 Practices in the United States 300
16.4 International Standardization 304

Bibliography
by Eduard A. Gerber and Arthur Ballato

Introduction 305
General Bibliography 306
Chapter Bibliographies 313

INDEX TO VOLUMES 1 AND 2 443

Contributors

Numbers in parentheses indicate the pages on which the authors' contributions begin.

DAVID W. ALLEN (223), Time and Frequency Division, National Bureau of Standards, Boulder, Colorado 80303

ARTHUR BALLATO (305), U.S. Army Electronics Technology and Devices Laboratory, Fort Monmouth, New Jersey 07703

RUDOLF BUSER (177), U.S. Army Night Vision Laboratory, Fort Belvoir, Virginia 22060

MARVIN E. FRERKING (99), Collins Defense Communications Division, Rockwell International, Cedar Rapids, Iowa 52498

JEAN-JACQUES GAGNEPAIN (287), Laboratoire de Physique et Métrologie des Oscillateurs du CNRS, 25000 Besançon, France

EDUARD A. GERBER[1] (305), U.S. Army Electronics Technology and Devices Laboratory, Fort Monmouth, New Jersey 07703 (Retired)

ERICH HAFNER[2] (1, 297), U.S. Army Electronics Technology and Devices Laboratory, Fort Monmouth, New Jersey 07703 (Retired)

HELMUT HELLWIG (113), Frequency and Time Systems, Beverly, Massachusetts 01915

WALTER KOECHNER (177), Science Applications, Inc., McLean, Virginia 22102

THOMAS E. PARKER (66), Research Division, Raytheon Company, Lexington, Massachusetts 02173

WARREN L. SMITH (45, 79), AT&T Bell Telephone Laboratories, Allentown, Pennsylvania 18103

[1]Present address: 11 Community Drive, West Long Branch, New Jersey 07764.
[2]Present address: 881 Sycamore Avenue, Tinton Falls, New Jersey 07724.

SAMUEL R. STEIN[3] (191), Time and Frequency Division, National Bureau of Standards, Boulder, Colorado 80303
F. L. WALLS (275, 287), Time and Frequency Division, National Bureau of Standards, Boulder, Colorado 80303

[3]Present address: Efratom Division, Ball Corporation, Broomfield, Colorado 80020.

Preface

The editors take pleasure in presenting this two-volume work on precision frequency control. The title encompasses the spectrum of frequency-determining and frequency-selective devices, subject to the constraint imposed by the adjective. A simple circuit consisting of an inductance and a capacitance can function as a frequency-controlling element. Its precision, however, is completely insufficient for modern electronic equipment. Different physical phenomena must be utilized to meet today's requirements. The discussion and explication of these phenomena and their applications are the main purposes of these books.

The aims are twofold: first, to offer a concise compendium of the state of the art to researchers and specialists engaged in a rapidly expanding and complex field of technology. It will enable them to work efficiently in their fields and to develop devices that meet the requirements of the equipment and systems engineer.

A second purpose of the books is to furnish information concerning properties and capabilities of frequency-control devices to users of these devices, such as equipment and systems designers. The volumes will also be very useful for technical managers who will be able to find, in a single publication, a description of the world of precision frequency control, written by experts, and an entree to the full literature of the field.

The idea of these books originated several years ago when the editors recognized that the literature in the field of frequency control was increasing at an explosive rate and that it would be extremely difficult, particularly for a novice in this field, to attain without guidance an essential level of knowledge in a reasonable time. Another incentive for compiling this text is the fact that there is no single book available on the world market that treats all precision frequency-control devices and allows the reader to weigh the advantages or disadvantages of the various technical approaches against one another.

The number of experimental observations and theoretical investigations in the field of precision frequency control has increased steadily over the past 60 years and has led, particularly during the past few years, to a deluge of original publications that is becoming more and more difficult to absorb in its totality, even for the trained specialist. In view of this, our aim is not to attempt to offer a textbook on the subject, but rather to provide a tutorial and coherent treatment of the more recent developments in the field, supported by an extensive literature reference list covering approximately the past fifteen years. The individual chapters are written by experts in their respective specialities. The editors feel that the fundamentals of this field, starting with the seminal works of the Curies, Voigt, Cady, Townes, Ramsey, and others, are very well represented in older textbooks and in many voluminous review papers and handbook articles whose titles the reader will find in the bibliography.

The material of the work is presented in two volumes, "Acoustic Resonators and Filters" (Volume 1) and "Oscillators and Standards" (Volume 2). The reader will find in the introduction to the bibliography, included in both volumes, some suggestions on how to use the chapter bibliographies to best advantage. The 16 chapters of the text can be read independently of one another. Their topics have been chosen to maximize the readability of the book, with lengths governed jointly by the number of publications pertinent to each chapter and by the importance the editors attach to each topic, although obviously it is impossible to discuss in the text all of the more than 5000 publications referenced. The selection of specific areas discussed is to a certain extent subjective, but we feel that they give a good indication of the overall progress in our field.

The reader will find glossaries of letter symbols—whenever necessary—at the beginning of each chapter and, in certain instances, introducing a section. These characters, as well as graphic symbols used in the book, correspond as much as possible to those specified in the following IEEE Standards:

IEEE 260	1978	Letter Symbols for Units of Measurement
IEEE 280	1968	Letter Symbols for Quantities Used in Electrical Science and Electrical Engineering
IEEE 315	1975	Graphic Symbols for Electrical and Electronics Diagrams
IEEE 176	1978	Piezoelectricity
IEEE 177	1966	Definitions and Methods of Measurement for Piezoelectric Vibrators

Copies of these standards may be obtained from The Institute of Electrical and Electronics Engineers, 345 East 47th Street, New York, New York 10017.

The editors wish to express their sincere thanks to the authors of the various chapters for their cooperation and enjoyable collaboration, the editorial and production staffs of Academic Press for their patience and support, Mrs. Carolyn Clever for her typing, and the personnel of the U.S. Army Electronics Technology and Devices Laboratory, Fort Monmouth, for much encouragement and assistance. They wish to thank, in particular, Mrs. Gloria Gatling for doing a careful and patient job of typing the final version of the bibliography, Miss Betsy Hatch for her computer work, and Mr. Ted Lukaszek for his steady and manifold help prior to and during the preparation of the text. Finally, the editors gratefully acknowledge stimulating discussions over many years with R. D. Mindlin (Columbia University) and R. A. Sykes (AT&T Bell Laboratories), who, by the synthesis of their theoretical and experimental work and by their education of students and colleagues, helped substantially to make a science out of an art in the field of crystal frequency control.

E. A. Gerber
West Long Branch, New Jersey

A. Ballato
Long Branch, New Jersey

Contents of Volume 1

1 Properties of Piezoelectric Materials

List of Symbols
1.1 An Overview
by Larry E. Halliburton and Joel J. Martin
1.1.1 Structural Requirements
1.1.2 Electroelastic Relations
1.1.3 Materials of Current Interest
1.2 Physical Properties of Quartz
by Larry E. Halliburton, Joel J. Martin, and Dale R. Koehler
1.2.1 Crystallography
1.2.2 Crystal Growth and Extended Defects
1.2.3 Point Defects
1.2.4 Thermal Properties
1.2.5 Material Evaluation Techniques

2 Theory and Properties of Piezoelectric Resonators and Waves

List of Symbols for Sections 2.1 and 2.2
2.1 Bulk Acoustic Waves and Resonators
by Thrygve R. Meeker
2.1.1 Introduction
2.1.2 Basic Quasi-Static Theory of a Piezoelectric Elastic Material
2.1.3 Linear Theory
2.1.4 Nonlinear Theory
2.1.5 The Christoffel Plane-Wave Solutions for the Linear Quasi-Static Piezoelectric Crystal
2.1.6 Thickness Modes
2.1.7 Contour Modes in Thin Plates and in Thin and Narrow Bars
2.1.8 Theory for Combined Thickness and Contour Modes
2.1.9 Electrical Effects in Piezoelectric Resonators

2.1.10 Equivalent Electrical Circuits for Piezoelectric Resonators
2.1.11 Properties of Modes in Crystal Resonators
2.1.12 Piezoelectric Materials
2.1.13 Conclusion
2.2 Properties of Quartz Piezoelectric Resonators
by Thrygve R. Meeker
2.2.1 Temperature Coefficient of Resonance Frequency
2.2.2 Dependence of Crystal Inductance on Temperature
2.2.3 Tabulation of Properties of Quartz Resonators
2.2.4 Conclusion
List of Symbols for Section 2.3
2.3 Surface Acoustic Waves and Resonators
by William R. Shreve and Peter S. Cross
2.3.1 Introduction
2.3.2 Resonator Design
2.3.3 Fabrication
2.3.4 State-of-the-Art Performance
2.3.5 Conclusion

3 Radiation Effects on Resonators
by James C. King and Dale R. Koehler

3.1 Introduction
3.2 Radiation Effects and Modeling
3.2.1 Substitutional Al^{3+} Defect Center
3.2.2 Frequency Changes
3.2.3 Optical Effects
3.2.4 Elastic Modulus Changes
3.3 Dynamics of Radiation Effects
3.3.1 Hydrogen and Transient Effects
3.3.2 ESR and IR Studies
3.3.3 Trap Characterization
3.3.4 Material Quality and Anelastic Losses
3.3.5 Thermal Effects

4 Resonator and Device Technology
by John A. Kusters

4.1 Resonator Material Selection
4.2 Sawing
4.2.1 Natural Quartz
4.2.2 Cultured Quartz
4.3 X-Ray Orientation
4.4 Mechanical Operations
4.5 Cleaning
4.6 Vacuum Deposition
4.7 Mounting and Sealing
4.8 Special Fabrication Considerations for SAW Devices
4.9 Novel Resonator Techniques
4.10 Environmental Effects

5 Piezoelectric and Electromechanical Filters

List of Symbols for Sections 5.1 and 5.2
5.1 General
by Robert C. Smythe
5.2 Bulk-Acoustic-Wave Filters
by Robert C. Smythe
5.2.1 Introduction
5.2.2 Crystal Filters
5.2.3 Electromechanical Filters
List of Symbols for Sections 5.3 and 5.4
5.3 Surface-Acoustic-Wave Filters
by Robert S. Wagers
5.3.1 Introduction
5.3.2 Interdigital Transducer Admittance
5.3.3 Relation of Normal-Mode Theory Admittance to the Impulse Model
5.3.4 Limitations on the Use of Electrostatic Fields
5.3.5 Electromechanical Coupling Constant k
5.3.6 Electrical Q and Insertion Loss
5.3.7 Bulk-Wave Modeling of Interdigital Transducers
5.3.8 Advanced Bulk-Wave Models
5.4 SAW Bandpass and Bandstop Filters
by Robert S. Wagers
5.4.1 Introduction
5.4.2 Impulse-Response Realizations
5.4.3 SAW Bandpass Filter Capabilities
5.4.4 SAW Bandstop Filters

6 Long-Term Stability and Aging of Resonators
by Eduard A. Gerber

6.1 Low-Frequency Bulk-Wave Devices
6.2 High-Frequency Bulk-Wave Devices
6.2.1 Causes of Aging
6.2.2 Progress through Holder Design
6.2.3 Progress through Mounting and Crystal Plate Design
6.2.4 Isolation of Aging Causes
6.2.5 Influence of Temperature
6.2.6 Influence of Radiation
6.3 Surface-Wave Devices
6.3.1 SAW Resonators
6.3.2 SAW Delay Lines

Bibliography
by Eduard A. Gerber and Arthur Ballato

Introduction
General Bibliography
Chapter Bibliographies

Introduction

The history of precision frequency control provides a good example of how technological maturity follows upon the prior accomplishment of scientific groundwork. The foundations of modern frequency control began with discovery of the piezoelectric effect by the brothers Curie in 1880, which found theoretical treatment in Voigt's classic book (1910). Founded on these accomplishments, the development of devices using the piezoelectric effect started during World War I and has proceeded since at an accelerating rate. Quartz crystals used for frequency control developed from rather simple, unevacuated, pressure-mounted units of the 1920s and 1930s to the present highly sophisticated plated units operating in ultrahigh vacua with temperature-compensating or temperature-controlling arrangements. Influences of the environment, such as mounting structure, pressure, and acceleration, have been greatly reduced by using doubly rotated crystal plates. Similarly, great progress has been made in the development of frequency-control devices based on atomic or molecular processes since Essen built and described the first cesium-beam frequency standard in 1957. They have progressed from the original 8-ft giant to the currently commercially available equipment of modest size and weight.

It is no accident that the flowering of our field has coincided with the advent of the space age. No stretch of the imagination is required to see the demands placed on oscillator stability by rocket and satellite environments; and in few applications is the need for precision so severe. Concurrently, similar requirements were imposed in the fields of communication and guidance systems, both commercial and military. For instance, systems for frequency- and time-division multiplex communication, satellite-assisted positioning, as well as remote surveillance and collision avoidance, would be impossible without precision frequency-control and timing devices.

In the dozen years from the launching of the first artificial satellite about the earth to the first manned lunar landing, the frequency-control field and its correlate areas of selection, signal processing, timing, and time distribution experienced an enormous period of development and growth. The advances made during this time turned out, in retrospect, to be only a prelude to the developments of the next decade. The interval following the first Apollo landing initiated what might justly be called the golden age of frequency control. The editors made no predictions as to the extent and duration of this exciting period—certainly it is continuing; but one may well question if we shall soon see a decade in which the development of both accuracy and precision will experience such favorable conditions as have been met within the area of frequency control.

The attribute "precision" in the title restricts the contents of this work to those devices whose Q value and frequency stability far exceed that of an ordinary LC circuit. Consequently, the reader will not find ceramic resonators and filters discussed. Material on polycrystalline and similar devices is included only if it bears on the behavior of high-Q devices (e.g., the theory of vibration of anisotropic bodies). On the other hand, superconductive LC devices with their high Q are properly included. One other remark regarding selection of material is pertinent: The main application of bulk-wave monocrystalline devices is to frequency control, whereas surface-acoustic-wave devices are being used in many other fields. We therefore discuss the fundamental properties of bulk-wave devices and their materials to a fuller extent. As far as surface-wave monocrystalline devices are concerned, only those aspects of material and resonator properties considered pertinent to precision frequency control are covered.

7 Resonator and Device Measurements

Erich Hafner

U.S. Army Electronics Technology and Devices Laboratory (Retired)
Fort Monmouth, New Jersey

List of Symbols 2
7.1 Introduction 2
7.2 The Crystal Unit and Its Equivalent Circuit 4
7.2.1 The Resonator-Equivalent Electrical Circuit 4
7.2.2 Device Properties of the Crystal Unit 6
7.2.3 The Characteristic Parameters of a Crystal Unit 11
7.2.3.1 Motional-Arm Resonance 14
7.2.3.2 Resonance and Antiresonance 15
7.2.3.3 Parallel Resonance 15
7.2.3.4 Maximum and Minimum Admittance 16
7.2.3.5 Minimum Reflection Coefficient 16
7.3 Crystal-Resonator Measurements 16
7.3.1 General 16
7.3.2 Resonator Measurement Instruments 19
7.3.2.1 Crystal Impedance Meters 19
7.3.2.2 The Zero-Phase π Network 22
7.3.2.3 Bridge-Type Instruments 25
7.3.2.4 Analyzers 31
7.3.3 Measurement Methods 33
7.3.3.1 The Sweep Mode 33
7.3.3.2 Measurement of the Characteristic Parameters 34
7.3.3.3 Measurement of Frequency–Temperature Characteristics and Aging 37
7.4 Summary and Conclusions 38
Appendix I: The Generalized Equivalent Circuit 41
Appendix II: Two-Port Relations for the IEC-444 π Network 43
Appendix III: Two-Port Relations for a Transmission Bridge 44

PRECISION FREQUENCY CONTROL
Oscillators and Standards

Copyright © 1985 by Academic Press, Inc.
All rights of reproduction in any form reserved.
ISBN 0-12-280602-6

LIST OF SYMBOLS

C_1, L_1, R_1, C_0	Parameters of lumped-element-equivalent electrical circuit for piezoelectric resonator
C_1', L_1', R_1', C_0'	Parameters of modified resonator circuit, transformed values of C_1, L_1, R_1, and C_0 due to presence of C_{HA} and C_{HB}
C_{HA}, C_{HB}	Holder capacitances, from resonator electrodes to enclosure (ground)
G, B	Coordinates of admittance plane
R, X	Coordinates of impedance plane
R_{sub}	Value of substitution resistor
R_γ	Resistance at ω_γ
$X_1(\omega)$	Reactance of resonator motional arm; $X_1' = \alpha X_1$ is the transformed value due to C_{HA}
$\bar{X}_0, \bar{B}_0$	Reactance, susceptance of all (lossless) elements in parallel with motional arm; $\bar{B}_0 = 1/\bar{X}_0$; $\bar{X}_0'$ is the transformed value of $\bar{X}_0$ due to C_{HA}
$\bar{X}_1, \bar{B}_1$	Reactance, susceptance of all (lossless) elements in series with crystal resonator
Z	Impedance
Z_0	Characteristic impedance
Z_k	Network impedances, $k = 1, 2, \ldots, 6$
Z_{Tk}	Terminating impedances, $k = 1, 2$
α	Transformation constant to account for C_{HA}
Γ	Reflection coefficient of impedance Z_x relative to impedance Z_0; $\Gamma = (Z_x - Z_0)/(Z_x + Z_0)$
ω_a, R_a	Frequency and resistance at antiresonance ($X_a = 0$)
ω_L, R_L	Frequency and resistance at resonance with load capacitance
ω_m, R_m, X_m	Frequency, resistance, and reactance at maximum admittance, minimum impedance
ω_n, R_n, X_n	Frequency, resistance, and reactance at minimum admittance, maximum impedance
ω_p, R_p	Frequency and resistance at parallel resonance [$X_1(\omega_p) = -\bar{X}_0$, $X_p = \bar{X}_0$, $R_p = \bar{X}_0^2/R_1$]
ω_r, R_r	Frequency and resistance at resonance ($X_r = 0$)
ω_s, G_s	Frequency and conductance at motional arm resonance [$X_1(\omega_s) = 0$, $G_s = 1/R_1$, $B_s = 1/\bar{X}_0$]
ω_{sL}, G_{sL}	Frequency and conductance at resonance of motional arm with load capacitance [$B_{sL} = \bar{X}_0\bar{X}_L/(\bar{X}_0 + \bar{X}_L)$]
ω_γ, Γ_n	Frequency and reflection coefficient at minimum Γ

7.1 INTRODUCTION

The classic literature on crystal resonators attests to an intense interest in the subject of resonator measurements ever since the first use of these devices for frequency control and selection. The efforts expended to gain an understanding of the behavior of piezoelectric devices as circuit elements led also, in time, to a clear appreciation of the basic principles of measurement (Cady, 1964, pp. 392ff). Fundamental to all measurements, then as now, are the equivalent electrical circuit and its immittance diagrams. The implementation of specific techniques is, naturally, a function of the state of technology

of components and instrumentation at any given time. The continuing evolution of new techniques is documented in the numerous articles on the subject cited in the bibliography to this chapter. Snapshots of the state of the art at various times are provided by the review papers by Horton and Boor (1965) and Horton *et al.* (1981).

Although the conventional equivalent circuit of the piezoelectric resonator is composed of capacitors, coil, and resistor, they are of a magnitude (not encountered in conventional devices) that sets resonator measurements apart from measurements on nearly all other electronic components. For quartz crystal units, the commercially most important crystal resonator, the capacitance values involved are in the femtofarad range, with the inductance ranging from many henrys at 1 MHz and below to millihenrys in the 100-MHz range. Consequently, the techniques and instrumentation for resonator measurements are subject to requirements not usually encountered with normal components. This in turn has led to the development, largely driven by speed and economic considerations, of specialty instruments specifically tailored, and generally restricted, to the measurement of crystal resonators. An example is the family of crystal impedance meters. Economic considerations will continue to assure a role for specialty instruments. However, the remarkable progress in measurement-system automation in general, coupled with the availability of new and useful circuit components, gives cause now for a fundamental change in philosophy. The amount and quality of labor in data accumulation and the computational effort in data reduction (previously of very major importance in the selection of a particular technique) can now be reduced to the point of insignificance, due to these developments, for nearly any resonator measurement technique considered. The selection can thus, in principle, be made on the basis of the intrinsic limitations of the various techniques; in practice it will be limited by the availability of instruments at any given time and, of course, by cost.

The present chapter first considers the equivalent circuit of crystal resonators and then proceeds with a discussion of the more important measurement instruments and techniques. An effort was made, thereby, to emphasize the common aspects of the operating principles of most of the relevant instruments, to discuss the basic facts involved in their calibration, and to alert the reader to the generic sources of measurement errors. Although resonator measurements are also used for the determination of material constants, the instrumentation and techniques specifically oriented to this purpose, such as the pulse-echo techniques (McSkimin and Bateman, 1969), are not included here.

Except for the respective frequency ranges involved, the measurement of surface acoustic wave (SAW) resonators is no different from that of the more conventional bulk-acoustic-wave resonators. The generic discussions of the instruments and techniques, therefore, apply equally to both types of

resonators. Moreover, many of the techniques to be discussed use the crystal resonator in a transmission network. The discussions of the error sources intrinsic to these types of measurements apply equally to the measurement of crystal filters, but filter measurements *per se* are not included here.

7.2 THE CRYSTAL UNIT AND ITS EQUIVALENT CIRCUIT

7.2.1 The Resonator-Equivalent Electrical Circuit

The key to the proper application of crystal resonators in electrical circuits is a thorough understanding of their equivalent electrical circuit. Yet, the conceptual difficulties in relating a crystal resonator—a disk of solid dielectric between electrodes, to all appearance a capacitor—to its behavior as a circuit element are often found to handicap the more casual user in his appreciation of the significance and utility of the equivalent electrical circuit. Therefore, a brief review of the basic facts behind it might well be in order.

A familiar electrical analog of a mechanically vibrating system with a single degree of freedom is shown in Fig. 7-1. A coil, a capacitor, and a resistor represent a mass, a spring, and a damping element (dashpot) (Cady, 1964, para. 62). Charge on the capacitor corresponds to displacement of the mass, current to its velocity, and voltage to the driving force. The two systems are described by the same differential equation, and this is, in fact, the only link between them. In Fig. 7-2a, however, the mass on the spring is assumed to be a magnet, suspended inside a coil. Now the electrical analog of the mass–spring system assumes a very direct meaning. To an observer at the coil terminals, the mass–spring system behaves as though it were (it is equivalent to) an electrical

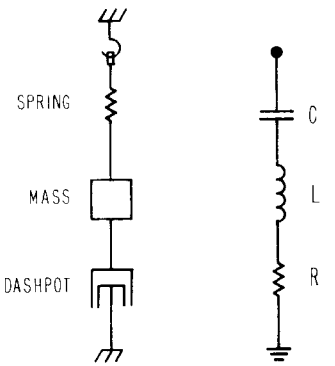


FIG. 7-1 Electrical analog of a vibrating mass. The correspondence is mass–coil, spring capacitor, and dashpot–resistor.

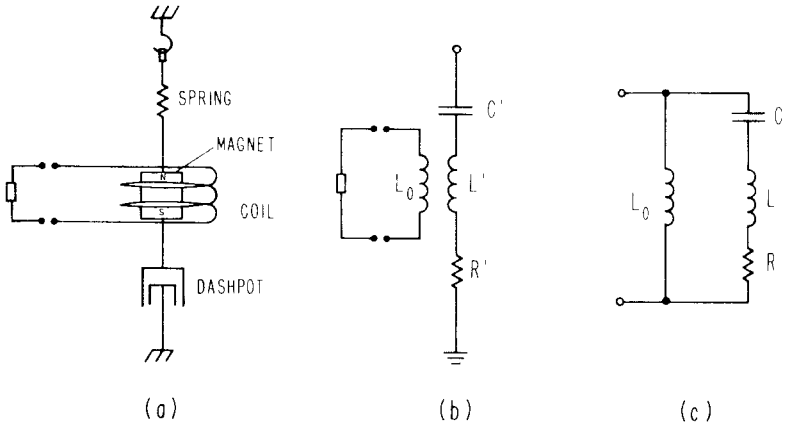


FIG. 7-2 Vibrating magnet in the vicinity of a coil. Voltage and current at the coil terminals in (a) are indistinguishable from those at the terminals of the "equivalent" cricuits in (b) or (c) if the parameters are chosen appropriately.

circuit. Two possible configurations present themselves immediately, as shown in Figs. 7-2b and c. The parameters of the "motional arm," C'–L'–R' in Fig. 7-2b and C–L–R in Fig. 7-2c, are related by such quantities as the strength of the magnet, the number of turns of the driving coil, and the distance of the coil from the vibrating magnet, that is, by the physical parameters of the magnetomechanical system; the values of mass, spring constant, and damping are already reflected in the values L', C', and R', respectively. If these physical parameters are not known a priori, then Fig. 7-2c is the simplest form for a circuit that provides a full description of the electrical behavior of the system in Fig. 7-2a.

A crystal resonator, too, is a mechanically vibrating system with a direct link to the electrical world. Here, the link is provided by the piezoelectric effect. Like any elastic body with finite dimensions, a crystal resonator is capable of a very large number of mechanical resonance vibrations. In general, only one of these "modes" is important, and desirable, for a particular application. For this one mode, the distributed mass and elastic properties of the body can, as a first approximation, again be represented as a lumped-mass–spring system, as in Fig. 7-1. If the material is piezoelectric, then a charge appears on the surface of the resonator when it is mechanically deformed. This charge is proportional, in magnitude and sign, to the deformation of the body. Conversely, the application of a charge to the body at rest causes it to deform. The appropriate piezoelectric constant for the type of motion involved establishes the numeric relationship between charge and deformation. Electrodes applied to certain parts of the surface of the resonator integrate the charges over the

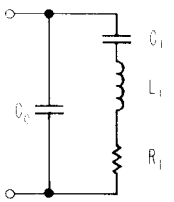


FIG. 7-3 Equivalent electrical circuit of a piezoelectric resonator. C_0 is the static capacitance of the electrodes. The L_1–C_1–R_1 branch is the *motional arm*, the electrical equivalent of the mechanical vibrating body of the resonator, coupled into the circuit by virtue of the piezoelectric effect.

covered areas and thus provide the means to link the mechanical vibrations of the body to the electrical world, in much the same fashion as discussed above for the magnet vibrating inside a coil. The circuit corresponding to Fig. 7-2c is the equivalent electrical circuit for the piezoelectric resonator shown in Fig. 7-3 (Butterworth, 1915). The L_1–C_1–R_1 branch is known as the "motional arm" of the equivalent electrical circuit of the crystal resonator. Approximate relations for the parameters L_1, C_1, R_1, and C_0 in terms of the effective elastic, piezoelectric, and dielectric material constants of the crystal resonator, its geometry, and the overtone order can be found in various references [e.g., Cady (1964, para. 256), Hafner (1974), and Bottom (1982, p. 98)].

The concept of a lumped-mass–spring system, coupled piezoelectrically to the electrodes, is a very useful aid in interpreting many aspects of the behavior of crystal resonators. The resulting lumped-element-equivalent electrical circuit in Fig. 7-3, with frequency-independent parameters, provides an excellent approximation to the electrical performance of crystal resonators made of materials with small piezoelectric coupling coefficients and low losses, such as quartz. Arbitrarily large coupling coefficients and, in fact, fairly large losses can be handled by the same formalism used in the following to analyze the circuit in Fig. 7-3 if the motional-arm reactance is suitably reinterpreted. This is demonstrated in Appendix I.

Numerous other forms of equivalent electrical circuits for crystal resonators have been developed (Mason, 1942; Meeker, 1972; Stevenson and Redwood, 1969; Ballato, 1972, 1977). These can provide, for certain applications, a more suitable representation of the resonator behavior. The one shown in Fig. 7-3, as extended in the following section, is adequate for all aspects considered here.

7.2.2 Device Properties of the Crystal Unit

The term "crystal resonator" is used to describe the appropriately shaped piece of crystalline material with electrodes on or near selected parts of its

surface. The term "crystal unit" refers to the packaged circuit component. The crystal unit consists of the crystal resonator, its support structure, and its (generally hermetic) enclosure. It is the finished product. Specifications generally deal with the device at that level. Of particular interest to the user are, next to the properties of the enclosure, the electrical characteristics of the unit at its terminals. The latter are dominated by the crystal resonator but also affected by the mounting structure needed to support the resonator inside the enclosure and by stray capacitances. An examination (Hafner, 1969) of the effects of these elements shows that, under fairly liberal assumptions which are nearly always met, the equivalent electrical circuit of a crystal unit reduces to the circuit between the terminals 1, 2, and 3 in Fig. 7-4a, where the values of L_1, C_1, R_1, and C_0 are very nearly equal to those of the like quantities in Fig. 7-3.

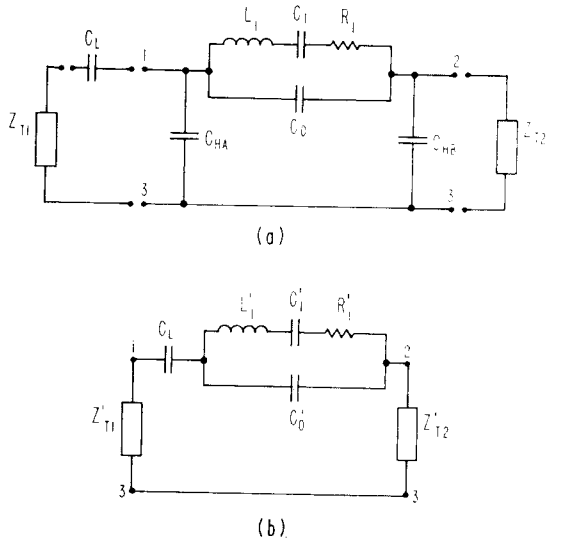


FIG. 7-4 Equivalent electrical circuit of a crystal unit, including the holder capacitances C_{HA} and C_{HB}, a series load capacitor C_L, and low-impedance terminations representing the using circuit. $|Z_{T1}|, |Z_{T2}| \ll 1/\omega C_{HA}$. The circuit in (a) can be transformed into (b), where $Z'_{T1} = Z_{T1}$, $1/Z'_{T2} = 1/Z_{T2} + j\omega C_{HA}$, $L'_1 = \alpha L_1$, $R'_1 = \alpha R_1$, $C'_1 = C_1/\alpha$, $C'_0 = C_0/\alpha$. When $|Z_{T2}| > 0$, $\alpha = (1 + C_{HA}/C_L)$, $C'_0 = C_0$; when $|Z_{T2}| = 0$, $\alpha = 1$, $C'_0 = C_0 + C_{HA}$.

With the transformation shown in Fig. 7-4b, it follows that the transfer characteristic of a crystal unit in a network with low terminating impedances is determined by the network in Fig. 7-5, which is termed the "modified crystal resonator." The latter reverts to the crystal resonator in Fig. 7-3 when $\bar{X}_L = 0$, $\bar{X}_0 = -1/\omega C_0$, and $X_1 = \omega L_1 - 1/\omega C_0$.

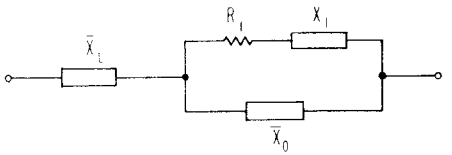


FIG. 7-5 The modified crystal resonator. X_1 and R_1 are the reactance and resistance, respectively, of the motional arm; $\bar{X}_0$ is the reactance of all (lossless) elements in parallel with the motional arm and $\bar{X}_L$ the reactance of all (lossless) elements in series with the crystal unit.

The admittance of the modified crystal resonator in Fig. 7-5, with $\bar{X}_L = 0$, is given by

$$Y = G + jB = j\bar{B}_0 + \frac{R_1}{R_1^2 + X_1^2} - j\frac{X_1}{R_1^2 + X_1^2}, \tag{7-1}$$

where $\bar{B}_0 = -1/\bar{X}_0$ and

$$X_1 = X_1(\omega). \tag{7-2}$$

As discussed in Appendix I, the frequency dependence of X_1 reflects the degree of approximation used in analyzing the mechanical motion of the resonator. In all cases

$$X_1(\omega_s) = 0. \tag{7-3}$$

When the crystal resonator is represented by Fig. 7-3,

$$\begin{aligned} X_1(\omega) &= \omega L_1 - 1/\omega C_1, \\ \omega_s &= 2\pi f_s = 1/\sqrt{L_1 C_1}. \end{aligned} \tag{7-4}$$

Separating the real and imaginary parts of Eq. (7-1) gives

$$G = \frac{R_1}{R_1^2 + X_1^2}, \qquad B = \bar{B}_0 - \frac{X_1}{R_1^2 + X_1^2}, \tag{7-5}$$

which, for any given R_1 and any given frequency, describe a point in the admittance (G, B) plane. Squaring and adding G and B in Eq. (7-5) gives $G^2 + (B - B_0)^2 = 1/(R_1^2 + X_1^2)$, which, when reinserted into Eq. (7-5) and after simple manipulations, leads to

$$(G - 1/2R_1)^2 + (B - \bar{B}_0)^2 = (1/2R_1)^2, \tag{7-6}$$

$$G^2 + (B - \bar{B}_0 + 1/2X_1)^2 = (1/2X_1)^2. \tag{7-7}$$

For finite $\bar{X}_L$ the corresponding equations are

$$\left(G - \frac{1}{2R_1}\frac{\bar{X}_0^2}{(\bar{X}_0 + \bar{X}_1)^2}\right)^2 + \left(B + \frac{1}{\bar{X}_0 + \bar{X}_L}\right)^2 = \left(\frac{1}{2R_1}\frac{\bar{X}_0^2}{(\bar{X}_0 + \bar{X}_L)^2}\right)^2, \tag{7-8}$$

$$G^2 + \left(B + \frac{1}{\bar{X}_0 + \bar{X}_L} + \frac{1}{2}\frac{\bar{X}_0^2}{(\bar{X}_0 + \bar{X}_L)^2}\frac{1}{X_1 + \bar{X}_0\bar{X}_L/(\bar{X}_0 + \bar{X}_L)}\right)^2 = \left(\frac{1}{2}\frac{\bar{X}_0^2}{(\bar{X}_0 + \bar{X}_L)^2}\frac{1}{[X_1 + \bar{X}_0\bar{X}_L/(\bar{X}_0 + \bar{X}_L)]}\right)^2 \tag{7-9}$$

In either set the resistive and reactive components of the motional arm, R_1 and X_1, are separated. The admittance (G, B) of the resonator at any particular frequency and for a particular R_1 is now defined as the intercept of the two circles given by the Eqs. (7-6) and (7-7) or, for finite $\bar{X}_L$, by (7-8) and (7-9). When the points of intercept for a given resonator (given R_1) are plotted three-dimensionally against the coordinates (G, B) and frequency f, a curve such as that shown in Fig. 7-6 is obtained (Ballato, 1970).

This applies to any circuit represented by the diagram in Fig. 7-5. In quartz crystals, however, the motional inductance L_1 is very large. This, in effect, makes X_1 infinitely large at all frequencies, except for a narrow range around the resonance frequency ω_s. Over the range in which X_1 assumes sensibly finite values, the values of $\bar{X}_0$ and $\bar{X}_L$ can be assumed to be constants with negligible error for most purposes. Over this range, which is called the resonance range, X_1 remains as the only frequency-dependent quantity in Eqs. (7-6) through (7-9). In particular, the R_1 = constant circles in Eqs. (7-6) and (7-8) are then independent of frequency. With $\bar{B}_0 = -1/\bar{X}_0$ = constant and $\bar{X}_L$ = constant, the admittance plot of the resonator forms a perfect circle, which is called the *admittance circle* of the crystal unit. All admittance values within the resonance range must lie on this circle. An example is shown in Fig. 7-7a.

Very similar considerations apply to the impedance of the crystal resonator, leading to the definition of the *impedance circle*, an example of which is shown in Fig. 7-7b. The impedance of the modified resonator, as shown in Fig. 7-5, is given by

$$Z = R + jX = j(\bar{X}_0 + \bar{X}_L) + \frac{R_1\bar{X}_0^2}{R_1^2 + (\bar{X}_0 + X_L)^2} - j\frac{\bar{X}_0^2(\bar{X}_0 + X_1)}{R_1^2 + (\bar{X}_0 + X_1)^2}. \tag{7-10}$$

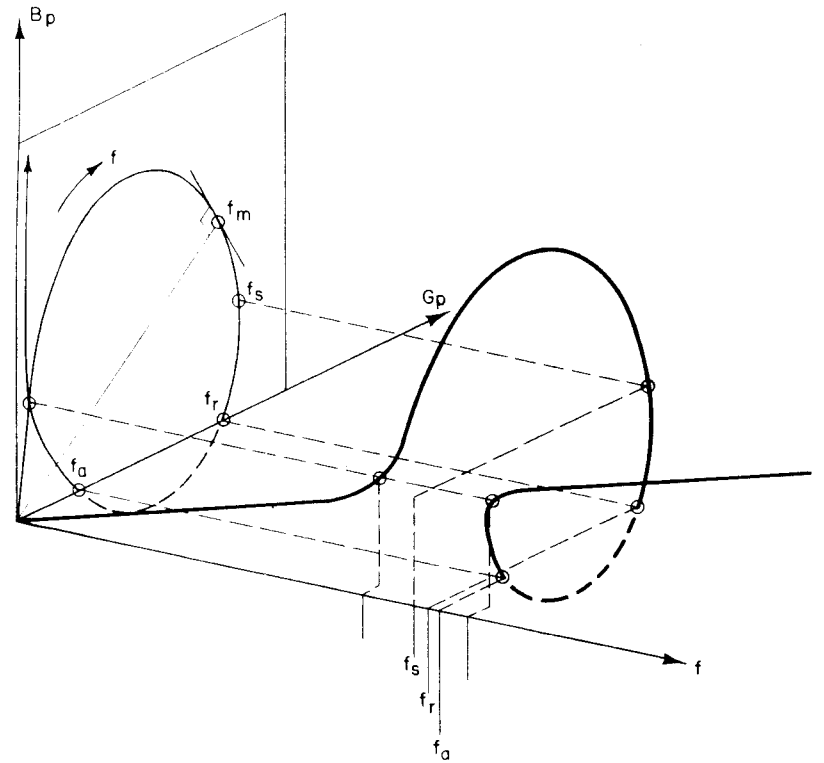


FIG. 7-6 The admittance of the modified resonator (with $\bar{X}_L = 0$) as a function of frequency. The projection of this curve onto the G–B plane is the admittance plot, the projections onto the G–f plane or the B–f plane are the conductance vs. frequency or the susceptance vs. frequency plots, respectively. [From Ballato (1970); © 1970 IEEE.]

Recasting the expressions for R and X into circle equations yields

$$\left(R - \frac{\bar{X}_0^2}{2R_1}\right)^2 + [X - (\bar{X}_0 + \bar{X}_L)]^2 = \left(\frac{\bar{X}_0^2}{2R_1}\right)^2,$$
$$R^2 + \left(X - (\bar{X}_0 + \bar{X}_L) + \frac{\bar{X}_0^2}{2(\bar{X}_0 + X_1)}\right)^2 = \left(\frac{\bar{X}_0^2}{2(\bar{X}_0 + X_1)}\right)^2. \tag{7-11}$$

These equations are again valid, regardless of the relative rate of change with frequency of the reactive elements in the circuit of Fig. 7-5. The generally cissoidal impedance plot described by Eqs. (7-11) becomes a perfect circle when the frequency dependence of $\bar{X}_0$ and $\bar{X}_L$ over the resonance range can be neglected, that is, when $\bar{X}_0$ = constant and $\bar{X}_L$ = constant can be assumed.

TABLE 7-1
Characteristic Parameters of a Crystal Resonator[a]

Parameter	Condition	Exact solutions: $\bar{X}_L = 0$, $\rho = 2R_1/\bar{X}_0$	Exact solutions: With load capacitor C_L, $\rho = \frac{2R_1'}{\bar{X}_0^2}(\bar{X}_0 + \bar{X}_L)$	Approximate solutions, $X_1 = \omega_s L_1(\omega/\omega_s - \omega_s/\omega)$: $\bar{X}_L = 0$, $\bar{X}_0 = -1/\omega_s\bar{C}_0$	Approximate solutions: With load capacitor C_L, $\bar{X}_0 = -1/\omega_s\bar{C}_0$, $\bar{X}_L = -1/\omega\bar{C}_L$
Resonance	$X = 0$	$R_r = \frac{2R_1}{1+\sqrt{1-\rho^2}}$	$R_L = \frac{(\bar{X}_0 + \bar{X}_L)\rho}{1+\sqrt{1-\rho^2}}$	$R_r = R_1$	$R_1 = R_1'(1 + \bar{C}_0/\bar{C}_L)^2$
		$X_1(\omega_1) = -R_1\frac{\rho}{1+\sqrt{1-\rho^2}}$	$X_1(\omega_1) = -\frac{\bar{X}_0\bar{X}_L}{\bar{X}_0 + \bar{X}_L} - \frac{R_1'\rho}{1+\sqrt{1-\rho^2}}$	$\frac{f_1 - f_s}{f_s} = \frac{1}{2}\frac{\omega_s\bar{C}_0R_1}{Q_0}$	$\frac{f_L - f_s}{f_s} = \frac{1}{2}\frac{C_1}{\bar{C}_0 + \bar{C}_L} + \frac{\omega_s\bar{C}_0R_1'}{2Q_0}\left(1 + \frac{\bar{C}_0}{\bar{C}_L}\right)$
Antiresonance	$X = 0$	$R_a = \frac{\bar{X}_0^2}{2R_1}(1+\sqrt{1-\rho^2})$	$R_{aL} = \frac{\bar{X}_0 + \bar{X}_L}{\rho}(1+\sqrt{1-\rho^2})$	$R_a = \frac{1}{\omega_s^2\bar{C}_0^2R_1}$	$R_{aL} = \frac{1}{\omega_s^2\bar{C}_0^2R_1'}$
		$X_1(\omega_a) = -\bar{X}_0 + \frac{R_1\rho}{1+\sqrt{1-\rho^2}}$	$X_1(\omega_{aL}) = -\bar{X}_0 + \frac{R_1'\rho}{1+\sqrt{1-\rho^2}}$	$\frac{f_a - f_s}{f_s} = \frac{C_1}{2\bar{C}_0} - \frac{\omega_s\bar{C}_0R_1}{2Q_0}$	$\frac{f_{aL} - f_s}{f_s} = \frac{C_1}{2\bar{C}_0} - \frac{\omega_s\bar{C}_0R_1'}{2Q_0}\left(1 + \frac{\bar{C}_0}{\bar{C}_L}\right)$
Motional-arm resonance	max G	$R_s = R_1$	$R_{sL} = R_1'(1 + \bar{X}_L/\bar{X}_0)^2$	$R_s = R_1$	$R_{sL} = R_1'(1 + \bar{C}_0/\bar{C}_L)^2$
		$X_1(\omega_s) = 0$	$X_1(\omega_{sL}) = \frac{\bar{X}_0\bar{X}_L}{\bar{X}_0 + \bar{X}_L}$	$f_s = \frac{1}{2\pi\sqrt{L_1C_1}}$	$\frac{f_{sL} - f_s}{f_s} = \frac{1}{2}\frac{C_1}{\bar{C}_0 + \bar{C}_L}$
Parallel resonance	max R	$R_p = \bar{X}_0^2/R_1$	$R_p = \bar{X}_0^2/R_1'$	$R_p = \frac{1}{\omega_s^2\bar{C}_0^2R_1}$	$R_p = \frac{1}{\omega_s^2\bar{C}_0^2R_1'}$
		$X_1(\omega_p) = -\bar{X}_0$	$X_1(\omega_p) = -\bar{X}_0$	$\frac{f_p - f_s}{f_s} \approx \frac{C_1}{2\bar{C}_0}$	$\frac{f_p - f_s}{f_s} = \frac{C_1}{2\bar{C}_0}$
Minimum reflection coefficient	min Γ	$R_\gamma = \frac{Z_0^2}{R_1}\frac{1}{1 + (Z_0/\bar{X}_0)^2}$		$R_\gamma = \frac{Z_0^2}{4R_1}$	$R_\gamma = \frac{Z_0^2}{R_1}\frac{1}{1 + Z_0^2\omega_s^2\bar{C}_0^2}$
		$X_1(\omega_\gamma) = -\bar{X}_0\left(\frac{Z_0}{\bar{X}_0}\right)^2\frac{1}{1 + (Z_0/\bar{X}_0)^2}$		$\frac{f_\gamma - f_s}{f_s} = \frac{1}{2}\frac{C_1}{\bar{C}_0}\frac{1}{1 + Z_0^2\omega_s^2\bar{C}_0^2}$	$\frac{f_\gamma - f_s}{f_s} = \frac{1}{2}\frac{C_1}{\bar{C}_0}\frac{Z_0^2\omega_s^2\bar{C}_0^2}{1 + Z_0^2\omega_s^2\bar{C}_0^2}$

[a] The "exact" relations are valid for the circuit in Fig. 7-5 regardless of the magnitude of the resistive and reactive components. The primed and unprimed quantities are related by the transformation in Fig. 7-4.

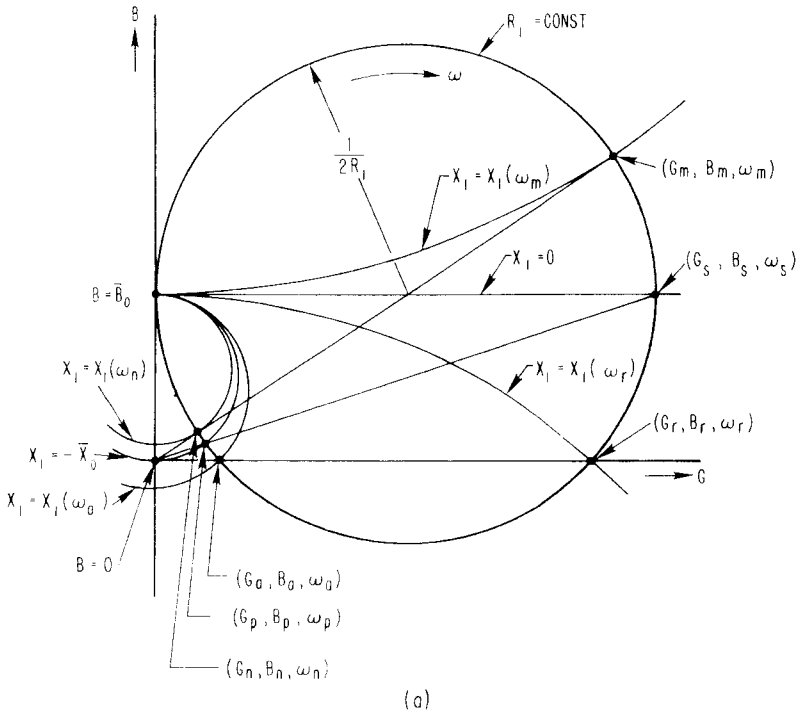


FIG. 7-7 (a) The admittance circle of the modified vibrator.

The admittance and impedance circles of the modified resonator are particularly convenient for defining the characteristic parameters of the resonator, many of which are indicated on the circles in Figs. 7-7a and b, and for visualizing the effects of parameter variations on the admittance–impedance of these devices, and hence, on their performance in a using circuit.

7.2.3 The Characteristic Parameters of a Crystal Unit

The characteristic frequencies of a (modified) crystal resonator are frequencies at which the impedance or admittance of the network in Fig. 7-5 assumes a unique value. A set of characteristic parameters consists of the characteristic frequency and the associated values of the resistive and reactive components of the immittance at that frequency. These are the parameters that are most significant for the application and, generally, the measurement of crystal units. The unique immittance points of the modified resonator, with $\bar{X}_L = 0$, are identified in Fig. 7-7a for the admittance and in Fig. 7-7b for the impedance.

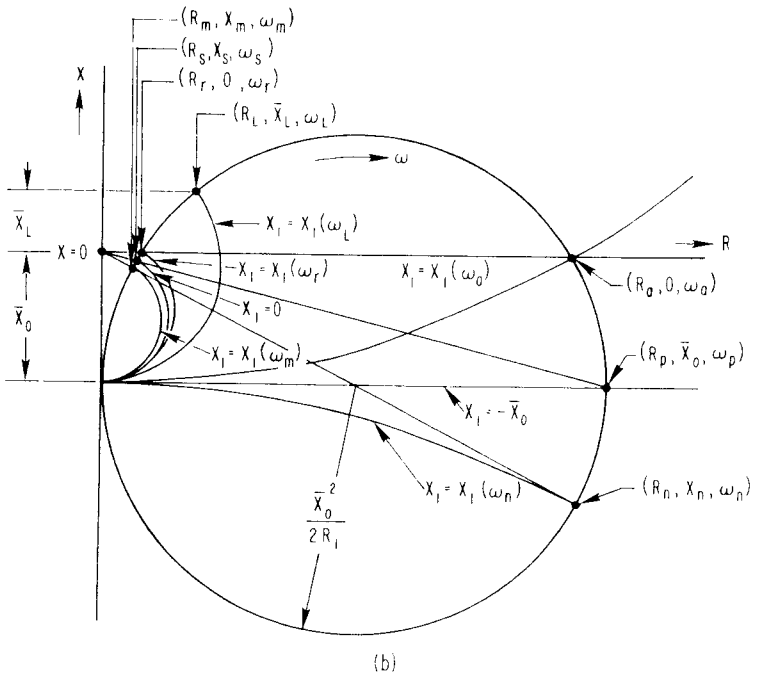


FIG. 7-7 (b) The impedance circle of the modified resonator. $\bar{X}_L = 0$ and $\bar{X}_0 \simeq$ const. are assumed. The figures (a) and (b) identify the characteristic parameters of the resonator. [From Hafner (1969); © 1969 IEEE.]

The analytic expressions for the resistance, reactance, and frequency at the points indicated are listed in Table 7-1 in the columns under the heading $\bar{X}_L = 0$. The corresponding expressions for the crystal unit with finite $\bar{X}_L$ are listed in the column headed "With load capacitor C_L." Although the term "load capacitor" is used, the general expressions under this heading are equally applicable for positive values of $\bar{X}_L$, that is, for inductive load elements. The expressions for the case where a coil is used to resonate with C_0 are found from those listed by letting $\bar{X}_0 \to \infty$. Whenever a finite $\bar{X}_L$ is used, it is important to consider the transformation shown in Fig. 7-4b.

All frequencies in Table 7-1 are referred to ω_s, the resonance frequency of the motional arm, defined by $X_1(\omega_s) = 0$ ($\omega_s = 1/\sqrt{L_1 C_1}$ for the circuit in Fig. 7-3). The exact solutions in Table 7-1 are valid for the network in Fig. 7-5 regardless of the magnitude of the circuit components. The quantity $\rho = 2R_1/\bar{X}_0$ or $\rho = 2R_1(\bar{X}_0 + \bar{X}_L)/\bar{X}_0^2$ is the ratio of the X coordinate of the center of the circle in Eq. (7-11) to the radius of that circle. With $\bar{X}_L = 0$ and

$\bar{X}_0 = -1/\omega_s \bar{C}_0$, the absolute value of ρ is equal to twice the inverse of the "figure of merit" of the crystal unit,

$$M = 1/R_1 \omega \bar{C}_0. \tag{7-12}$$

A general expression for the quality factor of the network in Fig. 7-5, valid at any point of its immittance plot, is given by (Hafner, 1964)

$$Q = \frac{\omega |\partial Y/\partial \omega|}{2 \operatorname{Re} Y}. \tag{7-13}$$

In the resonance range of a quartz crystal unit, where $\bar{X}_0$ = constant and $\bar{X}_L$ = constant can be assumed, this relation reduces to the familiar expression for the quality factor of the quartz resonator, $Q_0 = \omega_s L_1/R_1$.

The expressions in Table 7-1 are useful for the quantitative evaluation of the effects of series and/or parallel reactive elements, such as are added to the crystal resonator in circuit applications and in measurement sequences. They are also used for the determination of the equivalent-electrical-circuit elements L_1, C_1, R_1, and $\bar{C}_0$ of the (modified) crystal resonator. The values of L_1 and C_1 are usually determined, thereby, from the differences between characteristic frequencies under various conditions. When any of these conditions include finite values of $\bar{X}_L$, the relations shown in Fig. 7-4b have to be considered.

In the following, the sets of characteristic parameters shown in Figs. 7-7a and b will be described in somewhat greater detail. It should be noted that, as frequency is increased from the lower to the upper end of the resonance range, the sequence of the characteristic frequencies encountered is ω_m, ω_s, ω_r, ω_a, ω_p, ω_n. To a first approximation, when $M \gg 2$, $\omega_m = \omega_s = \omega_r$ and $\omega_a = \omega_p = \omega_n$.

7.2.3.1 MOTIONAL-ARM RESONANCE

The characteristic parameters at motional-arm resonance, with $\bar{X}_L = 0$, are $G_s = 1/R_1$, $B_s = \bar{B}_0$, and ω_s, with ω_s defined by $X_1(\omega_s) = 0$ per Eq. 7-2. The unique feature of the admittance plot at motional resonance is that the conductance is at its maximum value. There is no unique feature of the impedance plot at ω_s. The motional-arm resonance frequency is the one characteristic frequency that is intrinsic to the resonator; it is unaffected by the addition of series or parallel elements to the crystal unit. All other characteristic frequencies in Table 7-1 are referred to it. The frequency at maximum conductance of the modified resonator, with finite $\bar{X}_L$, will be called, by analogy, the "motional-arm resonance with load capacitor" and designated by ω_{sL}. The corresponding characteristic conductance is G_{sL}, the susceptance B_{sL}. The expressions for both are listed in Table 7-1.

7.2.3.2 RESONANCE AND ANTIRESONANCE

Resonance and antiresonance are the two points where the immittance circles of the resonator cross the real axis. The unique features, therefore, are purely resistive immittances. Resonance is the low-impedance zero crossing of the reactance of a resonator with $\bar{X}_L = 0$, antiresonance is the high-impedance zero crossing. The designations for the corresponding frequency and resistance are ω_r and R_r for resonance and ω_a and R_a for antiresonance. The low-impedance zero crossing of the reactance of the modified resonator, with $|X_L| > 0$, is called "resonance with load capacitor." It occurs at frequency ω_L, with resistance R_L. The high-impedance zero crossing of the resonator reactance with $|X_L| > 0$ is of little practical significance. The analytic expressions for ω_r, R_r, ω_a, R_a, ω_L, and R_L are listed in Table 7-1. When $R_1 \to 0$, then $\omega_r \to \omega_s$, $R_r \to R_1$, $\omega_a \to \omega_p$, and $R_a \to R_p \to \infty$.

Resonance and antiresonance can occur only when the immittance circle crosses the real axis, that is, for resonators with $\rho < 1$, $M > 2$. When $M \leq 2$, as is often encountered at frequencies above 100 MHz, a coil is usually placed in parallel with the crystal terminals to reduce the value of $\bar{B}_0$. Ideally, the coil inductance is dimensioned to resonate with $\bar{C}_0$ at the operating frequency. The relevant relations are then found from Table 7-1 with $\bar{X}_0 \to \infty$.

The antiresonance of a crystal resonator must not be confused with the so-called "antiresonance operation" of a crystal unit in a "parallel-resonance" oscillator (IEC, 1962). No practical oscillator operates the crystal unit in its high-impedance range, as had long been recognized (Heising, 1946; Awender and Sann, 1954). Rather, "antiresonance operation" refers to the use of a crystal unit with a series load capacitor, operated in the low-impedance range, that is, at ω_L, R_L. Proper terms for this type operation are "operation with load capacitor" and "resonance with load capacitor:" also acceptable is "positive reactance operation" of the crystal unit. The relations in Table 7-1 show that the frequency at resonance with series load capacitor C_L is equal, but only to a first approximation, to the antiresonance frequency of the resonator with the load capacitor placed in parallel with C_0, that is, with $\bar{C}_0 = C_0 + C_L$. Of course, the corresponding resistance values are, for reasonable values of M, vastly different.

7.2.3.3 PARALLEL RESONANCE

At parallel resonance, the resistive component of the resonator impedance is at its maximum, with value $R_p = X_0^2/R_1$ equal to the diameter of the impedance circle. The admittance shows no unique feature at the parallel-resonance frequency ω_p.

7.2.3.4 MAXIMUM AND MINIMUM ADMITTANCE

The characteristic parameters at maximum admittance (minimum impedance) are designated by subscript m, those at minimum admittance (maximum impedance) by subscript n. The corresponding points on the immittance circles in Fig. 7-7 [and the analytic expressions listed in Table I of Hafner (1969)] are derived geometrically by the "through-the-center method," which is valid only if the immittance plots are perfect circles. When this is not true, such as in resonators made of materials with very strong piezoelectric coupling and/or large losses, more elaborate relations must be used (Martin, 1954). Maximum and minimum admittance measurements have been used (IEEE, 1966) for the determination of the equivalent-electrical-circuit parameters of crystal resonators.

7.2.3.5 MINIMUM REFLECTION COEFFICIENT

The reflection coefficient $\Gamma = (Z - Z_0)/(Z + Z_0)$ is a useful quantity when the crystal resonator is at the end of a transmission line with characteristic impedance Z_0 (Stone and Baltzer, 1982). As is most easily visualized with Smith chart in hand, the reflection coefficient observed at the input of a (uniform and lossless) transmission line, terminated with an impedance Z, is independent of the length of the line. Since the impedance of a crystal resonator is a function of frequency, it follows that the reflection coefficient observed at a given frequency is independent of the length of the line. A unique value of the reflection coefficient in the resonance range of a crystal resonator is its minimum, which therefore qualifies as a characteristic parameter Γ_n. It occurs at a frequency designated as ω_γ (Horton and Smythe, 1983a,b). The values R_γ and ω_γ follow from Eqs. (34) and (35) of Hafner (1969) and are listed in Table 7-1.

7.3 CRYSTAL-RESONATOR MEASUREMENTS

7.3.1 General

The performance of crystal resonators as circuit elements is described by the equivalent electrical circuit. The purpose of the electrical measurements on crystal resonators is to evaluate the parameters of the equivalent circuit. Because the motional-arm parameters L_1, C_1, and R_1 and, hence, the characteristic frequencies, are functions of temperature, drive level, static acceleration, aging, etc. (Gagnepain, 1981; Nakazawa *et al.*, 1981), the conditions of measurement must be specified, and for most applications, the functional dependence on some or all of these variables must be determined.

For the latter purpose, it is usually adequate to measure the dependence of only one set of characteristic parameters, for example, resonance frequency and resistance, on the selected variable. The characteristic frequency chosen, nevertheless, should be close to the operating frequency of the device in its intended application, because the functional dependence is different for some variables, depending on which point on the immittance plot is observed. Thus, the frequency–temperature dependence of a quartz crystal resonator is slightly different for different values of the load capacitor (Ballato, 1978).

If the functional dependence of frequency on a particular variable, say, drive level, is measured at different points on the immittance circle, then the dependence of L_1 and C_1 on this variable can be determined separately, provided, of course, that the differences are large enough to be resolved with the available instrumentation. So it has been determined, for example (McKeown, 1958), that in VHF quartz crystal units the frequency change due to drive-level variations is due to changes in C_1, that is, to changes in the effective elastic constants. The ability to separate the changes in L_1 and C_1 can serve as a valuable diagnostic tool. In aging, for example, it would reveal the relative contributions of mass changes (changes in L_1) and stress relaxations (changes in C_1) to the overall effect. Sufficiently accurate measuring instruments for this latter purpose have, however, not been available in the past.

Nearly all crystal resonators have to be measured for frequency–temperature and for drive-level dependence. The former requires the crystal units to be measured remote from the instrument, in a temperature chamber or oven. The latter requires the instrument to be capable of measuring the crystal unit at normal and at extremely low drive levels. At drive levels in the nanowatt range and below, quartz crystal resonators are particularly susceptible to a variety of defects in the manufacturing process (Knowles, 1975; Bryan, 1975). These defects can manifest themselves in a resonance resistance value greatly in excess of the value found at normal drive levels (Bernstein, 1967), and can thus cause oscillators to fail to start oscillating on turn-on. In many cases, this problem is aggravated at low temperatures.

Nearly all crystal units must also be evaluated for their spurious-mode content. Strong spurious modes in oscillator crystals can compete successfully with the desired mode during start-up, resulting in oscillations at the wrong frequency; even weak modes in filter crystals cause unacceptable distortions in the filter response. The evaluation of the spurious modes requires instruments capable of sweeping the frequency range of interest and measuring, as a minimum, the resonance frequency and resistance of the unwanted mode.

The instrumentation for measuring crystal units must, therefore, be capable of (1) a sweep mode to display the main and spurious-mode spectrum with high resolution and of (2) measuring the frequencies and resistances at accurately defined points on the immittance plot of the resonator. The

measurements in (2) must be carried out at operating drive levels and at drive levels near the noise level, on the main mode and on spurious modes, and with the crystal unit at the test port of the instrument as well as in a remote position, such as in an environmental test chamber.

The major difficulty in measuring the characteristic frequencies of a crystal resonator is not, of course, the frequency measurement itself, even if attaining the high resolution frequently required in a short time is not always a trivial matter (Howe, 1981). The problem lies in knowing the precise impedance–admittance exhibited at the frequency measured. This requirement can be expressed, near resonance, in terms of phase angles. For a crystal unit with C_0 cancellation,

$$Q = \omega_s L_1/R_1 = \frac{\frac{1}{2}f_s}{f_{\phi_1} - f_{\phi_0}} (\tan \phi_1 - \tan \phi_0).$$

With $\phi_0 = 0$ it follows that

$$\frac{\Delta L_1}{L_1} - \frac{\Delta R_1}{R_1} + \frac{\Delta(f_{\phi_1} - f_{\phi_0})}{(f_{\phi_1} - f_{\phi_0})} = \frac{2}{\sin 2\phi_1} \Delta\phi. \tag{7-14}$$

Because the phase reading ϕ_1 is the difference between two individual phase settings $\phi = \phi_1$ and $\phi = 0 = \phi_0$, the phase error $\Delta\phi$ contains the errors in both, that is, $\Delta\phi = (\Delta\phi_1^2 + \Delta\phi_0^2)^{1/2}$ for random errors. If L_1, for example, should be determined with an accuracy of 1%, a marginal requirement for some applications, then one finds, under the most favorable conditions, that the instrumentation must be capable of identifying each phase setting with an accuracy of 0.2° at the operating frequency of the crystal unit. The relation for Q then shows, now with $f_{\phi_1} - f_{\phi_0} = \Delta f$ and $\phi_1 = \Delta\phi_0$, that an uncertainty of 0.2° in the knowledge of the $\phi = 0$ condition causes an uncertainty in the value of the resonance frequency of $\Delta f/f = 3.5 \times 10^{-8}$ for a crystal unit with $Q = 50{,}000$. Hence, the measurement of the resonance frequency, or any other characteristic frequency, with an accuracy of this order requires that the systematic phase errors be much smaller than the 0.2° in the present example. Reduction of the systematic errors to this level is a nontrivial problem.

Another difficulty in measuring crystal resonators also derives from their high quality factor. For a resonator with a Q value of 50,000, the half-power points of the resonance curve differ in frequency by only 20 ppm. On this scale nearly all of the operational and environmental parameters mentioned above have a large effect, even if their influence may be considered small in absolute terms. Special precautions are therefore always required to provide a controlled environment for the device being evaluated, whether electrically (e.g., drive level), thermally, or mechanically.

In the following two sections the major instruments and techniques for measuring crystal units will be discussed. In the instrument section the emphasis is on a description of the basic operating principles and their limitations. The methods section describes the principles of extracting the required data from the basic measurement results under the assumption (except in the case of ω_γ) that the crystal unit is directly at the measurement plane of the instrument. A discussion of the corrections required to account for a finite length of transmission line between the reference plane and measurement plane can be found in the relevant sections of Hafner (1969).

The instrument and measurement principles apply equally to any type of piezoelectric resonator, be it of the bulk-wave or SAW variety. The measurement of two-port devices, such as crystal filters, are not treated explicitly; however, all instruments capable of measuring the amplitude and phase of the signal transmitted through the test network are suitable for such measurements. All of the error sources to be discussed, with proper allowance for the differences in the network under test, apply equally to the filter measurements.

7.3.2 Resonator Measurement Instruments

7.3.2.1 CRYSTAL IMPEDANCE METERS

In principle, any oscillator circuit operating the crystal unit at series resonance could be used as the basis for the design of a test oscillator. Practical considerations limit the choice. The basic circuit of the test oscillator most widely used for several decades, the crystal impedance meter, or CI meter (Prichard and Bernstein, 1954), is shown in Fig. 7-8. The measurement follows the substitution principle: it can be made with or without a series load capacitor.

Several factors degrade the accuracy of the measurement.

(1) Real resistors are not perfect, zero-phase elements.

(2) Substitution resistors are available only in discrete steps, leaving, in general, a resistance error $\Delta R = (R_{sub} - R_t)$.

(3) Achieving a perfect frequency match is extremely time-consuming. In general, a frequency error $\Delta f = (f_{sub} - f_t)$ remains.

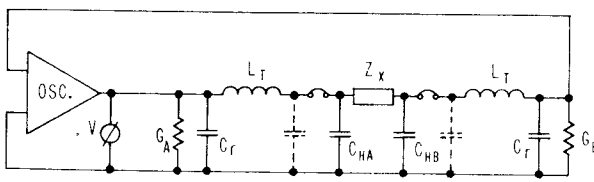


FIG. 7-8 Basic CI-meter circuit. The feedback element Z_x is either the crystal unit under test or a substitution resistor. Signal level and frequency of oscillation are the substitution process criteria.

The use of substitution elements with finite phase angles [error (1)] causes the measurement to be performed not at resonance, that is, zero phase, but at the phase angle of the substitution resistor. The frequency error caused by a parasitic inductance L_R of the resistor is $\Delta f/f = \frac{1}{2}L_R/L_1$. As an example, in uncompensated composition or film resistors, L_R can be around 16 nH, causing, with an $L_1 = 8 \times 10^{-3}$ H, a $\Delta f/f = 1 \times 10^{-6}$. This error can be reduced by the use of compensated resistors, that is, resistors with capacitors of value $C = L_R/R^2$ placed in parallel with them (IEC, 1973). Yet, an $L_R < 1$ nH is possible in leadless microcircuit-chip resistors, causing, with the same L_1, a $\Delta f/f < 6 \times 10^{-8}$. Thus, if the physical construction of the interface between the instrument and the crystal unit permits clamping such microcircuit-chip resistors into the CI meter terminals (not possible with most currently available instruments), then the use of compensated resistors may not be necessary for most practical purposes. On the other extreme, substitution resistors built into some CI meters, to be connected to the test terminals through switches, are bound to cause fairly large errors. The use of these resistors as substitution elements should be avoided. In the following it will be assumed that the substitution resistors are compensated for zero phase angle or are physically small enough for their reactive component to be neglected.

The ΔR error in (2) above causes the crystal to exhibit a reactance $\Delta X = \Delta R \tan \delta$, where δ is the loop phase error in the oscillator, which is due to deviations from 180° in the phase of the active device and to deviations from 90° in the phase of the terminating capacitors in Fig. 7-8 caused by the conductances G_A and G_B. When ΔR is large, drive-level differences cause further phase errors due to the nonlinearities in the active device and due to the drive-level dependence of the crystal frequency. The Δf error in (3) above translates into an error in the determination of the resonance frequency of the crystal unit given by $(f_r' - f_r) = (1/S)\,\Delta f$, where S is the stabilization factor of the oscillator. Reduction of this error, in the configuration of Fig. 7-8, requires increased labor in the measuring process.

In the majority of CI-meter measurements carried out in the field, a very

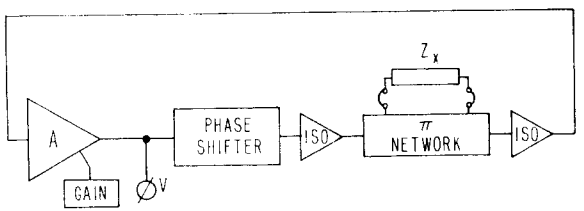


FIG. 7-9 Alternate CI-meter configuration. The amplifier is broadband, the phase shifter is a narrow-band tunable filter; the isolation amplifiers are matched to the low-impedance, resistive π network. The substitution process is the same as with the configuration in Fig. 7-8.

much-abbreviated substitution process is employed as a matter of expediency. The results obtained are correspondingly less than the optimum attainable with these instruments.

Several of the problems intrinsic to the CI meter in Fig. 7-8 can be addressed successfully, at least in principle, in the configuration show in Fig. 7-9. Here the basic operations on the signal in an oscillator are separated out and assigned to discrete circuits, that is, amplifier–limiter, phase shifter, and feedback network. Low impedances at the crystal port reduce the errors due to C_{HA} and C_{HB}. The loop-phase error δ will be small if

(1) the π network is purely resistive and has nearly constant input and output impedances regardless of the value of the (resistive) unknown Z_x,

(2) the isolation amplifiers have purely resistive output–input impedances, closely matched to the input–output of the π network, and

(3) the isolation amplifiers have very high reverse attenuation.

A π network approximating the stated requirements was described by Franx (1969) (IEC, 1973). The use of a vector-ratio meter, as in Fig. 7-10, will reduce the error in (3) above in a significantly shortened measurement time. Its primary function is to serve as a phase indicator, which permits substituting phase for frequency as the observed parameter during the tuning operation. The phase-shifter tuning can be implemented automatically (Frerking, 1969), as indicated by the dashed lines in Fig. 7-10.

Measurements with the crystal unit remote from the instrument are not practical with the CI-meter configuration in Fig. 7-8. With the CI meters in either Fig. 7-9 or Fig. 7-10, the π network, with crystal unit, can be connected to the rest of the instrument by well-shielded coaxial cables with their characteristic impedance matched to the isolation amplifiers and the π network.

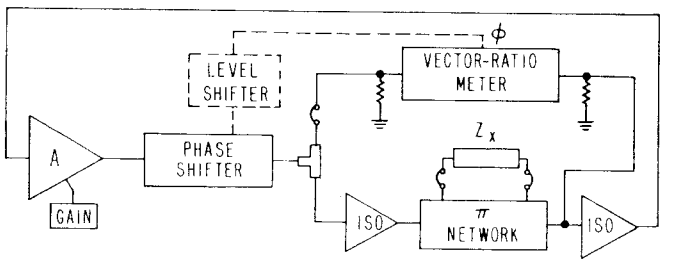


FIG. 7-10 Extension of the CI meter in Fig. 7-9. Frequency as a substitution criterion is now replaced by phase, set to zero with the substitution resistor in circuit. The proper value of substitution resistor to be used for accurate crystal measurements can be calculated from ratio-meter amplitude readings. The phase output of the ratio meter can be used for automatic frequency adjustments. (From Frerking, 1969.)

CI-meter-type instruments are basically well suited for testing crystal units at low drive levels. In the configuration of Fig. 7-10, however, the phase meter remains useful only for as long as its test channel has adequate sensitivity.

7.3.2.2 THE ZERO-PHASE π NETWORK

The use of a π network for the measurement of crystal-resonator parameters, as described by Gerber and Koerner (1958), was based on the measurement of the frequencies of maximum and minimum transmission, f'_m and f'_n, through the network with crystal unit inserted. It formed the basis for the Institute of Electrical and Electronics Engineers' (IEEE) standard on crystal measurements (IEEE, 1966). The addition of a phase meter to the transmission test set (Adams *et al.*, 1968; Grenier, 1968) created the capability to perform measurements at the "zero-phase" condition of the resonator, that is, at resonance, and also to generate a control signal to automatically tune the signal generator to the zero-phase condition. A number of configurations for the transmission network were explored (Horton *et al.*, 1981), which emphasized the importance of the detailed electrical and mechanical design of these devices for the validity of the results obtained. The need to incorporate attenuators into the π network and to use a power splitter to create separate channels for the reference and test signals was recognized by Franx (1969). The resulting configuration is shown in Fig. 7-11; the schematic for the π network itself is shown in Fig. 7-12. This implementation of the zero-phase π-network system is now recommended by the International Electrotechnical Commission (IEC) for the measurement of resonance resistance and frequency of crystal resonators with and without load capacitors (IEC, 1973).

Resonator measurements with the setup in Fig. 7-11 are again based on the substitution principle, with the phase meter used as an indicator for the correct frequency setting of the signal generator. The similarity between Figs. 7-10 and 7-11 is obvious—only the signal sources are different, and no isolation

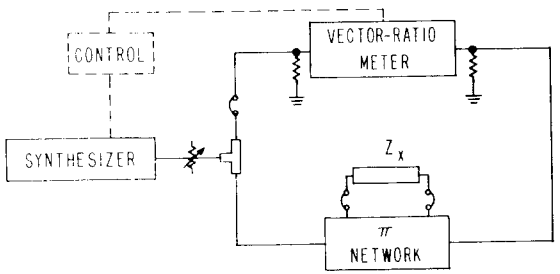


FIG. 7-11 The *zero-phase π-network* system. This system differs, in principle, from the CI meter in Fig. 7-10 only by the manner of test-signal generation: it differs from a manual network analyzer in that here the phase meter is used only as an indicator of the zero-phase condition.

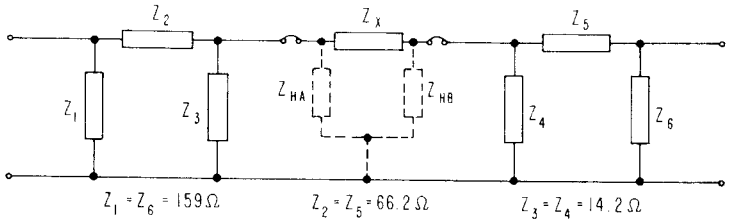


FIG. 7-12 Schematic of the IEC-177 π network (IEC, 1973). The attenuators Z_1–Z_3 and Z_4–Z_6, with values as shown, assure low reflection coefficients at input and output for all values of Z_x. Physical implementation with all impedances purely resistive is required for optimum results. Holder and stray capacitances Z_{HA} and Z_{HB} cause unavoidable residual errors.

amplifiers are used in Fig. 7-11. Moreover, it will become apparent in Section 7.3.3.4 that the setup in Fig. 7-11 has all the elements of a manually operated network analyzer. The zero-phase π-network technique just does not need the phase meter to be calibrated. Many of the system errors, exclusive of those associated with the vector-ratio meter itself, apply equally to network analyzers.

The error source to be considered first is ΔR, the difference between R_{sub}, the value of the substitution resistor, and R_r, the resistance of the crystal unit. A minimum number of substitution-resistor values is desirable in the interest of measurement speed. In many practical applications only one substitution element, a short circuit, is used.

The block diagram in Fig. 7-11 with Fig. 7-12 shows that a change in the value of Z_x will cause a level change in the output signal from the π network as well as a change in the reflection coefficient at the network input. The phase accuracy of most vector-ratio meters is highest for equal signal levels at the reference and test ports and decreases with increasing difference in the two levels. A change in the relative levels usually causes an apparent change in phase. The magnitude of this error depends on the instrument used. A finite reflection coefficient at the input of the π network causes a part of the test-channel signal to be reflected across the power splitter into the reference channel. Even if this reflected signal is, for example, 55 dB below the desired signal in the reference channel, it can, depending on the phase relationship, cause a shift of 0.1° in the reference phase. The attenuation across the power splitter is usually on the order of 30 to 40 dB; hence, the reflection coefficient at the π-network input has to be less than 0.06 (VSWR < 1.13), with any value resistor in the unknown terminal, for this error to be less than 0.1°. The π network in Fig. 7-12 has a reflection coefficient of $\Gamma = 0.22$ with $Z_x = 0$, $\Gamma = 0.05$ with $Z_x = 40\,\Omega$, and $\Gamma = 0.01$ with $Z_x = 100\,\Omega$, provided all elements are truly resistive, with the values as shown. A phase error of 0.4° can therefore result due to this effect alone if the measurement of a crystal

resonator with an $R_r = 40\,\Omega$ is referred to the initial adjustment of the phase meter with a short circuit. The maximum possible phase error due to this cause will be smaller if the zero adjustment of the phase meter is performed with a microcircuit-chip resistor in the 50-ohm range, instead of with a short-circuit element. Much larger errors are likely with measuring networks that do not have built-in attenuators to reduce the VSWR in the test channel.

Analysis of the diagram in Fig. 7-12 shows further (see Appendix II) that the ratio of input to output voltage for the network can be represented by

$$V_{in}/V_{out} = A + BZ_x, \tag{7-15}$$

where A and B are functions of all the impedances in the π network and of the terminating impedance. Unless all these impedances are purely resistive, A and B will be complex quantities. Plotting the vector $A + BZ_x$ in the complex plane shows immediately that the phase angle of the quantity B introduces an error proportional to ΔR. Thus, for the zero-phase π-network technique to be applicable with only one, or at most a few, substitution resistors, all impedances in Fig. 7-12 should be purely resistive. This requirement, coupled with the need for neglible crosstalk between the input and output section of the π network, places very stringent constraints on the physical construction of the device.

The physical implementation of not only the measuring network but of all of the various system components is important for the final accuracy of the results. Consideration of the system block diagram makes it clear that the zero-phase π-network measurement or, more generally, any network-analyzer measurement depends on all elements in the entire setup, including power splitter, cables and connectors, and, of course, the vector-ratio meter. Thus, the connectors should be of the precision type, with VSWRs of less than 1.04, to avoid adding to the reflection-coefficient problem just mentioned; the cables should be well shielded to reduce the problems of leakage and stray pickup; and the length of the cables should be chosen to provide for equal electrical length in the test and reference channels to make the phase balance independent of frequency.

Of special concern here, as well as in other instruments for crystal-resonator measurements, are the details of the interface to the unknown element. A major difficulty is the requirement to accommodate the load capacitors. Approaches to the physical construction of the load-capacitor jig have been described by Hughes *et al.* (1978) and by Horton *et al.* (1981). The problem is in finding the optimum compromise between the physical size of available load capacitors and the requirements that

(1) the base of the crystal enclosure be 2 mm from the measuring plane of the instrument,

(2) the crystal unit be, electrically, in the same relative position to the measuring plane with and without the load capacitor,

(3) the stray capacitance from the crystal–load-capacitor junction to ground be minimal, and

(4) there be no increase in crosstalk between the input and output sections of the network when the load capacitor is inserted.

The zero-phase π network is well suited for the display of spurious modes: their measurement is possible when $M > 2$. Since the π network is connected through cables to the rest of the system, the technique is also suited for the measurement of crystal units in environmental chambers. The measurement at low drive levels is limited by the sensitivity of the vector-ratio meter, which, for currently available instruments, ranges from -86 to less than -120 dB, as discussed further in Section 7.3.3.4. The insertion loss of the π network in Fig. 7-12 is 26 dB for $Z_x = 0$ and 37 dB for $R_r = 40\,\Omega$.

7.3.2.3 BRIDGE-TYPE INSTRUMENTS

By definition (IEEE, 1977), the term "bridge" applies to networks with branches that can be adjusted to obtain zero output. It is, nevertheless, applied also to networks with fixed branches that are operated in the transmission mode. For the presesnt purposes, the two uses shall be differentiated by the terms "transmission bridge" and "balanced bridge." One specific example of each will be discussed in the following.

7.3.2.3.A. Transmission Bridges. A transmission bridge such as that shown in Fig. 7-13 (Ichino *et al.*, 1980) can take the place of the π network in Fig. 7-11. The relation for the vector ratio of output voltage over input voltage,

$$\gamma = \frac{V_{out}}{V_{in}} = \left(\frac{Z_{in} - Z_2}{Z_{in} + Z_2}\right)\left(\bar{A} - \frac{\bar{B}}{Z_{in} + Z_2}\right), \tag{7-16}$$

follows from a straightforward analysis of the network. The values of the three constants Z_2, $\bar{A}$, and $\bar{B}$ can be determined by using open, short, and $Z_0 = 50\,\Omega$ terminations at the measuring port. These constants are functions of the network impedances $Z_1 = Z_3$, Z_2, and Z_T, as shown in Appendix III. Alternatively, (7-16) can be recast to express the voltage ratio in terms of the reflection coefficient of Z_m referred to the test termination Z_0, $\Gamma = (Z_m - Z_0)/(Z_m + Z_0)$, as

$$\gamma = V_{out}/V_{in} = A + B\Gamma/(1 - C\Gamma), \tag{7-17}$$

where A, B, and C are again functions of the network impedances $Z_1 = Z_3$, Z_2, and Z_T. In either case the measured quantity is γ. When Z_x is at the end of a transmission line, the relationship between Z_x and Z_m follows from standard

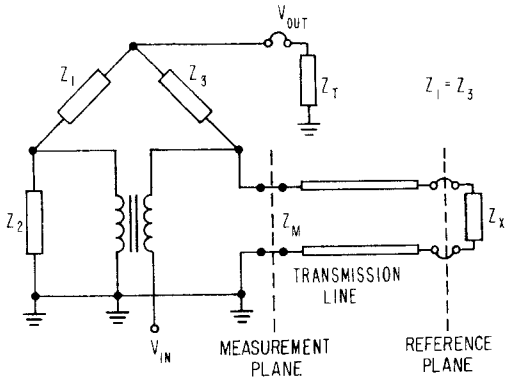


FIG. 7-13 Schematic of a transmission bridge network [after Ichino *et al.*, (1980); © 1980 Hewlett Packard Company; adapted with permission]. The value of Z_M is determined from the magnitude and phase of the vector ratio V_{out}/V_{in} and the values of the bridge impedances Z_k, $k = 1, 2, 3, T$. V_{out}/V_{in} is equal to one-half the reflection coefficient of Z_m with respect to Z_2 if $Z_1 = Z_3$ and $Z_T \to \infty$.

transmission-line theory, with the necessary constants determined by using open, short, and Z_0 terminations again, now at the far end of the transmission line. Equations (7-16) and (7-17) are exact subject to the conditions that the transformer in Fig. 7-13 is ideal (i.e., has unity coupling, infinite inductance, and no stray elements), that $Z_1 = Z_3$, and that there are no strays between the elements of the bridge network.

Under these conditions the accuracy of the system depends on the accuracy of the vector-ratio meter, the extent to which reflections from the network input, cables, and connectors reach the reference channel, and the extent to which crosstalk between the input and output lines of the test network are excluded. The reflection coefficient of the network input ranges (with $Z_k = 50\,\Omega$, $k = 1, 2, 3, T$) from zero to 0.43.

Even when the system imperfections are large, use of the three standard terminations, open, short, and 50 Ω, will always yield values for the three constants in either of the Eqs. (7-16) or (7-17), forcing the measurement results to be accurate at these three points on the impedance plane for the drive level and at the frequency used in the calibration. The three constants, however, are not necessarily valid for any other point on the impedance plane (i.e., for any other value of Z_m). In the general case, the system accuracy at other points can be determined only by the use of independently calibrated transfer standards. Nevertheless, a measure of the system imperfections lies in the behavior of the three constants as a function of frequency and/or drive level. It should reflect the frequency dependence of only the network impedances Z_K, $K = 1, 2, 3, T$, in Fig. 7-13 according to the relations in Appendix III, and ideally there should

be no dependence on signal level. Deviations therefrom are caused by error sources that may reside anywhere in the entire setup.

When used for substitution measurements such as the measurement of resonance frequency and resistance of a crystal resonator, with the phase obtained with the $Z_0 = 50\,\Omega$ termination as a reference [$\Gamma = 0$ in Eq. (7-17)], a phase error equal to $(R_r - Z_0)\tan\delta$ will normally be encountered, with δ a function of the phase angles of B and C in Eq. (7-17). The sources of the phase angles of B and C are not restricted to the elements of the bridge network but include all parts of the system. Yet, only the former are included in mapping the Γ plane onto the γ plane by means of Eq. (7-17): the latter cause mapping errors that increase with increasing distance from the three calibration points at $\Gamma = 0$ and ± 1.

The magnitude of any one of the errors discussed above is obviously a direct function of the details of implementation of every one of the components of the entire measurement system. However, everything else being equal, one advantage of the transmission bridge in Fig. 7-13 over the π network in Fig. 7-12 is the fact that one terminal of the unknown impedance is at ground potential and the impedance range of maximum sensitivity is around $Z_0 = 50\,\Omega$.

7.3.2.3.B. Balanced Bridges. A balanced bridge contains continuously variable elements, usually reactive elements, that are used to change the current distribution within the circuit. At balance, the current through the output branch is zero. An example is the Schering bridge shown in Fig. 7-14 (containing varactors as the variable capacitors), which permits electronic tuning (Hafner and Riley, 1976). The basic block diagram of a balanced-bridge measuring setup is shown in Fig. 7-15. Here the sole function of the receiver is

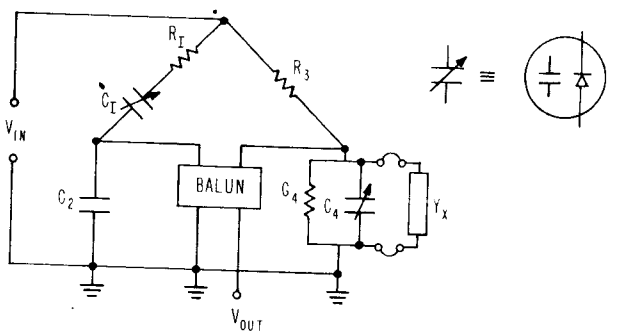


FIG. 7-14 Schematic of a balanced-bridge network. Varactors are used as variable capacitors (Hafner and Riley, 1976). The value of Y_x is determined from the dc voltages applied to C_1 and C_4 and the values of the fixed bridge elements. The magnitude of V_{out} at balance is zero. $G_x = (C_2/R_3)(1/C_{11} - 1/C_{10})$, $C_x = C_{40} - C_{41}$, $G_4 = (C_2/R_3)(1/C_{10})$, $C_{40} = (C_2/R_3)/R_1$.

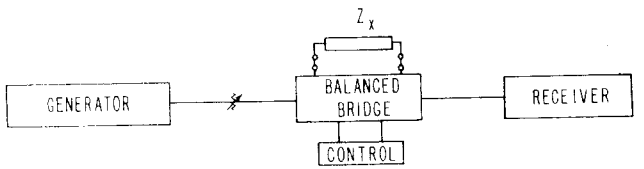


FIG. 7-15 Basic balanced-bridge measurement system.

to detect an absence of signal in the output from the bridge. The length and properties (aside from shielding) of the cables connecting the bridge to the generator and receiver are unimportant. Provided there are no leakage signals bypassing the bridge and entering the receiver input, all sources of measurement errors are within the bridge itself.

The basic equation for bridge balance is

$$Y_x + Y_4 = (Z_1/Z_3)Y_2. \tag{7-18}$$

It is valid when the output transformer is ideal, that is, when it has unity coupling and no stray elements (especially no strays that change with tuning) and there is no crosstalk between the various bridge arms. Microcircuit construction techniques permit these conditions to be approximated rather closely. Since the balanced bridge has no means for measuring phase, Eq. (7-18) is used only with all impedances represented in terms of their actual elements, for example, $Z_1 = R_1 - j(1/\omega C_1)$. Separation of real and imaginary components then yields two equations. When the bridge impedances are as shown in Fig. 7-14, the resulting equations for G_x and C_x are indicated in the legend to the figure, where the second subscripts zero and one refer to initial balance with $Y_x = 0$ and final balance with $Y_x = G_x + j\omega C_x$, respectively.

The power of the balance condition (7-18) is such as to reduce the calibration of the balanced-bridge network to the measurement of frequencies and dc voltages and the calibration of the dc value of a single resistor. This can be demonstrated as follows. Assume that $Y_x = 1/(R_x + j\omega L_x)$, that is, that $G_x = R_x/(R_x^2 + \omega^2 L_x^2)$, and $C_x = -L_x/(R_x^2 + \omega^2 L_x^2)$. Also assume at first that the relationships between the varactor capacitances C_1 and C_4 and the respective dc control voltages V_1 and V_4 are known. Using the relations in the legend to Fig. 7-14, the values of C_2/R_3, R_1, G_4, and L_x can be determined from initial balance and final balance at a single frequency ω_1 if only the value of R_x is known a priori. Balance at an additional frequency is already redundant. However, if the relationship between C_1 and V_1 is nonlinear and contains four constants, with C_4 vs. V_4 likewise, balance at four additional frequencies can be used to determine the values for these eight constants, four each from the real and imaginary parts of Eq. (7-18). Thus, balance at five frequencies with

$Y_x = Y_x(\omega)$ together with the initial balance $Y_x = 0$ permits the determination of all bridge elements in terms of the resistance value R_x.

Similar considerations apply if the residual reactive elements in the bridge arms are taken into consideration, with each additional frequency providing two equations for two more parameters to be determined. Actual results obtained on a microcircuit bridge for the 1–220-MHz range show (Malinowski and Hafner, 1978) that the most prominent residual elements are inductances in series with C_2 and C_4 of about 0.5 nH each. The largest cross-term element is an inductance of about 0.05 nH in series with R_3.

The resolution of balanced-bridge measurements is determined by $P_{D_{min}}$, the minimum detectable signal power at the receiver input, the bridge attenuation α, and the power applied to the bridge, P_{sig}, according to the relation

$$|\Delta Y|_{min} = \frac{1}{\alpha}\left(\frac{P_{D_{min}}}{P_{sig}}\right)^{1/2}, \tag{7-19}$$

where $|\Delta Y|_{min}$ is the bridge unbalance that produces an output signal power of $P_{D_{min}}$. The bridge attenuation α is on the order of 0.05 for the microcircuit bridge and ranges from 0.01 to 0.1 for most rf bridges. Equation (7-19) can be translated into phase angle resolution, to facilitate comparison with other measurement techniques, by assuming that ΔY_{min} represents the minimum detectable susceptance of a nominally pure conductance of value $1/R_x$, for example, a crystal resonator at resonance. Then,

$$\tan \phi_{min} = \frac{R_x}{\alpha}\left(\frac{P_{D_{min}}}{P_{sig}}\right)^{1/2}. \tag{7-20}$$

With strictly manual operation of the setup in Fig. 7-15 using a broadband detector, $P_{D_{min}}/P_{sig}$ is usually limited to about 40 dB due to the harmonic content of the generator. When the generator signal is suitably frequency- or phase-modulated, synchronous detection can be employed to attain $P_{D_{min}}/P_{sig}$ values greater than 100 dB (Linzer and Stockelsberry, 1973). However, a series of precautions has to be taken in this case. These have to do with the response of a high-Q circuit to a frequency-modulated signal (Barnes, 1970; Hewlett-Packard, 1976), the harmonics of the modulating signal, and the asymmetry of the bridge output for frequencies around the balance point (Hahn, 1970), all matters that have been studied extensively in connection with the high-Q atomic resonators used for frequency standards (see Chapter 10).

However, heterodyne receivers are usually used as the detectors for balanced-bridge measurements. Special care is thereby required to exclude the test signal from the local-oscillator channel and vice versa. An automated

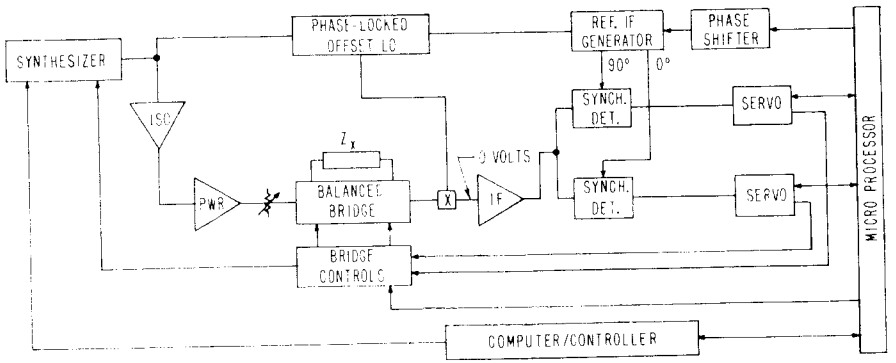


FIG. 7-16 Automatic balanced-bridge measurement system. Use of phase-locked offset local oscillator permits high-sensitivity synchronous detection of bridge output. The outputs of two orthogonal synchronous detectors are used for operating the resistive and reactive balance controls of the bridge. At balance, the input to the test-channel IF amplifier is zero. The phase of the reference IF is needed only to provide polarity information to the balancing servos.

system for measurements with the electronically tunable microcircuit bridge is shown in Fig. 7-16. It again has some similarity with a network analyzer; however, there are very significant differences in its operation. In a network analyzer the phase of the reference IF signal carries the all-important reference information for the accuracy of the phase measurement, and the test and reference signal amplitudes must be measured accurately. In the balanced-bridge measurement system no calibrated amplitude measurement is needed. The reference-signal phase is needed only for setting the proper polarity of the bridge-balancing servocontrol signals. Even if the reference-signal phase is $\pm 45°$ off its most desirable value, the only penalty is a somewhat reduced sensitivity of the servos. In the actual implementation of the system in Fig. 7-16, the extensive use of isolation amplifiers, with high reverse isolation, assures freedom from crosstalk between the signal and LO channels to the point where a usable (open-loop) $P_{D_{min}}$ of less than -150 dBm is attained (Hafner and Riley, 1976). Other schemes are, of course, possible.

Bridge networks are very well suited for the observation and measurement of spurious modes in crystal resonators, and they can readily be used for the measurement of resonators in environmental chambers. The balanced bridge should be located in the chamber for this latter purpose, while the transmission bridge, with its wider range for the unknown impedances, can accommodate the resonator at the end of a transmission line of generally limited but essentially random length. Resonator measurements at very low drive levels are limited in either bridge by the sensitivity of the detector used. Balanced-bridge measurements have been made successfully with crystal drive levels below the nanowatt range.

7.3.2.4 ANALYZERS

The basic elements of an rf network analyzer are (as shown in Fig. 7-17) a signal source whose output is split into reference and test channels, a vector-ratio meter to compare the amplitude and phase of the signals exciting the two channels, and a test network. The latter is either the unknown, as in filter measurements, or is a test fixture, for example, a π network, into which the unknown is inserted. For scattering parameter measurements, the test network is further embedded in a suitable arrangement of directional couplers and rf switches. Most network analyzers include analog-to-digital converters to prepare the amplitude and phase readings for subsequent digital processing and a computer–controller for automating the test sequence and for presenting the results in nearly any format that may be desired. Usually the computational facilities are also used to process the raw data through extensive error-correcting routines before the results are displayed on the readout devices. Frequently the user is presented the output terminal of the generator and the input terminals of the vector-ratio meter and is responsible for the remainder of the system between these terminals. The essence of the network analyzer, therefore, is the vector-ratio meter (with associated digital processor, in most cases).

The vector-ratio meter in Fig. 7-17 is based on the heterodyne principle (Nelson, 1972); other widely used devices are based on the sampling principle (Weinert, 1966; Ichino *et al.*, 1980). Also available are instruments with wideband characteristics, generally restricted to the low-frequency range, and

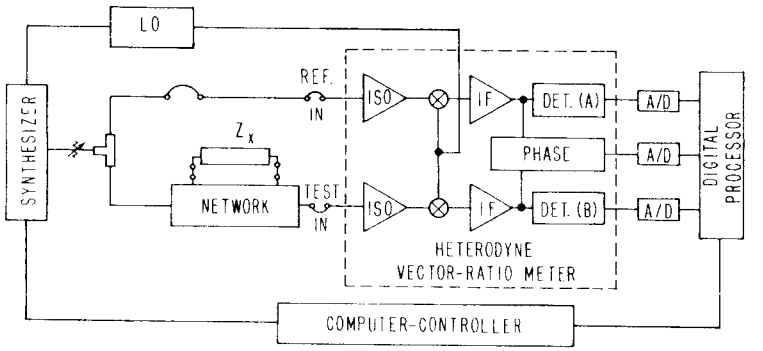


FIG. 7-17 Automatic network-analyzer system. The key element is the vector-ratio meter. It measures the magnitude and phase of the signal at its test-channel input relative to the reference-channel input signal and, thus, the transfer characteristics of the network under test. Numerous different operating principles are in use for the ratio meters: the one shown here is heterodyne with square-law amplitude detection. The primary data acquired is always analog. Subsequent digital analog conversion interfaces with the computer-controller for automation of test sequence and data presentation.

analyzers that use magnitude information only. Errors in the amplitude measurements are mostly due to deviations from the desired linear or logarithmic characteristics of the amplifiers. The techniques used for the phase measurement range from measuring the time difference between the zero crossings of the IF signals in the reference and test channels to formation of the sine and cosine components of the test-channel IF signal relative to the phase of the reference IF, with subsequent computation of magnitude and phase of the test-channel IF signal. The error sources differ depending on the detailed implementation of the different techniques. Potential error sources common to all techniques, however, are insufficient reverse isolation and crosstalk between the reference and test channels in both the rf and IF sections. These cause the phase of the respective signals to be affected by the signal in the opposite channel.

Several of the error sources present in conventional vector-ratio meters are avoided by the use of the IF substitution method (Weinert, 1980). A block diagram of this system is shown in Fig. 7-18. In a manner similar to that in Fig. 7-16, the IF signal, for example, in the test channel, is decomposed by means of two synchronous detectors into orthogonal components that are used, by

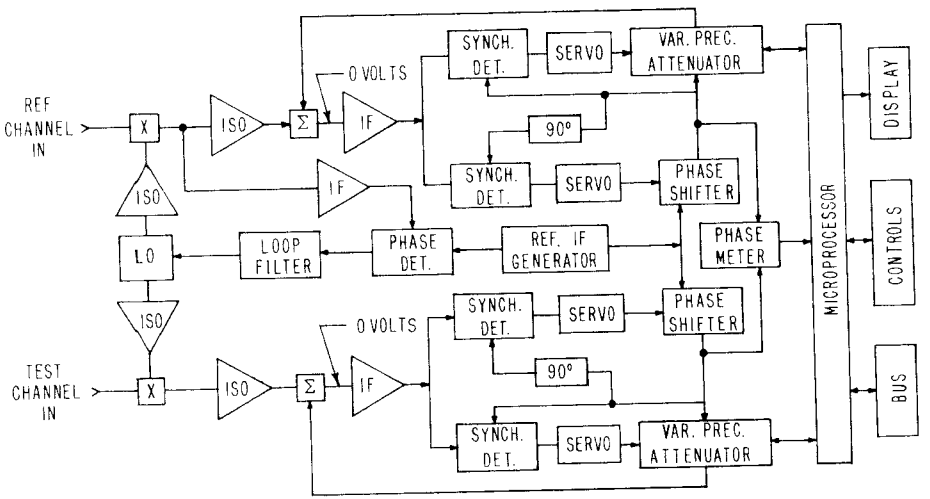


FIG. 7-18 Vector-ratio meter based on the IF substitution principle [after Weinert (1980); © 1980 IEEE] and using a phase-locked local oscillator. The outputs of two orthogonal synchronous detectors are used to adjust the phase and amplitude of an auxiliary IF signal to be equal and opposite to the input channel IF. The former is added to the latter to produce zero input to the channel IF amplifier. Test and reference channels are built identically. Amplitude readings are defined by the variable-precision attenuator settings and are not dependent on the amplifier characteristics.

means of appropriate controls, to force the input to the IF amplifier to zero. In the present case this is accomplished by adjusting a phase shifter and a precision attenuator, both operating on a signal at the IF frequency, such that the resulting signal is exactly equal and opposite to the test-channel IF signal. Signal amplitude is now measured by the setting of a precision attenuator, phase by a phase meter operating always at constant signal amplitude. The block diagram indicates that potential problems with the behavior of mixers (Huchital and Tomanic, 1980), isolation amplifiers, and the phase properties of the precision attenuators still exist but are mitigated by the identical configuration of the test and reference channels.

The impedance analyzer (Ichino *et al.*, 1980) is a network analyzer with a 50-Ω transmission bridge, such as shown in Fig. 7-13 and discussed in Section 7.3.2.3.A, as the test network. The associated vector-ratio meter is based on the sampling principle. The fundamental difference from a conventional network analyzer is in the fact that here the test network is an integral part of the instrument, with only the test port itself accessible to the user.

The accuracy and resolution of network analyzers can only be stated in terms of the capabilities of the vector-ratio meter. Both are very critical functions of the detailed design and depend on a variety of parameters such as signal level, frequency range, etc. Not all instrument makers provide accuracy information; where such data are available they range from degrees to around 0.5° for phase accuracy, while phase resolution reaches down to 0.01° in several cases. The accuracy of the amplitude ratio is usually in the 0.5-dB range, that is, around 10%. In the IF substitution instrument, the accuracy of the precision attenuator governs and is around 0.01 dB.

7.3.3 Measurement Methods

7.3.3.1 THE SWEEP MODE

All of the instruments described in the preceding section, except the CI meters, are suitable for displaying the main- and spurious-mode spectrum of a crystal resonator on an oscilloscope or recorder. An estimate of the sweep rate needed for a nearly true display of the mode spectrum can be obtained by observing that the output of a single-tuned filter with quality factor Q in response to a suddenly applied sine wave at the center frequency is $1 - \exp(-f_s t/Q)$. If the filter bandwidth $\Delta f = f_s/Q = BW$ is swept in a period Δt equal to one time constant, that is, when $\Delta t = \tau = Q/\pi f_s$, then the sweep rate is $\Delta f/\Delta t = \pi(f_s/Q)^2 = \pi(BW)^2$ and the signal amplitude at time $t = \tau$ is approximately $(1 - e)$. Hence, if the sweep rate is $\pi(BW)^2$, the response peak in the display is approximately 4 dB below its true value. If a $\Delta t = \pi\tau$, that is, a sweep rate of $(BW)^2$, is used, the error is reduced to about 0.4 dB. This agrees

fairly well with the results obtained by rigorous analysis (Hewlett-Packard, 1976). The latter results also include values for the shift in peak frequency of the display as a function of the sweep rate.

The sweep mode is used mostly for locating the response to be evaluated. Since the response height is a function of the measuring network, it is meaningless to state in general terms that a spurious mode is so many decibels below the main mode. The minimim description of a spurious mode must include its motional-arm resonance frequency and resistance.

7.3.3.2 MEASUREMENT OF THE CHARACTERISTIC PARAMETERS

7.3.3.2.A. The Zero-Phase Method. Any of the instruments discussed in Section 7.3.2 can be used for resonator measurements at zero phase angle. The zero-phase condition is established by use of one or more "purely resistive" substitution elements; in the case of the balanced bridge this may be an open circuit. All instruments except the CI meters in Figs. 7-8 and 7-9 have some means for measuring the value of the resistive component at zero phase; in CI meters it is determined by the value of the substitution resistor that matches the unknown. The determination of the equivalent-electrical-circuit parameters by the zero-phase technique requires measurement of resonance frequency and resistance at least twice, once with and once without a load capacitor. The data obtained are f_r, R_r and f_L, R_L. The relations in Table 7-1 are then used to determine R_1, C_1, and L_1. If the approximate relations in the table apply, then one obtains

$$
\begin{aligned}
R_1 &= \alpha R_1 \Big/ \left(1 + \frac{C_0 + C_{HA}}{C_L}\right)^2, \\
C_1 &= 2[(f_L - f_r)/f_s - \varepsilon](C_0 + C_{HA} + C_L), \\
L_1 &= 1/\omega_s^2 C_1, \\
Q_0 &= 1/\omega_s C_1 R_1, \\
f_s &= f_r(1 - \omega_s \bar{C}_0 R_1/2Q_0), \\
\varepsilon &= (\omega_s \bar{C}_0 R_1/2Q_0)(C_{HA} + C_0)/\alpha C_L .
\end{aligned}
\tag{7-21}
$$

Here $\alpha = 1 + C_{HA}/C_L$ and $\bar{C}_0 = C_0$ if the resonator appears as a two-port in the instrument or $\alpha = 1$ and $\bar{C}_0 = C_0 + C_{HA}$ if it is used as a one-port (see Fig. 7-4). The values of C_0, C_{HA}, and C_{HB} can be determined with a three-point capacitance bridge at low frequencies for most purposes. A somewhat better approximation for C_0 is obtained as the average of measurements above and below the resonance range (Smythe, 1981) or from f_L measurements using two different load capacitors (IEEE, 1973).

Zero-phase measurements are possible on resonator modes with $M \leq 2$ if a coil is used in parallel with C_0. A particular approach for implementing a tunable inductor for such purposes has been described by Fischer and Schulzke (1977). The relations for R_1, C_1, and L_1 appropriate to this case can be derived from Table 7-1 with $\bar{X}_0 \to \infty$.

In all cases it is important that the frequency measurements that are used in the equations for C_1 are made at the same drive level or at a drive level low enough for errors due to the frequency–drive-level effect to be negligible.

7.3.3.2.B. The Offset Method. Any instrument with phase measuring capability is suitable in principle for measurements at other than zero phase. Use of a load capacitor for the purpose of parameter evaluation can then be replaced by measurement of the resonator frequency at a finite phase angle ϕ, with C_1 determined from f_r and f_ϕ or from $f_{\phi 1}$ and $f_{\phi 2}$, if two different offset phase angles are used, for example, $\pm 45°$. More generally, offset methods involve measurement of the magnitude and phase of the test-network input–output voltage ratio at points on the resonator immittance plot that are not on the real axis. Depending on the instrument or the operator's choice, this may involve measurements at preset phase values or at preset frequencies. In either case the relation for the input–output voltage ratio for the particular measuring network used, such as Eq. (7-15) for the "zero-phase" π network, yields the resistive and reactive components of the resonator immittance corresponding to the observed voltage ratio. The value of the motional-arm reactance at the observed frequency then follows from either Eq. (7-1) or Eq. (7-10). Any two such values for X_1, with the corresponding frequencies, yield two of the constants in the equation for X_1, such as the values of f_s and the motional inductance L_1 when Eq. (7-4) is appropriate. A third measurement can be used to determine the value of $\bar{C}_0$. The degree to which each group of a multiplicity of such measurements on a well-isolated and well-behaved resonance mode of a crystal resonator yields the same values for these constants may be considered a measure of the internal consistency of the data obtainable with the instrument used. In general, the immittance plot of such a resonance mode covers a fairly large area of the immittance plane. The particular expression used for X_1 must, of course, thereby be assumed. In all cases the measurements should be carried out at a drive level that is sufficiently low for errors due to the frequency drive-level effect to be negligible. If such a drive level is less than the specified drive level of the crystal unit, a separate measurement of the specified resonance frequency, f_r or f_L, may be required. If the latter is f_L, the use of a physical load capacitor rather than a measurement at a large phase angle is recommended.

7.3.3.2.C. Balanced-Bridge Measurements. The resonance frequencies and resistances with and without load capacitor, f_r, R_r and f_L, R_L, respectively, are found by balancing the bridge while the reactance–susceptance control remains at the position found during initial balance. The values of the equivalent-circuit parameters can then be evaluated from the approximate Eqs. (7-21) in the same manner as discussed above for the zero-phase measurements. The resonance frequency and series resistance of the motional arm, f_s and R_1, respectively, can also be measured directly, with no approximations involved, if an admittance bridge is balanced by means of the f and G controls while the susceptance control is left at the setting needed to balance the susceptance of the parallel capacitance $\bar{C}_0$. When this same procedure is used on a crystal unit with load capacitor, that is, when the bridge is balanced with the susceptance control left at the setting needed to balance $\bar{C}_0$ and C_L in series, the resulting frequency and resistance are ω_{sL} and R_{sL}. According to Table 7-1 the relations for ω_{sL} are independent of R_1 and, hence, quite simple. When Eq. (7-4) is appropriate one finds, without further approximation,

$$C_1 = 2\left(\frac{\omega_{sL} - \omega_s}{\omega_s}\right)(C_0 + C_{HA} + C_L). \tag{7-22}$$

Numerous other techniques for bridge measurements on crystal resonators, including offset methods, are described by Hafner (1969).

7.3.3.2.D. Automatic-Analyzer Measurements. Because of the prodigious computational facility of automatic network analyzers, any of the techniques in Sections 7.3.3.2.A–C can be implemented on these instruments (Pustarfi and Smith, 1973; Smythe, 1981). Basically, each involves measuring the vector difference between two or more points on the immittance plot of the crystal resonator, along with the corresponding frequencies, and fitting the analytic expressions for the resonator immittance to this data by proper choice of the parameters. This is a task that most properly programmed automatic analyzers can perform with great resolution and repeatability. Also important is their ability to rapidly acquire a great deal of calibration data on the instrument and to use it in accuracy-enhancement routines. Regardless how powerful the digital and computational part of the instrument, the accuracy of the results is nevertheless a function of the detailed physical implementation of each of the components comprising the analog section of the system, as discussed in Section 7.3.2.

A description of the particulars of any specific analyzer technique for resonator measurements would have to be tailored to a given instrument. This is beyond the scope of this chapter.

7.3.3.3 MEASUREMENT OF FREQUENCY–TEMPERATURE CHARACTERISTICS AND AGING

The principal problems with precision frequency–temperature and aging measurements are knowledge of temperature and recent temperature history of the resonator and evaluation of the behavior of the resonator apart from that of any associated components or circuitry. Ideally, the latter requires that the measuring head of the instrument be located inside the temperature chamber or oven and that the initialization or calibration of the instrument be repeated periodically. Since in most cases calibration requires the use of substitution elements at the measuring head, mechanical means for manipulating the crystal resonator and/or these elements are needed. The only exception is balanced-bridge measurement of f_s, where the proper setting of the conductance control can be verified by off-resonance balance of $\bar{C}_0$ without necessarily removing the resonator from the test terminals. Several approaches to this manipulation have been reported, and pertinent papers are listed in the bibliography to this chapter. Among them are only a few attempts to avoid the use of auxiliary devices, such as switches, wiper arms, or sections of coaxial cables, between the resonator and the measuring head. In some cases separate sets of coaxial cables provide outside access to each crystal resonator in the chamber. The results are very much a function of the detailed implementation of the setup. When auxiliary devices are used, the results represent the behavior of the resonator plus that device.

For both frequency–temperature and aging testing, the most desirable system from the standpoint of economy will permit a multiplicity of crystal units in the same chamber. High-precision aging measurements in particular, however, require an extraordinary degree of temperature stability, which has not yet been demonstrated in a multicrystal chamber. Hence individual ovens, one for each resonator, are frequently employed for such tests (Beetley *et al.*, 1981), usually each with its own oscillator. Only the aging of crystal plus oscillator can be determined by this method. Whether continuous or intermittent operation of the crystal unit during the aging test period is preferable, and whether they can provide equivalent results, is still an open question (Euler and Yannoni, 1981; see also, Chapter 6 of Volume 1).

The dependence of resonator frequency on temperature contains a static and a dynamic part (Ballato and Vig, 1978; Sinha and Tiersten, 1980; Gagnepain, 1981), with the latter responsible for comparatively large frequency excursions, even in regions where the static frequency–temperature curve is nearly flat. Precision aging measurements therefore require an exceptionally stable temperature (successful modeling of the effects of temperature fluctuations has not yet been demonstrated), and frequency–temperature measurements require a very slow ramp or sufficient stabilization

time at each temperature for the gradients to decay. The time scale is determined by the magnitude of the dynamic effect for the type of resonator under study.

The frequency–temperature characteristics of crystal resonators are further complicated by hysteresis (Hammond *et al.*, 1968). Hysteresis manifests itself as a dependence of the resonator frequency at any given temperature on the thermal history of the unit. While large hysteresis effects, on the order of 0.5 ppm for quartz crystal units, mostly found at low temperatures, are apparently always caused by improper processing during manufacture, all resonators appear to be affected to some degree. The measurement of hysteresis effects is best performed at the upper and lower turnover temperatures following a temperature profile that includes storage of the units at the extremes of the operating temperature range for prolonged periods of time between the measurements.

The frequency–temperature and aging measurements on crystal resonators nearly always require a number of compromises depending on the particular aspect of major concern in any given test series. The validity of the chosen approach must be evaluated individually for each case.

7.4 SUMMARY AND CONCLUSIONS

The electrical performance of a piezoelectric crystal resonator vibrating in a single mode is fully described by the equivalent electrical circuit consisting of a *motional arm*, a resistor R_1 in series with a frequency-dependent reactance X_1, shunted by the *static capacitance* C_0. In the lumped-element approximation, valid for small-coupling-coefficient materials such as quartz, X_1 is the reactance of a series LC circuit with constant parameters $L = L_1$ and $C = C_1$. For higher-coupling-coefficient materials, the frequency dependence of X_1 is determined by the appropriate $(\tan X)/X$ function following from the theory of vibration of elastic materials with distributed properties. In either case the equivalent electrical circuit contains four constants.

The values of these four constant parameters can be determined from frequency and immittance measurements in the resonance range of the resonator. Such measurements are generally more difficult than those on conventional circuit elements, principally because of the exceedingly high rate of change of the value of X_1 with frequency which, of course, is a direct consequence of the high quality factor of these devices. For a quartz crystal resonator with a Q of 50,000, for example, the half-power points of the resonance curve differ in frequency by 20 ppm. Not only must the frequency stability and resolution of the measuring signal be very high, therefore, but nearly all operational and environmental factors acting on the crystal

resonator have a large effect on this scale, even if their influence may be considered small in absolute terms. For example, a 1-mW change in drive level causes a 1-ppm change in the resonance frequency of a typical AT-cut quartz crystal resonator, and frequency–temperature coefficients of 1 ppm/°C are quite commonly encountered at room temperatures. Special precautions are therefore always required to assure a reasonably constant environment for the resonator, and the signal source should preferably be locked to the device under test. Moreover, sufficient time must be allowed after changes in test frequency to permit the high-Q transients to decay.

With the resonator environment held constant and the test signal stable, the measurement of a crystal resonator proceeds in much the same manner as that of a conventional circuit element, except that for the latter there is rarely a need to measure a composite resonance circuit—the individual components are usually accessible directly. The subject of resonator parameter measurements can thus be divided further into the aspects dealing with the fact that the desired data must be extracted from the behavior of the complete equivalent electrical circuit and the aspects generic to the measurement of immittances at and near the resonance frequency of the device. Both of these aspects have been dealt with in this chapter.

Measurement techniques are usually based on the fact that the immittance of a crystal resonator as a function of frequency exhibits a number of unique features, such as the maxima of the magnitudes of the resistive and conductive components, etc. The most commonly used feature is zero reactance (phase angle) in the low-impedance range, that is, the resonance of the resonator, with or without series reactive elements. At resonance the resonator immittance is purely resistive, a feature that lends itself much more readily to substitution measurements than any other complex values of the impedance: zero phase, for instruments with phase-indicating or phase-measuring capability, is a much more readily established reference or calibration condition than any finite value. Nevertheless, the realization of substitution or calibration elements that exhibit zero phase at the resonator–instrument interface is a nontrivial problem.

All of the measuring instruments discussed in this chapter are capable of being used for the measurement of resonance frequency and resistance by the substitution technique. Within the limits of the substitution elements, the resonator–instrument interface, and the resolution of the indicating meters, the results obtained thereby will be equally accurate for all instruments if the substitution process is carried to completion. Meeting this latter condition, however, is tedious and requires in the limit an infinite number of substitution elements. One measure of the relative merits of the various instruments available for resonator measurements, therefore, is the degree to which they are capable of interpolating the true value of the resonator impedance between

more or less widely spaced values of the substitution elements: the latter would now more commonly be regarded as the calibration elements. To a large measure the magnitudes of the systematic errors encountered in any particular measuring system are a direct function of the imperfections in the detailed electrical and mechanical implementation of the basic system concept involved. Any value judgment of one system over another can thus apply only to the very specific implementations being compared.

Nevertheless, some generally valid observations are possible. In the context of this chapter, these must be restricted to the analog part of the system, where the basic accuracy is determined. Although digital processing, programming, and computational facilities are an important part of modern instrumentation, they have not been dealt with in this chapter nor, for that matter, have the many different schemes for test-signal generation been dicussed. Just as a purer signal will result in better data, so will error-correction routines provided by a computer be more effective the lower the basic errors in the analog section of the instrument.

The observations concern the relative difficulty in implementing any particular system concept electrically and mechanically, such as to minimize the more prominent sources of systematic measurement errors. A few examples must suffice. All of the principal system concepts considered, except the balanced bridge, employ vector-ratio meters with the crystal resonator in some kind of transmission network; the π network and the 50-Ω transmission bridge are the two examples discussed most extensively. All else being equal, including the vector-ratio meter and plumbing, use of the latter would appear to offer an advantage in that one of the unknown terminals is at ground potential and the range of maximum sensitivity is around 50 Ω. When comparing a transmission-type measuring system with a balanced-bridge system, it can be observed that the vector-ratio meter with the currently highest performance also employs the zero-balancing principle. Nevertheless, the sources of potential measurement errors in the transmission system include all elements of the entire analog signal train, including cables, connectors, etc., whereas in the balanced-bridge system they are restricted to the bridge proper. The latter would thus appear to have the advantage.

Other very pertinent measures of the relative merits of a particular measuring system, next to accuracy, are versatility, speed of operation, sensitivity–resolution and, last but not least, cost. Of these, only versatility in terms of the basic capability to satisfy the various resonator measuring needs has been discussed in this chapter. All other aspects are very much a function of the state of technology at any given time and, thus, subject to frequent changes in the future.

APPENDIX I: THE GENERALIZED EQUIVALENT CIRCUIT

Let the reactance of the motional arm in the lumped-element-equivalent electrical circuit in Fig. 7-3 be

$$X_{1L}(\omega) = \omega L_1 - 1/\omega C_1. \tag{7-23}$$

The admittance for a lossless ($R_1 = 0$) resonator is then

$$Y = j\omega C_0(1 - 1/\omega C_0 X_1). \tag{7-24}$$

The pole and zero frequencies are ω_s, the resonance frequency of the motional arm, and ω_p, the parallel-resonance frequency of the resonator, with ω_s and ω_p defined by

$$X_1(\omega_s) = 0 \qquad X_1(\omega_p) = 1/\omega C_0. \tag{7-25}$$

The plane-wave approximation for the vibration of resonators with distributed-mass, elastic, and piezoelectric properties yields the admittance expressions (Yamada *et al.*, 1970: IEEE, 1978)

$$\begin{aligned} Y_S &= j\omega C_0 \frac{1}{[1 - k_S^2(\tan A_S\omega)/A_S\omega]}, \\ Y_U &= j\omega C_0[1 + k_U^2(\tan A_U\omega)/A_U\omega] \end{aligned} \tag{7-26}$$

for piezoelectrically stiffened and piezoelectrically unstiffened resonators, respectively. These expressions can be recast into the form of Eq. (7-24), which leads to the definition of the corresponding generalized motional-arm reactances:

$$\begin{aligned} X_{1S}(\omega) &= \frac{1}{\omega C_0}\left(1 - \frac{A_S\omega}{k_S^2 \tan A_S\omega}\right), \\ X_{1U} &= -\frac{1}{\omega C_0}\frac{1}{k_U^2}\frac{A_U\omega}{\tan A_U\omega}. \end{aligned} \tag{7-27}$$

If the pole and zero frequencies are again defined by Eqs. (7-25), the constants in Eqs. (7-27) are determined as

$$\begin{aligned} A_S &= \frac{n\pi}{2\omega_p}, \qquad k_S^2 = \frac{(n\pi/2)(\omega_s/\omega_p)}{\tan[(n\pi/2)(\omega_s/\omega_p)]}, \\ A_U &= \frac{n\pi}{2\omega_s}, \qquad k_U^2 = \frac{(-n\pi/2)(\omega_p/\omega_S)}{\tan[(n\pi/2)(\omega_p/\omega_S)]}, \end{aligned} \tag{7-28}$$

with the overtone order n being an odd integer.

For small piezoelectric coupling, $k^2 \ll 1$, and Eqs. (7-27) can be approximated by

$$X_{1S} \simeq \frac{1}{\omega C_0}\left(1 + \frac{\omega - \omega_p}{\omega_s}\right)\left(\frac{\omega - \omega_s}{\omega_p - \omega_s}\right),$$
$$X_{1U} \simeq \frac{1}{\omega C_0}\frac{\omega}{\omega_p}\left(\frac{\omega - \omega_s}{\omega_p - \omega_s}\right), \tag{7-29}$$

while the reactance of the lumped-element circuit [Eq. (7-23)] with Eqs. (7-25) can be written as

$$X_{1L} = \frac{1}{\omega C_0}\left(\frac{\omega^2 - \omega_s^2}{\omega_p^2 - \omega_s^2}\right). \tag{7-30}$$

The values X_1 of the motional reactance according to the relations (7-27) with (7-28) and according to (7-29) are exactly the same as for the lumped-element circuit in Eq. (7-30) at the two frequencies ω_s and ω_p. The differences are in the frequency dependence outside these values for ω; they become increasingly important as k^2 increases. For quartz crystal resonators, as an example, the frequency ω determined from Eq. (7-30) for a given value of X_1 differs from the frequency found from the applicable relation in Eqs. (7-29), for the same value of X_1, by less than 1.5 parts per 10^6 over a range of ± 1 part per 10^3 from ω_s. Certainly, for materials with large coupling coefficients, the use of the applicable relation in Eqs. (7-27) in place of Eq. (7-30) for X_1 is advisable.

To provide for arbitrary losses in the resonator material (Holland, 1967) requires solution of the complex eigenvalue problem, which has apparently not yet been reported. Small viscous losses, however, can be accounted for by replacing, for example, A_S by $\bar{A}_S = A_S(1 - j\omega\tau/2)$ in Eqs. (7-26) and (7-27) (Lamb and Richter, 1966; Ballato, 1977), where $\tau = 1/\omega_s Q_0$ is the motional time constant (for quartz τ is on the order of 10^{-14} sec). When, further, X_1 in Eq. (7-24) is replaced by $Z_1 = R_1 + jX_1$ and the abbreviations

$$A_x = A_S\omega, \qquad A_r = A_S\omega^2\tau/2,$$
$$H = \frac{1}{k^2}\frac{\tan A_x(1 - \tanh^2 A_r)}{(\tan^2 A_x + \tanh^2 A_r)}, \qquad K = \frac{1}{k^2}\frac{\tanh A_r(1 + \tan^2 A_x)}{(\tan^2 A_x + \tanh^2 A_r)} \tag{7-31}$$

are used, one can find from Eq. (7-27) that

$$X_{1S} = \frac{1}{\omega C_0}(1 - A_x H - A_r K), \qquad R_1 = \frac{1}{\omega C_0}(A_x K - A_r H). \tag{7-32}$$

Within the limits of their validity, that is, arbitrary k^2 and $\omega\tau \ll 1$, the Eqs. (7-32) can nearly always be approximated by

$$X_{1S} = \frac{1}{\omega C_0}\left(1 - \frac{A_S\omega}{k^2 \tan A_S\omega}\right), \qquad R_1 = \frac{n^2\pi^2}{8k^2}\frac{\tau}{C_0}\left(\frac{\omega}{\omega_p}\right)^2, \tag{7-33}$$

demonstrating that the expressions for X_1 in Eqs. (7-27) are valid even in the presence of losses and, further, that the equivalent electrical circuit in Fig. 7-5, with X_1 and R_1 as just defined, is valid for most resonators of practical significance.

APPENDIX II: TWO-PORT RELATIONS FOR THE IEC-444 π NETWORK

The input–output relations for a four-terminal network are

$$V_1 = a_{11}V_2 + a_{12}I_2,$$
$$I_1 = a_{21}V_2 + a_{22}I_2. \tag{7-34}$$

For the network in Fig. 7-12, the matrix elements are

$$a_{11} = \left(1 + \frac{Z_2}{Z_3}\right)\left(1 + \frac{Z_5}{Z_6}\right) + \frac{Z_2(Z_4 + Z_5 + Z_6)}{Z_4Z_6} + Z_x\left(1 + \frac{Z_2}{Z_3}\right)\left(\frac{Z_4 + Z_5 + Z_6}{Z_4Z_6}\right),$$
$$a_{12} = Z_5\left(1 + \frac{Z_2}{Z_3}\right) + Z_2\left(1 + \frac{Z_5}{Z_4}\right) + Z_x\left(1 + \frac{Z_2}{Z_3}\right)\left(1 + \frac{Z_5}{Z_4}\right),$$
$$a_{21} = \left(\frac{Z_1 + Z_2 + Z_3}{Z_1Z_3}\right)\left(1 + \frac{Z_5}{Z_6}\right) + \left(\frac{Z_4 + Z_5 + Z_6}{Z_4Z_6}\right)\left(1 + \frac{Z_2}{Z_1}\right) + Z_x\left(\frac{Z_1 + Z_2 + Z_3}{Z_1Z_3}\right)\left(\frac{Z_+ + Z_5 + Z_6}{Z_4Z_6}\right),$$
$$a_{22} = \left(\frac{Z_1 + Z_2 + Z_3}{Z_1Z_3}\right)Z_5 + \left(1 + \frac{Z_2}{Z_1}\right)\left(1 + \frac{Z_5}{Z_4}\right) + Z_x\left(1 + \frac{Z_5}{Z_4}\right)\left(\frac{Z_1 + Z_2 + Z_3}{Z_1Z_2}\right).$$

The determinant $a_{11}a_{22} - a_{12}a_{21} = 1$. When the network in Fig. 7-12 is terminated with Z_T, $I_2 = V_2/Z_T$: the input–output voltage ratio then becomes

$$V_1/V_2 = a_{11} + a_{12}/Z_T = A + BZ_x.$$

The input impedance is given by

$$Z_{in} = V_1/I_1 = (a_{11}Z_T + a_{12})/(a_{21}Z_T + a_{22}).$$

If all elements in Fig. 7-12 are resistive with the values as shown and $Z_T = 50\,\Omega$, then $A = 30.03\,\Omega$ and $B = 1.24\,\Omega^{-1}$.

APPENDIX III: TWO-PORT RELATIONS FOR A TRANSMISSION BRIDGE

The chain matrix elements for the network in Fig. 7-13 are

$$a_{11} = \frac{(Z_1 + Z_3)(Z_2 + Z_M)}{Z_2Z_3 - Z_1Z_M},$$

$$a_{12} = \frac{Z_1Z_2(Z_3 + Z_M) + Z_3Z_M(Z_1 + Z_2)}{Z_2Z_3 - Z_1Z_M},$$

$$a_{21} = \frac{Z_1 + Z_2 + Z_3 + Z_M}{Z_2Z_3 - Z_1Z_M},$$

$$a_{22} = \frac{(Z_1 + Z_2)(Z_3 + Z_M)}{Z_2Z_3 - Z_1Z_M}.$$

If $Z_1 = Z_3$ the input–output voltage ratio becomes

$$\frac{V_1}{V_2} = 2\frac{Z_2 + Z_M}{Z_2 - Z_M} + \frac{Z_3 + 2Z_2}{Z_T} - \frac{1}{Z_T}\frac{2Z_2^2}{Z_2 + Z_M}.$$

The output–input voltage ratio can then be written as in Eq. (7-16). When Eq. (7-16) is solved for Z_M and the quantity $(Z_M - Z_0)/(Z_M + Z_0) = \Gamma$ is formed, Eq. (7-17) is found by solving for γ.

8 Precision Oscillators

Warren L. Smith

AT&T Bell Laboratories
Allentown, Pennsylvania

Thomas E. Parker

Research Division
Raytheon Company
Lexington, Massachusetts

List of Symbols for Section 8.1 46
8.1 Bulk-Acoustic-Wave Oscillators 47
by Warren L. Smith
8.1.1 General Characteristics of Crystal-Controlled Oscillators 47
8.1.1.1 Requirements for Oscillation 48
8.1.1.2 Sources of Frequency Instability 48
8.1.1.3 Classification of Oscillators and Their Performance Characteristics 51
8.1.2 Circuit Configurations for Crystal-Controlled Oscillators 53
8.1.2.1 Bridge Circuits 54
8.1.2.2 Modified Pierce Oscillator Circuits 56
8.1.2.3 Common-Collector Oscillator Circuits 58
8.1.2.4 Common-Base Oscillator Circuits 59
8.1.2.5 Emitter-Coupled Oscillators 60
8.1.3 Temperature-Control Techniques for Precision Oscillators 61
8.1.3.1 Temperature Stability Requirements 61
8.1.3.2 Proportional Temperature-Control Techniques 63
8.1.4 Temperature-Compensation Methods for Semiprecision Oscillators 63
8.1.5 Miniature Integrated-Circuit Oscillators 64
List of Symbols for Section 8.2 65
8.2 Surface-Acoustic-Wave Oscillators 66
by Thomas E. Parker
8.2.1 Introduction 66
8.2.1.1 What is a SAW Oscillator? 66
8.2.1.2 What is the Value of a SAW Oscillator? 66
8.2.1.3 State of the Art 66

PRECISION FREQUENCY CONTROL
Volume 2
Oscillators and Standards

Copyright © 1985 by Academic Press, Inc.
All rights of reproduction in any form reserved.

ISBN 0-12-280602-6

8.2.2 The Basic SAW Oscillator—A Physical Point of View 67
8.2.2.1 Conditions for Oscillation 67
8.2.2.2 Oscillator Using a SAW Delay Line 68
8.2.2.3 Oscillator Using a SAW Resonator 70
8.2.3 Frequency Stability 72
8.2.3.1 Introduction 72
8.2.3.2 Short-Term Stability 72
8.2.3.3 Temperature Stability 75
8.2.3.4 Long-Term Stability—Aging 76
8.2.4 Multifrequency Oscillators 76
8.2.5 Electronic Amplifiers and Other External Components 77
8.2.6 Advantages and Disadvantages of SAW Oscillators 78
8.2.7 Conclusion 79
List of Symbols for Section 8.3 79
8.3 Quartz Frequency Standards and Clocks—Frequency Standards in General 79
by Warren L. Smith
8.3.1 Design Considerations 80
8.3.1.1 Choice of Resonator 81
8.3.1.2 Oscillator-Circuit Considerations 82
8.3.1.3 Temperature-Control Requirements 86
8.3.1.4 Minimizing Ambient Mechanical Effects 88
8.3.2 Measurement and Specification of Frequency Stability 89
8.3.2.1 Measurement of Frequency 89
8.3.2.2 Interpretation of Frequency Measurements 93
8.3.2.3 Measures of Short-Term Frequency Stability (Time Domain) 93

LIST OF SYMBOLS FOR SECTION 8.1

$\mathbf{A}$	Amplifier gain, vector quantity
C_0	Resonator shunt (static) capacitance
C_1	Resonator motional capacitance
$\mathbf{e}$	Vector voltage
f	Frequency
f_r	Resonance frequency
f_s	Series resonance frequency
L_1	Resonator motional inductance
Q	Quality factor
R_1	Resonator motional resistance
R_e	Resonator resistance at the operating condition
$\bar{Y}$	Electrical admittance
$\bar{Z}$	Electrical impedance
$\boldsymbol{\beta}$	Feedback voltage ratio, vector quantity

8.1 BULK-ACOUSTIC-WAVE OSCILLATORS[§]

One of the most important applications of bulk-wave quartz crystal resonators is the stabilization of time–frequency generators. These generators provide the carrier signals and pilot signals for electronic communications and navigation systems, the clock signals for data processing and digital communications systems, and the reference signals for numerous special-purpose systems and instruments. The frequency accuracy and stability requirements placed on these signal sources are as diverse as the applications and range all the way from the $\pm 0.1\%$ tolerance often quoted for microprocessor clocks to the $\pm 5 \times 10^{-11}$ tolerance needed, for example, by high-speed digital telecommunication switching machines. Specific circuit designs are as diverse as their requirements.

In spite of the wide range and large numbers of designs, however, the crystal-controlled oscillators in common use may be broadly categorized for purposes of discussion. In addition, there are basic considerations that generally apply to crystal-controlled oscillator circuits of all types. In the following discussion, we attempt to proceed from the general to the more specific.

8.1.1 General Characteristics of Crystal-Controlled Oscillators

Nearly all crystal-controlled oscillator circuits may be considered to consist of two essential parts: an amplifier, or gain circuit, and a feedback network that provides positive feedback at the frequency of oscillation. Such a generalized conceptual circuit is shown in Fig. 8.1-1. The amplifier portion

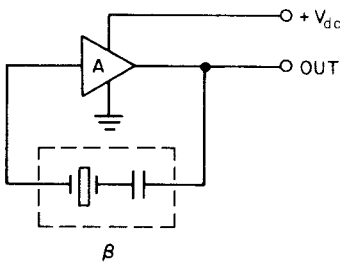


FIG. 8.1-1 Functional concept of the positive-feedback crystal-controlled oscillator.

usually consists of one or more active devices and the necessary biasing networks and may also include a band-limiting network together with impedance-matching elements. The crystal unit appears in the feedback

[§] Section 8.1 was written by Warren L. Smith.

network, which may contain other components as well. With this concept in mind, we shall examine some of the general characteristics of such circuits.

8.1.1.1 REQUIREMENTS FOR OSCILLATION

In the circuit of Fig. 8.1-1, consider for the moment that a signal **e** exists at the input of the amplifier. Letting **A** represent the gain of the amplifier (when loaded by the feedback network in shunt with the applied load), the signal appearing at the output terminal is $\mathbf{e} \cdot \mathbf{A}$. If we let $\boldsymbol{\beta}$ represent the transmission of the feedback network (when loaded by the input impedance of the amplifier), the resulting signal at the amplifier input is $\mathbf{e} \cdot \mathbf{A} \cdot \boldsymbol{\beta} = \mathbf{e}'$. When $\mathbf{e}'$ has the same phase as **e** and $|\mathbf{e}'| \geq |\mathbf{e}|$, the circuit oscillates. Writing $\mathbf{A} = Ae^{j\Theta_A}$ and $\boldsymbol{\beta} = \beta e^{j\Theta_\beta}$, we see that this requirement can be formulated as

$$\mathbf{A} \cdot \boldsymbol{\beta} = A\beta \exp[j(\Theta_A + \Theta_\beta)] \geq \exp[j(2n\pi))], \qquad n = 0, 1, 2, \ldots. \tag{8.1-1}$$

The frequency of oscillation is determined by the phase condition $(\Theta_A + \Theta_\beta) = 2n\pi, n = 0, 1, 2, \ldots$. At this frequency the magnitude of the loop gain vector $\mathbf{A} \cdot \boldsymbol{\beta}$ must be greater than unity for the signal level in the loop to build up. The signal level in the loop will continue to increase until the amplifier gain is reduced, either by nonlinearities in the active elements or by some automatic level-control method.

When initially energized, the only signal present in the circuit is "white" electrical noise associated with the components (mainly the active devices) in the circuit. That component of noise whose frequency satisfies the phase condition for oscillation is propagated around the loop with increasing amplitude. The rate of increase of amplitude depends on the excess gain of the loop as well as on the bandwidth of the crystal network.

8.1.1.2 SOURCES OF FREQUENCY INSTABILITY

The instantaneous frequency generated by any real oscillator circuit changes from one instant to another due to several causes that may be broadly considered as two categories. First are those variations produced by the sustaining circuit, which include loop-phase perturbations due to mechanical and electrical environments influencing the active elements as well as the R, L, and C parameters of the networks. Also, the phase stability of the loop is corrupted by the presence of intrinsic electrical noise generated in active elements and thermal noise associated with resistance elements. Long-term drift (aging) of the components in the sustaining circuit produces changes in the circuit-transfer phase characteristic, which in turn produces corresponding long-term changes in operating frequency.

In the second general category are those changes due to variations in the controlling resonator itself. The series-resonance frequency of the crystal unit will be influenced by its temperature environment, by mechanical disturbances, and by drive level. Long-term changes in its frequency (aging) can be the result of relaxation of electrode and mounting-system stresses, surface and subsurface changes (such as the propagation of microcracks left by shaping operations), diffusion of metal electrode systems, and adsorption–desorption of residual gases and vapors in the sealed crystal enclosure (see Chapter 6).

Consider, for example, the simple oscillator circuit of Fig. 8.1-2. Assume that the active devices are nearly ideal, so that the initial operating condition is at the resonance frequency f_r of the crystal unit and both Θ_A and Θ_β are therefore zero. The effective, or loaded, Q of the crystal unit, since it is loaded at either port by the transistor emitter resistance R_E, is

$$Q_e = \omega L_1/(R_1 + 2R_E). \tag{8.1-2}$$

At some later time a perturbation of supply voltage or some other variation results in a phase change in the active circuit of an amount $\Delta\Theta_A$. The operating frequency then changes until the phase shift in the crystal network is exactly equal in magnitude and opposite in sign:

$$\Delta\Theta_A + \Delta\Theta_\beta = 0. \tag{8.1-3}$$

The change in the crystal-network phase $\Delta\Theta_\beta$ can be approximated as

$$\Delta\Theta_\beta = \frac{\Delta X}{R_1 + 2R_E} = \frac{2\,\Delta\omega L_1}{R_1 + 2R_E}, \tag{8.1-4}$$

where L_1 is the equivalent motional inductance of the crystal unit, $\Delta\omega$ the incremental change in angular frequency, R_1 the motional resistance of the

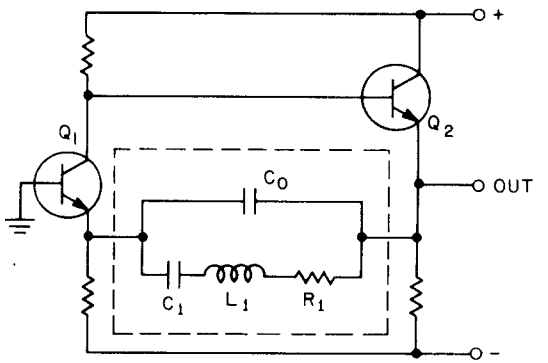


FIG. 8.1-2 A simple series-resonance crystal-oscillator circuit.

crystal, and R_E the effective emitter impedance of the transistor stage. Consequently, in order to satisfy the loop-phase conditions for oscillation,

$$\Delta\Theta_\beta = \frac{2\,\Delta\omega L_1}{R_1 + 2R_E} = -\Delta\Theta_A. \tag{8.1-5}$$

Or, solving for the fractional change in frequency,

$$\Delta\omega/\omega = -\Delta\Theta_A/2Q_e, \tag{8.1-6}$$

where we have used Q_e to represent the effective, or loaded, quality factor of the crystal embedded in the network.

Consequently, for any specific circuit configuration for which we can calculate the network transfer phase, we can relate frequency change to a particular parameter change, assuming that the crystal parameters remain invariant. Similar results can be obtained for operating conditions other than series resonance, although the relation between network phase and frequency change becomes more complex as the operating point moves further away from series resonance, as evidenced by the equivalent-circuit representation of the crystal unit shown in Fig. 8.1-3. If $\omega_0 = 1/\sqrt{L_1C_1}$ and $\omega = 2\pi f$, then using the angular frequency offset $\Delta\omega = \omega - \omega_0$ we see that very near series resonance the equivalent impedance can be expressed as

$$\bar{Z}_{12} \simeq R_1 + j(2\,\Delta\omega L_1). \tag{8.1-7}$$

Over a wider frequency range, admittance can be approximated by (neglecting C_{13} and C_{23})

$$\bar{Y}_{12} = \frac{R_1}{R_1^2 + (2\,\Delta\omega L_1)^2} + j\left[\omega C_0 - \frac{2\,\Delta\omega L_1}{R_1^2 + (2\,\Delta\omega L_1)^2}\right]. \tag{8.1-8}$$

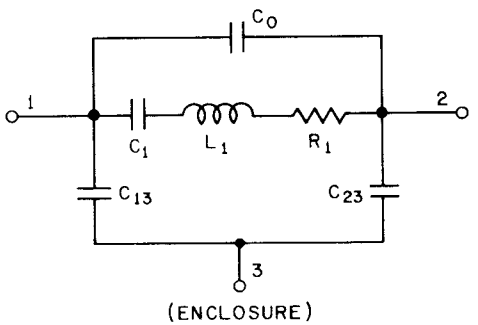


FIG. 8.1-3 Equivalent electrical circuit of a piezoelectric resonator at frequencies near resonance.

The admittance (or impedance) of a well-behaved crystal unit, when expressed in this way, is found to be nearly invariant under conditions of mechanical, electrical, or thermal disturbance: nor does it change appreciably with time. Consequently, any changes of crystal frequency due to aging or environment are seen directly in the operating frequency of the oscillator whether it operates the crystal unit near series resonance or in a positive-reactance region.

Actual circuits are usually found to undergo changes of several parameters simultaneously. As a practical result, the isolation of specific factors contributing to overall frequency instability can be a difficult task. In the case of very stable oscillators, this task is rendered even more difficult by the unavoidable presence of electrical noise. Analyzing the effect of this noise is a complex task and will not be considered here other than to say that it results in a nondeterministic random phase-fluctuation spectrum that is best treated by statistical methods (Barnes *et al.*, 1971: Cutler and Searle, 1966).

8.1.1.3 CLASSIFICATION OF OSCILLATORS AND THEIR PERFORMANCE CHARACTERISTICS

Crystal-controlled oscillators have been designed and produced in widely varying types, sizes, and circuit configurations—the possibilities are nearly unlimited (Edson, 1953; Frerking, 1978). For purposes of discussion, however, they can be broadly grouped into some general categories.

(1) *Packaged crystal oscillators* include those which do not provide means for reducing the frequency–temperature performance of the controlling crystal unit. These oscillators range from the miniature types used as clocks for microprocessors to the high-power, high-frequency exciters for radars or microwave generators. They may sometimes include a manual frequency adjustment to permit field recalibration.

(2) *Voltage-controlled crystal oscillators* are those frequency generators that provide a means for electrically controlling frequency over some narrow range, usually by means of a varactor diode used as tuning capacitor. These oscillators are commonly used in phase-locked-loop applications or as FM generators in communications systems.

(3) *Temperature-compensated crystal oscillators* make use of special circuits to improve the frequency–temperature performance that would be achieved with the crystal unit alone. Many techniques have been developed for this purpose. In general terms, a temperature sensing device is used to regulate a variable reactance in the crystal network so that at any temperature within the design range a nearly constant output frequency is obtained. Some commonly used techniques will be described in Section 9.2.

(4) *Temperature-controlled crystal oscillators* provide the highest degree of frequency stability. Either single or two-stage "ovens" or temperature-stabilized enclosures are used to maintain the crystal and oscillator circuit at a very stable temperature, thus eliminating frequency changes due to thermal environments. Such precision oscillators usually include sophisticated circuits to maintain stable, low-level crystal drive and to protect the oscillator circuit from the effects of external load and power supply variations as well.

Clearly, this categorization is very general, and an almost unlimited number of variations and combinations are possible. Packaged crystal oscillators, for example, may include frequency multipliers or dividers, provisions for multiple- or submultiple-frequency simultaneous outputs, etc. Temperature-compensated or oven-stabilized crystal oscillators are often also provided with voltage-control capabilities. The frequency-stability performance to be expected, however, can be generally correlated to the categorical types given above.

Packaged crystal oscillators and voltage-controlled oscillators provide frequency-stability performance determined mainly by the crystal resonator used. Typical frequency temperature curves of several commonly used crystal types are shown in Fig. 8.1-4. Using an AT-cut resonator, for example, a frequency tolerance of $\pm 25 \times 10^{-6}$ can be realized over a temperature range from about -40°C to 90°C.

The performance of temperature-compensated crystal oscillators is limited by the accuracy of the compensation method and by frequency aging of the crystal unit employed as well as by unavoidable environmental effects. Analog

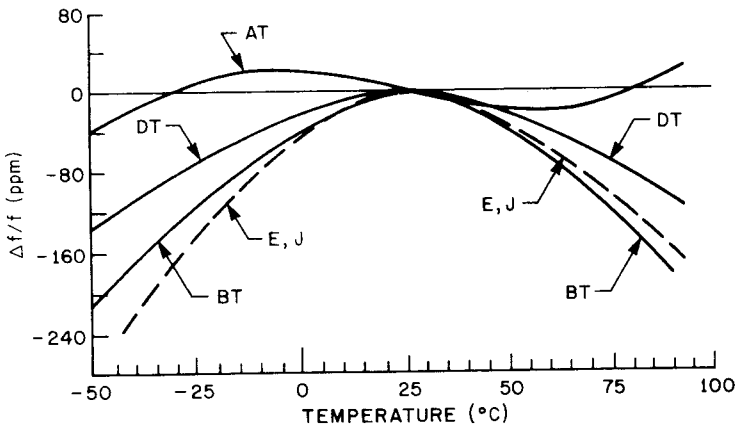


FIG. 8.1-4 Typical frequency variation as a function of temperature of several commonly used types of quartz crystal.

compensation methods are practically capable of maintaining frequency tolerances of about $\pm 5 \times 10^{-7}$ over a temperature range from -30°C to 80°C. With digital methods the frequency stability that can be achieved is theoretically limited only by the retrace characteristics and aging of the crystal unit. Practically, it also depends on the accuracy of the temperature sensor–digitizer, the thermal coupling between crystal unit and sensor, and the precision of the processor used. Tolerances of about $\pm 1 \times 10^{-7}$ over a wide temperature range are possible with present state-of-the-art sensors and microprocessor equipment using the best crystal units available (Frerking, 1978).

Oven-stabilized crystal oscillators commonly use proportional-temperature-control techniques, which allow the cavity temperature to be maintained with high accuracy and to be virtually free of thermal transients. A single-stage oven of this type can provide a temperature-stabilization ratio of as much as 1000 or more (i.e., an internal temperature change of no more than 0.01°C for an ambient variation of 10°C), while two-stage systems can achieve stabilization ratios of 50,000 or more. When used with precision overtone-mode crystal units and carefully designed circuitry, these oscillators can maintain frequency within $\pm 5 \times 10^{-12}$ per day, or even better, limited only by the aging of the crystal resonator (Flint and Pustarfi, 1974).

Some of the parameters of different types of oscillators are summarized in Table 8.1-1.

TABLE 8.1-1
Comparison of Oscillator Types

Type	Temperature range	Frequency deviation	Input power
Miniature, packaged discrete, voltage controlled	-40–100°C	$\geq 2.5 \times 10^{-5}$	5–100 mW
	0–70°C	$\geq 1.5 \times 10^{-5}$	5–100 mW
Temperature compensated	-40–100°C	$> 3 \times 10^{-6}$ to 5×10^{-7}	15–200 mW
	0–70°C	$> 1 \times 10^{-6}$ to 3×10^{-7}	15–200 mW
Temperature stabilized	0–70°C	1×10^{-7} to 2×10^{-10}	2–40 W

8.1.2 Circuit Configurations for Crystal-Controlled Oscillators

Many different circuit configurations have been used for crystal-controlled-oscillator applications. One class of sustaining circuits uses the crystal unit as a series-resonant feedback element with a noninverting amplifier. Such circuits are readily realized as silicon integrated circuits and have found extensive

application in miniature packaged oscillators. Another class of oscillator circuits makes use of inverting amplifiers, thus requiring that the crystal unit be combined with other elements in a feedback network capable of providing approximately π radians of phase shift. These networks may be bridge-type circuits or some form of bandpass structure. Phase-inverting feedback circuits can also be realized with divided-electrode crystal units or with monolithic crystal filters.

Some of the circuits which have been widely used are described in the following sections.

8.1.2.1 BRIDGE CIRCUITS

The bridge-type feedback network has been widely used in the past for precision crystal-controlled oscillators. Vacuum-tube amplifiers having tuned plate and grid transformers were employed in order to achieve impedance matching to the low-impedance bridge and thus realize high gain. Modern designs use an integrated amplifier circuit, which minimizes the need for impedance matching; however, a single tuned transformer, as shown in Fig. 8.1-5, is useful for suppressing wideband noise as well as for providing assurance that oscillation will not occur at some undesired crystal mode of vibration.

The advantage of the bridge circuit is that it provides simultaneously for positive and negative feedback around the sustaining amplifier. The negative-feedback portion serves to stabilize the operation of the active circuit and also provides a convenient means to achieve automatic level control. For example, if the resistive element connected between point C and ground in Fig. 8.1-5

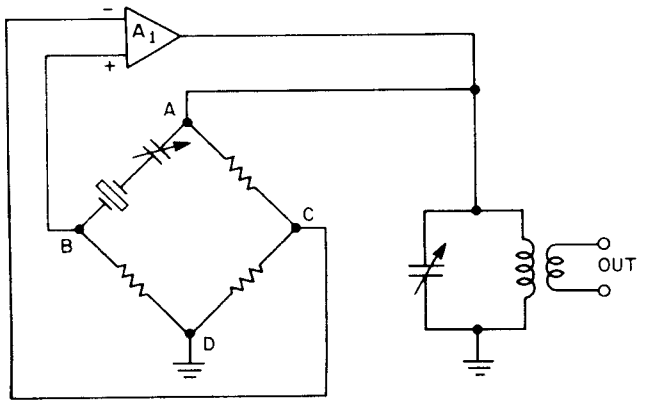


FIG. 8.1-5 Functional schematic of a bridge-type oscillator circuit using a differential-input integrated amplifier.

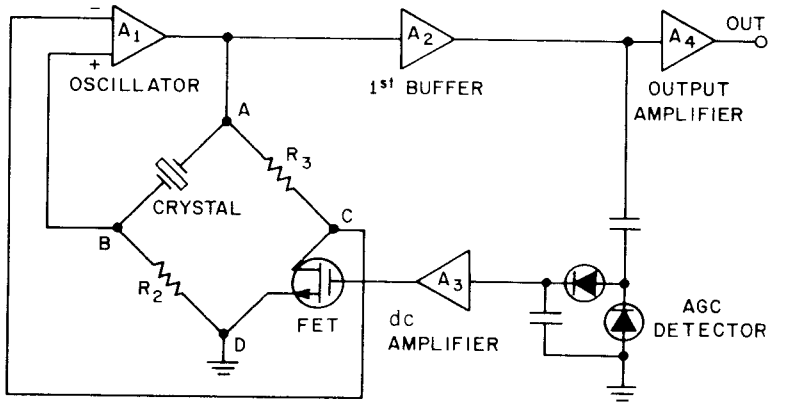


FIG. 8.1-6 One technique for application of automatic-level control to a bridge-type oscillator circuit.

consists of a variolosser diode or a field-effect transistor (FET), its effective resistance can be electrically controlled to maintain a constant output level. As $R_{C,D}$ is increased, the negative-feedback factor increases and the loop gain of the amplifier decreases. Figure 8.1-6 shows one way of accomplishing the level-control function. The FET device is initially biased to its high-conductivity state, producing a low value of negative feedback and therefore a maximum value of excess loop gain. As the oscillation level increases, the signal amplitude is detected by the diode rectifiers, amplified, and used to control the conductivity of the FET at the equilibrium gain condition.

The open-loop gain of the sustaining amplifier (A_1) can be very high (10^4 or greater), so that the transfer function of the oscillator loop is dependent almost entirely on the negative-feedback parameters; consequently, very stable operation is possible. Frequency stability is determined mainly by the phase-slope characteristics of the positive-feedback portion of the bridge, consisting of the crystal unit in series with R_2. The conditions for stable operation can be expressed as:

$$\frac{R_2}{R_1 + R_2} \simeq \frac{R_{FET}}{R_3 + R_{FET}}, \tag{8.1-9}$$

where R_1 is the motional resistance of the crystal unit and R_{FET} the dynamic impedance of the FET device. The crystal drive level at which this condition prevails is determined by the buffer-amplifier (A_2) gain and the characteristics of the diode detector, AGC amplifier (A_3), and the FET impedance characteristic.

Residual phase errors in the bridge components and circuit wiring give rise to a frequency offset from crystal-unit resonance,

$$\Delta f = f_0 - f_r = \frac{\Delta\Theta(R_2 + R_1)}{4\pi L_1}, \tag{8.1-10}$$

where $\Delta\Theta$ is the circuit phase error and L_1 the crystal-unit motional inductance. Rearranging and differentiating, the phase-slope function is found to be

$$\frac{\partial(\Delta\Theta)}{\partial(\Delta f)} = \frac{4\pi L_1}{(R_2 + R_1)}, \tag{8.1-11}$$

which is a measure of the stability characteristic of a crystal-controlled oscillator.

Although not extensively used in current commercial oscillators, the bridge circuit can provide highly stable oscillators and can easily be adapted to integrated differential-input amplifier circuits.

8.1.2.2 MODIFIED PIERCE OSCILLATOR CIRCUIT

The modified Pierce oscillator is currently one of the most widely used circuit configurations for highly stable crystal-controlled-oscillator applications. It is readily adapted for use with virtually any inverting amplifier, single-stage vacuum tube, bipolar transistor, or FET device and can easily be designed to operate the overtone mechanical modes of the crystal unit. Figure 8.1-7 is a schematic diagram of a bipolar-transistor Pierce oscillator with provision for automatic level control. In this configuration the crystal unit and

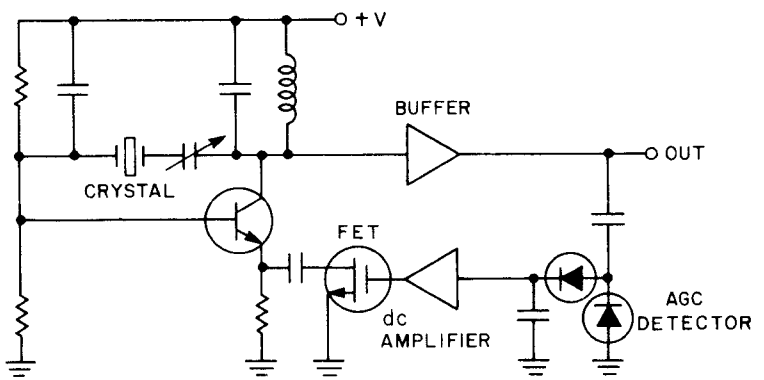


FIG. 8.1-7 Functional schematic of a modified Pierce oscillator circuit with automatic level control.

its associated trimming capacitor form the series branch of a bandpass phase-inverting feedback network. At moderate frequencies the transfer phase of the transistor exceeds 180° (i.e., at 10 MHz a transistor with a 900-MHz cutoff frequency exhibits about a 200° measured phase shift). Thus, the feedback filter network must provide an additional 160° phase delay in order to satisfy the loop-phase condition for oscillation, which occurs within the passband of the feedback filter section.

In order to satisfy the loop-phase conditions for oscillation with a π-network circuit of this kind, it is necessary that the two shunt reactance elements be of the same sign at the frequency of operation and the series element be of the opposite sign. In the modified Pierce configuration, the two shunt elements are capacitive, which forces the crystal branch to operate in a positive reactance condition, assuring the maximum phase slope for the network. For overtone operation of the crystal, it is only necessary that the L–C configuration in the collector circuit of Fig. 8.1-7 be resonant at a frequency between the desired mode frequency and the next lower odd overtone mode (i.e., between the fundamental and third overtone to assure third-overtone operation, etc.).

For best long-term frequency stability, the insensitivity of oscillator frequency to changes in transistor characteristics, load impedance, etc., is improved by choosing the shunt reactance elements as small as possible (large capacitance values), restricted only by the requirement that adequate loop gain be maintained. In this way the phase slope of the network is kept at a maximum. Analysis of the effective rf circuit (Figure 8.1-8) yields the following approximate expression for the minimum value of the terminating capacitive reactance at the operating frequency (Smith, 1960):

$$X_c^2 \geq \frac{R_e R_{in}}{A}\left[1 + \frac{f^2}{f_b^2}\right]^{1/2}, \tag{8.1-12}$$

where R_{in} is the effective input resistance of the amplifier stage, R_e the crystal-unit resistance at the operating condition, A the current gain (magnitude) of the amplifier stage, f the oscillator frequency, and f_b the beta cutoff frequency of the amplier stage.

The phase slope of the feedback network under these conditions is given by

$$\partial\Theta/\partial f \simeq 4\pi L_1/R_e, \tag{8.1-13}$$

which is the maximum that can be achieved with the given crystal-unit parameters (Felch and Israel, 1955).

A disadvantage of the modified Pierce oscillator is the relatively high current carried by the crystal unit. The magnitude of the crystal current can be easily restricted by automatic-level-control techniques, but the ratio of output power to crystal drive is quite low.

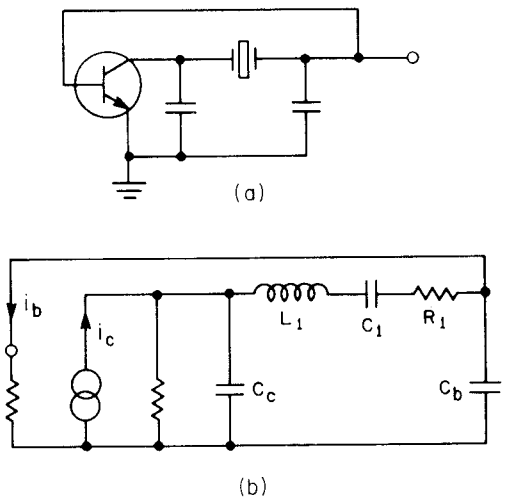


FIG. 8.1-8 Simplified ac equivalent circuit of the modified Pierce oscillator: (a) simplified schematic; (b) a linear analytic model, where $i_c = i_b\beta$ represents the current transfer function of the bipolar transistor.

8.1.2.3 COMMON-COLLECTOR OSCILLATOR CIRCUITS

A circuit configuration which offers some advantages makes use of a common-collector transistor stage as the sustaining amplifier. As evidenced by the schematic in Fig. 8.1-9, this configuration allows one side of the frequency-trimming reactance to be at ground potential, which is especially useful for varactor-diode tuning devices. This circuit is in fact a modification of the Pierce circuit, having the transistor collector rather than emitter at rf ground, and can be adapted to overtone-mode operation in the same way. Application

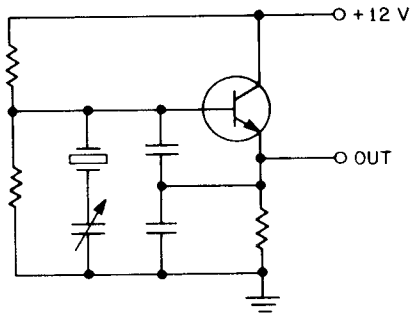


FIG. 8.1-9 Schematic of a bipolar common-collector oscillator circuit.

of AGC is somewhat complicated by the presence of rather large rf voltages at the emitter. Also, it will be noted that the base biasing network appears in shunt with the (nearly) parallel-resonant base circuit and can potentially degrade the Q factor of the network to a greater extent than in the Pierce circuit.

This circuit is especially well suited for use with a dual-gate field-effect device, where the second gate provides a convenient gain-control element and the biasing networks can use very high resistance values. Operation of this circuit is essentially the same as that of the modified Pierce circuit described previously.

8.1.2.4 COMMON-BASE OSCILLATOR CIRCUITS

The oscillator-circuit configurations described above are widely used at moderate frequencies, that is, below 30 or 40 MHz. For VHF use, however, the common-base transistor circuit shown in Fig. 8.1-10 has proven to be quite useful. The transfer phase of the common-base stage remains near zero for frequencies as high as 20% of the transistor unity-gain frequency. Also, the impedance presented to the crystal circuit by the emitter is relatively low, so that the phase slope of the feedback network is not seriously degraded.

The tuned network in the collector circuit effectively limits the bandwidth of the oscillator, making it useful with overtone-mode crystal units. The resonant network is tuned to the operating frequency, and coupling to the load (as well as the feedback ratio) can be chosen to optimize the ratio of output power to crystal current within the available gain limitations of the active device.

This circuit is particularly useful for those applications, such as microwave carrier generation, where stringent (wideband) signal-to-noise requirements are imposed. In contrast to the previously described circuits, the crystal unit in this circuit is not the resonant network and therefore does not carry circulating currents. Consequently, much greater output power results from the same crystal drive power.

A disadvantage of this circuit is that application of automatic gain control is not easily accomplished. Generally, the operating level is set by choosing the

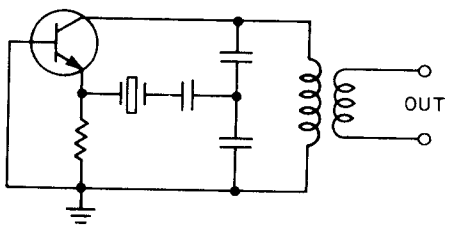


FIG. 8.1-10 Schematic of a common-base, tuned-collector oscillator circuit.

dc operating point of the transistor, and the device nonlinearity makes the circuit self-limiting. An alternative technique uses clamping diodes across the collector-tank circuit to limit oscillation amplitude. At the expense of added complexity, an electronically controlled loss pad can be introduced in series with the crystal unit.

8.1.2.5 EMITTER-COUPLED OSCILLATORS

A noninverting amplifier having good high-frequency performance and which can be realized with a minimum of reactive elements is the emitter-coupled circuit. Shown in Fig. 8.1-11, this is a transistorized adaption of the vacuum-tube circuit called the Butler oscillator. In this arrangement the crystal feedback path is connected between the emitters of the two transistors, thus minimizing the phase-slope degradation when using low-resistance crystal units. Since the transfer phase of both the common-base and common-collector stages is nearly zero even at high frequencies, the net amplifier phase errors are small, and phase stability is good. High loop gain results from the use of two active stages, allowing relatively large ratios of output power to crystal drive current. As shown, the circuit can be readily adapted for operation with overtone-mode crystal units by using a tuned circuit as the interstage coupling network. However, the most common application of the emitter-coupled oscillator is in single-chip silicon integrated-circuit oscillators (Embree *et al.*, 1980). In this application, circuits that operate over the entire frequency range of fundamental-mode AT-cut resonators can be realized without the need for any discrete components. This capability greatly simplifies the fabrication of the miniature oscillators used for data processing applications. The same silicon integrated circuit can also incorporate other functions, such as line drivers, frequency dividers, display drivers, and phase-locked loops.

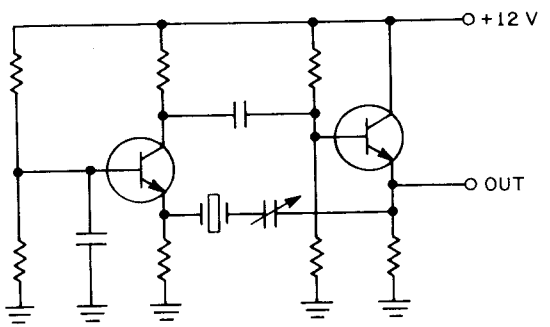


FIG. 8.1-11 Schematic of an emitter-coupled, series-resonance oscillator circuit.

Emitter-coupled oscillators do not provide the same degree of frequency stability as can be achieved with other types, such as the modified Pierce circuit. For example, the use of two active stages results in increased sensitivity to supply voltage and ambient temperature. The circuit is not conveniently provided with automatic-gain-control capabilities.

In spite of these shortcomings, this circuit can be very useful for applications requiring only moderate frequency stability with a minimum of space required for the oscillator circuit.

8.1.3 Temperature-Control Techniques for Precision Oscillators

Most precision crystal-controlled oscillators being manufactured today use some form of the modified Pierce circuit configuration, make use of either third- or fifth-overtone thickness-shear resonators of AT- or SC-cut quartz, and operate at a frequency in the range from about 5 to 10 MHz. These resonators exhibit Q-factors of 2.5 to 3 $\times$ 10^6 and under carefully maintained operating conditions can produce frequency generators of very high stability, for example, fractional frequency deviations of as little as 1 to 3 $\times$ 10^{-12} per day have been reported.

In order to achieve good frequency stability, it is essential to provide a very stable thermal environment for the crystal unit and the critical oscillator-circuit components. Other factors must also be carefully controlled, as discussed below, but temperature control is the most important single factor. A more detailed discussion of temperature-control techniques can be found in Chapter 9.

8.1.3.1 TEMPERATURE STABILITY REQUIREMENTS

As discussed in earlier chapters, the frequency of a quartz crystal resonator is a function of its temperature. In fact, frequency depends on both the instantaneous temperature and the rate at which the temperature is changing. The exact dependence is a function of many factors, including the crystallographic orientation of the plate, the mode of vibration, the shape of the plate, the distribution and amount of plating, and the method of mounting the resonator in the enclosure.

In particular, the AT-cut resonator exhibits a static frequency vs. temperature (f/T) characteristic that is quite closely approximated by expressing frequency change as a cubic function of temperature, as shown in Fig. 8.1-12. The inflection points of this curve are always located near 27°C, but the "turnover" temperatures (points of zero slope) depend on the exact orientation of the plate as well as on other fabrication parameters. For the specific example of Fig. 8.1-12, it is apparent that maintaining the temperature very close to the

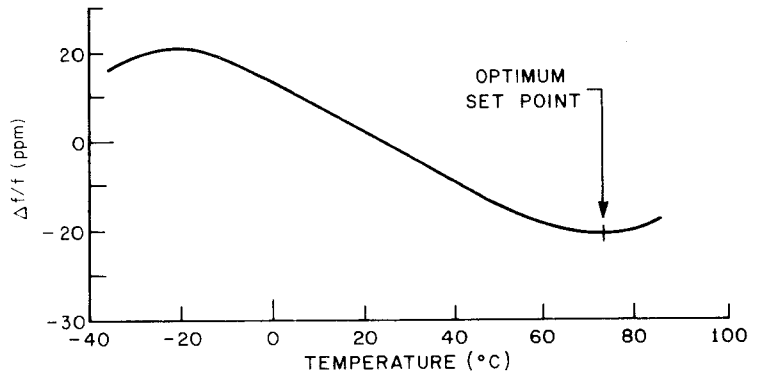


FIG. 8.1-12 Frequency vs. temperature characteristics of an AT-cut crystal unit designed for oven operation, showing the desired temperature of operation.

"turnover" point would result in minimizing frequency changes due to temperature drift. The first requirement to be met by the crystal oven device, then, is that it be carefully adjusted to maintain the crystal temperature as close as possible to the exact turnover of the crystal unit. The approximate location of the turnover point is controlled by the design of the crystal unit, but manufacturing tolerances on plate orientation, contouring, etc., usually result in a range of several degrees for devices of the same nominal design. If the set point of the oven drifts with time, the frequency changes according to the static f/T curve. For example, if the turnover temperature of an AT crystal unit were 75°C, then a drift of 1°C in either direction would cause a frequency change of about 1×10^{-8}. However, if the initial setting were 2°C away from the true turnover point, then a 1°C drift would cause as much as a 4.4×10^{-8} change.

The requirements on dynamic performance of the temperature-control system are not as easily specified. In this case, the SC-cut device is much more tolerant than the AT-cut resonator, which represents the most significant difference between the two types of crystal units. If we are to consider the AT-cut device, then empirical data are available to serve as a guide. It was reported (Smith and Spencer, 1963) that temperature changes of about 0.5°C within several minutes would cause the frequency of a 5.0-MHz fifth-overtone AT-cut resonator to be offset about 8×10^{-9}; increasing temperature causes the frequency to decrease, while decreasing temperature produces an increase in frequency. Very little quantitative data is available for very low rates of change; however, observation of relatively large frequency transients immediately following small adjustments of oven temperature have often been reported.

Certainly, if it is desired to maintain frequency within 5×10^{-11} using AT-cut crystal units, then it will be necessary to require the maximum rate of change of oven temperature to be no more than about 10^{-4}°C/hr. This requirement can probably be relaxed between one and two orders of magnitude if SC-cut resonators are employed; even so, the residual frequency fluctuations observed with most crystal-controlled precision oscillators over the time periods ranging from several minutes to several hours may well be caused by random fluctuations of oven temperature.

8.1.3.2 PROPORTIONAL TEMPERATURE-CONTROL TECHNIQUE

From the preceding discussion, we conclude that the ovens used to stabilize the temperature of crystal units in precision oscillators must be individually adjusted to the turnover temperature of the specific crystal unit used and, further, they must maintain that temperature with a minimum of fluctuations after being adjusted. These requirements can best be satisfied by a proportional controller, that is, one that supplies power to the oven heater continuously at a rate that is just sufficient to maintain constant temperature. "On–off" types of control, such as bimetallic or mercury-column thermostats, are not easily adjusted to a particular set point, usually exhibit a drift of set point with time, and always generate appreciable temperature gradients as they cycle between their on and off conditions.

The components used to provide temperature-control circuits, sensors, heating elements, and thermally stabilized enclosures constitute a system and must be designed as such. For further discussion on this subject, the reader is referred to Chapter 9.

8.1.4 Temperature-Compensation Methods for Semiprecision Oscillators

Requirements for frequency stability better than that achieved by crystal units alone can often be met by the use of temperature-compensated crystal-controlled oscillators. The temperature-compensated oscillator (TCXO) makes use of a thermally controlled reactance connected in series with the controlling crystal unit, which tunes the oscillating loop in such a manner as to maintain a (nearly) constant frequency as the surrounding temperature changes. The techniques employed to accomplish this function are widely varied, ranging from the use of negative-coefficient ceramic capacitors as combined sensor-variable reactance to highly sophisticated multiple-sensor–resistor networks supplying a thermally controlled bias to a varactor diode. Most recent developments in this area have been directed toward digital

computation methods for generation of the compensating reactance, although nearly all TCXOs manufactured up to the present time make use of some form of analog method.

The subject of temperature compensation will be discussed in detail in Chapter 9; consequently, only a few comments will be made at this point. The main advantages of temperature compensation over temperature control include reduced power requirements and physical size as well as a minimal warm-up time to achieve frequency accuracy. The requirements placed on the crystal unit, however, are in many respects much more severe because operation over the full ambient temperature range is needed with complete absence of spurious frequency deviations from a smooth, predictable function. Also, the crystal unit is repeatedly exposed to thermal cycling environments, so that nearly perfect retrace is necessary.

8.1.5 Miniature Integrated-Circuit Oscillators

The recent rapid growth of data processing, digital communication systems, and applications of microprocessor systems has led to a greater demand for low-cost, miniature crystal-controlled timing sources of moderate stability and precision. These oscillators are usually totally contained in a single, dual-in-line package (DIP), operate from standard logic-level 5-V power sources, and provide so-called TTL-compatible output waveforms, that is, positive pulses of greater than +2.5 V peak amplitude, a minimum level less than +0.5 V, and a nearly 50% duty cycle at the 1.4-V level.

These miniature oscillators generally use one or more silicon integrated circuits: a linear amplifier circuit as the oscillator stage and digital circuits for additional signal processing, which may be a simple buffer–line driver function but can also include frequency division and provision for simultaneous output of several submultiple frequencies. The crystal resonator must be of small physical size in order to be accommodated by the interior dimension of the package. AT-cut resonators at frequencies above approximately 6 MHz are readily accommodated, and specially designed resonators (beveled, contoured, etc.) have been successfully made at frequencies as low as 3 MHz. Extensional-mode and width-shear resonators can be used for frequencies from about 250 kHz to 1.5 MHz, and flexure-mode resonators of special design (X–Y bar, tuning forks, etc.) allow design of miniature oscillators at frequencies as low as 20–30 kHz.

Frequency stability performance of these miniature oscillators depends primarily on the f/T characteristics of the resonator used, the initial frequency adjustment tolerances, and subsequent frequency aging. All of these variables must be considered, since there is usually no way of adjusting frequency after the oscillator package is sealed. Fortunately, most data processing timing

requirements allow reasonable tolerances. Current commercial products usually range from 1×10^{-3} to 1×10^{-4} as overall frequency accuracy.

Several different approaches have been used in the design and selection of the integrated circuits used in miniature oscillators, although very little design information has been published (Embree *et al.*, 1980; Dubey and Singh, 1974). Many designs employ discrete transistor chips together with miniature discrete components for the oscillator function and then use available synchronous- or ripple-counter frequency dividers, which may be either bipolar or MOS circuits.

In some cases specially designed silicon integrated circuits are used that include a linear amplifier and digital shapers and frequency dividers on a single silicon chip. This approach greatly simplifies the assembly of the oscillator, since the number of interconnections is considerably reduced.

One technique which has been rather widely used is the use of a logic gate as an oscillator stage. Unfortunately, however, logic gates are not usually specified for linear operation, so that very wide deviations in their parameters must be tolerated. Since the logic gate may be made up of as many as 10 or more equivalent transistors with complex interconnections, the transfer phase, when biased in the linear operating region, can be far from ideal for an oscillator application (Holmbeck, 1977) and can lead to large frequency correlation errors or operation on resonator vibrational modes other than those intended.

As applications for miniature oscillators increase, more sophisticated integrated-circuit designs can be expected. It is presently within the state of the art to generate special circuits that would include voltage-control capability, frequency synthesis with programmable dividers and phase-locked loops, and even temperature-compensation circuits realized with only a few integrated circuits, all housed within the mechanical limitations of the dual-in-line miniature package. These circuit techniques, combined with new resonator technologies, will provide increasingly sophisticated miniature frequency–time sources in the future.

LIST OF SYMBOLS FOR SECTION 8.2

f	Frequency	N	Frequency multiplication factor
f_m	Modulation frequency	P_c	Carrier power level at amplifier output
f_o	Oscillator frequency	P_{sb}	Single-sideband noise power in a 1-Hz bandwidth
f_x	Flicker frequency		
f_t	Oscillator feedback bandwidth	Q	Quality factor (loaded)
F	Amplifier noise figure	t_R	Effective cavity length (in seconds) of SAW resonator
G	Amplifier gain ($\simeq$ SAW insertion loss)		
k	Boltzmann's constant	T	Temperature (kelvins)

α	Flicker noise constant (sec^{-1})	ϕ_e	Transmission phase shift for electrical components other than SAW device
σ_A	Fractional frequency deviation (σ_A^2 is the Allan variance)	ϕ_L	Transmission phase shift for entire oscillator circuit (open loop)
τ	Group delay (phase slope) of SAW device	ω	Angular frequency ($\omega = 2\pi f$)
ϕ_D	Transmission phase shift of SAW delay line	ω_m	Modulation (Fourier) frequency ($=2\pi f_m$)

8.2 SURFACE-ACOUSTIC-WAVE OSCILLATORS[§]

8.2.1 Introduction

8.2.1.1 WHAT IS A SAW OSCILLATOR?

In order to operate correctly, a stable feedback oscillator requires a feedback element with a long delay time and proper filtering in the frequency domain. In acoustic oscillators the long delay is provided by the propagation of acoustic energy in an appropriate medium. Through the proper design of the acoustic device, the required filtering is also obtained. The surface-acoustic-wave (SAW) oscillator, like the familiar quartz crystal oscillator, uses an acoustic device as the feedback element; however, the SAW oscillator uses an acoustic mode propagating on the surface of the substrate rather than a mode propagating in the bulk of the medium, as in the quartz crystal oscillator. The SAW resonator is analogous to the bulk-wave resonator and behaves much the same when used in an oscillator. With surface waves, however, narrow-band delay lines can also be used as feedback elements in oscillators.

8.2.1.2 WHAT IS THE VALUE OF A SAW OSCILLATOR?

The advantage of using a SAW delay line or resonator, as opposed to a bulk-wave resonator, is that the SAW device is most conveniently fabricated in the 100-MHz to 2-GHz range, which is considerably higher than the typical bulk-wave resonator. Offering frequency stability similar to quartz crystal oscillators, the SAW oscillator can be used to reduce multiplier requirements in stable high-frequency sources. In certain regions of the noise spectrum, clearly superior performance can be obtained; however, the temperature and long-term stability of SAW oscillators are generally not as good as those obtained with high-quality quartz crystal oscillators.

[§] Section 8.2 was written by Thomas E. Parker.

The high operating frequency of SAW oscillators is in itself of great importance, but in addition the planar construction of SAW oscillators and the choice of either delay lines or resonators offers a new dimension in flexibility to oscillator design. The delay-line oscillator provides a tuning capability of up to several tenths of a percentage point while maintaining a reasonably large Q value. Delay lines can also be operated in such a manner as to provide multiple-frequency operation. Multiple paths on the substrate surface have been used to provide a novel means of temperature compensation, and layers of different materials can be used to alter many device properties.

8.2.1.3 STATE OF THE ART

The concept of using SAW devices as controlling elements in oscillators was first published by Maines and co-workers in 1969, so the technology is very young compared with bulk-wave oscillators. At present, most SAW oscillators have been produced as research devices, and they are not yet widely available on the commercial market. Active areas of research are high frequencies, maximizing Q, packaging, aging mechanisms, $1/f$ noise, temperature stability, vibration and g sensitivity, and circuit design.

The SAW oscillator appears to have considerable potential, since it nicely fills the gap between bulk-wave oscillators and microwave cavity oscillators. SAW oscillators are being developed for a number of military applications, and many of the initial problems such as long-term stability and frequency setting are being reduced or eliminated.

8.2.2 The Basic SAW Oscillator—A Physical Point of View

8.2.2.1 CONDITIONS FOR OSCILLATION

For the feedback oscillator shown in Fig. 8.2-1, there are only two conditions required to obtain oscillation. One is that the total phase shift around the loop equal a multiple of 2π. The other is that the gain of the amplifier exceed the combined loss of the delay element and other circuit components such as the output coupler. These conditions must be satisfied simultaneously. In terms of oscillator performance, the parameters of the SAW device that are the most important are insertion loss and phase slope or group delay ($\tau = d\phi/d\omega$). In the next two sections, we shall examine how the conditions for oscillation are met for a SAW delay line and a two-port SAW resonator. For the most part these conditions will be discussed for the open-loop circuit shown in Fig. 8.2-1b.

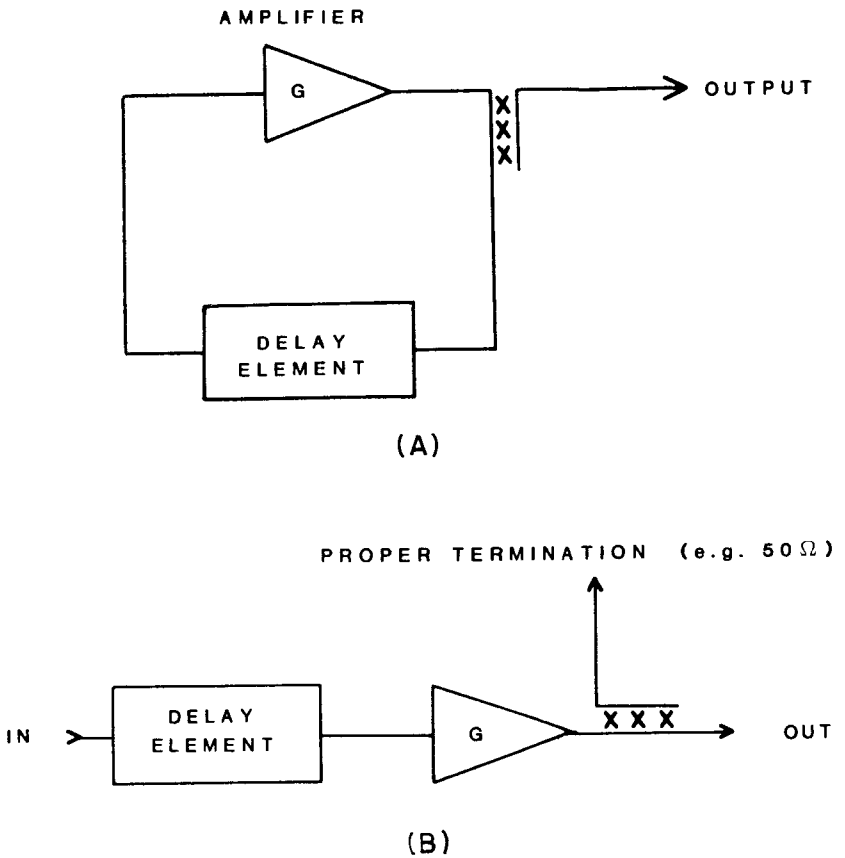


FIG. 8.2-1 Block diagram of a simple feedback oscillator. (A) Closed loop; (B) open loop.

8.2.2.2 OSCILLATOR USING A SAW DELAY LINE

The delay-line oscillator very clearly illustrates how the conditions for oscillation are met. For an idealized delay line the transmission phase shift ϕ_D is a function of frequency and can be expressed as

$$\phi_D = -2\pi f\tau, \tag{8.2-1}$$

where f is the frequency and τ the delay time of the delay line. The phase condition for oscillation then becomes

$$\phi_L = 2\pi N = -2\pi f\tau + \phi_e, \tag{8.2-2}$$

where ϕ_L is the total phase shift through the circuit in Fig. 8.2-1b, N an integer, and ϕ_e the sum of all phase shifts due to components other than the delay line. Figure 8.2-2b illustrates Eq. (8.2-2). The figure shows that the condition $\phi_L = 2\pi N$ is met at many frequencies (zero crossings are equivalent to multiples of 2π). In fact, the condition is met at frequency intervals equal to $1/\tau$. In order to determine which of the many frequencies will oscillate, the transducers of the delay line must be designed in such a manner as to provide only a narrow passband centered around one of the zero crossings. Typically,

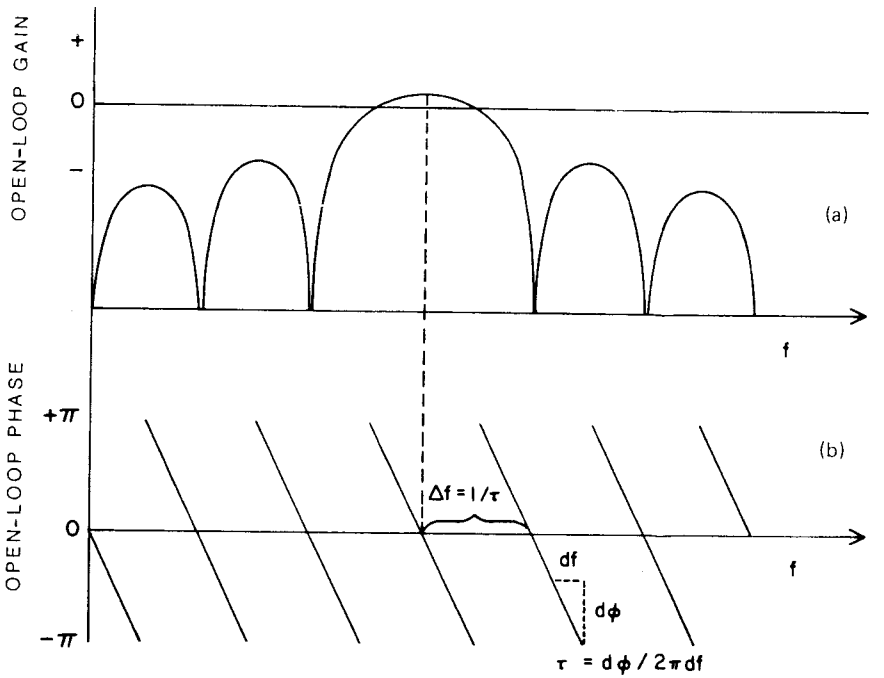


FIG. 8.2-2 Open-loop gain and phase for an SAW delay-line oscillator.

this is accomplished by making the length of one of the transducers approximately the same as the center-to-center distance between the transducers (Crabb *et al.*, 1973). Physical size, design requirements, or both usually limit the length of a transducer to less than 1000 acoustic wavelengths and therefore limit the delay length of a single-mode device to approximately the same value.

The minimum insertion loss of the delay line will normally be in the range of 15 to 20 dB and, of course, must be overcome by the gain of the amplifier.

Assuming that the amplifier gain is flat over the frequency range of interest, the open-loop gain of the delay line and amplifier will be similar to that shown in Fig. 8.2-2a. Note that the gain is positive only over a small frequency range that includes only one of the phase zero crossings. The excess open-loop gain is typically 2 to 3 dB. Once the loop is closed (Fig. 8.2-1a), oscillation starts, and the signal amplitude increases until the amplifier saturates and the loop gain is reduced to exactly 0 dB. The equilibrium power level of the oscillator is then at the 2 3-dB compression point of the amplifier. Furthermore, the bandpass filter built into the SAW delay line guarantees that only the desired frequency will oscillate.

The precise frequency of oscillation is determined by Eq. (8.2-2). By changing ϕ_e with a phase shifter or short piece of transmission line, the oscillator can be made to operate over nearly the entire range of frequency where the open loop gain is positive. Thus, the oscillator can be tuned or frequency modulated. Care must be taken, however, that the zero crossing is not pushed too far from the point of maximum gain. When the zero crossing at which the circuit is oscillating is moved, all of the other zero crossings also move. As the frequency of oscillation is moved from the point of maximum gain, either the next higher or the next lower zero crossing moves closer to the range of positive gain. If the phase shift is too large, the frequency of oscillation may actually jump to the next zero crossing. In less extreme cases (i.e., in the presence of a zero crossing at a point where the gain is negative, but not by a large amount) an increase in oscillator noise may be observed (Browning and Lewis, 1976). If a zero crossing is suppressed by 10 dB, an increase in the noise spectrum of not more than 3 dB may be observed at that frequency.

8.2.2.3 OSCILLATOR USING A SAW RESONATOR

The delay element in Fig. 8.2-1 can be a SAW resonator as well as a delay line. A SAW resonator also provides a large stable group delay and the appropriate filtering to ensure stable oscillation. In the following paragraphs we shall examine how a two-port SAW resonator meets the conditions for oscillation that were stated in Section 8.2.2.1.

The SAW resonator has many similarities to the bulk-wave resonator, but there are also some differences. A major difference is that the cavity on a SAW resonator is generally more than 100 wavelenghts long and therefore is operating at a high longitudinal mode. However, the grating is a distributed reflector and can provide the necessary frequency selectivity to limit the resonance to one longitudinal mode. Unlike the bulk-wave resonator, the SAW resonator couples equally well to odd or even modes. For transmission through a two-port SAW resonator, there is a 180° phase difference between odd or even modes. Figure 8.2-3 shows the open-loop gain and phase shift for

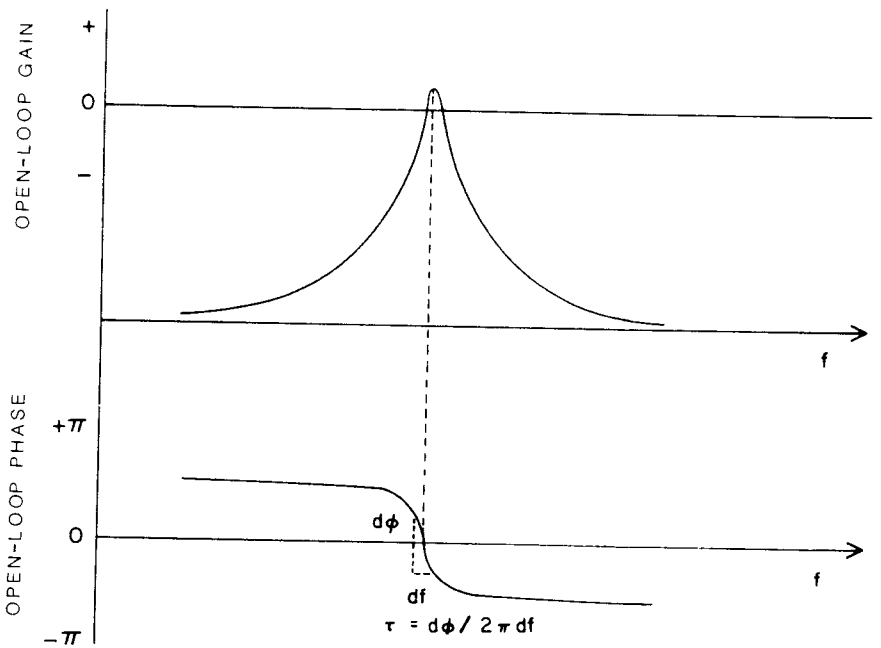


FIG. 8.2-3 Open-loop gain and phase for an SAW two-port resonator oscillator.

a SAW oscillator using a two-port resonator. As before, we shall assume that the amplifier gain is flat over the frequency range of interest and that it is large enough to provide a positive loop gain of 2 to 3 dB at the point of minimum insertion loss of the resonator. An arbitrary phase shift ϕ_e has been added in the loop to bring the phase zero crossing to the frequency of minimum insertion loss (ϕ_e is typically about $+70°$ or $-110°$, depending on whether the resonant mode is odd or even).

A major difference between the SAW delay line and SAW resonator is the relationship between frequency response and phase. With the delay line the bandpass is determined by transducer length and finger spacing, while the delay (and hence phase shift) is determined by the separation of the two transducers. The two can be varied nearly independently of each other. This, of course, is not the case with the resonator, which is a highly dispersive device. At resonance the insertion loss is at its minimum and the phase slope $d\phi/df$ is at its maximum. If the cavity length is changed, the resonance frequency will move. As a result both the insertion-loss and phase curves will be moved along the frequency axis by the same amount and maintain the same relative relationship.

When the loop is closed, oscillation takes place in the same fashion as for the delay line. The signal level increases until the amplifier gain saturates and the loop gain drops to exactly 0 dB. A change in ϕ_e results in a change in the frequency of oscillation, but this moves the point of oscillation away from the minimum insertion loss and maximum group delay. For a delay line the 3 dB bandwidth is approximately equal to $1/\tau$, while for the resonator the 3 dB bandwidth is equal to $1/\pi\tau$. Thus, for equivalent values of group delay τ, the resonator has about one-third of the tuning range and, of course, the phase is not linear with respect to frequency as it is with the delay line.

A SAW resonator may also be designed with only one interdigital transducer; it is then referred to as a one-port resonator. At resonance the impedance of this transducer changes rapidly. This change may be used to control an oscillator in much the same manner as a bulk-wave resonator. In principle, the same oscillator performance can be obtained from either a one- or two-port resonator, but the latter seems to be more generally used.

8.2.3 Frequency Stability

8.2.3.1 INTRODUCTION

Of major importance for any oscillator technology is the degree of frequency stability that is obtained. In this section we shall discuss or summarize three major aspects of frequency stability of SAW oscillators, aspects which have been the subject of many investigations. They include short-term stability (or noise), temperature stability, and aging.

8.2.3.2 SHORT-TERM STABILITY

Following approximately the treatment of Leeson (1970), the single-sideband phase-noise spectral density of a feedback oscillator can be written as

$$\frac{P_{sb}}{P_c} = 10\log\left[N^2\left(\frac{\alpha}{\omega_m} + \frac{GFkT}{P_c}\right)\left(\frac{1}{\omega_m^2\tau^2} + 1\right)\right] \tag{8.2-3}$$

$$= 10\log\left[N^2\left(\frac{\alpha}{\omega_m^3\tau^2} + \frac{GFkT}{P_c\omega_m^2\tau^2} + \frac{\alpha}{\omega_m} + \frac{GFkT}{P_c}\right)\right], \tag{8.2-4}$$

where P_{sb} is the single-sideband noise power in a 1-Hz bandwidth, P_c the carrier power level at amplifier output, N the frequency multiplication factor, G the amplifier gain ($\approx$ SAW insertion loss), F the amplifier noise figure, kT the thermal noise (4.00×10^{-18} mW/Hz), τ the group delay (phase slope) of the SAW device, $\omega_m = 2\pi f_m$ the modulation (Fourier) frequency, and α the flicker noise constant ($\sec^{-1}$). (The ratio P_{sb}/P_c is given in decibels relative to the carrier, dBc.)

In Eq. (8.2-3) the terms enclosed in the left-hand set of parentheses represent the open-loop phase noise, while the terms enclosed in the right-hand set represent the oscillator transfer function when the loop is closed (a phase servo with positive feedback). Multiplying the terms in the two sets of parentheses gives Eq. (8.2-4), which shows that the noise spectrum has regions of varying dependence on ω_m.

Close to the carrier (small f_m), the $\alpha/\omega_m^3\tau^2$ term dominates, while far from the carrier the $GFkT/P_c$ term, which is independent of ω_m, dominates. Of the two middle terms the one that dominates depends on the values of the various parameters. In this respect two values of f_m are of particular importance. The value of f_m when $\alpha/\omega_m = GFkT/P_c$ is called the flicker frequency and is equal to

$$f_\gamma = \alpha P_c/2\pi GFkT. \tag{8.2-5}$$

The value of f_m when $1/\omega_m^2\tau^2 = 1$ is called the oscillator-feedback bandwidth frequency and is equal to

$$f_\tau = 1/2\pi\tau. \tag{8.2-6}$$

For resonators, the relation between group delay and loaded Q,

$$Q = \pi f_0\tau, \tag{8.2-7}$$

can also be used, where f_0 is the oscillator frequency, and f_τ can then be written as

$$f_\tau = f_0/2Q. \tag{8.2-8}$$

When $f_\tau > f_\alpha$, the $1/\omega_m^2$ term in Eq. (8.2-4) dominates. If $f_\tau < f_\alpha$, then the $1/\omega_m$ term dominates.

Figure 8.2-4 shows typical phase-noise spectra for 300- and 400-MHz resonator and delay-line SAW oscillators (Parker, 1977b). For most delay lines $f_\tau > f_\alpha$ and therefore there is no region of $1/\omega_m$ dependence. The equation for the phase-noise spectral density of delay lines reduces to

$$\frac{P_{sb}}{P_c} \simeq 10\log\left\{N^2\left[\frac{\alpha}{\omega_m^3\tau^2} + \frac{GFkT}{P_c}\left(\frac{1}{\omega_m^2\tau^2} + 1\right)\right]\right\}. \tag{8.2-9}$$

The noise curve for the resonator looks very similar except that it is lower because of its lower insertion loss and larger value of τ (higher Q value). In general, resonators provide a higher group delay than delay lines up to about 1 GHz. Therefore, in applications where frequency tuning or modulation is not required, resonators usually give the best short-term stability.

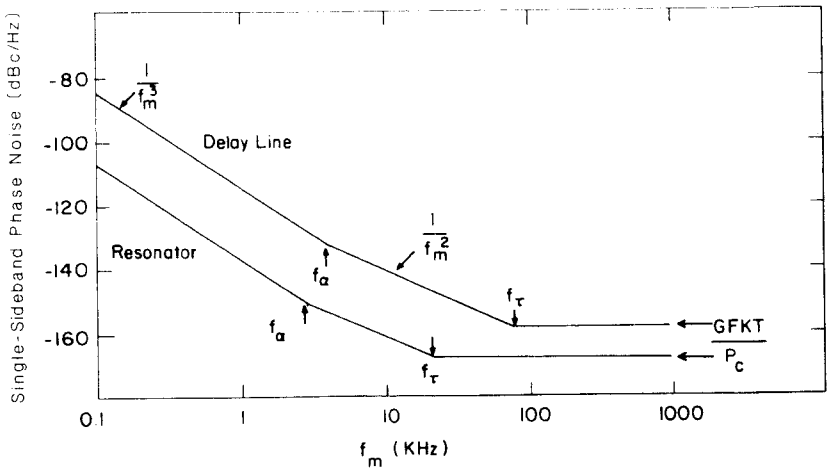


FIG. 8.2-4 Single-sideband phase-noise spectral density for a 400-MHz delay-line oscillator and a 310-MHz two-port resonator oscillator. (Values in the figure are given in decibels relative to the carrier, dBc.) The appropriate device parameters are the following: for the 400-MHz delay-line oscillator, $N = 1$, $G = 160$ (22 dB), $F = 4$ (6 dB), $P_c = 20$ mW (+13 dBm), $\tau = 2.0$ μsec, and $\alpha = 2.5 \times 10^{-12}$ sec^{-1}; for the 310-MHz resonator oscillator, $N = 1$, $G = 15.8$ (12 dB), $F = 4$ (6 dB), $P_c = 20$ mW (+13 dBm), $\tau = 8.0$ μsec, $\alpha = 6.0 \times 10^{-15}$ sec^{-1}, and $t_R = 1.3$ μsec.

The close-to-carrier region of the curve (slope = $1/f_m^3$) requires special comment, since it involves the so-called $1/f$, or flicker, noise. For delay lines the SAW device has been identified as the dominant source of flicker noise (Parker, 1979b). Thus, the value of the constant α is determined by the SAW device and must be measured experimentally. Since α is not a design parameter but is related to fabrication variables, it can be controlled to some extent by surface treatments. For delay lines, values of α have been found to range from about 6×10^{-13} to 2×10^{-10} sec^{-1}.

For resonators, the dominant source of $1/f$ noise may be either the SAW device or the amplifiers. If the SAW device is the dominant source, the first term in Eq. (8.2-3) becomes $\tau^2\alpha/t_R^2\omega_m$, where t_R is the cavity length (in seconds) of the resonator (Parker, 1979). As a result, f_α becomes

$$f_\alpha = \frac{\tau^2}{t_R^2}\frac{\alpha P_c}{2\pi GFkT}. \tag{8.2-10}$$

If $f_\tau > f_\alpha$, then Eq. (8.2-3) reduces to

$$\frac{P_{sb}}{P_c} \simeq 10\log\left\{N^2\left[\frac{\alpha}{\omega_m^3 t_R^2} + \left(\frac{GFkT}{P_c}\right)\left(\frac{1}{\omega_m^2\tau^2} + 1\right)\right]\right\}. \tag{8.2-11}$$

The significance of the SAW being the source of $1/f$ noise is that the close-to-carrier noise no longer depends on τ and therefore is independent of the loaded Q. As with delay lines, α is an empirical constant that must be measured. If the amplifier is the dominant source of $1/f$ noise, then in a resonator oscillator Eq. (8.2-3) holds as its stands (Penavaire *et al.*, 1980). For $f_\tau > f_\alpha$, the result for resonators is the same as Eq. (8.2-4). If $f_\tau < f_\alpha$, then the equation becomes

$$\frac{P_{sb}}{P_c} \simeq 10\log\left\{N^2\left[\frac{\alpha}{\omega_m}\left(\frac{1}{\omega_m^2\tau^2} + 1\right) + \frac{GFkT}{P_c}\right]\right\}. \tag{8.2-12}$$

In cases when the SAW resonator was identified as the source of $1/f$ noise, values of α ranging from 6×10^{-15} to 2×10^{-13} have been observed. When the amplifiers were the source of $1/f$ noise, the values of α range from 1×10^{-12} to 1×10^{-11}.

In addition to the phase-noise spectral density discussed above, another common way of specifying short-term frequency stability is the fractional frequency deviation σ_A, which is derived from the Allan variance. Without going into details, values of σ_A for delay-line oscillators range from 7×10^{-11} to 1×10^{-8} for gate times of 0.01 to 10 sec. For resonator oscillators values of σ_A range from 2×10^{-11} to 3×10^{-10}.

8.2.3.3 TEMPERATURE STABILITY

The temperature stability of the frequency of SAW-controlled oscillators is mainly determined by the material on which the SAW device is fabricated. As discussed in Volume 1, Chapter 2, Section 2.3.4, the most commonly used material is ST-cut quartz, which has a parabolic temperature dependence similar to that of BT-cut bulk-wave resonators. The electronic components of an oscillator tend to shift the turnover point to lower temperatures, but this can be corrected by slight changes in cut angle. Other newly discovered surface-wave cuts of quartz offer somewhat better temperature stability than ST-cut quartz (Williams *et al.*, 1980; Browning and Lewis, 1978a), but none has yet been discovered that is equivalent to the AT-cut bulk-wave resonator. A layered structure of SiO_2 on (YZ) $LiTaO_3$ (Parker and Wichansky, 1979) does offer such temperature stability, but a severe problem with long-term stability has not yet been eliminated.

In the absence of materials with improved temperature stability, various compensation techniques have been used to demonstrate temperature stability equivalent to that of AT-cut quartz (Lewis, 1979). Compensated oscillators using voltage-controlled phase shifters and thermistors have been tested (Kinsman, 1978; Lee, 1979). A novel technique using two different propagation paths on a single substrate has also been used for temperature compensation (Browning and Lewis, 1978b).

8.2.3.4 LONG-TERM STABILITY—AGING

As with temperature stability, the long-term stability of a SAW oscillator is primarily determined by the stability of the SAW device. This topic was discussed in Volume 1, Chapter 6, Section 6.3 and so will not be covered here in detail. Aging is the subject of a number of investigations and substantial improvement has been made over the last few years. At this time research devices are showing aging rates as low as a few tenths of a part per million per year, with aging rates of an average device on the order of 1 to 2 ppm per year (Parker, 1980). Improvements to date have been gained primarily through the use of better packaging techniques. As greater understanding of specific aging mechanisms is gained, it will be reasonable to expect further improvement.

8.2.4 Multifrequency Oscillators

Up to this point the discussion has been confined to single-frequency oscillators: however, the great flexibility in designing SAW devices has led to the development of several designs for multiple-frequency SAW oscillators. One scheme, described by Gilden *et al.* (1975), uses a wideband SAW delay line and a nonlinear element in the oscillator loop to generate a comb of frequencies via a circulating pulse. An oscillator operating at 300 MHz has generated a comb of more than ten frequencies (Gilden, 1977) and has been stabilized by injection locking. A similar wideband delay line has been used in a circuit without the nonlinear element to produce a cw oscillator that can be made to hop to any of a large number of oscillator modes (Browning *et al.*, 1975). The advantage of such operation is to provide a wide tuning range simultaneously with a long delay time. An oscillator operating from 54 MHz to 92 MHz in steps of 435 kHz ($\tau = 2.3$ μsec) has been demonstrated (Bale *et al.*, 1975). One disadvantage of this technique is that when the oscillator is operating at one mode, noise spikes appear at the frequencies of the other modes (Browning and Lewis, 1976). By using two separate acoustic paths of different lengths, these spurious noise spikes can be suppressed. Such an oscillator still provides a wide frequency range of oscillations along with a large delay time. An oscillator operating at 155 MHz with an effective group delay of 5 μsec has demonstrated eleven distinct frequencies spaced at 100-kHz intervals (Parker and Sage, 1976).

Multiple-frequency operation is not confined totally to delay lines. Since the SAW resonator operates at a high longitudinal mode, it is easy to design a device with more than one resonance simply by increasing the length of the cavity. In the most useful configuration, the device has just two resonances. The principle of multiple-frequency operation is most easily illustrated for a two-port resonator. Figure 8.2-5 shows that, in transmission, a two-port

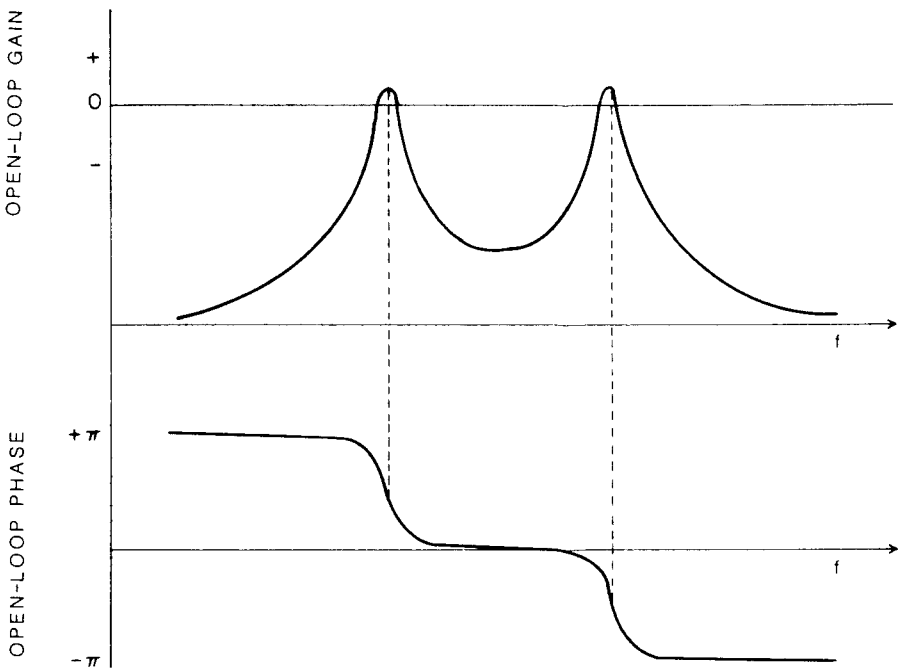


FIG. 8.2-5 Open-loop gain and phase for a two-port resonator oscillator having two resonances.

resonator has a 180° phase difference between the two resonances. Inserting either a $+90°$ or a $-90°$ phase shift in the loop circuit produces oscillation at either resonance. The unused resonance causes virtually no degradation in oscillator noise level.

8.2.5 Electronic Amplifiers and Other External Components

Because of the relatively high insertion loss (~ 20 dB) and short delay time ($\lesssim 2$ μsec) of typical SAW delay lines, highly stable commercial wideband amplifiers have generally been used in delay-line oscillators. These amplifiers offer high gain but still have a very small group delay, which is ideal for minimizing the contribution of electronic components to the total group delay. When voltage control of the frequency is required for modulation or temperature compensation, an electronic phase shifter can be used. Both commercial phase shifters and custom-designed circuits using varactor diodes have been used.

One disadvantage of wideband commercial amplifiers is that they are very inefficient (typically less than 2% dc-to-rf efficiency). Amplifiers designed around silicon and GaAs dual-gate FETs (Leja and Parker, 1979) have shown substantially higher efficiency (9% and 40%, respectively). One problem encountered with the GaAs FETs was their very high $1/f$ noise levels, which substantially degraded the short-term frequency stability of the oscillator.

The lower insertion loss and more convenient impedance levels of SAW resonators has made amplifier design for resonator oscillators considerably easier. In some cases wideband commercial amplifiers have been used but, as mentioned, they are very inefficient and also relatively expensive. For these reasons many people have designed their own one-transistor amplifiers with equally good success (Dolochycki *et al.*, 1979). It must be kept in mind, however, that the Q value of SAW delay lines or resonators is considerably less than that of low-frequency bulk-wave quartz crystal resonators, and therefore the stability of electronic circuit components has a proportionally larger influence on overall oscillator stability.

8.2.6 Advantages and Disadvantages of SAW Oscillators

The main reason for interest in SAW-controlled oscillators is the high frequency range (100 MHz to 2 GHz) in which they operate. They can be considered for all applications where the final frequency is above the normal range of bulk-wave devices. The use of SAW oscillators reduces the need for multiplication and the associated filtering and amplification.

With regard to short-term stability, a SAW oscillator offers some definte advantages. For noise sidebands that are more than 1–10 kHz from the carrier, the SAW oscillator offers considerably better performance than a multiplied bulk-wave oscillator. Only close to the carrier does the higher Q value of bulk-wave devices offer low noise levels, even after multiplication.

For other aspects of frequency stability, the performance of SAW oscillators is somewhat less than that of quartz crystal oscillators. For temperature stability the typical SAW oscillator is similar to BT-cut quartz; as yet, there is no equivalent to AT-cut quartz. The long-term stability of SAW oscillators has improved considerably over the last few years and is now running around 1 ppm/yr for laboratory models. However, there remains considerable improvement to be made before SAWs can compete with the best quartz crystal resonators. Other aspects of frequency stability, such as sensitivity to vibration and acceleration, are just now coming under investigation. Little data exists at this time and some of it is contradictory. However, the author has observed (Parker and Callerame, 1981) that with proper mounting of the substrate, vibration sensitivity comparable to that of AT-cut quartz can be obtained with ST-cut substrates.

8.2.7 Conclusion

The technology of SAW oscillators is still very young when compared with that of bulk-wave devices. Nevertheless, there is considerable potential for SAW oscillators in many high-frequency applications where frequency stability requirements are not extremely tight. In certain portions of the noise spectrum, SAW oscillators have demonstrated a definite performance advantage, and further advances in other aspects of frequency stability will continue to increase their usefulness. SAW oscillators will not replace quartz crystal resonators in low-frequency applications, nor microwave cavities at very high frequencies, but a UHF technology that offers moderate Q values and stability similar to that of quartz crystals can fill the gap advantageously.

LIST OF SYMBOLS FOR SECTION 8.3

$B_2(r, \mu)$	Bias function for correction of measured variances obtained with dead-time
C_0	Crystal unit shunt (static) capacitance
C_1	Crystal unit motional capacitance
C_α	Coefficient depending on the type of noise
f	Reference oscillator frequency
f_0	Frequency under test
f_2	Signal frequency (or Fourier frequency)
f_h	Cutoff frequency of a measurement system
h_α	Coefficient of a noise process characterized by a power spectral-density dependence f^α
L_1	Crystal-unit motional inductance
M	Total number of measurements of Y_k
Q	Resonator quality factor
R_1	Crystal-unit motional resistance
$S_y(f)$	Power spectral density of frequency deviations
$S_\phi(f)$	Power spectral density of phase deviations
Y_k	kth measurement of a frequency difference
α	Integer exponent of Fourier frequency f
μ	$= -(\alpha + 1)$
$\sigma_y^2(\tau)$	Expectation value of the two-sample variance of frequency deviations for sample averaging interval τ
τ	Sampling time
ϕ	Phase

8.3 QUARTZ FREQUENCY STANDARDS AND CLOCKS—FREQUENCY STANDARDS IN GENERAL[§]

Precision quartz-crystal-controlled oscillators have long filled a vital need as frequency standards and clocks throughout the electronics industry. They are not absolute standards of frequency: their frequency of operation can be adjusted over at least narrow ranges with ease and they are subject to more or less long-term drift (aging). However, they can be manufactured over a

[§] Section 8.3 was written by Warren L. Smith.

realtively wide range of frequencies and can therefore be designed and calibrated to produce very precisely a particular reference frequency signal without further processing. In concept and in realization, the electronic circuits required are relatively simple, resulting in operational frequency standards of excellent reliability and dependability.

Early crystal-controlled reference standards were designed using crystal units in the frequency range of about 50 to 100 kHz, usually X-cut or GT-cut resonators. However, development of the thickness-shear AT-cut overtone-mode crystal resonators resulted in considerable improvement in performance (Warner, 1960). Oscillators designed to use fifth-overtone AT-cut crystal units operating in the frequency range from 2.5 to 10 MHz became the accepted standard reference frequency sources (Gerber and Sykes, 1966). At the present time, overtone-mode AT-cut crystal units operating in carefully designed and adjusted oscillators can provide frequency drift rates of a few parts times 10^{-12} day^{-1} and can exhibit short-term stability of better than 1×10^{-12} for averaging times as short as one second.

Recent work has been directed toward the design of improved crystal resonators. The SC cut, a doubly rotated thickness-shear resonator, has been shown to be much less sensitive to both thermal environment and mechanical disturbances than the AT cut. The stability of oscillators using SC-cut resonators has been reported to be better than that achieved with AT-type crystal control.

Considerable success has also been reported when "electrodeless" crystal resonators are used to control the frequency of precision oscillators. For these devices excitation fields are established by means of electrodes placed near, but not on, the surfaces of contoured, precision overtone-mode resonators. By also making the mounting structures from crystalline quartz of the same orientation, thermal stresses are minimized. Removal of the metal electrodes from the vibrating system improves its quality factor as well as eliminates the possibility of frequency changes due to electrode film-stress relaxation and intermetallic diffusions (Besson *et al.*, 1980).

The frequency stability achieved by crystal-controlled precision oscillators certainly depends in large part on the stability characteristics of the controlling resonator. However, in order to achieve this stability, the mechanical, electrical, and thermal design of the oscillator must be optimized for the particular type of resonator used. This section will deal in general with some of the methods for minimizing the effects of temperature, electrical disturbances, and component instabilities on the performance of the completed oscillator.

8.3.1 Design Considerations

The choice of resonator type, circuit operating point, and crystal oven design all depend on the specific intended application. If long-term stability

(frequency aging) is the principal objective, for example, the circuit parameters should be chosen to drive the crystal unit at a very low level and the ovens designed to assure the best long-term temperature stability. For best short-term stability (lowest phase noise), however, considerably higher crystal drive current would be indicated as well as good isolation from any mechanical disturbances. Some of the trade-offs that can be made are discussed in the following paragraphs.

8.3.1.1 CHOICE OF RESONATOR

The crystal resonator to be used in a precision oscillator should provide a high mechanical quality factor Q, exhibit minimum sensitivity of frequency to small changes in drive level, be insensitive to mechanical disturbances, and have near-zero frequency vs. temperature characteristics at the temperature of operation. In addition, it must exhibit minimum long-term frequency aging. Overtone-mode AT-cut crystal units operating at frequencies in the range from about 2.5 to 10 MHz, designed to have a *turnover temperature* in the range from 60 to 80°C, are capable of providing good performance with most commercial precision oscillators. The AT-cut crystal is generally operated on its fifth overtone in order to realize Q values near the intrinsic material limitations and still permit sufficient frequency adjustment in the oscillator circuit to allow compensation for manufacturing tolerances as well as expected frequency aging over an extended operational life.

Generally, realizable Q values are inversely dependent on frequency, ranging from about 5×10^6 at 2.5 MHz to about 1×10^6 at 10 MHz; however, much larger plates are required at lower frequencies, and the commonly used 5-MHz frequency region represents a practical compromise.

Recent work with doubly rotated Y cuts, such as the SC cut and FC cut, has demonstrated that these resonators are capable of providing oscillators having better performance than the AT-cut crystals. However, at the present time these units are not as readily available and are considerably more costly. These doubly rotated resonators are capable of somewhat higher Q values than the AT cut and can also be designed to have considerably reduced frequency vs. temperature characteristics at normal oven operating temperatures. Also, they show much lower transient frequency perturbations when subjected to small temperature fluctuation, so that the stability required of the crystal oven for a given frequency tolerance is somewhat reduced.

The frequency-adjustment range of the doubly rotated crystals is smaller than that of the singly rotated AT types because of the reduced value of the piezoelectric coupling coefficients. In some applications this may be a critical factor; in any case, it requires that a closer finished-frequency tolerance be specified. For example, a 5-MHz fifth-overtone AT-cut crystal can be specified to an initial tolerance of about $\pm 1 \times 10^{-6}$ and still allow a using oscillator to

be adjusted precisely to specified frequency over a 20-year lifetime. This tolerance may be reduced by a factor of two or more if the crystal is a doubly rotated SC cut.

8.3.1.2 OSCILLATOR-CIRCUIT CONSIDERATIONS

In order to realize the best possible frequency stability, it is essential that the sustaining circuit used for the precision oscillator have as little influence on the operating frequency as possible. Since the oscillator frequency is determined by the loop phase condition, this implies the following objectives.

(1) The slope of the transfer phase versus frequency characteristic of the sustaining circuit should be as small as possible over a frequency range near the operating frequency.
(2) The transfer phase of the circuit should be essentially independent of supply voltage, ambient temperature, and mechanical disturbances.
(3) The circuit should introduce as little excess noise as possible.
(4) The circuit should introduce as little resistive loading into the crystal feedback network as possible in order to realize the maximum phase slope of the frequency-controlling resonator.

To assure oscillation at the desired overtone mode of the crystal unit, the circuit must also be arranged to prevent the possibility of operation at lower overtone modes, since the crystal unit may well exhibit lower resistance at these lower-frequency modes. Use of a narrow-band circuit can suppress the available gain at these lower frequencies, or a crystal feedback network can be used that does not provide the required phase shift at the lower frequencies. Usually, the latter approach results in a lower phase-slope value for the sustaining circuit and provides the better choice.

One commonly used circuit configuration is the modified Pierce circuit shown in Fig. 8.3-1. In order to provide the required loop-phase closure, the feedback network must exhibit a phase shift of nearly 180°. This can only occur when the shunt impedance from point 1 to ground is a capacitive reactance, so that oscillation will only occur at some frequency above the parallel resonance of the L_2-C_2 tank circuit. Consequently, the values for L_2 and C_2 are chosen to provide the desired value of negative reactance at the operating frequency and to be resonant between the operating frequency and the next lower crystal mode (i.e., for fifth-overtone 5-MHz crystal operation, the resonance of L_2-C_2 must lie between 3 and 5 MHz). In the interest of minimizing the phase slope of the network, this resonance should be set only slightly above the next lower crystal mode.

Other possible circuit configurations are shown in Fig. 8.3-2. In Fig. 8.3-2a, L_2 is chosen such that the combination of crystal unit and load capacitor C_L

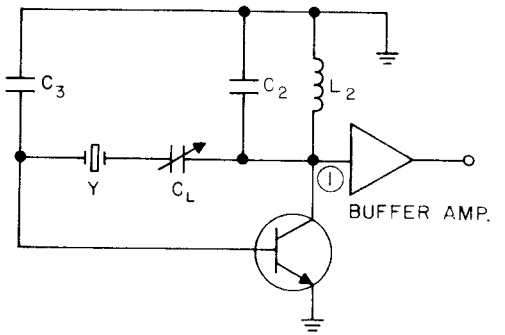
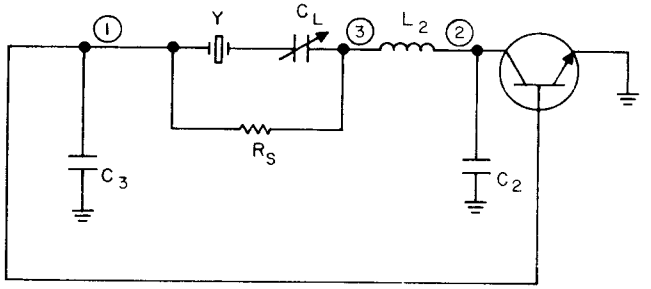
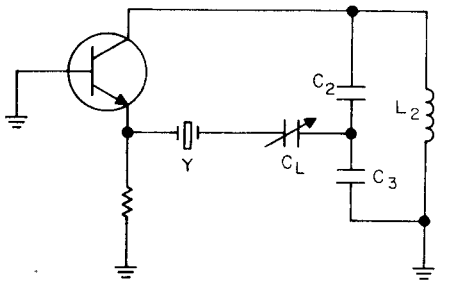


FIG. 8.3-1 Pierce-type oscillator circuit modified for overtone-mode crystal operation.



(a)



(b)

FIG. 8.3-2 Some alternate arrangements for overtone-mode crystal operation: (a) use of a shunt resistor to suppress oscillation at lower crystal modes; (b) use of a tuned, common-base amplifier for overtone-mode operation.

operates very near series resonance. At lower crystal modes, however, a considerable effective inductance will be required between points 1 and 3. The resistance R_s is then chosen to suppress oscillation at the lower frequency, but it has little effect at the operating frequency. In Fig. 8.3-2b, the resonant collector-tank circuit provides a narrow-band gain characteristic, so that the available gain at the lower frequencies is insufficient to sustain oscillation. Both of these networks, however, are more sensitive to the value of the inductive element and also introduce more resistive loading than the network of Fig. 8.3-1. The configuration of Fig. 8.3-2b, however, is useful when the ratio of signal power to wideband noise is critical, since it provides a much higher output level for the same crystal drive current than can be realized by the other networks discussed. Phase-fluctuation noise within one or two bandwidths of the feedback network, however, may be enhanced due to the reduction of the effective feedback-network Q value, so this advantage really exists only for those applications, such as communication systems, where wideband additive noise is of importance.

To protect the oscillator circuit from the effects of external loading and to provide useful output power levels, buffer amplifiers are required following the oscillator stage. These amplifiers should be designed to minimize their contributions to both phase fluctuations and additive noise and to provide good isolation. These attributes are usually accomplished through the use of considerable negative-feedback factors.

Since crystal resonators exhibit frequency change with variations in drive current, some form of automatic level control (ALC) of the oscillator stage is required. Ideally, this ALC function should influence only the transfer gain of the sustaining circuit, without affecting the transfer phase. In actuality, this

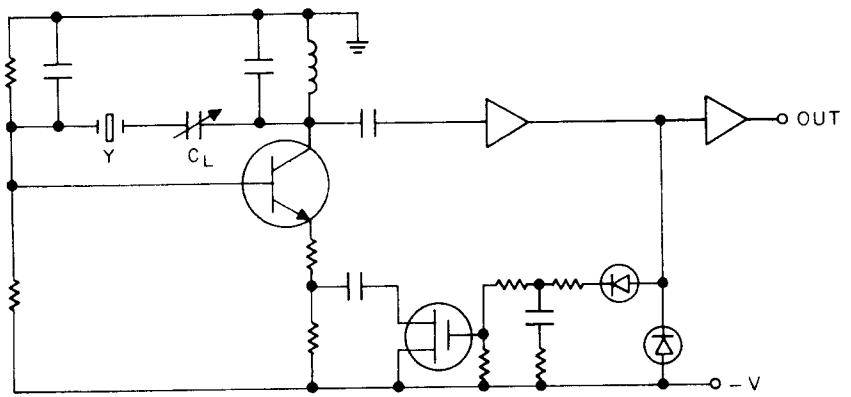


FIG. 8.3-3 Application of ALC to a modified Pierce crystal-controlled oscillator.

condition can never be perfectly satisfied; however, the use of a variable resistive element, such as the field-effect device introduced into the emitter circuit of the configuration in Fig. 8.3-3, is generally superior to methods based on variable-bias current control, since both the transfer phase and noise figure of the transistor stage are quite sensitive to bias current. The stability of the ALC circuitry is also of vital concern and usually requires the use of negative feedback in any amplifier stages used in the circuit. Care in the design of the low-pass networks required must also be exercised.

A typical arrangement of a complete oscillator circuit for use with a 5-MHz fifth-overtone AT-cut precision resonator is shown in Fig. 8.3-4. This circuit uses two broadband buffer amplifiers, with the drive for the ALC provided by the first buffer. Gain control of the oscillator stage is accomplished by use of the variable-resistance characteristic of the field-effect transistor (FET) as a negative-feedback resistor in the emitter of the oscillator stage. Some voltage delay in the ALC is provided by the forward-breakdown voltage of the rectifier diodes at its input. Additional delay can easily be provided by addition of a reverse-polarity voltage introduced in series with the diodes or by a pre-bias cutoff voltage incorporated in the ALC amplifier.

It is important that the oscillator stage be biased to operate in a very linear

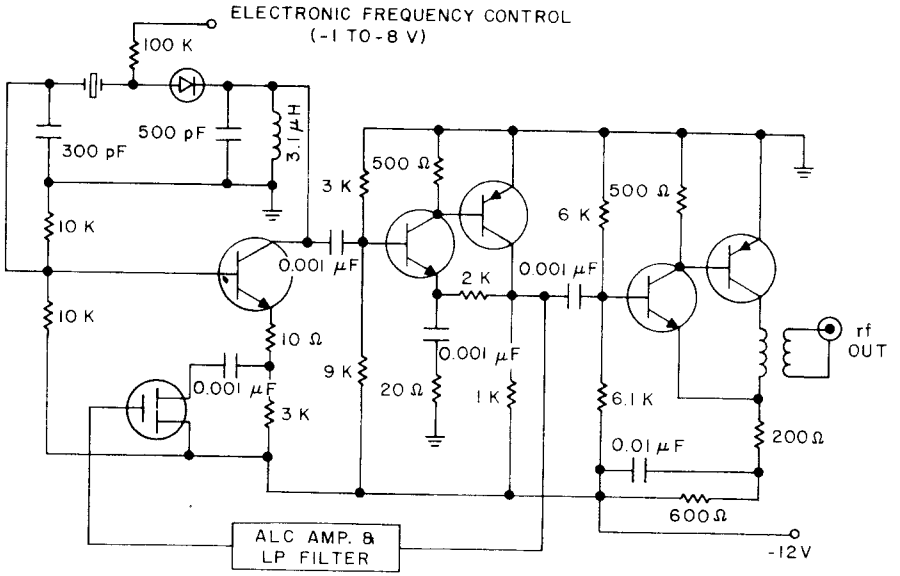


FIG. 8.3-4 Schematic of a modified Pierce 5-MHz oscillator circuit with electronic frequency control and output buffer amplifiers.

region to reduce the amount of phase modulation of the signal caused by low-frequency noise currents. Also, the first stage of the buffer amplifier should be carefully selected to reduce wideband additive noise.

The use of varactor-diode frequency adjustment is quite common in precision oscillators. This eliminates the need for mechanical access through the oven shells and also allows use of electronic frequency control to permit phase locking to a reference signal or remote control of system frequency. Care must be taken in the selection of these devices, however, to ensure that they do not add phase- and frequency-modulation noise. The reverse leakage current of a varactor is inherently noisy and thus produces a noise-voltage component superimposed on the frequency-control voltage. Varactors chosen should exhibit low values of leakage current at the oven operating temperature, and the effective resistance of the biasing circuit should be kept as low as possible. For the same reason, it is necessary to avoid noise signals being introduced via the tuning-voltage circuits themselves. Typical tuning sensitivity obtained with a 30-pF nominal-value hyper-abrupt junction varactor used with a 5th-overtone 5-MHz AT-cut resonator is about 3×10^{-7} per volt. Simple arithmetic shows that voltage variation of a few microvolts, then, can cause frequency fluctuation of 1×10^{-12} or more.

High-quality, on-board regulation circuits to stabilize the dc supply voltages for all of the rf circuits are also good practice, since in use, voltage supplies are often found to be influenced by other equipment having both long-term variations and transient voltages present.

8.3.1.3 TEMPERATURE-CONTROL REQUIREMENTS

The quartz crystal unit is usually operated at a temperature very near its *turnover* point, that is, the temperature at which the first derivative of its frequency vs. temperature characteristic is zero. This, of course, implies that it is placed in some kind of thermally controlled environment. The other components on the oscillator circuit are also temperature sensitive to some degree; thus, the entire circuit should be maintained at a stable, fixed temperature. Consequently, the thermal and mechanical design of the stabilizing oven structures, as well as the electrical design of the electronic control circuits required to maintain the interior temperature, are of major importance.

Two methods are commonly used to provide thermal isolation of the stabilized region from ambient conditions. One method is the use of a Dewar vacuum-insulated structure made of stainless steel shells, while the other is the use of rigid expanded-foam material to support one metallic shell within an outer enclosure. The vacuum-barrier method, in principle, provides superior insulation and requires less total space for the oscillator. The vacuum

structures, however, are susceptible to long-term degradation due to small leaks and/or outgassing of the materials. The urethane foam materials, on the other hand, have been shown to have excellent long-term stability. In addition, they provide excellent mechanical support for the interior structure.

The quartz crystal itself imposes the most stringent requirements for temperature stabilization. An overtone-mode AT-cut crystal unit, for example, exhibits a frequency offset on the order of 1×10^{-9} when exposed to a transient temperature ramp of about 0.01°C/hr; thus, the crystal oven must maintain steady temperature environments with deviation rates no more than about 10^{-5} °C/hr if frequency deviations are to be kept below 1×10^{-12}. The SC cut is much less sensitive to thermal variations, but tolerances on the orientation angles of the plate make it difficult to assure better than a ten- or twenty-fold improvement, thus relaxing the requirement to perhaps about 10^{-4} °C/hr. Circuit-element stability, however, can be maintained with a temperature stability on the order of 0.1°C, providing reasonable care is taken in the selction of components.

These requirements, then, dictate that, if a single-stage oven system is used to control the environment of the entire oscillator, it is essential that the crystal unit be tightly coupled to the temperature control. Even with very-high-gain control circuits, it becomes difficult to maintain the required stability in a single-stage device, since stabilization ratios in excess of 10^5 are required. It is generally much easier to obtain the needed stability if only the crystal unit, or at most, the rf circuits, are included within an inner-oven enclosure. This inner oven, together with voltage regulators, temperature control circuits, and power output stages, is then housed in an outer-oven structure, as shown symbolically in Fig. 8.3-5. This approach requires more space and more power, but leads to improved performance with less "fine tuning" of the thermal structure and temperature-control circuits. For example, a stabilization ratio of only 500 for the outer oven will result in maintaining a temperature stability of 0.1°C in the outer chamber. Then, it is quite reasonable to achieve a stabilization ratio in excess of 1000 for the inner oven, thus providing temperature stability better than 10^{-4} °C for the inner oven for an ambient temperature range of −10 to 50°C. Depending on the thermal design of the structure and the total power dissipation, it may be necessary to control the outer chamber at least 10 to 15°C above the maximum ambient temperature. Similarly, if the rf circuits are included in the inner chamber, it must operate some 10°C or more above the temperature of the outer chamber. Consequently, if ambient temperatures as high as 50°C are expected, the crystal unit must be designed to operate at a temperature above about 75°C.

The temperature-control circuits used in precision oscillators must, of course, be of the proportional type, and they are generally based on a resistance bridge circuit having temperature-sensitive elements in one or two

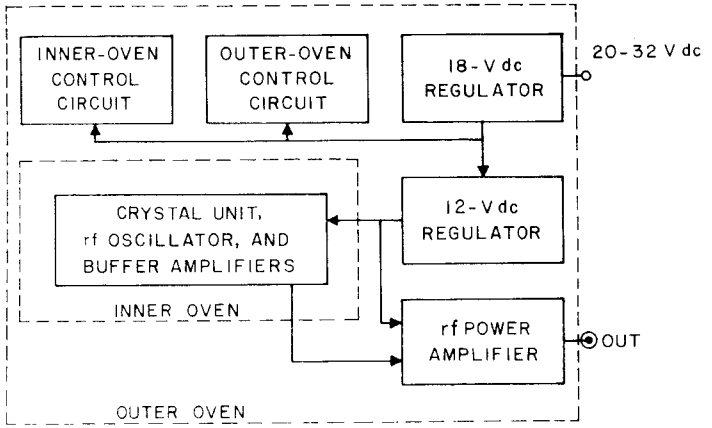


FIG. 8.3-5 Arrangement of circuit modules to provide near-optimum stabilization of frequency with wide variations in both ambient temperature and supply voltage.

of the bridge arms. Either dc or low-frequency ac excitation voltages may be applied to the bridge, and high-gain feedback-stabilized amplifiers sense the unbalance of the bridge circuit and provide heater power proportional to the unbalance. The gain of such a system must be finite, but can be very high. To avoid hunting (thermal oscillation) of the system, it is necessary to obtain very close coupling and rapid response time between heater and sensor as well as to limit the maximum rate of change of temperature of the controlled cavity by limiting the available power and using a structure for the chamber that has a large heat capacity. The permissible thermal insulation between ambient and the outer chamber is determined by the power dissipation within the outer chamber and the allowable temperature difference between the maximum ambient temperature and the outer chamber set point (some power must always be provided by the heating element). If only the crystal unit is contained in the inner chamber, then the thermal insulation between it and the outer chamber is limited only by the available space. When active circuits are included in the inner chamber, then the same conditions must be satisfied as for the outer chamber, although the temperature difference is well established by the set point of the outer chamber and the turning-point temperature of the crystal unit.

8.3.1.4 MINIMIZING AMBIENT MECHANICAL EFFECTS

All crystal-controlled oscillators are subject to frequency perturbations caused by mechanical shock and vibration. AT-cut overtone resonators of plano-convex design show acceleration coefficients on the order of $1 \times 10^{-9}/g$ for acceleration applied normal to the plane of the plate and varying coefficients for accelerations in the plane of the plate, depending on the direction of the applied acceleration and the type of mounting system used. These coefficients can be reduced significantly for some doubly rotated orientations; however, some acceleration-induced frequency changes will still be present (Bloch and Vulcan, 1976).

The response of the electrical circuits to mechanical disturbances can be minimized by careful mechanical design of circuit boards, oven structures, etc. When applications imply particularly severe mechanical stresses, special techniques have been found useful. For example, when high linear acceleration is expected, such as during the launching of spacecraft, the crystal unit may be carefully positioned to place the expected acceleration vector in the plane of the plate and very near one of the zero-coefficient axes. If severe vibrational environments are expected, energy-absorbing damping materials may be used to isolate the crystal oven chamber from high-frequency vibrations. In normal laboratory environments, vibration isolators and shock-absorbing mountings can be used to reduce the effects of building vibrations or vibrations produced by rotating machinery.

8.3.2 Measurement and Specification of Frequency Stability

The stability (or more correctly, instability) of the frequency of a signal refers to the deviation of that frequency from a constant value. Precision crystal-controlled oscillators generally produce a signal whose frequency drifts, or changes, slowly and monotonically with time. Usually measured over periods of days or months, this gradual change is commonly called frequency aging or long-term frequency stability. Alternatively, if the duration of each successive period of the signal could be measured with perfect precision, it would be observed that these durations would differ from each other by small, more or less random amounts. Such deviations, measured over sample intervals ranging from a single period to hundreds of seconds, are commonly referred to as short-term frequency stability. The precise sample interval marking the boundary between short- and long-term measurements is quite vague, thus requiring more specific definition in particular applications.

8.3.2.1 MEASUREMENT OF FREQUENCY

In order to determine the deviations of frequency from a constant value, it is implied that a perfectly constant reference is available. Assuming for the moment that such a reference were available, then there are basically two methods that are commonly used to measure the frequency of a source under test.

The first method makes use of the frequency reference to generate a precisely known time interval (gate time), and then the number of periods of the test source occurring in this time interval are counted electronically. Dividing the number of occurrences by the known gate time provides the average frequency for that sample time. However, since the reference signal and the test signal are uncorrelated, the best precision that can be obtained corresponds to a deviation of plus or minus one occurrence during the observation. This means, for example, that a 10-MHz source measured in this way during a precise 1-sec gating interval could be measured to a precision of ± 1 Hz, or $\pm 1 \times 10^{-7}$.

Alternatively, it is possible to let the test signal establish the gate time while the reference frequency periods are counted. In this way the duration of one period (or more) of the test frequency is determined to a resolution of ± 1 period of the reference. Some commercial counters now available utilize a 500-MHz reference in this mode of operation, allowing measurement of time intervals to a resolution of $\pm 2 \times 10^{-9}$ sec. Even this mode, however, enables a precision of only $\pm 2 \times 10^{-9}$ for 1-sec sample intervals.

In order to improve the resolution of frequency measurement, then, additional signal-processing techniques must be employed. One commonly used technique is the *beat-frequency* method, in which a small difference frequency is provided between the reference signal and the test-source signal; a mixer is used to detect this difference frequency (commonly set to a value of 100 Hz or less). The difference frequency is then measured using the reciprocal-frequency, or period, method of measurement, as shown in Fig. 8.3-6. The output of the mixer then consists of

$$df = (f_1 - f_0) + \Delta f(t),$$

which contains the total frequency deviation between the two signals in addition to the difference between the two nominal frequencies. The signal df can now be measured to a precision of $\pm 2 \times 10^{-9}$ in 1 sec; however, if the nominal value of $f_1 - f_0$ is only 100 Hz, the resolution is $\pm 2 \times 10^{-7}$ Hz. Consequently, deviations in the f_1 signal of $\pm 2 \times 10^{-7}$ Hz with respect to the reference f_0 are resolved. If the nominal value of f_1 is 10 MHz, the fractional resolution is $(\pm 2 \times 10^{-7})/10^7 = \pm 2 \times 10^{-14}$ in 1 sec or $\pm 2 \times 10^{-12}$ in 10 msec. In this way frequency fluctuations between even the best of crystal-controlled oscillators can easily be resolved with only limited frequency multiplication required.

When the two signals to be compared have precisely the same frequency, a slightly different technique is appropriate, as described by Saxena and Mathur (1980). This dual-mixer technique introduces the use of a third signal source (which need not have as good stability as the sources being compared) and two separate mixers to generate two channels with the same nominal frequency, as shown in Fig. 8.3-7. However, the phase deviations between the two channels

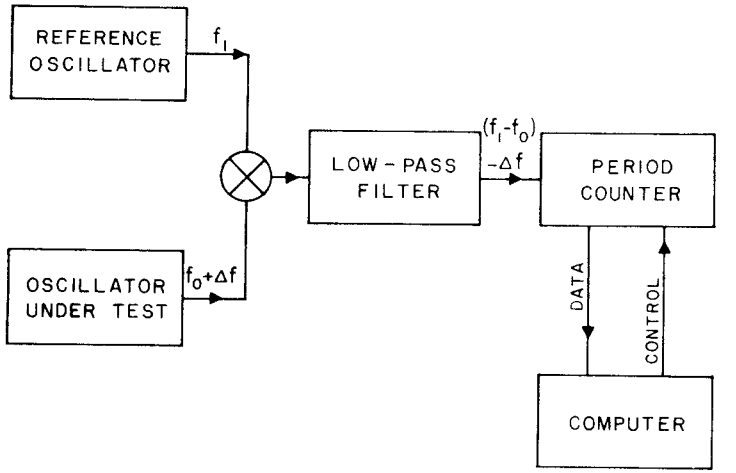


FIG. 8.3-6 Use of a period counter and an offset reference frequency source for the measurement of frequency and frequency fluctuations.

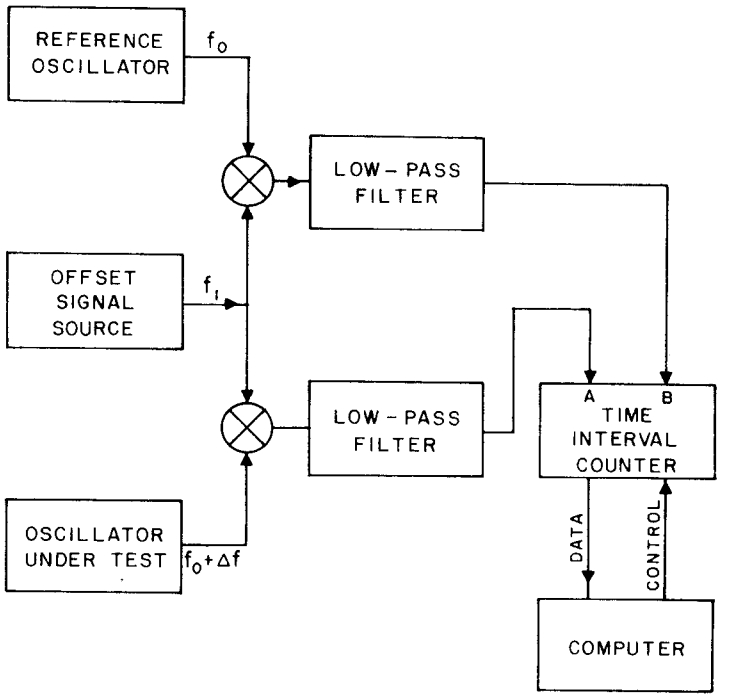


FIG. 8.3-7 The dual-channel time-difference method of measuring frequency fluctuations between two oscillators having exactly the same mean frequency.

can be related to the frequency deviations between the two signal sources. It has been reported (Saxena and Mathur, 1980) that residual measurement-system noise is lower for this method than for those previously described. A second benefit is that measurements are made without dead-time, so no corrections need be made to the data (Barnes *et al.*, 1971).

Another technique that has been used for improving the sensitivity of frequency measurement is shown in Fig. 8.3-8. This method makes use of extensive frequency multiplication and mixing to produce an output signal at the same frequency as the test signal but with an increased frequency-error component. However, the repeated multiplication is a probable source of added noise, and the method is probably not capable of as low a measurement-system noise contribution as those previously described.

The above are some of the more commonly used techniques for making high-resolution measurements of frequency differences between two signal sources of the same (or nearly the same) frequency. We have referred to one

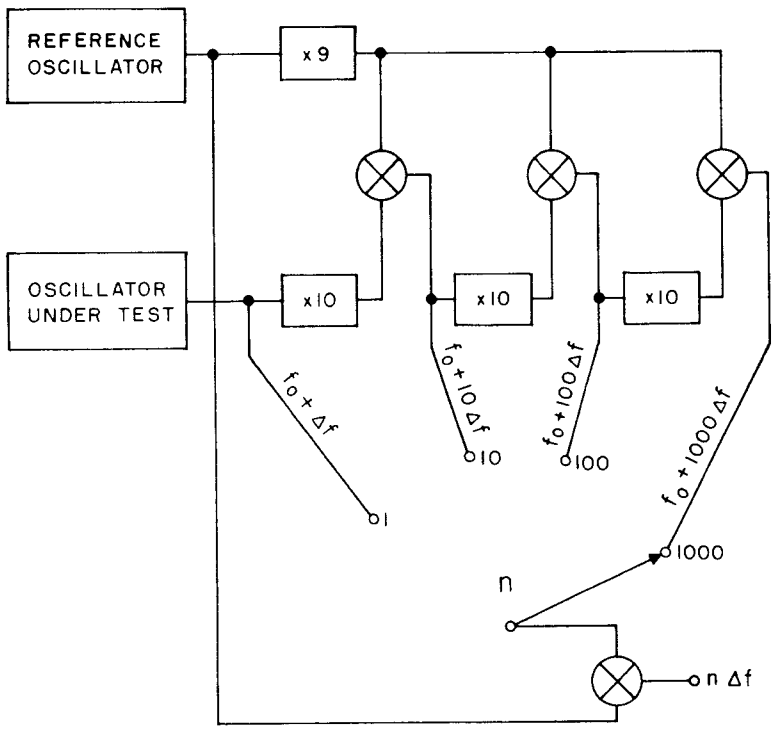


FIG. 8.3-8 Principle of the frequency-deviation multiplier method of increasing the sensitivity of frequency measurement.

source as a "reference;" in actuality, when dealing with precision oscillators the two sources will often be of like stability, and we are really determining the relative deviations between the two. For measurements having very long sample intervals (hours or days), an atomic source (cesium-beam standard, hydrogen maser, etc.) may be used as an essentially zero-drift reference or local quartz references may be calibrated to one of several broadcast signals, thus providing an essentially drift-free reference for long-term measurements. For short-term measurements (sample intervals of 100 seconds or less), however, precision quartz sources provide exceptional stability and can really only be compared to one another.

8.3.2.2 INTERPRETATION OF FREQUENCY MEASUREMENTS

Having obtained measurements over some span of observation of the frequency deviation between an oscillator signal and a reference, some analysis of the data is required in order to describe the oscillator's performance. This is usually done by determining its aging, or long-term frequency drift, and by reporting the results of some kind of statistical analysis of the set of measured data.

The long-term-drift characteristic is commonly expressed as an expected change of the "average" frequency in fractional parts per day (or week). For this determination quite long sample intervals (100–1000 sec) are usually used and the daily value assigned to the frequency is the mean of the values observed during that day. In its usual meaning, then, aging of a crystal oscillator is more precisely the change in its mean observed frequency per unit of time (rate of change of the mean). Analysis of data resulting from short-term measurements of frequency deviation is not so simply described. A considerable amount of work has been done in this area (Barnes *et al.*, 1971; Cutler and Searle, 1966; Rutman, 1978; Saxena and Mathur, 1980).

8.3.2.3 MEASURES OF SHORT-TERM FREQUENCY STABILITY (TIME DOMAIN)

In many applications of crystal-controlled oscillators (as well as other precision frequency generators), the fluctuation of frequency from its average value is of more use when expressed in terms of its time and time-average characteristics rather than in terms of its Fourier-frequency characteristics.

The fundamental time-domain definition of short-term frequency stability is based on the two-sample variance of the average relative deviation of the instantaneous frequency:

$$\sigma_y^2(\tau) = \langle \tfrac{1}{2}(\bar{Y}_{k+1} - \bar{Y}_k)^2 \rangle, \qquad (8.3\text{-}1)$$

where $\sigma_y^2(\tau)$ is the two-sample variance of the frequency deviations for a sampling interval τ, $\langle\ \rangle$ indicates an average calculated for an infinite number of measurements, and τ is the sampling period over which the average relative deviation of the instantaneous frequency $\overline{Y}_k$ is obtained. The successive measurements of $\overline{Y}_k$ shall be obtained without dead-time between measurements.

For the different kinds of noise that can disturb an oscillator, it has been shown that the relative uncertainty of the variance value calculated from a finite number of measurements is of the form

$$\Delta(\sigma_y^2)/\sigma_y^2 = C_\alpha/M \qquad \text{for} \quad M > 10,$$

where M is the total number of measurements of $\overline{Y}_k$ used for the calculation and C_α a coefficient depending on the type of noise ($C_\alpha \leq 1$). The variance is then defined by

$$\sigma_y^2(M, 2, \tau, \tau) = \sigma_y^2(\tau) = \frac{1}{2(M-1)} \sum_{k=1}^{M-1} [\overline{Y}_{k-1} - \overline{Y}_k]^2, \tag{8.3-2}$$

with

$$\Delta(\sigma_y^2)/\sigma_y^2 = C_\alpha/M.$$

At present, there are thought to be five independent noise processes that can disturb an oscillator. For these types of noise, the coefficient C_α is as follows.

Noise	C_α
Random-walk-frequency noise	0.75
Frequency-scintillation noise	0.77
Frequency white noise	0.87
Phase-scintillation noise	0.99
Phase white noise	0.99

The average relative deviation of instantaneous frequency is the summation over the time τ of the relative deviation of instantaneous frequency:

$$\overline{Y}_k = \frac{1}{\tau} \int_{t_k}^{t_k+\tau} Y(t)\, dt.$$

Therefore,

$$\overline{Y}_k = \frac{1}{2\pi f_0 \tau} \int_{t_k}^{t_k+\tau} Y(t)\, dt = \frac{1}{2\pi f_0 \tau} (Y_{t_k+\tau} - Y_{t_k}). \tag{8.3-3}$$

The two-sample variance without dead-time for M measurements can then be written as

$$\sigma_y^2(\tau) = \sigma_y^2(M, 2, \tau, \tau) = \frac{1}{2(M-1)} \frac{1}{(2\pi f_0 \tau)^2} \times \sum_{k=1}^{M-1} [(Y_{t_k+1+\tau} - Y_{t_k+1}) - (Y_{t_k+\tau} - Y_{t_k})]^2. \tag{8.3-4}$$

The expression "without dead-time" means that

$$t_{k+1} = t_k + \tau.$$

Further, the phase fluctuation $Y(\tau)$ can be replaced by the total phase $\phi(t)$ because the phase components $2\pi f_0 \tau$ can be removed, and therefore

$$\sigma_y^2(\tau) = \frac{1}{2(M-1)} \frac{1}{(2\pi f_0 \tau)^2} \times \sum_{k=1}^{M-1} [(\phi_{t_k+2\tau} - \phi_{t_k+\tau}) - (\phi_{t_k+\tau} - \phi_{t_k})]^2. \tag{8.3-5}$$

The time-domain representation of short-term frequency stability commonly consists of the curve $\sigma_y(\tau) = f(\tau)$, where $\sigma_y(\tau)$ is the square root of the two-sample variance defined above.

It has been found that there are five independent noise processes that can usually be found to closely approximate the experimental short-term stability measured for an oscillator. These noise processes are characterized in the frequency domain by power spectral-density functions having integer-exponent dependence on the Fourier frequency:

$$S_y(f) = \frac{f^2}{f_0^2} S_\phi(f) = \sum_{\alpha=-2}^{2} h_\alpha f^\alpha, \tag{8.3-6}$$

where $S_y(f)$ is the power spectral density of frequency noise, $S_\phi(f)$ the power spectral density of phase noise, h_α the coefficient of the noise process represented by the frequency dependence f^α, and α an integer exponent of the Fourier frequency f. Whenever the power spectral density of the noise spectrum can be adequately represented by a linear combination of power terms [as in Eq. (8.3-6)], the time-domain variance function can be written in the form

$$\sigma_y^2(2, \tau, \tau) = \sigma_y^2(\tau) = h_{-2}\left[\frac{4\pi^2 t}{6}\right] + h_{-1}[2 \ln 2] + h_0\left[\frac{1}{2\tau}\right] + h_1\left[\frac{1}{4\pi^2\tau^2}\right][1.038 + 3 \ln(2\pi f_h \tau)] + h_2\left[\frac{3f_h}{4\pi^2\tau^2}\right]. \tag{8.3-7}$$

where the h's are the coefficients of the different noise processes as defined above.

According to the two relations (8.3-6) and (8.3-7), the conversion of the measurements for each of the five noise processes from the frequency domain to the time domain and conversely can be made on the assumption that

$$2\pi f_h \tau \gg 1 \qquad \text{and} \qquad 0 < f \leq f_h$$

by the coefficients in Table 8.3-1. It is noted that the two frequency-domain functions $h_2 f^2$ and $h_1 f$ give rise to the same slope for the $\sigma_y(\tau)$ function; one must resort to frequency-domain measurements to discriminate between them.

Figure 8.3-9 shows the slopes of the $\sigma_y(\tau)$ function resulting from each of the noise types. In actual data more than one process is usually present, although frequently a single process is found to dominate in a particular range of τ. Figure 8.3-10 is a plot of measured values of $\sigma(\tau)$ for a pair of precision 5-MHz oscillators.

The above discussion has been based on the assumption that the time-domain measurements are made without dead-time. In practice, this is not always possible to achieve. However, measured data may be corrected for

TABLE 8.3-1

Conversion of Power-Law Spectral-Density Processes between the Time Domain and the Frequency Domain[a]

Noise process	Time domain		Frequency domain	
	μ	$\sigma_y^2(\tau)$	α	$S_y(f)$
Frequency random walk	1	$A[f^2 S_y(f)]\tau$	−2	$\frac{1}{A}[\tau^{-1}\sigma_y^2(\tau)]f^{-2}$
Frequency scintillation	0	$B[fS_y(f)]$	−1	$\frac{1}{B}[\sigma_y^2(\tau)]f^{-1}$
White frequency	−1	$C[S_y(f)]\tau^{-1}$	0	$\frac{1}{C}[\tau\sigma_y^2(\tau)]$
Phase scintillation	−2	$D[f^{-1}S_y(f)]\tau^{-2}$	1	$\frac{1}{D}[\tau^2\sigma_y^2(\tau)]f$
White phase	−2	$E[f^{-2}S_y(f)]\tau^{-2}$	2	$\frac{1}{E}[\tau^2\sigma_y^2(\tau)]f^2$

[a] τ is the sampling time, f is the Fourier frequency, f_h is the system cutoff frequency, $A = 4\pi^2/6$, $B = 2 \ln 2$, $C = 1.2$, $D = [1.038 + 3 \ln(2\pi f_h \tau)]/4\pi^2$, and $E = 3f_h/4\pi^2$.

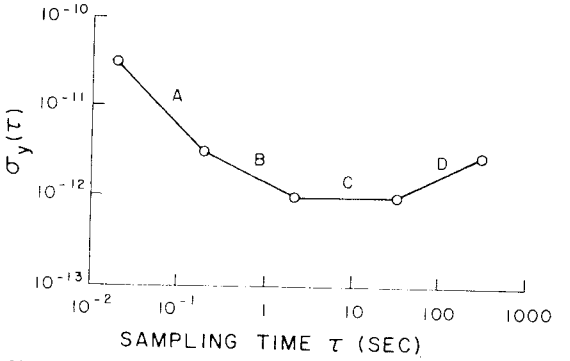


FIG. 8.3-9 Characteristic σ/τ plots corresponding to the five common power-law noise processes: A, white phase noise and phase scintillation noise, slope = −1; B, white frequency noise, slope = −1/2; C, frequency scintillation noise, slope = 0; D, random walk of frequency, slope = 1/2.

dead-time as described in NBS Technical Note 375 (Barnes, 1969). The corrected value is obtained by dividing the measured value by a constant obtained from the tables:

$$\sigma_y^2(M, 2, \tau, \tau) = \sigma_y^2(M, 2, T, \tau)/B_2(r, \mu),$$

where T is the time between the start of successive samples, τ the sample averaging time, $r = T/\tau$, and $\mu = -(\alpha + 1)$, α being the exponent of the predominant noise power law (except that $\mu = -2$ when $\alpha = 2$).

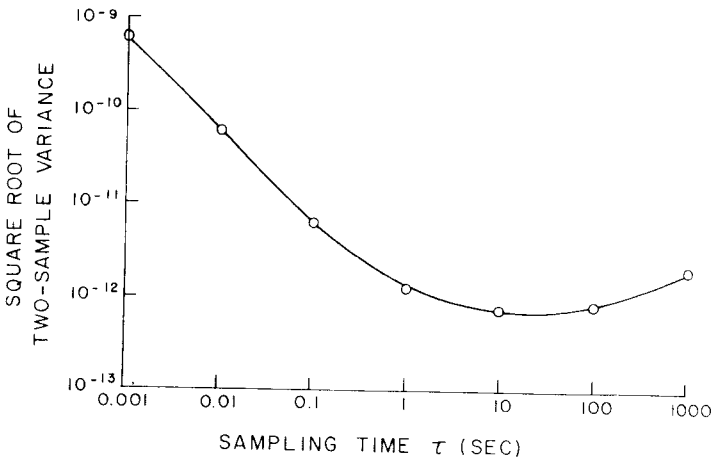


FIG. 8.3-10 Typical short-term stability performance of a precision crystal-controlled oscillator.

Values of $B_2(r, \mu)$ for some commonly encountered values of r and μ, where

$$B_2(r, \mu) = \frac{1 + \frac{1}{2}[2(r)^{\mu+2} - (r+1)^{\mu+2} - (r-1)^{\mu+2}]}{2(1 - 2^{\mu})},$$

are given in Table 8.3-2.

TABLE 8.3-2
Values of $B_2(r, \mu)$ Frequently Encountered

	$r = T/\tau$			
μ	1.00	1.01	1.10	2.0
2	1.000	1.020	1.2100	4.0000
1	1.000	1.015	1.1500	2.5000
0	1.000	1.010	1.0890	1.5660
−1	1.000	1.000	1.000	1.0000
−2	1.000	0.6667	0.6667	0.6667

9 Temperature Control and Compensation

Marvin E. Frerking

Collins Defense Communications Division
Rockwell International
Cedar Rapids, Iowa

List of Symbols 99
9.1 Temperature Control 101
9.1.1 Thermal Loss 105
9.1.2 Warm-Up Considerations 107
9.2 Temperature Compensation 108
9.2.1 Analog Temperature Compensation 109
9.2.2 Digital Temperature Compensation 110
9.2.3 Microprocessor Temperature Compensation 111

LIST OF SYMBOLS

A	Cross-sectional area of thermal path
A_1	Crystal linear temperature coefficient in parts per unit per degree Celsius
A_2	Crystal quadratic temperature coefficient in parts per unit per degree Celsius squared
A_3	Crystal cubic temperature coefficient in parts per unit per degree Celsius cubed
b	Number of bits
B	Exponential temperature coefficient of thermistor
c	Specific heat in joules per degree Celsius per gram
d	Diameter of Dewar flask
f	Frequency in hertz
Δf	Frequency deviation from nominal value in hertz
$(\Delta f/f)_m$	Maximum frequency excursion of crystal over temperature range
l	Length of thermal path
m	Oven mass in grams
P	Power loss in watts
R_{eq}	Equivalent thermal resistance of crystal mount in degrees Celsius per watt
$R_{th}(T)$	Thermistor resistance at absolute temperature T in kelvins

PRECISION FREQUENCY CONTROL
Volume 2
Oscillators and Standards

Copyright © 1985 by Academic Press, Inc.
All rights of reproduction in any form reserved.
ISBN 0-12-280602-6

S	Slope of crystal curve
T	Temperature in degrees Celsius or kelvins, as specified
T_0	Reference temperature in degrees Celsius for crystal equation
T_p	Turning-point temperature of crystal
ΔT	Temperature difference between crystal oven and ambient temperature
W	Thermal mass in joules per degree Celsius
V_{ref}	Voltage reference for thermistor bridge
β	Exponential temperature coefficient
θ_0	Reference angle for a specific crystal type
ε	Emissivity of surface
$\Delta\theta$	Crystal angle of cut in degrees from the angle producing a zero slope at the reference temperature T_0
λ	Thermal conductivity of wire or insulation
σ	Stefan–Boltzmann constant $= 0.56687 \times 10^{-7}$ W/m$^2 \cdot$K^4

Temperature control and temperature compensation are the two primary means by which the frequency stability of a crystal oscillator can be improved over a temperature range. Without one of these techniques the frequency stability is generally limited to about ± 1 ppm over a limited temperature range (0–50°C) and perhaps ± 15 ppm from -55 to 105°C. Temperature control results in the highest stability; however, there are many applications where temperature compensation has been used to great advantage, particularly in communications equipment, where the requirements are often in the 0.5–5-ppm frequency-stability range. Temperature compensation can be used to achieve stabilities approaching $\pm 5 \times 10^{-8}$, as demonstrated by Buroker and Frerking (1973) and Mroch and Hykes (1976). As the requirements approach these values, however, the compensation becomes difficult and the use of temperature control may result in a more economical design. Temperature control has several disadvantages that make it unsuitable for some applications, and the choice of which technique to use must often be determined by the constraints of the application.

The primary disadvantages of temperature-controlled oscillators are the following.

(1) A relatively large volume is required because of the thermal insulation.
(2) An initial stabilization period is required after turn-on while the oven warms up.
(3) The power consumption, particularly at cold temperatures, is higher than for temperature-compensated oscillators due to the thermal loss.
(4) The reliability of the components in the oven may be reduced in applications that require the oscillator to be turned on and off at frequent intervals.
(5) Operation of the oven at elevated temperatures tends to accelerate the aging rate of the crystal.

Various degrees of temperature control have been used in different applications. At one end of the spectrum only the crystal is placed in the oven, with the oscillator exposed to the external ambient temperature. The higher-precision standards require both the oscillator and the crystal to be in the controlled environment. Double-oven arrangements have also been used in ultraprecision applications in which one oven is placed within the other. These variations are discussed further in Section 9.1. A frequency stability of $\pm 1 \times 10^{-8}$ is typical for a single-oven frequency standard over a wide temperature range, while stabilities of parts per 10^{10} have been achieved with double ovens.

9.1 TEMPERATURE CONTROL

Temperature control of a crystal oscillator is nearly always accomplished by placing the unit in an oven. The oven temperature is set above the highest ambient temperature, and a control circuit is provided to hold the temperature constant. The temperature is selected or adjusted to be near a turning point of the crystal, where the slope of the frequency vs. temperature curve is nearly zero. The crystal curve can be described by an equation of the form

$$\Delta f/f = A_1(T - T_0) + A_2(T - T_0)^2 + A_3(T - T_0)^3, \qquad (9\text{-}1)$$

where T_0 is an arbitrarily chosen reference temperature, usually selected to be in the 20 to 30°C range, and A_1, A_2, and A_3 are constants for a given angle of cut and a given reference temperature T_0.

Table 9-1 lists the coefficients as a function of the angle $\Delta\theta$, measured in degrees from the angle θ_0 producing a zero slope at the reference temperature, for AT-, FC-, IT-, and SC-cut resonators. The reference temperature was chosen to be 25°C. Curves are shown for AT-cut resonators in Fig. 2.2-4 (Volume 1).

TABLE 9-1

Coefficients of Eq. (9-1) for Various Quartz Crystal Cuts[a]

Cut	Reference angle θ_0	A_1 (°C^{-1})	A_2 (°C^{-2})	A_3 (°C^{-3})	Inflection temperature
AT	35.25°	$-5.08 \times 10^{-6}\,\Delta\theta$	-0.45×10^{-9}	108.6×10^{-12}	26.4°C
FC	34.33°	$-4.32 \times 10^{-6}\,\Delta\theta$	-5.55×10^{-9}	82.2×10^{-12}	47.5°C
IT	34.08°	$-3.98 \times 10^{-6}\,\Delta\theta$	-10.1×10^{-9}	68.4×10^{-12}	74.2°C
SC	33.93°	$-3.78 \times 10^{-6}\,\Delta\theta$	-12.3×10^{-9}	58.2×10^{-12}	95.4°C

[a] Data from Ballato (1977).

Equation (9-1) can also be used to determine the degree of temperature control required for a given frequency stability. Unfortunately, AT-cut resonators are extremely sensitive to temperature gradients, and small differences in temperature between the crystal pins or between the pins and the holder can completely overshadow the frequency behavior in the region around the turning point. Doubly rotated crystals are less sensitive to gradients than AT-cut resonators and consequently exhibit superior performance in a crystal oven.

As previously indicated, it is desirable to set the oven temperature to the turning point of the crystal where it has a zero slope. This may not always be practical in production, and it is interesting to calculate the slope of the crystal as a function of temperature offset from the actual turning-point temperature. This can be accomplished by differentiating Eq. (9-1) to determine the slope. By setting the slope equal to zero at the turning-point temperature T_p, one can solve for the coefficient A_1. Substituting this value into the equation for the slope gives

$$S = 2A_2(T - T_p) + 3A_3[(T^2 - T_p^2) - 2T_0(T - T_p)], \qquad (9\text{-}2)$$

where S is the slope of the curve, T the temperature in degrees Celsius, T_p the turning-point temperature in degrees Celsius, and T_0 the reference temperature used in determining the coefficients A_2 and A_3 (25°C for Table 9-1).

Figure 9-1 is a plot of Eq. (9-2) in the vicinity of the turning point for various crystal cuts with 85°C turning points. From the graph it is obvious that the doubly rotated resonators require a lesser degree of temperature control than AT-cut resonators. It cannot be overemphasized, however, that small temperature gradients across the crystal, which may change with the ambient temperature, can completely mask the effect illustrated in Fig. 9-1. Similar curves can be plotted for other turning-point temperatures using Eq. (9-2).

The temperature control resulting from a single oven is usually in the 0.5 to 0.01°C range for units operating over wide ambient temperatures. Improved temperature control can be achieved by using a double oven, that is, a second oven within the first. Ideally, two independent control circuits are used for the inner and outer ovens, and temperature stabilities in the 0.001 to 0.0001°C range are possible. A considerable improvement over a single oven is also possible by using a single control circuit with two ovens. Both the inner-oven heater and the outer-oven heater are controlled by the same sensor. The improvement here results primarily because of a reduction in the temperature gradients in the inner oven.

A typical crystal-oven control circuit is shown in Fig. 9-2. The fast warm-up heaters are optional. Initially, at turn-on, the oven is cold and the thermistor R_{th} has a high resistance given by

$$R_{th}(T) = R_{th}(T_0) \exp \beta(1/T - 1/T_0), \qquad (9\text{-}3)$$

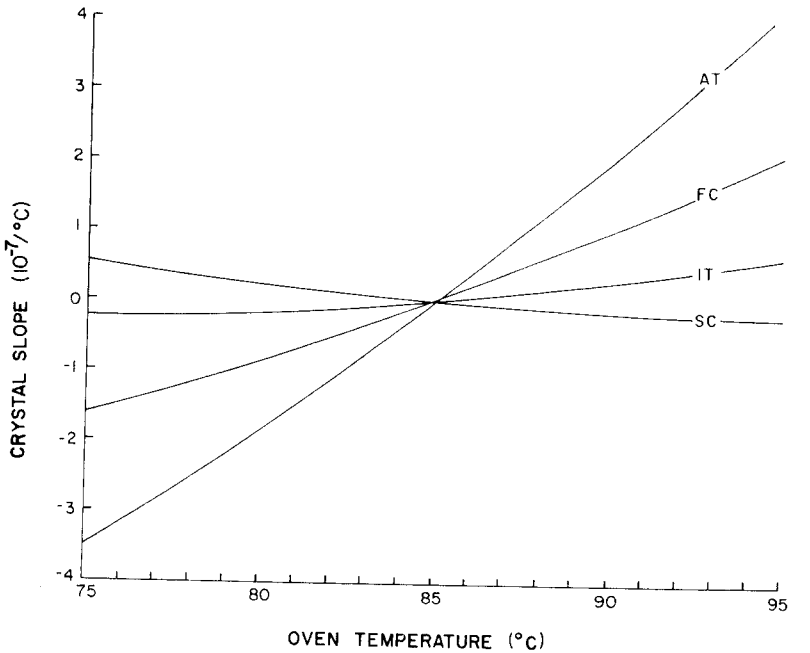


FIG. 9-1 Rate of change of frequency vs. temperature for crystals with 85°C turning points. [Data from Ballato (1977).]

where $R_{th}(T_0)$ is the thermistor resistance at the reference temperature T_0, normally chosen to be 298 K (25°C), T the thermistor temperature in kelvins, and β the exponential temperature coefficient.

The voltage V_1 is initially high and causes the amplifier to supply power to the oven. As the oven warms up, the thermistor resistance decreases until the voltage V_1 approaches the reference voltage V_{ref}. When this occurs, the amplifier output V_2 decreases, causing a reduction in the heat produced in R_1. An equilibrium is reached when the voltage V_1 is just sufficiently above V_{ref} so that the heater power equals the thermal loss. The gain of the amplifier determines how large the voltage offset will be. If the ambient temperature changes so that the heat loss increases or decreases, a corresponding oven temperature change will result. The oven temperature change results in a change in the thermistor resistance R_{th}, which in turn causes V_1 to vary and readjust the heater power to correct for the temperature error. Obviously, V_1 must stabilize at a slightly different voltage than the initial value to produce a different heater power. The amount of change is a function of the gain of the amplifier. It is not difficult to calculate the gain necessary to achieve a given

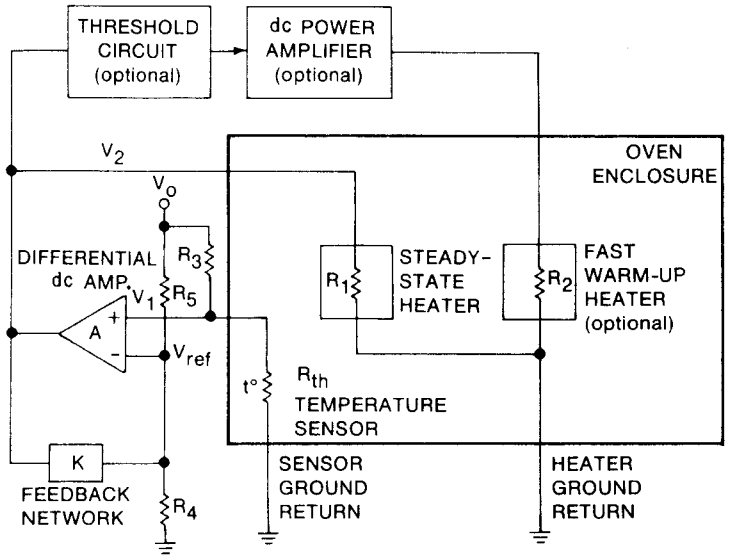


FIG. 9-2 Block diagram of temperature-control circuit for a crystal oven.

degree of temperature control at the thermistor. It is simply necessary to determine the required voltage change across the heater as the ambient temperature varies and divide this by the voltage change in V_1 caused by the allowable temperature variation at the thermistor. The feedback network for the amplifier is designed to provide the required value of gain. It is highly desirable to connect the reference voltage-divider to the same voltage source used by the sensor network. This results in the common-mode rejection of the amplifier, reducing the voltage-regulation requirements of the control circuit. In some applications it may be desirable to design the feedback network with a capacitor, so that the amplifier becomes an integrator (Hamatsuki *et al.*, 1973). This gives essentially infinite gain at dc.

A serious degradation in temperature control may result in practice because of various thermal considerations, and several of the more troublesome of these are enumerated below. It is of utmost importance that the oven temperature be uniform. Not only does this minimize the temperature gradients across the crystal, but it also ensures that the thermistor, which contacts the oven at only one point, will sense the true crystal temperature. A good design also assures that the thermistor and all lead wires to or from the oven are adequately heat-sinked to the oven enclosure.

Another important aspect of the design is the selection of a suitable location for the heater and the thermistor on the oven. It is desirable to distribute the

heater resistance over the oven surface in such a way that the heat is applied proportionately to the thermal loss. In practice this is never achieved perfectly, and some temperature gradient will be present across the oven. The sensor location is selected so that it sees the same average temperature as the crystal. Additionally, the sensor must be closely coupled to the heater or a thermal oscillation will occur, resulting in poor short-term frequency stability.

In many applications, particularly those of higher precision, the resistor R_3 will be located within the oven enclosure to eliminate the effects associated with its temperature coefficient. The differential dc amplifier may be placed in the oven as well; this involves trade-offs of increased stability vs. oven volume. A technique using a dual-mode oscillator with a single crystal serving as its own temperature sensor has also been reported (Kusters *et al.*, 1978) and may ultimately overcome some of these difficulties.

In many designs it is possible to eliminate the heater resistor R_1 and allow the output stage of the oven amplifier to perform the function of the heater. A more uniform heat distribution can be obtained by using two power transistors, one on each side of the oven (Burgoon and Wilson, 1979). Some form of current limiting is normally required to protect the heater transistors during warm-up. One method is to place a small resistor in series with the power transistor. An operational amplifier or a transistor can be used to sense the voltage across the resistor. If this voltage exceeds a predetermined threshold, the protective device reduces the drive power to the heater transistor.

The use of power transistors for the heater improves the efficiency of the oven circuit, since nearly all of the input power is then used to heat the oven. The technique has the disadvantage, however, that the heat is not uniformly applied to the oven, and a more massive oven enclosure may be required to minimize temperature gradients.

9.1.1 Thermal Loss

The input power required by a temperature-controlled oscillator is largely the result of thermal loss, and consequently most designs tend to minimize this quantity. Even in applications where the power consumption is unimportant, it is desirable to control the heat loss, since it affects the temperature gradients across the oven and also determines the size of the control amplifier. Precision crystal oscillators tend to employ foam insulation or a Dewar flask to minimize the heat loss. Foam insulation has the advantage of being more rugged and lower in cost; however, the heat loss is significantly greater and the size of the final package is larger. A Dewar flask, on the other hand, minimizes the thermal loss but must be carefully mounted in high-vibration or shock environments. It also tends to require a round oven design, which may be less

convenient to manufacture. The input power for a foam-insulated oven may typically run from 5 to 10 W at the cold temperature extremes in military equipment, while that for a unit using a small Dewar flask may be in the 1-W range. The approximate heat loss for a crystal oven with foam insulation can be calculated using the formula

$$P = \lambda A\, \Delta T/l \tag{9-4}$$

on each of the six surfaces and for each of the wires going into the oven. Here λ is the thermal conductivity of the wires or insulation, A the cross-secttional area for the volume under consideration, l the length of the thermal path, that is, the wire length or insulation thickness, and ΔT the difference between oven and ambient temperatures.

The approximate heat loss for a Dewar flask can be calculated from the dimensions if the thermal properties of the materials are known. Figure 9-3 shows the cross-sectional view of a typical unit. The heat loss results primarily from conduction along the inner glass wall of length l_2 and diameter d_1, from radiation loss across the vacuum, from loss in the foam cork, and from loss in the connecting wires. The conductive losses can be computed using Eq. (9-4) with the proper thermal conductivity for the materials used. The radiation loss can be computed using

$$P = \sigma \varepsilon_t A(T_i^4 - T_o^4), \tag{9-5}$$

where P is the thermal radiation loss in watts, σ the Stefan–Boltzmann constant $= 0.56687 \times 10^{-7}\ \mathrm{W/m^2 \cdot K^4}$, A the total surface area of outer glass in the vicinity of the oscillator assembly, ε_t the total emissivity factor, given by

$$\varepsilon_t = \frac{1}{(1/\varepsilon_i + 1/\varepsilon_o - 1)}, \tag{9-6}$$

ε_i the emissivity of the silvered inner glass, ε_o the emissivity of the silvered outer glass ($\varepsilon_i = \varepsilon_o = 0.01$–$0.02$ for deposited silver), and T_i and T_o the temperature of the inner and outer glass, respectively, in kelvins.

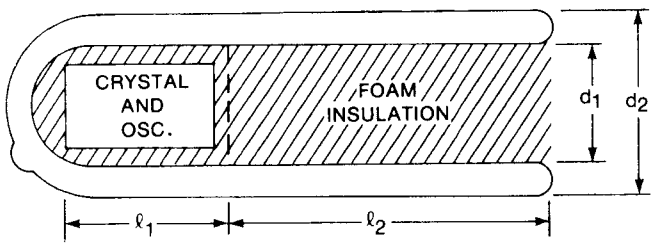


FIG. 9-3 Cross-sectional view of a Dewar-flask insulated oven.

9.1.2 Warm-Up Considerations

The stabilization time required by a temperature-controlled crystal oscillator may vary greatly depending on the type of design and the requirements of the application. Warm-up periods of 15 to 30 min are not uncommon for precision crystal oscillators, although when requirements dictate, much shorter intervals can be achieved. A considerable amount of work has been done to achieve fast warm-up, and stabilization periods of 2 to 5 min have been achieved for frequency stabilities within a few parts per 10^8.

Many factors enter into the warm-up time for a precision oscillator. The first consideration is to produce enough heat in the oven to raise the temperature of the associated mass from the ambient temperature to the oven operating temperature. This, unfortunately, is only part of the requirement. An equally important consideration, particularly with ultrafast warm-up, is to develop an oven and heater design so that the residual temperature gradients equalize quickly after the warm-up power is cut off. Finally, the crystal design must be such that internal stress in the quartz blank resulting from minute temperature gradients will not cause transient frequency excursions beyond the specification limit. AT-cut crystals are particularly susceptible to temperature transients and are generally not used in applications requiring the fastest warm-up. Here the doubly rotated crystals exhibit superior performance, and the closer one comes to the angle for an SC-cut crystal the better the performance. The crystal mount obviously influences the behavior of the unit as well, and a relatively massive mount is desirable.

The time required to heat the crystal blank to the oven temperature can be approximately calculated using the equivalent circuit of Fig. 9-4. Here the heater is represented by a current source of P joules per second (watts); W_0 is the thermal mass of the oven in joules per degree Celsius given by $W_0 = mc$, where m is the oven mass and c the average specific heat of the oven; W_x is the thermal mass of the crystal blank itself; and R_{eq} represents the thermal resistance of the crystal mount in degrees Celsius per watt. R_{eq} consists primarily of the supports in the crystal holder given by $R_h = l/\lambda A$, where l is the length of the supports, A the cross-sectional area, and λ the thermal conductivity. The equivalent thermal resistance of the quartz blank must be

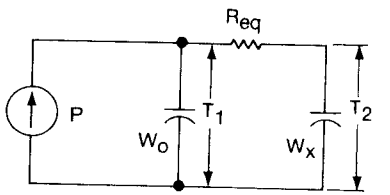


FIG. 9-4 Approximate equivalent circuit of crystal in oven.

added to R_h to find the value of R_{eq}. This is difficult to calculate accurately, and in practice it may be easier to measure the time constant of the crystal or an indentically constructed AC-cut crystal.

9.2 TEMPERATURE COMPENSATION

Many applications exist for crystal oscillators which require greater stability over the operating-temperature range than can be achieved with an uncompensated crystal exposed to the ambient temperature, but where it is desirable to overcome the disadvantages associated with temperature control. This can often be accomplished by using temperature compensation to stabilize the frequency of the oscillator. Frequency stabilities in the parts-per-10^7 range have been achieved over wide temperature ranges using this technique and about $\pm 5 \times 10^{-8}$ over limited or controlled temperature ranges (Buroker and Frerking, 1973; Kusters *et al.*, 1978).

Work is continuing on temperature-compensated crystal oscillator (TCXO) development at the time of this writing both to reduce the compensation effort for precision units and also to improve the accuracy of compensation.

A considerable number of techniques for temperature compensation have been proposed, with varying degrees of success. One of the earliest was to apply physical force to the crystal to correct its frequency using one or more bimetal supports (Gerber and Miles, 1961). Another method uses several crystals in parallel with different turning-point temperatures to improve the resultant temperature coefficient (Hirama, 1972). Capacitors shunted by thermistors have also been used in series with the crystal to achieve compensation. The most widely used technique, and the one producing the best stability over a wide temperature range, is that of electrical compensation.

Electrical temperature compensation of a crystal oscillator is accomplished by placing a voltage-variable capacitor (varactor) in the oscillator and pulling the frequency by precisely the amount, but in the opposite direction, that it drifts due to temperature. Much of the initial work using this technique was performed by Newell at Collins Radio during the early 1960s. Following the initial investigation, a practical three-thermistor network, tracking the crystal temperature coefficient (TC) from -55 to 75°C, was derived by Broadhead and Hykes, and this network is still used in many present-day TCXOs (Hykes and Newell, 1961). Newell continued working on TCXOs and developed a segmented approach that eased some of the tracking problem but required many components (Newell and Hinnah, 1969). As work continued, digital approaches were developed to achieve true segmentation of the network. One of the most interesting approaches uses a hybrid analog–digital scheme in which a coarse analog compensation network is used to reduce the frequency excursion to less than 1 ppm and a digital fine-correction system is then used

to correct the remaining TC (Buroker and Frerking, 1973). A purely digital approach was nearly simultaneously worked out as well (Prak and Peduto, 1972). Subsequent development has been accomplished using microcomputers to produce the compensation voltage (Frerking, 1978; Onoe *et al.*, 1978). A technique using two crystal modes simultaneously, one as the temperature sensor, has been reported to have a potential stability performance in the parts-per-10^8–10^9 region (Kusters *et al.*, 1978). Work has also continued with analog compensation, and a two-varactor approach was developed to linearize the voltage required around the crystal turning point (Schodowski, 1970). A great deal of unpublished work was performed during this period to develop proprietory networks for the various crystal-oscillator manufacturers.

An overview of electrical temperature compensation is presented below and will allow the reader to grasp the fundamental concepts of the various techniques. For more detailed design information, the reader is directed to a book covering this specific subject (Frerking, 1978, especially Chapter 10).

9.2.1 Analog Temperature Compensation

A very large number of TCXOs have been manufactured using analog compensation, and at the time of this writing analog techniques dominate TCXO production. A diagram depicting this approach is shown in Fig. 9-5.

A considerable variety of thermistor-network configurations have been used to produce the required compensation voltage as a function of temperature, primarily for AT-cut resonators with curves as shown in Fig. 2.2-4 (Volume 1). A typical network is shown in Fig. 9-6. This network is well suited for crystals with 30–35-ppm frequency excursions between the turning points. The thermistor values are chosen so that at cold temperatures, R_{T2} and R_{T3} are effectively open circuits, and the compensation voltage V_0 is determined by R_2 and R_{T1}. In the room-temperature region, R_{T1} is an effective short, while R_{T3} is still essentially an open circuit. The behavior is then determined by R_{T2} and R_1. Finally, at high temperatures R_{T2} and R_{T1} are effective shorts, and the behavior is most strongly influenced by R_3 and R_{T3}. A considerable degree of independence is thus achieved in designing the network to cover a wide temperature range.

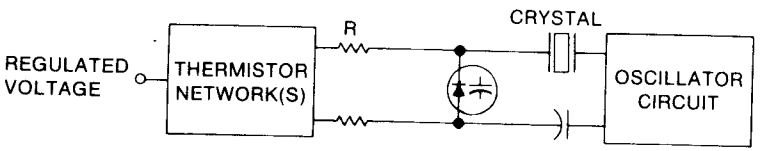


FIG. 9-5 An analog-compensated TCXO.

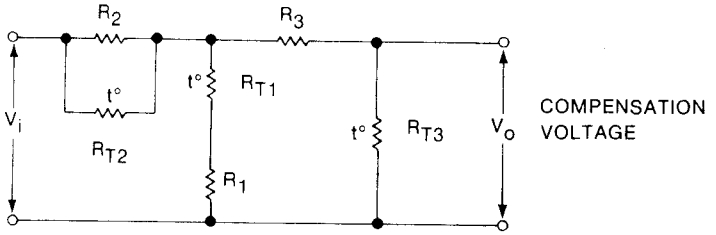


FIG. 9-6 A three-thermistor temperature-compensation network.

9.2.2 Digital Temperature Compensation

Another approach to temperature compensation involves the use of digital compensation. A block diagram showing the basic configuration is presented in Fig. 9-7. The temperature sensor develops an approximately linear voltage as a function of temperature. The voltage is converted to a digital word in the A/D converter. The digital temperature word is then used as an address for the programable read-only memory (PROM). A specific ambient temperature thus results in a specific address to the PROM. The PROM is preprogrammed so that the cell being addressed at any temperature contains the correction voltage required at that temperature. The digital output of the PROM is then converted to an analog voltage in the D/A converter and applied to the varactor in the oscillator circuit. It can be shown that the minimum memory size required to achieve a given frequency stability occurs if the number of bits b in the correction words satisfies the relationship (Frerking, 1978, p. 156)

$$2^b = \frac{(\Delta f/f)_m(1 + b \ln 2)}{2(\Delta f/f)}. \tag{9-7}$$

Then the number of memory locations (words) required is given by

$$n = \frac{ST}{2(\Delta f/f - (\Delta f/f)_m/2^b)}, \tag{9-8}$$

where S is the maximum frequency vs. temperature slope of the crystal in parts per million per degree Celsius, T the total temperature range in Celsius degrees over which the oscillator must operate, $(\Delta f/f)_m$ the maximum peak-to-peak frequency excursion of the crystal in parts per million, and $\Delta f/f$ the desired frequency stability in parts per million.

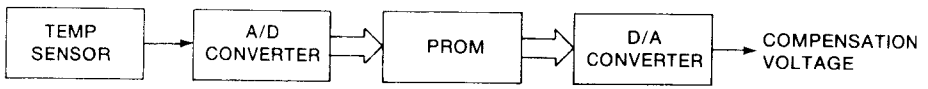


FIG. 9-7 Block diagram of a digital compensation network.

9.2.3 Microprocessor Temperature Compensation

A third approach to temperature compensation uses a microprocessor to replace the PROM of Fig. 9-7. A relatively small table of stored frequency corrections is used, and the microcomputer is programmed to interpolate between them to find the required correction at any temperature. The processor can also be programmed to calculate corrections from the cubic equation of the crystal directly if the accuracy requirements are not too great. Microprocessor compensation has not been extensively used to date because of economic considerations. It appears to have considerable potential, however, since the cost of integrated-circuit components continues to fall. Advantages in accuracy over digital compensation may also be possible by the use of programs to compensate for secondary effects. It can be shown (Frerking, 1979) that the cost of the A/D and D/A converters is minimized if the number of bits in the A/D converter is chosen to be

$$b_t = \log_2 \frac{1}{2(\Delta f/f)}\left(ST + \sqrt{ST\left(\frac{\Delta f}{f}\right)}\right) \tag{9-9}$$

and the number of bits in the D/A converter is chosen to be

$$b_v = \log_2 \frac{(\Delta f/f)_m}{2(\Delta f/f)}\left(1 + \sqrt{\frac{ST}{(\Delta f/f)}}\right), \tag{9-10}$$

assuming that the combined cost of the two converters is proportional to

$$C = 2^{b_t} + 2^{b_v}. \tag{9-11}$$

Each of the techniques for compensation described in this chapter depends on the crystal and oscillator to produce the same temperature curve regardless of the past thermal history of the crystal. In practice, crystals tend to exhibit a certain degree of hysteresis, which becomes troublesome as the required accuracy of the compensation is increased. It is not unusual to select crystals for low hysteresis to produce TCXOs with specifications in the region of a few parts per 10^7 or better. Even in the part-per-million range hysteresis can be troublesome for some manufacturing techniques.

Temperature-compensated crystal oscillators are susceptible to frequency excursions as a result of rapid temperature transients, making them unsuitable for some applications. It should also be noted that the compensation voltage tends to become slightly mismatched with the crystal TC curve after significant frequency adjustments for aging (Galla and McVey, 1980). This phenomenon can usually be minimized by using crystals with a low aging rate.

Temperature compensation has been widely used because of its small size and low power consumption as well as the absence of a warm-up stabilization period. Aging rates less than 1 ppm/yr have been achieved in many units, and typical aging of a few parts per 10^7 per year after the first year is common for units with well-processed crystals.

10 Microwave Frequency and Time Standards

Helmut Hellwig

Frequency and Time Systems, Inc.
Beverly, Massachusetts

List of Symbols 114
10.1 Concepts, Design, and Performance 115
10.1.1 Historical Perspective 115
10.1.2 Concept of an Atomic Resonator 116
10.1.3 Design Principles 119
10.1.4 Performance Principles 123
10.1.5 Active and Passive Electronic Systems 125
10.1.6 Phase-Lock Servos 128
10.1.7 Frequency-Lock Servos 128
10.1.7.1 Fast Modulation 130
10.1.7.2 Offset in Mixer Output and Input to Integrator 131
10.1.7.3 Distortion in FM 131
10.1.7.4 Square-Wave Frequency Modulation 132
10.1.7.5 Higher-Harmonic Locks 132
10.1.8 Electronic Systems 133
10.2 Passive Beam Standards 137
10.2.1 Beam Generation 137
10.2.2 Spatial State Selection 138
10.2.3 Microwave Interrogation 139
10.2.4 Detection of Atoms 142
10.2.5 The Cesium-Beam Standard 143
10.2.6 Other Passive Beam Standards 148
10.2.7 New Horizons 149
10.3 Gas-Cell Standards 150
10.3.1 Gas-Cell Principles 150
10.3.2 Optical State Selection 152
10.3.3 The Rubidium Gas-Cell Standard 153
10.3.4 Other Gas-Cell Standards 157
10.3.5 New Horizons 158
10.4 Hydrogen Masers 159
10.4.1 Hydrogen-Maser Principles 159
10.4.2 Active and Passive Masers 161
10.4.3 Frequency Stability and Accuracy 163
10.4.4 Other Masers 165
10.4.5 New Horizons 166

PRECISION FREQUENCY CONTROL
Volume 2
Oscillators and Standards

Copyright © 1985 by Academic Press, Inc.
All rights of reproduction in any form reserved.
ISBN 0-12-280602-6

10.5 Other Microwave Frequency Standards 169
10.5.1 The Ammonia Maser 169
10.5.2 Trapped Ions 169
10.6 Comparison of Frequency Standards 171
10.7 Applications 171
10.7.1 Metrology and Science 171
10.7.2 Technology 175

LIST OF SYMBOLS

b	Amplitude of driving field
c	Speed of light
E	Electric field
F	Hyperfine-energy-level quantum number
g	Gyromagnetic ratio
h	Planck's constant
$\hbar$	$h/2\pi$
B	Magnetic flux density
I	Nuclear spin quantum number
J	Electron spin quantum number
K_1	Second-order Zeeman coefficient
K_2	First-order Zeeman coefficient (microwave resonance)
K_3	First-order Zeeman coefficient (low-frequency resonance)
k	Wave vector ($k = (2\pi/c)\nu$)
L	Length of interaction region (between microwave field and atoms)
m	Atomic orientation (magnetic) quantum number
M	Atomic mass
n	Number of events
Q	Quality factor ($Q = \nu/\Delta\nu$)
Q_c	Quality factor of microwave cavity
Q_l	Quality factor of atomic resonance
S	Signal level
S_R	Signal-to-noise ratio
t	Time
T	Absolute temperature
v	Atomic velocity
V	Voltage
W	Energy (of an atomic energy level: ΔW is the energy separation)
x	Magnetic field parameter [$x = (g_J - g_I)\mu_0\pi/\Delta W$]
y	Fractional frequency
$\Delta\nu_l$	Linewidth
$\Delta\nu_m$	Amplitude of frequency modulation
ν_M	Magnetic-field-dependent atomic resonance frequency
ν_0	Nominal frequency
ν_R	Atomic resonance frequency
i	Number of events per unit time

μ_0	Bohr magneton
ϕ	Phase angle
$\sigma_y^2(\tau)$	Two-sample (or Allan) variance
τ	Sample (or averaging) time
ω	Angular frequency ($\omega = 2\pi\nu$)

10.1 CONCEPTS, DESIGN, AND PERFORMANCE

10.1.1 Historical Perspective

Atomic and molecular beam physics, which began with the experiment of O. Stern and W. Gerlach in 1921, is the foundation of today's atomic time and frequency standards. I. I. Rabi's (1937) idea to use an oscillator-driven magnetic field to induce transitions led to successful atomic beam resonance experiments by J. Zacharias, P. Kusch, J. M. B. Kellog, and N. Ramsey between 1938 and 1940. Today's atomic cesium-beam frequency standards are strikingly similar to these first atomic beam devices.

The idea of atomic clocks, that is, clocks based on natural resonance phenomena in atoms and molecules, was actively studied after World War II when the necessary microwave technology became widely available. At that time accuracies in the 10^{-9}–10^{-10} range were predicted. For the first time it appeared possible to build a clock better than the rotating earth. Working experimental devices based on the ammonia molecule and the cesium atom were built and tried.

In the mid-1950s it was experimentally shown that cesium devices were indeed usable as clocks surpassing the performance of astronomical clocks (Essen and Parry, 1956). This ultimately led to an international agreement and the redefinition of the second as the duration of 9,192,631,770 periods of the radiation corresponding to the transition between the two hyperfine levels of the ground state of the cesium-133 atom. The first quantum electronic oscillator was the ammonia maser, built in 1954 by E. Gordon, H. Zeiger, and C. Townes. It was relegated to a place in history by the atomic hydrogen maser, built and operated for the first time in 1960 by M. Goldenberg, D. Kleppner, and N. Ramsey.

Other atoms than ammonia, cesium, and hydrogen and techniques different than atomic beams have had an impact on the development of atomic clocks. Optical pumping, developed by A. Kastler in 1950, led to the development of the rubidium gas-cell frequency standard. The resonances of cesium, rubidium, and hydrogen in the microwave region have dominated the atomic time and frequency standard field since they matured in the 1960s. In fact, rubidium and cesium standards have now been commercially available for two decades (Hellwig, 1975; Ramsey, 1972) and have undergone numerous

improvements and refinements. The 1960s saw refinements in atomic clock design and the use of atomic clocks in many scientific applications and in metrology, including the generation of time on a worldwide basis. The 1970s were characterized by fundamental physical and design breakthroughs and the beginning of large-scale system use of atomic time and frequency standards reaching far beyond scientific studies, making possible today's communication and navigation systems.

10.1.2 Concept of an Atomic Resonator

An atomic time and frequency standard consists of three elements: the external interfaces, the electronic systems, and the atomic resonator. The atomic resonator is the heart of the atomic standard and serves the same function as the pendulum in a mechanical clock, with one most fundamental difference: the atomic resonance frequency itself is determined by nature; it will not drift, nor will it age according to all of our present experimental and theoretical knowledge. Furthermore, all atoms of a given elemental type are the same; thus, atoms operating in a frequency standard today will give precisely the same performance as atoms to be used tomorrow. A standard built independently from another standard will show the same characteristics and the same frequency as its predecessors or as standards in different locations. Atomic clocks feature an a priori accuracy; therefore, atomic clocks and frequency standards are often called primary standards.

The frequency of the emitted or absorbed radiation is related to the energy difference between the two atomic energy levels being used. In the three alkali atoms which are most prominently in use today (as they have been for several decades), hydrogen, rubidium, and cesium, the magnetic hyperfine transition in the ground state ($^2S_{1/2}$) is being used. Table 10-1 shows a summary of these three standards and their characteristic frequencies. The transitions occur between energy levels that are created by the spin–spin interaction between the atomic nucleus and the outer electron in the ground state of the atom. As such, the separation of the two energy levels, that is, the transition frequency, is a function of the magnetic field. This dependency is described by the Breit–Rabi equation (Ramsey, 1956),

$$W_{F,m_F} = \frac{-\Delta W}{2(2I+1)} + \mu_0 g_I m_F B_0 \pm \frac{\Delta W}{2}\left[1 + \frac{4m_F x}{(2I+1)} + x^2\right]^{1/2}, \quad (10\text{-}1)$$

where ΔW is the hyperfine separation in zero field ($\Delta W = h\nu_R$) between the states $F = I + \frac{1}{2}$ and $F = I - \frac{1}{2}$, x the magnetic field parameter $(g_J - g_I)\mu_0 B_0/\Delta W$, μ_0 the Bohr magneton, h Planck's constant, $\nu_R = \Delta W/h$ the resonance frequency, I the quantum number of the nuclear spin, m_F the quantum number characterizing the orientation in the magnetic field, and g_I and g_J the g factors and m_I and m_J the magnetic quantum numbers of the nucleus and electron, respectively. Transitions follow the quantum mechanical selection rules of $\Delta F = 0, \pm 1$; $\Delta m_F = 0, \pm 1$. Since minimizing magnetic perturbations is essential for high-performance clock operations, the clock transition is characterized by $\Delta F = 1, \Delta m_F = 0$. (This transition is sometimes called the sigma transition and the $\Delta m_F = \pm 1$ transitions are called π transitions, but these names are not in accordance with the normal designations of atomic physics.)

TABLE 10-1

Summary of the Most Widely Used Atoms in Atomic Clocks

Atom	Atomic mass	Nuclear spin	ν_R (Hz)
Hydrogen (H)	1	1/2	1,420,405,752
Rubidium (Rb)	87	3/2	6,834,682,608
Cesium (Cs)	133	7/2	9,192,631,770

There are two consequences that result from the fact that magnetic dipole transitions are used: the first relates to the sensitivity of the transition frequency with respect to the magnetic field in which the atom is imbedded; the second is the fact that forces are exerted on atoms in an inhomogeneous magnetic field. We shall discuss both of these effects in more detail later. In order to define the precise resonance frequency, the external magnetic field has to be well defined and must usually be kept constant. This necessitates magnetic shielding, which is a characteristic design feature of all presently used atomic frequency standards. The shielding can be quite elaborate; it reduces the external magnetic fields, foremost the earth's magnetic field, to 1% or less of its normal value. It is obvious that only the $\Delta m_F = 0$, the so-called clock transition, can provide highly stable reference frequencies. The probability for this transition must be maximized, and the corresponding probabilities for all other magnetic-field-dependent transitions must be minimized. This is done by applying a constant magnetic field, the C field.[§] In order to force the $\Delta m_F = 0$ transition, the magnitude of the C field is typically at least an order of magnitude above all anticipated residual field components, and its orientation is such that its vector is parallel to the vector of the oscillating magnetic field that is coupled to the resonance of the atom. The resulting frequency shift can range up to parts per 10^9 of the frequency of the atom in a zero magnetic field.

[§] The name "C field" originates from naming the three fields necessary in a magnetic resonance experiment (Ramsey, 1956) where, in addition, A and B fields have to be applied corresponding to the state-selecting magnetic fields. This will be discussed later.

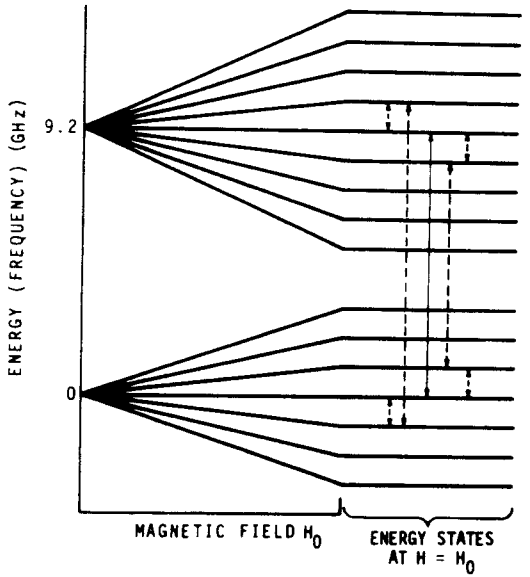


FIG. 10-1 Magnetic field dependence of the hyperfine energy levels (nine in the upper state, seven in the lower state) in the ground state of the cesium atom. Energy is plotted as frequency; the magnetic field is plotted up to the value H_0. The solid arrow represents the "clock" transition; the dashed arrows depict the magnetic-field-sensitive (Zeeman) transitions.

The magnitude of the field can be measured quite precisely, to an accuracy that is much better than required in view of all other frequency-stability limitations. Such a measurement is done by using the atom itself as the magnetometer. In Fig. 10-1, which illustrates the hyperfine energy levels of cesium for regions of relatively low magnetic field (Mockler, 1961), the clock transition is indicated by the solid line. The magnetic flux density B can then be measured precisely by measuring the magnetic-field-dependent or Zeeman resonances at higher or lower frequencies, as indicated by the dashed lines between the energy levels. The corresponding magnetic field dependencies are given by the following equations (ν and f are in hertz, B is in tesla) for the shift in the clock transition,

$$\begin{aligned} \nu - \nu_0 &= K_1 B^2, \qquad \text{Rb}{:}K_1 = 5.73 \times 10^{10}, \\ \text{H}{:}K_1 &= 27.5 \times 10^{10}, \qquad \text{Cs}{:}K_1 = 4.27 \times 10^{10}; \end{aligned} \tag{10-2}$$

for the magnetic-field-dependent resonance,

$$\begin{aligned} \nu_M - \nu_0 &= K_2 B, \qquad \text{Rb}{:}K_2 = 1.4 \times 10^{10}, \\ \text{H:none}, \qquad \text{Cs}{:}K_2 &= 0.7 \times 10^{10}; \end{aligned} \tag{10-3}$$

and for the low-frequency resonance,

$$\begin{aligned} f_M &= K_3 B, \qquad \text{Rb}{:}K_3 = 0.7 \times 10^{10}, \\ \text{H}{:}K_3 &= 1.4 \times 10^{10}, \qquad \text{Cs}{:}K_3 = 0.35 \times 10^{10}. \end{aligned} \tag{10-4}$$

It should be noted that we can measure a magnetic flux density B by measuring at microwave frequencies ($\nu_M - \nu_0$) or, alternately, by injecting a low-frequency f_M. The field H can be calculated and the proper frequency-shift correction and zero-field clock transition can be calculated using the first of the above equations.

The number of magnetic sublevels is determined by the quantum number $F = I \pm \frac{1}{2}$, where I is the nuclear spin. The projection of F on the external magnetic field is an integer. This yields the quantum number m_F. Thus, each F level has $2F + 1$ sublevels, with the $m_F = 0$ state being the centrally located one. As a result of the fact that hydrogen has a nuclear spin of $I = \frac{1}{2}$ and therefore has no magnetic hyperfine splitting in the $F = 0$ state, the magnetic-field-dependent resonance $\nu_M - \nu_0$ does not exist in the case of hydrogen. If a precise calculation of the magnetic-field-induced frequency shift in the clock transition is called for, Eqs. (10-4) or, more precisely, the K factors are insufficient. The Breit–Rabi equation must be solved exactly for this case, and higher-order terms in H must be included. With increasing magnetic fields, the magnetic coupling between the nuclear spin and the electron spin weakens until the high-field condition is achieved, where F is no longer a good quantum number but rather I and the electron spin are quantized separately in the external magnetic field. Again, the Breit–Rabi equation describes the total range and is graphically depicted for cesium in Fig. 10-2. At high fields, therefore, we have approximately a constant magnetic dipole moment with a positive sign for eight of the nine magnetic sublevels of the upper state and a negative sign for all seven of the magnetic sublevels of the lower state plus the one remaining (lowest) sublevel of the upper state.

As is well known, a magnetic dipole moment μ causes a force to be exerted on the carrier particle. This force is given by $F = \mu \operatorname{grad} B_0$. Since, strictly speaking (and as shown in Fig. 10-2), the magnetic dipole moment is not a constant but is dependent on the magnetic field itself, μ_{eff} is used in the above equation. The fact that this force exists was discovered in the first beam experiments of Stern and Gerlach using spatial state selection, and it is still the basis for all atomic beam machines.

10.1.3 Design Principles

Atomic frequency standards are fundamentally devices that allow the measurement of a microwave frequency with very high resolution and accuracy. The fundamental limitation to high-precision spectral measurements

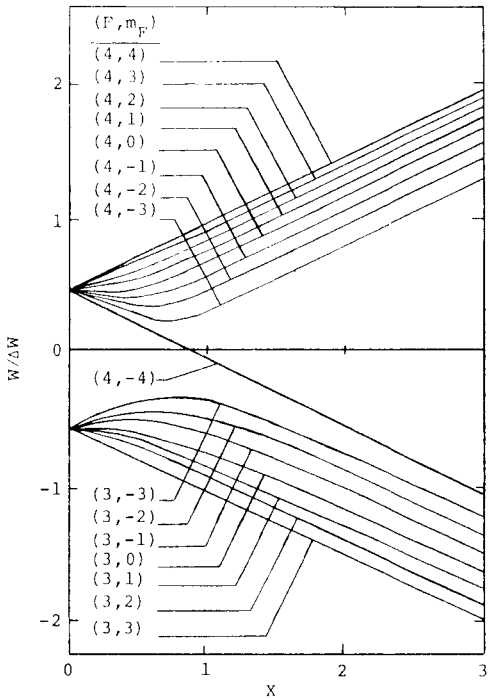


FIG. 10-2 Energy-level diagram of ^{133}Cs in the $^2S_{1/2}$ ground state as a function of the applied magnetic field. The energy W is normalized to the hyperfine separation ΔW. The dependence plotted is according to the Breit–Rabi equation. F is the hyperfine quantum number; the magnetic quantum numbers of the electron, nucleus, and atom are m_J, m_I, and m_F, respectively.

is the first-order Doppler effect. A moving atom sees a frequency shift $\Delta f/f = \pm v/c$. The Dopler effect represents perhaps the most important problem limiting the accuracy and resolution of frequency standards. In the usual way we can say that if an absorber of radiation moves relative to the source, the observed resonance frequency is shifted to the value (Hellwig *et al.*, 1978)

$$\omega_{\text{abs}} \simeq \omega_0 + \mathbf{k}\cdot\mathbf{v} - \tfrac{1}{2}\omega\left(\frac{v}{c}\right)^2 + \frac{\hbar\omega^2}{2Mc^2}, \tag{10-5}$$

where the velocity $\mathbf{v}$ and wave vector $\mathbf{k}$ are measured relative to the source. The first-order Doppler shift ($\mathbf{k}\cdot\mathbf{v}$), the second-order Doppler shift $\frac{1}{2}(v/c)^2$, and the recoil shift (the last term, where M is the atomic mass) can be understood in terms of conservation of energy and momentum in the emission or absorption process. Specifically, the so-called second-order Doppler shift is merely the

relativistic time-dilation factor resulting from the movement of the atom relative to the apparatus. Its effect is small but ultimately important. We can describe the first-order Doppler shift in terms of the time dependence of an ordinary electromagnetic wave as seen by an atom. We have for the oscillating electromagnetic field,

$$E(x, t) = E_0 \sin(\mathbf{k}\cdot\mathbf{x} - \omega t + \phi), \tag{10-6}$$

where $\mathbf{x}$ is the atom position, $\mathbf{k}$ the field wave vector, and ϕ an arbitrary phase vector. If $\mathbf{x} = \mathbf{v}_x t$, that is, the particle is moving with velocity v in the x direction, then

$$E(t) = E_0 \sin[(\mathbf{k}\cdot\mathbf{v}_x - \omega)t + \phi] \tag{10-7}$$

and the atom sees a sinusoidally varying field of frequency $\omega' = \omega - \mathbf{k}\cdot\mathbf{v}_x$.

Typically, the atoms in a sample, say, in a gas cell, have velocities in all spatial directions and a Maxwellian velocity distribution. The result is the familiar Doppler broadening that leads to a distribution of ω values. The width of the corresponding distribution of frequencies, that is, the full Doppler broadening, is then directly related to the mean velocity of the atoms. As a result, for room-temperature atoms which, for atomic weights of around 100, have a mean velocity of about 300 m/sec, we have for the fractional linewidth $\Delta\nu/\nu_0 \simeq 10^{-6}$. In summary, the first-order Doppler effect in a normal sample of atoms causes a fractional linewidth of about 1 ppm and systematic frequency shifts, depending on preferential directions of electromagnetic energy flow, of up to 1 ppm. We define Q as the quality factor of the resonance, where $Q = \nu_0/\Delta\nu$. Atomic frequency standards are thus characterized by extremes in the reduction of the first-order Doppler effect in terms of Doppler broadening and systematic Doppler frequency shifts as well as in terms of maximizing the line Q. In principle, the reduction of the first-order Doppler effect is achieved by confining the atom within a number of dimensions x less than k^{-1}. Such a condition is called the *Dicke regime*. Figure 10-3 shows the resulting spectral narrowing of the resonance spectrum, which now has a sharp central feature with a linewidth corresponding to the natural linewidth (see below). This effect, first noted experimentally by Lamb in 1939, was discussed and explained in an important paper by Robert Dicke (Dicke, 1953).

It is quite interesting to note that the Dicke regime has also been realized in the optical as well as in the gamma-ray region of the spectrum, where it is the basis for the Mössbauer effect; as in the microwave case, the photon recoil momentum is transferred to the whole lattice and therefore does not appear as a frequency shift, allowing highly precise measurements. Earlier, the term "natural linewidth" was used. This normally refers to the emission of visible light, where the natural linewidth describes the spectral linewidth associated with an optical transition. Lifetimes of optical transitions can be calculated

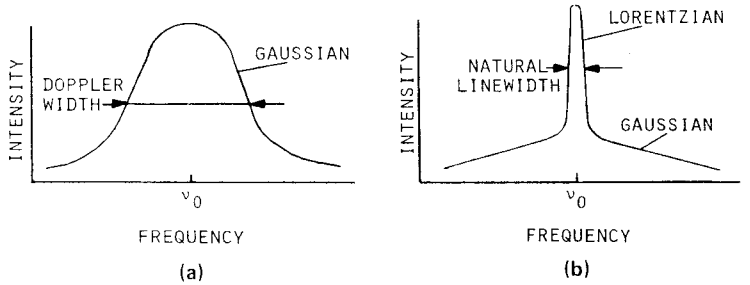


FIG. 10-3 Spectrum of an atomic transition. (a) The situation when the atoms are unbound and the resonance feature has the full Doppler width $\Delta\nu_0 \approx (v/c)\nu_0$. (b) When the atom is confined to dimensions less than the wavelength, the Doppler profile is suppressed and the central feature has the natural linewidth $\Delta\nu$.

from quantum mechanics using Planck's equation for the blackbody radiator, yielding average lifetimes in the nanosecond region. The lifetime in a given state is proportional to the frequency cubed; thus, at microwave frequencies we are faced with natural lifetimes of the states involved on the order of hundreds of seconds.

Heisenberg's uncertainty relationship gives $\Delta W\,\Delta t \geq h/2$, where ΔW is the energy uncertainty and Δt the conjugate uncertainty in time. Since $\Delta W = h\,\Delta\nu$, where h is Planck's constant, we obtain from this uncertainty relationship the linewidth $\Delta\nu$. Natural transition times of hundreds of seconds, therefore, yield very small fractions of a hertz as $\Delta\nu$. In other words, the natural linewidth is unmeasurably small in the microwave region as compared to other limitations on Δt or $\Delta\nu$. As a consequence, one may interpret for microwave frequency standards that Δt is the observation time allowed by the frequency-standard apparatus or atomic resonator to coherently observe the atomic radiation. In general, this lifetime is limited by either of two general effects: the atom enters and leaves the apparatus after a time Δt, or the atom stops oscillating due to a collision with other atoms or with the walls of the container after a time Δt. Thus, atomic frequency standards are characterized by maximizing Δt and, with it, the line Q.

In summary, the basic design principles of atomic resonators are the confinement of the atom to well within a wavelength of the electromagnetic radiation and the principle of maximizing the coherent observation time, that is, confinement of the atoms in an unperturbed radiating state for as long as possible. In the microwave region, the natural lifetime of the atomic state is so long that the designer does not worry about this as a limitation. This is in contrast to the situation found at optical frequencies, where metastable states are needed to have lifetimes sufficient to take advantage of available confinement techniques.

Fundamentally related to this, again via Planck's equation, is the fact that the population difference between the two levels separated by microwave frequencies is very small. The population difference is a function of ν. In the low gigahertz region, where $h\nu \ll kT$, the population difference is only a very small fraction of 1%. Thus, in a natural ensemble, that is, in a gas, the total number of upper-state atoms is nearly equal to the total number of lower-state atoms. This has an important consequence. If this gas is placed in an external magnetic field that oscillates at the atomic resonance frequency, all atoms will undergo transitions. However, approximately half of the atoms receive (absorb) energy from the field; the other half emit (add) energy of an equivalent amount to the field. Thus, it is obvious that the net effect is essentially zero. The gas as a whole acts as if it has no resonance, although the individual atoms do resonate. In order to observe the atomic resonance, it is therefore a common design principle in microwave frequency standards to modify the population in the upper and the lower state. One or the other has to be significantly depopulated. The result is an atomic ensemble that either has a significant net emission or net absorption of energy. The way in which this is accomplished is a significant determinant in the design of an atomic resonator.

In summary, the design of an atomic resonator is characterized by the particular method of maximizing the coherent observation time, minimizing first-order Doppler effects, and achieving a significant net population difference between the two microwave energy levels.

10.1.4 Performance Principles

Time and frequency standards can be characterized in numerous ways. However, most frequently a time-domain characterization is most lucid and useful. The quantity measured (Barnes *et al.*, 1971) is the two-sample (or Allan) variance $\sigma_y^2(\tau)$, defined as

$$\sigma_y^2(\tau) = \langle \tfrac{1}{2}(\bar{y}_{k+1} - \bar{y}_k)^2 \rangle, \tag{10-8}$$

where y is the fractional frequency of adjacent measurements, each with a sample time τ. The brackets $\langle\ \rangle$ denote an infinite time average.

An idealized presentation (Hellwig, 1975) for all precise time and frequency standards is shown in Fig. 10-4. Part I of the stability plot can be characterized by the equation $\sigma_y(\tau) = k_1\tau^{\alpha_1}$. It is determined by the fundamental noise processes present in the standard. Part II is called the flicker of frequency floor, which describes an independence of $\sigma_y(\tau)$ from the averaging time. We shall call this value σ_{yF}. Its level depends on the particular frequency standard and its physical basis is not fully understood but relates to fluctuations in the value of critical, frequency-determining parameters of the standard. Section III can be characterized by $\sigma_y(\tau) = k_2\tau^{\alpha_2}$. The coefficients k_2 and α_2 cannot

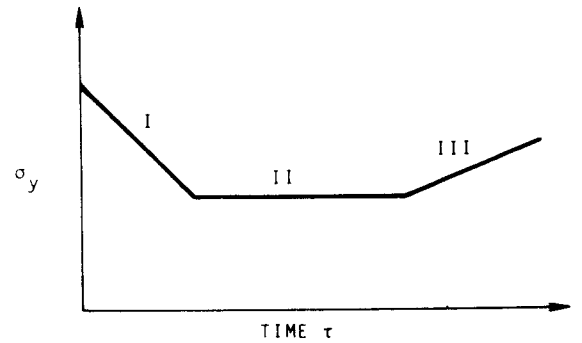


FIG. 10-4 Typical frequency stability behavior of a frequency standard. The two-sample or Allan variance is $\sigma_y^2(\tau)$. I: $\sigma_y \sim \tau^{-1}$, white or flicker-of-phase noise; $\sigma_y \sim \tau^{-1/2}$, white frequency noise. II: σ_y = constant, flicker "floor" (flicker-of-frequency). III: $\sigma_y \sim \tau^{\alpha}$; $0 \leq \alpha \leq 1$, typical; $\alpha = 1$, pure frequency drift (aging).

usually be determined very accurately because of the long measurement times needed in order to obtain statistical confidence. These coefficients are largely subject to environmental effects and thus are not stable. If linear frequency drift is present, $\alpha_2 = +1$. Of course, drift is always caused by some systematic change in a frequency-determining parameter with time. In contrast, regions I and II have more quantifiable physical relationships. The approximate relationship between frequency stability in region I and the signal-to-noise ratio available in the device can be given by $\sigma_y(\tau) \simeq (QS_R)^{-1}$, where S_R is the signal to noise ratio which, of course, is a function of the sampling time τ. The quality factor of the resonance line enters as a key determining factor: the larger the Q, the better the stability. However, Q and S_R can be traded against one another. A device with a relatively low Q and a large S_R gives the same short-term stability performance as a device with a high Q and a low S_R. The ratio S_R can be expressed in terms of physical parameters of the atomic resonators, which typically are shot-noise limited: if i is the number of signal events per unit time, $S_R = \sqrt{i\tau}$.

In order to achieve excellence in region I, the number of signal events per unit time as well as the resonance Q must be maximized. The stability performance then improves as $\tau^{-1/2}$ (if shot-noise limited) or as τ^{-1} (if white-phase-noise limited). The flicker floor (σ_{yF}), region II in Fig. 10-4, is fundamentally related to the Q value of the resonance. Qualitatively, this is not surprising. Atomic resonators with Q values of 10^8 or higher may be expected to have accuracies of one part per 10^8 or better because the linewidth is acting as an ultimate limit on the variability of the frequency of the resonance. It appears that the Dicke limit forms the actual limitation for σ_{yF}, that is, the ultimate stability limit or accuracy of the device appears to be governed by the

atomic resonator Q. The result is a speculative relationship $\sigma_{yF} = 1/CQ^m$, where C is a constant of order 10^6 and m an integer of order unity (Hellwig, 1979).

In the following detailed discussions of atomic frequency standards, we will see that in all cases the Q value of a resonator is the scale factor (or multiplier) for almost all perturbing effects on the frequency of the atomic resonator. We can summarize thusly: a high resonator Q is essential to achieve high accuracy and ultimate stability. Thus, the time-keeping potential of an atomic clock is governed by the Q value and not by the signal-to-noise ratio. The signal-to-noise ratio is only important to assure sufficient short-term frequency stability so that measurement periods of acceptably short duration are needed to realize the available accuracy. As a practical guideline, the maximum reasonable sampling time to achieve ultimate measurement precision or accuracy (realizing σ_{yF}) may be taken as 10^4. Using this experimental guideline and the above empirical equation for σ_{yF} and combining it with the equation for $\sigma_y(\tau)$, we can easily calculate an empirical guideline for the number of signal events per unit time, n. We find that $n \approx 10^8$, independent of the resonator Q. Increased resonator Q leads to increased accuracy and long-term stability only as long as the atomic signal intensity is maintained at $n = 10^8$ events/sec or better. Frequency-standard concepts and designs are thus based on the following four principles:

(1) minimized Doppler shifts and line broadening,
(2) freedom from perturbations, that is, a free atom,
(3) as high a line Q as possible, and
(4) as high a signal-to-noise ratio as possible but not less than 10^8 signal events/sec.

Unfortunately, these four principles are mutually contradictory. Thus, the actual performance of an atomic resonator is a compromise. For example, the obvious ideal situation is a single atom at rest in free space observed for an infinite length of time. This would fulfill three of the above requirements but the signal-to-noise ratio would be zero and thus not yield a useful standard.

10.1.5 Active and Passive Electronic Systems

The basic purpose of the electronics of an atomic clock is to provide an oscillatory output signal that is both accurate and stable in time. Atomic-based oscillators have the desirable features of high Q and relative insensitivity to environmental factors to give good stability. They also carry their own internal calibration, that is, the resonance frequency is identical for all atoms of the same species, and therefore they provide accuracy. However, at some level the environment affects the observed resonance frequency and therefore

the electronics must reduce the effects of this environment to yield high accuracy and stability.

Auxiliary functions must also be provided, and therefore the complete electronics must include

(1) a reference oscillator,
(2) cavity control,
(3) servo electronics to control the reference-oscillator output frequency,
(4) synthesizers and multipliers,
(5) temperature control,
(6) provision for a good magnetic environment (magnetic field supplied by stable current plus magnetic shielding), and
(7) other electronics such as power supply and logic.

As is common practice, it is useful to make a distinction between two types of electronic principles.

(1) *Active maser oscillator.* In the maser oscillator the power for the oscillator is provided by the atoms themselves (e.g., atomic hydrogen maser). For reasons outlined below it is desirable to lock a reference oscillator (e.g., a crystal oscillator) to the maser oscillator. Therefore two oscillators are actually present in the configuration.

(2) *Passive atomic standard.* In this configuration the interrogating frequency for the atomic resonator is provided externally (e.g., by the multiplied output of the reference oscillator). In this case the atoms act as a frequency discriminator or passive filter to which the reference oscillator is locked.

In principle, a reference oscillator is not necessary in the case of a maser oscillator. One could think of merely synthesizing the desired output frequency from the output of the maser. The reason this is not done is that in general a high spectral purity (good short-term stability) is desired in the output of the device; a reference oscillator is used to give good short-term stability and is locked to the master oscillator in order to give good long-term stability and accuracy. The same philosophy governs the design of a passive atomic oscillator. Qualitatively, in both cases it is desirable to lock the reference oscillator to the atomic resonance in a time approximately equal to the time when the stability of the reference oscillator becomes worse than the stability provided by the atomic resonance (Walls and Stein, 1976).

The choice of reference oscillator and reference-oscillator frequency is in principle arbitrary but in practice is determined by the cost and availability of suitable reference oscillators. Quartz crystal oscillators have been the best choice for many years; the performance of these oscillators has been optimized at frequencies from 5 to 10 MHz and, therefore, they have been used almost exclusively in atomic clock oscillators.

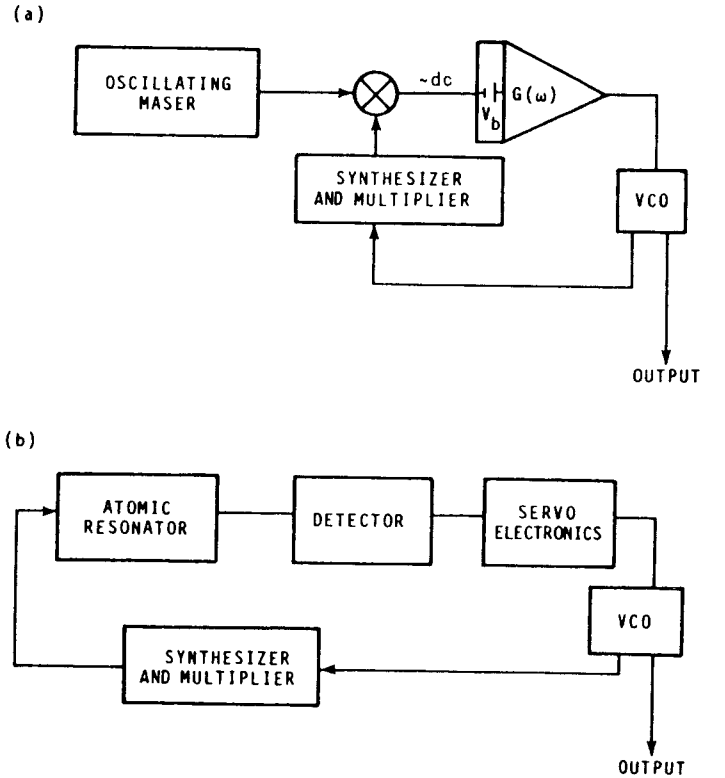


FIG. 10-5 Simplified block diagram for frequency servo electronics: (a) for a maser oscillator, (b) for a passive atomic standard.

Finally, the reference oscillator must be tunable. It is, of course, desirable to make it voltage tunable; this is usually accomplished by coupling a varactor to the oscillator. We can therefore call the reference oscillator a voltage-controlled (crystal) oscillator (VCO or VCXO).

Figure 10-5 depicts the general concept of the overall design of an atomic standard where the atomic resonator serves as the frequency reference for a slave oscillator (usually a quartz crystal) in a servo-loop configuration.

The basic goal of the frequency servo electronics is to steer the reference oscillator so that its output is related to the atomic resonance frequency in an unambiguous way. For simplicity, we shall assume that the frequency of the reference oscillator is a subharmonic of the atomic frequency. In practice a synthesizer is usually incorporated into the system so that the frequency of the reference oscillator is nominal (e.g., 5 MHz).

10.1.6 Phase-Lock Servos

In general, direct phase comparison is used to lock one oscillator to another. It is used in the maser oscillator to lock the reference oscillator to the output of the maser. Referring to Fig. 10-5a, we assume that the signal from the maser oscillator is given by $A\cos\omega_0 t$, where $\omega_0 = 2\pi\nu_0$ and ν_0 is the atomic resonance frequency. We assume the frequency of the reference is near that of the maser, and we therefore write the reference signal as $B\sin[\omega_0 t + \phi(t)]$, where $\dot{\phi} \ll \omega_0$. To first order the output of the mixer gives a signal V_0 proportional to the two input signals multiplied together. We have

$$\begin{aligned} V_0 &= 2C\sin[\omega_0 t + \phi(t)]\cos\omega_0 t + D \\ &= C\{\sin[2\omega_0 t + \phi(t)] + \sin\phi(t)\} + D, \end{aligned} \tag{10-9}$$

where C is a function of A, B, and the mixer efficiency and D is an offset term that depends on A and B and mixer asymmetries. These asymmetries may depend on environmental parameters such as temperature. Only terms near dc are important; therefore, the first term (near 10 MHz in most cases) is easily filtered. The voltage V_0 is then a sinusoidal function of $\phi(t)$ that can be used to servo the reference oscillator (VCO) to the frequency of the maser. This can be accomplished with the scheme shown in Fig. 10-5a; V_b is the equivalent input offset voltage of the feedback amplifier. This amplifier serves to amplify the error voltage V_0 and therefore steer the VCO so that its output frequency coincides with that of the maser. If the gain $G(\omega)$ is very high near dc, then the voltage at the input to the amplifier is driven to zero, so that $\phi(t) \simeq -(D + V_b)/C$. As an example, if the mixer efficiency is $C = 3$ mV/deg, then a change in D or V_b as large as 1 mV gives a change in phase of 0.3° at 5 MHz. This corresponds to a change of $0.3°/(360° \times 5 \times 10^6) = 0.17$ nsec. Therefore, offset problems are usually solved easily using phase-locked loops.

10.1.7 Frequency-Lock Servos

Frequency-lock servos, as depicted in Fig. 10-5b, are used in passive atomic clocks (e.g., cesium-beam and rubidium gas cells) to steer the frequency of the reference oscillator so that it coincides with that of the atomic transition. The atomic resonator behaves similarly to a simple bandpass filter followed by a square-law detector. Therefore, in the following we will assume that the *lineshape* of the detected signal $S(\omega)$ versus applied rf frequency is Lorentzian, that is,

$$S(\omega) = S_0[1 + (\nu - \nu_0)^2/\Delta\nu_l^2]^{-1}, \tag{10-10}$$

where ν_0 is the atomic frequency, $\Delta\nu_l$ the linewidth, and ν the frequency of the source (multiplied reference oscillator). The signal $S(\omega)$ is plotted in Fig. 10-6.

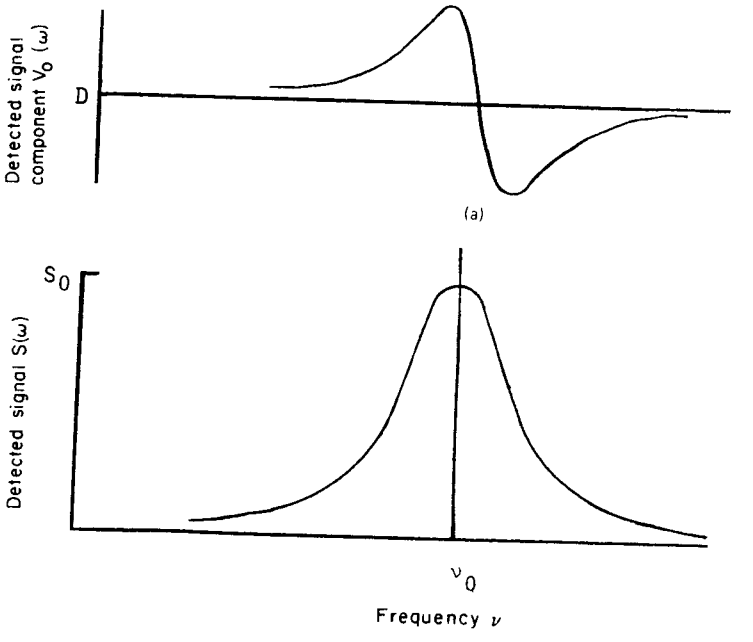


FIG. 10-6 Plot of atomic resonance feature assuming a Lorentzian lineshape. (a) The detected signal component $V_0(\omega)$ (at modulation frequency ν_m), where ω is the rf frequency in the vicinity of the atomic resonance. (b) The detected signal $S(\omega)$.

Some devices do not exhibit such line shapes; however, the results discussed below still apply qualitatively. We can use the $S(\omega)$ curve as a frequency discriminator; one common way is to use sine-wave frequency modulation (FM) on the source. Figure 10-7 is a more detailed block diagram of the principle shown in Fig. 10-5b. For sine-wave FM, $\nu = \nu_s + \Delta\nu_m \sin\omega_m t$, where ν_s is the source frequency, $\Delta\nu_m$ the FM swing, and $\omega_m = 2\pi\nu_m$ the modulation frequency.

If we assume $\omega_m/2\pi \ll \Delta\nu_l$ (the *steady-state* approximation), then the resulting signal is given by

$$S(\omega) = S_0[1 + (\Delta\nu_m \sin\omega_m t + \nu_s - \nu_0)^2/\Delta\nu_l^2]^{-1}, \tag{10-11}$$

where ν_s is the frequency of the interrogating signal.

If $\Delta\nu_m \ll \Delta\nu_l$, then the sinusoidal component of $S(\omega)$ at frequency ω_m is given by

$$S(\omega) = -\frac{2\,\Delta\nu_m \sin\omega_m t S_0(\nu_s - \nu_0)}{(\Delta\nu_l)^2\{1 + [(\nu_s - \nu_0)/\Delta\nu_l]^2\}^2}. \tag{10-12}$$

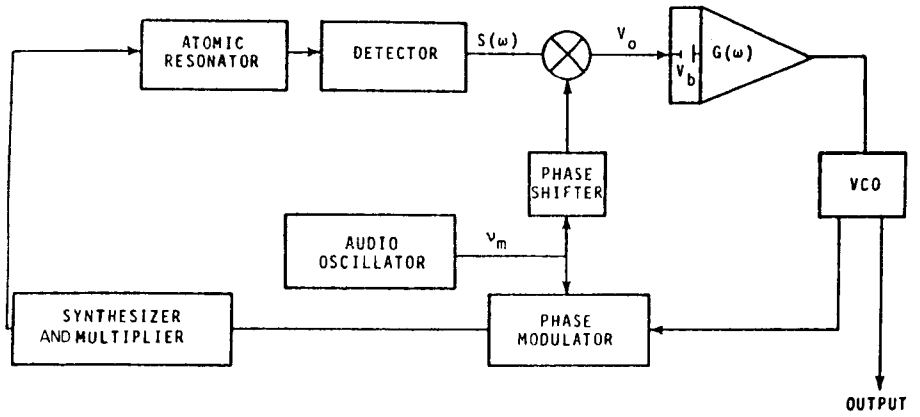


FIG. 10-7 Block diagram of an atomic clock with a frequency-lock servo. $S(\omega)$ is the resonator demodulated ac signal, ν_m the modulation frequency, V_0 the phase-detector output voltage, V_b a dc bias voltage, and $G(\omega)$ the electronic gain.

If we now mix this signal with a reference signal proportional to $\sin \omega_m t$, as shown in Fig. 10-7, then the output of the mixer has output near dc (i.e., neglecting $2\omega_m$ terms) of

$$V_0 = -F \frac{\Delta\nu_m(\nu_s - \nu_0)}{(\Delta\nu_l)^2\{1 + [(\nu_s - \nu_0)/\Delta\nu_l]^2\}^2} + D, \tag{10-13}$$

where F depends on the input levels to the mixer and the mixer efficiency and D is a possible mixer-output offset. This output voltage is plotted as a function of frequency in Fig. 10-6. Since the sign of V_0 depends only on the sign of $\nu_s - \nu_0$, this output voltage can be used to servo the frequency of the (multiplied) oscillator (VCO), as shown in Fig. 10-7. For good long-term stability and accuracy, we want the gain $G(\omega = 0) \to \infty$; therefore, this part of the servo is usually an integrator. Figure 10-7 shows that the FM is accomplished with a phase modulator; it may also be accomplished by applying FM to the VCO directly.

The above technique is sometimes called the first-derivative lock since the first term in the expression for V_0 is proportional to the derivative of $S(\omega)$. There are more potential problem areas with the frequency-lock servo than for the phase-lock servo. Some of these problems are discussed below.

10.1.7.1 FAST MODULATION

When $\nu_m = \omega_m/2\pi \simeq \Delta\nu_l$, the expression for $S(\omega)$ should be modified. The important point to note, however, is that $S(\omega)$ still remains symmetric and the basic dispersionlike character of the output of the mixer (V_0) is still preserved.

10.1.7.2 OFFSETS IN MIXER OUTPUT AND INPUT TO INTEGRATOR

These effects were discussed above for the phase-lock servo; for the frequency-lock servo we again assume that the gain $G(\omega)$ is very high near dc, and therefore $(V_0 + V_b) \to 0$, where V_b is the biasing voltage (offset). Thus, the source frequency (ν_s) for the locked condition is

$$\nu_s - \nu_0 = \frac{\Delta\nu_l}{F\,\Delta\nu_m}(D + V_b) \tag{10-14}$$

when $(\nu_s - \nu_0) \ll \Delta\nu_l$. This equation illustrates the need to use large FM swings ($\Delta\nu_m$); in practice, it is desirable to make $\Delta\nu_m \simeq \Delta\nu_l$; therefore,

$$\frac{\nu_s - \nu_0}{\nu_0} \simeq \frac{D + V_b}{Q_l F}, \tag{10-15}$$

where $Q_l \equiv \nu_0/\Delta\nu_l$. This equation is only approximately true since we assumed $\Delta\nu_m \ll \Delta\nu_l$. In a properly designed mixer (demodulator), F can be large; if we assume $F = 10\,V$ and $Q_l = 10^7$ (approximately true in a commercial cesium standard), then D and V_b must be constant to $1\,\mu V$ to obtain 10^{-14} frequency stability. This requirement is rather severe and therefore work continues to find better demodulators. Digital techniques, which are better than the analog demodulators in state-of-the-art lock-in amplifiers by more than an order of magnitude, have been used.

10.1.7.3 DISTORTION IN FM

Ideally, the frequency of the source is modulated according to $\nu = \nu_s + \Delta\nu_m \sin \omega_m t$. In practice, this equation does not hold precisely and offsets can occur. If the signal from the "audio" oscillator (Fig. 10-7) has, for example, second-harmonic content, then offsets can occur. Even if we assume that the modulation signal to the phase or frequency modulator is perfectly sinusoidal, there could still be distortion in the modulation if the phase or frequency modulator is nonlinear. This is often the case in practice since the modulation is usually accomplished with a varactor diode coupled to the phase modulator or oscillator. This type of distortion leads to a source frequency described by

$$\nu = \nu_s + \Delta\nu_m \sin \omega_m t + \beta\,\Delta\nu_m \sin(2\omega_m t + \phi), \tag{10-16}$$

where we assume $\beta \ll 1$. Considering that D and V_b are negligible and $\Delta\nu_m \simeq \Delta\nu_l$; then, if $\phi \simeq \pi/2$, there may be an offset

$$\frac{\nu_s - \nu_0}{\nu_0} = \frac{\beta}{2Q_l}. \tag{10-17}$$

If the source or detector efficiency is frequency dependent, then amplitude modulation may occur at the modulation frequency ν_m. For example, if the output of the source is frequency dependent and assuming $\nu_s = \nu_0$, as the source frequency is swept back and forth, one side of the atomic resonance receives more power than the other. This implies that a signal component (at frequency ν_m) exists at the detector; therefore, the servo will shift ν_s to compensate for this effect. This problem usually only occurs when the atomic line Q, Q_l, is fairly low (i.e., $\Delta\nu_m$ is large) and when the source has tuned circuit elements that are therefore frequency sensitive (Wineland *et al.*, 1977).

10.1.7.4 SQUARE-WAVE FREQUENCY MODULATION

Square-wave modulation provides an attractive alternative to sine-wave modulation. For example, the second-harmonic problems do not exist. The experimental problems are now the following: how to switch the frequency without any transients and how to keep the power constant. Problems in both areas would, of course, shift the lock point of the VCO away from line center. The optimum way to process the signal in this case is through an integrator that is switched synchronously with the FM. If the reference level of the integrator is the average of the two signal levels, then this system is even independent of small differences in the time spent at the two frequencies. Also, the line can be split to higher precision with square-wave than with sine-wave modulation; square-wave modulation gives a signal that is approximately twice as strong.

10.1.7.5 HIGHER-HARMONIC LOCKS

When using sine-wave frequency modulation, the strongest signal component at the detector occurs at frequency ν_m. When $\Delta\nu_m \simeq \Delta\nu_l$, however, we note that higher harmonics of ν_m also occur in the output. For example, the signal at $2\nu_m$ is strongest when $\nu_s = \nu_0$; this second-harmonic signal is used in commercial standards to indicate that the correct lock point has been achieved. Also interesting are the higher-order harmonic signals (at $3\nu_m$, $5\nu_m$, ...) which, when demodulated, exhibit dispersionlike character. Figure 10-8 shows the dispersion curves obtained after demodulation (i.e., at the output of the mixer in Fig. 10-7) for the first, third, and fifth harmonics when $\Delta\nu_m$ is adjusted to give maximum slope near the center of the curve (Wineland *et al.*, 1977). (The vertical scales are different for each part of Fig. 10-8.) One can then use the dispersion curves of the higher harmonics to lock to line center, the principal advantage of using these higher-harmonic locks is that offsets due to slopes in the background (e.g., the tails of the magnetic-field-sensitive $\Delta m = 0$ transitions in cesium) are highly suppressed (Wallard, 1972).

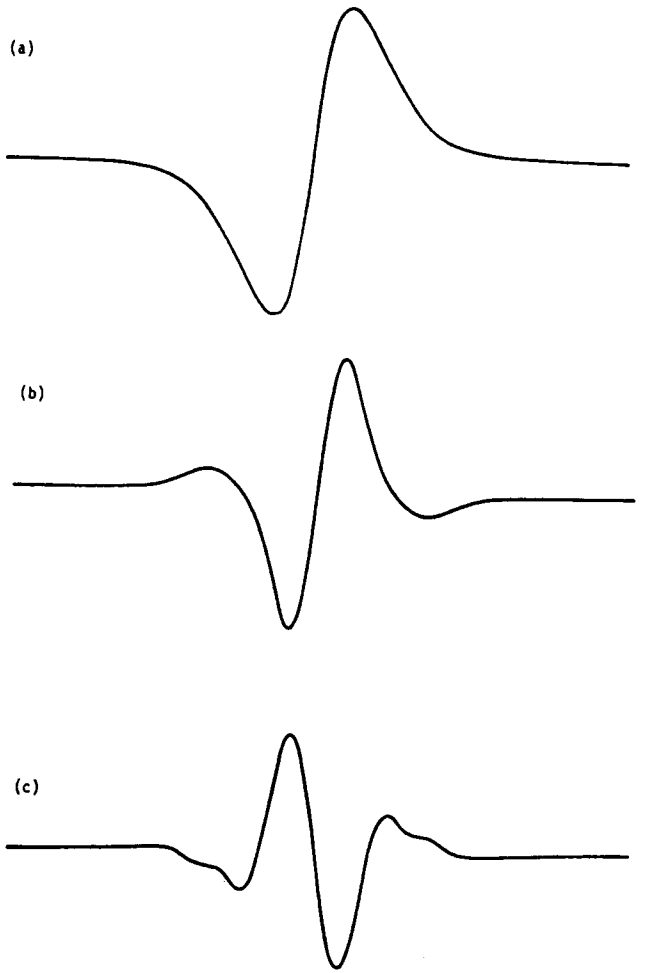


FIG. 10-8 Dispersion curves obtained at the output demodulator for different harmonics: (a) fundamental, (b) third harmonic, (c) fifth harmonic. Vertical scales are different in the three cases and curve (c) has an (arbitrary) 180° phase shift introduced.

10.1.8 Electronic Systems

The synthesizer–multiplier–modulator of Figs. 10-5b and 10-7 are depicted in more detail in Figs. 10-9 and 10-10, respectively. Figure 10-9 shows the simplest solution. The frequency modulation is imposed on the rf. This modulation can be a frequency modulation or a phase modulation and may

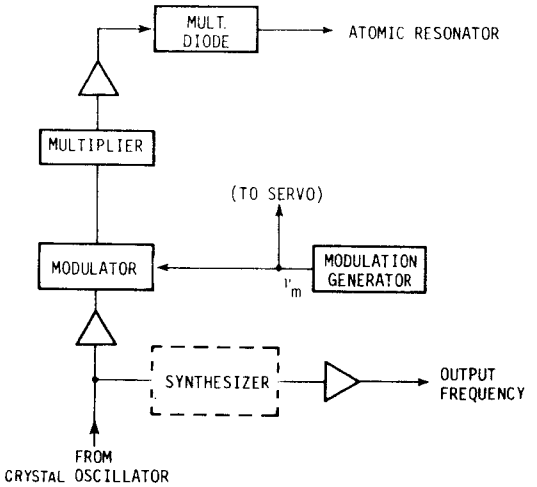


FIG. 10-9 Block diagram of the multiplier, synthesizer, and modulator electronics of the system in Fig. 10-5b. The crystal oscillator operates at a direct subharmonic of the atomic frequency; the standard output frequency is generated in an output synthesizer. ν_m, modulation frequency.

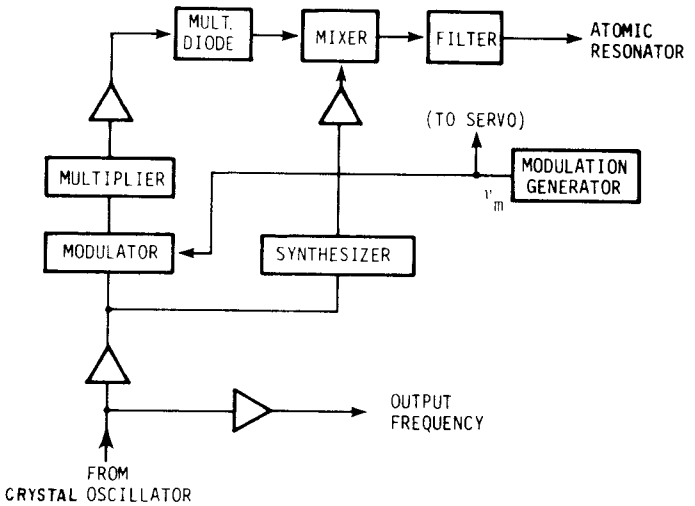


FIG. 10-10 Block diagram of the multiplier, synthesizer, and modulator electronics of the system in Fig. 10-7. The crystal oscillator operates at a standard frequency; the atomic resonance is synthesized by mixing and filtering. ν_m, modulation frequency.

be a sinusoidal or square wave. The modulation frequency must be lower than the linewidth of the atomic resonance. As an example, in commercial cesium atomic standards the linewidth is a few hundred hertz. Thus, the modulation frequency is typically of the same order. The modulated rf is then multiplied to a frequency of several hundred megahertz before it is fed into a step-recovery diode for further multiplication to the gigahertz range.

For an optimum signal-to-noise ratio, the FM amplitude of the modulation is equal to half the linewidth of the atomic resonance. In this most simple synthesizing scheme of Fig. 10-9, the crystal oscillator operates at a direct subharmonic of the atomic resonance frequency. This often means that its frequency is not a standard 5 MHz. In order to create a standard 5-MHz output, a synthesizer may have to be inserted before the output frequency is generated. The main loop containing the atomic resonator is often called the primary loop. The synthesized output, if another oscillator is used for spectral purity, is called the secondary loop.

Figure 10-10 depicts an alternate system that is often found in commercial standards. Here the synthesis is done in the primary loop. In other words, the crystal oscillator is at a standard (e.g., 5-MHz) frequency. The signal is again multiplied to several hundred megahertz, then further multiplied in a step-recovery diode. The final frequency does not match with the atomic resonance frequency; therefore, a sideband must be created at the atomic resonance frequency by mixing a synthesized lower frequency to the gigahertz carrier. A filter may be necessary to clean up the spectrum before the signal reaches the atomic resonator.

As discussed in Section 10.1.5, it is possible to operate an atomic standard as an active maser oscillator. It is necessary, nevertheless, to include frequency synthesis and electronic servo principles in such a device because the output signal is not a standard frequency and, typically, has a very low power level (on the order of picowatts).

The electronic system of a maser-oscillator frequency standard is depicted in Fig. 10-11. The output of the maser is amplified in a wideband amplifier and then fed into a double-heterodyne receiver, which ultimately translates the frequency down to dc. This dc voltage is used to control the frequency of the crystal oscillator that drives the double-heterodyne system. In other words, the crystal oscillator is phase-locked to the maser frequency. The output frequency, typically at about 5 MHz, is buffered, and a clock-tick can be obtained by passing this frequency through a divider and an output buffer. Such frequency standards are called *active* devices (in contrast to the *passive* principles discussed above) because they are based on an active maser oscillator and the standard 5 MHz is obtained via phase-locking techniques.

In both passive as well as active systems, the slave oscillator is of special importance because its performance determines, in part, the frequency

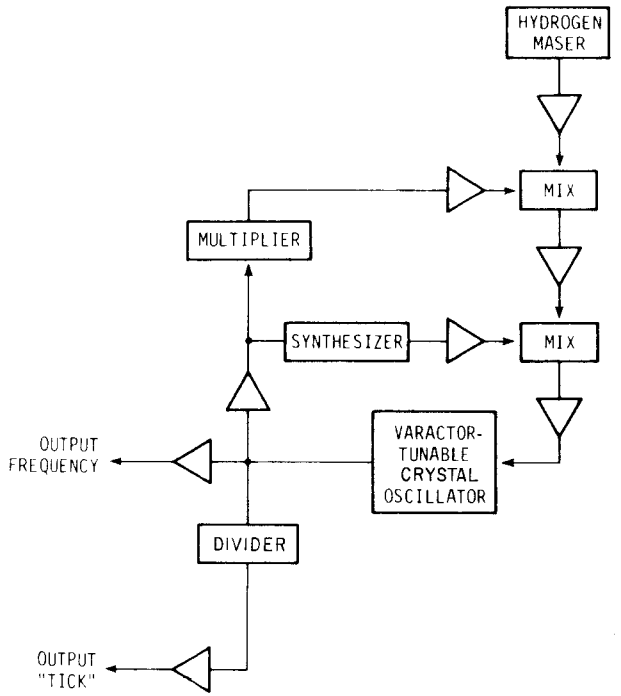


FIG. 10-11 Schematic diagram of a maser-oscillator frequency standard. The maser generates an output frequency that is detected in a double-superheterodyne receiver; the crystal oscillator is therefore phase locked to the maser oscillator.

stability of the whole standard. For averaging times of less than those corresponding to the unity gain of the servo loop, the frequency stability is essentially that of the slave oscillator; for times larger than that, the atomic resonator dominates the stability performance. It must be noted here that an inferior slave oscillator, that is, an oscillator with a frequency stability worse than that of the atomic resonator at the unity-gain point, will correspondingly reduce the frequency stability of the system for some range of averaging times. Thus, in the design of a complete frequency standard, the choice of the stability characteristics of the slave oscillator (as well as the atomic resonator) in combination with the selection of the time constant of the servo loop or bandwidth, which determines the unity-gain point, is critical to achieve optimum system performance.

10.2 PASSIVE BEAM STANDARDS

10.2.1 Beam Generation

An atomic beam device features the following essential components (Hellwig, 1970a; Kartaschoff, 1978): a source for the generation of an atomic beam; a first state selector for the purpose of accomplishing a sufficient population difference between the upper and the lower state; the interrogation region, in which the atoms interact with the electromagnetic field; a second state selector serving as an analyzer to detect and sort spatially the atoms that have undergone a transition in the interaction region; and finally, a detector for the purpose of converting an impinging neutral atomic beam into an electrical signal.

The basic principle of a source is a container for the atoms or molecules and an output channel for the formation of the beam. Since it is desirable to minimize waste of atoms while, at the same time, minimizing the need for pumping capacity, a long, narrow channel is typically used to provide molecular-flow conditions. The use of such channels can give collimation factors well above one in the forward direction as compared to the cosinusoidal output distribution of a simple aperture. It is difficult to achieve forward enhancement factors significantly exceeding 10 because of the difficulty in maintaining molecular-flow conditions while achieving sufficient output in very long and narrow channels. Often multiple channels are used, giving adequate forward directivity while increasing the total output. Bundled channels are realized by featuring hundreds of adjacent channels using precision hole-drilling techniques or assembly techniques based on combining wrinkled-foil structures. Target-acceptance angles (detector width divided by the distance between source and detector) of 10^{-2} to 10^{-3} are typically encountered, leading to waste factors of 1000 to 100,000. In Section 10.1.4 the minimum necessary signal flux was estimated at 10^{8} events/sec; thus, source outputs of not less than 10^{11} atoms/sec and, more likely, much higher are typical. This, combined with a need for molecular-flow conditions, leads to an internal gas pressure of the source for acceptable performance of 10^{-3} Torr. If permanent gases are used, a regulator device is found between the gas container and the source to achieve this pressure. A substance which is in the liquid or solid state at room temperature requires an oven in order to heat the substance to the necessary vapor pressure. Normally, a two-chamber oven is built: one chamber contains the liquid or solid phase, the other chamber contains the output channels for the vapor phase. Such a two-chambered source would feature a temperature gradient with high temperature at the output channels and the lower temperature in the second chamber, which

contains the bulk material. The output of such a source is typically a modified Maxwell distribution (Howe, 1976b), modified due to surface effects in the output channel, which deplete the slow velocity tail of the Maxwell distribution. Thus, all beam sources suffer from a deficiency in slow velocities that becomes noticeable or significant at about 30% of the most probable velocity.

10.2.2 Spatial State Selection

The state selector provides an inhomogeneous electric or magnetic field. This results in forces acting on the atoms or molecules that carry an electric or magnetic dipole moment. The two states that are coupled by the clock transition are spatially separated because they differ by the sign of the electric or magnetic dipole moment. For a constant dipole moment, a constant force can be created over some spatial region by a two-wire field (Ramsey, 1972). This is actually realizable by passing current through two parallel wires. However, the most common realization of the two-wire field is the magnetic dipole configuration depicted in Fig. 10-12; this figure also shows the basic effect of separation of states resulting in spatially and angularly separated beams containing the two different states. A great variety of state selectors has been devised, all based on the same fundamental principle of opposing forces on dipole moments of opposite sign. They include double dipoles or multiple dipoles (to form more than one beam) as well as axially symmetric configurations such as quadrupoles, hexapoles, or higher-order poles (Becker, 1976b; Hyatt *et al.*, 1971; Emmons and Rogers, 1979; Xue and Yang, 1980).

Axially symmetric state selectors have both advantages and disadvantages. The advantages include providing an axially symmetric beam as well as high field strengths, allowing more efficient spatial collection of atoms emanating from the source. One disadvantage lies in the fact that along the axis only

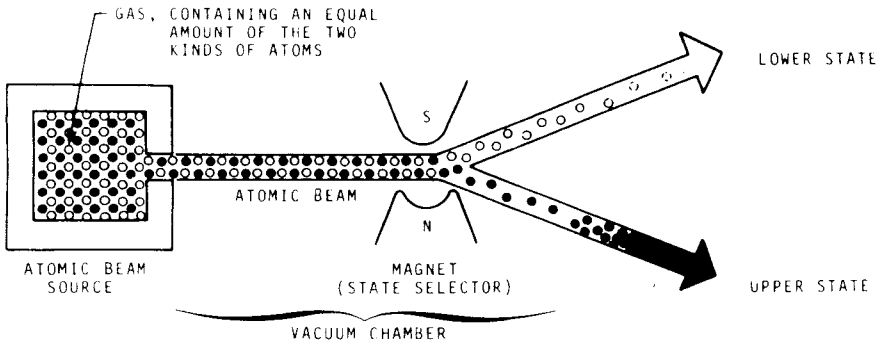


FIG. 10-12 Spatial state selection.

minimal forces are exerted; thus beam stops are mandatory to avoid line-of-sight, successful trajectories between source and detector containing atoms that are not state selected.

Often focusing or optical-collection properties using dipole optics are mentioned. Indeed, atoms emanating from a point source with a single velocity and a constant dipole moment will be focused by a hexapole magnet into an image point. However, the practical application of this limited focusing is not overly important because none of the assumptions are fulfilled in practice. Sources with adequate intensity can rarely be considered point sources. All such sources emit a Maxwellian-type velocity distribution and, as was discussed in Section 10.1.3, the dipole moment as described by the Breit–Rabi equation is a function of the magentic field strength, which is not constant in any practically realizable state-selection field. Thus, calculations of trajectories, that is, beam-optics calculations, that address the problem of successful trajectories between source and detector are nontrivial. Because of the multiplicity of variables involved, only approximations are possible and these require computer-assisted calculations. In general, we can state that the location of an atom hitting the image plane is dependent on the following variables: the coordinates of the source plane, the distance between the source and the first state selector, the distance between the first and second state selectors, the distance between the second state selector and the detector plane, the velocity as well as the velocity vector, the coordinates of location of trajectory within each state selector, and the dependence of the atomic dipole moment on the coordinates within each state selector.

10.2.3 Microwave Interrogation

The interrogation region, in its simplest form, is a cavity filled with an electromagnetic signal of the correct frequency. For historical reasons this single cavity is often called a Rabi cavity. Since we saw previously that the all-important line Q can only be reasonably large with a long interaction region, a relatively long cavity must be built. This leads to the problem that the cavity contains multiple wavelengths of the radiation in a standing-wave pattern. It can be easily seen that this leads to first-order Doppler effects, giving rise to substantial frequency shifts. Any attempts to build a very-high-precision frequency standard, based on the premise that the wave fronts of the standing-wave pattern and the atomic beam can be aligned to a high precision, are bound to fail if one realizes that for a sufficient signal-to-noise ratio, beam dispersions of about 10^{-3} are needed. The corresponding reduction in the first-order Doppler effect, then, is only approximately three orders of magnitude. Thus, frequency shifts of parts per 10^{10} have been encountered in attempts to use single cavities in atomic beam frequency standards.

A solution to this problem was developed by Ramsey and realized in Ramsey's separated-oscillatory-field technique, which is now universally used in high-performance devices. The atoms with velocity vector $\mathbf{v}$ interact with the radiation in two phase-coherent, spatially separated interaction regions. In each region the condition $(\mathbf{k} \cdot \mathbf{v})\,\Delta t \lesssim 1$ is satisfied, where Δt is the transit time through one of the interaction regions. The Q of this device is calculated from the much larger transit time between the interaction regions. It should be noted here that the same technique can be applied not only by using spatially separated interaction regions but also by using temporally separated oscillatory fields, that is, by applying radiation pulses separated in time to an ensemble of atoms.

Figure 10-13 shows the essential relationships of a Ramsey cavity and its effect on linewidth and line Q. The resonance spectrum of this technique is also shown. The broad feature with a linewidth of $W \simeq v/l$ is often called the Rabi pedestal. It is caused by the independent interaction of the atoms with each region of length l. The coherent interrogation of the atoms by both regions causes a much narrower spectral line of width $W \approx v/L$ that is centered on the Rabi pedestal.

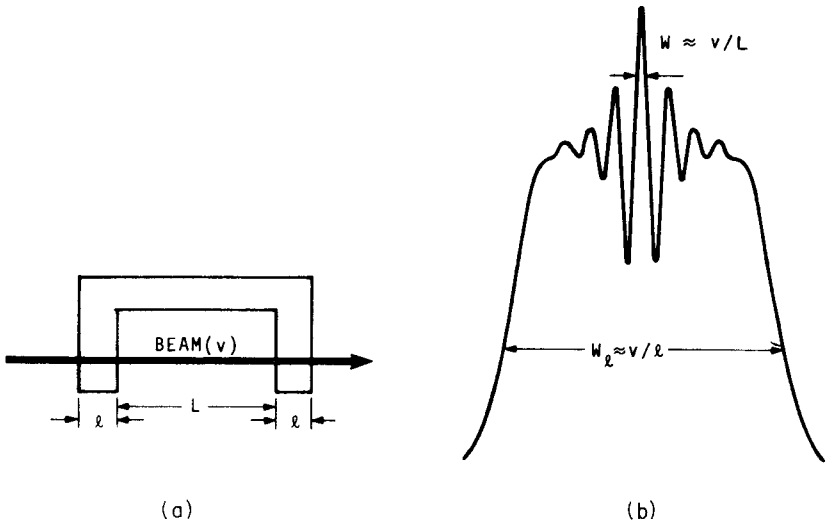


FIG. 10-13 (a) Ramsey cavity and (b) the corresponding atomic resonance spectrum. The broad resonance (Rabi pedestal) of the spectral width $W \approx v/l$ originates from the independent interaction between atoms and the electromagnetic field in each interaction region of length l; the oscillating feature is caused by the coherent interaction of both interaction regions. The central peak has a width of about $W \approx v/L$. v is the average atomic velocity.

If the phase difference of the electromagnetic field in both interaction regions is zero, then atoms will see maximum excitation at their resonance frequency. If the frequency is offset in such a way that the atoms, stimulated in the first interaction region and continuing at their natural resonance frequency, see a 180° phase shift in the second cavity as a result of the elapsed time of flight between the two interaction regions, then destructive phase relationships result, leading to a minimum in the pattern. If the frequency is further offset, phase relationships of 360° result, leading to another maximum in the signal level. Thus, we see a sine–square spectrum, as shown in Fig. 10-13, with a period of L/v, where L is the separation between the two interaction regions. Since we are not dealing with a single velocity but with a velocity distribution, the sine–square pattern of the monovelocity case is attenuated by an envelope reflecting the velocity distribution (Hellwig *et al.*, 1973b; Jarvis, 1974). It may be noted that it is possible to lock to this envelope using two-frequency excitation in separated oscillatory fields, that is, by driving the two interaction regions with two slightly offset frequencies (Garvey *et al.*, 1978), which of course must have a stable, time-varying phase relationship. If the phases in the two interaction regions are not the same, then the center peak will be displaced from the atomic resonance and, for example, with a 180° phase shift, be fully inverted as a pattern. The signal intensity I, that is, the number of atoms having performed a transition from one state to another, is proportional to the square of the transition probability and is given by $I \simeq \sin^2 bt$, where t is the duration of exposure of the atom to a driving field at the resonance frequency with an amplitude b. It is obvious that maxima of I exist for $bt = (2n - 1)(\pi/2)$. It is equally obvious that for a given velocity and dimension l of the region, that is, for a given transit time t through the region, preferred microwave drive levels b exist that maximize or minimize the signal. The first maximum, $bt = \pi/2$, is called the *optimum power*. Since we never encounter, truly, a single velocity but a velocity distribution, the interaction time t is not the same for every atom. As a result, the signal does not follow a sine–square function in relation to bt but washes out with increasing n. However, the first peak, that is, the optimum power, is always quite pronounced, even when encountering the full Maxwellian velocity distribution.

The microwave cavity is itself a resonator; thus, we may have an additional frequency-determining element besides the atoms. Over a limited frequency range the cavity and atoms can be characterized by a single resonant frequency for each. (Over a large frequency range the cavity has other resonant modes that are important and the atoms may have other resonance transitions.) Therefore, the atoms and cavity can be thought of as comprising a system of two coupled oscillators; the coupling occurs through the radiation field. In general, in a system of coupled oscillators, the frequency of each can be shifted by the presence of the other; in the atomic oscillator this means that the cavity

must be tuned to the atomic resonance frequency or else a systematic frequency shift in the output will occur. The result is cavity pulling: the apparent resonance frequency, that is, the maximum signal intensity, lies between the resonance of the atom and that of the cavity if these resonances are different. For beam devices using atom detection the cavity pulling can be approximated by

$$\nu - \nu_0 \simeq k(Q_c/Q_l)^2(\nu_c - \nu_0). \tag{10-18}$$

In this equation Q_l is the resonance Q of the atoms, Q_c the cavity Q, ν_c the resonance frequency of the cavity, and ν_0 the resonance frequency of the unperturbed atom. The factor k is on the order of unity and depends on the power parameter b: k can be shown to be zero for optimum power (Holloway and Lacey, 1964). Cavity pulling in beam devices thus can be reduced to unimportance by choosing a line Q as high as possible, a cavity Q as low as possible, and optimum power.

10.2.4 Detection of Atoms

The atoms that leave the cavity as an atomic beam have a modified population distribution as compared to thermal equilibrium. A second state selector is positioned following the cavity, which again spatially sorts the atoms. A suitable atom detector is placed to intercept one of these beams, that is, one of the two states as shown in Fig. 10-14. The output of the detector thus

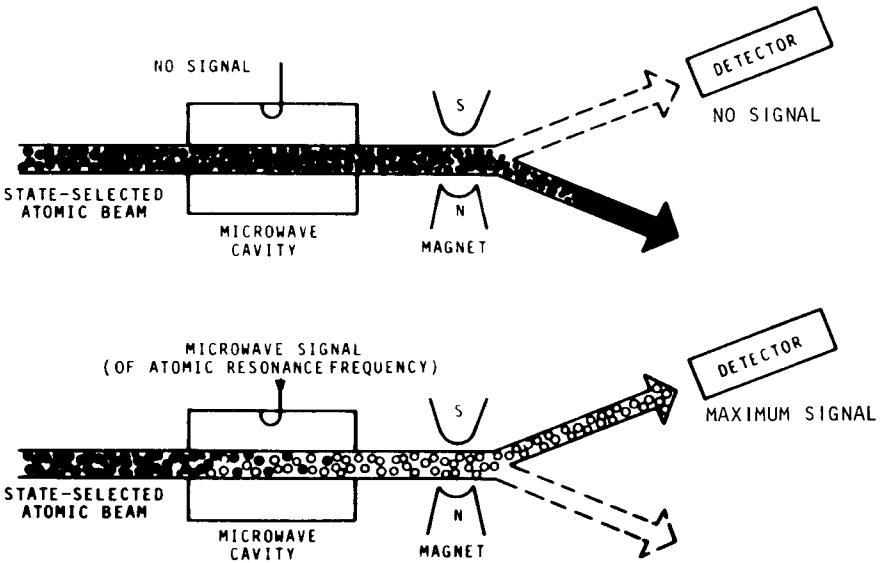


FIG. 10-14 Atom detection.

indicates the number of atoms in the upper state or lower state, depending on which beam it intercepts. If the system is arranged in such a way that with no application of microwave power to the interrogation region no atoms reach the detector and atoms only reach the detector if microwave power is applied, the system is called a *flop-in* system. If the converse is true, and application of optimum power corresponds to a minimum in the detected signal, we have a *flop-out* system. The detector itself is a device suitable to convert atoms into ions, which then are collected on an electrode. The resulting electrical current is used as the signal input for the electronic servo system. Since the deflection angles of neutral atomic beams are not very large, but only on the order of 10^{-3} radians, the actual placement of the detector can be critical, and its dimensions are typically comparatively small in order to avoid interception of portions of the unwanted beam emanating from the analyzing state selector.

10.2.5 The Cesium-Beam Standard

The cesium standard was the first and still is the most important of all atomic standards. Developed in the early 1950s, its first operational use as a laboratory clock came about in 1955 at the National Physical Laboratory in the United Kingdom, and its first commercial use took place in 1958 at the National Company in Massachusetts. Today, a variety of laboratory-type and commercial standards exist (Hellwig, 1975), and the world's internationally coordinated time system is based on a large number of cesium standards of worldwide distribution. The laboratory devices, or primary standards, are used to define the unit of time, the second. This is done by constructing the apparatus in such a way that most known perturbing parameters can be independently and separately measured. Then, corrections can be applied to the output frequency in order to realize, as best as possible, the unperturbed resonance frequency of the cesium atom at rest in free space (Granveaud and Azoubib, 1976).

The atomic resonance of cesium is 9,192,631,770 Hz. Since cesium is a very reactive metal, special provisions have to be made in supplying cesium to the source. Figure 10-15 depicts the schematic design of a cesium-beam standard, omitting the electronic systems. The oven is constructed in such a way that an ampule containing cesium can be inserted and opened inside of the oven via a remote mechanism after the beam device has been evacuated to very low pressures. Pressures of better than 10^{-7} Torr are needed to allow a sufficient mean free path from source to detector. Oven temperatures used vary between 60 and 120°C, providing vapor pressures in the range from 10^{-4} to 10^{-2} Torr inside the oven. The state selectors for a cesium beam are typically dipole magnets, but multiple-dipole, double-dipole, and hexapole magnets have been used. Most devices use the flop-in technique to maximize the signal-to-noise ratio. However, in the case of a hexapole device such as used in the

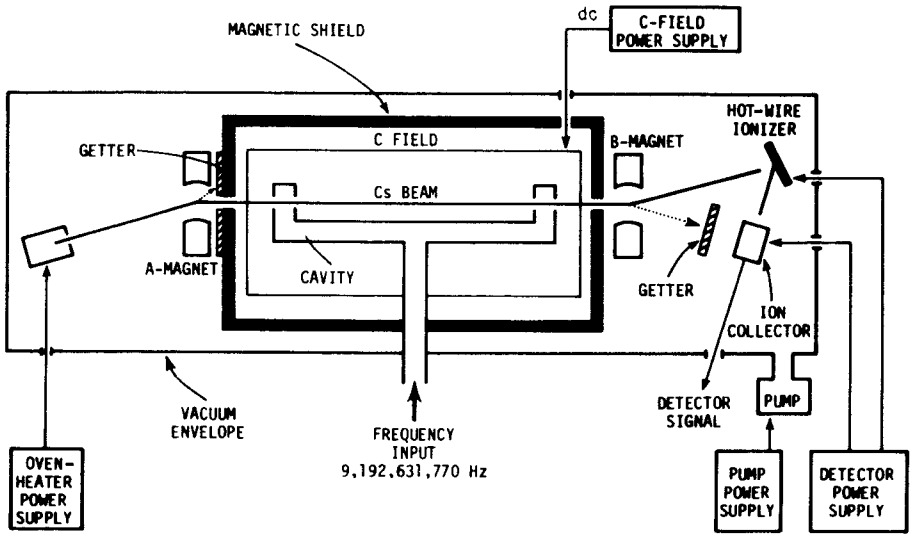


FIG. 10-15 Schematic diagram of a cesium atomic beam resonator. The frequency input is derived from a quartz crystal oscillator (typically at 5 MHz) with a frequency multiplier and synthesizer to generate the atomic resonance frequency. A feedback servo from the detector output then controls the oscillator.

primary standard of the PTB in Germany (Becker, 1977), the flop-out technique had to be used because of the characteristics of the hexapole magnets.

Vacuum is typically maintained by ion pumps; these feature rather sizable pump capacities in the case of laboratory-type standards, but are as small as 0.1 l/sec for internal pumps in the case of commerical cesium standards. These small pumps serve only to scavenge residual gases, most importantly noble gases. Since a commercial tube is baked prior to permanent seal-off, at high temperatures there is very little evolution of gases inside of the tube. Furthermore, the expended cesium acts as an effective getter for many gases. The waste cesium itself is gettered by graphite in solid as well as in surface deposition form. Thus, cesium standards are characterized by strategic placement of graphite apertures and graphite-coated surfaces, especially in the vicinity of the oven and the detector (in order to minimize residual cesium background) as well as at the entrance to the cavity, in order to avoid deposition of metallic cesium inside of the microwave structure.

Dual-beam devices have been built that utilize simultaneously the upper and lower state by generating two different beams deflected in opposing directions (Wineland *et al.*, 1976b). The detector in cesium standards is typically a hot wire. The low ionization potential of the cesium atom makes it

possible to surface-ionize cesium atoms on metals with a sufficiently large work function. Metals that are being used include tungsten, niobium, and tantalum as well as platinum–iridium alloys. Since most of these metals contain significant amounts of contaminants, in particular potassium, the ions formed at the surface of the hot wire are extracted through a mass spectrometer. The mass spectrometer is typically a magnetic field that bends the ions by 90° out of the original path of the incoming neutral atoms. Fields of about 0.1 T and voltages on the order of 10 to 20 volts are sufficient. The ions are collected on an electrode. In some high-intensity-beam laboratory devices, the current is directly detected by an electronic amplifier (Becker, 1977; Wineland *et al.*, 1976; Mungall *et al.*, 1976), typically with a field-effect transistor front end. In all commercial devices, however, an internal electron multiplier is used. Thus, the collector electrode becomes the first dynode of the multiplier. The electron multiplier provides sufficient gain to raise the signal level by orders of magnitude above the noise level of electronic amplifiers. The surface ionization efficiency, together with the low noise of an electron multiplier, allow essentially noise-free detection of single atoms in cesium-beam devices. The C field in cesium devices is typically perpendicular to the beam axis if conventional cavities (TE_{01} mode) and dipole optics are used. However, with hexapole optics, an axial, long-coil field is preferable.

Cesium is preferred over other atoms because of its convenient frequency, which permits the use of readily available electronic techniques while featuring a sufficiently high resonance frequency for achieving high Q values; cesium has an ideal vapor pressure not far above room temperature, and the detectability of cesium by surface ionization is nearly 100% efficient. The speed of the atoms and the length of the interaction region determine the Q of the cesium resonator. Atomic velocities at the most probable thermal velocity are 200–250 m/sec. In many practical cesium-beam tubes, a lower velocity is selected by the beam optics, typically close to 100 m/sec. Thus, we find Q values ranging from a few times 10^7 to a few times 10^8 over the spectrum of commercial and laboratory devices. Typical beam intensities at the detector are on the order of 10^7 to 10^8 atoms/sec, corresponding to electric currents on the order of a picoampere. The resulting signal-to-noise ratio for averaging times of 1 sec is on the order of 1000 and allows fractional frequency stabilities at 1 sec in the range from 10^{-12} to 10^{-10}. The most common electronic synthesis technique for cesium-beam standards is the injection of 12.631 MHz as a sideband on the multiplied carrier frequency of 9.180 GHz, followed by filtering. The spectrum of the cesium resonator (Glaze *et al.*, 1977) is shown in Fig. 10-16, which contains all $\Delta m_F = 0$ transitions, of which there are seven. Only the center transition is first-order magnetic-field independent and thus forms the clock transition. The relative decrease in the Ramsey-pattern amplitude of the more magnetic-field-sensitive transitions is a result of

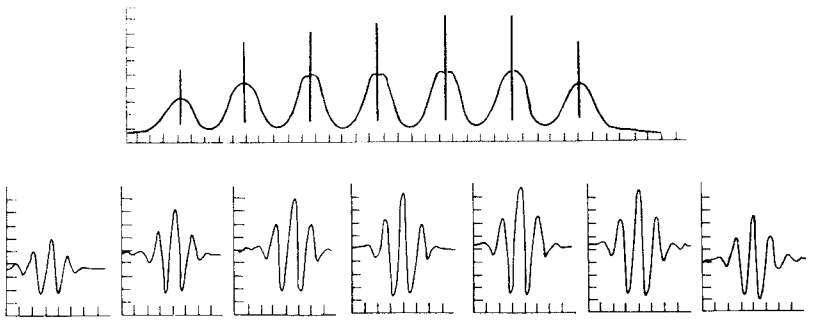


FIG. 10-16 Microwave spectrum of the σ transitions (quantum mechanical selection rules: $\Delta F = 1, \Delta m_F = 0$) of a laboratory cesium tube (the primary standard of the U.S. National Bureau of Standards, NBS-6). The microwave power was set to the optimum level for the "clock" transition, that is the $(F = 4, m_F = 0) \leftrightarrow (F = 3, m_F = 0)$ transition. In the upper recording all seven Rabi pedestals are shown with the respective Ramsey patterns at full amplitude. The frequency axis is 8.9 kHz/division. In the lower recording, the vertical scale and sweep rate are exactly the same as in the upper recording. The only difference is that the chart speed was increased to give an expanded frequency axis of 50 Hz/division, so that the character of the Ramsey patterns can be seen.

magnetic field inhomogeneities across the axis of the atomic beam. Field inhomogeneities across the beam axis result in different trajectories seeing different net magnetic fields (and thus different frequency shifts), washing out the Ramsey patterns. The relative offset of the Ramsey resonance as compared to the Rabi pedestal (Fig. 10-13) is a result of magnetic field inhomogeneities in the axial direction, causing the average magnetic field that determines the Ramsey resonance to differ from the effective magnetic field in the two interacting regions that determines the Rabi resonance. The resulting frequency shifts can be estimated (see Section 10.1.3) but typically are not limiting; the very high sensitivity of the magnetic-field-dependent transitions would require rather large offsets and asymmetries, and complete washouts will occur before the clock transition is measurably perturbed. Spectrum diagnostics is therefore a very sensitive method. The C field is typically set at around 6×10^{-6} T, corresponding to a separation of the transition in intervals of about 40 kHz. The major reason for this C field choice is the occurrence of frequency pulling of the center clock transition by the tails of the neighboring resonances. At 40 kHz the net offset is on the order of 10^{-5} of the linewidth of the center Ramsey resonance. If the spectrum itself were totally symmetric around the center clock transitions, then no net frequency shift would occur. However, this is not the case because the differences in effective magnetic dipole moment cause the available number of atoms within the interrogation region to have a nonsymmetric distribution, as reflected in Fig. 10-16. A further, minor reason for this C-field is that the resulting offset of the

TABLE 10-2

Tabulation of Contributions to the Frequency Inaccuracy in the Primary Frequency Standard NBS-6 of the U.S. National Bureau of Standards[a]

	Bias	Bias (Δy)	Uncertainty
(1)	Servo-system offsets		
	(a) Amplifier offsets	0	0.02×10^{-13}
	(b) Second-harmonic distortion	0	0.15×10^{-13}
(2)	Magnetic-field effects		
	(a) Offset due to finite field	536×10^{-13} (typical)	0.03×10^{-13}
	(b) Magnetic field inhomogeneity	0.02×10^{-13}	0.02×10^{-13}
	(c) Majorana transitions	0	0.03×10^{-13}
(3)	Pulling by neighboring transitions	0.4×10^{-13}	0.20×10^{-13}
(4)	Cavity pulling	0	0.01×10^{-13}
(5)	rf spectrum	0	0.02×10^{-13}
(6)	Second-order doppler shift	-3.1×10^{-13} (typical)	0.10×10^{-13}
	Cavity phase shift (for a particular direction)	0.25×10^{-13}	0.80×10^{-13}
(7)	Total error due to systematic frequency biases		
	(a) Root mean square	—	0.85×10^{-13}
	(b) Sum of errors	—	1.38×10^{-13}
(8)	Random uncertainty	0	0.31×10^{-13}

[a] From Wineland *et al.* (1976b).

clock transition allows for a simple and elegant rational-number-ratio synthesis of the atomic transition frequency from a standard 5-MHz oscillator. The total frequency offset of the "standard" C-field setting on the clock transition is 1.6×10^{-10} fractional frequency. As a result, the C-field power supply must be stabilized to better than 10^{-4} fractional current stability in order not to limit the frequency stability of the cesium standard. Collisions between the atoms in the beam do not occur at normal beam intensities, which provide for mean free paths of many meters in regard to cesium–cesium collisions. In order to highlight the different frequency-perturbing effects, an error budget (Wineland *et al.*, 1976) of one of the world's primary standards, NBS-6 at the National Bureau of Standards in Boulder, Colorado, is given in Table 10-2. As must be expected, perturbations scale in most cases with approximately the Q of the resonance; thus, commercial standards have error budgets of an order of magnitude or more greater than that shown in Table 10-2.

10.2.6 Other Passive Beam Standards

Other beam approaches were being pursued after cesium had reached a certain degree of maturity in design in the early 1960s. None of these have led to a working clock. Most notable among the cesium alternatives is the use of the thallium atom (Beehler and Glaze, 1966; Lacey, 1967). Thallium was chosen to overcome some perceived limitations of the cesium-beam resonator, in particular its alleged sensitivity against magnetic fields. It is true that thallium has a much lower magnetic dipole moment ($K_1 = 0.21 \times 10^{10}$; see Section 10.1.2) and thus reacts with correspondingly lower frequency shifts if exposed to changes in the C field, as could be caused by external magnetic field changes coupling through the magnetic shielding. In retrospect, it must be realized that this lower magnetic dipole moment is no basic advantage because cesium-beam resonators have been equipped with sufficient shielding to make magnetic field perturbations not a practical concern and, in case of exposure to unusual magnetic environments, further shielding could arbitrarily reduce any negative effects. Another advantage of the thallium atom is its higher resonance frequency, more than a factor of two higher than cesium ($\nu_0 =$ 21.311 GHz) with a corresponding increase in line Q. This is partly nullified, however, by the fact that thallium requires a much higher source temperature and thus features higher atomic velocities.

As compared to cesium, the thallium atom posed several rather difficult technical problems as well as fundamental limitations. These include the difficulty of building a high-temperature oven; conventional heating means were not practical and indirect electron-bombardment-type heating was used. The lower magnetic dipole moment caused a correspondingly reduced effectiveness of the state selector, requiring longer magnets with higher field strength and thus heavier magnets while still featuring reduced spatial deflection as compared to cesium. The most difficult problem in the thallium-beam tube proved to be the higher ionization potential of thallium as compared to cesium, making surface ionization relatively ineffective. Ionization effectiveness was increased by providing a constantly oxidizing surface through a metered oxygen leak in the detector vicinity; however, the surface ionization efficiency became a time-varying, relatively unstable parameter. As a result of all these limitations, thallium work was discontinued in the late 1960s.

An alternative to cesium seemed to be the use of electric dipole moments, rather than the magnetic hyperfine structure of alkali atoms. Such transitions are available at low frequency in molecules and, as a result, barium oxide (Hellwig *et al.*, 1968; Andresen *et al.*, 1968) and ammonia devices (Wineland *et al.*, 1977) were proposed and built. With these devices the alleged advantages are total insensitivity against magnetic fields, no requirement for magnetic

shielding, and much lighter state selectors based on electrostatic effects. The difficulties with barium oxide proved to be similar to those encountered with thallium: the relative inefficiency of surface ionization and, more importantly, the difficulties in achieving the very high oven temperature. In the case of ammonia, efficient detection with a simple detector proved to be next to impossible, in addition to the limitations posed by the ammonia molecule due to its complex energy-level structure (see Section 10.5.1). Both ammonia and barium oxide were pursued experimentally, but work was terminated in the 1970s. It should be noted that none of the cesium alternatives offered a significant improvement in the fundamental limitations of any frequency standard and, particularly as compared to cesium, there was no significant improvement in resonance Q nor in signal-to-noise ratio. Looking back at these developments, it appears that beams alternative to cesium are likely to be doomed because there is no fundamental hope to improve the essential basic parameters and because of the unlikelihood of improving on the existing technical elegance of the cesium-beam machine: low oven temperatures, efficient state selection, and very efficient surface ionization detection.

10.2.7 New Horizons

As was pointed out above, it appears to be difficult to improve on the cesium-beam atomic resonator. Fundamental improvements in both Q and signal-to-noise ratio appear to be possible only by the use of higher frequencies, including infrared and optical frequencies. If it is assumed that these higher frequencies do not pose additional technical problems, the advantages are obvious: for the same length of the device, the Q improves with the resonance frequency. Thus, a device with a resonance at 100 GHz and otherwise similar dimensions has a 10-times-improved Q as compared to cesium and, in the near-infrared and visible regions, an enhancement by a factor of 10,000 is available. With such enhancement factors, Q could be traded against the signal-to-noise ratio by building shorter tubes, making more efficient use of the spatial acceptance limitations, or by multiple interrogation of the atoms or molecules, cycling each atom several times through its two states. Another technically elegant solution is optical pumping for state selection and possibly also detection. Optical pumping was tried on the rubidium beam (Arditi and Cérez, 1972) and, more recently, on the cesium beam (Arditi and Picqué, 1980), originally with rf-excited lamps but more recently with lasers, ranging from diode lasers to dye lasers. The principal advantage of this technique is that it removes the distributed cavity phase-shift limitation (Lewis *et al.*, 1980; Wineland, 1977). The distributed cavity phase shift arises from the fact that the cavity phase is distributed along the axis as well as across both coordinates of the plane perpendicular to the beam. As a

result, different trajectories sample different cavity phases in each of the two interrogation regions, and the cavity phase difference, which affects the shift of the Ramsey pattern, becomes trajectory dependent. Since with spatial state selection, that is, magnetic state selectors, the trajectories are velocity dependent, we have a two-parameter dependence of the effective cavity phase shift, and thus of the apparent resonance frequency; since the distributed cavity phase shift can be assumed to be on the order of 10^{-4} to 10^{-3} radians, cesium tubes suffer from this effect, depending on their resonance line Q, anywhere between 10^{-13} and 10^{-11}; since optimum power is a function of the velocity, power changes in the microwave driving field lead to favoring different velocities. As a result, we have a change of the average trajectory location with microwave power, and therefore frequency shifts as a function of microwave power. Other related shifts include temperature-gradient-related frequency shifts, acceleration- or gravitation-induced frequency shifts, vibration-induced perturbations, and voltage-related frequency shifts (Wineland, 1977), for example, those caused by changes in the collector voltage potential near the hot wire (causing a sampling of different regions of the hot wire corresponding to different atomic trajectories (Allan *et al.*, 1977). Thus, state selection and detection, which are uniform across the beam and retain the spatial isotropy of the velocity distribution, would essentially remove all effects related to the distributed cavity phase shift. Optical pumping appears to be an elegant means to this end. At this point in time, there are insufficient experimental data to make a judgment of optical pumping as it relates to these advantages. Optical detection would be a combined function of the second state selector which, if optically executed, would interrogate the population levels and act as a photon transformer for the detection of microwave-induced atomic transitions. If high-frequency beams were chosen, the second state-selection region could be merged with the interrogation region and detection executed as monitoring the fluorescence resulting from the interaction of the driving interrogating field with the atoms and molecules. Remember that at microwave frequencies the fact that the photon energies $h\nu_0$ are small compared to kT causes noise problems if the resonance is to be detected via absorption or emission of the microwave signal itself. This is the only reason why, for example, cesium-beam tubes resort to a second state selection and detection process in order to achieve noiseless detection of every single atom that makes a transition.

10.3 GAS-CELL STANDARDS

10.3.1 Gas-Cell Principles

If atoms are confined in a container such as a storage vessel, then they will collide with each other as well as with the walls of the container. Except under special circumstances, such a collision will terminate coherent interaction

between a radiation field and the atomic resonance. Thus, the normal case of a storage vessel inside of a cavity extending over more than one-half wavelength will be that of a Doppler-broadened (or pressure-broadened or wall-collision-broadened) line. In addition, reradiation from atoms is absorbed by other atoms, causing radiation quenching. In principle, three steps can be taken to minimize all of the above effects.

(1) The walls of the vessel can be coated with a surface layer, providing for essentially elastic collisions; such surface layers are characterized by saturated chemical bonds, high molecular mass (polymers), and lack of chemical reactivity with the gas in question.

(2) The introduction of buffer atoms of a different species that is inert can result in elastic collisions between the radiating gas and the buffer gas. Such buffer gases include noble gases as well as species such as nitrogen and methane.

(3) Confinement within less than one-half the wavelength of the microwave radiation can be accomplished by placing the storage vessel inside of a cavity and reducing the size of the storage vessel to conform to the necessary conditions. An alternate way is connected to the use of buffer gas. If buffer gas of sufficient pressure is used, the radiating atoms will have a sufficiently small mean free path between collisions and, thus, will not move freely any more through the storage container. The radiating atoms, during their radiative lifetime, are restricted to a very small region of space; their residual spatial movement may be characterized not by free flight but by diffusion.

As we have seen, the introduction of buffer gas is critical to the success of a closed storage system, that is, a gas cell (Davidovits and Novick, 1966). It provides the following functions: elastic collisions that increase the radiative lifetime of the atoms, confinement to less than one-half wavelength, quenching of reradiation, and near elimination of wall collisions. Nevertheless, each collision with a buffer-gas atom results in a small, phase-perturbing effect that accumulates until the atomic radiation is quenched. Typically, anywhere from 10 to several hundred collisions can occur before relaxation of the radiating atom occurs, yielding relaxation times on the order of milliseconds.

Since the density of buffer gas in the cell is so high, any given atom is essentially fixed in position for a duration sufficient to allow stimulated emission. As was pointed out above, this allows a usable signal-to-noise ratio as well as a high line Q. However, under these conditions the resonance frequency of the atoms in one part of the cell will be different from that in other parts of the cell due to the fact that the atoms are localized in their particular "environment" (Risley and Busca, 1978). This environment may be somewhat different due to gradients in cell temperature, gas density, magnetic field microwave power (mode structure), population inversion, etc. A change in any of these parameters will then change the weighting of the sampling of the

cell and result in a frequency change. This is a line-inhomogeneity effect, and it is this effect which is a principal limitation of gas-cell frequency standards.

Since gas cells cannot be fabricated with the same precision as beam tubes, because the buffer-gas filling has the effect of shifting the frequency by parts per 10^8, the atomic resonance frequency is only an approximate determinant of the operating frequency of the gas cell. Depending on the particular choice of buffer gas, differently manufactured gas cells will differ by parts per 10^8; gas cells of the same manufacture will also show a distribution of resonance frequencies (on the order of 10^{-9}) due to the variability of the manufacturing process. This has the following consequences.

(1) The frequency synthesizer in the electronic system of the standard must be adjustable over the range of variability or the gas cell itself must be tunable over this range. The latter can be achieved by operating at a high magnetic field to provide, via adjusting the C field, sufficient range for tuning.

(2) Changes in buffer-gas composition may occur as a time-dependent effect due to absorption, diffusion, and gas evolution at the container walls. This causes frequency-drift (or aging) phenomena.

10.3.2 Optical State Selection

Since in gas-cell standards we have a self-contained, permanently closed system, effective interrogation can only be made by optical means. Thus, the functions of achieving sufficient population differences between the two levels and the detection of changes in that population difference are done by optical means. Optical pumping is typically used as illustrated in Fig. 10-17. This requires a three-level atomic system where the transition between levels 1 and 2 corresponds to the microwave ("clock") transition and optical frequencies correspond to transitions between level 3 and either microwave level 1 or 2. If filtered light of sufficient intensity at the frequency ν_{31} is used and no light is

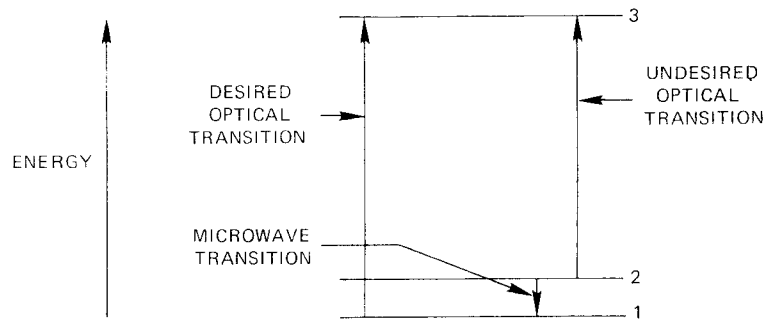


FIG. 10-17 Idealized three-level system for optical pumping.

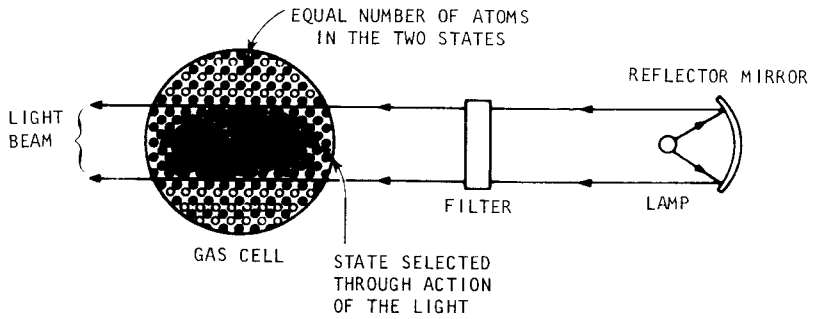


FIG. 10-18 Optical state selection.

present at frequency ν_{32} (filter action), population inversion between levels 2 and 1 occurs, that is, referring to Fig. 10-18, the net result of the optical pumping is to overpopulate state 2 with respect to state 1. If microwave radiation at a frequency corresponding to the 2–1 transition is then applied, the ensemble is moved back toward thermal equilibrium. When the microwave frequency ν_{21} is on resonance, the total light transmitted through the cell to the photodetector is somewhat smaller than if it is off resonance. If ν_{21} is swept through resonance, an absorption curve results, the position of whose peak defines the resonant frequency of the system as illustrated for the atomic ensemble in Fig. 10-19. This procedure leads to very efficient detection and a good signal-to-noise ratio because, in principle, for every microwave photon an optical photon is detected. Optical photons, in turn, can be detected essentially noise-free using photoresistive or photovoltaic cells.

10.3.3 The Rubidium Gas-Cell Standard

The traditional design of a rubidium standard features a lamp filled with rubidium-87 isotope, a filter with rubidium-85 isotope, and the cell again featuring rubidium-87 isotope (Davidovits and Novick, 1966). As illustrated in Fig. 10-20, it is a happy coincidence that one of the optical absorption lines of rubidium-85 largely overlaps one of the hyperfine splitting components of the rubidium-87 pumping light; thus, the insertion of the rubidium-85 filter effectively suppresses the light that otherwise would couple to the upper microwave level of rubidium-87. This results in efficient optical pumping, that is, saturation in the population of the upper microwave level while the lower level is essentially fully depopulated. Figure 10-21 shows the schematic of a rubidium gas-cell frequency standard.

In order to achieve the full efficiency of the system, the vapor pressure in the gas cell must be adequately high; partial pressures of 10^{-6} to 10^{-5} Torr are a

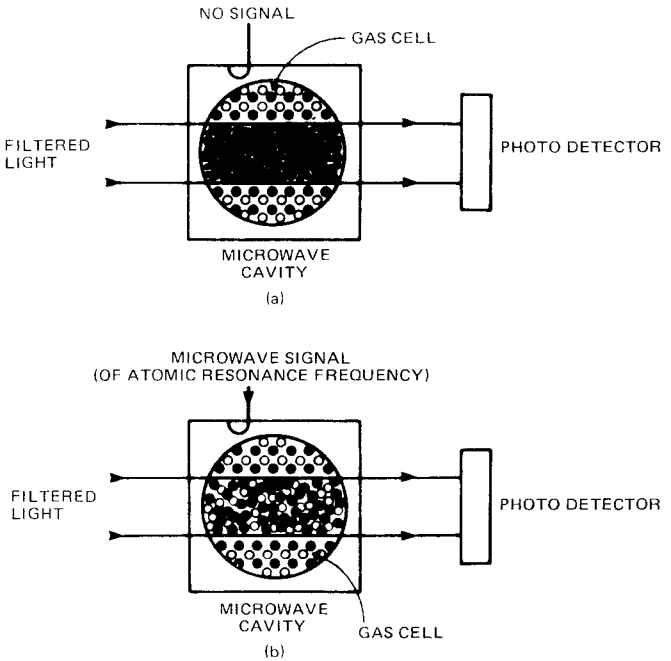


FIG. 10-19 Optical detection: (a) maximum signal, (b) minimum signal.

reasonable compromise between achieving good signals while avoiding significant numbers of spin-exchange collisions between rubidium atoms, which would lead to frequency shifts (Têtu *et al.*, 1976a) and also shorten the relaxation time and thus the line Q. In order to obtain the necessary light intensity, the rubidium pressure in the lamp must be at a higher level and, typically, temperatures between 120 and 180°C in the lamp are used. The filter temperature is adjusted to a temperature between those of the lamp and the gas cell. The gas cell features a buffer-gas mixture typically containing two components, one with a positive pressure shift on the rubidium frequency and the other with a negative shift, compensating each other's temperature coefficients (Missout and Vanier, 1975a). Table 10-3 lists three of the most widely used buffer-gas constituents. In this table the temperature coefficient $\Delta\nu_T$ is given at constant volume, while the pressure shift (at zero light intensity I_L) $\Delta\nu_p$ is given for a temperature of 333 K.

Since the $\Delta\nu_p$ and $\Delta\nu_T$ values are additive, it is obvious that a zero-temperature coefficient can be achieved using a proper mixture at some total pressure. In practice, the residual temperature coefficient is not much less than 1 part per 10^{10}.

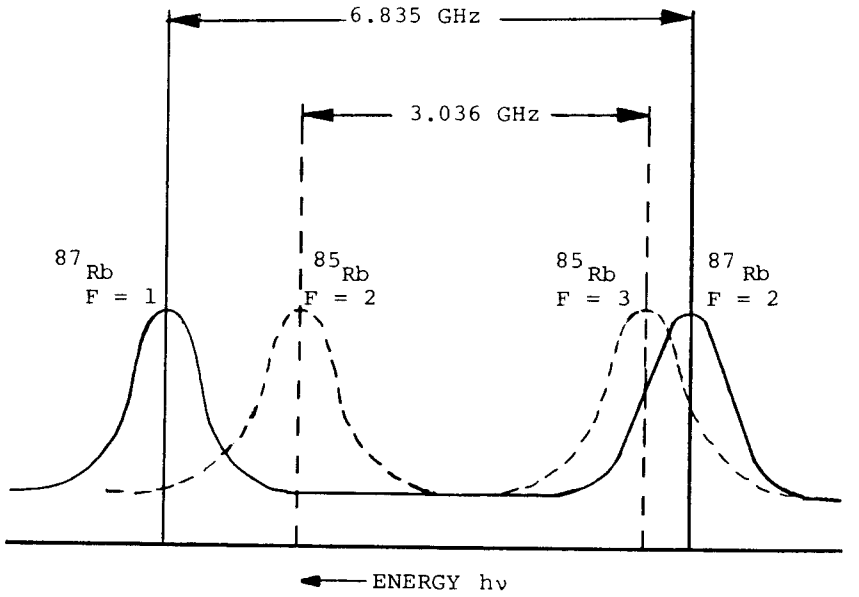


FIG. 10-20 Optical emission corresponding to the desired ($F = 1$) and the undesired ($F = 2$) states of ^{87}Rb (solid curves) and absorptions corresponding to the filter action of ^{85}Rb (dashed curves).

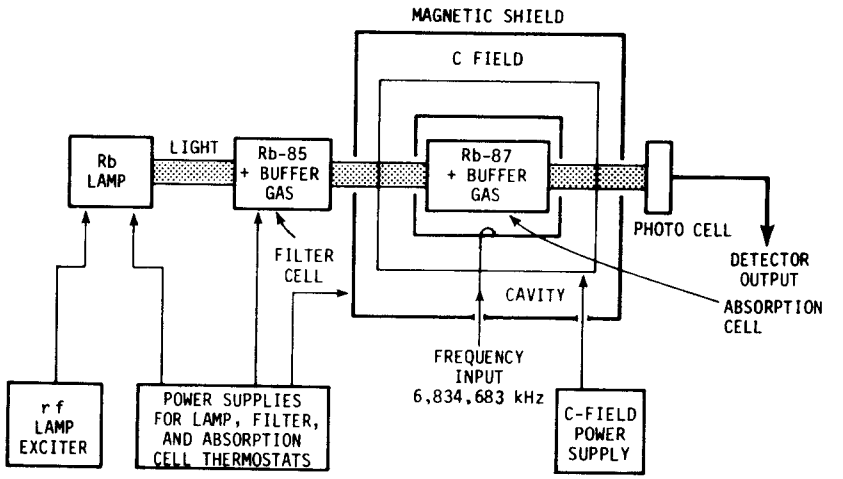


FIG. 10-21 Schematic diagram of a rubidium gas-cell frequency standard.

TABLE 10-3
Buffer Gases versus Rubidium-87 Transition Frequency

Gas	$\Delta\nu_p$ (Hz/Torr)[a]	$\Delta\nu_T$ (Hz/K · Torr)
Argon	−60	−0.35
Krypton	−600	−0.59
Nitrogen	560	0.54

[a] $T_0 = 333$ K, $I_L = 0$.

Usually, the rubidium is in a liquid–gas phase equilibrium provided by a relatively cooler appendix in the rubidium gas cell. The appendix is cooled by thermoelectric cooling or by providing a thermal-gradient oven with higher temperature for most of the gas cell (with the exception of the appendix). Alkali-resistant glass must be used to minimize reaction as well as absorption and diffusion of rubidium into the glass. Some diffusion of rubidium into the glass always exists: thus, overfilling with rubidium is typically the procedure used in manufacturing the lamp as well as the filter and the gas cell. Rubidium depletion into the glass is responsible for the fact that the rubidium vapor pressure is not in true equilibrium with the liquid phase, as would be calculated from the temperature of the appendix containing the liquid phase. Typically, the actual rubidium density is less than that calculated. Since depletion of rubidium into the glass is highly temperature sensitive, such effects are much more pronounced in the rubidium lamp, where rubidium saturation may be the only method capable of achieving long lifetimes of the rubidium lamp.

Another problem in the optical package is condensation of liquid rubidium, which can occur on cooled surfaces and is particularly likely in the filter-cell walls facing the rubidium cell. Careful design for thermal radiance characterizes most rubidium standards. The lamp is typically excited by an rf discharge in the 100-MHz range. The rubidium gas cell is housed in a cavity with a low Q (i.e., $Q_c \approx 100$). The microwave signal can be generated externally or by harmonic generation internal to the cavity using a varactor diode. A separated filter cell is not absolutely necessary. If the rubidium gas cell is filled with an isotope mixture of rubidium-85 and rubidium-87, the light of the lamp penetrating the first layers of this isotope mixture will shift in its spectral characteristics in such a way as to pump effectively the remainder of the gas cell. In other words, this *integrated* gas cell (Jechart, 1973) acts like a filter cell at the side facing the lamp and, on the opposite side, like the gas-cell resonator. This design approach lends itself to a more compact and simpler design but further aggravates the effects of gradients and inhomogeneities discussed in Section 10.3.1. The detector is typically a photocell, that is, a photovoltaic device, that has a surface area commensurate with the effectively used light

beam (on the order of 1 cm diameter). Unlike the case of the cesium standard, there is no optimum power. The reason for this is the fact that we have no transit-time phenomena as in a cesium beam, but rather the relaxation spectrum of the rubidium atoms due to collisions or radiation phenomena. These are exponential processes, and therefore increasing the microwave power will always result in some fast-relaxing atoms being optimally pumped. Increasing microwave power causes a monotonic and asymptotic increase in the signal intensity. However, as the signal increases with applied microwave power, line broadening occurs due to the fact that fast-relaxing atoms are preferentially selected. Best conditions are obtained by selecting the microwave power in such a way that the product of the signal-to-noise ratio and the line Q is optimized.

As discussed above, the atomic ensemble does not perform spatial averaging but rather acts as a superposition of the individual resonance frequencies of the spatially fixed atoms, leading to an inhomogeneous resonance line. As a result, dependencies occur against all parameters that are spatially selective. This includes light intensity, magnetic field gradients across the cell, microwave power due to the mode structure of the microwave cavity, and other effects as discussed above. In summary, the rubidium gas-cell standard is a less "primary" device than the cesium-beam tube. Basic frequency shifts due to buffer gas and light are on the order of parts per 10^9 to parts per 10^8. The rubidium standard is therefore sensitive against the stability in time of the parameters that cause these shifts (Cerez and Hartmann, 1977). It is therefore no surprise that rubidium gas-cell standards show systematic frequency changes on the order of 10^{-13} to 10^{-12} per day, corresponding to parameter changes as a function of time on the order of 10^{-4} to 10^{-5} per day.

10.3.4 Other Gas-Cell Standards

Because of its simplicity, it is not surprising that the rubidium gas-cell approach has a great attractiveness. Other atoms have been tried, but with no practical success. Most notably, this includes cesium (Rovera *et al.*, 1976). The basic advantage of the rubidium atom over all other known alternatives is that it features relatively elastic collisions with readily available buffer gases and offers the isotopic overlap in the optical spectrum for effective pumping. In an optically pumped cesium system, one faces the necessity of creating population inversion by other means, which include discrimination between the two hyperfine levels by their different polarizations or resorting to spectrally narrow light sources such as lasers. Both approaches are technically much less elegant and practical. Cesium is heavier than rubidium and suffers more under collisions. In fact, the relaxation times under similar conditions are factors of 5 to 10 less than in the case of rubidium. Of course, an atom such as

hydrogen would perform much better. However, hydrogen atoms cannot easily be maintained in a stable condition: the need to continuously dissociate molecular hydrogen runs against the gas-cell concept of a closed system (see Section 10.4). Of course, gas-cell standards are readily possible in the optical region because population inversion naturally exists. Thus, the requirements for effective filtering can be dropped and simple absorption can be used with any one of the many gas resonances available in the infrared and visible radiation regions.

10.3.5 New Horizons

One of the primary limitations of the rubidium gas-cell standard is the fact that it features an inhomogeneous line. In order to transfer the rubidium gas cell into a standard with a homogeneous line, the buffer gas must essentially be removed to realize effective spatial averaging of the individual atoms. As a result, wall collisions dominate, as was shown experimentally using certain high-polymer coatings such as paraffin and polyethylene as wall materials (Busca *et al.*, 1975). This approach allows the removal of the buffer gas while retaining the optical-pumping principle with a separate filter or isotope mixture in the gas cell. Unresolved at this time is the stability in time of the coating materials when exposed to rubidium.

Another limitation of rubidium standards appears to be the residual light shift. One portion of the light shift is due to the inhomogeneous line, that is, the atomic resonance frequency is dependent on the light intensity, which is dependent on the location of the peak of pumping efficiency. It would be cured with the wall-coating approach and spatial averaging. The other remaining light shift is due to the insufficient overlap of the rubidium-85 absorption and the rubidium-87 emission (Fig. 10-20). This leads to an asymmetric spectral filtering of the rubidium-87 line that pumps the lower microwave level. This light shift could be removed if a light source were employed that is centered and symmetrically coupled to the upper microwave level. Obviously, this can only be a laser source. In order to arrive at a practical device, dye-laser approaches cannot be considered, although they have been tried, but rather solid-state lasers must be used. The limitation of a practical standard would then be the stability of the laser frequency with temperature. An effective centering of the solid-state-laser pumping line would probably require a frequency stabilizing servo to the rubidium resonance. Finally, one should consider, with regard to fundamental improvements, the criteria. Does it improve the basic resonance Q and the signal-to-noise ratio? As long as the answer to both is not affirmative, there will be no significant improvement in the rubidium standard's performance. Substitution of cesium for rubidium, if anything, will lead to a lowering of the line Q because of the greater effect

on the relaxation processes. The most promising approach appears to be a combination of a good alkali-resistant wall coating with some residual buffer gas in order to quench reradiation so that both a high signal-to-noise ratio and a high line Q can be maintained while achieving spatial averaging (a homogeneous line). A practical solid-state laser light source could then be envisioned to remove the other, secondary limitation, the light shift.

10.4 HYDROGEN MASERS

10.4.1 Hydrogen-Maser Principles

As discussed above for the case of rubidium versus cesium in a gas cell, the heavier atom suffers much more from effects of collisions on relaxation time. Correspondingly, a lighter atom has a more elastic collision with surfaces or other atoms than a heavier atom would have. Thus, atomic hydrogen appears ideal for devices that contain atoms by relying on elastic collisions. The technical difficulty posed by atomic hydrogen is that it is not a stable gas, and contained or enclosed systems using atomic hydrogen are difficult to envision. The first experiments with containing atoms, in fact, were done using the cesium beam. In these experiments, the broken-beam experiments at Harvard University in the late 1950s (Goldenberg *et al.*, 1960), paraffin-coated obstructions were placed into the path of cesium atoms, forcing the atoms to undergo one or more collisions before proceeding onward toward the detector. The high degree of inelasticity of the cesium–wall collisions led N. Ramsey to use atomic hydrogen. The atomic hydrogen storage bulb was born, a storage container lined with a surface coating that provides for elastic wall collisions of atomic hydrogen. It remains as an open system, that is, an external atomic hydrogen source that replenishes the atomic hydrogen in the storage bulb after it is allowed to escape or recombine to molecular hydrogen is used. Today's practical devices rely exclusively on teflon (a fluorocarbon) as the wall-coating material. Different types of teflon polymers exist with somewhat varying wall properties but not significantly differing effects on relaxation time.

A schematic diagram of an atomic-hydrogen maser is depicted in Fig. 10-22. Shown is operation as an active maser oscillator (compare with Section 10.1.8). The beam source is a glass container in which atomic hydrogen is created in a radio-frequency discharge from molecular hydrogen. Molecular hydrogen is supplied from a hydrogen source such as a bottle or, in some more recent experiments, from metal hydrides at elevated temperatures. The hydrogen beam is formed by a collimator, which can have a single-channel or multichannel design. The hydrogen-beam intensity is determined by the power

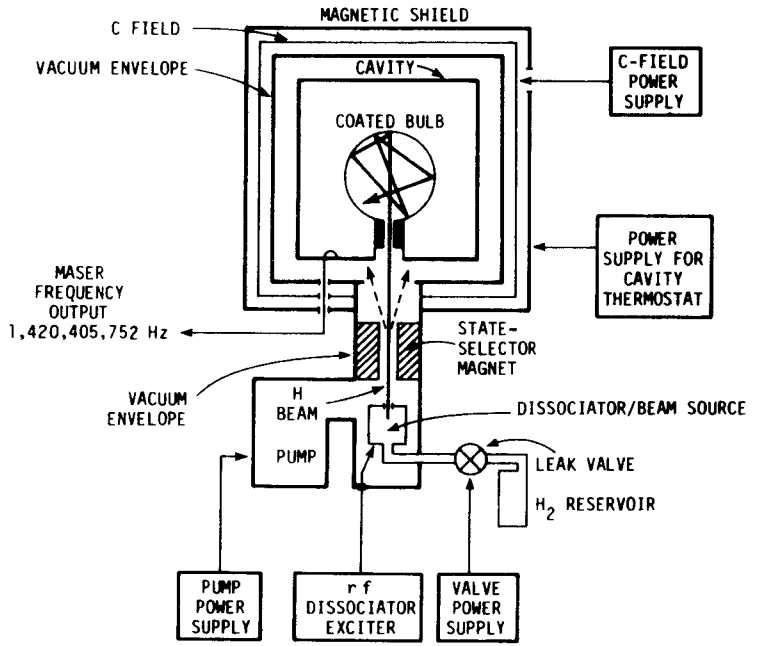


FIG. 10-22 Schematic diagram of an atomic-hydrogen-maser frequency standard (active oscillator).

of the dissociating discharge as well as the flux of molecular hydrogen. In order to achieve stable beam intensities, it is mandatory to regulate both the power of the dissociating discharge and the supply of molecular hydrogen. The former is done by electronic means, the latter either by a mechanical servo valve or by using a palladium leak. Palladium metal has the property that, at elevated temperature, it has a very high diffusion coefficient for molecular hydrogen while remaining essentially impermeable for all other gases. Thus, via temperature changes it can operate as a regulated leak while at the same time purifying and rejecting impurities in the hydrogen gas. For effective dissociation the typical pressure in the source, which operates at around 100 MHz, is 10^{-3} Torr.

The beam, which is formed at the output of the source, must be state-selected (Kleppner *et al.*, 1965). The state selector almost always is a multipole, axially symmetric magnet, which achieves high field strengths while providing an axially symmetric state-selected beam as well as some limited spatial focusing. The most probable velocity is focused on the entrance aperture of the storage bulb. The storage bulb is placed inside of a TE_{011} cavity. In order to retain a high cavity Q, the storage bulb is typically made out of quartz,

which shows very low dielectric losses. Atomic hydrogen can collide with the inside, teflon-coated surfaces of the storage bulb numerous times. Typically, several thousand to more than 10,000 collisions can take place before sufficient phase error is accumulated to decorrelate the radiation process. If the cavity Q is high enough, that is, if cavity losses are low and the supply of state-selected hydrogen is sufficiently high, then the energy transferred into the cavity by the state-selected hydrogen atoms exceeds the energy losses of the cavity and its associated electronics: the maser becomes an oscillator, providing a frequency close to the atomic resonance frequency of atomic hydrogen at 1,420,405,752 Hz. It is desirable to achieve oscillations at the lowest possible beam intensities to make the storage time in the storage bulb as long as possible. Since storage times in excess of 1 sec are possible, the escape relaxation time of the bulb, that is, the flow of gas in or out of the bulb, is arranged in such a way as to be just below the wall-collision relaxation time of the hydrogen atoms for optimum performance. Storage times of about 1 sec lead to line Q values greater than 10^9. These are the highest Q values in all presently used atomic standards and are the basic reason for the exceptional performance of the atomic hydrogen maser. The output of the device is a signal at the picowatt level.

10.4.2 Active and Passive Masers

For an active maser oscillator, a crystal oscillator is still needed in order to provide a standard frequency output. A signal that is derived from the crystal oscillator is generated at the frequency of the atomic hydrogen maser. This signal is compared to the output of the atomic hydrogen maser using a superheterodyne multistage receiver, as was discussed in Sections 10.1.6 and 10.1.8. Ultimately, the output of a phase detector is used to servo the crystal oscillator to be phase coherent with the output signal of the atomic hydrogen maser. For this type of servo, which is phase sensitive, the frequency stability improves as the inverse of the averaging time τ, as compared to a $\tau^{-1/2}$ dependency for frequency-lock servos such as those in the passive cesium-beam and hydrogen-maser standards and the rubidium gas-cell standards. In an active device cavity pulling is more pronounced (Viennet *et al.*, 1972). Cavity pulling was discussed for passive devices in Section 10.2.3. For active devices it can be approximately described by the following equation:

$$\nu - \nu_0 = (Q_c/Q_l)(\nu_c - \nu_0). \tag{10-19}$$

We note that the pulling factor translating the cavity offset into the frequency offset of the standard is the simple ratio of the cavity Q and the line Q, as contrasted to the square of this ratio for passively operating devices (devices operating far below the oscillating threshold). Thus, cavity pulling is much

more pronounced. The pulling factor in typical hydrogen masers is on the order of 10^{-5} for the translation of cavity-frequency offsets into output-frequency offsets. Thus, active hydrogen masers are characterized by elaborate designs to stabilize the microwave cavity. This stabilization can be done by using low-thermal-expansion materials such as pure quartz as the cavity material. In addition, the temperature coefficient of the cavity can be improved by using temperature-compensation techniques such as specially mounted end plates, which produce temperature coefficients essentially close to zero for a given temperature. In any case, it is required to place the cavity inside of a high-performance thermally stabilized enclosure. Such ovens may yield temperature stabilities of better than 1 mK.

An alternate way to stabilize the microwave cavity's resonance frequency is to modulate the coefficient in the pulling equation, that is, modulate the line Q of the hydrogen resonance (Kleppner *et al.*, 1965). This method is called spin-exchange cavity tuning. By increasing the amount of hydrogen supplied to the storage bulb, an increasing number of spin-exchange collisions between the hydrogen atoms take place, shortening the radiation lifetime of the hydrogen atoms. The result is a broadening of the resonance line, that is, a decrease in the line Q. If the cavity is not tuned perfectly, the pulling equation leads to a frequency change as a result of the change in Q due to spin exchange. Thus, a modulation of the hydrogen-beam intensity results in a modulation of Q that can be used to determine the point where $\nu - \nu_0'$ becomes zero and the cavity is properly tuned. This requires monitoring the output frequency of the device to a very high degree of precision, which ultimately requires the use of a second similar device to achieve the full accuracy needed. Thus, an auto-tuned maser system, consisting of two hydrogen masers modulated in their hydrogen-beam intensity, may achieve very good long-term stabilities by keeping their microwave cavities tuned to the hydrogen resonance over long time periods.

For hydrogen-beam intensities insufficient to provide self-sustained oscillations, microwave radiation, that is, its amplification, can be detected by using a microwave receiver, and a crystal oscillator can be servoed to the atomic resonance signal (Hellwig and Bell, 1972b). In this process, frequency or phase modulation in conjunction with either the absorption feature or the dispersion feature of the atomic resonance can be used to generate the reference signal for locking the crystal oscillator. This is the principle of the passive atomic hydrogen maser (Walls and Hellwig, 1976). Since the detection of the atomic resonance still relies on the (phase-sensitive) measurement of the atomic radiation, the pulling equation for the active maser still applies (as an approximation). Therefore, cavity stabilization is as important for a passive maser as for an active one, with the only difference being that lower cavity Q values may be used. An elegant method for cavity stabilization, which is applicable to the active maser as well but appears to be easier in the passive

mode, is the absolute probing of the cavity resonance by injecting sidebands into the wings of the cavity resonance and detecting any mistuning of the cavity. This is shown in Fig. 10-23, where two servos are employed: one at a high frequency above 10 kHz to probe the cavity resonance (independently stabilizing it) and a much slower modulation probing the hydrogen resonance, for example, below 1 Hz, locking the crystal oscillator to the atomic reference frequency.

10.4.3 Frequency Stability and Accuracy

It must be noted that one of the exquisite features of the atomic-hydrogen maser in the active mode is its exceptional frequency stability. A simple calculation will show that the 1-sec stability of such a device is always in the 10^{-13} range; thus, in very short averaging times extremes of stability are achievable with the hydrogen maser. Stabilities of 10^{-15} at 1000 sec have been achieved and stabilities in the 10^{-16} range have been repeatedly reported. We are reminded that the main reason for the superb performance of the hydrogen maser is the line Q, which exceeds that of the longest cesium-beam tube by almost an order of magnitude. Remember that the concept of optimum power, so convenient in the case of the cesium atomic resonator, is absent in the case of the hydrogen storage principle, as it was in the case of the rubidium gas cell. Again, we have an exponential relaxation phenomenon in the storage bulb which, if properly designed, is due to the escape of atomic hydrogen out of the storage bulb. Thus, increasing microwave power leads to interrogation of atoms with lesser relaxation times and corresponding line broadening, much as in the case of the rubidium gas cell. Again, in the passive hydrogen maser, the microwave power is set in such a way as to maximize the product of the line Q and the signal-to-noise ratio.

Accuracy and long-term stability are limited by a perturbation discussed by Crampton and Wang (1974). The perturbation is caused by the presence of radial rf and dc magnetic field components in the storage region coupled to the difference in the population of the two Zeeman levels.

One way to reduce substantially this effect is to operate at very low fields (e.g., 10^{-6} T). However, this solution may not be practical for achieving long-term stability, since it requires extreme stability of the residual magnetic fields (e.g., 10^{-11} T). A more elegant scheme is to use double state selection, which removes both the 1, 1 and 1, −1 states (Audoin *et al.*, 1974a, b). Double state selection would, in principle, totally eliminate this effect. This is more feasible with the passive system than in an active maser because of the reduced requirements on beam intensity. Another approach to reduce this effect is via careful centering of the storage bulb.

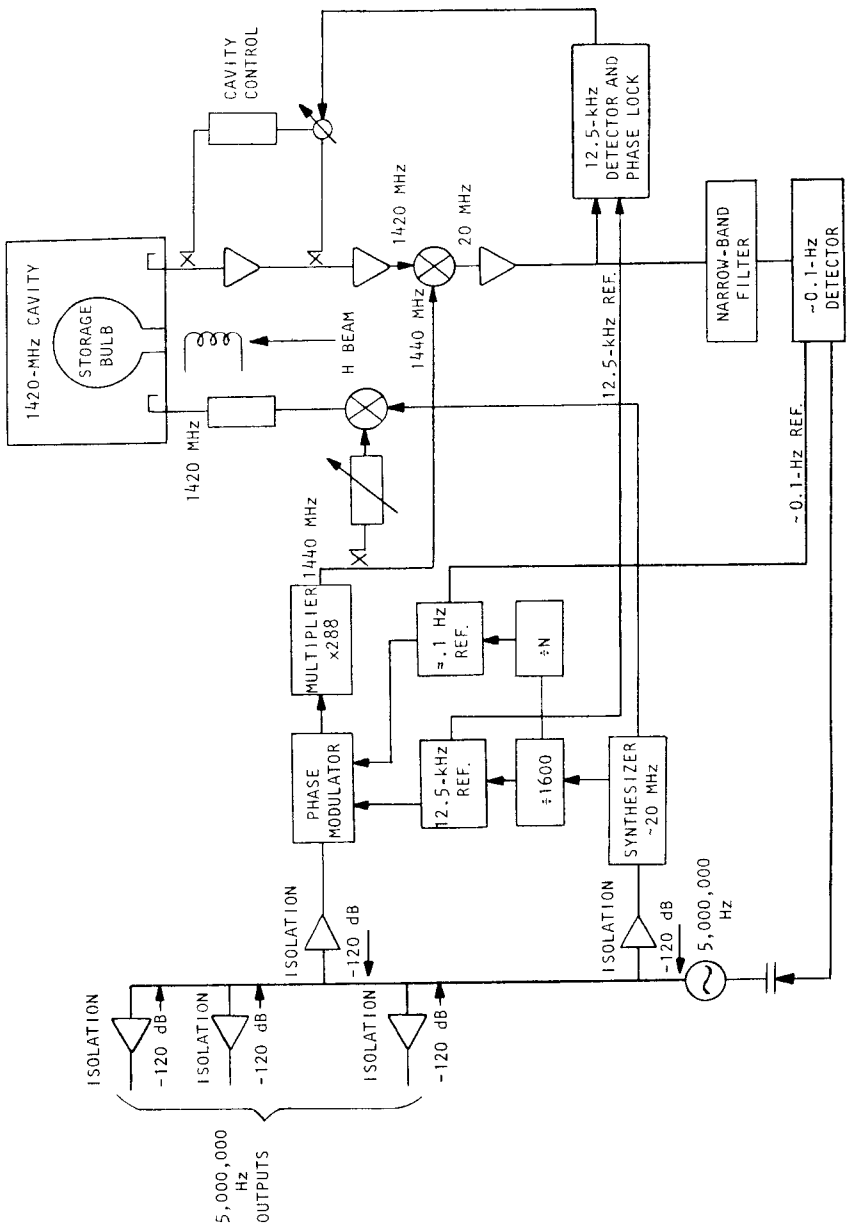


FIG. 10-23 Block diagram of a passive-hydrogen-maser frequency standard. The crystal oscillator is locked to the hydrogen resonance using a first modulation frequency of 0.1 Hz; the cavity resonance is independently stabilized using a much faster, second modulation of 12.5 kHz, which is separated from the first modulation by filtering.

As a consequence of the storage of hydrogen atoms and the resulting large number of wall collisions, a frequency offset is encountered. This wall shift is given by the mean phase shift in the radiating atom per collision divided by the average time between collisions (time of flight across the storage bulb). For fluorocarbon surfaces and a typical one-liter storage bulb, the resulting fractional frequency offset, or wall shift (Vanier and Larouche, 1978), is in the 10^{-11} range. Smaller bulbs have higher wall shifts and larger bulbs lower wall shifts. In addition, the phase shift per collision is temperature dependent (Vessot and Levine, 1970a). Precise measurements of the wall shift have been made by using a series of bulbs of different volumes in a hydrogen maser and extrapolating the measured frequency values to infinite size of the storage bulb (Hellwig *et al.*, 1970). Such a measurement is depicted in Fig. 10-24, which yielded an absolute accuracy of 10^{-12}. Thus, hydrogen masers, despite the available high line Q and the resulting excellent frequency stability, do not feature the frequency accuracy that is available from cesium-beam tubes.

10.4.4 Other Masers

In principle, all quantum electronic devices can be operated as masers, since population inversion leads to stimulated emission of radiation and thus operation as an amplifier. This includes the cesium, rubidium, and other passive standards discussed above. It may be useful here to mention only those devices and principles that actually achieved maser oscillations or came very close to it. Most notable among these is the rubidium maser (Busca *et al.*, 1975). This device is built very much like the hydrogen maser, including

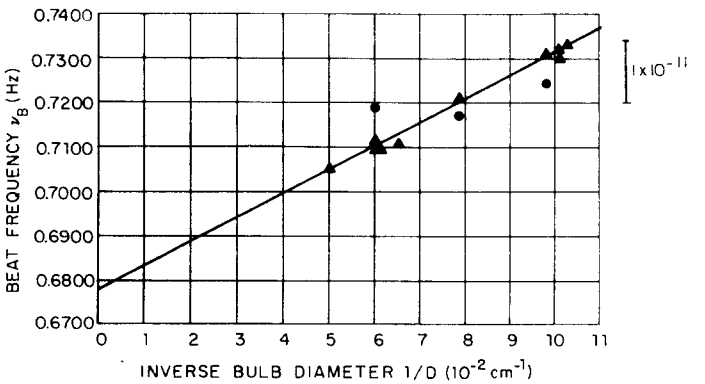


FIG. 10-24 Wall-shift measurement using the hydrogen maser. Plotted is the beat frequency ν_B between the maser under test and a reference oscillator. The test maser was successively equipped with different storage bulbs of varying diameter D. The resulting data points are extrapolated to $D \to \infty$. ▲, good data points; ●, excluded data points.

rubidium source, state-selecting magnet, cavity, magnetic shielding, cavity thermostat, and storage bulb. Among others, paraffin and polyethylene have been used as coating materials. Maser oscillations have been achieved by using sufficiently large beam intensities (Busca *et al.*, 1973b) and substantial lamp powers in order to pump actively and saturate sufficiently large volumes of the storage bulb. Frequency stabilities of 10^{-13} have been achieved; however, no convincing results for medium- or long-term stability have been reported. The stability deteriorates beyond 10 sec with $\tau^{+1/2}$ to τ^{+1}. Another maser device that has been operated is the deuterium maser (Wineland and Ramsey, 1972); it operates very much like the atomic hydrogen maser except it is adapted to the much lower frequency of the hyperfine resonance in atomic deuterium. Other maser devices include the cesium maser, based on the gas-cell principle using optical pumping; however, its limitations are more severe than those of rubidium, as discussed previously. In principle, almost any quantum electronic system can be operated as a maser oscillator because the requirement for active maser oscillation can normally be fulfilled: the gain must exceed the losses. All lasers, of course, are maser oscillators (Siegmann, 1971). Their use as frequency standards is discussed in Chapter 11.

10.4.5 New Horizons

It is difficult to imagine a storage-type device with a performance exceeding that of the hydrogen maser. This is based on the fact that the hydrogen atom is the smallest of all atoms and permits a maximum number of collisions with minimum relaxation. Therefore, the question may be asked, How can the atomic hydrogen maser be improved further in order to achieve higher line-Q values or other performance improvements? Efforts to reduce size, as illustrated in Fig. 10-25, may lead to less costly, more practical, and smaller devices (Peters, 1978; Wang, 1979, 1980; Mattison *et al.*, 1979; Howe *et al.*, 1979; Hellwig and Pannaci, 1968). However, the reduced cavity volume (e.g., of a dielectric cavity) leads to less available volume for the storage container and thus increased wall relaxation and consequential reduction in the line Q. Also, the need to stabilize a dielectric cavity, with its less-controlled mode structure, leads to a disparity between the nominally controlled cavity frequency as compared to the atomic hydrogen transition frequency. This may cause cavity-pulling-related shifts, even though the cavity itself is stabilized. Conversely, the wall relaxation can be decreased and the line Q improved using much larger storage volumes; however, size, cost, and practicality rapidly decline with this approach. Line Q values of 10^{10} have been achieved at Harvard University with an external storage bulb (Uzgiris and Ramsey, 1968a), where the excitation is done in a cavity containing a normal-size storage bulb that is in communication with an external, very large storage

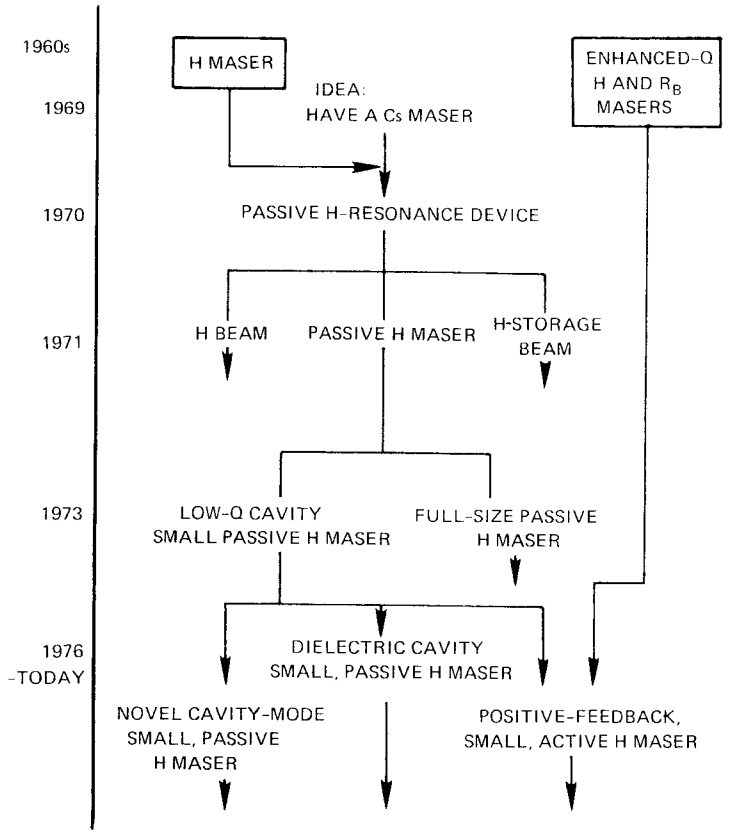


FIG. 10-25 Passive-hydrogen-maser family tree.

volume. The excited atoms diffuse out of the cavity into the large storage container and return back into the cavity, producing a Ramsey-type separated oscillatory-field resonance. However, a device of this kind is big and costly. More fundamental improvements may be possible by using more efficient wall coatings and by further decreasing wall relaxation, allowing, even in conventional devices, the storage of atoms for periods far exceeding 1 sec. The short-term stability could be further increased were it not for the low frequency of the hydrogen resonance: at 1.4 GHz receiver noise is predominant, masking the beam shot noise and cavity noise that actually limits the atomic hydrogen's stability. Optical pumping or even optical state selection and detection may be an interesting solution to this problem. The key to this is the availability of adequately stable and (in frequency) correctly placed ultraviolet

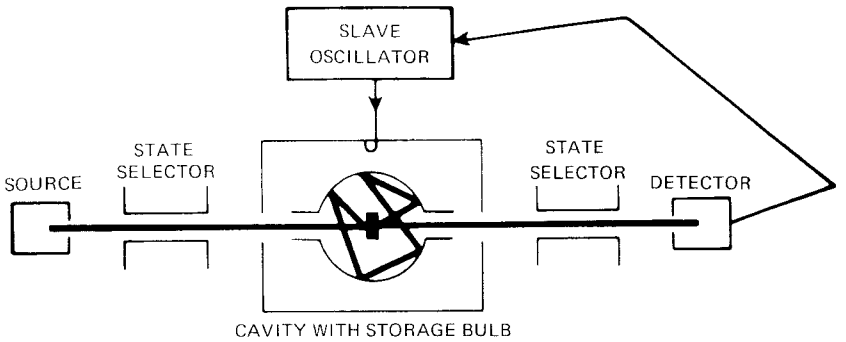


FIG. 10-26 Hydrogen-storage beam. $Q \approx 2 \times 10^9$; $\nu_0 = 1.4$ GHz.

laser devices. New material-property problems may be expected due to the dissociative action of ultraviolet light on materials, including glasses.

Another alternative is the hydrogen storage beam tube (Hellwig, 1970), which was tried but not further pursued because of the absence of an efficient hydrogen detector. This principle is shown in Fig. 10-26. The storage principle is actually retained but the hydrogen atoms are exiting again into a state-selecting and detecting scheme. This latter system can be conventional, using dipole or hexapole spatial state selection and atomic hydrogen detection. The basic advantage would be the reduction of cavity pulling, since the square of the ratio of cavity and line Q would be the pulling factor. This scheme was actually tried (Hellwig and Bell, 1972b), but the very high ionization potential of atomic hydrogen makes detection with other than universal-pressure-gauge or electron-bombardment-type detectors difficult. These detectors are not very efficient (not better than 1%) and do not sufficiently discriminate against different species of atoms or molecules. The only effective method, again, would be optical pumping combining state selection and detection.

As we have discussed many times, the very high line Q of the hydrogen storage principle leads to a very low flicker-of-frequency floor as well as to excellent long-term timekeeping performance. The key to frequency fluctuations in the medium and long term is cavity pulling. The elimination of cavity pulling appears to be most elegant with the passive maser principle (and the use of particle detection, as discussed above). The passive principle also allows small, low-Q cavities with resulting reduced resonance line Q. Unfortunately, for the purpose of this discussion, it appears that the reduced sensitivity to cavity pulling due to the lower cavity Q and the passive-control principle is compensated by the lower line Q, which leads to increased susceptibility against frequency-perturbing parameter changes. Thus, it may be concluded that for excellence in clock performance (a very high line Q), a so-called full-size passive hydrogen maser appears to be the most promising device realization.

10.5 OTHER MICROWAVE FREQUENCY STANDARDS

10.5.1 The Ammonia Maser

Although the ammonia maser is no longer important, it must be mentioned here because of its historical role as the first of all quantum electronic devices known today (Gordon *et al.*, 1955). The basic device complexity is low. Ammonia can be stored easily and can be produced as a beam from any suitable source. The transition used is the inversion transition of the ammonia molecule, which corresponds to a vibrational tunneling of the nitrogen atom through the potential well established by the plane of the three hydrogen atoms (Townes and Schawlow, 1955). Because of this tunneling of the nitrogen atom, the resulting molecular-vibration spectrum is moved to the microwave region and lies between 18 and 26 GHz. This is a very attractive frequency for frequency standards from an electronic design viewpoint. As a vibrational transition it is, of course, an electric-dipole transition. Thus, electric-multipole state selectors were used, ranging from quadrupoles to many-pole systems. The cavity featured a simple TM_{010} mode, with the electric field axially oriented and of maximum intensity along the central axis. In order to compensate first-order Doppler effects due to the flow of microwave energy along the cavity axis, double-beam devices were used. A complete beam-generating system was placed on either side of the cavity. Due to the difficulty in fully symmetrizing the beam, the resulting reduction in first-order Doppler effect was not substantial, with the consequence of rather limited accuracy and a long-term stability on the order of 10^{-11}. If the number of state-selected ammonia molecules is sufficiently large, the device starts maser oscillations.

The limitations of this device relate to the complex spectrum of ammonia, giving rise to fine and hyperfine structure. This results in frequency offsets that depend on the mixture of states as a result of state-selector action. The residual first-order Doppler effect, as was pointed out, cannot be completely removed by compensation techniques such as the double-beam technique. The Ramsey cavity was not usable for maser oscillators because of insufficient cavity Q and molecular-filling factor. In addition, residual electric fields, including thermoelectric effects and surface charges, produced very substantial frequency shifts. Also, the beam densities required for oscillation were of such a magnitude that significant numbers of collisions within the beam occurred, leading to pressure shifts. Passive, beam-type devices, including the Ramsey cavity, were studied. Their practicality, however, was doomed due to the difficulty in selectively detecting ammonia.

10.5.2 Trapped Ions

Figure 10-27 shows a schematic diagram of a possible ion-storage configuration. Because of the great variety of not fully explored possibilities of injecting a microwave signal into the ion ensemble, of interrogating this ion

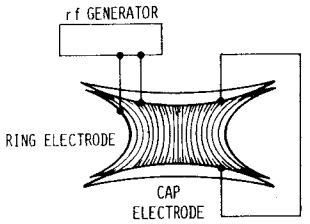


FIG. 10-27 Trapped-ion principle. The rf generator creates, together with the donut-shaped electrodes (ring electrodes), a potential well that traps charged particles. Ionization and excitation (particle preparation) must be done within this trap. The Doppler shift is its major limitation. $Q \approx 10^8$–10^{10}; ν_0 is in the gigahertz region.

ensemble, and of state selection, these features are omitted in the schematic. Ion storage is capable of featuring very high line Q's well in excess of 10^{10}. Although ions with resonance frequencies in the infrared or visible radiation region are typically considered, very attractive resonances can be found in the gigahertz region. Most importantly, this includes mercury at about 26 and 40 GHz (Schuessler, 1971; McGuire, 1977). The achievement of very high line Q's is a result of stable storage in electromagnetic fields (Dehmelt, 1967). Two types of ion traps are possible. The Penning trap, using a constant magnetic field and an oscillating electric field, is very similar to the Penning vacuum gauge. However, for effective storage it requires substantial magnetic fields over extended regions of space and thus may be impractical. A more attractive and elegant solution is the radio-frequency ion trap, a doughnut-shaped ring with two capped electrodes, as shown in Fig. 10-27, and with an oscillating field applied between the caps and the ring electrode. An analysis of the frequency shifts due to this confinement method has shown their influence to be less than 10^{-14}. The main drawback of this method is the difficulty in determining the speed of the ions, which is needed to calculate the second-order Doppler effect.

Both the first- and second-order Doppler shifts could be reduced in a fundamental way if the atoms could be slowed down or cooled. This cooling was attempted by Zacharias in 1953 in his so-called fountain experiment in which only the very slow atoms from a diffusive cesium source were selected by gravity. As was discussed, the number of slow atoms available from an effusive source is too small to be useful, but ion traps offer the possibility of using radiation pressure to cool. Dehmelt has long pointed out the advantages of the stored-ion technique, where the confining forces are relatively benign and the conditions of Fig. 10-3 (Dicke regime) can be realized without substantial perturbations. More recently, tunable, narrow-band optical sources that make detection of the small number of ions much easier than in the past are available. Typically, not many more than 10^4 ions can be stored. Cooling

of electromagnetically confined atoms or ions has been demonstrated (Wineland *et al.*, 1978; Neuhauser *et al.*, 1978). Optical pumping appears to be necessary to interrogate effectively any stored-ion ensemble without perturbation. Other auxiliary techniques include the generation or injection of ions, which appears best if done by providing a relatively weak electron beam through the ion trap. The relative vapor pressure of the ion species must then be controlled largely by the residual vapor pressure of the neutral atoms corresponding to the ions. This is not easy considering the low ion density required. Since ion traps that are less than one-half the microwave wavelength in their dimension can be built, it appears not difficult to inject the microwave radiation. A simple microwave horn may be the device of choice.

10.6 COMPARISON OF FREQUENCY STANDARDS

Tables 10-4–10-7 give, in a summary fashion, a comparison of the frequency standards that have been constructed and tested extensively. Included are both laboratory-type and commercially available devices as well as quartz crystal oscillators. Individual units may give better or worse performance than indicated by the numbers in the table; the primary intent is the comparison of types of devices.

10.7 APPLICATIONS

10.7.1 Metrology and Science

The application that has now become a classical use of precision time and frequency standards is the generation of time. The increasing availability of commercial clocks since the late 1950s caused an increasing number of laboratories to generate atomic time scales. The demonstrated timekeeping uniformity exceeded that of astronomical time by orders of magnitude. This led to the redefinition of the duration of the second in terms of the cesium resonance in 1967 (Seances, 1968). Internationally coordinated time scales are now maintained, including international atomic time (TAI) and coordinated universal time (UTC). TAI and UTC are the bases for official or legal time in different countries. A very important application is radio astronomy, in particular very-long-baseline interferometry (VLBI). In a typical VLBI experiment, two or more radio antennas receive signals from one or more stellar radio sources. The larger the distance between the locations of the radio antennas, the higher the resolution. However, it is essential to provide for coherence between these remote sites. The coherence can be provided by

TABLE 10-4

Comparison of Fractional Frequency Stability and Time between Resynchronization

Device	Fractional frequency stability				Time between resynchronization for timekeeping of	
	1 sec	1 hr	1 day	10 days	1 μsec	1 msec
Crystal oscillator						
Oven-controlled	1×10^{-11}	1×10^{-10}	5×10^{-10}	10^{-9} range	One hour	Several days
High-performance (oven-controlled)	1×10^{-12}	1×10^{-12}	5×10^{-11}	10^{-10} range	Several hours	One month
Cesium beam						
Typical	5×10^{-12}	5×10^{-13}	1×10^{-13}	10^{-14} range	Month	Many years
High-performance	5×10^{-12}	1×10^{-13}	5×10^{-14}	10^{-14} range	Month	Many years
Laboratory	1×10^{-12}	2×10^{-14}	1×10^{-14}	10^{-14} range	Month	Many years
Rubidium gas cell (small commercial)	5×10^{-12}	1×10^{-13}	3×10^{-13}	10^{-12} range	Several days	Several months
Hydrogen maser						
Laboratory (active)	5×10^{-13}	1×10^{-15}	1×10^{-14}	10^{-14} range	Month	Many years
Laboratory (passive)	1×10^{-12}	2×10^{-14}	$(3 \times 10^{-15})^a$	10^{-14} range	Month	Many years

[a] Insufficient data.

TABLE 10-5

Comparison of Fractional Frequency Accuracy and Principal Environmental Effects

Device	Warm-up	Fractional frequency accuracy		Principal environmental effects
		Retrace		
Crystal oscillator				
Oven-controlled	10–60 min	10^{-8}	As manufactured, worse than 10^{-6}	Accelerations (g forces, shock, vibration), temperature changes, ionizing radiation
High-performance (oven-controlled)		10^{-9}		
Cesium beam				
Typical	20–60 min	10^{-12}	$0.7–2 \times 10^{-11}$	Strong magnetic fields, large temperature changes
High-performance			7×10^{-12}	
Laboratory			1×10^{-13}	
Rubidium gas cell (small commercial)	5–30 min	10^{-11}	5×10^{-10}	Strong magnetic fields, temperature changes, atmospheric pressure, ionizing radiation
Hydrogen maser	Hours	10^{-12}	1×10^{-12}	Strong magnetic fields, temperature changes

TABLE 10-6

Comparison of Causes of Long-Term Instability and Resonator-Limited Lifetime

Device	Principal causes for long-term instability	Resonator-limited lifetime
Crystal oscillator	Aging of crystal resonator and electronic components, environmental effects	Not limited by crystal resonator
Cesium beam		
Typical		3–10 yr
High-performance	Environmental effects (some units continue to improve in stability without apparent limitation)	1.5–5 yr
Laboratory		Insufficient data (3 months–3 yr)
Rubidium gas cell	Aging of optical package and electronic components, environmental effects	3–10 yr
Hydrogen maser	Cavity pulling, wall and spin-exchange shifts, environmental effects	Insufficient no. of units; some have operated continuously for much longer than one year

TABLE 10-7

Comparison of Basic Modular Standards

Device	Basic modular standard			
	Volume (cm^3)	Weight (kg)	Power demand (W)	Estimated selling price for 1984[a] ($1000)
Crystal oscillator				
Oven-controlled	100–1000	0.1–0.5	Several watts	0.6–2
High-performance (oven-controlled)	1000	0.5	Several watts	2–4
Cesium beam				
Typical	10,000	10	25	20
High-performance	10,000	10	25	25
Laboratory	1,000,000	1000	100	300
Rubidium gas cell	1000	1	15	5
Hydrogen maser	200,000 to 1,000,000	50–1000	40	150

[a] Assuming no special parts or environmental requirements.

highly stable time bases located at each antenna site. These clocks independently provide phase coherence over observation times of sometimes many hours. The recorded signals can then be compared at any time after the actual observation: interference fringes are produced by comparison of the two or more recordings. Since the observations are made in the microwave region and observation times of many hours are common, clock stabilities of 10^{-14} or even better have been required in VLBI. Of particular use in this regard have been hydrogen-maser standards.

An obvious major application in science is relativity. Fundamental experiments that observe changes in frequency and in accumulated time of clocks moving relative to each other and in different gravitational potentials have been made. Such experiments include clocks in airplanes and proposals for spacecraft experiments. Of particular interest (Haefele and Keating, 1972) have been experiments of clock ensembles flown in commercial airliners around the world, demonstrating experimentally about a 400-nsec time difference between clocks flown with the rotation of the earth compared with clocks flown against the rotation of the earth. A hydrogen-maser space probe was sent 10,000 km into space in a 4-hr flight, returning in a ballistic trajectory back to earth. This latter experiment (Vessot *et al.*, 1980) has provided an accuracy of 10^{-4} in the validity of the gravitational red shift.

10.7.2 Technology

Two general areas that benefit from the availability of accurate time and frequency are *Navigation* (position location) and *Communication*. Navigation has been a driving force in clock development for many centuries. In the past, new clocks often led to improved or novel navigational systems. Challenges facing navigational systems designed today demand new clocks that offer increased precision, system reliability, and insensitivity to adverse environmental perturbations.

Navigation makes use of accurate time to establish instantaneous position, most often via ranging techniques. In general, locating an object such as a vehicle, airplane, ship, or spacecraft involves the knowledge of three coordinates, for example: longitude, latitude, and altitude. If all three coordinates are unknown, the knowledge of the ranges (distances) to three reference stations will provide the necessary information. These three stations are typically radio transmitters located on earth, in space, or on moving platforms.

The range between the object to be positioned and the reference stations can be obtained by measuring the time of arrival of signals from these three stations. The signals travel at the speed of light, approximately 300 m/μsec. A timing accuracy of 1 μsec allows a positioning accuracy of ± 300 m. The total contribution of this timing error comes from the user clock, the reference-station clock, changes in propagation delays, and other systematic errors.

Timing accuracy as used in navigation usually refers to the time differential between the reference-station clock and the user clock. In principle, clocks can be set very accurately (synchronized) when they are directly compared. For navigational needs the question is, How well can a clock keep time accurately after such synchronization? In many cases clock synchronization and resynchronization can be accomplished using radio signals. However, propagation delay fluctuations and other delays often severely limit the accuracy achieved. Equally important, the user may need to be independent from radio links (at least for some period of time) for reasons of reliability, security, or signal availability.

State-of-the-art high-performance atomic clocks offer time errors of approximately 10 nsec/day, 10 μsec/month, and 100 μsec/yr after synchronization. These data mean that a vessel can establish its position using such a clock to within 3 m if only one day has passed since synchronization with the station clocks, deteriorating to 3000 m after one month of sailing. To limit the maximum error, periodic resynchronizations to within 1 μsec, via rf links, assure a position accuracy to within 300 m. Unfortunately, for many purposes 300 m is clearly inadequate, causing a need for better clocks and resynchronization systems.

TABLE 10-8

Navigation Needs

Vehicle type	Desired positioning accuracy (m)	Approximate timing accuracy (ns)
Small boats	1000	3000
Large commercial and military ships	100	300
Downed aircraft or persons	100	300
Commercial aircraft in flight	10–100	30–300
Deep-space probes	10–100	30–300
Special military vessels	<10	<30
Location of radio emitters	10	30
Natural resource exploration	10	30
Commercial aircraft during landing approach	1-10	3–30
Military aircraft	1–10	3–30
Spacecraft in earth orbit	1–10	3–30
Geophysical measurements	<1	<3

A major space-based navigation system is presently being deployed. It makes use of atomic clocks on board orbiting satellites (Institute of Navigation, 1980). Rubidium and cesium standards are currently in operation on board space vehicles, and improved rubidium and cesium standards, or even hydrogen devices, are envisioned for the final system.

Table 10-8 is a list of typical positioning-accuracy requirements. Our examples show that today's available clocks and radio navigation systems are in many cases quite inadequate in terms of their timing accuracy, size, weight, survivability, or a combination of these factors.

In communications, knowing the frequency of one transmitter in relation to other transmitters, as well as the ability to maintain a certain given frequency over time, is important. The following are examples of where high-frequency stability and accuracy are required:

(1) maintaining intelligible information such as radio and television transmission;
(2) signal separation to avoid interference;
(3) link-up of two television studios for split-screen interviews, etc., without noticeable deterioration of picture quality;
(4) high-data-rate digital communications;
(5) for pooling of electric power, line frequencies must be identical to prevent destructive power surges;
(6) secure communication requires a precise frequency standard to ensure an a priori knowledge of the frequency and/or precise time of transmission.

11 Laser Frequency Standards

Rudolf G. Buser

U.S. Army Night Vision Laboratory
Fort Belvoir, Virginia

Walter Koechner

Science Applications, Inc.
McLean, Virginia

11.1 Introduction 177
11.2 The Potential Role of Lasers 179
11.3 Basic Laser Configuration 181
11.4 Stabilization of Lasers 182
11.4.1 He–Ne Laser Stabilized with a Ne Cell 184
11.4.2 He–Ne Laser with an I_2 Cell 185
11.4.3 He–Ne Laser and Methane Absorption Cell 185
11.4.4 CO_2 Laser with a CO_2 Absorption Cell 185
11.5 Measurement of Optical Oscillation Frequencies 185
11.6 Future Prospects and Problems 189

11.1 INTRODUCTION

In this chapter we shall concentrate on the use of the laser as a viable concept for frequency standards, discuss the main means of approach and their results, and speculate on future developments. At present, the primary frequency standard that has the highest accuracy is based on an atomic transition of ^{133}Cs. (The $F = 4, m_F = 0 \rightarrow F = 3, m_F = 0$ transition of ^{133}Cs corresponds to 9.19263177 GHz). Atomic frequency standards are based on a fundamental property of nature. The interaction of electromagnetic radiation with atoms or molecules leads to interchanges of energy in discrete steps, changing the energy of the absorbing or emitting particle between discrete

PRECISION FREQUENCY CONTROL
Volume 2
Oscillators and Standards

Copyright © 1985 by Academic Press, Inc.
All rights of reproduction in any form reserved.

ISBN 0-12-280602-6

energy levels. The frequency ν_0 of the emitted or absorbed photon is related to the energy difference between levels p and q by the relation

$$h\nu_0 = W_q - W_p, \tag{11-1}$$

where $h \approx 6.63 \times 10^{-34}$ J sec is Planck's constant. For unperturbed atoms or molecules, the energies W_p and W_q and, therefore, the frequency ν_0 can be regarded as constants.

Time and frequency are closely interrelated, the unit of one being the inverse of the other. However, since the introduction of primary atomic frequency standards, the basic quantity of interest is the frequency related to the atomic resonance. Time intervals can then be defined by counting definite numbers of periods. By combining continuously running frequency sources with counters and storage and display devices, we obtain clocks.

The standard of length, the meter, is defined in terms of the vacuum wavelength of the 0.6058-μm (4.95×10^5 GHz) radiation from the krypton atom. (One meter equals 1,650,763.730 times the wavelength of the $2p_{10}$–$5d_5$ transition of ^{86}Kr.) The accuracy of the length measurement, which is limited by diffraction and optical imperfection, is about 4×10^{-9}. In the microwave region, where the second is defined, direct frequency-measurement techniques are accurate to about 10^{-13}. Descriptions of these primary standards can be found in Chapter 10.

The development of lasers has opened the way to the use of quantum transitions in atomic and molecular systems in the 10^{13}–10^{15}-Hz frequency range as frequency standards. Lasers have fractional linewidths close to those of radio and microwave sources; at the same time, they have orders of magnitude higher spectral radiance as compared to incoherent sources. These characteristics produce an important consequence: the laser can be considered not only a candidate length standard but also a time–frequency standard. High-precision, high-S/N interferometric measurements are easily implemented with lasers, and the results allow a connection with existing international standards of length. Similarly, frequency-measuring techniques are only limited by the accuracy of the fundamental standard and the stability of the source, and there indeed exists the promise of quantum-optical frequency standards. It therefore becomes, at least in principle, possible to build a combined single standard for length and time, thus avoiding the problem encountered in the determination of the international unit of length and time resulting from the use of two different spectral lines.

From a practical point of view, this availability of a single transportable time–frequency and length standard is highly desirable for large-scale availability to the technical community. As a further consequence, the existence of a single standard for length and time–frequency impacts upon the precision determination of the speed of light and other physical constants involving the speed of light. Overviews of the use of lasers in time and frequency standards are given by Kartaschoff and Barnes (1972), Hellwig *et al.* (1978), and Halford and Hellwig (1972).

11.2 THE POTENTIAL ROLE OF LASERS

We can categorize the possibilities that exist for lasers to either improve or augment existing standards as follows:

(1) replacement of the krypton-based wavelength standard,
(2) replacement of the cesium frequency standard or extension of the frequency standard into the visible regime, or
(3) application of the laser as a precision yardstick that can be used to translate a frequency standard into a length standard.

At present, separate standards for frequency and length exist, for which the wavelength measurement is several orders of magnitude less precise compared to frequency or time. Stabilized lasers have an accuracy that is potentially several orders of magnitude better than that of a krypton light source. The reason for the higher accuracy stems mainly from the much greater coherence and spectral power of the laser compared to the incoherent radiation of the krypton line. The laser offers, therefore, the potential of a more accurate wavelength standard whose accuracy could approach the frequency standard.

Frequency measurements do not suffer from instrumental limitations as do wavelength measurements; rather, the uncertainties are imposed by the sources themselves. The laser, due to its coherence and spectral power, lends itself to frequency measurements. Therefore, if use of separate standards for length and frequency were to continue, the most accurate value could possibly come from a frequency measurement of the laser, which is then used as a length standard. Figure 11-1 illustrates the application of a laser as an improved length standard.

As a frequency standard the laser offers the possibility of relating the standard defined in the microwave frequency range to the infrared or visible portion of the spectrum. Highly accurate frequency synthesis among the microwave, infrared, and visible radiation (MR, IR, and VR) portions of the

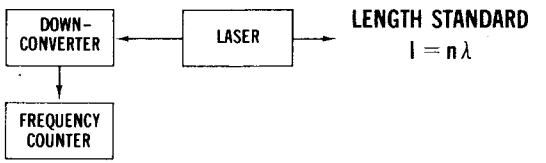


FIG. 11-1 The laser as an improved length standard: (l, length; λ, wavelength; n, integer).

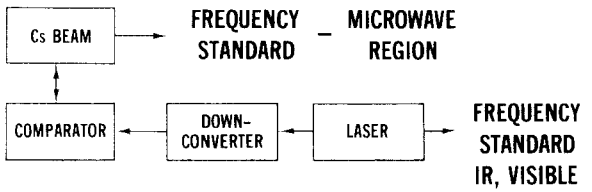


FIG. 11-2 The laser as an extended frequency standard for the IR and visible region.

frequency spectrum are possible. This ability, coupled with the possibility of transduction between frequency and wavelength in the IR and visible region, will give metrologists some new options for highly accurate measurements. In fact, with frequency-difference measurement techniques, stabilities approaching 10^{-14} are possible with the 3.39-μm He–Ne laser. Therefore, it may be possible that the laser will replace the Cs atomic transition as a frequency standard in the infrared and visible region, as illustrated in Fig. 11-2.

If one defines the speed of light by assigning a numerical value to c, the standard for length can be derived from the very precise ^{133}Cs frequency standard. This way a unified standard for frequency, time, and length would be created. We can only take the step of defining the speed of light in order to derive the length standard if we have an experimental possibility of measuring frequency and wavelength with a precision satisfactorily exceeding the accuracy of the inferior length standard. Figure 11-3 illustrates the use of a laser to relate a frequency measurement via the speed of light to the measurement of length. The laser would serve as a precision yardstick to provide a reliable basis for the measurement of length based on the frequency standard.

Actually, the International Committee of Weights and Measures is proposing to redefine the speed of light and therefore the meter. They have proposed to define the speed of light as $c = 299{,}792{,}458$ m/sec and the meter as

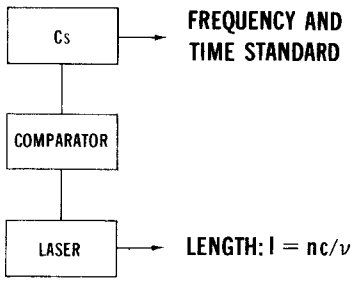


FIG. 11-3 Length measurement based on time and speed-of-light standards: c, defined quantity; ν, defined by Cs standard; l, derived from frequency.

the distance light travels in 1/299,792,458 sec. This proposed standard was considered by the General Conference for Weights and Measures in Paris in October 1983 (Quinn, 1982).

11.3 BASIC LASER CONFIGURATION

The purpose of a frequency standard is always the generation of a periodic signal having a frequency that is as stable and accurate as possible. Laser oscillators generally do not provide very stable frequencies; the frequency can vary within the Doppler- and pressure-broadened gain curve of the laser medium. This gain curve might have a width from less than a hundred to several thousand megahertz, depending on the laser. Therefore, even though the instantaneous frequency of the laser can be measured with high precision, there is no reference point other than the broad gain curve whose center cannot be located very precisely. A solution to this problem was the development of the technique of saturated absorption, which allows sub-Doppler observation of atomic and molecular resonances.

First recognition of the laser's potential, and specifically the proposed use of the narrow resonance produced by the saturation of the absorption process in a low-pressure gas cell, was provided by Lee and Skolnick (1967), followed by an extensive wave of research and investigations.[§] Figure 11-4 shows

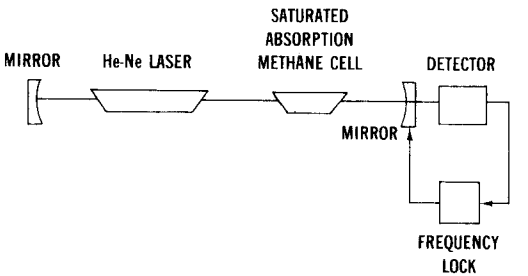


FIG. 11-4 Principle of methane-saturated absorption.

schematically the design of a laser frequency standard. As an example, we use the He–Ne laser stabilized by a methane cell (Kartaschoff and Barnes, 1972). A gas cell filled with methane is mounted with a ^{3}He–^{20}Ne gain medium between the two mirrors of a laser cavity. The He–Ne laser can be made to

[§] Birnbaum (1967), White (1967), Hall (1968), Polanyi and Tobias (1968), Basov and Letokhov (1968a), Mielenz *et al.* (1968), Bloom and Wright (1966), Sosnowski and Johnson (1968), Smith *et al.* (1967), Bagaev *et al.* (1968a), Barger and Hall (1969b), and Ezekiel and Weiss (1968).

oscillate at a frequency of approximately 88 THz (a wavelength of 3.39 μm), which coincides with a resonance of the methane molecule. With appropriate methane pressure, strong absorption occurs over the whole range of oscillation of the laser. Methane molecules in the cell interact with both running waves forming the standing-wave pattern, provided that their velocity is nearly perpendicular to the laser beam (i.e., parallel to the wave fronts). With sufficient intensity, these molecules are saturated and a narrow "hole" is "burned" in the absorption profile. This results in a corresponding narrow peak in the output of the laser–methane cell combination. A Q factor of 10^9 is easily obtained. A photodetector provides the resonance signal used for locking the laser frequency to the resonance.

How does a laser differ from a conventional atomic frequency standard? In the traditional atomic frequency standard, signals derived from crystal oscillators interrogate microwave hyperfine resonances in atoms. In the infrared and visible radiation regions, signals derived from laser oscillators interrogate atomic and molecular resonances ranging from electronic transitions in atoms to molecular rotations and vibrations.

11.4 STABILIZATION OF LASERS

To be able to provide a quantum-optical frequency standard, we need an atomic–molecular reference frequency in the optical frequency band. There are several necessary conditions: the reference must be stable and reproducible to the same performance as required of the standard, and the relative width of the reference line should be commensurate with the required stability. To achieve a frequency stability and reproducibility on the order of 10^{-13}, which is representative of the microwave range, one requires a spectral resonance with the same stability and reproducibility of the line and a relative width of 10^{-9}–10^{-10}. In principle, the stability is achievable in a variety of atomic–molecular quantum transitions, which are in an environment where the levels of the transitions involved are negligibly perturbed by external fields, collision processes, or other interferences. This then leads automatically to low-pressure (10^{-3} Torr) envelopes. However, conventional Doppler broadening, the usual major contributor to broadening, does prevent us from reaching the required goal, and spectral techniques have to be applied to narrow optical spectral lines.

Homogeneous as well as inhomogeneous broadening in gas lasers results in gain curves that are typically many megahertz wide, while the cavity linewidths are about 1 MHz. Therefore, the frequency of the gas laser is in first order determined by the optical length of the cavity. The fractional frequency instability is proportional to fractional changes in optical pathlength;

$dl/l \sim 10^{-7}$ is typically possible, leading to frequency drifts of megahertz over periods of time of less than 1 sec for passively stabilized lasers. Use of cavity materials with zero expansion coefficient, cavity temperature control, and acoustic isolation, together with highly stable power supplies, leads to an optimization of this approach. As it turns out, with appropriate effort "passive" stabilization leads to short-term linewidths on the order of kilohertz. Long-term stability of laser oscillators invariably requires active control.

The optical field inside a laser resonance is normally a standing wave (represented by two waves traveling in opposite directions). In the Doppler-broadened regime and in the case of inhomogeneous line broadening, the optical laser field interacts only with those atoms of the Doppler distribution, the Doppler frequency of which exactly matches the tuning of the field frequency. Laser action unavoidably induces saturated gain, that is, the optical field alters the population of the active level. As a consequence, the power-level distribution changes in a very specific fashion as a function of frequency (hole-burning effects). Since this interaction is fundamental for the frequency-stabilizing techniques in lasers, we must briefly discuss the related physics.

An atom, moving with a constant Doppler velocity v component parallel to the electromagnetic field of frequency ν, will experience a shifted frequency (as compared to a stationary atom); specifically, it is

$$\nu_D = \nu - (v/c)\nu. \tag{11-2}$$

Since in a laser oscillator we have two waves traveling in opposite directions, two holes are eaten in the profile of its power input, equidistant from the line center, because the to and fro running waves have the right Doppler frequencies for atoms with opposite thermal velocities. These holes are caused by a selective saturation of the inhomogeneously broadened line at frequencies of

$$\nu_D = \nu_0/(1 \pm v/c) \approx \nu_0(1 \mp v/c). \tag{11-3}$$

If the cavity is tuned to the center ν_0 of the optical linewidth ($\nu_D = \nu_0$), then only those atoms that have vanishing velocity components parallel to the resonator axis ($v = 0$) interact with the electromagnetic field. This results in a resonance dip in the center of the line, the so-called "Lamb dip." As it turns out, the width of the Lamb dip is at least one order of magnitude smaller than the Doppler width. From this concept stems the idea of combining within a cavity the gain medium with a separate low-pressure absorption cell, the latter providing a narrow *absorption* dip at the center of the Doppler-broadened line. Its origin can be explained by considerations very similar to those used above for the interpretation of the Lamb dip. This absorption dip results in a narrow peak in the center of the gain curve of the laser–absorber arrangement as shown in Fig. 11-5.

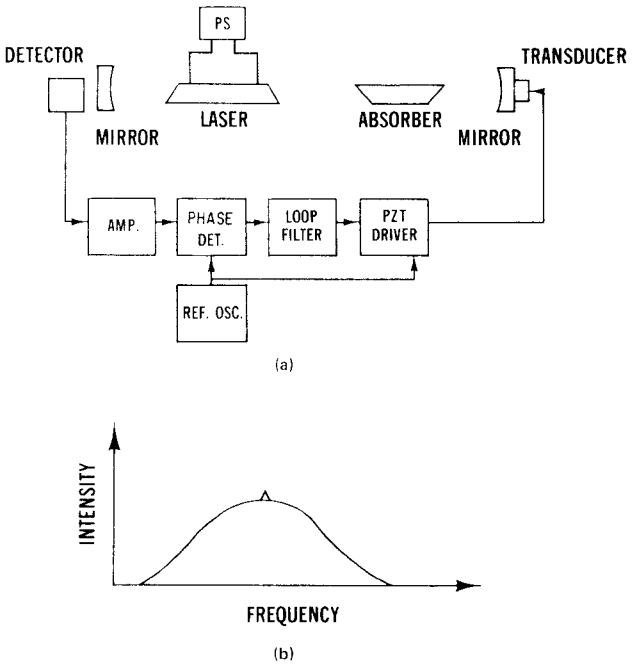


FIG. 11-5 Schematic diagram of laser stabilization by the technique of molecular saturated absorption: (a) servocontrolled laser; (b) gain curve of the laser–absorber combination.

This approach then allows us to satisfy all required conditions inasmuch as absorption may occur in transitions from the ground or nearby states to long-lived excited states with extremely small radiative widths. Furthermore, the population of ground states is normally high, providing significant absorption even at very low pressure: optical resonances of 10^4–10^5 Hz are obtainable. In addition, the absence of excitation within the absorption cell positions the absorption line in a rather stable way. The major search at this point, then, is to determine appropriate matches of laser gain and gas absorption and to establish the practical capabilities of this concept.

We shall now summarize several combinations of laser and absorption cells and report on the experimental results.

11.4.1 He–Ne Laser Stabilized with a Ne Cell

The first experimental investigation of frequency stabilization using nonlinear absorption involved the He–Ne laser (0.6328 μm) coupled with a pure Ne cell (0.1 Torr). An electric discharge populated the appropriate Ne level.

Precision tuning to 0.1 MHz, corresponding to 1/300 of the resonance width, was achieved. Frequency reproducibility was basically limited by the collision-induced shift of the absorption line (6 MHz/Torr), the discharge current, and other secondary effects. Short-term stability of 10^{-9} was obtained during a period of 10^{-3} sec (Lee and Skolnick, 1967; Letokov, 1967).

11.4.2 He–Ne Laser with an I_2 Cell

Limitations in the frequency stability with reproducibility of the He–Ne laser with a Ne cell combination led to a search for improvements. As a result, the resonance of the He–Ne line (0.6328 μm) with the absorption line of I_2 [R(127) line] was discovered (Hanes and Dahlstrom, 1969). Frequency stability of 10^{-11} with 10^3-sec integration times has been achieved, and reproducibility was on the order of 2×10^{-10}.

11.4.3 He–Ne Laser and Methane Absorption Cell

Better results in frequency-stabilization gas have been obtained in the combination of a He–Ne laser at 3.39 μm with methane as the absorbing medium (Hall, 1968). Optimization was achieved by pressure tuning or isotope selection (^{22}Ne). The frequency stability and reproducibility obtained was 10^{-11}; the width of 200 kHz at 300 K led to a long-term stability of 10^{-13} Ultimate frequency reproducibility of 10^{-14} may be possible.

11.4.4 CO_2 Laser with a CO_2 Absorption Cell

Experiments with CO_2 lasers ($CO_2 + N_2 + He$) in the presence of a CO_2 absorption cell led to the following: frequency reproducibility reached 10^{-10}, short-term stability reached 10^{-10}, and long-term stability reached 10^{-11} for 100-sec integration (Freed and Javan, 1970). For comparison, representative results are combined in Table 11-1.

11.5 MEASUREMENT OF OPTICAL OSCILLATION FREQUENCIES

Given that one has a stable oscillator, in principle the frequency measurement requires a determination of the number of zero crossings per second of the electromagnetic wave, which reduces to a counting of the number of cycles in a given period. Advanced electronics permits direct counting of up to 1 GHz, the timing being derived by a crystal oscillator or cesium clock. At higher frequencies a heterodyne technique is required, where the known and

TABLE 11-1

Performance Characteristics of Saturation-Absorption-Stabilized Lasers

Characteristic	Wavelength (μm)			
	0.6328	0.6328	3.39	10.6
Laser/cell	He–Ne/Ne	He–Ne/I_2	He–Ne/CH_4	CO_2/CO_2
Limiting effect/broadening; shift	6 MHz/Torr	13 MHz/Torr	100 MHz/mTorr	
Cell pressure (Torr)	0.1	0.1	10^{-2}	
Temperature (K)	300	300	300	400
Short-term stability (10^{-2}–10^{-3} sec)	10^{-9}	10^{-10}	10^{-11}	10^{-10}
Stability averaged over X sec	—	2×10^{-11} (10^3 sec)	10^{-13} (100 sec)	4×10^{-11} (100 sec)
Frequency	10^{-9}	2×10^{-10}	10^{-11}	10^{-10}
Reproducibility	—	2×10^{-11}	(10^{-13} best)	—

unknown frequencies are mixed and the period of difference frequency then becomes measurable. The known "base" frequency may be extended to a higher frequency via nonlinear devices as an exact harmonic of a directly countable lower-frequency oscillation.

There are, of course, signal-to-noise considerations that determine the number of steps required to proceed from a directly countable frequency to the frequency domain of the unknown source where heterodyning is practical. Furthermore, it is clear that as the frequency becomes higher, the appropriate harmonic-generator–mixer diode must be deployed to provide the necessary frequency resolution. The extension of frequency measurements into the IR, visible, and possibly beyond is, in fact, only possible by the invention of metal-on-metal point-contact diodes and their further development.

In view of the significance of frequency measurements in the optical regime, we shall describe the technique employed by Jimenez and Peterson (1977). Figure 11-6 illustrates the approach taken in order to compare the cesium frequency standard with the He–Ne-laser frequency. This figure is greatly simplified to show only the essentials.

To measure the frequency of methane, a chain of oscillators extending from the cesium frequency standard to the methane-stabilized He–Ne laser is used. Conventional silicon point-contact harmonic generator–mixers were used up to the frequency of the HCN laser. Above this frequency tungsten-on-nickel diodes were used as harmonic generator–mixers.

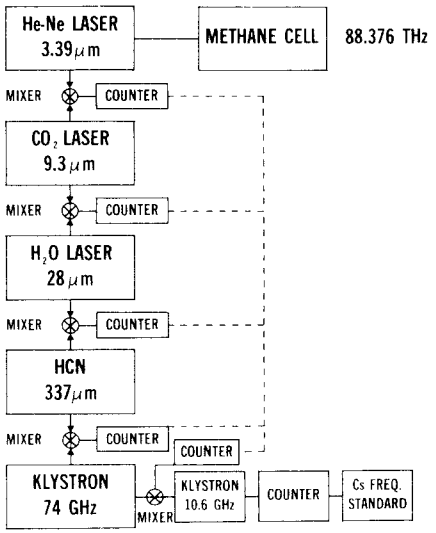


FIG. 11-6 Stabilized-laser frequency-synthesis chain used to compare the absorption frequency of the methane cell with the Cs standard (greatly simplified).

Conventional klystrons are used to generate the four difference frequencies between the lasers, all stabilized by standard phase-lock techniques, and their frequencies are determined by cycle counting at X band.

An interpolating counter controlled by a cesium frequency standard on the NBS atomic time scale counts the 10.6-GHz klystron in the transfer chain. This same standard is used to calibrate the other counters and the spectrum-analyzer tracking generator. All difference frequencies in this chain are either measured simultaneously or held constant. Each main chain oscillator has its radiation divided so that all beat notes in the chain can be measured simultaneously. The experiment was carried out as follows. The 10.6-GHz klystron was phase locked to the 74-GHz klystron, which in turn was phase locked to the free-running HCN laser. The free-running H_2O-laser frequency was monitored relative to the stabilized CO_2-laser frequency, and the beat frequency between the H_2O and HCN lasers was measured on the spectrum analyzer. The frequency of the P(7) line in methane was measured relative to the CO_2 wavelength. More recently, the infrared measurements have been extended to 260 THz with the measurement of the 1.15-μm laser line in ^{20}Ne. The frequency was synthesized in nonlinear crystals of $CdGeAs_2$ and Ag_3AsS_3 from stabilized CO_2 and the 1.15-μm laser line of ^{20}Ne (Jennings *et al.*, 1979a,b).

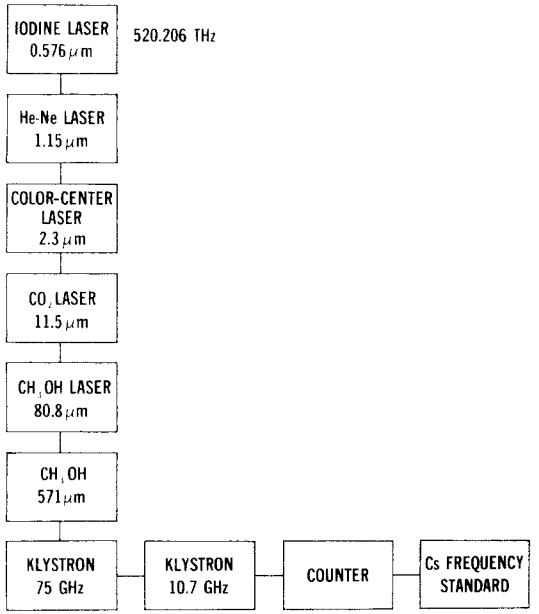


FIG. 11-7 Laser frequency-synthesis chain (greatly simplified, mixers and combiners not shown).

Further efforts are underway to push frequency standards further towards shorter wavelengths. An example using the more recently developed millimeter-wave lasers and a color-center laser is given in Fig. 11-7. The output wavelength from dye lasers can be varied continuously over a fairly wide range. This increases the probability that a substance having optimal properties as a nonlinear absorber can be found. Up to now the fixed-wavelength gas lasers had to be matched with a suitable nonlinear absorption medium. The number of suitable pairs of amplifying and absorbing elements is relatively small. Therefore, the tunable dye laser offers new possibilities in achieving high stabilities. Further articles on frequency synthesis can be found in Wells *et al.* (1972), Evenson *et al.* (1970, 1972a), Hull (1978), and McDonald *et al.* (1971). An excellent review of microwave-to-infrared frequency chains was recently given by Baird (1983).

It should be noted that tunable lasers can greatly simplify a frequency synthesis and measurement system. This is one of the reasons why Soviet research in frequency synthesis in the optical range has concentrated on the development of cw color-center lasers. Tunable lasers utilizing color centers in LiF crystals, emitting in the region of 1 μm, are particularly valuable. Tunable radiation can be generated in different parts of the spectrum by transforming

the frequencies of F-center lasers via sum and difference frequencies. The use of color-center lasers for the synthesis and measurement of near-infrared and visible frequencies removes a number of difficulties and may make it possible to implement specific optimized systems with a minimum number of oscillators and nonlinear devices. Frequency synthesis schemes utilizing F-center lasers are described by Bagaev *et al.* (1982).

11.6 FUTURE PROSPECTS AND PROBLEMS

Progress so far has made the laser the most stable and reproducible source of electromagnetic oscillation. However, the long-term frequency stability of better than 10^{-14} and the reproducibility of 10^{-13} do not represent the ultimate limits. For example, the use of narrow resonances in atomic and molecular beams would probably reduce the effect of collisions significantly (but also increase complexity). A search for quantum transitions without hyperfine structure but with sufficient absorption should be actively pursued. Coupled with this is the need for practical fine- and coarse-tunable lasers, where there is a renewed emphasis in conjunction with other applications. Other nonlinear processes in multiple quantum transitions using possibly forbidden transitions need exploration and if successful may, in fact, lead to frequency reproducibility in the 10^{-15}–10^{-16} range. Perhaps most significantly, the chain process in the context of frequency synthesis must be simplified. For example, it has been recently proposed that it may be feasible to obtain a one-step frequency division from optical or infrared laser frequencies to a subharmonic in the microwave regime (Wineland, 1979). In this concept the cyclotron orbit of a single electron in a Penning discharge is driven with a laser beam of Gaussian cross section focused to a spot diameter on the order of the pump wavelength. The laser subharmonic frequency is measured from the electron synchrotron radiation. This approach, aside from its conceptual simplicity, has other significant advantages. It is known that in frequency multipliers of order N the noise spectral density increases with N^2 relative to the carrier. With the technique considered here (frequency divider), the noise decreases relative to the carrier and basically appears to be limited by the electronic circuit noise within the detection schemes.

In addition, new concepts pushing the performance potential of frequency (and time) standards to its ultimate are under consideration. For example, it has been proposed to locate an individual ion in the center of a small rf quadrupole trap, where the ion may be put into a complete state of rest without any external interference (Dehmelt, 1981). Similarly, the location and charge of appropriate ions in a Penning trap and the application of laser cooling may lead to optical frequency standards better than 1 part per 10^{15}

and frequency stabilities at least 10 times better. Ultimately, of course, there is the Heisenberg uncertainty principle, which limits all physical effects.

In a slightly different vein, one interesting approach has been pursued by Facklam (1982). His work involves the combination of a high-accuracy He–Ne ring-laser gyro and a high-accuracy clock.

In summary, laser technology and concepts so far have led to frequency standards in the visible region, and if pushed they may be developed at still higher frequencies. It is equally true that the prospects of reaching the 10^{15} range within the next decade are excellent. These results will significantly impact upon time–length-standard development and to wherever the ultimate accuracy of physical standards is important. From a more practical point of view, a significant development effort (in addition to basic work) will still have to be invested before the laser frequency standard can be used in system applications on a large scale.

12 Frequency and Time—Their Measurement and Characterization

Samuel R. Stein

Time and Frequency Division
National Bureau of Standards
Boulder, Colorado

List of Symbols 192
12.1 Concepts, Definitions, and Measures of Stability 193
12.1.1 Relationship between the Power Spectrum and the Phase Spectrum 195
12.1.2 The IEEE Recommended Measures of Frequency Stability 195
12.1.3 The Concepts of the Frequency Domain and the Time Domain 203
12.1.4 Translation between the Spectral Density of Frequency and the Allan Variance 203
12.1.5 The Modified Allan Variance 205
12.1.6 Determination of the Mean Frequency and Frequency Drift of an Oscillator 207
12.1.7 Confidence of the Estimate and Overlapping Samples 210
12.1.8 Efficient Use of the Data and Determination of the Degrees of Freedom 213
12.1.9 Separating the Variances of an Oscillator from the Reference 216
12.2 Direct Digital Measurement 217
12.2.1 Time-Interval Measurements 217
12.2.2 Frequency Measurements 219
12.2.3 Period Measurements 219
12.3 Sensitivity-Enhancement Methods 220
12.3.1 Heterodyne Techniques 220
12.3.2 Homodyne Techniques 221
12.3.2.1 Discriminator and Delay Line 222
12.3.2.2 Phase-Locked Loop 223
12.3.3 Multiple Conversion Methods 227
12.3.3.1 Frequency Synthesis 227
12.3.3.2 The Dual-Mixer Time-Difference Technique 229
12.3.3.3 Frequency Multiplication 231
12.4 Conclusion 231

PRECISION FREQUENCY CONTROL
Volume 2
Oscillators and Standards

ISBN 0-12-280602-6

LIST OF SYMBOLS

df	Number of degrees of freedom
f	Fourier (cycle) frequency
$G_{eq}(j\omega)$	Open-loop transfer function of a phase-locked loop
F(s)	Transfer function of the loop filter of a phase-locked loop
$H(f - f_0)$	Transfer function of a filter
K_d	Sensitivity of a linear phase detector in volts per radian
P	Number of counts accumulated by a time-interval counter
Q	Quality factor of a resonance, equal to the ratio of the stored energy to the energy lost in one cycle
s	Independent variable of the Laplace transform
s_y^2	Estimate of the two-sample or Allan variance
$S_y(f)$	One-sided power spectral density of the fractional-frequency deviations
$S_\phi(f)$	One-sided power spectral density of the phase deviations
$S_\phi^{TS}(f)$	Two-sided power spectral density of the phase deviations
$S_{\phi,c}^{TS}(f)$	Two-sided power spectral density of the phase deviations of the carrier
$S_{\phi,p}^{TS}(f)$	Two-sided power spectral density of the phase deviations of the pedestal
$S_V^{TS}(f)$	Two-sided power spectral density of the instantaneous voltage
V_0	Peak voltage of a signal generator
V_d	Output voltage of a phase detector
V_f	Voltage applied to the tuning element of the voltage-controlled oscillator of a phase-locked loop
$V(t)$	Instantaneous voltage of a signal generator or other device
$x(t)$	Time deviation required by a signal generator operating at nominal frequency ν_0 to accumulate phase equal to $\phi(t)$.
$X(f)$	Fourier transform of $x(t)$
$y(t)$	Instantaneous fractional-frequency offset from nominal
$\bar{y}_k$	Mean fractional-frequency offset over the kth interval
α	Exponent of f for a power-law spectral density
$\Delta\nu_Q$	Frequency uncertainty due to the quantization of measurements
ζ	Damping constant of a phase-locked loop
μ	Exponent of τ for a power-law Allan variance
$\nu(t)$	Instantaneous frequency
ν_0	Nominal frequency of a signal generator
$\bar{\nu}(t_1; t_2)$	Mean frequency over the interval $t_1 \le t \le t_2$
ν_H	Heterodyne frequency or difference frequency between two oscillators
$\rho(\chi^2)$	Probability density of the chi-squared distribution
$\sigma_y^2(N, T, \tau)$	Sample variance of N fractional-frequency deviations, each averaged over a period τ spaced at intervals T
$\sigma_y^2(\tau)$	The two-sample or Allan variance of the fractional-frequency deviations
mod $\sigma_y^2(\tau)$	Modified Allan variance
τ	Averaging time
τ_c	Period of the time base of a counter
$\phi(t)$	Instantaneous phase deviation
χ^2	Chi-squared distribution
ω	Fourier (angular) frequency
ω_n	Natural frequency of a phase-locked loop

12.1 CONCEPTS, DEFINITIONS, AND MEASURES OF STABILITY

This chapter deals with the measurement of the frequency or time stability of precision oscillators. It is assumed that the average output frequency is determined by a narrow-band circuit so that the signal is very nearly a sine wave. To be specific, it is also assumed that the output is a voltage, which is conventionally (Barnes *et al.*, 1971) represented by the expression

$$V(t) = [V_0 + \varepsilon(t)] \sin[2\pi\nu_0 t + \phi(t)], \tag{12-1}$$

where V_0 is the nominal peak voltage amplitude, $\varepsilon(t)$ the deviation of amplitude from nominal, ν_0 the nominal fundamental frequency, and $\phi(t)$ the deviation of phase from nominal.

When either specifying or measuring the noise in an oscillator, one must consider the nature of the reference. This may be either a passive circuit such as a narrow-band filter, another similar oscillator, or a set of oscillators, synthesizers, and other signal-generating equipment. A reference with lower noise than the device under test may be available, and in this case the expressions developed in this chapter describe the noise in the oscillator alone. However, a state-of-the-art device will have lower noise than any available reference. In this case all the expressions below refer to the sum of device and reference noise. The most common approach to solving this problem is to compare two or more nearly identical devices. Under most circumstances it is then reasonable to assume that each oscillator contributes half of the measured noise.

The most direct and intuitive method of characterizing the properties of a signal is to determine the two-sided spectrum of $V(t)$, which is denoted $S_V^{TS}(f)$ (Rutman, 1978). The variable f is called a Fourier frequency and is very closely related to the concept of a modulation frequency. A positive f indicates a frequency above the carrier frequency ν_0, while a negative f indicates a frequency lower than the carrier. Since the noise can in theory modulate the carrier at all possible frequencies, a continuous function is required to describe the modulation of $V(t)$. S is called a spectral density and $S_V^{TS}(f)$ is the mean-square voltage $\langle V^2(t)\rangle$ in a unit bandwidth centered at f. It is proportional to the rf power per unit bandwidth delivered by the oscillator to a matched load. The total signal power is proportional to the mean square voltage, which is also called the variance of the signal since the mean value of $V(t)$ is zero. The variance is therefore equal to the two-sided spectral density integrated over all frequencies.

The two-sided spectrum is usually measured by an rf spectrum analyzer, a device that functions like a bandpass filter followed by a bolometer, as shown

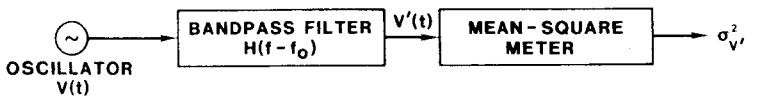


FIG. 12-1 An rf spectrum analyzer. The device produces an output proportional to the mean-square value of the signal passing through a tunable narrow-band filter centered at frequency f_0.

in Fig. 12-1. The spectrum of the filtered voltage $V'(t)$ is equal to the square of the magnitude of the filter transfer function $H(f - f_0)$ multiplied by the spectrum of the input signal (Cutler and Searle, 1966). The variance of the filtered voltage is obtained from Parseval's theorem:

$$\sigma_{V'}^2(f_0) = \int_{-\infty}^{\infty} |H(f - f_0)|^2 S_V^{TS}(f)\, df. \tag{12-2}$$

If the bandpass filter is sufficiently narrow, so that $S_V^{TS}(f)$ changes negligibly over its bandwidth, then Eq. (12-2) may be inverted. With this assumption, the power spectrum is estimated from the measurement using Eq. (12-3):

$$S_V^{TS}(f_0) = \sigma_{V'}^2(f_0)/B, \tag{12-3}$$

where $B = \int_{-\infty}^{\infty} |H(f' - f_0)|^2\, df'$ is the noise bandwidth of the filter and f_0 its center frequency. Figure 12-2 shows a typical two-sided rf spectrum. For many oscillators the spectrum has a Lorentzian shape, that is,

$$S_V^{TS}(f) = \frac{2\langle V^2\rangle/\pi\, \Delta f_{3dB}}{1 + (f/(\Delta f_{3dB}/2))^2}. \tag{12-4}$$

The Lorentzian lineshape is completely described by the mean square voltage $\langle V^2\rangle$ and the full width at half maximum Δf_{3dB}.

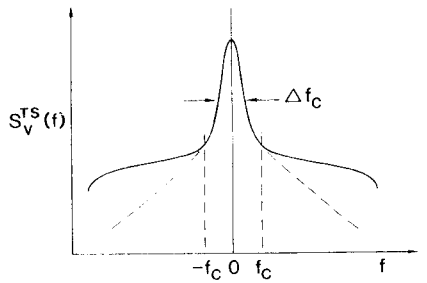


FIG. 12-2 The rf spectrum of a signal. It is often useful to divide the spectrum into the carrier and the noise pedestal. The spectral density of the carrier exceeds that of the noise pedestal for Fourier frequencies smaller in magnitude than f_c.

12.1.1 Relationship between the Power Spectrum and the Phase Spectrum

The power spectrum differs from a delta function $\delta(f)$ due to the presence of the amplitude- and phase-noise terms, $\varepsilon(t)$ and $\phi(t)$, respectively, included in Eq. (12-1). Usually the noise modulation separates into two distinct components, so that one observes a very narrow feature called the carrier above the level of a relatively broad pedestal. The frequency that separates the carrier and pedestal is denoted f_c. Below this frequency the spectral density of the carrier exceeds that of the pedestal. Assuming that the amplitude noise is negligible compared to the phase noise and that the phase modulation is small, the relationship between the power and phase spectra is given by (Walls and DeMarchi, 1975)

$$S_V^{TS}(f) \cong \frac{V_0^2}{2} e^{-I(f_c)} \times \begin{cases} \delta(f), & \text{if } -f_c < f < f_c, \\ S_\phi^{TS}(f), & \text{otherwise.} \end{cases} \tag{12-5}$$

$S_\phi^{TS}(f)$ is the two-sided spectrum of the phase fluctuations, which divides into a carrier component $S_{\phi,c}^{TS}(f)$ and a pedestal component $S_{\phi,p}^{TS}(f)$: $I(f_c)$ is given by

$$I(f_c) = \int_{f_c}^{\infty} S_{\phi,p}(f)\, df \simeq \int_{f_c}^{\infty} S_\phi(f)\, df \tag{12-6}$$

since above f_c the pedestal dominates the noise spectrum. The variance of the carrier is equal to $(V_0^2/2)e^{-I(f_c)}$, with the remaining variance in the pedestal. If $\Delta\nu_p$ is the width of the pedestal and $\Delta\nu_c$ the width of the carrier, then the power density in the carrier is equal to that in the pedestal when $I(f_c) = \ln(\Delta\nu_p/\Delta\nu_c)$. For the pedestal, one may use the 3-dB linewidth for $\Delta\nu_p$ provided that $\int_{f_c}^{\infty} S_\phi(f)\, df < \ln 2$. Otherwise the pedestal width is estimated from $\int_{\Delta\nu/2}^{\infty} S_\phi(f)\, df = \ln 2$. For the carrier, the linewidth is estimated by calculating $\int_{\Delta\nu_c/2}^{\infty} S_{\phi,c}(f)\, df = \ln 2$.

The foregoing analysis makes it possible to draw certain conclusions concerning detection of the carrier. We use $\int_p df$ to denote the integral over the phase noise pedestal. If $\int_p S_\phi(f)\, df < \ln 2$, then the carrier may be resolved irrespective of detector bandwidth. When $\ln(\Delta\nu_p/\Delta\nu_c) > \int_p S_\phi(f)\, df > \ln 2$, the carrier may be resolved by restricting the detection bandwidth. But when $\int_p S_\phi(f)\, df > \ln(\Delta\nu_p/\Delta\nu_c)$, the carrier can no longer be distinguished from the pedestal since its spectral density is smaller.

12.1.2 The IEEE Recommended Measures of Frequency Stability

By the mid-1960s the problem of the specification of precision oscillators had become extremely important, but there was very little uniformity among manufacturers, metrologists, and applications engineers in the methods of

performing measurements or the description of measurement results. This situation was complicated by the difficulty of comparing the various descriptions. A measure of stability is often used to summarize some important feature of the performance of the standard. It may therefore not be possible to translate from one measure to another even though the respective measurement processes are fully described and all relevant parameters are given. This situation resulted in a strong pressure to achieve a higher degree of uniformity.

In order to reduce the difficulty of comparing devices measured in separate laboratories, the IEEE convened a committee to recommend uniform measures of frequency stability. The recommendations made by the committee are based on the rigorous statistical treatment of ideal oscillators that obey a certain model (Barnes *et al.*, 1971). Most importantly, these oscillators are assumed to be elements of a stationary ensemble. A random process is stationary if no translation of the time coordinate changes the probability distribution of the process. That is, if one looks at the ensemble at one instant of time, then the distribution in values for a process within the ensemble is exactly the same as the distribution at any other instant of time. The elements of the ensemble are not constant in time, but as one element changes value other elements of the ensemble assume previous values. Thus, it is not possible to determine the particular time when the measurement was made.

The stationary noise model has been adopted because many theoretical results, particularly those related to spectral densities, are valid only for this case. It is important for the statistician to exercise considerable care since experimentally one may measure quantities approximately equal to either the instantaneous frequency of the oscillator or the instantaneous phase. But the ideal quantities approximated by these measurements may not both be stationary. The instantaneous angular frequency is conventionally defined as the time derivative of the total oscillator phase. Thus,

$$\omega(t) = \frac{d}{dt}[2\pi\nu_0 t + \phi(t)], \tag{12-7}$$

and the instantaneous frequency is written

$$\nu(t) = \nu_0 + \frac{1}{2\pi}\frac{d\phi}{dt}. \tag{12-8}$$

For precision oscillators, the second term on the right-hand side is quite small, and it is useful to define the fractional frequency

$$y(t) = \frac{\nu(t) - \nu_0}{\nu_0} = \frac{1}{2\pi\nu_0}\frac{d\phi}{dt} = \frac{dx}{dt}, \tag{12-9}$$

where

$$x(t) = \phi(t)/2\pi\nu_0 \tag{12-10}$$

is the phase expressed in units of time. Alternatively, the phase could be written as the integral of the frequency of the oscillator:

$$\phi(t) = \phi_0 + \int_0^t 2\pi[\nu(0) - \nu_0]\, d0. \tag{12-11}$$

However, the integral of a stationary process is generally not stationary. Thus, indiscriminate use of Eqs. (12-7) and (12-11) may violate the assumptions of the statistical model. This contradiction is avoided when one accounts for the finite bandwidth of the measurement process. Although a more detailed consideration of the statistics goes beyond the scope of this treatment, it is very important to keep in mind the assumption that lie behind the statistical analysis of oscillators. In order to analyze the behavior of real oscillators, it is necessary to adopt a model of their performance. The model must be consistent with observations of the device being simulated. To make it easier to estimate the device parameters, the models usually include certain predictable features of the oscillator performance, such as a linear frequency drift. A statistical analysis is useful in estimating such parameters to remove their effect from the data. It is just these procedures for estimating the deterministic model parameters that have proved to be the most intractable. A substantial fraction of the total noise power often occurs at Fourier frequencies whose periods are of the same order as the data length or longer. Thus, the process of estimating parameters may bias the noise residuals by reducing the noise power at low Fourier frequencies. A general technique for minimizing this problem in the case of oscillators actually observed in the laboratory is discussed below.

It has been suggested that measurement techniques for frequency and time constitute a hierarchy (Allan and Daams, 1975), with the measurement of the total phase of the oscillator at the peak. Although more difficult to measure with high precision than other quantities, the total phase has this status owing to the fact that all other quantities can be derived from it. Furthermore, missing measurements produce the least deleterious effect on a time series consisting of samples of the total phase. Gaps in the data affect the computation of various time-dependent quantities for times equal to or shorter than the gap length, but have a negligible effect for times much longer than the gap length. The lower levels of the hierarchy consist of the time interval, frequency, and frequency fluctuation. When one measures a quantity somewhere in this hierarchy and wishes to obtain a higher quantity, it is necessary to integrate one or more times. In this case the problem of missing data is quite serious. For example, if frequency is measured and one wants to

know the time of a clock, one needs to perform the integration in Eq. (12-11). The missing frequency measurements must be bridged by estimating the average frequency over the gap, resulting in a time error that is propagated forever. Thus, it is preferable to always make measurements at a level of the measurement hierarchy equal to or above the level corresponding to the quantity of principle interest. In the past this was rather difficult to do. Measurement systems constructed from simple commercial equipment suffered from dead time, that is, they were inactive for a period after performing a measurement. To make matters worse, methods for measuring time or phase had considerably worse noise performance than methods for measuring frequency. As a result, many powerful statistical techniques were developed to cope with these problems (Barnes, 1969; Allan, 1966). The effect of dead time on the statistical analysis has been determined (Lesage and Audoin, 1979b). Other techniques have been developed to combine short data sets so that the parameters of clocks over long periods of time could be estimated despite missing data (Lesage, 1983). The rationale for these approaches is considerably diminished today. Low-noise techniques for the measurement of oscillator phase have been developed. Now, commercial equipment is capable of measuring the time or the total phase of an oscillator with very high precision. Other equipment exists for measuring the time interval. These devices use the same techniques that were previously employed for the measurement of frequency and are very competitive in performance.

The proliferation of microcomputers and microprocessors has had an equally profound effect on the field of time and frequency measurement. There has been a dramatic increase in the ability of the metrologist to acquire and process digital data. Many instruments are available with suitable standard interfaces such as IEEE-583 or CAMAC (IEEE, 1975) and IEEE-488 (IEEE, 1978). As a result, there has been a dramatic change in direction away from analog signal processing toward the digital, and this process is accelerating daily. Techniques once used only by national standards laboratories and other major centers of clock development and analysis are now widespread. Consequently, this chapter will focus first on the peak of the measurement hierarchy and the use of digital signal processing. But the analysis is directed toward estimating the traditional measures of frequency stability. Considerable attention will be paid to problems associated with estimating the confidence of these stability measures and obtaining the maximum information from available data.

The IEEE has recommended as its first measure of frequency stability the one-sided spectral density $S_y(f)$ of the instantaneous fractional-frequency fluctuations $y(t)$. It is simply related to the spectral density of phase fluctuations since differentiation of the time-dependent functions is equivalent to

multiplication of their Fourier transforms by $j\omega$:

$$S_y(f) = (f/\nu_0)^2 S_\phi(f) = (2\pi f)^2 S_x(f). \tag{12-12}$$

Section 12.1.1 on the relationship between the power spectrum and the phase spectrum described the analog method for the measurement of a spectral density. If a voltage V is the output of the oscillator, then the result of the measurement is proportional to the rf power spectral density. But if the voltage were proportional to the frequency or phase of the oscillator, then the result of the measurement would be proportional to the spectral density of the frequency or phase. The most common units of $S_\phi(f)$ are radians squared per hertz.

Alternatively, the spectral density can be obtained by digital analysis of the signal. For example, the quantity $S_x(f)$ can be calculated from the Fourier transform of $x(t)$. The relevant continuous Fourier-transform pair is defined as follows:

$$X(f) = \int_{-\infty}^{\infty} x(t) e^{-j2\pi ft}\, dt \tag{12-13}$$

and

$$x(t) = \frac{1}{2\pi} \int_{-\infty}^{\infty} X(f) e^{j2\pi ft}\, df. \tag{12-14}$$

However, one does not generally have continuous knowledge of the phase of the oscillator. Since it is relatively easy to measure $x(t)$ at equally spaced time intervals, we assume the existence of the series x_l, where $x_l = x(l\tau)$ for integer values of l. The discrete Fourier transform is defined by analogy to the continuous transform (Cochran *et al.*, 1967):

$$X(f) = \sum_{l=-\infty}^{\infty} x(l) e^{-j2\pi fl}. \tag{12-15}$$

In practice the time series has finite length T consisting of N intervals of length τ, and it is not possible to compute the infinite sum. Nevertheless, it remains possible to compute a spectrum that is not continuous in f but rather has resolution Δf, where

$$\Delta f = 1/T = 1/N\tau. \tag{12-16}$$

The need to sum over all values of the index l is removed by assuming that the function $x(t)$ repeats itself with period T. The resulting spectrum contains no information on the spectrum at Fourier frequencies less than $1/T$. Truncation of the time series also introduces spurious effects due to the turn-on and turn-off transients. These problems can be minimized through the use of a window function. The computed spectrum is actually the square of the magnitude of

the window function multiplied by the desired spectrum. The use of a window function reduces the variance of the spectrum estimate at the expense of smearing out the spectrum to a small degree. With these changes but no window function, we arrive at the discrete finite transform

$$X(n\,\Delta f) = \frac{1}{N}\sum_{k=0}^{N-1} x(k\tau)e^{-j2\pi n\,\Delta f\,k\tau}. \tag{12-17}$$

The spectral density of $x(t)$ is computed from Eq. (12-17) by squaring the real and imaginary components, adding the two together, and dividing by the total time T:

$$S_x(m\,\Delta f) = \frac{\{R[X(m\,\Delta f)]\}^2 + \{I[X(m\,\Delta f)]\}^2}{T}. \tag{12-18}$$

The digital method of estimating spectral densities has many advantages over analog signal processing. Most important is the fact that it may be computed from any set of equally spaced samples of a time series. As a result, the technique is compatible with other methods of characterizing the signal, that is, the sampled data can be stored and processed using a variety of algorithms. In addition, each record of length T produces a single estimate of the spectrum for each of the N frequencies $\Delta f, 2\,\Delta f, \ldots, N\,\Delta f$. It is therefore possible to estimate the entire spectrum much more quickly using the digital technique than it would be using analog methods. The fast Fourier transform, a very efficient algorithm for the computation of the discrete finite transform, has opened the way to versatile self-contained, commercial spectrum analysis. It is also very straightforward to compute the spectrum from data acquired by computerized digital data acquisition systems.

A result of the finite sampling rate is that the upper frequency limit of the digital spectrum analysis is $1/2\tau$, called the Nyquist frequency (Jenkins and Watts, 1968). Power in the signal being analyzed that is at frequencies higher than the Nyquist frequency affects the spectrum estimate for lower frequencies. This problem is called aliasing. The out-of-band signal is rejected by only approximately 6 dB per octave above the Nyquist frequency. Thus, when significant out-of-band signals exist, they must be reduced by analog filtering. One or more low-pass filters are usually sufficient for this purpose.

As its second measure of frequency stability, the IEEE recommended the sample variance $\sigma_y^2(\tau)$ of the fractional-frequency fluctuations. It is a measure of the variability of the average frequency of an oscillator between two adjacent measurement intervals. The average fractional-frequency deviation $\bar{y}_k$ over the time interval from t_k to $t_k + \tau$ is defined as

$$\bar{y}_k = \frac{1}{\tau}\int_{t_k}^{t_k+\tau} y(t)\,dt, \tag{12-19}$$

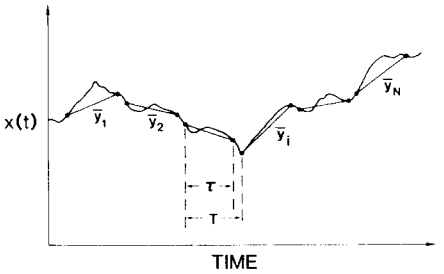


FIG. 12-3 Measurement process for the computation of the sample variance. The phase difference between two oscillators is plotted on the ordinate. The measurement yields a set of frequencies averaged over equal intervals τ separated by dead time $T - \tau$.

from which it follows that

$$\bar{y}_k = \frac{x(t_k + \tau) - x(t_k)}{\tau}. \tag{12-20}$$

The quality τ is often referred to as the sampling time or the averaging time. Equations (12-19) and (12-20) are not the only way to define mean frequency, but they are the simplest. Other definitions lead to alternative measures of stability that may have desirable properties.

Suppose that one has measured the time or frequency fluctuations between a pair of precision oscillators and a stability analysis is desired. The process is illustrated in Fig. 12-3. These are N values of the fractional frequency $\bar{y}_i$. Each one is measured over a time τ, and measurements are repeated after intervals of time T. If the measurement repetition time exceeds the averaging time, then there is a dead time equal to $T - \tau$ between each frequency measurement, during which there is no information available.

There are many ways to analyze these data. A fairly general approach is the N-sample variance defined by the relation

$$\langle\sigma_y^2(N, T, \tau)\rangle = \left\langle \frac{1}{N-1}\sum_{n=1}^{N}\left(\bar{y}_n - \frac{1}{N}\sum_{k=1}^{N}\bar{y}_k\right)^2\right\rangle, \tag{12-21}$$

where the angle brackets denote the infinite time average. Frequently, Eq. (12-21) does not converge as $N \to \infty$, since some noise processes in oscillators diverge rapidly at low Fourier frequencies. This implies that the precision with which one estimates the variance does not improve simply as the sample size is increased. For this reason, the two-sample variance with no dead time is preferred. Also called the Allan variance, it converges for all the major noise types observed in precision oscillators. It may be written as

$$\sigma_y^2(\tau) = \langle\tfrac{1}{2}(\bar{y}_{k+1} - \bar{y}_k)^2\rangle. \tag{12-22}$$

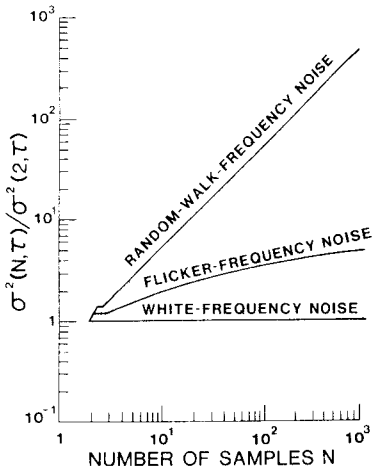


FIG. 12-4 N-sample variance versus Allan variance. The two-sample variance converges for the important types of noise observed in frequency standards but the ratio of the traditional variance to the two-sample variance is an increasing function of sample size for flicker frequency noise and random-walk frequency noise.

The dependence of the classical variance on the number of samples is shown in Fig. 12-4 for the case of no dead time. The quantity plotted is the ratio of the N-sample variance to the Allan variance. Note that $\sigma_y^2(\tau)$ has the same value as the classical variance for the white-noise frequency modulation. However, the classical variance grows without bound for flicker-frequency and random-walk-frequency noises.

One may combine Eqs. (12-20) and (12-22) to obtain an equation for $\sigma_y(\tau)$ in terms of the time-difference or time-deviation measurements:

$$\sigma_y^2(\tau) = \langle \tfrac{1}{2}\tau^{-2}[x(t + 2\tau) - 2x(t + \tau) + x(t)]^2 \rangle. \tag{12-23}$$

N discrete time readings may be used to estimate the variance

$$\sigma_y^2(\tau) \cong \frac{1}{2(N-2)\tau^2} \sum_{i=1}^{N-2} (x_{i+2} - 2x_{i+1} + x_i)^2, \tag{12-24}$$

where i denotes the number of the measurement in the set of N and the nominal spacing between measurements is τ. Since it has been assumed that there is no dead time between measurements, one can write τ in Eq. (12-24) as an integer multiple of τ_0, that is, $\tau = m\tau_0$, where τ_0 is the smallest spacing of the data. In this case

$$\sigma_y^2(m\tau_0) \cong \frac{1}{2(N-2m)m^2\tau_0^2} \sum_{i=1}^{N-2m} (x_{i+2m} - 2x_{i+m} + x_i)^2. \tag{12-25}$$

12.1.3 The Concepts of the Frequency Domain and the Time Domain

Spectral densities are measures of frequency stability in what is called the frequency domain since they are functions of Fourier frequency. The Allan variance, on the other hand, is an example of a time-domain measure. In a strict mathematical sense, these two descriptions are connected by Fourier transform relationships (Cutler and Searle, 1966). However, for many years the inadequacy of measurement equipment created artificial barriers between these two characterizations of the same noise process. As a result, many specialized techniques have been developed to translate between the various measures of stability (Allan, 1966; Burgoon and Fischer, 1978). The preceding sections have demonstrated how easily both types of stability measures can be computed from the same data provided that the measurement process provides complete information. For example, both $\sigma_y^2(m\tau_0)$ and $S_x(m\,\Delta f)$ can be computed from evenly spaced samples of $x(t)$. However, incomplete information can result from either measurement dead time or interruptions in the data acquisition process. In these cases translation techniques remain valuable.

Both the spectral density and the Allan Variance are second-moment measures of the time series $x(t)$. However, it is only possible to translate unambiguously from the spectral density to the Allan variance, not the reverse. To calculate the spectral density it is necessary to use the autocorrelation function of the phase. The following discussion on power-law noise processes further demonstrates this dichotomy. As we shall see, the Allan variance for a fixed measurement bandwidth does not distinguish between all of the noise processes that are commonly observed in precision oscillators.

12.1.4 Translation between the Spectral Density of Frequency and the Allan Variance

The power-law model is most frequently used for describing oscillator phase noise. It assumes that the spectral density of frequency fluctuations is equal to the sum of terms, each of which varies as an integer power of frequency. Thus, there are two quantities that completely specify $S_y(f)$ for a particular power-law noise process: the slope on a log–log plot for a given range of f and the amplitude. The slope is denoted by α and therefore f^α is the straight line on a log–log plot that relates $S_y(f)$ to f. The amplitude is denoted h_α. When we examine a plot of the spectral density of frequency fluctuations, we represent it by the addition of all the power-law processes (Allan, 1966; Vessot *et al.*, 1966) with the appropriate coefficients:

$$S_y(f) = \sum_{\alpha=-\infty}^{\infty} h_\alpha f^\alpha. \tag{12-26}$$

TABLE 12-1

Correspondence between Common Power-Law Spectral Densities and the Allan Variance[a]

Noise type	$S_y(f)$	$\sigma_y^2(\tau)$
White phase	$h_2 f^2$	$3f_h h_2/(2\pi)^2\tau^2$
Flicker phase	$h_1 f$	$\dfrac{[1.038 + 3\ln(2\pi f_h\tau)]}{(2\pi)^2} h_1 \dfrac{1}{\tau^2}$
White frequency	h_0	$\frac{1}{2}h_0(1/\tau)$
Flicker frequency	$h_{-1}f^{-1}$	$2\ln(2)h_{-1}$
Random-walk frequency	$h_{-2}f^{-2}$	$\frac{1}{6}(2\pi)^2 h_{-2}\tau$

[a] Where necessary for convergence the spectral density has been assumed to be zero for frequencies greater than the cutoff frequency f_h.

This technique is most valuable when only a few terms in Eq. (12-26) are required to describe the observed noise and each term dominates over several decades of frequency. This situation often prevails. Five power-law noise processes (Allan, 1966; Vessot *et al.*, 1966) are common with precision oscillators:

(1) random-walk frequency modulation $\alpha = -2$
(2) flicker frequency modulation $\alpha = -1$
(3) white frequency modulation $\alpha = 0$
(4) flicker phase modulation $\alpha = 1$
(5) white phase modulation $\alpha = 2$

The spectral density of frequency is an unambiguous description of the oscillator noise. Thus, the spectrum can be used to compute the Allan variance (Barnes *et al.*, 1971):

$$\sigma_y^2(\tau) = \frac{2}{(\pi\nu_0\tau)^2}\int_0^\infty S_\phi(f)\sin^4(\pi f\tau)\,df. \tag{12-27}$$

However, Eq. (12-27) shows that the Allan variance is very sensitive to the high frequency dependence of the spectral density of phase, thereby necessitating a detailed knowledge of the bandwidth-limiting elements in the measurement setup. The integral has been computed for each of the power-law noise processes, and the results are summarized in Table 12-1 (Barnes *et al.*, 1971). For α in the range $-2 \le \alpha \le 0$, the Allan variance is proportional to τ^μ, where $\mu = -\alpha - 1$. When the log of the Allan variance is plotted as a function of the log of the averaging time, the graph also consists of straight-line segments with integer slopes. However, Table 12-1 also shows that even if

the oscillator is reasonably modeled by power-law spectra, it is not practical to distinguish between white phase noise and flicker phase noise from the dependence of the Allan variance on τ. In both cases $\sigma_y^2 \simeq 1/\tau^2$.

12.1.5 The Modified Allan Variance

Table 12-1 also shows that the Allan variance has very different bandwidth dependence for white phase noise and flicker phase noise. Therefore, these noise types have been distinguished by varying the bandwidth of the measurement system. If $x(t)$ were measured, the noise type could be identified by computing the spectrum. However, both the approach of making measurements as a function of bandwidth and the computation of the spectrum can be avoided by calculating a modified version of the Allan variance. The algorithm for this variance has the effect of changing the bandwidth inversely in proportion to the averaging time (Snyder, 1981; Allan and Barnes, 1981).

Each reading of the time deviation x_i has associated with it a measurement-system bandwidth f_h. Similarly, we can define a software bandwidth $f_s = f_h/n$, which is $1/n$ times narrower than the hardware bandwidth. It can be realized by averaging n adjacent x_i's. Based on this idea it is possible to define a modified Allan variance that allows the reciprocal software bandwidth to change linearly with the sample time τ:

$$\operatorname{mod}\sigma_y^2(\tau) = \frac{1}{2\tau^2}\left\langle\left[\frac{1}{n}\sum_{i=1}^{n}(x_{i+2n} - 2x_{i+n} + x_i)\right]^2\right\rangle, \tag{12-28}$$

where $\tau = n\tau_0$. Equation (12-28) reduces to Eq. (12-23) for $n = 1$. One can see that mod $\sigma_y^2(\tau)$ is the second difference of three time values, each of which is a nonoverlapping average of n of the x_i's. As n increases the software bandwidth decreases as f_h/n.

For a finite data set of N readings of x_i ($i = 1$ to N), mod $\sigma_y^2(\tau)$ can be estimated from the expression

$$\operatorname{mod}\sigma_y^2(\tau) \cong \frac{1}{2\tau^2 n^2(N - 3n + 1)}\sum_{j=1}^{N-3n+1}\sum_{i=j}^{n+j-1}(x_{i+2n} - 2x_{i+n} + x_i)^2, \tag{12-29}$$

which is easy to program but takes more time to compute than the corresponding equation (12-24) for $\sigma_y^2(\tau)$.

Table 12-2 gives the relationship between the time-domain measure mod $\sigma_y^2(\tau)$ and its power-law spectral counterpart. In the right-hand column are the asymptotic values of the ratio of the modified Allan variance to the Allan variance. It is clear from the table that mod $\sigma_y^2(\tau)$ is very useful for white

TABLE 12-2

Correspondence between Common Power-Law Spectral Densities and the Modified Allan Variance[a]

Noise type	$S_y(f)$	mod $\sigma_y^2(\tau)$	mod σ_y^2/σ_y^2
White phase	$h_2 f^2$	$h_2 \frac{3f_h}{n(2\pi)^2}\frac{1}{\tau^2}$	n
Flicker phase	$h_1 f$	$h_1 \frac{[1.038 + 3\ln(2\pi f_h \tau)]}{(2\pi)^2}\frac{1}{\tau^2}$	1
White frequency	h_0	$h_0 \frac{1}{4\tau}$	0.5
Flicker frequency	$h_{-1} f^{-1}$	$h_{-1}(0.936)$	0.674
Random-walk frequency	$h_{-2} f^{-2}$	$h_{-2}(5.42)\tau$	0.824

[a] Where necessary the spectral density has been assumed to be zero for frequencies greater than the cutoff frequency f_h. The constant n is the number of adjacent phase values that are averaged to produce the bandwidth reduction. The values in the last two columns are for the asymptotic limit $n \to \infty$. In practice, n only needs to be 10 or larger before the asymptotic limit is approached within a few percent. When $n = 1$ the ratio in the last column is 1 in all cases.

phase modulation and flicker phase modulation, but for $\alpha \leq 1$ the conventional Allan variance gives both an easier-to-interpret and an easier-to-calculate measure of stability.

It is interesting to make a graph of α versus μ for both the ordinary Allan variance and the modified Allan variance, such as the one shown in Fig. 12-5.

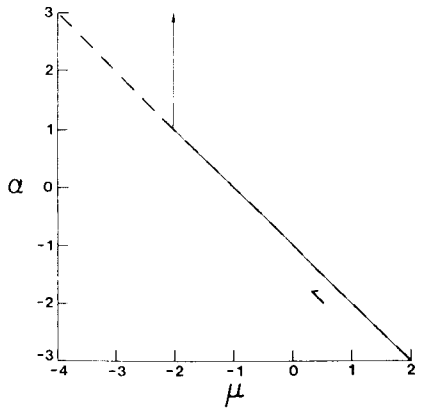


FIG. 12-5 Relationship between a power-law spectral density whose slope on a log–log plot is α and the corresponding sample variance whose slope on a log–log plot is μ. The solid line describes the behavior of the Allan variance, while the dashed line shows the advantage of the modified Allan variance for white phase noise and flicker phase noise.

This graph allows one to determine power-law spectra for noninteger as well as integer values of α. In the asymtotic limit the equation relating μ and α for the modified Allan variance is

$$\alpha = -\mu - 1 \qquad \text{for} \quad -3 < \alpha < 3. \tag{12-30}$$

12.1.6 Determination of the Mean Frequency and Frequency Drift of an Oscillator

Before the techniques of the previous four sections can be meaningfully applied to practical measurements, it is necessary to separate the deterministic and random components of the time deviation $x(t)$. Suppose, for example, that an oscillator has significant drift, such as might be the case for a quartz crystal oscillator. With no additional signal processing, the Allan variance would be proportional to τ^2. The variance of the Allan variance would be very small, further demonstrating that deterministic behavior has been improperly described in statistical terms and the oscillator's predictability is much better than the Allan variance indicated. Unfortunately, it is difficult to estimate the oscillator's deterministic behavior without introducing a bias in the noise at Fourier frequencies comparable to the inverse of the record length. In practice, it has been sufficient to consider two deterministic terms in $x(t)$:

$$x(t) = x_0 + (\Delta\nu/\nu_0)t + \tfrac{1}{2}Dt^2 + x_1(t) \tag{12-31}$$

The first term on the right-hand side is the synchronization error. The second term is due to imperfect knowledge of the mean frequency and is sometimes called syntonization error. The quadratic term, which results from frequency drift, is the most difficult problem for the statistical analysis because the Allan variance is insensitive to both synchronization and syntonization errors.

For white noise, the optimum estimate of the process is the mean. Therefore, a general statistical procedure that can be followed is to filter the data until the residuals are white (Allan *et al.*, 1974; Barnes and Allan, 1966). For example, at short times the frequency fluctuations of atomic clocks are usually white. Taking the first difference of Eq. (12-31), we find that

$$\bar{y}(t) = \frac{\Delta\nu}{\nu_0} + Dt + \frac{x_1(t+\tau) - x_1(t)}{\tau}, \tag{12-32}$$

and a linear least square fit to the frequency data yields the optimum estimate of $\Delta\nu$. However, the drift in atomic clocks is generally so small that the value obtained for D will not be statistically significant when τ is small enough to

satisfy the assumption of white frequency noise. Thus, we are led to consider the first difference of the frequency,

$$\frac{\bar{y}(t+\tau) - \bar{y}(t)}{\tau} = D + \frac{x_1(t+2\tau) - 2x_1(t+\tau) + x_1(t)}{\tau^2}. \quad (12\text{-}33)$$

Many atomic clocks are dominated by random walk of frequency noise for long averaging times. Thus, the first difference of the frequency data (the second difference of the phase data) is white, and the optimum estimate of the drift is just the simple mean. If instead, a linear least square fit were removed from the frequency data in this region of τ, then the random-walk residuals would be biased, and it is likely that an optimistic estimate of $\sigma_y(\tau)$ would be obtained.

The optimum procedure would be different if the dominant noise type were flicker of frequency, rather than random walk. But there is no simple prescription that can be followed to estimate the drift in that case. Fortunately, a maximum likelihood estimate of the prameters for some typical cases has shown that the mean second difference of phase is still a good estimator of frequency drift in the sense that it introduces negligible bias in the Allan variance. Thus, in practice there is a simple prescription for computing the Allan variance in the presence of significant drift. Starting with the phase data, one forms the second difference and uses the simple average to estimate the mean. The value of τ chosen for creating these second differences must be long enough so that the predominant noise process is random-walk frequency modulation. After subtracting this estimate, the second-difference data is integrated twice to recover phase data with drift removed, and further analysis, including the computation of the Allan variance, may proceed. Figures 12-6 through 12-10 illustrate the estimation of drift. The quadratic dependence of the phase data in Fig. 12-6 nearly obscures the noise. The first difference of this data produces the nearly linear frequency dependence shown in Fig. 12-7, and the second difference produces the residuals shown in Fig. 12-8, which appear to be nearly white. Rigorous statistical analysis of this data indicates that the first difference of the frequency is indeed white with 90% confidence. Next, the mean frequency difference is subtracted. Then the residuals of Fig. 12-8 are integrated twice, and the result is the estimate of the phase deviation with drift removed shown in Fig. 12-9. Fig. 12-10 illustrates the Allan variance of this data calculated by three techniques. The squares were computed from the data of Fig. 12-6, while the open circles were computed following the recommended procedure for estimating the drift. The validity of the approach is illustrated by the black dots, which are the result of a statistically optimum parameter estimation procedure.

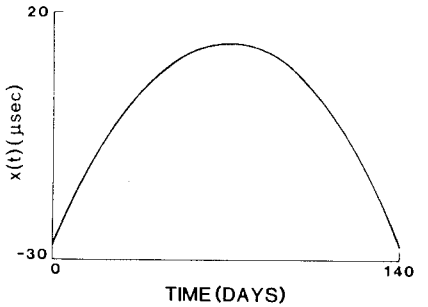


FIG. 12-6 Measured phase difference between a frequency standard and a reference during a 140-day experiment. The nearly quadratic form of the data effectively obscures the noise.

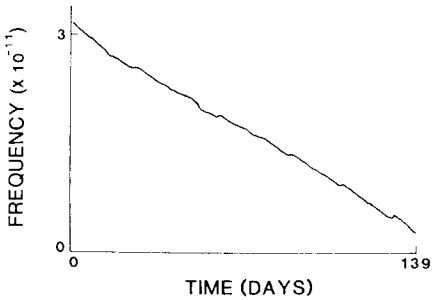


FIG. 12-7 One-day frequency averages obtained by taking the first differences of the data in Fig. 12-6. The ordinate is the fractional difference of the daily frequency from a nominal value. The nearly linear change in frequency with time is apparent, although the random deviations are visible.

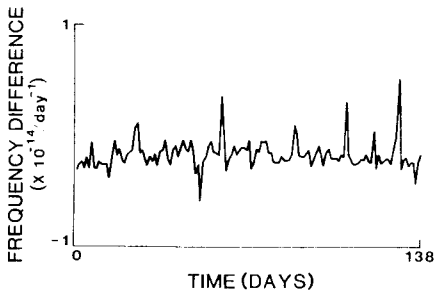


FIG. 12-8 Second difference of the data in Fig. 12-6. The second difference operation has removed the nonrandom behavior and the residuals appear to be nearly white.

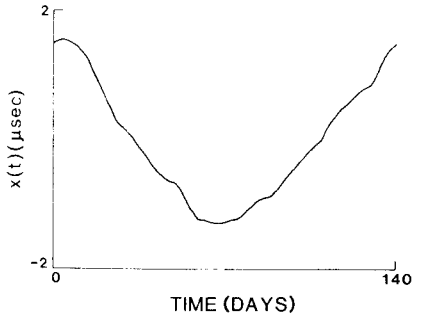


FIG. 12-9 Phase variations of the frequency standard due to the residuals, obtained by performing two integrations on the data of Fig. 12-8. The ordinate scale is expanded approximately 10 times compared to Fig. 12-6.

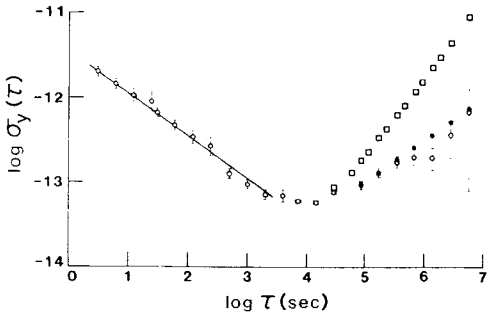


FIG. 12-10 Logarithm of the square root of the Allan variance as a function of the logarithm of the averaging time for three different computation methods. The squares were computed from the data of Fig. 12-6 and show the effect of the drift. The open circles were computed from the data of Fig. 12-9. The closed circles were computed using an optimum-parameter estimation procedure.

12.1.7 Confidence of the Estimate and Overlapping Samples

Consider three phase or time measurements of one oscillator relative to another at equally spaced intervals of time. From this phase data one can obtain two adjacent values of average frequency and one can calculate a single sample Allan variance (see Fig. 12-11). Of course, this estimate does not have high precision or confidence, since it is based on only one frequency difference.

For most commonly encountered oscillators, the first difference of the frequency is a normally distributed variable with zero mean. However, the square of a normally distributed variable is not normally distributed. This is so because the square is always positive and the normal distribution is

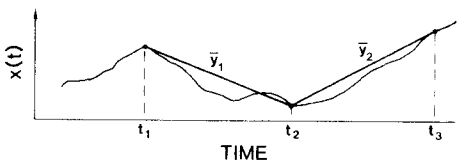


FIG. 12-11 Calculation of two average frequencies $\bar{y}_1$ and $\bar{y}_2$ by measuring the phase of an oscillator $x(t)$ at times t_1, t_2, and t_3.

completely symmetric, with negative values being as likely as positive ones. The resulting distribution is called a chi-squared distribution, and it has one "degree of freedom" since the distribution was obtained by considering the squares of individual (i.e., one independent sample), normally distributed variables (Jenkins and Watts, 1968).

In contrast, from five phase values four consecutive frequency values can be calculated, as shown in Fig. 12-12. It is possible to take the first pair and calculate a sample Allan variance. A second sample Allan variance can be calculated from the second pair (i.e., the third and fourth frequency measurements). The average of these two sample Allan variances provides an improved estimate of the true Allan variance, and one would expect it to have a tighter confidence interval than in the previous example. This could be expressed with the aid of the chi-squared distribution with two degrees of freedom.

However, there is another option. One could also consider the sample Allan variance obtained from the second and third frequency measurements, that is, the middle sample variance. This last sample Allan variance is not independent of the other two, since it is made up of parts of each of the others. But this does not mean that it cannot be used to improve the estimate of the true Allan variance. It does mean that the new average of three sample Allan variances is not distributed as chi squared with three degrees of freedom. The

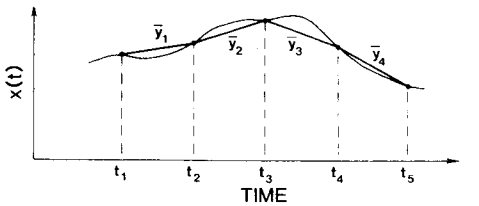


FIG. 12-12 Calculation of four frequency values $\bar{y}_1$, $\bar{y}_2$, $\bar{y}_3$, and $\bar{y}_4$ from five phase measurements at times t_1, t_2, t_3, t_4, and t_5. The sample variance formed from $\bar{y}_1$ and $\bar{y}_2$ and the one formed from $\bar{y}_3$ and $\bar{y}_4$ are independent. The sample variance formed from $\bar{y}_2$ and $\bar{y}_3$ is not independent of the other two but does contain some additional information useful in estimating the true sample variance.

number of degrees of freedom depends on the underlying noise type, that is, white frequency, flicker frequency, etc., and may have a fractional value.

Sample Allan variances are distributed as chi square according to the equation

$$\chi^2 = (\mathrm{df})s_y^2/\sigma_y^2, \tag{12-34}$$

where s_y^2 is the sample Allan variance, df the number of degrees of freedom (possibly not an integer), and σ_y^2 the true Allan variance, which we are interested in knowing but can only estimate imperfectly.

The probability density for the chi-squared distribution is given by the relation (Jenkins and Watts, 1968)

$$\rho(\chi^2) = \frac{1}{2^{\mathrm{df}/2}\Gamma(\mathrm{df}/2)}(\chi^2)^{\mathrm{df}/2-1}e^{-\chi^2/2}, \tag{12-35}$$

where $\Gamma(\mathrm{df}/2)$ is the gamma function, defined by the integral

$$\Gamma(t) = \int_0^\infty x^{t-1}e^{-x}\,dx. \tag{12-36}$$

A typical distribution is shown in Fig. (12-13).

Chi-squared distributions are useful in determining confidence intervals for variances and standard deviations, as shown in the following example. Suppose one has a sample variance $s^2 = 3.0$ and it is known that this variance has 10 degrees of freedom. The object is to calculate a range around the sample value of $s_y^2 = 3.0$ that *probably* contains the true value σ_y^2. The desired confidence is, say, 90%. That is, 10% of the time the true value will actually fall outside of the stated bounds. The usual way to proceed is to allocate 5% to the low end and 5% to the high end for errors, leaving 90% in the middle. This is arbitrary and a specific problem might dictate a different

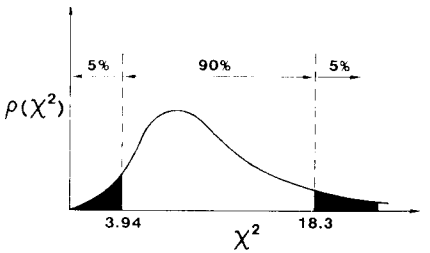


FIG. 12-13 Approximate form of a typical chi-squared distribution. For 10 degrees of freedom, 5% of the area under the curve corresponds to values of χ^2 less than 3.94, and an additional 5% corresponds to values of χ^2 greater than 18.3.

allocation. By referring to tables of the chi-squared distribution, one finds that for 10 degrees of freedom (df = 10) the 5% and 95% points correspond to

$$\chi^2(0.05) = 3.94, \qquad \chi^2(0.95) = 18.3. \tag{12-37}$$

Thus, with 90% probability the calculated sample variance $s_y^2 = 3$ satisfies the inequality

$$3.94 < (\mathrm{df})s_y^2/\sigma_y^2 < 18.3, \tag{12-38}$$

and this inequality can be rearranged in the form

$$1.64 < \sigma_y^2 < 7.61. \tag{12-39}$$

The estimate $s_y^2 = 3$ is a *point* estimate. The estimate $1.64 < \sigma_y^2 < 7.61$ is an *interval* estimate and should be interpreted to mean that 90% of the time the interval calculated in this manner will contain the true σ_y^2.

12.1.8 Efficient Use of the Data and Determination of the Degrees of Freedom

Typically, the sample variance is calculated from a data set using the relation

$$s^2 \cong \frac{1}{N-1}\sum_{n=1}^{N}(z_n - \bar{z})^2, \tag{12-40}$$

where it is implicitly assumed that the z_n's are random and uncorrelated (i.e., white) and where $\bar{z}$ is the sample mean calculated from the same data set. If all of this is true, then s^2 is chi-squared distributed and has $N - 1$ degrees of freedom.

Consider the case of two oscillators being compared in phase with N values of the phase difference obtained at equally spaced intervals τ_0. From these N phase values one obtains $N - 1$ consecutive values of average frequency, and from these one can compute $N - 2$ individual sample Allan variances (not all independent) for $\tau = \tau_0$. These $N - 2$ values can be averaged to obtain an estimate of the Allan variance at $\tau = \tau_0$.

The variance of this Allan variance has been calculated (Lesage and Audoin, 1973; Yoshimura, 1978). This approach is less versatile than the method of the previous section since it yields only symmetric error limits. However, it is simple and easy to use. Let $\Delta(N)$ be the relative difference between the sample Allan variance and the true value. Thus,

$$s_y^2 = [1 + \Delta(N)]\sigma_y^2(\tau). \tag{12-41}$$

TABLE 12-3

Variance of the Relative Difference between the Sample Allan Variance and the True Value $(C_\alpha/N)^a$

Noise type	α	C_α
White phase	2	3.88
Flicker phase	1	3.88
White frequency	0	2.99
Flicker frequency	−1	2.31
Random-walk frequency	−2	2.25

[a] N is the number of phase measurements. The result is accurate to better than 10% for N larger than 10.

The quantity $\Delta(N)$ has mean zero. For N larger than 10, the variance of Δ is approximately

$$\sigma^2(\Delta) = C_\alpha/N. \tag{12-42}$$

Table 12-3 gives the constant C_α for the five major noise types.

Using the same set of data it is also possible to estimate the Allan variances for integer multiples of the base sampling interval $\tau = m\tau_0$. Now the possibilities for overlapping sample Allan variances are even greater. For a data set of N phase points, one can obtain a maximum of exactly $N - 2m$ sample Allan variances for $\tau = m\tau_0$. Of course only $(N - 1)/2m$ of these are generally independent. Still, the use of all of the data is well justified since the confidence of the estimate is always improved by so doing. Consider the case of an experiment extending for several weeks in duration with the aim of getting estimates of the Allan variance for τ values equal to a week or more. As always, the purpose is to estimate the "true" Allan variance as well as possible, that is, with as tight an uncertainty as possible. Thus, one wants to use the data as efficiently as possible. The most efficient use is to average all possible sample Allan variances of a given τ value that one can compute from the data. This procedure is illustrated in Fig. 12-14.

In order to calculate confidence intervals for a sample variance, it is necessary to know the number of degrees of freedom. This has been done by both analytical and Monte Carlo techniques, and empirical equations have been found that are accurate to 1% for white phase, white frequency, and random-walk frequency modulation. The tolerance is somewhat larger for flicker frequency and phase modulation (Howe *et al.*, 1981). The empirical equations for the degrees of freedom are given in Table 12-4. Table 12-5 gives the degrees of freedom for selected values of N, the total number of phase values, and m, the number of intervals averaged. Figure 12-15 illustrates the number of degrees of freedom for all noise processes as a function of τ for the case of 101 total phase measurements.

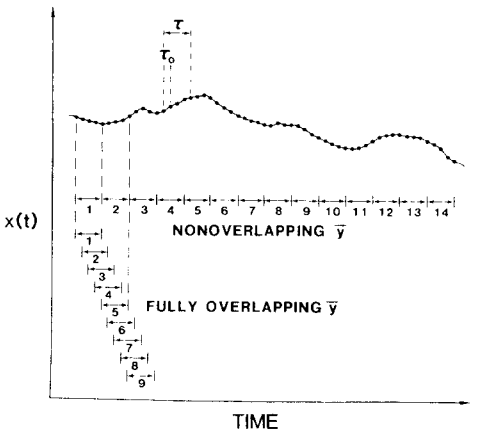


FIG. 12-14 Illustration of the case of $\tau = 4\tau_0$, for which the ratio of the number of fully overlapping to nonoverlapping estimates of the variance is more than 8 for the 57 phase points shown. When the averaging time for the computation of mean frequencies τ exceeds the sampling time τ_0, the number of fully overlapping mean frequencies is far larger than the number of nonoverlapping frequencies. In general, for large N approximately $2m$ times as many estimates of the sample variances can be computed using the fully overlapping technique.

TABLE 12-4

Number of Degrees of Freedom for Calculation of the Confidence of the Estimate of a Sample Allan Variance[a]

Noise type	df
White phase	$\dfrac{(N+1)(N-2m)}{2(N-m)}$
Flicker phase	$\exp\left[\ln\left(\dfrac{N-1}{2n}\right)\ln\left(\dfrac{(2m+1)(N-1)}{4}\right)\right]$
White frequency	$\left[\dfrac{3(N-1)}{2m} - \dfrac{2(N-2)}{N}\right]\dfrac{4m^2}{4m^2+5}$
Flicker frequency	$\dfrac{2(N-2)}{2.3N-4.9}$ for $m = 1$
	$\dfrac{5N^2}{4m(N+3m)}$ for $m \geq 2$
Random-walk frequency	$\dfrac{N-2}{m}\dfrac{(N-1)^2 - 3m(N-1) + 4m^2}{(N-3)^2}$

[a] For $\tau = m\tau_0$ from N phase points spaced τ_0 apart.

TABLE 12-5

Number of Degrees of Freedom for Calculation of the Confidence of the Estimate of a Sample Allan Variance for the Major Noise Types[a]

N	m	White phase	Flicker phase	White frequency	Flicker frequency	Random-walk frequency
9	1	3.665	4.835	4.900	6.202	7.000
	2	3.237	3.537	3.448	3.375	2.866
	4	1.000	1.000	1.000	1.000	0.999
129	1	65.579	79.015	84.889	110.548	127.000
	2	64.819	66.284	71.642	77.041	62.524
	4	63.304	52.586	42.695	36.881	29.822
	8	60.310	37.306	21.608	16.994	13.567
	16	54.509	22.347	9.982	7.345	5.631
	32	44.761	9.986	4.026	2.889	2.047
	64	1.000	1.000	1.000	1.000	1.000
1025	1	526.373	625.071	682.222	889.675	1023.000
	2	525.615	543.863	583.622	636.896	510.502
	4	524.088	459.041	354.322	316.605	253.755
	8	521.038	366.113	186.363	156.492	125.398
	16	514.952	269.849	93.547	76.495	61.241
	32	502.839	179.680	45.947	36.610	29.210
	64	478.886	104.743	21.997	16.861	13.288
	128	432.509	50.487	10.003	7.281	5.516
	256	354.914	17.429	4.003	2.861	2.005
	512	1.000	1.000	1.000	1.000	1.000

[a] N is the number of equally spaced phase points that are taken m at a time to form the averaging time.

12.1.9 Separating the Variances of the Oscillator and the Reference

A measured variance contains noise contributions from both the oscillator under test and the reference. The individual contributions are easily separated if it is known a priori that the reference is much less noisy than the device under test or equal to it in performance. Otherwise, the individual contributions can be estimated by comparing three devices (Barnes, 1966). The three possible joint variances are denoted by σ_{ij}^2, σ_{jk}^2, and σ_{ik}^2, while the individual device variances are σ_i^2, σ_j^2, and σ_k^2. The joint variances are composed of the sum of the individual contributions under the assumption that the oscillators are independent:

$$\begin{aligned} \sigma_{ij}^2 &= \sigma_i^2 + \sigma_j^2, \\ \sigma_{jk}^2 &= \sigma_j^2 + \sigma_k^2, \\ \sigma_{ik}^2 &= \sigma_i^2 + \sigma_k^2. \end{aligned} \tag{12-43}$$

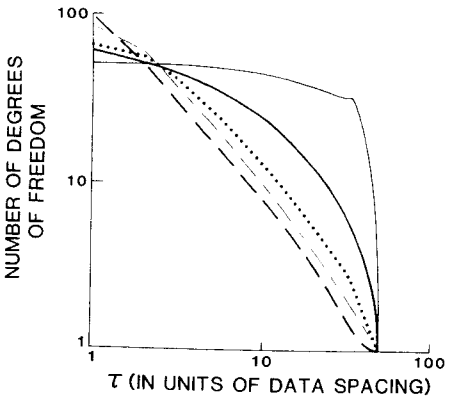


FIG. 12-15 Number of degrees of freedom as a function of averaging time for the case of 101 phase measurements: The heavy broken line is for random-walk frequency noise, the light broken line is for flicker frequency noise, the dotted line is for white frequency noise, the heavy solid line is for flicker phase noise, and the light solid line is for white phase noise.

An expression for each individual variance is obtained by adding two joint variances and subtracting the third:

$$\begin{aligned} \sigma_i^2 &= \tfrac{1}{2}(\sigma_{ij}^2 + \sigma_{ik}^2 - \sigma_{jk}^2), \\ \sigma_j^2 &= \tfrac{1}{2}(\sigma_{jk}^2 + \sigma_{ij}^2 - \sigma_{ik}^2), \\ \sigma_k^2 &= \tfrac{1}{2}(\sigma_{jk}^2 + \sigma_{ik}^2 - \sigma_{ij}^2). \end{aligned} \tag{12-44}$$

This method works best if the three devices are comparable in performance. Caution must be exercised since Eqs. (12-44) may give a negative sample Allan variance despite the fact that the true Allan variance is positive definite. This is possible because the confidence interval of the estimate is sufficiently large to include negative variances. Such a result is an indication that the confidence intervals of the sample Allan variances are too large and that more data is required.

12.2 DIRECT DIGITAL MEASUREMENT

12.2.1 Time-Interval Measurements

A common technique for measuring the phase difference between oscillators having nearly equal nominal frequencies is the use of direct time-interval measurements. In this section and those that follow, the symbols ν_{10} and ν_{20} are used to indicate the nominal values of ν_1 and ν_2, respectively. In the simplest form of this technique, a time-interval counter is started on some

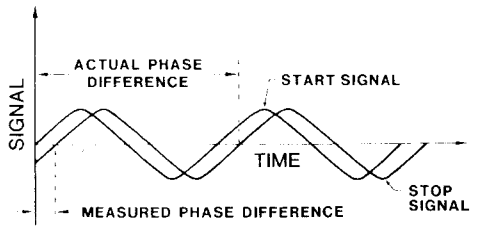


FIG. 12-16 The phase difference measured by a time-interval counter is the phase difference between the start signal and the stop signal modulo the period of the stop signal.

arbitrarily selected positive-going zero crossing of the signal from one oscillator (started on ν_{10} at time t_1) and stopped in the next positive-going zero crossing of the second oscillator (stopped on ν_{20} at time t_2). The measured time difference is

$$x_2(t_1) - x_1(t_1) \cong -P\tau_c[1 + (\nu_{20} - \nu_{10})/\nu_{10}], \tag{12-45}$$

where P is the reading of the time-interval counter and τ_c the period of its time base (Allan *et al.*, 1974). The units of the time difference is seconds of oscillator number 1. Equation (12-45) demonstrates an important characteristic of both time- and phase-difference measurements. Because of distortion the phase of an oscillator is generally not well known except at zero crossings. Thus, the quantity usually measured is $x_2(t_2) - x_1(t_1)$. However, all analysis techniques require the phase difference at the same time, and the translation requires a correction that takes into account the difference in frequency between the two oscillators. This correction is the reason for the second term in the brackets on the right-hand side of Eq. (12-45).

The simple scheme described above measures a maximum accumulated phase difference of one cycle of the signal. When the phase difference exceeds one cycle the counter reading is periodic, as shown in Fig. 12-16. This ambiguity can be reduced by dividing the signals from each oscillator before the time-interval measurement. The complete system is shown in Fig. 12-17. The effect of the divider is to increase the time interval before an ambiguity

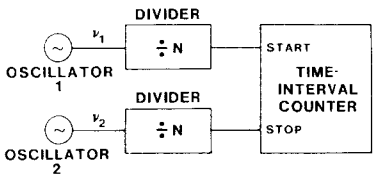


FIG. 12-17 Schematic diagram of the dividers used in conjunction with a time-interval counter to increase the maximum measurable phase difference to N cycles of the stop signal.

occurs to N/ν_{10}, where N is the divisor. Such measurement systems are used at many standards laboratories for the long-term measurement of atomic clocks, whose output is usually divided down to 1 pulse/sec. Since time-interval counters with resolution better than 0.1 nsec are available, this measurement scheme is suitable for long-term performance monitoring, yielding frequency-measurement precision of 10^{-14} for 1-day averages.

12.2.2 Frequency Measurements

Average frequency is measured most directly using a frequency counter. Used this way, the counter determines the number of whole cycles M occurring during a time interval τ given by the counter's time base. Thus

$$\bar{\nu}(0;\tau) = (M + \Delta M)/\tau \simeq M/\tau, \tag{12-46}$$

where $\bar{\nu}(t_1;t_2)$ denotes the average frequency over the interval from t_1 to t_2 and ΔM, the fractional cycle, is not measured by the counter. The starting time is arbitrarily called $t = 0$. Thus, the quantization error is given by

$$\Delta\nu_Q/\langle\nu\rangle < 1/M. \tag{12-47}$$

12.2.3 Period Measurements

For low frequencies, the number of cycles counted may be small and the quantization error can be very large. By measuring the period instead of the frequency, it is possible to decrease the error without increasing the duration of the measurement. A period counter measures the duration of M whole cycles of the signal as N cycles of the time base τ_c. The fraction of a cycle ΔN is not measured. Thus, we have

$$M = \bar{\nu}(0;M/\nu_0)(N + \Delta N)\tau_c, \tag{12-48}$$

and therefore

$$\bar{\nu}(0;M/\nu_0) \cong M/N\tau_c \tag{12-49}$$

and the quantization error is

$$\Delta\nu_Q/\langle\nu\rangle < 1/N. \tag{12-50}$$

Frequency measurements are almost never used to characterize precision oscillators, but period measurements are very common. A straightforward extension of this method eliminates the bias potentially introduced by the quantization error and permits the measurement of accumulated phase. The counter must be capable of being read without halting the counting process.

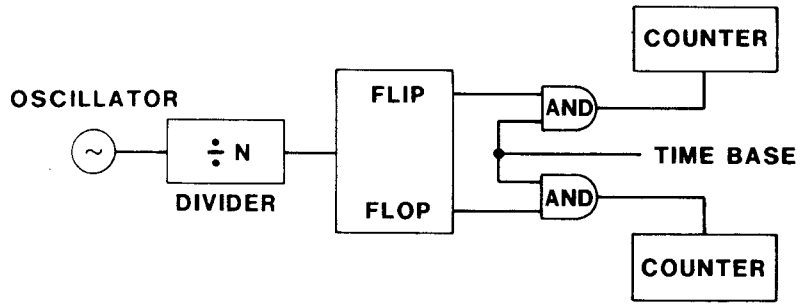


FIG. 12-18 Two-counter system to eliminate dead time in period measurements. The two counters alternately count the number of cycles of the time base in N periods of the oscillator under test.

Alternatively, a second counter may be used to begin counting the same time base when the first counter stops. The second approach is illustrated in Fig. 12-18. This type of measurement system is sometimes called a chronograph.

12.3 SENSITIVITY-ENHANCEMENT METHODS

12.3.1 Heterodyne Techniques

It is possible for oscillators to be very stable, and values of $\sigma_y(\tau)$ can be as small as 10^{-16} in some state-of-the-art standards. Thus, one often needs measuring techniques capable of resolving very small fluctuations in $y(t)$. One of the most common techniques is the heterodune or beat-frequency technique. In this method the signal from the oscillator under test is mixed with a reference signal of almost the same frequency so that one is left with a lower average frequency for analysis without reducing the frequency (or phase) fluctuations themselves.

In principle, it is possible to analyze the most general measurement case, where no restrictions are placed on the average frequency or phase difference between the two oscillators under test. Equation 12-1 can be inverted as

$$2\pi\nu_0 t + \phi(t) = \arcsin[V(t)/V_0] \tag{12-51}$$

and used to obtain the series $\phi(m\tau)$ by sampling the voltage at regular time intervals. This direct technique is not used, because it requires unobtainable mixer performance characteristics. The high-level rf signals that are required for low-noise phase measurements produce significant harmonic distortion, so that the output of the phase detector deviates significantly from a sine wave. Furthermore, the distortions are generally sensitive to level and environmental perturbations. However, the phase relationships among the various harmonics are very stable, so it is possible to use the repetition of one

point on the waveform in order to count cycles. The positive-going zero crossings are normally chosen in order to provide immunity from changes in both the amplitude and symmetry of the waveform.

Consider two signals whose frequency difference is much less than the frequency of either oscillator:

$$V_1(t) = V_{10}\sin[2\pi\nu_{10}t + \phi_1(t) + \phi_{10}]$$

and

$$V_2(t) = V_{20}\sin[2\pi\nu_{20}t + \phi_2(t) + \phi_{20}], \tag{12-52}$$

where $|\nu_{10} - \nu_{20}| \ll \nu_{10}$ and the constants ϕ_{10} and ϕ_{20} represent the nominal phases of the two signals.

Suppose that the two signals are mixed in a linear product detector and filtered so that the signal at the sum frequency $\nu_{10} + \nu_{20}$ is highly attenuated. The result is

$$V(t) \cong V_0\cos[2\pi(\nu_{10} - \nu_{20})t + \phi_{10} - \phi_{20} + \phi_1(t) - \phi_2(t)], \tag{12-53}$$

which may be characterized by any of the measurement techniques discussed in Section 12.2. The amplitude V_0 of the mixer output is a function of the mixer design, the input amplitudes, and the output termination (Walls *et al.*, 1976). Using the definition (12-10), we find that for the heterodyned signal

$$x_H(t) = (1/2\pi\nu_H)\,\Delta\phi(t), \tag{12-54}$$

where

$$\nu_H = |\nu_{10} - \nu_{20}| \tag{12-55}$$

and

$$\Delta\phi(t) = \phi_1(t) - \phi_2(t). \tag{12-56}$$

Equation (12-54) may be rewritten as

$$x_H(t) = (\nu_0/\nu_H)x(t), \tag{12-57}$$

from which we conclude that a given phase change corresponds to a larger time deviation for the heterodyne signal than for the original signal. As a result, the quantization error for the period measurement technique is reduced by the factor ν_H/ν_0.

12.3.2 Homodyne Techniques

The limit of the heterodyne method, called homodyne, occurs when $\nu_{10} = \nu_{20}$. In this case the output of the phase detector is given by

$$V(t) \cong V_0\cos[\phi_{10} - \phi_{20} + \phi_1(t) - \phi_2(t)]. \tag{12-58}$$

The analysis of phase noise is accomplished by arranging that $\phi_{10} - \phi_{20} = \pi/2$, which can be achieved with a phase shifter. Then,

$$V(t) \cong -V_0 \sin[\phi_1(t) - \phi_2(t)] \cong V_0[\phi_2(t) - \phi_1(t)]. \tag{12-59}$$

There are various methods by which one can control the signal $V_2(t)$ so that $\nu_{10} = \nu_{20}$ without producing significant correlation between $\phi_2(t)$ and $\phi_1(t)$. When any one of these methods is used, it is possible to use $V(t)$ as a measure of $\phi(t)$. Two methods, delay lines and phase-locked loops (Gardner, 1966), are described below.

12.3.2.1 DISCRIMINATOR AND DELAY LINE

The circuit of a discriminator or delay-line system for measuring phase noise is illustrated in Fig. 12-19. The delayed signal is given by

$$V_2(t) = V_1(t - t_d) = V_{20} \sin[2\pi\nu_{10}(t - t_d) + \phi_1(t - t_d) + \phi_{10} + \phi_s]. \tag{12-60}$$

When the phase shifter is set for quadrature, $\phi_s - 2\pi\nu_{10}t_d = \pi/2$ and

$$V_2(t) = V_{20} \sin[2\pi\nu_{10}t + \phi_1(t - t_d) + \phi_{10} + \pi/2]. \tag{12-61}$$

The output of the phase detector is given by

$$V(t) = V_0[\phi_1(t - t_d) - \phi_1(t)]. \tag{12-62}$$

Substituting Eq. (12-62) into Eq. (12-20), we obtain

$$\bar{y}(t - t_d; t) = -V(t)/2\pi\nu_0 V_0 t_d \tag{12-63}$$

and we see that the delay-line method can be used to produce samples of $\bar{y}(m\tau_0)$ by varying the delay time. However, the technique is used more frequently with a fixed delay by restricting its application to the region of τ much greater than the delay time, so that $\bar{y}(t - t_d; t)$ is a good approximation for the instantaneous frequency. Under this assumption spectrum analysis of

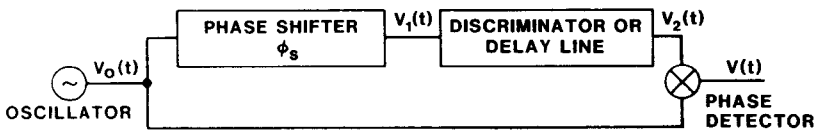


FIG. 12-19 A delay-line phase-noise-measurement system. When the phase shifter is adjusted so that $V_2(t)$ is in phase quadrature with $V_0(t)$, the output of the phase detector is approximately equal to the instantaneous frequency deviation of the oscillator. The spectral density of the source may be estimated for Fourier frequencies small compared to the inverse of the delay time.

the signal from the mixer can be used to estimate the spectral density of the frequency fluctuations:

$$S_y(f) \cong \frac{1}{(2\pi\nu_0 t_d)^2} S_{V/V_0}(f) \qquad \text{for } f \ll 1/\pi t_d. \tag{12-64}$$

Frequency discriminators are applied in an analogous fashion. A resonant circuit is often used to provide discrimination since it produces a phase shift proportional to the frequency deviation from the resonant frequency. For example, the phase shift on reflection from a resonance with loaded quality factor Q is

$$\phi = \arctan(2Qy) \cong 2Qy, \tag{12-65}$$

provided that the frequency deviation is small compared to the bandwidth of the resonance and the applied signal is nearly at the center frequency of the discriminator. This can be accomplished either manually or with a frequency-locked loop. The design of such a loop is similar to the phase-locked loop of the next section. Once again, one can spectrum analyze the signal from the mixer to obtain

$$S_y(f) \simeq \frac{1}{(2Q)^2} S_{V/V_0}(f) \qquad \text{for } f \ll \nu_0/Q. \tag{12-66}$$

The noise floor for measurements made with either a delay line or discriminator normally results from white voltage noise in the analysis circuitry and is independent of the Fourier frequency. We denote the noise floor S_{V/V_0} (minimum) and find the noise floor for frequency or phase measurements by

$$S_\phi(\text{noise limit}) = \frac{\nu_0^2}{f^2} S_y(\text{noise limit}) = \frac{\nu_0^2}{f^2(2Q)^2} S_{V/V_0}(\text{minimum}). \tag{12-67}$$

Consequently, the discriminator or delay-line technique is limited in sensitivity since the output voltage is proportional to the frequency deviations. Greater sensitivity is possible using two oscillators in a phase-locked loop. The noise in the reference is an important consideration, even though the reference is passive in the case of a discriminator or a delay line. If the oscillator has sufficiently low noise, then the circuits described measure the variations of the discriminator center frequency or the delay variations in the delay line.

12.3.2.2 PHASE-LOCKED LOOP

The block diagram for the most general phase-locked loop that will be considered here is shown in Fig. 12-20. The noise voltage summed into the loop is a schematic way of representing $\phi_n(t)$, the open-loop phase noise of the

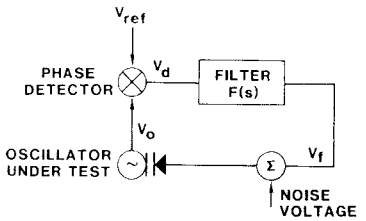


FIG. 12-20 Block diagram of a phase-locked loop. The order of the loop is determined by the filter transfer function. For convenience, noise in the oscillator under test is introduced at the summing junction.

oscillator under test. Phase noise in the reference oscillator is denoted by $\phi_{ref}(t)$.

The purpose of using a phase-locked loop is simply to guarantee that the two oscillators are, on the average, in phase quadrature. When the oscillators are near quadrature, the voltage output of the phase detector is proportional to the difference in phase between the two output signals.

Analysis of the phase-locked loop yields the result

$$\phi_0(s) = \phi_n(s)\left[\frac{1}{1 + G_{eq}(s)}\right] + \phi_{ref}(s)\left[\frac{G_{eq}(s)}{1 + G_{eq}(s)}\right], \tag{12-68}$$

where $G_{eq}(s)$ is the open-loop transfer function defined by

$$G_{eq}(s) = \frac{K_0 K_d F(s)}{s} \tag{12-69}$$

and $\phi_n(s)$ and $\phi_{ref}(s)$ are the Laplace transforms of the corresponding time-varying quantities. We can also calculate the voltage output of the phase detector,

$$V_d(s) = \frac{K_d[\phi_{ref}(s) - \phi_n(s)]}{1 + G_{eq}(s)}, \tag{12-70}$$

as well as the feedback voltage to the varactor,

$$V_f(s) = F(s)V_d(s) = \frac{sG_{eq}(s)}{G_{eq}(s)}[\phi_{ref}(s) - \phi_n(s)]. \tag{12-71}$$

Assuming that the phase noise of the two oscillators is not correlated,

$$S_{V_d}(\omega) = \frac{K_d^2}{|1 + G_{eq}(j\omega)|^2}[S_{\phi_{ref}}(\omega) + S_{\phi_n}(\omega)], \tag{12-72}$$

$$S_{V_f}(\omega) = \frac{\omega^2 G_{eq}(j\omega)^2}{|1 + G_{eq}(j\omega)|^2}[S_{\phi_{ref}}(\omega) + S_{\phi_n}(\omega)]. \tag{12-73}$$

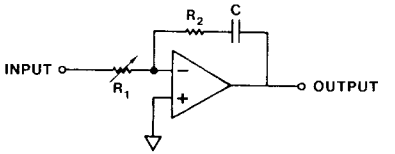


FIG. 12-21 Circuit diagram of the most common loop filter for a second-order phase-locked loop. Resistor R_2 is required for stable operation. Capacitor C provides the low-frequency gain needed to reduce the phase errors of the first-order loop.

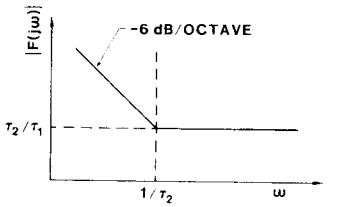


FIG. 12-22 Bode plot for the loop filter of Fig. 12-21.

Thus, if we know the behavior of $G_{eq}(j\omega)$, then we can relate the measured spectrum of the voltage at the output of the phase detector or at the varactor tuner to the sum of the spectral densities of the phase noise of the two oscillators.

The loop filter is often chosen to be a pure gain. The resulting first-order loop has a significant drawback: the two oscillators are offset from quadrature by a phase shift proportional to their open-loop frequency difference. In order to maintain system calibration, the operator must remove the frequency offset from time to time. This problem can be eliminated by using a second-order loop. Figure 12-21 illustrates one loop filter that can be used to achieve the desired frequency response. The transfer function of this filter is

$$F(s) = (1 + s\tau_2)/s\tau_1, \tag{12-74}$$

where $\tau_2 = R_2C$ and $\tau_1 = R_1C$. Figure 12-22 shows the Bode plot of the frequency-response function of this filter. Substitution of Eq. (12-74) into Eq. (12-69) yields the open-loop frequency-response function

$$G_{eq}(j\omega) = -\frac{\omega_n^2 + 2j\zeta\omega_n\omega}{\omega^2}, \tag{12-75}$$

where

$$\omega_n = [K_0K_d/\tau_1]^{1/2} \tag{12-76}$$

and

$$\zeta = \tfrac{1}{2}\tau_2\omega_n. \tag{12-77}$$

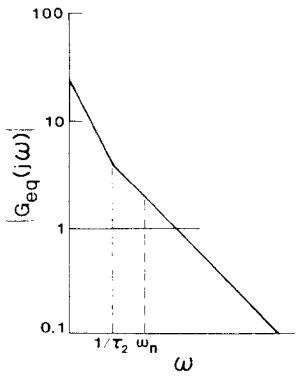


FIG. 12-23 Bode plot of the open-loop frequency-response function for a phase-locked loop having the loop filter of Fig. 12-21. Parameters were chosen to illustrate a stable condition.

The first requirement to be satisfied by the loop parameters is that the closed loop be stable. Since the transfer function $G_{eq}(s)$ has no poles or zeros for $s > 0$, a sufficient requirement for the phase-locked loop to be stable is that the slope of the Bode plot of $|G_{eq}(j\omega)|$ be less steep than -12 dB/octave at the point where $|G_{eq}(j\omega)| = 1$. The Bode plot of $|G_{eq}(j\omega)|$ is shown in Fig. 12-23 for a case where the loop operation is stable.

It is desirable for the loop to be nearly critically damped, that is, $\zeta = 1$. At critical damping the natural frequency of the loop is related to τ_2 by

$$\omega_{n,\zeta=1} = 2/\tau_2. \tag{12-78}$$

Under the same conditions the unity gain frequency is

$$\omega_{1,\zeta=1} = 4.12/\tau_2. \tag{12-79}$$

The second requirement to be satisfied by the phase-locked loop is related to the accuracy with which spectral-density measurements can be made. Substitution of Eq. (12-75) into Eq. (12-72) yields

$$S_{V_d}(\omega) = \frac{K_d^2\omega^4}{(\omega^2 - \omega_n^2)^2 + 4\zeta^2\omega^2\omega_n^2}[S_{\phi_{ref}}(\omega) + S_{\phi_n}(\omega)]. \tag{12-80}$$

Since the proportionality factor has a high pass response, it is possible to use an essentially constant calibration to relate $S_{V_d}(\omega)$ and $S_\phi(\omega)$. For example, if we require that

$$S_{V_d}(\omega) \cong K_d^2[S_{\phi_{ref}}(\omega) + S_{\phi_n}(\omega)] \tag{12-81}$$

with no more than 10% error for all Fourier frequencies greater than 2π rad/sec, then for the critically damped loop the requirement on τ_2 is $\tau_2 > 1.4$ sec.

The third requirement on loop performance is that the frequency offset between the two oscillators produce negligible phase shift of the oscillators from quadrature. In the ideal loop the phase error for a frequency error $\Delta\nu$ introduced at time $t = 0$ is

$$\phi_{error} = 2\pi\,\Delta\nu t\, e^{-\omega_n t}.$$

However, in the actual circuit there is a finite phase error due to the limited loop gain of the amplifier of Fig. 12-21. Nevertheless, the phase error is reduced by 10^5 compared to its value for a first-order loop. Typically, the error is less than the residual phase error due to the voltage offset at the mixer output and should be much less than 1°.

The feedback loop reduces the sensitivity of the system for measurements of the phase spectral density for Fourier frequencies less than the unity-gain frequency of the phase-locked loop. One way to avoid this problem is to utilize the feedback voltage V_f. Substituting Eq. (12-75) into Eq. (12-73), we find that

$$S_{V_f}(\omega) = \frac{2\pi\nu_0^2(\omega_n^4 - 4\zeta^2\omega_n^2\omega^2)}{(\omega^2 - \omega_n^2)^2 + 4\zeta^2\omega_n^2\omega^2}[S_{y_{ref}}(\omega) + S_{y_n}(\omega)]. \tag{12-82}$$

For this case, the proportionality factor has a low pass response and a constant calibration factor may be used to relate $S_{V_f}(\omega)$ to $S_y(\omega)$.

12.3.3 Multiple Conversion Methods

Quite often the beat frequency between the signal under test and the laboratory reference is unsuitable or inconvenient for frequency-stability measurements. The frequency may be too high for the available counters or the heterodyne factor may be too small to yield the required noise enhancement. Under these circumstances a second mixing stage in series with the first can be used to produce the desired beat frequency. On the other hand, the direct beat frequency between two oscillators may be too small. For example, the frequencies of commercial cesium-beam frequency standards are usually so close together that the beat frequency between two devices would be near 1 cycle/day, making it impossible to observe the stability at shorter times. This limitation can be overcome by the use of two parallel mixing stages.

12.3.3.1 FREQUENCY SYNTHESIS

A commercial frequency synthesizer is usually the most convenient way to produce arbitrary reference frequencies for stability measurements. A mixing stage preceding the synthesizer can be used both to bring the signal into the

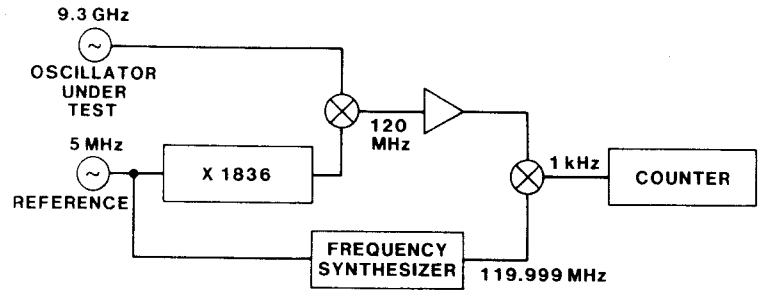


FIG. 12-24 Use of frequency synthesis to measure oscillators whose frequency differs significantly from the available low-noise reference. It may be necessary to use a frequency multiplier to bring the signal into the range of the available synthesizer or to overcome the synthesizer's phase noise.

appropriate range and to enhance the oscillator noise compared to the short-term phase noise of the synthesizer. Figure 12-24 demonstrates both aspects of the technique.

The initial mixing stage from the microwave frequency to the rf results in a substantial heterodyne factor, 77.5 for the example chosen. The output of the first conversion stage lies within the range of low-noise commercial frequency synthesizers, which makes it possible to obtain a fixed, low beat frequency over a wide range of input frequencies. The initial mixing stage also reduces the frequency synthesizer's contribution to the measurement-system noise. Figure 12-25 shows the typical phase excursions of a high-quality commercial synthesizer operated near 5 MHz.

Under some circumstances a frequency divider may be used to provide the signal for the second mixing stage, as shown in Fig. 12-26. This technique has the disadvantage of requiring a custom divider but results in much lower measurement noise than the direct use of a synthesizer with a single heterodyne stage.

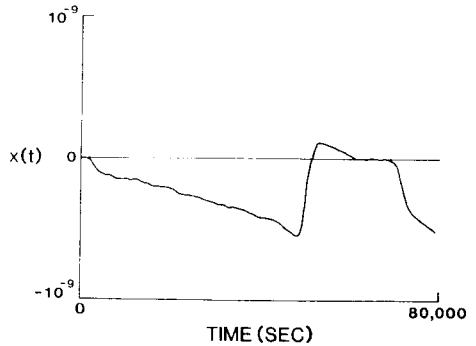


FIG. 12-25 Typical phase excursions of a commercial frequency synthesizer.

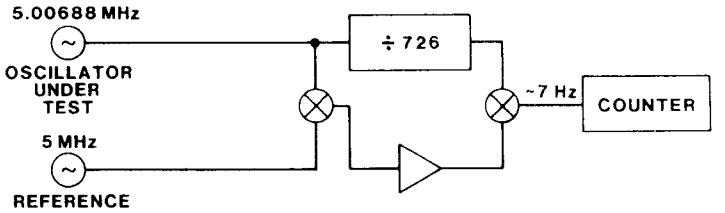


FIG. 12-26 Use of a simple divider as a substitute for a commercial frequency synthesizer in a heterodyne measurement system. Better noise performance can result from the initial mixing stage.

12.3.3.2 THE DUAL-MIXER TIME-DIFFERENCE TECHNIQUE

There is no best answer to the question of how to make frequency-stability measurements. However, by combining versatility with low-noise performance, the dual-mixer time-difference technique (Cutler and Searle, 1966: Allan and Daams, 1975) shown in Fig. 12-27 comes close to the ideal. The original motivation for this method was to use a transfer oscillator and two mixers in parallel to permit short-term frequency-stability measurements between oscillators that have an inconveniently small frequency difference. The transfer oscillator is most easily realized with a frequency synthesizer locked to one of the oscillators, designated oscillator 1 in Fig. 12-27. By convention the frequency of the synthesizer is set low compared to the oscillator under test, so we write the frequency of the synthesizer as

$$\nu_s = \nu_1(1 - 1/R). \tag{12-83}$$

The constant R is equal to the heterodyne factor, which can be seen by calculating the beat frequency between oscillator 1 and the synthesizer:

$$\nu_{B1} = \nu_1 - \nu_s = \nu_1/R. \tag{12-84}$$

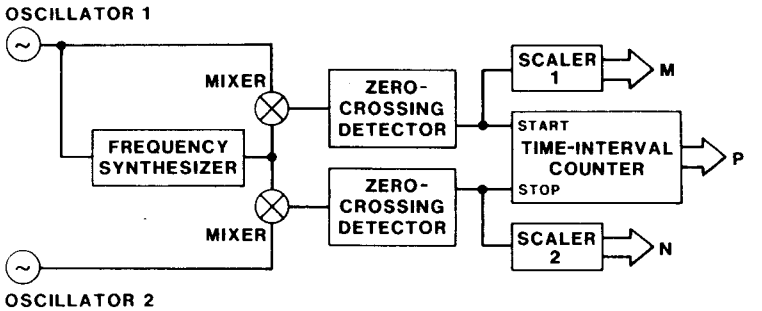


FIG. 12-27 A dual-mixer measurement system. The scalars measure the number of whole cycles of elapsed phase, while the time-interval counter measures the fractional cycle.

The combination of oscillator, frequency synthesizer, and mixer functions as a divider and scaler 1 functions as the system clock, recording elapsed time in units of cycles of oscillator 1.

The signals from oscillators 1 and 2 are represented according to Eq. (12-52) with $\phi_{10} = \phi_{20} = 0$, and the signal from the synthesizer is written

$$V_s(t) = V_{s0} \cos[2\pi\nu_{s0}t + \phi_s(t)]. \tag{12-85}$$

The phase of the synthesizer retards nearly linearly in time compared to the phase of oscillators 1 and 2. At time t_M the synthesizer reaches phase quadrature with oscillator 1 and the beat signal crosses zero (in the positive direction), producing a pulse from the zero-crossing detector and starting the time-interval counter. At a later time t_N the continued sweep of the synthesizer has brought it into quadrature with oscillator 2, and a pulse is produced that stops the time-interval counter. The phase difference between the oscillators can be written in terms of the three counter readings:

$$\phi_2(t_M) - \phi_1(t_M) = 2(N - M)\pi - 2\pi[\bar{\nu}_{B2}(t_M; t_N)]\tau_c P, \tag{12-86}$$

where N is the reading of scaler 2, M the reading of scaler 1, P the reading of the time-interval counter, and τ_c the period of its time base (Stein *et al.*, 1983). Comparison with Eq. (12-45) for direct time-interval measurements reveals that the role of the scalers is to accumulate the coarse phase difference between the oscillators, while the time-interval counter provides fine-grain resolution of the fractional cycle. This process is illustrated in Fig. 12-28. The advantage of the technique over direct time-interval measurements is that the noise performance is improved by the large heterodyne factor, allowing time resolution of 0.1 psec to be obtained. The synthesizer degrades the noise performance very little since it contributes to the noise only over the interval $\tau_c P$.

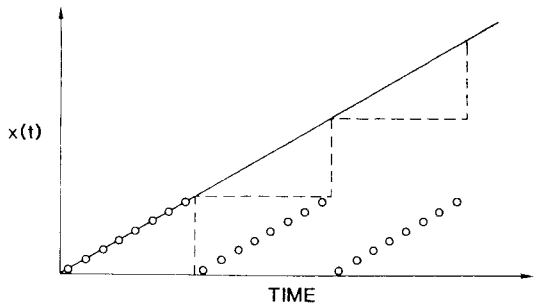


FIG. 12-28 Total elapsed phase measured by the dual-mixer system of Fig. 12-27 (solid line). This phase measurement consists of two components: the number of full cycles that have elapsed is the step function plotted as a dashed line; the fractional cycle is the saw-tooth function plotted as open circles.

The average beat frequency $\bar{\nu}_{B2}(t_M; t_N)$ cannot be known exactly, but it may be estimated with sufficient precision if it changes slowly compared to the interval between measurements. If the primed and unprimed variables represent two independent measurements, then

$$\bar{\nu}_{B2}(t_M; t_N) \cong (N' - N)/[R(M' - M)/\nu_{10} + \tau_c(P' - P)]. \tag{12-87}$$

12.3.3.3 FREQUENCY MULTIPLICATION

A frequency multiplier produces n full cycles of the output signal for each cycle of the input signal, where n is an integer determined by the design of the device. Such a device is also a phase multiplier, that is, the total phase accumulation of the output signal is n times as great as the phase accumulation of the input signal:

$$\Phi_{out} = 2\pi\nu_{out}t + \phi_{out}(t) = 2\pi(n\nu_{in})t + n\phi_{in}(t). \tag{12-88}$$

It follows that the spectral density of the output signal is enhanced by a factor of n^2 compared to the input signal,

$$S_{\phi_{out}}(f) = n^2 S_{\phi_{in}}(f),$$

making it easier to perform the necessary noise measurements. Similarly, it is also easier to make Allan-variance measurements. If the oscillator under test and the reference are both multiplied by the same factor, the beat frequency will be n times larger than with no multiplication but the heterodyne factor will be the same. The zero crossings that must be detected by the counter have n times higher slope and more easily overcome the voltage noise in the counter trigger circuits. The ability to measure frequency stability is only enhanced if the multipliers have extremely low phase noise themselves. This is the case for many modern multipliers that are triggered by the zero crossings of the input signal. As a result, the use of multipliers can reduce the performance requirements on the phase detector and the following low-noise amplifiers.

12.4 CONCLUSION

The IEEE recommendations have achieved the goal of introducing substantial uniformity in the specification of oscillator performance. The Allan variance and the one-sided power spectral density of phase have proved sufficient to evaluate oscillators for all common applications. In a few cases more specialized measures are helpful in relating performance to the specific application. For example, the rms time-prediction error is helpful in judging a clock's ability to keep time over long intervals (Allan and Hellwig, 1978).

However, the specialized performance measures are generally calculable in terms of the IEEE recommended measures.

Significant progress has been made during the last 15 years in measurement techniques and data processing. These advances have obscured the dividing line between the frequency domain and the time domain. Today the spectral density and the variance are most often computed from the identical input data set, the equally spaced time series of the phase deviations. The choice of a specific measurement setup can be made mostly on a cost versus performance basis. Perhaps the biggest advance in commercially available equipment is the introduction of heterodyne measurement techniques for time-domain (counter-based) measurements. As a result, the noise performance of these systems has improved dramatically.

One recommendation that should be made is to perform measurements as high up in the measurement hierarchy as possible. Direct measurement of the phase deviation is most desirable. This approach places the largest share of the burden on the measurement equipment, minimizes long-term errors, and maximizes data processing flexibility.

13 Frequency and Time Coordination, Comparison, and Dissemination

David W. Allan

Time and Frequency Division
National Bureau of Standards
Boulder, Colorado

List of Acronyms 233
13.1 Introduction 234
13.1.1 Historical Perspectives and Methods of Comparison 234
13.1.2 Time and Frequency Standards 235
13.2 Terrestrial Time and Frequency Comparison or Dissemination Methods 237
13.2.1 High and Medium Frequency 237
13.2.2 Low- and Very-Low-Frequency Transmissions 237
13.2.3 Other Methods 250
13.3 Extraterrestrial Time and Frequency Comparison or Dissemination Methods 253
13.3.1 Operational-Satellite Techniques 253
13.3.2 Experimental-Satellite Techniques 258
13.3.3 Deep-Space Radio-Source Techniques 268
13.4 Coordinate Time for the Earth 268
13.5 Levels of Sophistication and Accuracies for the Users 270
13.5.1 Typical User Applications 272
13.5.2 Sophisticated and High-Accuracy Techniques 272
13.6 Summary 272

LIST OF ACRONYMS

BIH	Bureau International de l'Heure
ESA	European Space Agency
GOES	Geostationary Operational Environmental Satellite
GPS	Global Positioning System

PRECISION FREQUENCY CONTROL
Volume 2
Oscillators and Standards

ISBN 0-12-280602-6

LASSO	Laser synchronization from stationary orbit
NASA	National Aeronautics and Space Administration
NBS	National Bureau of Standards
NOAA	National Oceanic and Atmospheric Administration
OTS-2	Orbital Test Satellite No. 2 by ESA
TAI	International Atomic Time
TDRS	Tracking and data-relay satellites
USNO	United States Naval Observatory
UT1	Universal time scale obtained by correcting UT0 for polar motion, where UT0 is the mean solar time at the Greenwich meridian plus 12 hr.
UT2	Universal time scale obtained by correcting UT1 for secular variations (e.g., annual and semiannual) in the rate of rotation of the earth
UTC	Universal Coordinate Time
VLBI	Very-long-baseline interferometry

13.1 INTRODUCTION

The purpose of this chapter is to review both the current and some anticipated metrology techniques useful in comparing or calibrating remotely located time and frequency (T/F) standards. Typically, the interest in this regard is to make available to a remote user some primary frequency or time standard reference. The techniques usually employed to accomplish this either involve the transport of a secondary standard or the propagation of time and frequency information carried on an electromagnetic signal. The accuracy, reasonable coverage areas, convenience to the user, and, in some cases, nominal cost of some of these techniques of comparison and dissemination will be reviewed (Beehler, 1981; Sperry Gyroscope Co. Staff, 1967; Jespersen *et al.*, 1972; Kamas and Howe, 1979).

Time and frequency coordination is the process of combining primary standards to generate coordinated T/F standards for the world or for a particular country. Coordination is important in the generation of International Atomic Time (TAI) and Universal Coordinate Time (UTC) (Smith, 1972). State-of-the-art comparison methods are usually employed to accomplish this coordination. T/F dissemination, on the other hand, occurs at a wide variety of accuracy levels and is typically provided as a service to a largely unknown receiving audience (Allan *et al.*, 1972c). The more useful methods of T/F coordination, comparison, and dissemination will be discussed in this chapter.

13.1.1 Historical Perspectives and Methods of Comparison

We see four basic eras as we review methods of measuring oscillators and clocks at remote locations. The first era employed astronomical observations. The second, which is perhaps highlighted in its early years by the Harrison chronometer, involved the transport of the best chronometer

possible to do accurate navigation. The third era is associated with the advent of time and frequency information on electromagnetic signals that could be transmitted from a known fixed site to any general receiver location to measure clocks and oscillators at that location. The fourth era is just now dawning and is a marriage of the concepts from the second and third eras in which we have very good clocks whose signals can be transported or transponded via satellite. This opens up new opportunities and possibilities because of the different parts of the electromagnetic spectrum that can be utilized. Greater bandwidths are now available. In contrast to earth-fixed transmitters, line-of-sight paths are natural from the earth to a satellite, which can be used to give worldwide coverage with extremely accurate time and frequency signals.

13.1.2 Time and Frequency Standards

The time and frequency standard for the world is generally accepted as International Atomic Time (TAI), generated and maintained at the International Time Bureau, Bureau Internationale de l'Heure (BIH) (Guinot and Granveaud, 1972). The rate of TAI is periodically adjusted to be within one part of 10^{13} or better of the rates as given by primary frequency standards at key laboratories in the world (Granveaud and Guinot, 1978). Currently these laboratories are the National Bureau of Standards (NBS) in Boulder, Colorado, the National Research Council (NRC) in Ottawa, Canada, and the Physikalisch-Technische Bundesanstaldt (PTB) in Braunschweig, Federal Republic of Germany. The current accuracies of these three standards are eight parts in 10^{14}, four parts in 10^{14}, and two parts in 10^{14}, respectively. The TAI is generated by a computer algorithm (called ALGOS) that combines the time readings of about 100 remote clocks from various laboratories and observatories in North America and Europe (Guinot, 1974; Bureau International de l'Heure, 1981). The remote time readings of these clocks are transferred to the BIH mostly via Loran-C, as outlined above. Satellite techniques are coming more into use (Costain *et al.*, 1979b; Allan *et al.*, 1985). Loran-C limits the locations and the accuracies that can be achieved (Allan *et al.*, 1972a). The new era will greatly improve the accuracy with which T/F data can be transferred from remote areas of the earth. The rates of the clocks participating are determined from historical data so that the rate of TAI (ALGOS output) is in agreement with the primary standards. The second, as generated by the primary standards, is "the duration of 9 192 631 770 periods of the radiation corresponding to the transition between the two hyperfine levels of the ground state of the cesium-133 atom." The time origin of TAI is 00 hours, 1 January 1958, at which time it was made synchronous with the earth time scale UT2. Since

that date TAI has been independent of earth time and astronomical data. However, the time scale UTC (Universal Coordinate Time), as generated by the BIH, is constrained to within 0.9 sec of the earth time scale UT1 by adding *leap seconds* as needed. UT1 is dependent on the spin of the earth and is the most useful time scale for most navigators. By keeping UTC nominally synchronous with UT1, UTC has utility for both the navigator and the precision T/F metrologist who wishes to base his measurements on the definition of the second. As of 1 July 1983 the time difference TAI − UTC = 22 sec. Most countries have adopted UTC as civil time and generate within their country a near-synchronous equivalent to UTC, usually denoted UTC(i), where i denotes the laboratory or observatory where the time scale is generated.

In the following sections we shall discuss some of the ways in which one can calibrate the time or frequency of a local clock, oscillator, or resonator with respect to the UTC(i)'s and frequency standards available. The most popular method of receiving the UTC T/F signals is via the standard T/F transmitters located around the earth. The relative merits and accuracies of different techniques will be indicated as well as some other techniques that hold promise in the foreseeable future.

A useful variation on the above is for two sites, A and B, to receive time and/or frequency signals T from a transmitter in common view to both sites. A time difference can be simultaneously measured at the two sites: $A - T + D_A$ and $B - T + D_B$, where D_A and D_B are the delays in propagating the signal to A and B, respectively. Differencing these two measures yields $A - B + \Delta D$, where ΔD is the differential delay. The transmitter acts as a transfer standard (i.e., a standard to transfer T/F from A to B or vice versa) and its errors do not contribute to measurements of the difference between the standards, $A - B$. Furthermore, if there are delay variations that are the same for both paths, these errors cancel. This simultaneous common-view technique is very useful (Allan, 1972; Allan *et al.*, 1972b; Allan and Weiss, 1980; Inouye and Nara, 1975). For example, it is used in the construction of International Atomic Time (TAI), with the transmitter being the Loran-C navigation chain (Shapiro, 1968; Doherty *et al.*, 1961). This particular technique is utilized in several other systems that we will discuss in this chapter, for example, TV line 10, OTS-2 satellite (Hoffman, 1982), GPS satellites in common view, and very-long-baseline interferometry (VLBI).

The frequency-standard field is fairly unique in that the cesium atom provides an intrinsic frequency standard. That is, if one has access to either a commercial or laboratory cesium resonator, then one has access to the standard, and it is not necessary to relate the frequency standard back to some standards laboratory (within some accuracy limits). The accuracy of commercial cesium devices is typically only one order of magnitude worse than that available in laboratory devices. Current commercial cesium accuracies are as good as 7 parts in 10^{12}. Time, on the other hand, is not generated intrinsically with respect to anything but is based on definitions and procedures.

13.2 TERRESTRIAL TIME AND FREQUENCY COMPARISON OR DISSEMINATION METHODS

We shall define terrestrial methods as those confined to the surface of the earth or within its atmosphere. In several of these methods the ionosphere plays a key role, either acting as a reflective layer or one surface of a waveguide to propagate the electromagnetic signal that carries the time and frequency information. Because the ionosphere has significant diurnal variations, changing in its electron density with the day–night solar exposure, significant propagation-delay variation results on these terrestrial-bound signals (Winkler, 1972; Joyner and Butcher, 1977; Fleer and Vorob'eu, 1976). As a result of these diurnal variations, it is very often the case that one can average the signal at a quiet time each day, reducing the fluctuations due to the diurnal term by very significant amounts (Allan *et al.*, 1970a).

13.2.1 High and Medium Frequency

The transmissions listed in Table 13-1 are from 27 high-frequency (HF) transmitters located throughout the world. The accuracy of the signals as transmitted is typically on the order of one part in 10^{10} or better, and the time that is transmitted may be synchronous with UTC to within 10 or 20 μsec (Milton, 1974). However, the received accuracy will be greatly degraded due to the propagation fluctuations. Time synchronizations can be achieved on the order of 1 msec and frequency accuracies range between one part in 10^9 and a few parts in 10^7 depending on the distance from the transmitter, the propagation conditions, and the averaging times involved (Kobayashi *et al.*, 1968). For HF and medium-frequency (MF) transmissions, making measurements at the same time each day will reduce the effect of some of the diurnal fluctuations (Sen, 1977).

Transmissions can be received at most locations at any time even though HF and MF propagation is often adversely affected by ionospheric disturbances. See Fig. 13-1 for frequency-stability comparisons (Allan *et al.*, 1974).

13.2.2 Low- and Very-Low-Frequency Transmissions

Table 13-2 lists 17 low-frequency (LF) broadcast stations throughout the world. The accuracies of the frequencies generated at each location are also listed because the long-term phase stability of a propagation signal measured

TABLE 13-1

Standard Frequency- and Time-Signal Broadcasts in the High and Very High Frequency Bands

Station	Latitude and longitude	Power (kW)	Antenna	Standard frequencies used: Carrier (MHz)	Standard frequencies used: Modulation (Hz)	Times of UT transmissions
ATA	New Delhi, India 28°34′ N 77°19′ E	8	Horizontal Folded dipole	5.0 10.0 15.0	1: 1000	Continuous
BPM	Pucheng, China 35°0′ N 109°31′ E	10–20	Omni-directional	5.0 10.0 15.0	1: 1000	15/30 9/30 (UTC) (UT1)
BSF	Taiwan, Peoples Republic of China 24°57′ N 121°9′ E	2		5.0 15.0		Continuous except interruption between minutes 35 and 40
CHU	Ottawa, Canada 45°18′ N 75°45′ W	3 10 3	Omni-directional	3.330 7.335 14.670	1	Continuous
DAM	Elmshorn, Federal Republic of Germany 53°46′ N 9°40′ E	10 15 5 10 5 15		8.6385 16.9804 4.2650 8.6385 6.4755 12.7635		1155–1206 2355–2406 from 21 Oct. to 26 March 2355–2406 from 27 March to 20 Oct.
FFH	Paris, France 48°33′ N 2°34′ E	5	Vertical dipole	2.5	1	Continuous
IAM	Rome, Italy 41°47′ N 12°27′ E	1	Vertical dipole $\lambda/4$	5.0	1	Continuous
IBF	Torino, Italy 45°2′ N 7°46′ E	5	Vertical dipole $\lambda/4$	5.0	1	Continuous
JJY	Sanwa, Sashima, Ibaraki, Japan 36°11′ N 139°51′ E	2	Vertical dipole $\lambda/4$	2.5 5.0 10.0 15.0	1: 1000	Continuous
LOL	Buenos Aires, Argentina 34°37′ S 58°21′ W	2	Horizontal 3-wire folded dipole	5.0 10.0 15.0	1: 440: 1000	Continuous
MSF	Rugby, United Kingdom 52°22′ N 1°11′ W	5	Horizontal quadrant dipoles (vertical monopole, 2.5 MHz)	2.5 5.0 10.0	1	5 in each 10
OMA	Praha, Czechoslovakia 50°7′ N 14°35′ E	1	T	2.5	1: 1000	15 in each 30
PPR	Rio de Janeiro, Brazil 22°54′ S 43°11′ W			4.244 4.350 8.634 13.105 17.1944 22.603		During 5 min preceding 0130, 1430, 2130

Table continues

TABLE 13-1 (continued)

Station	Latitude and longitude	Power (kW)	Antenna	Standard frequencies used: Carrier (MHz)	Standard frequencies used: Modulation (Hz)	Times of UT transmissions
RCH	Tashkent, USSR 41°19′ N 69°15′ E	1	Horizontal dipole	2.5	1; 10	39 in each 60
RID	Irkutsk, USSR 52°46′ N 103°39′ E	1	Horizontal dipole	5.004 10.004 15.004	1; 10	41 in each 60
RIM	Tashkent, USSR 41°19′ N 69°15′ E	1	Horizontal dipole	5.0 10.0	1; 10	39 in each 60
RTA	Novosibirsk, USSR 55°04′ N 82°58′ E	5	Horizontal dipole	10.0 15.0	1; 10	41 in each 60
RWM	Moscow, USSR 55°19′ N 38°41′ E	5 5 8	Horizontal dipole	4.996 9.996 14.996	1; 10	39 in each 60
SAJ	Stockholm, Sweden 59°15′ N 18°6′ E	0.02	Omni-directional	150.0	—	10(20)
VNG	Lyndhurst, Victoria, Australia 38°3′ S 145°16′ E	10	Omni-directional	4.5 7.5 12.0	1; 1000	Continuous
Y3S	Nauen, German Democratic Republic 52°39′ N 12°55′ E	5	Omni-directional	4.525	—	Continuous
YVTO	Caracas, Venezuela 10°30′ N 66°56′ W			6.1		Continuous
WWV	Ft. Collins, Colorado 40°41′ N 105°2′ W	2.5 10.0 10.0 10.0 2.5	Vertical $\lambda/2$ dipole arrays	2.5 5.0 10.0 15.0 20.0	1; 440; 500; 600	Continuous
WWVH	Kekaha, Kauai, Hawaii 21°59′ N 159°46′ W	5.0 10.0 10.0 10.0	Phased vertical half-wave dipole arrays	2.5 5.0 10.0 15.0	1; 440; 500; 600	Continuous
ZLFS	Lower Hutt, New Zealand 41°14′ S 174°55′ E	0.3		2.5	—	—
ZUO(′)	Olifantsfontein, Republic of South Africa 24°58′ S 28°14′ E	4	Vertical monopole	2.5 5.0	1	Continuous
ZUO(″)	Olifantsfontein, Republic of South Africa 24°58′ S 28°14′ E	0.06	Omni-directional	100	1	Continuous

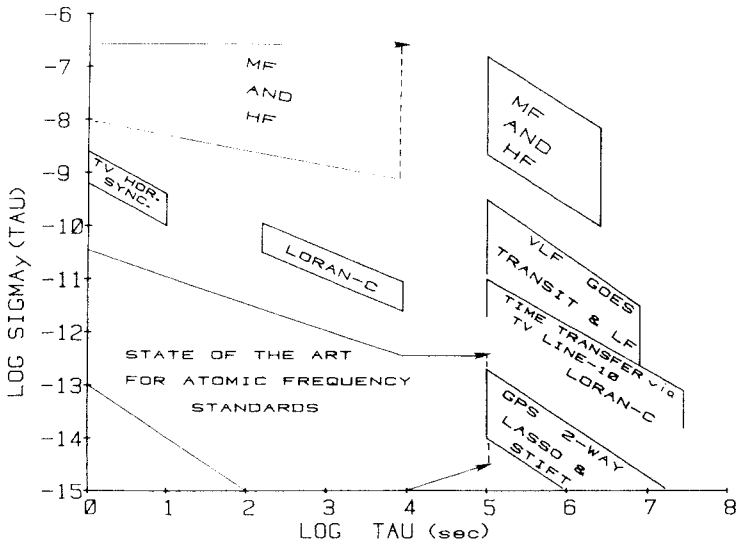


FIG. 13-1 Fractional-frequency stability as a function of averaging time for various T/F dissemination and coordination techniques.

during the same time each day is good enough to transfer frequency to high accuracies (see Fig. 13-1) (Allan and Barnes, 1967). In this case the ionosphere is acting like a waveguide that is quite stable and reproducible from day to day at the same time each day, for example, at noon on the path between the transmitter and the receiver. The coverage of the LF broadcast services, however, is not nearly so great as the very-low-frequency (VLF) and HF services (Weiss, 1976a,b,c; Feichtinger, 1977; Pierce, 1957; Guétrot *et al.*, 1969; Becker and Kramer, 1969; Fey and Looney, 1966). Typical coverage for LF may be a few thousand kilometers from the transmitter. For example, the radio broadcast services of the NBS radio station WWVB are nominally limited to North America.

In general, the user of LF signals wants both frequency and time information. Typical users include industrial, military, and civilian standards labs, electric power companies, calibrators of electronic-counter time bases, and a variety of other moderate-accuracy oscillators (and certifiers of communication-system frequencies as required by law). Typical uses of LF signals, where the emphasis is on time information, include the synchronization of communication systems (Kartaschoff, 1977), time coordination within electric power networks, event dating in electric power networks as an aid in fault analysis, and provision of a general time base in the simultaneous recording of geophysical data at many remote locations. A variety of

TABLE 13-2
Standard Frequency- and Time-Signal Broadcasts in the Low and Very Low Frequency

Station	Latitude and longitude	Power (kW)	Antenna	Standard frequencies used		Times of UT transmissions	Accuracy
				Carrier (kHz)	Modulation (Hz)		
DCF77	Mainflingen, Federal Republic of Germany 50°1′ N 9°0′ E	20	Omni-directional	77.5	1	Continuous	5×10^{-13}
EBC	San Fernando, Cadiz, Spain 36°28′ N 6°12′ W	1	Omni-directional	12.008 6.840	50	10	1×10^{-10}
GBR	Rugby, United Kindom 52°22′ N 1°11′ W	60 750	Omni-directional	15.95 16.00	1	4×5^{10} per day	2×10^{-12}
HBG	Prangins, Switzerland 46°24′ N 6°15′ E	20	Omni-directional	75	1	Continuous	1×10^{-12}
JG2AS JJF-2	Sanwa, Sashima, Ibaraki, Japan 36°11′ N 139°51′ E	10	Omni-directional	40	1	Continuous	1×10^{-11}
MSF	Rugby, United Kingdom 52°22′ N 1°11′ W	25	Omni-directional	60	1	Continuous	2×10^{-12}

Table continues

TABLE 13-2 (continued)

Station	Latitude and longitude	Power (kW)	Antenna	Standard frequencies used: Carrier (kHz)	Standard frequencies used: Modulation (Hz)	Times of UT transmissions	Accuracy
NAA	Cutler, Maine 44°39′ N 67°17′ W	1000	Omni-directional	17.8	—	—	1×10^{-11}
NDT	Yosami, Japan 34°58′ N 137°1′ E	50	Omni-directional	17.4	—	—	1×10^{-11}
NLK	Jim Creek, Washington 48°12′ N 121°55′ W	125	Omni-directional	18.6	—	—	1×10^{-11}
NPM	Cualualei, Hawaii 21°25′ N 158°9′ W	600	Omni-directional	18.6	—	—	1×10^{-11}
NSS	Annapolis, Maryland 38°59′ N 76°27′ W	400	Omni-directional	21.4	—	—	1×10^{-11}
NWC	Northwest Cape, Australia 21°49′ S 114°10′ E	1000	Omni-directional	22.3	—	—	1×10^{-11}
OMA	Podebrady, Czechoslovakia 50°8′ N 15°8′ E	5	T	50	1	23 hr per day	1×10^{-9}
RBU	Moscow, USSR 55°19′ N 38°41′ E	10	Omni-directional	66 2/3	1; 10	6 in each 60	1×10^{-11}
RTZ	Irkutsk, USSR 52°18′ N 104°18′ E	10	Omni-directional	50	1; 10	6 in each 60	1×10^{-11}
RW166	Irkutsk, USSR 52°18′ N 104°18′ E	40	Omni-directional	200	—	—	1×10^{-11}
UQC3	Khabarovsk, USSR 48°30′ N 134°51′ E	300	Omni-directional	25.6 25.1 25.5 23.0 20.5	1; 10; 40	40 min 4 times/day	
UTR3	Gorky, USSR 56°11′ N 43°58′ E	300	Omni-directional	25.0 25.1 25.5 23.0 20.5	1; 10; 40	40 min 4 times/day	
WWVB	Ft. Collins, Colorado 40°40′ N 105°3′ W	13	Top-loaded vertical	60	1	Continuous	1×10^{-11}

TABLE 13-3

Loran-C Chains

Chain name	Station name	Location		Station identification	Peak power (kW)
		Latitude	Longitude		
Great Lakes	Dana, IN	39°51′8″ N	87°29′12″ W	8970 M[a]	400
Great Lakes	Malone, FL	30°59′39″ N	85°10′9″ W	8970 W[a]	800
Great Lakes	Seneca, NY	42°42′51″ N	76°49′34″ W	8970 X[a]	800
Great Lakes	Baudette, MN	48°36′50″ N	94°33′18″ W	8970 Y	
U. S. West Coast	Fallon, NV	39°33′6″ N	118°49′56″ W	9940 M	400
U. S. West Coast	George, WA	47°3′48″ N	119°44′40″ W	9940 W[a]	1600
U. S. West Coast	Middletown, CA	38°46′57″ N	122°29′45″ W	9940 X	400
U. S. West Coast	Searchlight, NV	35°19′18″ N	114°48′17″ W	9940 Y	540
Northeast U. S.	Seneca, NY	42°42′51″ N	76°49′34″ W	9960 M[a]	800
Northeast U. S.	Caribou, ME	46°48′27″ N	67°55′38″ W	9960 W[a]	350
Northeast U. S.	Nantucket, MA	41°15′12″ N	69°58′39″ W	9960 X[a]	275
Northeast U. S.	Carolina Beach, NC	34°3′46″ N	77°54′47″ W	9960 Y[a]	550
Northeast U. S.	Dana, IN	39°51′8″ N	87°29′13″ W	9960 Z[a]	400
Southeast U. S.	Malone, FL	30°59′39″ N	85°10′9″ W	7980 M[a]	800
Southeast U. S.	Grangeville, FL	30°43′33″ N	90°49′44″ W	7980 W	800
Southeast U. S.	Raymondville, TX	26°31′55″ N	97°50′0″ W	7980 X	400
Southeast U. S.	Jupiter, FL	27°1′58″ N	80°6′54″ W	7980 Y	275
Southeast U. S.	Carolina Beach, NC	34°3′46″ N	77°54′47″ W	7980 Z[a]	550
West Coast of Canada	Williams Lake, BC	51°57′59″ N	122°22′2″ W	5990 M	400
West Coast of Canada	Shoal Cove, AK	55°26′21″ N	131°15′20″ W	5990 X[a]	540
West Coast of Canada	George, WA	47°3′48″ N	119°44′40″ W	5990 Y[a]	1600
West Coast of Canada	Port Hardy, BC	50°36.5′ N	127°21.5′ W	5990 Z	400
Central Pacific	Johnston Island	16°44′44″ N	169°30′31″ W	4990 M	275
Central Pacific	Upolo Point, HI	20°14′49″ N	155°53′10″ W	4990 X	275
Central Pacific	Kure, Midway Island	28°23′42″ N	178°17′30″ W	4990 Y	275
North Pacific	St. Paul, Pribiloff Is., AK	57°9′10″ N	170°14′60″ W	9990 M	275
North Pacific	Attu, AK	52°49′45″ N	173°10′52″ W	9990 X	275
North Pacific	Point Clarence, AK	65°14′40″ N	166°53′14″ W	9990 Y	1000
North Pacific	Narrow Cape, Kodiak Is., AK	57°26′20″ N	152°22′11″ W	9990 Z[a]	400
Northwest Pacific	Iwo Jima, Bonin Is.	24°48′4″ N	141°19′29″ E	9970 M	1800
Northwest Pacific	Marcus Island	24°17′8″ N	153°58′52″ E	9970 X	1000
Northwest Pacific	Hokkaido, Japan	42°44′37″ N	143°43′09″ E	9970 X	1000
Northwest Pacific	Gesashi, Okinawa	26°36′25″ N	128°8′56″ E	9970 Y	1000
Northwest Pacific	Yap, Carolina Is.	9°32′46″ N	138°9′55″ E	9970 Z	1000
Gulf of Alaska	Tok, AK	63°19′43″ N	142°48′32″ W	7960 M	540
Gulf of Alaska	Narrow Cape, Kodiak Is., AK	57°26′20″ N	152°22′11″ W	7960 X[a]	400
Gulf of Alaska	Shoal Cove, AK	55°26′21″ N	131°15′20″ W	7960 Y[a]	540
North Atlantic	Angissoq, Greenland	59°59′17″ N	45°10′27″ W	7930 M	760
North Atlantic	Sandur, Iceland	64°54′27″ N	23°55′22″ W	7930 W[a]	1500
North Atlantic	Ejde, Faroe Island	62°17′60″ N	7°4′27″ W	7930 X[a]	400
North Atlantic	Cape Race, Newfoundland	46°46′32″ N	53°10′28″ W	7930 Z[a]	1500
Norwegian Sea	Ejde, Faroe Island	62°17′60″ N	7°4′27″ W	7970 M[a]	400
Norwegian Sea	Boe, Norway	68°38′7″ N	14°27′47″ E	7970 X	165
Norwegian Sea	Sylt, F. R. Germany	54°48′30″ N	8°17′36″ E	7970 W	275
Norwegian Sea	Sandur, Iceland	64°54′27″ N	23°55′22″ W	7970 Y[a]	1500
Norwegian Sea	Jan Mayen, Norway	70°54′53″ N	8°43′59″ E	7970 Z	250
Mediterranean Sea	Sellia Marina, Italy	38°52′21″ N	16°43′6″ E	7990 M	165
Mediterranean Sea	Lampedusa, Italy	35°31′21″ N	12°31′30″ E	7990 X	325
Mediterranean Sea	Karga Barun, Turkey	40°58′21″ N	27°52′2″ E	7990 Y	165
Mediterranean Sea	Estartit, Spain	42°3′36″ N	3°12′16″ E	7990 Z	165

[a] These stations are members of two or more chains and are therefore dual or triple rated. They transmit on two (or three) rates with two (or three) pulse repetition periods.

commercial receiving equipment is available for either or both types of application.

The Loran-C navigation chain has found a lot of use in the time and frequency community (Hefley, 1972; Fujiwara *et al.*, 1972; Akatsuka *et al.*, 1977; Mazur, 1973; Potts and Wieder, 1972). As mentioned above, it is the current operational method of communicating the times of most clocks contributing to the generation of TAI and UTC. Although the coverage is presently limited, the long-term plan is to continue to increase this coverage. Most of the northern hemisphere is currently covered by ground-wave propagation from Loran-C transmitters, with the exception of parts of Asia (see Table 13-3) (Allan *et al.*, 1972a). Using the ground-wave-propagated signal, adequate Loran-C signal is receivable up to about 2500 km over land and 3200 km over ocean from the transmitter (Wieder, 1971). Using the sky-wave-propagated signal, reception up to and even beyond 8000 km is possible. The ground-wave accuracy, once the path is calibrated, is typically better than 1 μsec. The sky-wave accuracy is at least an order of magnitude worse than the ground-wave accuracy. Within ground-wave coverage of a Loran-C transmitter, frequency accuracies on the order of one part in 10^{13} can be achieved over long-term averages on the order of two months (see Fig. 13-1).

Although some very good time and frequency accuracies are available with Loran-C, it has not proven as useful to the average user because of the fairly high level of sophistication needed to use the receiver equipment (Kamas and Howe, 1979). A variety of commercial receiver equipment is available.

The Omega Navigation System (Pierce, 1965; Fey, 1971; Swanson and Kugel, 1972) has nominal worldwide coverage because of the frequencies that have been selected and the use of eight different transmitting stations. The Omega Navigation System is composed of a group of VLF radio stations operating in the 10–15-kHz range. Each station time-shares common frequencies used for navigation. In addition, each station may transmit some frequencies unique to that particular station. Table 13-4 lists the specifics of each transmitter.

If one wishes to use an Omega station for frequency calibration, a phase-tracking receiver is highly recommended (Palmer, 1970). If one of the navigation frequencies is to be used, then an Omega commutator must also be used. This is a device that turns the phase-tracking receiver on and off at the proper time to receive only the desired Omega station.

The frequencies and the format segments of the Omega stations are derived from cesium-beam oscillators. The U.S. Naval Observatory (USNO) monitors and reports the Omega stations' phase values. These stations radiate a nominal power of 10 kW. This power level should be sufficient to allow users to receive at least three stations no matter where they are located.

TABLE 13-4

Characteristics of the Omega Navigation System Stations[a]

Station	Location	Latitude, longitude	Power (kW)	Carrier frequencies	Accuracy
OMEGA Ω/A[b]	Alda, Norway	66°25′ N 13°09′ E	10	12.1[c] 10.2 A 11 1/3 C 13.6 B	5×10^{-12}
OMEGA Ω/B	Monrovia, Liberia	06°18′ N 10°40′ W	10	12.0[c] 10.2 B 11 1/3 D 13.6 C	1×10^{-12}
OMEGA Ω/C	Haiku, Oahu, Hawaii	21°24′ N 157°50′ W	10	11.8[c] 10.2 C 11 1/3 E 13.6 D	1×10^{-12}
OMEGA Ω/D	La Moure, North Dakota	46°22′ N 98°20′ W	10	13.1[c] 10.2 D 11 1/3 F 13.6 E	1×10^{-12}
OMEGA Ω/E	La Reunion	20°58′ S 55°17′ E	10	12.3[c] 10.2 E 11 1/3 G 13.6 F	1×10^{-12}
OMEGA Ω/F	Golfo Nuevo, Argentina	43°03′ S 65°11′ W	10	12.9[c] 10.2 F 11 1/3 H 13.6 G	1×10^{-12}
OMEGA Ω/G	Australia	38°29′ S 146°56′ E	10	13.0[c] 10.2 B 11 1/3 D 13.6 C	1×10^{-12}
OMEGA Ω/H	Tsushima Is., Japan	34°37′ N 129°27′ E	10	12.8[c] 10.2 H 11 1/3 B 13.6 A	1×10^{-12}

[a] All stations use omnidirectional antenna.

[b] A through H designate the eight time slots formatted over 10 seconds. The letter by the frequency designates the time slot in which that frequency is broadcast.

[c] Unique station frequency broadcast in the remaining five of the eight time slots.

All Omega transmitting stations are synchronized by means of very stable cesium-beam frequency standards to within a few microseconds. These standards or clocks are referenced to an atomic time scale that is TAI − 10 sec, which was the same as UTC time on 1 January 1972. Choosing not to insert the UTC leap seconds causes the Omega 10-sec format to move nearly 1 sec with respect to UTC with each leap second.

The propagation characteristics that permit the use of Omega at great range also introduce certain limitations (Kirby, 1970). Two areas that require special attention are normal time variations and modal interference. Since signals are propagated within the waveguide formed by the earth and ionosphere, changes in propagation parameters such as velocity may be expected as a result of changes in the ionosphere–ground waveguide (Burgess and Walker, 1970). These changes may be as much as one complete cycle at the carrier frequency. Sometimes, with stable reference clocks, one can predict across these apparent cycle jumps since these variations are often repeatable.

13.2.3 Other Methods

Television signals are probably one of the most cost-effective, precise T/F comparison methods available.[§] There are basically three schemes for using TV signals: two are associated with fixed transmitters and one with satellite transmission. For fixed transmitters one can use TV as a timing device, assuming fixed delays from transmitter to receiver, by extracting one of the horizontal synchronization lines such as line 10. One can also use it as a frequency calibration device. Since many of the transmitters have atomic oscillators for frequency control, TV techniques have been demonstrated to be very feasible for remote frequency calibration.

Using a horizontal synchronization pulse, after calibrating and removing systematic time delays, one can achieve stabilities and accuracies on the order of a few microseconds. Hence, long-term multiday frequency averages can be as good as a few parts in 10^{13} if averaged over a long enough period (see Fig. 13-1) (Allan *et al.*, 1972a; Allan *et al.*, 1970a). If the frequencies of the transmissions of the main-network TV stations are known with respect to some primary standard, then the TV methods can be used as common-view transfer standards, yielding accuracies potentially as good as a few parts in 10^{13}. The use of TV frame synchronizers has rendered the above two schemes nonviable except where common view of the same transmitter is utilized between the two sites being compared.

[§] Tolman *et al.* (1967), Saxena and Mathur (1977), Hundertmark *et al.* (1976), Palii *et al.* (1972), Gabry *et al.* (1977), Becker and Enslin (1972), Rovera (1972), Parcelier (1970), Fujiwara *et al.* (1975), Davis *et al.* (1970), Miller (1970), and Fedorov *et al.* (1977).

The third scheme is being developed extremely well by the Yugoslavians and is mentioned here in the context of TV methods (Kovacevic *et al.*, 1979). They locate the position of the satellite that is transmitting the TV signal and then use the encoding on the TV signal to perform the time transfer between two fixed points on the surface of the earth. They believe accuracies of a few nanoseconds can be achieved between two sites within the beam width of their satellite signal. This particular system is fairly exclusive to Yugoslavia. However, other countries are pursuing similar techniques (Takashashi, 1976b).

Microwave techniques have been utilized to perform submicrosecond time transfer (Phillips *et al.*, 1970, 1971; Curtwright, 1969). A line-of-sight path is chosen between two clocks and the signal is sent in both directions. Assuming reciprocity of the two directions allows calculation of the absolute delay between the two sights. The limiting accuracy is usually in the calibration of delays in the transmitters and receivers at each site and not in the assumption of reciprocity. When microwave repeaters are required for overland transmissions, the stability degrades due to the longer path through the atmosphere as well as the instabilities in the repeaters. If a repeater is changed along a given path, then it is extremely difficult to reproduce the total transmission delay to a few nanoseconds (Leschiutta, 1973; Souček, 1969). In the case of the television microwave system in the U. S., the delay may change several microseconds when components are changed in the microwave transmission system (Allan *et al.*, 1972a). With current technology it appears that one can calibrate the equipment delays to better than 10 nsec (Imae *et al.*, 1982). The errors in the assumption of reciprocity for line-of-sight paths are less than 1 nsec. Time stabilities for sampling intervals from 1 sec to several thousand seconds have been measured at the 100-psec level and below (Costain *et al.*, 1979b; Janes, 1970). If, in addition to the benefits of reciprocal transmissions, one can also calibrate the atmospheric effects, then stabilities as good as 1–10 psec can be achieved (Vessot and Levine, 1974; Levine, 1977; Allan, 1981).

Portable clocks have been used for centuries in one form or another to transfer time and frequency between remote locations. Currently, one of the better ways to communicate time between two remote sites is by portable clock. However, with the advent of extraterrestrial dissemination methods, described in the following sections, that may very well change.

The current most popular clocks are based on cesium resonators (Bodily and Hyatt, 1967). Rubidium has been tried with some success (Hellwig and Wainwright, 1975), but apparently most people feel that, considering the time and expense involved in making a trip, it is better to carry a cesium clock since cesium will outperform rubidium under transport. Portable clocks are usually carried to transport time, not frequency. Most people experience

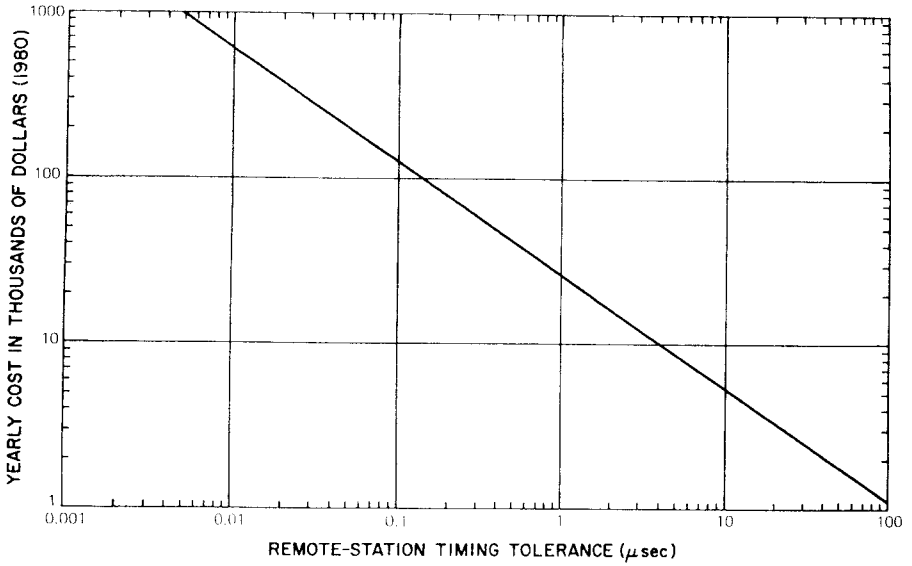


FIG. 13-2 An approximate estimate of yearly cost per station for time synchronization by portable clock as a function of remote-station timing tolerance.

fairly large inaccuracies when they try to transport frequency. However, this need not be the case, as will be discussed later.

Figure 13-2 gives an indication of the cost-effectiveness of portable clock transports. The accuracy of this method is as good as a few nanoseconds between points on the surface of the earth that are reasonably accessible to airports. Outlined in the references (Hafele and Keating, 1972b; Ashby and Allan, 1979; Hellwig and Wainwright, 1975) are some ways to achieve high accuracy using portable clocks.

Typically, portable clocks do not work well for frequency transfer between two locations, because of transport effects and environmentally induced instabilities. Some of the problems can be overcome. Some recovery time is required for the clock to reach thermal equilibrium. Also, a different magnetic field environment is usually encountered at each location. Often the frequency dividers that generate the one pulse per second (pps) from 5-MHz signals, for example, can have significant delay variations as a function of temperature (on the order of several nanoseconds in some cases). If one wishes to use a device for frequency transport, then there are two important steps. First, the delay between the 1-pps tick and the next zero-volt crossing of the 5- or 10-MHz sine-wave output should be measured. If the divider is perfect, then the delay should remain constant for the clock. The zero crossing will usually be a much better reflection of the cesium resonator

than will the 1-pps tick if it is properly terminated when measured and cable delays are taken into account. The 1-pps tick can be used to remove the 200- or 100-nsec ambiguity in the timing of the 5- or 10-MHz zero crossings, respectively. Second, the clock should be allowed to reach equilibrium (which usually takes a few hours), and then the magnetic field should be measured. This can be done on most commercial cesium clocks without opening the servo loop if it is done with care. The effect of the magnetic field can be measured to a few parts in 10^{14}. These measurements allow one to account for different magnetic field environments at the two locations. The clock should be measured for a few day's time at the secondary site before being carried back to the original site to give a total round-trip frequency and an average frequency for the trip. If these procedures are followed, then accuracies of a few parts in 10^{14} can be achieved for transferring frequency to remote sites (Endsley, 1982).

Coaxial techniques for communicating time and frequency to remote locations have been fairly well documented (Powers, 1974). One particularly new and promising area, however, is optical fibers. Time stabilities on the order of about 30 psec have been demonstrated over a three kilometer path (Moreau, 1977b; Lutes, 1981).

One of the most popular time-dissemination services offered in some countries is *telephone time of day*. These services can be accurate to better than 0.1 sec with time stabilities of a few milliseconds, which allows one to obtain frequency accuracies of about one part in 10^5 (Koide, 1966).

13.3 EXTRATERRESTRIAL TIME AND FREQUENCY COMPARISON OR DISSEMINATION METHODS

The word "extraterrestrial," is used here to refer to signals or clocks that are above the atmosphere of the earth. Such methods certainly include satellites and may also include deep-space radio sources. Over the last several years there has been a lot of interest in this area, and several interesting ideas have emerged.[§]

13.3.1 Operational-Satellite Techniques

As a complement to its other time and frequency services, the National Bureau of Standards (NBS) sponsors a satellite-disseminated time code using the Geostationary Operational Environmental Satellite (GOES) satellites of

[§] Cooper and Chi (1979), Taylor (1974), Hanson and Hamilton (1971a,b, 1973), Chi (1975), Fisher *et al.* (1976), Buisson (1973), Gatterer *et al.* (1968), and Nottarp *et al.* (1979), Allan *et al.* (1985).

the National Oceanic and Atmospheric Administration (NOAA) (Hanson *et al.*, 1979: Beehler *et al.*, 1979). This system is an example of how a meteorological satellite can be used for time dissemination. The time code is referenced to the UTC(NBS) time scale. Although the time code was designed to provide a means of dating environmental data collected by the GOES satellites, it can also be used as a general-purpose time reference for many other applications. The time code is operationally available nearly full time to the entire Western hemisphere from two satellites.

There are always at least three GOES satellites in orbit, two in operational status with a third serving as an in-orbit spare. The western satellite operates at 468.825 MHz and is located at 135° West longitude. The eastern satellite is received on 468.8375 MHz and is positioned at 75° West longitude. The spare is at 105° West longitude. Coverages of the two operational satellites are shown in Fig. 13-3.

The GOES satellites collect environmental data from remote sensors. The time code is part of the interrogation channel that is used to communicate with these sensors. The interrogation messages and time code are prepared and sent to the GOES satellites from Wallops Island, Virginia. The National Bureau of Standards maintains atomic clocks referenced to the UTC (NBS) time scale at this site to generate the time code. The time code includes a sync word, a time-of-year message (including day of year, hour, minute, and second), UT1 correction, and satellite position. A description of the time code and receiver is given in Cateora *et al.* (1978).

The GOES time code can be used at three levels of performance: uncorrected for path delay, corrected for mean path delay only, and fully corrected.

(1) *Uncorrected*: The path delay from the point of origin (Wallops Island, Virginia) to the earth via the satellite is approximately 260,000 μsec. Since the signals are advanced in time by this amount before transmission from Wallops Island, they arrive at the earth's surface on time to within 16 msec.

(2) *Corrected for mean path delay*: Accounting for the mean path delay to any point on the earth's surface but ignoring the cyclic (24-hr) delay variation generally guarantees the signal arrival time to within ±0.5 msec.

(3) *Fully corrected*: The cyclic delay variation is a result of the satellite orbit not being perfectly circular and not in the plane of the equator. The orbit is actually an ellipse and has a small inclination, usually less than 1°. To compensate for these and other effects, the satellite position is included with the time message for correction of path delay either by the user or automatically within the receiving equipment. This correction, in principle, provides path delays accurate to ±10 μsec, assuming the availability of good quality satellite tracking data. The ultimate accuracy of the recovered time,

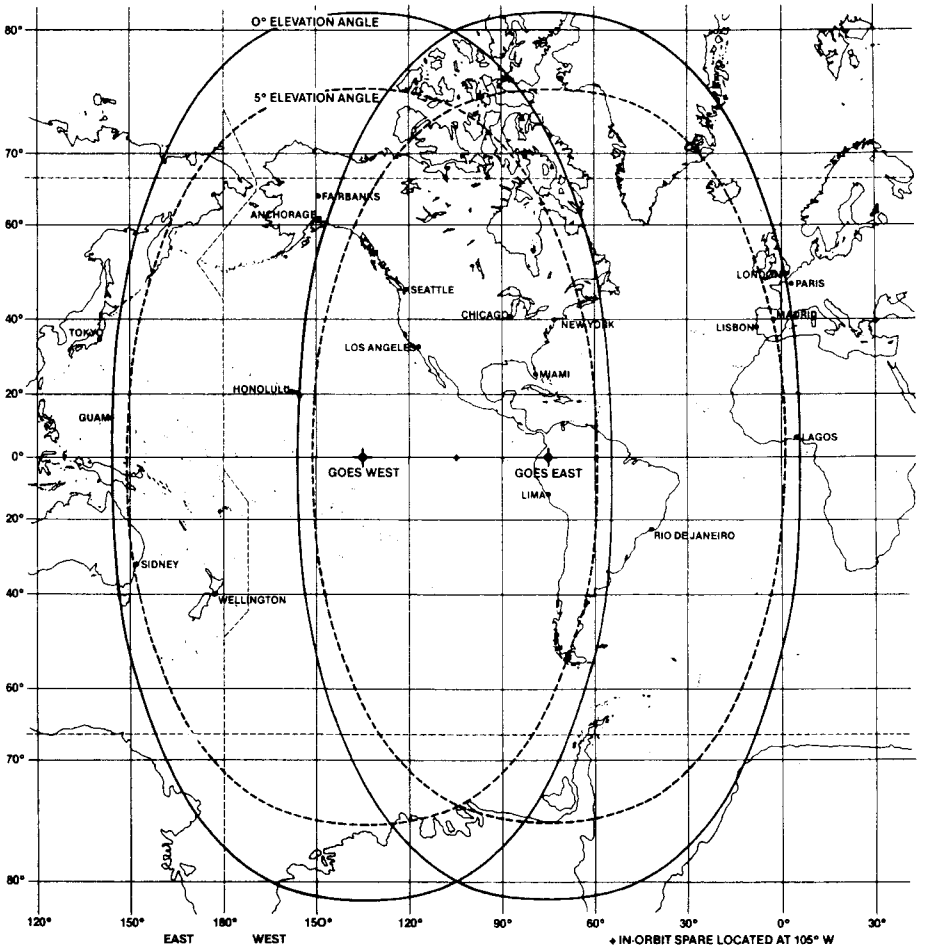


FIG. 13-3 Area covered on the surface of the earth by the two operational GOES satellite timing-signal transmissions.

however, depends on knowledge of the satellite's ephemeris, signal path delay, and user equipment delays and noise levels. Approximately five years of experience with this system has shown that much larger errors occasionally occur. These errors result from such sources as unusually poor-quality orbit elements for the satellites being supplied to NBS by the tracking organizations, unannounced shifts from one satellite to another, and satellite maneuvers. Occasional temporary time-code shifts due to such causes have

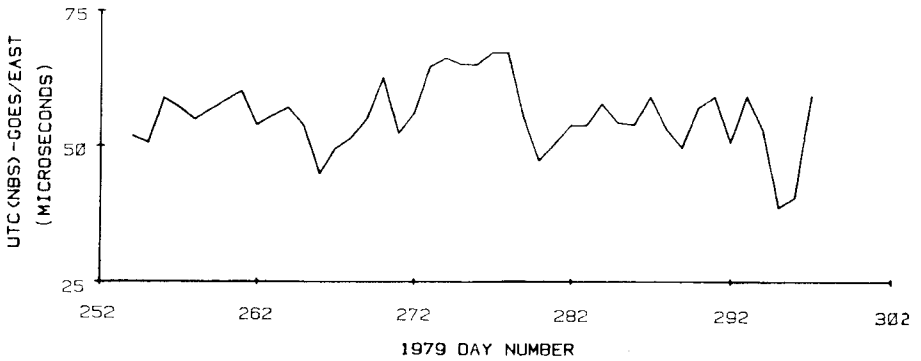


FIG. 13-4 Time-stability plot of filtered daily averages of GOES/EAST timing signal referenced to UTC (NBS), Boulder, Colorado.

been observed at the several hundred microsecond level. However, the timing signal can usually be relied on to remain within ± 50 μsec of UTC (NBS) over long periods of time, that is, months (Hanson *et al.*, 1979).

Figure 13-4 shows the variation of path-delay-corrected daily averages of UTC (NBS) − GOES (East) over a typical 45-day period. Figure 13-5 shows the performance of GOES (East) over a longer period of 258 days but based only on a single measurement made at 0000 UT each day. For comparison, Fig. 13-6 shows how the received time code varied over a period of about 6

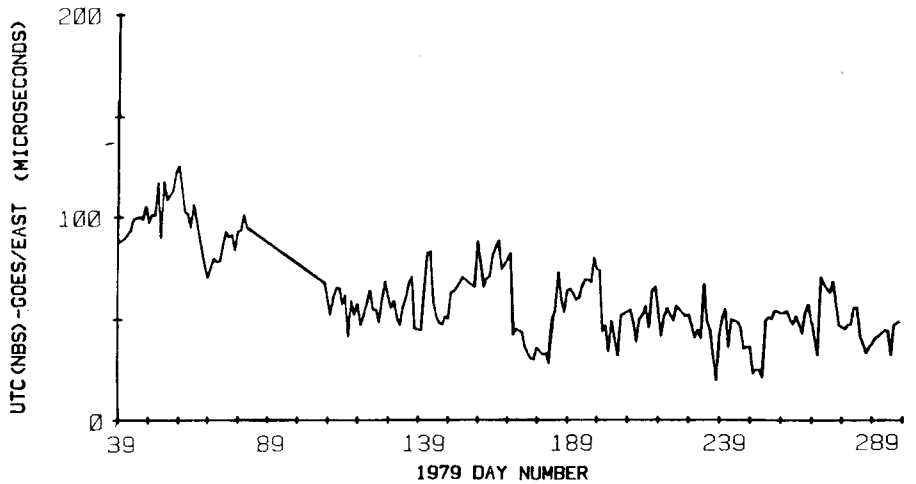


FIG. 13-5 Time stability of single daily measurements taken at 0000 UT of GOES/EAST timing signal referenced to UTC (NBS), Boulder, Colorado.

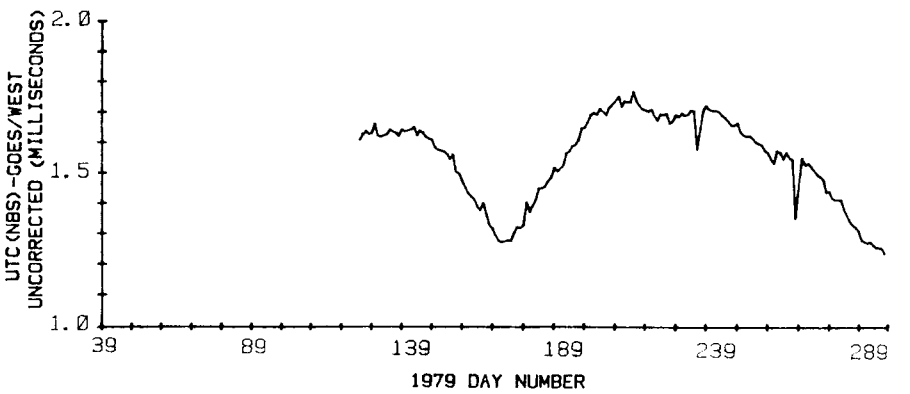


FIG. 13-6 Time stability of single daily measurements taken at 0000 UT uncorrected for path delay for the GOES/WEST timing signal referenced to UTC (NBS), Boulder, Colorado.

months for GOES (West) when no corrections were made to the data for path delay.

Commercial receivers are available at different levels of complexity and performance. Based on estimates of commercial receiver sales, there are currently more than 400 users of the GOES satellite time code. Applications vary widely, with special emphasis on those situations where multiple receiving sites are involved that must be synchronized over large geographical areas and where remote geographical areas are involved that are not well served by terrestrial-based T/F services. Examples include time coordination throughout large electric-power networks in South America, Central America, and Canada; provision of a widely accessible standard for comparing phase-angle measurements throughout electric-power networks; synchronization of communication-system sites, both on the ground and in aircraft; and correlation of extensive data collected from geophysical monitoring networks.

The worldwide meteorological satellite system, of which the GOES satellites are a part, also includes operational satellites for the European and Japanese regions; these are known as Meteosat and GMS, respectively. A number of new and upgraded satellites designed to replace those currently in operation are in the planning, design, and construction stages, thus assuring continued operation of the overall system well into the 1990s.

Although the time code is presently available only from the U.S. components of the international system, the appropriate bits in the data format needed for the time code are available on the other satellites. Some discussions have been held with European and Japanese T/F organizations and the European Space Agency concerning an international expansion of

the time-code capability, but firm decisions have not yet been made. Also, there is some possibility that an Indian Ocean satellite component of this overall system will be added at some later time, giving considerable improvement in the coverage of that region.

Also, in the future the operational GOES time-code system may be improved by arranging direct access by NBS to a NOAA computer in order to access satellite position information on a more current basis. The system would then be capable of about 10-μsec accuracy.

The TRANSIT, or NOVA, satellite system is the first to provide an operation worldwide timing system (Laidet, 1972; Stansell, 1971; Rueger, 1970, 1971; Beehler *et al.*, 1979). The system is also known as the Navy Navigational Satellite System (NNSS). It currently consists of a constellation of five satellites in polar orbits at altitudes of about 1000 km. This altitude gives a $1\frac{3}{4}$-hr orbit period, and the satellite longitudes are chosen so that any point on the surface of the earth can be covered by any of the satellites as the earth spins under their orbits. Two-minute intervals on the satellite transmissions are measured at Navy tracking stations, which in turn are coordinated with UTC (USNO). The corrections are uploaded for each satellite, so that the satellite signal can be traceable to UTC (USNO). By averaging over several of the satellites and a large number of passes, one can obtain the root-mean-square (rms) time errors with respect to UTC (USNO), which are less than 10 μsec (Beehler *et al.*, 1979). Figure 13-7 illustrates the improvement gained by averaging sequential passes, and Fig. 13-8 illustrates the stability obtained by averaging 30 passes over an 8-month period with UTC (NBS) as the reference. At any given single measurement the time difference with respect to UTC (USNO) should be less than 50 μsec. The transmission frequency for transit is 400 MHz, and commercial receivers are available in the $12,000 price range. One-day averages would allow a frequency calibration of better than one part in 10^{10}. The accuracy of calibration would nominally improve as the inverse of the averaging time.

13.3.2 Experimental-Satellite Techniques

There are several very interesting experiments that have been done comparing T/F at remote locations, and there are several experiments that are either in process or being planned. We shall look briefly at some of the experiments that show future potential.

Although T/F services such as those described earlier will continue to serve the needs of a great majority of users for many years to come, they are already proving to be deficient for applications demanding state-of-the-art accuracies. As more sophisticated technology continues to be introduced throughout most societies, T/F dissemination and coordination capabilities,

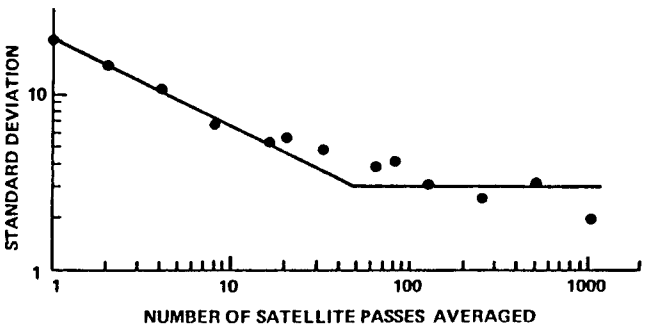


FIG. 13-7 Standard deviation of received transit signals as a function of the number of satellite passes averaged (all satellites included).

Day	Mean (μsec)	σ (μsec)
037–100	−3.9	6.6
100–165	−2.7	3.4
165–220	−8.2	6.1
221–268	−13.1	5.3
268–274	−22.8	3.8

which are important components in many cases, will have to show corresponding improvement. At least in the case of present terrestrial-based T/F services, however, such improvements will be extremely difficult and expensive or, in some instances, virtually impossible due to fundamental limitations. For example, the accuracy of time transfer via HF and LF radio propagation will, in general, always be limited to about the levels achievable now due to the uncertainties and disturbances introduced by the propagation

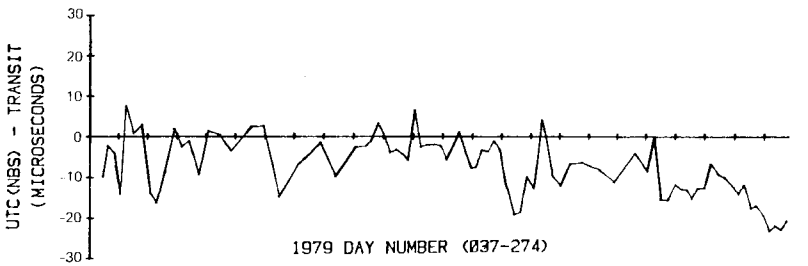


FIG. 13-8 Time stability of transit-timing signals averaging 30 satellite passes per point referenced to UTC (NBS), Boulder, Colerado.

media. Even in the case of a need for improved coverage, where one might expect to alleviate the problems by simply implementing more HF radio stations, we are already seeing the disadvantages of this approach, in some regions of the world, in the form of increased mutual interference.

In recognition of this need to explore other possibilities for improving time-transfer capabilities in the future, Study Group 7 of the Consultative Committee for International Radio (CCIR) has initiated a study of satellite-based alternatives for improving T/F dissemination and coordination. The emphasis of this study is on satellite systems and techniques that offer reasonable promise of supporting operational, long-term needs as contrasted with short-term experiments. A special Interim Working Party (IWP) 7/4 has been established to perform this study and, while this task is not yet concluded, some useful background information on various satellite alternatives has been accumulated and is being evaluated. Part of the work of this committee has been used in developing this section (CCIR, 1982).

The availability and use of communication channels provided by operational communication satellite systems is growing dramatically.[§] For high-accuracy, point-to-point time comparisons, two sites can arrange simultaneous exchange of timing signals through a satellite link. At each site the measurements consist of time differences between the transmitted and received time markers. Assuming that signal delays through the propagation medium, the satellite transponder, and the receiving–transmitting equipment are symmetrical, the time difference between the two sites can be computed simply from the measured time differences at each site without any knowledge of the satellite or user locations. Currently available communication satellites operate either in the 4/6-GHz or the 11/12/14-GHz allocated bands. The user has considerable flexibility in selecting the signal design and, in some cases, the channel bandwidth. With some systems entire 36-MHz-wide transponder channels must be leased; in others, each channel can be subdivided. In digitally oriented systems, data-bit rates of 56 kbit/sec are often available as a "standard" channel, but bit rates of 1.5 Mbit/sec and higher are often available. In one-hop two-way situations, time stabilities of less than 1 nsec have been achieved when taken over several minutes of data (Costain *et al.*, 1979b). The time-transfer accuracy is still being researched and investigated, but it appears that 6 nsec or better is achievable (Imae *et al.*, 1982).

The Global Positioning System (GPS), also known as NAVSTAR, is being developed by the U.S. Department of Defense as a high-accuracy, continuously available navigation–position-location system (Ward, 1976; Buisson *et al.*, 1976; Grenchik and Fang, 1977; Milliken and Zoller, 1978). The system will eventually include 18 operating satellites, arranged in 3 orbital planes at nominally 55° degrees inclination to the ecliptic. The 18 satellites in 12-hr orbits will result in several satellites being in view of any specific location at any time. Each satellite will contain atomic clocks (cesium, rubidium, and hydrogen devices are all being investigated) to generate extremely well-characterized timing signals as part of the navigation message format. The system will be supported by an extensive network of monitoring and control stations that will provide updated timing corrections to the onboard atomic clocks. GPS time will be kept within 100 nsec of UTC (USNO). The complex GPS signal format is transmitted to users on frequencies of 1575 and 1228 MHz and can be received with relatively small omnidirectional antennas. Coded information is included, giving clock corrections, ionospheric corrections, and satellite ephemeris data for calculating the one-way propagation delay. The GPS signal is designed to provide navigation and time information at two different accuracy levels.

[§] Steele *et al.* (1964), Smith *et al.* (1977), Markowitz *et al.* (1966), Saburi *et al.* (1976a,b), Easton *et al.* (1974), Yamamoto *et al.* (1976), Detoma and Leschiutta (1980), Mathur *et al.* (1980), and Brunet (1979).

It is important to understand that the U. S. Department of Defense has not yet formally announced decisions that could have a major impact on the time-transfer capabilities of GPS for nonmilitary users. Examples of questions that remain to be officially answered include the extent to which access to the GPS timing information may be controlled for nonmilitary users and the extent, if any, to which the full timing accuracy of the GPS may be intentionally deteriorated for nonmilitary users. Because this information is *not* available at present, the background information in this chapter is based on generally available publications and reasonable projections from a variety of (nonofficial) sources. In particular, where timing accuracies are projected or referred to, it must be understood that what eventually becomes available from the GPS, assuming full implementation of the system, could be substantially different from that expected to date or projected herein.

As of February 1983 six GPS satellites were in orbit and being evaluated. All carry rubidium standards and quartz crystal oscillators, and two also have cesium standards. Full implementation (18 satellites) is projected for the last quarter of 1988. A variety of GPS navigation and timing-receiver developments, intended for various applications, are in progress.

There are four basic approaches to using signals from the GPS satellites. The first three approaches utilize the *clear-access* signal. As shown in Fig. 13-9a, one simply extracts GPS time from the satellite. This approach should have an accuracy, internationally, of about 100 nsec. The second approach, shown in Fig. 13-9b, is what could be called the *clock flyover* mode; the same clock is used at both sites (Besson, 1970, 1974; Besson *et al.*, 1978). Any two sites on the surface of the earth would be able to observe the same clock

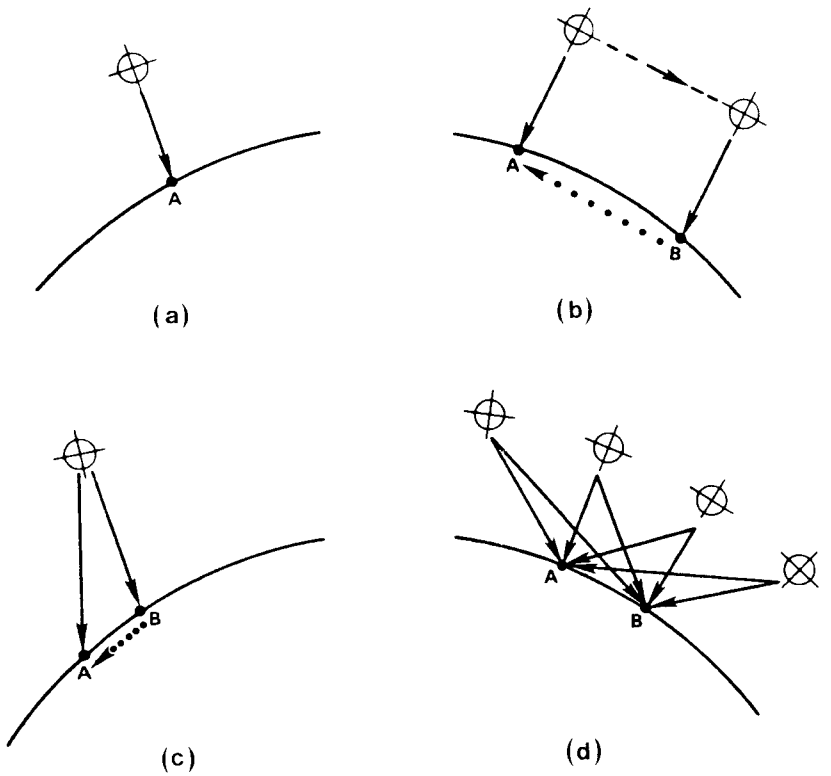


FIG. 13-9 Alternative methods of using GPS for time transfer. (a) GPS time (~ 100 nsec), (b) clock flyover (~ 50 nsec), (c) differential common view ($\lesssim$ 10 nsec), (d) VLBI techniques over short baselines ($\lesssim$ 1 nsec).

within a 12-hr interval. It is projected that accuracies on the order of 50 nsec could be achieved in this mode by comparing the received GPS times of the two ground-station clocks. The third approach, shown in Fig. 13-9c, is called the common-view approach, that is, both ground-station clocks observe the same satellite simultaneously (Allan and Weiss, 1980; Davis *et al.*, 1981; Starker *et al.*, 1982; Clements, 1982). In this case the time error of the satellite clock has no effect on the time-transfer error, and the ephemeris error is reduced by approximately an order of magnitude, depending on geometries and propagation circumstances. Accuracies of about 10 nsec are believed achievable using this approach. For short baselines, this approach should yield accuracies approaching 1 nsec as the common-mode cancellation of errors improves for both the satellite ephemeris error and the ionosphere

propagation errors. If the ionospheric delay could be measured, errors less than 1 nsec might be achievable (Buennagel *et al.*, 1982).

The last approach, shown in Fig. 13-9d, is being developed for geodesy purposes and is the same idea as that employed in very-long-baseline interferometry (VLBI) (Mac Doran, 1979). In this case, however, the baselines are very short and one simultaneously looks at four satellites from two ground stations using wideband receivers tuned to the full GPS signal. The potential accuracies are in the subnanosecond range, but the equipment employed is more complex than with the other methods, since a computer cross-correlator and radiometers similar to those used in VLBI are needed. The common-view approach is the most cost-effective. Figure 13-10 shows a calculated time transfer using the common-view approach, as would result from the satellite ephemeris errors between the BIH and NBS (with a baseline angle of 74.4°). There are time-transfer errors of about 4 nsec from a 25-nsec rms ephemeris uncertainty when the satellite is nominally midway between the two sites. Differential propagation fluctuations will add additional uncertainties of several nanoseconds to the measurement.

The laser synchronization from stationary orbit system (LASSO), as proposed to the European Space Agency (ESA) by the BIH, employs a laser retroreflector mounted on a suitable geostationary satellite and laser-telescope-equipped ground stations that are to be synchronized (Serène and Albertinoli, 1979). Each ground station arranges to transmit laser pulses to the spacecraft, detect the returned pulses, and measure the round-trip delay

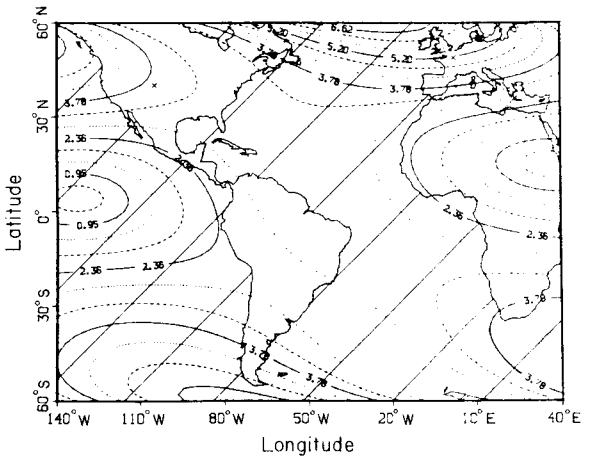


FIG. 13-10 Profile map showing the rms time-transfer error between Boulder, Colorado, and Paris, France, by simultaneously viewing the same GPS satellite, which has an rms position error equivalent to 25 nsec. The contour lines are for the overhead position of the GPS satellite.

time. On the spacecraft the pulses received from the ground stations are detected and their times of arrival are measured in terms of a spacecraft clock. These measured differences in the arrival time at the spacecraft are then combined with the measured round-trip delays from each ground station and the known time relationship of the emitted laser pulses to the local clock at each station to provide the time differences among the ground-station clocks. The spacecraft timing data can be sent to the ground stations after the fact by normal telemetry channels, and the ground stations can exchange their data via modern or other terrestrial links.

A spacelab experiment featuring cesium and rubidium atomic clocks is scheduled to be launched in June 1985. The work is being sponsored by the Bundesministerium für Forschung und Technologie of the Federal Republic of Germany and is a part of a joint agreement between ESA and NASA. The objectives of the experiment are to synchronize distant ground stations with an accuracy of better than 10 nsec. Spread-spectrum signals will be used (Starker *et al.*, 1982).

The NASA Office of Space and Terrestrial Applications (OSTA) is considering a Space Shuttle experiment called STIFT to demonstrate techniques for global high-precision comparison of clocks and primary frequency standards (Decher *et al.*, 1982). The experiment would involve a hydrogen-maser clock on board the Shuttle. Transmission of microwave and pulsed-laser signals would be used to compare the space clock in the Shuttle with a clock in a ground station. The goal of the proposed experiment is to demonstrate time transfer with accuracies of 1 nsec or better and frequency comparison of clocks at the 10^{-14}–10^{-16} accuracy level (Allan *et al.*, 1981).

There are special opportunities with communication satellites. One suggestion that has been made is to use to VHF transponders on such satellites for time dissemination. These transponders are used mainly during initial orbit-insertion maneuvers and thus may be available for other ancillary applications once the satellite is well established in its operational orbit.

In one specific case (India) an arrangement has been worked out for access by the National Physical Laboratory (NPL) in New Delphi to a portion of the communications spectrum on the Indian National Communications Satellite (INSAT) for the specific purpose of time dissemination on an operational basis. A 10-kHz channel will be made available on the *S*-band frequency channel, and planning is underway to provide a complete timing signal, including position information on the satellite for one-way path-delay correction by users. Experiments are still being conducted in preparation for implementing this T/F service on the INSAP-1B satellite (Jain and Kumar, 1981; Mathur, 1981).

Time-comparison experiments conducted with an experimental, improved TRANSIT (NOVA) satellite have indicated that accuracies of better than

100 nsec are achievable (Taylor, 1974; Rueger and Bates, 1979). This improved performance, relative to the *operational* TRANSIT results, is due mainly to use of spread-spectrum, pseudo-random-noise-coded satellite signals and sophisticated receivers.

One NOVA satellite was launched during 1981 with the pseudo-random-noise (PRN) capability. As of this writing, there is no approved operational requirement for keeping the PRN code turned on, and it remains uncertain whether such improved signals (for timing) will be available on a long-term basis.

The TDRS system is being implemented to provide two-way relay of tracking and other types of data between NASA ground facilities and low-altitude orbiting satellites in the 1980s. The system will include two operational geostationary satellites at 41° W and 171° W longitude and a dedicated spare in orbit with the master control center at White Sands, New Mexico. With these locations the TDRS system could provide timing links to laboratories all the way from Japan and Australia through North America, to and including all of Europe. While the TDRS system is mainly intended to communicate with orbiting spacecraft, some NASA tracking stations will also be in the system. The possibility may exist for timing organizations to also participate as users. In one possible high-accuracy, two-way mode each timing user could have an *S*-band ($\simeq$2-GHz) transponder with suitable auxiliary systems on-site. A timing signal consisting of an identified point in a PRN code sequence could be transmitted at *K* band from the master control station to the TDRS satellite and then to a timing user at *S* band. This user could then measure the time of arrival in terms of his local clock, encode this information onto the TDRS signal, and return the signal to the control station via the satellite once again. The user could also generate a local timing signal and transmit it to the control station. Propagation delays can be accurately dealt with, and time-transfer accuracies of about 10 nsec should be possible. For operational use, one could envision a periodic sequence of measurements comparing each timing laboratory in turn with the master clock reference in New Mexico. Such regular comparisons could perhaps be scheduled and coordinated by NASA, the BIH, or some other interested organization (Chi, 1979; Laios, 1972).

Fixed-location users on the earth might also have the option of using the TDRS signals in a lower-accuracy, one-way mode by making suitable computations and corrections for path delay. There is some possibility that a time-of-day code may be added to the TDRS capabilities.

The TDRS system is currently in the implementation stage with one of the two principal satellites in orbit. Since some operational aspects of the full TDRS system are still under discussion, the potential role for future time comparisons and distribution remains unclear.

Terrestrial time comparisons, both within local areas and over much longer distances, are conducted routinely in many countries by having two sites simultaneously observe a designated synchronization pulse within the normal TV transmission format. When both sites are within common view of a single TV transmitter, clock time differences can be measured to accuracies of $\simeq 100$ nsec or better, assuming the differential propagation path delay can also be determined. This method is also useful at larger distances, where two different TV transmitters that are interconnected in a TV network can be observed. With the present trend toward developing TV broadcast capabilities from dedicated satellites, it may become feasible to apply the same TV time-synchronization methods to the satellite TV case. The satellite TV pulses can certainly be received over larger areas and measured against local clocks with high resolution (a few nanoseconds). The accuracy with which two clocks can be compared, however, depends on knowing the differential propagation delay. One interesting idea is to accurately range the TV satellite via a few laser ranging stations and then use this information to compute the path delays. Another variation, suggested by the BIH, would use the LASSO technique to calibrate the emission time of the satellite TV pulse, which would then be used to transfer time to individual users via one-way reception of the pulse. A third possibility would be for several timing centers to provide their own high-accuracy satellite-position information by comparing the reception times of selected TV pulses. Still another approach for using TV broadcast satellites—in this case with more emphasis on general time dissemination—involves encoding time-of-day information into the TV signal vertical-blanking interval. It can then be received and decoded over wide reception areas with modest accuracy, which is sufficient for many public timekeeping needs.

Television broadcast satellites are currently under development to serve a number of countries and regions throughout the world. T/F dissemination experiments using such satellites are being conducted in Japan (Ishida *et al.*, 1979; Saburi *et al.*, 1979) and are planned for India and Europe. The vertical-interval time code has been tested experimentally in the United States and may be implemented later on some European TV satellites as they become operational.

A proposal for international time and frequency coordination using geostationary meteorological satellites is being pursued. An accuracy of 10 nsec worldwide as frequently as every 3 hr on a continual basis is anticipated.

The international system of satellites of interest is provided by Japan, the United States, and the European Space Agency (ESA). The satellites are all geostationary and include METEOSAT, operated by ESA and located 0° E longitude, Japan's Geostationary Meteorological Satellite (GMS), located at

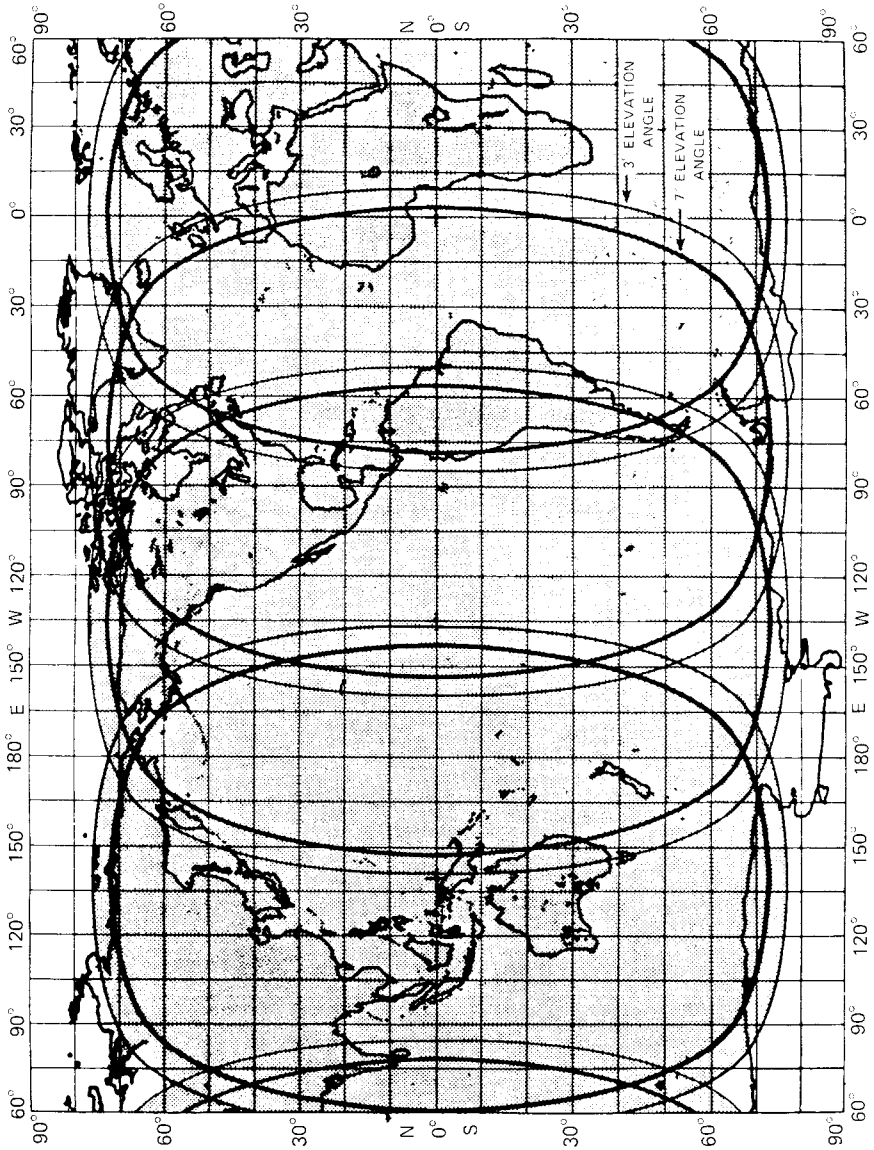


FIG. 13-11 Area coverage by the currently existing meteorological satellites, illustrating the near total coverage for time transfer possible if these satellites could be linked into a common timing system as is proposed.

140° E longitude, and two Geostationary Operational Environmental Satellites (GOES), operated by the United States and located at 225° E and 285° E longitude. Each of these satellites is supported by a ranging system for determining the satellite position at fixed intervals of time, usually every three to four hours. These data are then used to generate a set of orbital elements for the purposes of stationkeeping and position prediction. The approximate earth coverages of these satellite systems are shown in Fig. 13-11.

13.3.3 Deep-Space Radio-Source Techniques

Most deep-space experiments involved either geodesy or the study of deep-space signal sources. Most of these projects are involved with very-long-baseline interferometry (VLBI) techniques. In the long term a cooperative effort between the VLBI community and the T/F community could lead to significant benefits for both. The philosophy of the VLBI community is to use at each site very good frequency standards, typically hydrogen masers, whose frequencies are nominally syntonous (i.e., the frequencies are the same) with each other, and then to store the received radio-source data from large antenna on magnetic tape and cross-correlate the data after the fact. Once cross-correlated, they are in effect finding time resolution between the signals that is subnanosecond. Ten-picosecond resolution has been achieved. The potential for this technique to do extremely precise remote synchronization is incredibly high. The problem is to have real-time clocks at each site at that level of synchronization. Also, any of the techniques involved in studying deep-space radio sources have the very significant disadvantage that the signal strength is about 10^5 smaller than signals from satellites. Hence, almost all of these techniques require extremely sophisticated equipment, very-low-noise electronics, and usually very large antenna surfaces in order for the receiver to have adequate gain to receive the signals.

13.4 COORDINATE TIME FOR THE EARTH

As the accuracies of time and frequency methods for communicating between clocks at remote locations have improved, the relativistic corrections have become operational realities (Ashby, 1975; Ashby and Allan, 1979; Saburi *et al.*, 1976a,b). The September 1980 Consultative Committee for the Definition of the Second (CCDS) agreed upon a declaration establishing international atomic time (TAI) as a coordinate time scale to conform with the definition of the second as realized at the geoid (mean sea level) on the rotating earth and that the reference frame for this coordinate time scale would be a geocentric reference time frame. It was further declared that all of the appropriate relativistic correction be applied so that TAI could be

realized as a coordinate time scale on the surface of the earth. If TAI is used as a reference, the following equations allow one to reference to TAI unambiguously at nanosecond levels of accuracy. If clocks at two remote sites wish to have self-consistent coordinate measurements, then they must also use these equations if nanosecond or better accuracy and consistency are desired.

Since TAI has been designated as a coordinate scale (i.e., a time scale defined in space and time in the vicinity of the earth), this implies that UTC is also a coordinate scale, to be distinguished from Universal Time Coordinated. That is, UTC uses the same second based on the definition that TAI uses, but leap seconds are added to UTC so that it is "coordinated" with UT1 for navigational reasons.

When transferring time from point P to point Q by means of a portable clock, the coordinate time accumulated during transport is

$$\Delta t = \int_P^Q ds\left[1 - \frac{\Delta V(\mathbf{r})}{c^2} + \frac{v_e^2}{2c^2}\right] + \frac{2\omega}{c^2} A_E, \tag{13-1}$$

where c is the speed of light, ω the angular velocity of rotation of the earth, v_e the velocity of the clock with respect to the ground, $\mathbf{r}$ a vector whose origin is at the center of the geoid and whose terminus moves with the clock from P to Q, A_E the equatorial projection of the area swept out during the time transfer by the vector $\mathbf{r}$ as its terminus moves from P to Q, $\Delta V(\mathbf{r})$ the potential difference between the location of the clock at $\mathbf{r}$ and the geoid as viewed from an earth-fixed coordinate system, with the convention that $\Delta V(\mathbf{r})$ is positive when the clock is above the geoid, and ds the increment of proper time accumulated on the portable clock. The increment of proper time is the time accumulated on the portable standard clock as measured in the "rest frame" of the clock, that is, in the reference frame traveling with the clock. The area A_E is measured in an earth-fixed coordinate system. As the area A_E is swept, it is taken as positive when the projection of the path of the clock on the equatorial plane is eastward. When the height h of the clock is less than 24 km above the geoid, $\Delta V(\mathbf{r})$ may be approximated by gh, where g is the total acceleration due to gravity (including the rotational acceleration of the earth) evaluated at the geoid. This approximation applies to all aerodynamic and earthbound transfers. When h is greater than 24 km, the potential difference $\Delta V(\mathbf{r})$ must be calculated to greater accuracy as follows:

$$\Delta V(\mathbf{r}) = -GM_e\left(\frac{1}{r} - \frac{1}{a_1}\right) - \frac{1}{2}\omega^2(r^2 \sin^2\theta - a_1^2) + \frac{J_2 GM_e}{2a_1}\left[1 + \left(\frac{a_1}{r}\right)^3 (3\cos^2\theta - 1)\right]. \tag{13-2}$$

where a_1 is the equatorial radius of the earth, r the magnitude of the vector $\mathbf{r}$, θ the colatitude, GM_e the product of the earth's mass and the gravitational constant, and J_2 the quadrupole-moment coefficient of the earth, $J_2 = 1.083 \times 10^{-3}$.

When transferring time from point P to point Q by means of a clock whose distance from the center of the earth is less than 50,000 km (about 8 earth radii), the coordinate time elapsed during the motion of the clock is

$$\Delta t = \int_P^Q ds \left[1 - \frac{V(\mathbf{r}) - V_g}{c^2} + \frac{v^2}{2c^2} \right], \tag{13-3}$$

where $V(\mathbf{r})$ is the potential at the location of the clock and v is the velocity of the clock, both as viewed [in contrast to Eq. (13-1)] from a geocentric *nonrotating* reference frame, and V_g is the potential at the geoid, including the effect on the potential of the earth's rotational motion. Note that $\Delta V(\mathbf{r}) \neq V(\mathbf{r}) - V_g$, since $V(\mathbf{r})$ does not include the effect of the earth's rotation. This equation applies to clocks in geostationary orbits.

When transferring time from point P to point Q by means of an electromagnetic signal, the process can be viewed either from a geocentric, earth-fixed, rotating reference frame, or from a geocentric, nonrotating, local inertial frame. From the viewpoint of a geocentric, earth-fixed, rotating frame, the coordinate time elapsed between emission and reception of an electromagnetic signal is

$$\Delta t = \frac{1}{c} \int_P^Q d\sigma \left[1 - \frac{\Delta V(\mathbf{r})}{c^2} \right] + \frac{2\omega}{c^2} A_E, \tag{13-4}$$

where $d\sigma$ is the increment of standard length, or proper length, along the transmission path, $\Delta V(\mathbf{r})$ the potential at the point $\mathbf{r}$ on the transmission path less the potential at the geoid [see Eq. (13-3)] as viewed from an *earth-fixed* coordinate system, and A_E the area circumscribed by the equatorial projection of the triangle whose vertices are (1) at the center of the earth, (2) at the point P of transmission of the signal, and (3) at the point Q of reception of the signal. The area A_E is positive when the signal path has an eastward component. The second term amounts to about a nanosecond for an earth to geostationary satellite to earth trajectory. In the third term, $2\omega/c^2 = 1.6227 \times 10^{-6}$ nsec/km^2: this term can contribute hundreds of nanoseconds for practical values of A_E.

13.5 LEVELS OF SOPHISTICATION AND ACCURACIES FOR THE USERS

We shall divide the anticipated users into two groups. There are those who wish to buy commercially available equipment, "plug it in," and hope it works! The second group consists of those who are willing to expend some effort,

TABLE 13-5
Characteristics of the Major T/F Dissemination Systems

Dissemination techniques		Frequency syntonization accuracy	Time transfer accuracy	Ambiguity	Coverage for stated accuracy
VLF radio	GBR, NBA, OMEGA, etc.	1×10^{-11}	Envelope 1–10 msec	1 cycle	Nearly global
LF radio	Standard frequency broadcast (e.g., WWVB)	1×10^{-11} phase 24 h	Envelope 1–10 msec	Year	USA—limited (WWVB)
	LORAN-C	5×10^{-12}	1 μsec (ground) 50 μsec (sky)	TOC 15 min phase 10 μsec	Special areas
HF/MF radio	Standard frequency broadcast (e.g., WWV)	1×10^{-7}	1000 μsec	Code—year voice—1 day tick—1 sec	Hemisphere
Television (VHF/SHF radio)	Passive line-10	1×10^{-11}	1 μsec	33 msec	Network coverage
Satellite	GOES	3×10^{-10}	50 μsec	1 year	Western hemisphere
(UHF radio)	Transit	3×10^{-10}	30 μsec	15 min	Global
Portable clocks	Physical transfer	1×10^{-13}	100 nsec	N/A	Limited by transportation

TABLE 13-6

International Time and Frequency Comparison ($\ll 1$ μsec)

System	Time-transfer accuracy (nsec)	Time stability (nsec)	Frequency syntonization accuracy	Coverage for stated accuracy
GPS (common view)	10	1	$\lesssim 10^{-14}$	Global
Shuttle (STIFT)	1	0.001	$\lesssim 10^{-14}$	To $\pm 57°$ latitude
GOES (trilateration)	10	a few	$< 10^{-13}$	All but near the poles
LASSO	1	0.1	$\lesssim 10^{-14}$	Depends on implementation
GPS	40[a]	10	$\sim 3 \times 10^{-13}$	Global
2-way (communication satellite)	10	$\lesssim 1$	$\sim 10^{-14}$	All but near the poles
Portable clock	100	N/A	$\lesssim 10^{-12}$	Global (best accuracy within reasonable driving vicinity of airports)
Loran-C	500	$\lesssim 40$	$\lesssim 10^{-12}$	Excludes most of Asia and Southern Hemisphere

[a] This inaccuracy may increase if the GPS C/A code is deteriorated for strategic reasons.

perhaps because of broader coverage or higher levels of accuracy that may be needed in the particular comparison or dissemination system being employed.

13.5.1 Typical User Applications

Table 13-5 summarizes the main characteristics of major time and frequency dissemination systems. Specific examples are given for U.S. controlled systems. The entries in the table are nominal values. Depending on the specific technique employed, the actual accuracy values achieved may be as much as an order of magnitude better or worse than the nominal values listed, and there may be specific departures from the values given resulting from unusual circumstances.

13.5.2 Sophisticated and High-Accuracy Techniques

The techniques listed in Table 13-6 are experimental in nature and may be very labor intensive, requiring very sophisticated users on each end as T/F comparisons are made between clocks. The table gives some indication of the coverage and possible accuracies that might be achieved by the experimental systems that are being tested or are anticipated.

13.6 SUMMARY

Over the last several decades frequency standards have improved about one order of magnitude every seven years. The uses and needs of accurate time and frequency standards have, in a general sense, tracked this improvement. The use and need areas have usually been in the navigation and communication fields. As high technology continues to increase its demands on these and related fields, the need for improved T/F standards will persist as well as the need for improved methods of synchronization and syntonization between remote sites. These improved methods will draw heavily upon satellite techniques for comparing, calibrating, and measuring the improved clocks and oscillators. There are some attractive options being developed, and the potential appears nearly unlimited. With these increasing demands the use of terrestrial techniques will undoubtedly diminish, especially as radio interference becomes more and more of a problem.

To illustrate this trend, consider the backbone T/F dissemination techniques of the past. These have been the MF and HF transmissions, for example, JJY, CHU, WWV, and WWVH, with accuracies of about a millisecond in time and parts in 10^8–10^9 in frequency. These accuracies cannot be improved, because of terrestrial propagation problems, and the expense to run them soars with the energy costs. Increasing the transmission power only increases the costs and the radio frequency interference problems. In contrast, there is now being developed, using satellite techniques, a low-cost operational system with worldwide coverage that is anticipated to have 1-μsec accuracy in time and a few parts in 10^{12} in frequency. Experimental-satellite T/F systems have already demonstrated two to three orders of magnitude better accuracy performance than even this new anticipated operational satellite technique. On the "drawing boards" are satellite techniques with accuracies that push into the few picoseconds region in time and the parts in 10^{16} region in frequency. It has only been recently, with the advent of satellite techniques, that remotely located atomic clocks have been able to be compared at state-of-the-art levels of accuracy with averaging times of only a few days. With terrestrial means it took months.

In order for this congruency between remote T/F measurement methods and improving clocks to continue, it will clearly be necessary to continue developments in both fields. Fortunately, this seems to be happening.

ACKNOWLEDGMENTS

The author is indebted to Roger Beehler, Wayne Hansen, and Dr. Arthur Ballato for their careful reading of this chapter and for their valuable comments and contributions. Trudi Peppler helped greatly in updating and preparing some of the tables and references. This chapter draws upon the work of a large number of people to whom the author gives acknowledgment. The bibliography for this chapter gives reference to them. Figure 13-3 was kindly made available by True Time Instruments, a Division of Kinemetrics.

14 Other Means for Precision Frequency Control

Fred L. Walls

Time and Frequency Division
National Bureau of Standards
Boulder, Colorado

14.1 Introduction 275
14.2 Low-Frequency Devices 276
14.2.1 Quartz Tuning Forks 276
14.2.2 Other Low-Frequency Devices 279
14.3 Microwave Devices 281
14.3.1 Superconducting Cavities 281
14.3.2 Dielectrically Loaded Cavities 289

14.1 INTRODUCTION

In addition to the quantum electronic devices described in Chapter 10 and the bulk quartz and SAW oscillators discussed in Chapter 8, there are a number of other methods for precision frequency control. The frequency-controlling elements used in these techniques include high-Q tuning forks, high-Q LC circuits, superconducting cavities, and other high-Q resonators.

Techniques for frequency control with these devices have many similarities with those discussed in Chapters 8 and 10. General considerations outlined by Cutler and Searle (1966) can be used to estimate the limits of frequency stability due to wideband additive noise and thermal noise within the bandwidth of the resonator, that is, the frequency-determining element. Specifically,

$$\sigma_y(\tau) = \sqrt{\frac{kT}{2}\left(\frac{FB}{2\pi^2\nu_0^2 P_0 \tau^2} + \frac{1}{Q_l^2 P_b \tau}\right)}, \tag{14-1}$$

PRECISION FREQUENCY CONTROL
Volume 2
Oscillators and Standards
ISBN 0-12-280602-6

where k is Boltzmann's constant, T the noise temperature of the resonator, ν_0 the resonance frequency, F the noise figure of the first signal amplifier not filtered by the resonator, B the noise bandwidth of the receiver-plus-measurement system, P_0 the output power received at the first amplifier not filtered by the resonator, Q_l the loaded-resonator quality factor, P_b the total power dissipated in the resonator and its load, and τ the measurement interval. The first term on the right-hand side of Eq. (14-1) is due to additive noise of the receiver measurement system, whereas the second term is due to noise within the resonator bandwith perturbing the phase of oscillation. These two considerations therefore favor high-Q resonators operating at the highest possible power and frequency. Practical limitations come from systematic shifts or degradation in the resonator and/or degradation of receiver noise performance with increased resonator frequency and/or power levels. The following equation describes the empirical relationship between resonator Q factor and the best frequency stability observed with a given system, which seems to apply to many different techniques for frequency control [see, e.g., Table 3 of Hellwig (1979)]:

$$\Delta\nu/\nu_0 \cong \beta/10^7 Q, \qquad 2 < \beta < 100. \tag{14-2}$$

The empirical constant β is as low as 10 in many systems.

In addition to these random processes, many environmental parameters, such as temperature, excitation power, vibration, shock, radiation, outgassing, chemical processes, etc., affect the frequency and frequency stability of real devices. The performance of these devices indicated in the literature is often directly due to the technology available at the time and the constraints of the specific applications and as such may not apply to a new application due either to changes in technology or the presence of different constraints, such as size, power, weight, complexity, etc.

14.2 LOW-FREQUENCY DEVICES

In this section devices operating at frequencies under about 1 GHz are described.

14.2.1 Quartz Tuning Forks

The first low-frequency quartz resonators used for watch applications were flexure bars at 16 kHz and then at 32 kHz (Forrer, 1969; Musa and Daniels, 1971; Engdahl and Matthey, 1975). However, they were replaced by tuning forks, which typically have better long-term stability, are easier to mount, are more rugged, have less susceptibility to shock, have better frequency stability,

and occupy less volume than comparable flexure bars. As a consequence they have been widely used for highly stable, low-frequency oscillators.

The first quartz tuning forks were made in 1928 by Koga (1928). They were of proportions similar to the classical metal tuning forks and were operated at 1 kHz. More recently, the interest has been in obtaining much higher frequencies and much smaller size, but still with "bulky" tuning forks (Yoda *et al.*, 1972; Kanbayashi *et al.*, 1976; Bindal and Singhal, 1976; Schwartz, 1972).

The crucial breakthrough in terms of size and cost originated with Staudte (1973), who used photolithographic techniques to produce "thin" tuning forks with typical dimensions 6 mm long, 1 mm wide, and 0.025 mm thick. These devices can be made with fundamental frequencies from 10 to 300 kHz. Other frequencies can be obtained by using the first overtone (which is about 5.8 times higher than the fundamental) or by frequency multiplication or division. Much of the recent work has been done at $\nu = 2^{15} = 32{,}768$ Hz because of the straightforward division to one cycle per second and the convenient device parameters for the clock industry.

The flexural vibration is obtained by means of two opposite length-extensional vibrations. This requires double electrodes to apply the out-of-phase driving signals on the four faces (bulky tuning fork) or on the two faces (thin tuning fork) of each arm of the tuning fork (Fig. 14-1). As a consequence plating becomes more difficult to perform. The crystal plate can be rotated

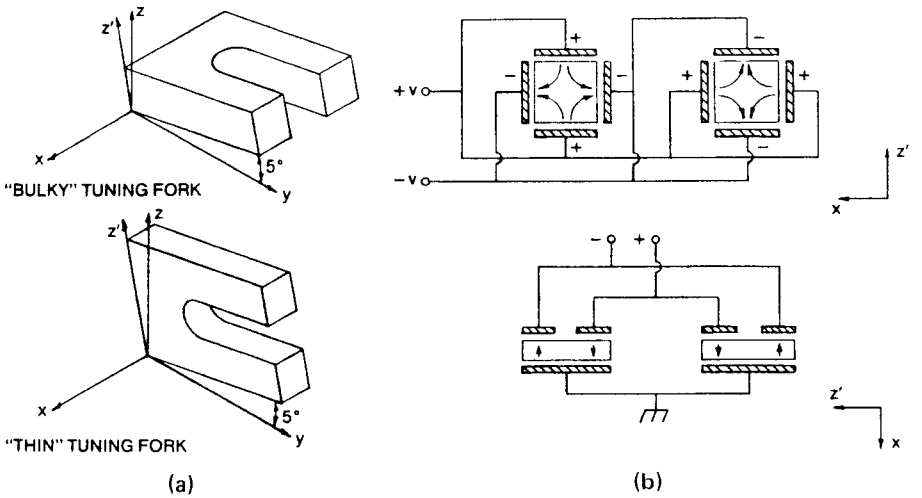


FIG. 14-1 (a) Orientation and (b) electrode configuration of "thin" and "bulky" tuning forks.

TABLE 14-1

Typical Characteristics of 32-kHz Quartz Tuning Forks

Parameter	Approximate value
Approximate size	6 mm × 1 mm × 0.2 mm
Q factor	30,000–120,000
Motional resistance	~10–400 kΩ
Temperature sensitivity	$\Delta\nu/\nu \cong 4 \times 10^{-8}(T - T_0)^2$
Frequency shift vs. power	$\Delta\nu/\nu \cong 10^{-5}/\mu W$
Tuning range	$\Delta\nu/\nu \cong 10^{-4}$
Acceleration sensitivity	$\Delta\nu/\nu \cong 10^{-7}/g$

around the x axis to obtain a 5° X-cut for instance, which would have a better frequency versus temperature characteristic.

In fact, today the choice between bulky and thin tuning forks is not yet clear and the choice is a function of compatibility with the pressure of industrial large-scale production, cost, and reproducibility of the parameters. Table 14-1 shows some approximate parameters for 32 kHz resonators (Engdahl and Matthey, 1975: Kanbayashi *et al.*, 1976; Kusters *et al.*, 1976; Yoda *et al.*, 1972).

Many studies have been made of various parameters versus cut angles and tuning-fork parameters. Temperature sensitivity is a critical point for most applications because these devices exhibit a parabolic frequency versus temperature characteristic rather than a cubic one as for AT-cut thickness-shear crystals. Attempts have been made to reduce this sensitivity, with only moderate success. Kusters *et al.* (1976) investigated first-order temperature-coefficient turnover point and Q factor versus length-to-width ratio at doubly rotated cut angles for 32-MHz tuning forks, and Kanbayashi *et al.* (1976) investigated the effects of asymmetry on frequency.

Limitations on frequency stability due to added noise for the high-series-resistance units characterized by Kusters *et al.* (1976) can be estimated using Eq. (14-1). For the purpose of calculation, let us assume an amplifier noise figure of $F = 2$, a dissipation power of 10^{-8} W, and a measurement bandwidth of 1 kHz. Equation (14-1) then shows that the frequency stability is dominated by the additive noise for times shorter than 10 sec:

$$\sigma_y(\tau) \cong 1.5 \times 10^{-10}\tau^{-1}.$$

The above performance has not, to our knowledge, ever been verified, since virtually all of the tuning forks have been used without protection from environmental effects such as temperature, supply variations, shock, etc. In addition, the CMOS oscillator circuit that is normally used limits the observed frequency stability to about 1×10^{-7} at 1 sec. In a more stable

circuit 1-sec frequency stability would be expected to improve by one to three orders of magnitude, limited by the thermal and vibrational environment. Frequency drift or aging of 1×10^{-7} per year or 3×10^{-10} per day has been reported for some types of tuning forks (see, e.g., Fig. 6-2) (Yoda *et al.*, 1972; Kanbayashi *et al.*, 1976).

The relatively low-drift, good short-term stability, and extremely low cost of modern tuning-fork fabrication and divider chips would seem to make this device an excellent candidate for low-cost timing applications and precision low-frequency oscillators.

14.2.2 Other Low-Frequency Devices

Several other techniques are capable of producing precision frequency sources with fractional-frequency stabilities of order 10^{-9}. These techniques can be typified by LC resonators with Q values of order 10^3 and relatively high oscillation powers. An example of this approach is seen in the tunnel-diode oscillators developed by Van Degrift (1975), shown schematically in Fig. 14-2. For an oscillator frequency of 3.7 MHz, resonator Q of $\cong 10^3$, and oscillator power of 10^{-8} W, he obtained the results shown in Fig. 14-3. In principle, even better results could have been obtained for times shorter than $\cong 10$ sec by going to a higher frequency, where the additive noise is less important. Another example is the stripline oscillator developed by D. A. Howe and described by Wineland *et al.* (1977). This oscillator, whose resonator cross section is shown in Fig. 14-4, produces 5 mW at about 500 MHz; however, similar designs can cover the range from $\cong 100$ MHz to several gigahertz. Figure 14-5 shows the frequency stability of a 500-MHz oscillator divided down to 5 MHz. The divider noise masks the stability for very short times. The performance at times longer than a few milliseconds is most likely dominated by fluctuations in the teflon-based laminate used for the stripline. The use of a different substrate material with better dimensional stability and comparable or lower losses, such as alumina, might significantly improve the frequency stability beyond about 10 msec. The improved

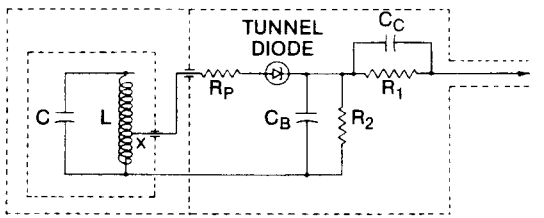


FIG. 14-2 Block diagram of tunnel-diode oscillator. [From Van Degrift (1975).]

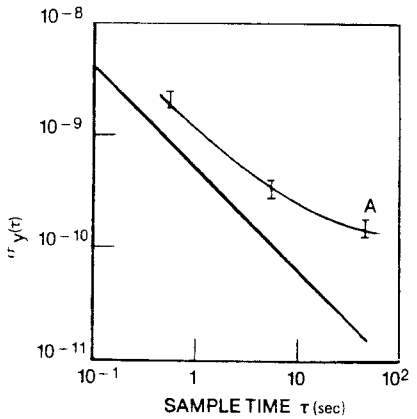


FIG. 14-3 Frequency stability $\sigma_y(\tau)$ versus averaging time for a cryogenic 3.7-MHz tunnel-diode oscillator with $P_0 = 10^{-8}$ W; the measurement bandwidth is 2.5 Hz. The stability at point A is probably limited by the measurement apparatus. [From Van Degrift (1975).]

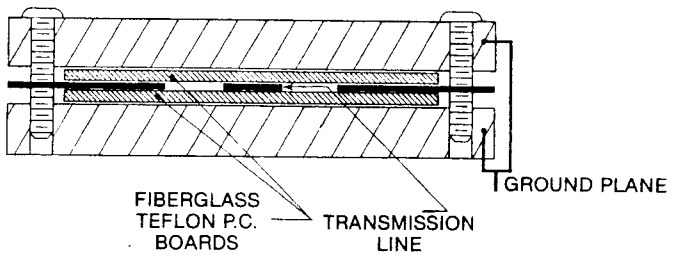


FIG. 14-4 Cross section of a stripline resonator for use at 500 MHz. The unloaded Q factor is about 500. [From Wineland *et al.* (1977).]

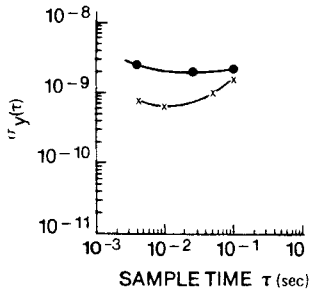


FIG. 14-5 Frequency stability of a 500-MHz stripline oscillator divided down to 5 MHz for a measurement bandwidth of 40 kHz (upper curve) and 400 Hz (lower curve). [From Wineland *et al.* (1977).]

stability from 1 to 10 msec, as compared to the tunnel-diode circuit, is due to the higher operating frequency and oscillation power. The limitations on fractional-frequency stability at 1 to 100 msec due to added thermal noise is totally negligible ($< 10^{-14}$) in this case.

In principle, this oscillator design can be made with a much lower sensitivity to vibration than a quartz-crystal-controlled oscillator. The unit shown in Fig. 14-4 achieved a sensitivity of approximately 5×10^{-10}/g for vibration at 40 Hz. The use of a more rigid substrate material and chip-bonding techniques should improve performance considerably. Such an oscillator might prove to be significantly superior to quartz crystal oscillators for use in systems with very high vibration and shock. A hybrid solution might be to use an LC oscillator locked to a quartz-crystal-controlled oscillator in order to reduce some of the vibration-induced sidebands and still retain the better long-term stability of the quartz-crystal-controlled oscillator.

14.3 MICROWAVE DEVICES

In this section devices operating at frequencies of about 1 GHz are described. Microwave cavities can be used in all the traditional ways low-frequency resonators have been used to stabilize the frequency of an oscillator. [See, for example, Stein (1975) and Jimenez and Septier (1973).] Superconductive cavities have the distinction of having the best combination of practically achievable power, Q factor, and operating frequency of all known microwave devices.

Recently, wide interest has developed in the use of dielectrically loaded microwave cavities to stabilize microwave oscillators and for various filtering applications. The term "dielectrically loaded" designates that a solid dielectric material is used instead of vacuum or air. Although the Q factor is not as high as in superconducting cavities, these devices handle higher power, operate over a very large temperature range, and are much cheaper.

14.3.1 Superconducting Cavities

In order to achieve the high Q values characteristic of superconductors, it is generally necessary to use cavity modes and assembly techniques that minimize surface imperfections and eliminate the need for rf current through the assembly joints. In the case of niobium, electron-beam welding techniques have been developed to a sufficient degree that the assembly joint can carry rf current without seriously degrading the Q factor. Figure 14-6 shows the measured Q values for X-band cavities fabricated from lead and niobium, the two most promising superconductors for microwave cavities. These two

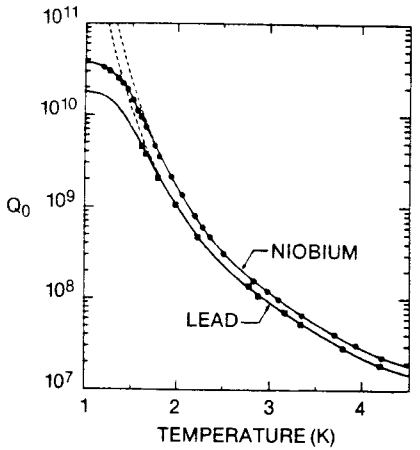


FIG. 14-6 Unloaded Q value of typical lead and niobium X-band cavities with a measurement bandwidth of 10^4 Hz. The dashed curves represent the theoretical behavior. [From Pierce (1974).]

metals are available commercially in sufficient purity and the fabrication techniques are well known (Turneaure and Weissman, 1968; Pierce, 1974). The superconducting transition temperature for lead is 7.19 K, whereas that for niobium is 9.25 K. Other superconductors with higher transition temperatures are known; however, they are generally brittle and difficult to fabricate. Lead cavities, on the other hand, are particularly easy to fabricate by electroplating. At Stanford niobium cavities have been fabricated using electron-beam welding followed by firing at 1900°C and chemical polishing (Turneaure and Weissman, 1968). Another technique developed at Siemens (Diepers *et al.*, 1971) uses chemical polishing followed by anodizing. The Q value produced by this latter technique may degrade in time, however (Pierce, 1974). The rf magnetic fields achieved without serious Q-factor degradation are approximately 60% higher in niobium than in lead cavities. From Eq. (14-1) it is seen that this yields somewhat better noise performance and is the primary reason for the predominant concentration on niobium cavities in the early work. Experimental results, however, show that in every practical application the environmental sensitivities dominate the frequency stability. The white-frequency level from Eq. (14-1) for a loaded Q value of 5×10^9, $P_b = 10^{-6}$ W, $T = 1$ K, and $\nu = 10^{10}$ Hz corresponds to $\sigma_y(\tau) \cong 10^{-20}\tau^{1/2}$, while the additive noise only contributes $\sigma_y(\tau) = 4 \times 10^{-20}\tau^{-1}$ for a 300-K sustaining circuit. Figure 14-7 shows the frequency stability of 8.4-GHz niobium cavities, whose characteristics are given in Table 14-2 (Stein, 1975). The environment was carefully controlled and yet the vibration–acceleration

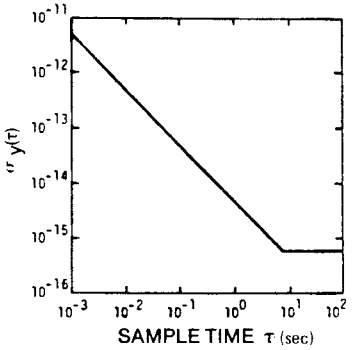


FIG. 14-7 Fractional-frequency fluctuations of an X-band superconducting-cavity-stabilized voltage-controlled oscillator. [From Stein (1975).]

sensitivity of approximately 10^{-9}/g limits the short-term stability. The long-term drift was of order 2×10^{-13}/day.

One approach having greater potential for better short-term stability is the all-cryogenic parametric oscillator stabilized by a superconducting-cavity transmission filter proposed by Stein (1975). This all-cryogenic-oscillator approach eliminates many of the long leads associated with earlier work. Frequency stabilities of order 1×10^{-16} at 1 sec appear feasible with this scheme, which also uses the superconducting cavity as a transmission filter. Superconducting cavities can also be used as transmission filters for conventional oscillators. The filtering process greatly improves the spectral purity (i.e., the phase noise for Fourier frequencies outside the bandpass of the cavity) and improves the short-term frequency stability for times long compared to the inverse linewidth of the cavity.

As indicated above, the primary disadvantages of superconducting cavities are their environmental sensitivities. In order to achieve a stability of 10^{-16} in the present TM_{010} X-band niobium cavities, the power must be fractionally

TABLE 14-2

Typical Characteristics of X-Band Niobium Superconducting Cavities

Parameter	Approximate value
Q factor	10^{10}–10^{11}
Operating power	10–100 μW
Temperature coefficient	$\Delta\nu/\nu \cong 4 \times 10^{-10}$/K at 1.4 K
Acceleration sensitivity	$\Delta\nu/\nu \cong 10^{-9}$/g
Energy shift	$\Delta\nu/\nu = 10^{-11}/10^{-7}$ J stored energy

stable to 10^{-5}, the acceleration constant to 10^{-7} g, and the temperature constant to 10^{-7} K at 1.3 K. Of these effects the vibration–acceleration sensitivity is presently the most serious limit on the short-term stability.

A new approach that might yield a major reduction in the vibration sensitivity is to plate lead on the inside of a ceramic cavity. The mechanical strength of several ceramics exceeds that of niobium by an order of magnitude. The small loss in Q factor should have an insignificant effect on the noise performance. Also, new cavity designs that are inherently less sensitive to mechanical deformation need to be studied. One such approach is being pursued by Dick and Strayer (1983). In their design the cavity is a sapphire sphere coated on the outside. The gain element is a ruby maser at about 3 GHz. This approach sacrifices cavity Q due to the losses within the sapphire dielectric; however, it has the nice features of parametric pumping and compactness suggested by Stein (1975).

14.3.2 Dielectrically Loaded Cavities

The use of dielectrically loaded cavities dates from the work of Richtmeyer (1939), but the early dielectrics suffered from large temperature coefficients. Recent materials have dielectric constants from 30 to about 100, temperature coefficients of order 10 to -10×10^{-6}/°C, and loss tangents less than 10^{-3}.

TABLE 14-3

Characteristics of Temperature-Compensated Dielectric-Resonator Materials at 7 GHz

	Material			
Parameter	Ba_2TiO_6, $Ba_2Ti_6O_{20}$	R–04C; series TiO_2–ZrO_2–SnO_2–(ZrSn)TiO_2; monoclinic	R-09C; series (BaPb)TiO_3	Ba(NiTa)O_3–Ba(ZrZnTa)O_3
Loss tangent	0.5×10^{-3}	1.6×10^{-4} from −55 to 100°C	10^{-3}	6.8×10^{-5}
$Q_{unloaded}$	2000 (minimum)	6300 (minimum)	1000	14500
Relative dielectric constant	37 ± 5%	36.8–38.9, selectable	90	30
Temperature coefficient of frequency from −50 to 100°C	−25 ppm/°C	0 possible selectable from −4 to 12 ppm/°C	0 possible selectable from −10 to 10 ppm/°C	0 possible selectable from 18 to −10 ppm/°C

The availability of temperature coefficients from 10 to -10×10^{-6}/°C allows one to compensate the entire resonator–gain system to $< 10^{-6}$/°C. The high dielectric constants greatly reduce the size of the resonator as compared to traditional vacuum dielectric cavities.

Table 14-3, from the review article of Stiglitz (1981) and a paper by Wakimo *et al.* (1983), compares several of the most interesting dielectric families for application in frequency metrology. Clearly there is great opportunity to make extremely stable miniature microwave resonators and oscillators with high signal-to-noise ratios and hence frequency stability. As an example, Wakimo *et al.* (1983) describes a 5-g, 11-GHz oscillator having an uncompensated frequency stability of ±1 MHz from −40 to 60°C. The size is 2.03 cm × 1.26 cm × 0.88 cm.

15 Special Applications

Fred L. Walls

Time and Frequency Division
National Bureau of Standards
Boulder, Colorado

Jean-Jacques Gagnepain

Laboratoire de Physique et Métrologie des Oscillateurs
Besançon, France

15.1 Microbalances, Thin-Film Measurement, and Other Mass-Loading Phenomena 288
15.2 Measurements of Force, Pressure, and Acceleration 290
15.2.1 Force 290
15.2.2 Pressure 291
15.2.3 Acceleration 291
15.3 Temperature Measurements 293

The high resolution achievable with frequency metrology often makes it attractive to connect the measurement of physical parameters to a frequency measurement via a suitable transducer. Quartz crystal resonators are sensitive to mass loading and, via nonlinear effects, to temperature and stress. The sensitivities are generally low; however, the excellent short-term stability of precision quartz resonators makes high-resolution measurements of temperature, pressure, vibration, acceleration, film thickness, some gas-phase chemical reaction rates, and absorption feasible.

PRECISION FREQUENCY CONTROL
Volume 2
Oscillators and Standards

ISBN 0-12-280602-6

15.1 MICROBALANCES, THIN-FILM MEASUREMENT, AND OTHER MASS-LOADING PHENOMENA

The sensitivity of quartz resonators to added mass has been widely studied and used to measure the deposition rate, thickness, etc., of various materials. This technique was first suggested by Sauerbrey (1959). Further analyses have been carried out by many researchers [see, e.g., Warner and Stockbridge (1963), Mueller and White (1968), EerNisse (1975a), and Lu (1975)].

For changes in crystal-resonator mass loading of several percent or less, the frequency change $\Delta\nu/\nu$ is linear, that is,

$$\Delta\nu/\nu = K\,\Delta m/m,$$

where K depends only on the crystal and deposition area. As the thickness of the coating grows, the elastic and inelastic properties of the coating and the inherent stress of the coating play increasingly important roles in determining the resonator frequency (EerNisse, 1975b; Lu, 1975). Ultimate resolution for coatings of aluminum and copper is typically about $\Delta m/m = 10^{-12}$.

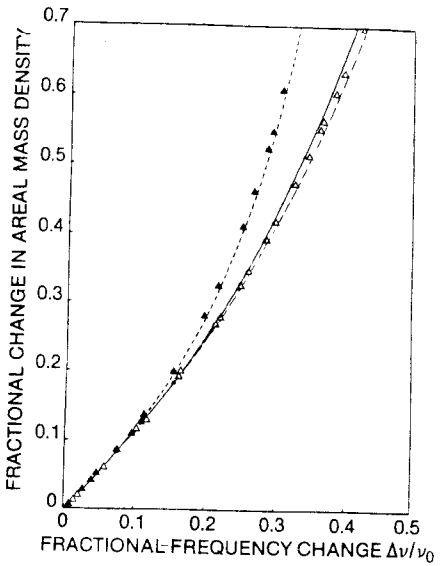


FIG. 15-1 Comparison of measured and computed fractional-frequency changes for quartz resonators loaded by copper and aluminium. The symbol ▲ denotes the experimentally measured points for copper, while △ denotes the experimentally measured points for aluminum. The theoretical curve for copper is shown as - - - -, that for aluminum is shown by — — —, and that for quartz is shown by a solid line. [From Lewis and Lu (1975).]

Film coatings ranging from a few picograms per square centimeter to 0.05 g/cm^2 (Lu, 1975) can be measured with accuracies that are typically better than 3% (see Fig. 15-1). Since quartz resonators are also sensitive to stress and temperature, schemes must be used to minimize these spurious effects. Usually these effects are compensated by using several resonators with either different exposures or different sensitivities [see, e.g., Warner and Stockbridge (1963), Warner *et al.* (1965), Mueller and White (1968), Shiojiri *et al.* (1969), Mecea and Bucur (1974), EerNisse (1975a), and Van Ballegooijen *et al.* (1978)] as frequency-determining elements in two or more oscillators in order to distinguish between the various effects.

A new possibility could be offered by doubly rotated crystals that exhibit, in addition to the regular C mode, a second resonance. The B mode (see Chapter 2) is very temperature sensitive and can therefore be used as a temperature probe for compensation in a dual-mode oscillator (Kusters *et al.*, 1978).

By using a cryogenically cooled pair of quartz resonators, Scialdone (1974) measured the outgassing of condensable gasses from a spacecraft. The high sensitivity to mass changes achievable with quartz resonators makes it possible to monitor chemical reactions between an electrode material and a gas. The sensitivity to mass change typically exceeds 10^{-3} monolayers. Benndorf *et al.* (1977) used such an arrangement to study the initial oxidation of aluminum. Warner *et al.* (1965) used this technique to study the effect of carbon dioxide on gold. Florio (1968) studied *alkali-antimonide* films. Shiojiri *et al.* (1969) studied sulfuration and oxidation of metal films, and Bucur *et al.* (1972) studied palladium–deuterium systems.

Mecea and Bucur (1974) showed that the amplitude of oscillation of a quartz crystal resonator decreases linearly with added mass and that many nonmetallic materials have a relatively larger effect than the same mass of copper. Water, for example, decreases the amplitude some 200 times faster than copper, while mineral oil decreases it about 60 times faster than copper. This inelastic effect is due to the added damping of the oscillation, which is due to dissipation within the coating. This technique could possibly be used to detect phase changes in coatings by simultaneously measuring changes in the amplitude and frequency of oscillation.

Quartz crystals can also be used as detectors by coating one electrode with a material that can absorb one specific gas (King, 1971). For instance, ambient-air hydrocarbons or auto-exhaust hydrocarbons can be analyzed in this manner. Generally, polymers are used as coating material. There is a potential for application in the field of meteorological monitors by employing simultaneously several sensors for humidity, temperature, and pressure measurements (Kertzman, 1971).

15.2 MEASUREMENTS OF FORCE, PRESSURE, AND ACCELERATION

When the propagation medium of an elastic wave is submitted to static or low-frequency mechanical perturbations, the quasistatic stresses and strains that are induced in the crystal are coupled to the high-frequency wave by the elastic nonlinearities of the crystal, thereby causing wave-velocity and frequency shifts.

15.2.1 Force

Force sensitivity was studied in the case of diametric or bending forces applied at the periphery of circular plates (Ballato, 1960; Gerber and Miles, 1961a,b; Keyes and Blair, 1967; Ratajski, 1966, 1968). These first measurements, made with AT-cut resonators, were then complemented by theoretical analyses and extended to doubly rotated cut resonators (EerNisse *et al.*, 1978; Lee *et al.*, 1976; Janiaud *et al.*, 1978). As an example, Fig. 15-2 shows the frequency change per diametrically applied force for an AT-cut plate as a function of the azimuth angle (Gerber and Miles, 1961a).

The temperature dependence of the force-sensitivity effect was also investigated (Dauwalter, 1972; EerNisse *et al.*, 1978, 1979), and in some particular cases attempts were made to use the force-sensitivity effect for temperature compensation (Gerber and Miles, 1961a,b).

This force sensitivity is typically on the order of 1.4×10^{-5}/N for AT-cut crystals under diametric forces along the x-axis. The force sensitivity depends on the directions of application of the forces. Particular azimuthal angles can be found either with zero or maximum force sensitivities. Quartz force

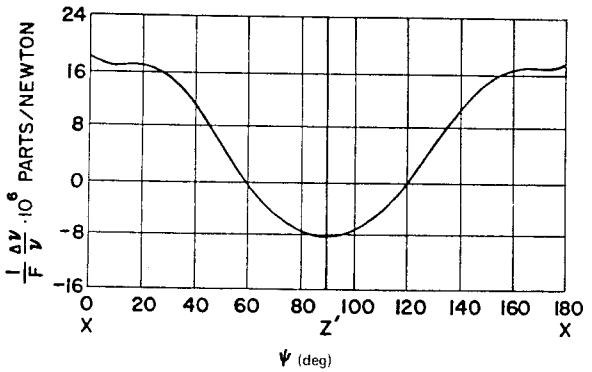


FIG. 15-2 Frequency change $\Delta v/v$ per applied force F as a function of the azimuth ψ for an AT-cut plate. [From Gerber and Miles (1961a).]

sensors were studied in this last case (Hammond and Benjaminson, 1969; Karrer and Ward, 1977).

Surface-acoustic-wave (SAW) devices also are sensitive to forces. Sensitivity to compressional and bending forces on rectangular plates and to diametric forces on circular plates were also investigated (Hauden *et al.*, 1980; Dias and Karrer, 1974). The largest sensitivity was obtained with bending forces (typically 1200 Hz/N for ST-cut quartz at 100 MHz). Such sensitivity opens the possibility of measuring pressures and accelerations through the force-frequency effect.

15.2.2 Pressure

Warner *et al.* (1965) and Stockbridge (1966) examined the sensitivity of quartz resonators to the hydrostatic pressure of inert gasses and found a sensitivity of about 1×10^{-7}/Pa for a 5th-overtone AT-cut resonator. This phenomenon of viscous damping on bulk-acoustic-wave (BAW) devices can be exploited to yield a pressure sensor. An example of this approach is illustrated by the work of Genis and Newell (1977). They used a bellows arrangement to isolate an X–Y-flexure watch crystal from humidity and contamination effects. The transfer gas was dry nitrogen. They achieved an accuracy of about 700 Pa over the range from 0 to 1.4×10^5 Pa.

A much different approach is that described by Hammond and Benjaminson (1969) and Karrer and Ward (1977), where the pressure is transformed to diametric forces applied on the periphery of a BT-cut resonator. They reported a sensitivity of about 70 Pa, an accuracy of order ± 5000 Pa $\pm$ 0.025%, and an operating range of 100 to 8×10^7 Pa. A very special feature of their resonator was an integral resonator–mounting structure machined out of a single piece of quartz. This gave a total pressure range extending over six orders of magnitude.

SAW devices can also be exploited as pressure–force sensors. Their sensitivity to hydrostatic pressure is relatively small. An ST-cut SAW device at 100 MHz yields sensitivities of order 3×10^{-3} Hz/Pa (Hauden *et al.*, 1980). By utilizing a small circular diaphragm, a differential pressure device has been built with a sensitivity of 0.4 Hz/Pa. This differential device also has excellent thermal properties, with offsets of order ± 400 Pa for temperatures from -40 to 80°C (Reeder and Cullen, 1976).

15.2.3 Acceleration

When a crystal is in an acceleration field, the body forces and the induced reaction forces (at the fixation points) also give a static or quasistatic deformation and, again through nonlinear coupling, the wave velocity is

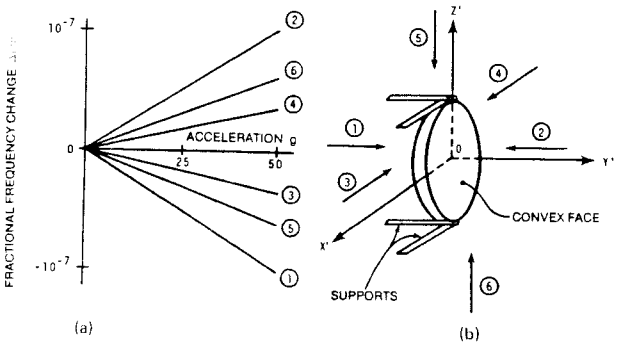


FIG. 15-3 (a) Frequency variation of a quartz resonator for several different directions of applied acceleration, shown schematically in (b). [From Valdois *et al.* (1974).]

changed. The result is a variation of the resonance frequency related to the applied acceleration field direction, as shown in Fig. 15-3 [Valdois *et al.* (1974): see also Ballato and Bechmann (1960)]. This effect, a major source of environmental disturbance in precision oscillators, can be used to produce an acceleration transducer. However, since the acceleration sensitivity varies widely (even polarity) depending on the direction of applied force, a single resonator provides little information on acceleration. By a careful choice of mounting several resonators, one can fabricate a sensor with calibrated sensitivity to only a single directional component of acceleration (vibration). The work of Onoe *et al.* (1977) describes one such approach. Two near-identical retangular plates are separated by a small distance and clamped along the same edge. Both are made to oscillate at their respective thickness-shear resonance. The beat frequency between the two oscillators, derived by mixing the two oscillator outputs, is proportional to the acceleration component perpendicular to the plane of the crystal plates. Other force components that normally produce a signal in single-resonator accelerometers cancel out to a high degree. They achieved a sensitivity of 500 Hz/g for the range from 0 to 100. Deviations from linearity were typically less than 0.2% of the full range, or 0.2 g.

SAW resonators exhibit a sensitivity to forces of order 1 kHz/N at 100 MHz, which can be used to fabricate an acceleration sensor by transforming the acceleration into a force using an auxiliary mass. Due to their relatively recent introduction and a preoccupation with using them for complex data processing, their application to acceleration measurement is not well developed yet.

An interesting aspect is the sensitivity of propagating acoustic waves to Coriolis acceleration: when a point mass moves with a velocity relative to a rotating frame, it experiences a Coriolis force. Thus, the velocity of a wave

therefore varies with the angular velocity of the substrate. This effect could be used for measuring rotation rates: however, it occurs only for propagating waves and not for standing waves. This necessitates the use of delay lines rather than resonators to control the frequency of the oscillator.

Theoretical evaluations of sensitivity to Coriolis forces have been made for surface acoustic waves and bulk flexure waves (Lao, 1980: Tiersten *et al.*, 1980). An interesting effect is the fact that reversing the propagation direction of the wave reverses the sign of the velocity or frequency shift. It is therefore possible to operate with a differential configuration that improves sensitivity and reduces some spurious effects.

15.3 TEMPERATURE MEASUREMENTS

The present accuracy limit of temperature measurements near 300 K is on the order of 50–100 μK and is obtained using platinum resistance thermometers (Riddle *et al.*, 1973). Thermistors used as thermal sensors yield a resolution of approximately 10 μK and a temperature stability of order 1 mK/100 days (Dror and Cannel, 1974: Wood *et al.*, 1978). Quartz crystal thermometers presently have a temperature resolution of order 2 μK and inherently yield a digital output; however, they are plagued by hysteresis effects due to thermal shock and cycling. Several new experimental quartz crystal resonators show promise of achieving temperature resolutions of less than 1 μK with daily variations of less than 10 μK and greatly reduced thermal-shock–cycling-induced hysteresis.

The potential for using a quartz crystal resonator to obtain a high-resolution digital thermometer has long been recognized (Gorini and Sortori, 1962; Hammond *et al.*, 1965; Hammond and Benjaminson, 1969; Holland, 1974). Indeed, Smith and Spencer (1963) used a high-quality quartz resonator as the frequency-determining element of an oscillator and obtained a temperature resolution of approximately 5 μK for a 10-sec measurement time and a drift of less than 100 μK/hr, as illustrated in Fig. 15-4. The frequency

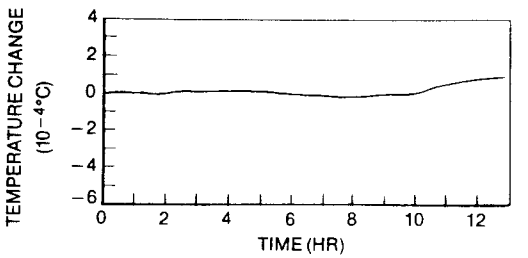


FIG. 15-4 Temperature variation of a double oven versus time measured using a 5° Y-cut quartz resonator. [From Smith and Spencer (1963).]

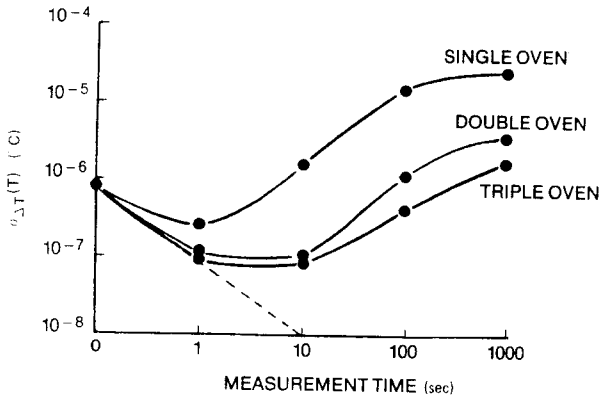


FIG. 15-5 Temperature stability of BVA SC-cut resonators contained in various ovens that were digitally controlled with an LC-cut quartz temperature probe. The dashed line shows the measurement limit due to noise. [From Marianneau and Gagnepain (1980).]

dependence was approximately 74.6 ppm/°C from −20 to 100°C. Presently available quartz thermometers are linear to within a few millikelvin from 0 to 200°C, have a time constant of order 10 sec, a resolution of order 2 μK, and a drift of only a few millikelvin per month (Hammond *et al.*, 1965). LC-cut quartz probes were used by Marianneau and Gagnepain (1980) for controlling the temperature of very stable ovens, as shown in Fig. 15-5. Temperature can also be measured by using the B mode of SC-cut crystals (Kusters *et al.*, 1978). Accurate temperature control and thermal filtering enable one to lower the residual temperature fluctuation of a vacuum-enclosed quartz crystal down to 0.1 μK over a few seconds.

However, LC-cut resonators suffer from thermal stress effects that result in spurious temperature readings on the order of 10 mK following thermal cycling (Fig. 15-6). The apparent temperature typically drifts approximately 10 mK over several days immediately following a temperature shock of many degrees. Because of these hysteresis effects, quartz crystal resonators have not generally been used in precision thermometry where temperature cycling is required.

Stress-induced frequency transients have received considerable attention in the past 5 years because they are responsible for much of the frequency instability of high-precision quartz crystal resonators used in frequency control (Holland, 1974; Ballato and Vig, 1978; Stein *et al.*, 1978; Theobald *et al.*, 1979). It appears likely that they are responsible for the thermal hysteresis as well as the noise in quartz sensors. In the past several years great strides have been made in designing crystallographic cuts that are less sensitive to

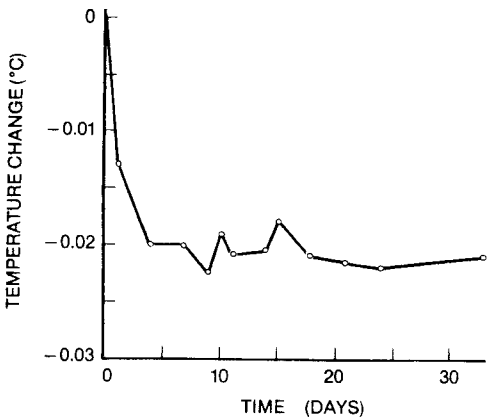


FIG. 15-6 Temperature error of an LC-cut quartz thermometer as a function of time after a temperature transient. [From Hammond *et al.* (1965).]

stress and in new mounting techniques that help to minimize temperature-induced (i.e., stress-induced) transients (EerNisse, 1975b, 1976; Besson, 1976, 1977; Kusters *et al.*, 1977).

For example, a fifth-overtone, 5-MHz quartz resonator has a parabolic static temperature sensitivity of approximately $\Delta\nu/\nu = 10^{-9}/\mathrm{K}^2$, yielding a linearized sensitivity of $\Delta\nu/\nu = 2 \times 10^{-8}/\mathrm{K}$, 1 K away from turnover. Since the frequency stability of such precision units is $\Delta\nu/\nu = 10^{-13}$, one would expect to achieve temperature resolution of 5 μK; however, the thermal-transient-induced response is $\Delta\nu/\nu = 10^{-5}\, dT/dt$, requiring that dT/dt be less than 0.01 μK/sec in order to achieve 1-μK temperature resolution and stability. Most ovens and test systems do not have the low-temperature transients required to use AT-cut resonators for temperature sensors.

The new SC-cut resonators (Besson, 1977; Kusters *et al.*, 1977; Theobald *et al.*, 1979) have a measured transient response that is 50–100 times smaller than that for AT-cut resonators. Therefore, dT/dt of only 0.5–1 μK/sec is required in order to resolve 1 μK. SC-cut resonators are therefore excellent candidates for thermal sensors. These new SC-cut resonators have another very interesting feature, namely, they can be made to oscillate on both the B and C modes simultaneously (Kusters *et al.*, 1978). The C mode can be made with $\Delta\nu/\nu = 10^{-9}/\mathrm{K}^2 + 10^{-7}\, dT/dt$, while the B mode has a linear response of $\Delta\nu/\nu = 2.5 \times 10^{-5}/\mathrm{K}$. It may be possible to use the C mode as the frequency reference for the microprocessor-based counter measuring the frequency of the B mode. With such a system temperature resolutions of approximately 0.1 μK are contemplated. Using only the B mode temperature stabilities of 1 μK over hours and 10 μK/day appear likely. The application

of the so-called BVA_2 technology developed by Besson (1977) to the LC cut (Hammond *et al.*, 1965) or the Y cut (Smith and Spencer, 1963) may yield a thermal sensor with resolution of order 0.1 μK, linearity of order 10 mK/100 K, and a daily stability of order $< 10\,\mu K$.

SAW devices are also sensitive to temperature. Hauden *et al* (1980) examined several cuts and found that a cut that is near $\phi = 11°24'$, $\theta = 59°24'$, and $\psi = 35°$ has a nearly linear frequency versus temperature curve. The first-order coefficient is ~ 31 ppm/°C or 3.2×10^{-4} °C/Hz at 93 MHz. The second-order coefficient was 2×10^{-3} ppm/°C^2. Given a typical SAW oscillator stability of 10^{-9} to a few parts in 10^{-10} would indicate possible resolutions on the order of 10 to 30 μK. Data on hysteresis effects appear to be nonexistent, but an interesting feature of such a SAW temperature probe is its short response time, which is typically 0.3 sec or less. This is 30 times shorter than for typical LC-cut sensors.

16 Specifications and Standards

Erich Hafner

U.S. Army Electronics Technology and Devices Laboratory (Retired)
Fort Monmouth, New Jersey

16.1 Specifications 297
16.2 Standards 299
16.3 Practices in the United States 300
16.4 International Standardization 304

16.1 SPECIFICATIONS

Specifications are the means by which manufacturers and users communicate regarding the properties of devices. A specification is a specific document applicable to a particular type of device, providing numeric values for all properties that affect its performance in a particular application. If the specification is complete, any unit that meets the specified requirements, regardless of manufacturer, can be substituted for any other like unit, with no adverse effect on the using equipment. Every numeric value for a property will have a tolerance associated with it that is no tighter than required for the intended application, and only the properties needed for that application are specified. In general, the values and tolerances in a specification should be the end result of intense consultation between the device manufacturers and the user. Most specifications also require that only materials of a certain type and quality be used in the manufacture of the item.

An important aspect of the specification is a complete description of the methods by which the various specified attributes are to be measured and the conditions under which the tests are to be performed. These descriptions must be sufficiently complete to assure agreement between the results of tests performed independently in the manufacturer's and user's plants. Disputes

PRECISION FREQUENCY CONTROL
Volume 2
Oscillators and Standards

Copyright © 1985 by Academic Press, Inc.
All rights of reproduction in any form reserved.
ISBN 0-12-280602-6

that arise, at times, especially about values near the limits of the specified tolerances, emphasize the need for clarity. A test should be devised for each attribute specified, and attributes that cannot be tested for objectively should not be included in the specification.

Generally, there are at least two types of attributes. One group includes those that depend primarily on the basic designs of the unit, the materials used, and the overall manufacturing process. Here, changes from unit to unit are rare; when failures occur, they often affect large quantities of units. In the second group are attributes that depend primarily on the detailed manufacturing operations performed on the individual units, with unit-to-unit variations a common occurrence. Further, not all attributes have equal weight. Failure of a unit to meet the requirement in regard to a particular attribute may be of critical, major, or minor importance for the performance of the device in its intended application, and inspections of some attributes can only be performed by destructive testing. Clearly, therefore, economy and common sense dictate that every product cannot, and need not, be inspected for every attribute specified. A suitable grouping of attributes and a sampling plan for each group are needed and must be included in the specification together with alternate sampling plans for reduced or tightened inspection, the latter to be based on (specified) experience factors.

A specification must also address the procedure by which a customer–vendor relationship is first established between a manufacturer and user, how it is to be maintained for continuous as well as for intermittent production, and what remedies are to be applied in the event that the product does not conform to the requirements of the specification. Establishing the customer–vendor relationship usually involves complete testing of an appropriate number of units that were produced using the equipment and procedures to be used in the subsequent manufacture of the items—at times these units are called "tool-made samples." Beyond that, it may involve establishing various kinds of controls on the production line which, in some cases, are to be maintained during the entire production period. Remedial actions generally range from retesting of failed lots, usually under tightened sampling procedures, to complete severance of the customer–vendor relationship, with the vendor incurring certain specified liabilities for any defective products delivered.

This latter aspect of the specification provides the means by which conformance to its technical content can be enforced and is of critical importance for the quality of the product. A defective product is costly—in the simplest case extensive retesting is required, but if the defects are systematic, it can mean a shutting down of the production line at the vendor and, for lack of product, at the customer's plant also. Hence, formulation of

the relevant sections of the specification involves policy-level decisions that are guided by the quality assurance philosophies of the participating parties and tempered by the nature of the consequential damages resulting from the use of defective devices.

Stand-alone specifications, that is, specifications that include, in themselves, all of the above factors, are rarely used. In most industries a great deal of the contents of a complete specification for one particular product applies equally to many other products, with one specification differing from another by only a few numeric values. To assure uniformity to the greatest extent possible, therefore, the common aspects are committed to a separate document, the applicable sections of which can then be referred to in the specifications for the individual product. These now vastly less voluminous detailed specifications contain the specific numeric values for the attributes of the particular products. The common document is the basic or general specification; it, in turn, may refer back to standards that are still broader documents.

It is important to recognize that a detailed specification, which may consist of no more than a single table of values and an outline drawing, is only a small part of the full specification of the product; for a partial specification to be complete, it must reference explicitly the basic specification to which it applies. Where no such basic specification exists or existing documents are, for valid reasons, not acceptable, they must be developed for the protection of both customer and vendor. Any implicit assumptions on the part of either are an open invitation for serious problems to develop, sooner or later.

16.2 STANDARDS

In the present context, standards are authoritative documents that promote mutual understanding and uniformity of practices for the benefit of researchers, developers, manufacturers, and users of frequency control devices. The term is used loosely and includes guides to the use of frequency control devices, precise definitions of terms, preferred dimensions and values, environmental test conditions and methods, quality assurance procedures, etc. Even though the use of standards documents, with notable exceptions, is voluntary, the basic reason for the existence of many is for them to be cited in the various product specifications. Once incorporated, their use is, de facto, mandatory whenever that specification is used.

In general, standards are self-contained documents that are sufficiently complete to provide definitive answers to relevant questions. Unlike specifications they do not, as a rule, refer to other documents as integral parts.

16.3 PRACTICES IN THE UNITED STATES

Formulation of standard documents relevant to frequency control devices in the United States is carried out by the Institute of Electrical and Electronics Engineers (IEEE), the Electronic Industries Association (EIA), and the Department of Defence (DOD). A listing of widely available standards currently in effect is shown in Table 16-1. Updated lists are provided yearly on the back pages of the Proceedings of the Annual Frequency Control Symposium. In addition, of course, proprietary documents are generated by many users for their own purposes. These are not considered in the following discussions. As indicated in Table 16-1, one of the current IEEE standards has been adopted by the American National Standards Institute (ANSI), a federation of national associations dealing with standardization. ANSI coordinates but does not, in itself, formulate standards.

The most recent IEEE standard, 176-1978, addresses basic properties of piezoelectric crystals. It deals with the determination of material constants, sign conventions for crystallographic axes, and theoretical concepts and mathematical relationships applicable to vibrations of piezoelectric bars and plates. The measurement method detailed in IEEE Standard 177-1966 is the precursor for the method later adopted, in modified form, by the IEC for Standard IEC-444. IEEE Standard 177-1966 will be revised in the future to embrace the latest gains in measurement practice.

The EIA publications listed in Table 16-1 deal with selected topics that are of interest to the manufacturers of crystal units. Standard RS-186-E is a broad-based document applicable to electronic components for commercial use.

The most comprehensive and self-consistent set of documents dealing with standardization of frequency control devices is contained in the Military Specification (MIL-SPEC) System. Its use is mandatory in all DOD-related procurements. Development of the basic system, which covers all electronic components, was completed in the decade following World War II; it is a dynamic system that is being kept up-to-date by periodic revisions and additions as needed. The standards and specifications issued are fully coordinated with the industries affected and thus represent a government–industry consensus to the greatest extent possible. The system will be explained with the documents applicable to quartz crystal units as an example.

Equipment designers in need of a quartz crystal unit are required to use MIL-STD 683, the military standard on "Quartz Crystal Units and Crystal Holders," to determine the standard crystal unit most appropriate for the intended application. MIL-STD-683 provides a listing of the standard crystal

TABLE 16-1
Specifications and Standards Relevant to Frequency Control

Institute of Electrical and Electronics Engineers
Order through: IEEE Service Center, 445 Hoes Lane, Piscataway, NJ 08854, (201)-981-0060

176-1978 Piezoelectricity

177-1966 Piezoelectric Vibrators, Definitions and Methods of Measurements for (ANSI C83.17-1970)

180-1962 Ferroelectric Crystal Terms, Definitions of

319-1971 Piezomagnetic Nomenclature

Electronic Industries Association
Order through: Electronic Industries Assn., 2001 Eye Street, N.W., Washington, D.C. 20006, (202)-457-4900

(a) Holders and Sockets
RS-192-A, Holder Outlines and Pin Connections for Quartz Crystal Units (standard dimensions for older types)

RS-367, Dimensional and Electrical Characteristics Defining Receiver Type Sockets (including crystal sockets)

RS-417, Crystal Outlines (standard dimensions and pin connections for current quartz crystal units—1974)

(b) Production Tests
RS-186-E (all sections), Standard Test Methods for Electronic Component Parts

(c) Application Information
Components Bulletin No. 6, Guide for the Use of Quartz Crystals for Frequency Control

(d) RS-477, Cultured Quartz (April, 1981)

International Electrotechnical Commission
Order through: American National Standards Inst., 1430 Broadway, New York, NY 10018

ANSI can quote prices on specific IEC publications on a day-to-day basis only. All IEC and ISO standards have been removed from its Standards Catalog. Call ANSI, NYC (212)-354-3300 for prices

IEC Publication 122-1 (1976) Quartz Crystal Units for Frequency Crystal and Selection. Part 1: Standard Values and Test Conditions (Second Edition)

IEC Publication 68 Basic Environmental Testing Procedures (in 48 parts)

IEC Publication 122-2 (1962) Section 3: Guide to the Use of Quartz Oscillator Crystals, including Amendment 1 (1969)

IEC Publication 122-3 (1977) Part 3: Standard Outlines and Pin Connections (second edition)

IEC Publication 283 (1968) Methods for the Measurement of Frequency and Equivalent Resistance of Unwanted Resonances of Filter Crystal Units

IEC Publication 302 (1969) Standard Definitions and Methods of Measurement for Piezoelectric Vibrators Operating Over the Frequency Range up to 30 MHz

IEC Publication 314 (1970) Temperature Control Devices for Quartz Crystal Units, including Supplement 314A Contents: General Characteristics & Standards; Test Conditions; Pin Connections

(*Continued overleaf*)

Table 16-1 (*Continued*)

IEC Publication 314A (1971) First Supplement to Publication 314 (1970) Contents: Guide to the Use of Temperature Control Devices for Quartz Crystal Units

IEC Publication 368 (1971) Piezoelectric Filters including Amendment 1, Amendment 2, and Supplement 368A and 368B Contents: General Information & Standards Values; Test Conditions

IEC Publication 368A (1973) First Supplement to Publication 368 (1971) Contents: Guide to the Use of Piezoelectric Filters

IEC Publication 368B (1975) Second Supplement to Publication 368 (1971) Contents: Piezoelectric Ceramic Filters

IEC Publication 444 (1973) Basic Method for the Measurement of Resonance Frequency and Equivalent Series Resistance Quartz Crystal Units by Zero Phase Technique in a π-Network

IEC Publication 483 (1976) Guide to Dynamic Measurements of Piezoelectric Ceramics with High Electromechanical Coupling

Department of Defense

Order through: Naval Publication & Form Center, 5801 Tabor Avenue, Philadelphia, PA 19120

MIL-C-3098 Crystal Unit, Quartz, General Specification for

MIL-H-10056 Holders (Enclosures), Crystal, General Specifications for

MIL-STD-683 Crystal Units, Quartz/and Holders, Crystal

MIL-F-28734 Frequency Standards, Cesium Beam, General Specification for

MIL-O-55310 Oscillators, Crystal, General Specification for

MIL-F-18327 Filters, High Pass, Low Pass, Band Pass Suppression and Dual Functioning, General Specification for

MIL-O-39021 Oven, Crystal, General Specification for

MIL-O-55240 Oscillators, Audio Frequency

MIL-F-28811 Frequency Standard, Cesium Beam Tube

MIL-STD-202 Test Methods for Electronic and Electrical Component Parts

units, the so-called CR (Crystal *R*esonator) types, in the order of the most essential parameters of interest to the equipment designer, such as frequency range, type of operation, temperature range, etc., and it shows drawings of the standard crystal holders, with maximum dimensions. A more complete detailed specification for each CR type is contained in the so-called "slash sheets" to MIL-C-3098, to be discussed below; the slash-sheet numbers for the various CR types are listed in MIL-STD-683. If one of the standard crystal units meets the requirements of the equipment, that crystal unit can be ordered, in single-unit or production quantities, from one of the so-called "qualified sources," following normal procurement procedures, with the purchase order listing no more than the CR number and the

nominal frequency. If, for good and valid reasons, none of the standard crystal units meet the equipment needs, the designer will prepare his own detailed specification and submit it for approval per the instructions in MIL-STD-683. Even when approved that crystal unit remains nonstandard unless, and until, it is converted into a CR type by the responsible military authorities. In most cases the nonstandard detailed specification will call out the closest standard (CR-type) crystal unit and list the required exceptions; in all cases it will specify that the requirements of the general specification MIL-C-3098 be met. Thus, the provisions of MIL-C-3098 apply in all cases.

MIL-C-3098, the general specification for quartz crystal units, defines the terms used and the attributes of the crystal units to be evaluated with respect to the numeric values given in the detailed specifications (slash sheets); it specifies the conditions under which these evaluations are to be performed and the measurement methods to be used. When these are common to most electronic components, such as many of the environmental test conditions, the details are defined by reference to the applicable MIL-STD documents, for example, MIL-STD-202, the standard for "Test Methods for Electronic and Electrical Component Parts." As a matter of policy, the specification relies on the performance of the product. Details of manufacture are not prescribed, as a rule. Thus, specific manufacturing practices are addressed only in cases where they are known to affect product performance, but the effects are difficult to evaluate adequately by reasonable testing procedures or within a reasonable testing period.

MIL-C-3098 also details the procedure to be followed by manufacturers to obtain qualifications as a supplier for any one, or all, of the various categories of standard crystal types. At the time of this writing, qualification requirements are waived for nonstandard crystal units, that is, crystal units covered by detailed specifications that are not slash sheets to MIL-C-3098. Procurements for such crystal units occur most frequently in cases where the crystal manufacturer is a subcontractor to an original equipment manufacturer (OEM) under contract with the government. That contract places the full burden for the quality of the materials used, including the crystal units, on the OEM. The OEM is constrained to obtain "first article" (tool-made sample) tests on the products of his subcontractors. These are the same tests as required for qualification. But, unless specifically requested by the crystal manufacturer, they are not counted toward qualification per the requirement of MIL-C-3098. The contract also assures government inspectors access to the OEM plant, including the relevant documentation. It does not, under normal conditions, assure government access to the subcontractor's plant, based on its relationship with the OEM. When problems develop with the subcontractor's product, however, the government inspector serving the OEM can request his counterparts in the subcontractor's area to conduct a

selective examination of the subcontractor's operations to determine if the requirements of MIL-C-3098 are met and to perform such tests as are considered necessary. If deficiencies are noted, the remedies prescribed by MIL-C-3098 are to be invoked. The selective examination does not constitute "government source inspection" and does not transfer responsibility for product quality from the OEM to the government.

Similar practices apply to the DOD standards-specifications for other frequency control devices and also for other electronic components and subsystems. (Special, much more rigorous practices are used for missile and space applications.) The DOD standards are effectively serving the function of national standards in the frequency control area in the United States and are, in fact, used extensively throughout the Western World.

16.4 INTERNATIONAL STANDARDIZATION

Voluntary international standards in the commercial arena are promulgated by the International Electrotechnical Commission (IEC), a worldwide organization whose work is conducted by various Technical Committees, each dealing with a particular speciality. The Technical Committee No. 49 (TC-49) of the IEC is responsible for "Piezoelectric Devices for Frequency Control and Selection." The standards documents prepared by TC-49 and currently in effect are listed in Table 16-1. IEC Publication No. 122 provides definitions of terms, standard values for temperature ranges, load capacitors, and drive levels, conditions of measurement, standard holder outlines, etc. IEC Publication No. 444 describes a specific method for the measurement of frequencies and equivalent electrical parameters of crystal units, along with a specific measuring device, the IEEE π-network used in the zero-phase mode.

IEC Publication No. 68 defines standard conditions for environmental testing of electronic components. Documents dealing with quartz crystal oscillators, filters, synthetic quartz properties, and other relevant topics are in various stages of preparation. An IEC Quality Assurance (Assessment) System is under consideration.

Bibliography

Eduard A. Gerber
Arthur Ballato

U.S. Army Electronics Technology and Devices Laboratory
Fort Monmouth, New Jersey

Introduction 305
General Bibliography 307
Books 307
Conference and Symposia Proceedings; Special Issues 308
General Papers; Reviews; Book Chapters 309
Chapter Bibliographies 313
Chapter 7 313
Section 8.1 321
Section 8.2 333
Section 8.3 339
Chapter 9 344
Chapter 10 349
Chapter 11 376
Chapter 12 399
Chapter 13 416
Chapter 14 432
Chapter 15 435
Chapter 16 442

INTRODUCTION

The editors have assembled a reasonably complete bibliography covering the years 1968–1982. More than 5000 references were found for this period. The pre-1968 period is covered by the inclusion of reviews and a selection of references to seminal articles. Science Abstracts A (Physics) and B (Electrical and Electronics) and Chemical Abstracts were particularly helpful in leading us to the pertinent literature. The organization of the main part of the bibliography follows that of the rest of the book, that is, the references are

PRECISION FREQUENCY CONTROL
Volume 2
Oscillators and Standards

Copyright © 1985 by Academic Press, Inc.
All rights of reproduction in any form reserved.
ISBN 0-12-280602-6

arranged in alphabetical order under each chapter heading. Thus, it will be easy for the reader to find the references quoted in the text. In the case of Chapters 2, 5, and 8, however, the arrangement is made according to sections, due to different authorships.

The references for the various chapters include papers on applications of specific devices, such as application of crystal units and filters. References describing more than one topic are listed under the chapter where that subject is predominant. Multi-subject papers without emphasis on a specific topic, items of a more general nature, survey papers, books, and chapters of books are listed separately in the general bibliography section.

Obviously, some overlap of topics is unavoidable. It is, therefore, recommended that the reader review related subjects in search for a paper of a specific nature. For instance, looking for a paper on the properties of a crystal unit, it would be well to search the bibliographies for Chapters 2 and 4.

In the area of quantum electronic devices and standards, we have included only references on gaseous masers. On the other hand, a large number of references may be found in the area of laser frequency standards. It is thought that in this rapidly developing field, valuable information is to be found in papers on gas lasers even though not directly concerned with frequency standards.

Papers on tuning forks, particularly for wristwatches, are considered to be a special case and are listed under Chapter 14; papers regarding their applications are listed under Chapter 15.

Where an article or book exists in English translation, normally only the English version is cited. This is particularly germane to the Russian literature, but since this book is primarily intended for the English-literate reader and since the original citation will appear in the translated journal, no essential information is omitted.

Certain documents, particularly U. S. government reports, are cited as obtainable from NTIS; these are usually catalogued according to a six digit number prefixed by the letters AD or ADA. The address is National Technical Information Service, U. S. Department of Commerce, 5285 Port Royal Road, Springfield, Virginia 22161, U.S.A.

References cited as *Proc. Annu. Freq. Control Symp.* refer to proceedings of the Annual Frequency Control Symposia, sponsored by the U. S. Army Electronics Research and Development Command, Fort Monmouth, New Jersey 07703, U.S.A. Proceedings from the 10th (1956) through the 31st (1977) may be obtained from NTIS. The 32nd through 35th are available through Electronic Industries Association, 2001 Eye Street, N.W., Washington, D.C. 20006, U.S.A. The 36th through 38th may be obtained from Systematics General Corporation, 2711 Jefferson Davis Highway, Arlington, Virginia 22202, U.S.A.

GENERAL BIBLIOGRAPHY

Books

Androsova, V. G., Bankov, V. N., Dikidzhi, A. N., Il'ichev, V. A., Karaul'nik, A. Ye., Pozdnyakova, P. G., Rakhmaninov, S. V., Fedotov, I. M., and Khristoforov, V. N. (1978). "Quartz Resonators Reference Book" (P. G. Pozdnyakova, ed.) Moscow: Svyaz', 288 pp. In Russian.

Auld, B. A. (1973). "Acoustic Fields and Waves in Solids," vols. 1 and 2. Wiley, New York.

Bennett, R. E. (1960). "Quartz Resonator Handbook: Manufacturing Guide for "AT" Type Units." Union Thermoelectric Division, Niles, Illinois. U.S. Army Contract DA36-039-SC-71061, 225 pp.

Blair, B. E. (1971). "Time and Frequency: a Bibliography of NBS Literature Published July 1955 to December 1970." Report Spec. Publ. 350, National Bureau of Standards, Washington, D.C., 50 pp.

Blair, B. E. (ed.) (1974). "Time and Frequency: Theory and Fundamentals." NBS Monograph 140. U. S. Government Printing Office, Washington, D.C.

Bottom, V. E. (1982). "Introduction to Quartz Crystal Unit Design." Van Nostrand-Reinhold, New York.

Buchanan, J. P. (1956). "Handbook of Piezo-Electric Crystals for Radio Equipment Designers." Wright Air Development Center, Wright-Patterson AFB, Ohio. Number WADC TR-56-156, 692 pp.

Cady, W. G. (1964). "Piezoelectricity," vols. 1 and 2, Dover Publications, New York.

Edson, W. A. (1953). "Vacuum Tube Oscillators." Wiley, New York.

Firth, D. (1965). "Quartz Crystal Oscillator Circuits Design Handbook," Magnavox Serial No. TP64-1072, Magnavox Company, Fort Wayne, Indiana. U. S. Army Contract No. DA-36-039-AMC-00043 (E).

Frerking, M. E. (1978). "Crystal Oscillator Design and Temperature Compensation." Van Nostrand-Reinhold, New York.

Groszkowski, J. (1964). "Frequency of Self-Oscillations." Macmillan, New York.

Heising, R. A. (1946). "Quartz Crystals for Electrical Circuits." Van Nostrand, New York.

Herrmann, G. (ed.) (1974). "R. D. Mindlin and Applied Mechanics." Pergamon, New York.

Herzog, W. (1949). "Siebschaltungen mit Schwingkristallen." Dieterich'sche Verlagsbuchhandlung, Wiesbaden, Germany. In German.

Holland, R., and EerNisse, E. P. (1969). "Resonant Piezoelectric Devices, Design of." MIT Press, Cambridge, Massachusetts.

Johnson, R. A. (1983). "Mechanical Filters in Electronics." Wiley, New York.

Kartaschoff, P. (1978). "Frequency and Time." Academic Press, London.

Mason, W. P. (1942). "Electromechanical Transducers and Wave Filters." Van Nostrand, New York.

Mason, W. P. (1950). "Piezoelectric Crystals and Their Application to Ultrasonics." Van Nostrand, New York.

Mason, W. P. (1966). "Crystal Physics of Interaction Processes." Academic Press, New York.

Mason, W. P., and Thurston, R. N. (eds.) (1964ff). "Physical Acoustics: Principles and Methods." (Vol. 1 (1964)–Vol. 16 (1983). Academic Press, New York.

Matthews, H. (ed.) (1977). "Surface Wave Filters." Wiley, New York.

Matthys, R. J. (1983). "Crystal Oscillator Circuits." Wiley, New York.

Mindlin, R. D. (1955). "An Introduction to the Mathematical Theory of Vibrations of Elastic Plates." U. S. Army Signal Corps Engineering Laboratories, Fort Monmouth, New Jersey. Contract No. DA-36-039 SC-56772.

Parzen, B. (1983). "Design of Crystal and Other Harmonic Oscillators." Wiley, New York.
Post Office Research Station Staff (R. Bechmann, *et al.*) (1957). "Piezoelectricity." Her Majesty's Stationery Office, London.
Ramsey, N. F. (1969). "Molecular Beams." Oxford Univ. Press (Clarendon), London and New York.
Ristic, V. M. (1983). "Principles of Acoustic Devices." Wiley, New York.
Sanders, J. H., and Wapstra, A. H. (1976). "Atomic Masses and Fundamental Constants." Plenum, New York.
Scheibe, A. (1938). "Piezoelektrizitaet des Quarzes." Steinkopff, Dresden and Leipzig. In German.
Sheahan, D. F., and Johnson, R. A. (eds.) (1977). "Modern Crystal and Mechanical Filters." IEEE Press, New York.
Siegmann, A. E. (1971). "An Introduction to Lasers and Masers." McGraw-Hill, New York.
Smagin, A. G. (1964). "Precision Quartz Resonators." Izdatyelestvo Standarfov, Moscow. In Russian.
Tiersten, H. F. (1969). "Linear Piezoelectric Plate Vibrations." Plenum, New York.
Townes, C. H., and Schawlow, A. L. (1955). "Microwave Spectroscopy." McGraw-Hill, New York.
Vanier, J. (1971). "Basic Theory of Lasers and Masers." Gordon and Breach Science Publishers, London and New York.
Vigoureux, P. (1939). "Quartz Oscillators and Their Applications." His Majesty's Stationery Office, London.
Vigoureux, P., and Booth, C. (1950). "Quartz Vibrators and Their Applications." His Majesty's Stationery Office, London.
Voigt, W. (1928). "Lehrbuch der Kristallphysik." B. G. Teubner, Leipzig und Berlin. In German.
Vuylsteke, A. A. (1965). "Elements of Maser Theory." D. Van Nostrand Co., Inc., New York.
Zverev, A. I. (1967). "Handbook of Filter Synthesis." Wiley, New York.

Conferences and Symposia Proceedings; Special Issues

Cooper, M. (1967). The quartz crystal comes of age. *18th Annual Conference of the IEEE Vehicular Technology Group (New York: IEEE)*, pp. 72–77.
First open symposium on Time and Frequency of URSI Commission A. *Radio Sci.* **14**, (4), July–August 1979, 519–731.
Gagnepain, J. J., Meeker, T. R., Nakamura, T., and Shuvalov, L. A. (eds.) (1982). Special Issue on Piezoelectricity. *Ferroelectrics*; **40** (3/4), 123–256 (Part I); **41** (1/2/3/4), 1–254 (Part II); **42** (1/2/3/4), 1–246 (Part III); **43** (1/2), 1–96 (Part IV).
IEEE (1965). Special issue on ultrasonics. *Proc. IEEE* **53**, 1292–1680.
IEEE (1966). Special issue on frequency stability. *Proc. IEEE* **54**, 103–338.
IEEE (1967). Special issue on radio measurement methods and standards. *Proc. IEEE* **55**, 741–1126.
IEEE (1969). Special issue on microwave acoustics. *IEEE Trans. Microwave Theory Tech.* **MTT-17**, 800–1046.
IEEE (1976). Special issue on surface acoustic wave devices and applications. *Proc. IEEE* **64**, 581–807.
IEEE Ultrasonics Symposium Proceedings (1972ff). IEEE Group on Sonics and Ultrasonics, IEEE, 345 East 47th Street, New York, New York 10017.
Proceedings of the Annual Frequency Control Symposium (1956ff). U. S. Army Electronics Research and Development Command, Fort Monmouth, New Jersey 07703.
Proceedings of the Annual Precise Time and Time Interval Applications and Planning Meeting (1969ff). NASA Goddard Space Flight Center, Greenbelt, Maryland 20715.

Proceedings of the IEEE–NASA Symposium on Short-Term Frequency Stability (1964). Report NASA SP-80. Goddard Space Flight Center, Greenbelt, Maryland 20715.

General Papers; Reviews; Book Chapters

Allan, D. W., Gray, J. E., and Machlan, H. E. (1974). The National Bureau of Standards atomic time scale: Generation, stability, accuracy and accessibility. *In* "Time and Frequency: Theory and Fundamentals" (B. E. Blair, ed.), pp. 205–231. Natl. Bur. Stand. Monogr. 140.
Allan, D. W., Shoaf, J. H., and Halford, D. (1974). Statistics of time and frequency data analysis. *In* "Time and Frequency: Theory and Fundamentals (B. E. Blair, ed.), pp. 153–204. Natl. Bur. Stand. Monogr. 140.
Alley, C. (1979). Relativity and clocks. *Proc. 33rd Annu. Freq. Control Symp.*, pp. 4–39.
Anonymous (1969). Applications of mechanical oscillations in communication technology. *Technica* **18**, 1451–1454. In German.
Anonymous (1973). Piezoelectronics. *Pr. Inst. Tele-Radiotech.* **17**, 72–83. In Polish.
Anonymous (1976). The technology of surface acoustic waves and their applications. *Elettron. Oggi (Italy)* (10), 1269–1277. In Italian.
Anonymous (1979). The SAW [surface acoustic wave] technology. [function theory]. *Mikrowellen Mag.* (4), 235–238. In German.
Anonymous (1980). Quartz crystals for accuracy. *Telonde* (1), 38–41.
Balek, R., and Bunc, V. (1975). The applicability of surface elastic waves. *Sdelovaci Tech.* **23**, 130–132. In Czech.
Ballato, A. (1977). Doubly rotated thickness mode plate vibrators. *In* "Physical Acoustics," vol. XIII, (W. P. Mason and R. N. Thurston, eds), pp. 115–181. Academic Press, New York.
Ballato, A., and Gerber, E. A. (1979). Piezoelectricity. *In* "Digest of Literature on Dielectrics" (M. R. Wertheimer and A. Yelon, eds.), vol. 41, pp. 393–436. National Academy of Sciences, National Research Council, Washington, D.C. 20418.
Ballato, A., Staudte, J. H., Horton, W. H., Takeuchi, T., and Fischer, R. (1981). The future of the quartz crystal industry—worldwide. *Proc. 35th Annu. Freq. Control Symp.*, pp. 576–595.
Barnes, J. A. (1974). Basic concepts of precise time and frequency. *In* "Time and Frequency: Theory and Fundamentals" (B. E. Blair, ed.), pp. 3–14. Natl. Bur. Stand. Monogr. 140.
Barnes, J. A., and Winkler, G. M. R. (1974). The standards of time and frequency in the U.S.A. *In* "Time and Frequency: Theory and Fundamentals" (B. E. Blair, ed.), pp. 317–327. Natl. Bur. Stand. Monogr. 140.
Beehler, R. E. (1974). A historical review of atomic frequency standards. *In* "Time and Frequency: Theory and Fundamentals" (B. E. Blair, ed.), pp. 85–100. Natl. Bur. Stand. Monogr. 140.
Beehler, R. E. (1974). Recent progress on atomic frequency standards. *In* "Time and Frequency: Theory and Fundamentals" (B. E. Blair, ed.), pp. 101–109. Natl. Bur. Stand. Monogr. 140.
Bidart, L. (1982). New design of very high frequency sources. *Ferroelectrics* **40**, 231–236.
Blair, B. E. (1974). Time and frequency dissemination: An overview of principles and techniques. *In* "Time and Frequency: Theory and Fundamentals" (B. E. Blair, ed.), pp. 233–313. Natl. Bur. Stand. Monogr. 140.
Bowers, K. D. (1971). Ultrasonics in communications. *Bell Lab. Rec.* **49**, 139–145.
Butler, M. B. N. (1980). Surface acoustic wave devices. I [analogue signal processing]. *Electron. Eng.* **52**, 37–39, 41, 43–44.
Butler, M. B. N. (1980). Surface acoustic wave devices. II. *Electron. Eng.* **52**, 57, 59, 61, 63, 65.
Butler, M. B. N. (1981). Surface acoustic wave devices III. Applications. *Electron Eng.* **53**, 54–63.
Chao, G. (1977). Surface acoustic wave devices move into high-volume markets. *EDN* **22**, 96–99.
Cometta, M. (1974). Piezoelectricity, (devices) and its applications. *Elettrificazione* (2), 71–75. In Italian.

Contoni, A. (1981). Surface acoustic wave devices I. *Antenna* **53**, 435–438. In Italian.
Cook, W. R., and Jaffe, H. (1979). Piezoelectric, electrostrictive and dielectric constants, and electromechanical coupling factors of piezoelectric crystals. *In* "Landolt–Boernstein, New Series" (K.-H. Hellwege, ed.), pp. 287–470. Springer-Verlag, Berlin, Heidelberg, New York.
De Klerk, J. (1975). Elastic surface wave devices. *In* "Physical Acoustics," vol. XI (W. P. Mason and R. N. Thurston, eds.), pp. 213–244. Academic Press, New York.
Dressner, J. M., and Del Vecchio, J. P. (1969). Frequency control requirements for the Mallard communication system. *Proc. 23rd Annu. Freq. Control. Symp.*, pp. 1–7.
Essen, L. (1971). Electrical standards in terms of frequency and physical constants. *Alta Freq.* **40**, 693–696.
Eykholt, A., and Lipetz, N. (1970). Surface acoustic wave devices—an emerging technology. *Proc. Natl. Electron. Conf.*, p. 991.
Fisk, J. R. (1971). New acoustic surface-wave devices. *Electron. Aust.* **33**, 24–27.
Folts, H. (1972). Precise time and frequency in a communication system. *Proc. 26th Annu. Freq. Control Symp.*, pp. 4–7.
Forsbergh, P. W., Jr. (1956). Piezoelectricity, electrostriction and ferroelectricity. *In* "Handbuch der Physik," vol. XVII (S. Flugge, ed.), Springer Verlag, Berlin, Gottingen, Heidelberg.
Franx, C. (1970). A report on IEC technical committee TC-49. *Proc. 24th Annu. Freq. Control Symp.*, pp. 172–176.
Gerber, E. A. (1948). Piezoelektrische Eigenschaften (piezoelectric properties). *In* "Physik des festen Korpers (Physics of Solids)" (G. Joos, ed.), Chapter 52. Dieterich'sche Verlagsbuchhandlung, Wiesbaden, Germany.
Gerber, E. A., and Sykes, R. A. (1966). State of the art—Quartz crystal units and oscillators. *Proc. IEEE* **54**, 103–116.
Gerber, E. A., and Sykes, R. A. (1967). Quartz frequency standards. *Proc. IEEE* **55**, 783–791.
Gerber, E. A., and Sykes, R. A. (1971). A quarter century of progress in the theory and development of crystals for frequency control and selection. *Proc. 25th Annu. Freq. Control Symp.*, pp. 1–45.
Gerber, E. A., and Sykes, R. A. (1974). Progress in the development of quartz crystal units and oscillators since 1966. *In* "Time and Frequency: Theory and Fundamentals" (B. E. Blair, ed.), pp. 59–66. Natl. Bur. Stand. Monogr. 140.
Glaze, D. J. (1974). Improvements in atomic cesium beam frequency standards at the National Bureau of Standards. *In* "Time and Frequency: Theory and Fundamentals" (B. E. Blair, ed.), pp. 111–117. Natl. Bur. Stand. Monogr. 140.
Glaze, D. J., Hellwig, H., Jarvis, S., Wainwright, A. E., and Allan, D. W. (1974). The new primary cesium beam frequency standard. *In* "Time and Frequency: Theory and Fundamentals" (B. E. Blair, ed.), pp. 121–124. Natl. Bur. Stand. Monogr. 140.
Greebe, C. A. A. J. (1974). Electromagnetic, elastic and electro-elastic waves. *Philips Tech. Rev.* **33**, 311–349.
Hafner, E. (1972). Frequency control aspects in Army communications and surveillance. *Proc. 26th Annu. Freq. Control Symp.*, pp. 15–19.
Hawkins, D. T. (1973). Absolute configuration of piezoelectrics—A bibliography. *Ferroelectrics* **5**, 111–123.
Hearman, R. F. S. (1979). The elastic constants of crystals and other anisotropic materials. *In* "Landolt Boernstein, New Series" (K.-H. Hellwege, ed.), pp. 1–244. Springer-Verlag, Berlin, Heidelberg, New York.
Hearman, R. F. S. (1979). The third- and higher-order elastic constants. *In* "Landolt Boernstein, New Series" (K.-H. Hellwege, ed.), pp. 245–286. Springer-Verlag, Berlin, Heidelberg, New York.

Hellwig, H. (1974). Areas of promise for the development of future primary frequency standards. *In* "Time and Frequency: Theory and Fundamentals" (B. E. Blair, ed.), pp. 125–136. Natl. Bur. Stand. Monogr. 140.
Hellwig, H., and Halford, D. (1974). Accurate frequency measurements: Relevance to some other areas of metrology. *In* "Time and Frequency: Theory and Fundamentals" (B. E. Blair, ed.), pp. 137–149. Natl. Bur. Stand. Monogr. 140.
Henaff, J. (1980). Applications of surface-acoustic-wave devices in satellite communication systems. *Proc. 10th European Microwave Conf.*, pp. 202–207.
Holland, M. G., and Claiborne, L. T. (1974). Practical surface acoustic wave devices. *Proc. IEEE* **62**, 582–611.
Inamura, T., and Yoshikawa, S. (1976). Applications of surface acoustic wave devices. *Oyo Buturi* **45**, 718–728. In Japanese.
Ivanek, F. (1979). New developments in frequency control for microwave communications. *3rd World Telecommunication Forum. Pt. II (Switzerland: Telecommunication Union)*, p. 1.3.3/1–8.
Joshi, N. K., and Singh, A. (1978). Surface acoustic wave devices in electronic warfare. *Def. Sci. J.* **27**, 157–162.
Kartaschoff, P. (1977). Frequency control and timing requirements for communication. *Proc. 31st Annu. Freq. Control Symp.*, pp. 478–483.
Kentley, E. (1972). The practical aspects of international standardization in the frequency control field. *Proc. 26th Annu. Freq. Control Symp.*, pp. 159–163.
Kino, Y., Nakayama, Y., Furuya, N., Watanabe, Y., Aihara, Y., and Inaba, R. (1976). Application for surface acoustic waves. *Natl. Tech. Rep. (Japan)* **22**, 644–650. In Japanese.
Kinsman, R., and Gunn, D. (1981). Frequency control requirements for 800 MHz mobile communication. *Proc. 35th Annu. Freq. Control Symp.*, pp. 501–510.
Kurokawa, S. (1978). Japan's quartz crystal industry sees international cooperation as its panacea. *JEE J. Electron. Eng.* (144), 28–30.
Lagasse, P. E. (1980). State of the art in design and technology of SAW devices. *Electrocompon. Sci. Technol.* **6**, 199–204.
Langer, E. (1979). The piezoelectric effect and its applications. A simple tutorial on the physics and techniques for piezoelectric devices. IV. *Nachr. Elektron.* **33**, 237–238. In German.
Langer, E. (1979). The piezoelectric effect and its applications. V. *Nachr. Elektron.* **33**, 273–274. In German.
Lawrence, M. W. (1975). Surface acoustic waves and their applications. *Aust. Electron. Eng.* **8**, 19–22.
Lawrence, W. D. (1972). Frequency control requirements for remote sensor systems. *Proc. 26th Annu. Freq. Control Symp.*, pp. 113–119.
Lemanov, V. V., and Ilisavsky, Yu. V. (1982). Piezoelectricity and acoustoelectronics. *Ferroelectrics* **42**, 77–101.
Lubimov, L. A., and Zhoukina, L. I. (1975). Piezoelectric devices. *Eltek. Aktuell Elektron.* **18**, 59–61.
Lubimov, L. A., and Zhourkina, L. I. (1975). Piezoelectric devices. *IEC Bull* **9**, 1–2.
Lundbom, P.-O. (1974). On the activities of URSI Commission I [for radio measurements and standards] during the last 20 years and plans for the future. *CPEM Digest: Conference on Precision Electromagnetic Measurements (London: IEE)*, p. 330.
Maines, J. D. (1977). Surface wave devices for radar equipment. *In* "Surface Wave Filters" (H. Matthews, ed.), pp. 443–476. Wiley, Chichester, England.
Maines, J. D., and Paige, E. G. S. (1976). Surface acoustic-wave devices for signal processing applications. *Proc. IEEE* **64**, 639–652.

Mason, W. P. (1964). Use of piezoelectric crystals and mechanical resonators in filters and oscillators. *In* "Physical Acoustics," vol. 1, Part A (W. P. Mason, ed.), pp. 336–417. Academic Press, New York.

Mason, W. P. (1975). Professor Walter G. Cady's contributions to piezoelectricity and what followed from them. *J. Acoust. Soc. Am.* **58**, 301–309.

Mason, W. P. (1981). Piezoelectricity, its history and applications. *J. Acoust. Soc. Am.* **70**, 1561–1566.

McDermott, J. (1973). Focus on piezoelectric crystals and devices. *Electron. Des.* **21**, 44–54.

McQuiddy, D. N., Jr. (1981). Frequency stability requirements for a 95 GHz instrumentation radar system. *Proc. 35th Annu. Freq. Control Symp.*, pp. 516–524.

Mockler, R. C. (1961). Atomic beam frequency standards. *In* "Advances in Electronics and Electron Physics," vol. 15, pp. 1–71. Academic Press, New York.

Nekrasov, M. M., Lavrinenko, V. V., Bozhko, A. A., Kartashev, I. A., Koval, V. S., Miroshinchenko, A. P., and Yakimenko, Yu. I. (1971). Elements of piezo-electronics and prospects of application in electrical engineering. *Elec. Technol. USSR* **4**, 134–135.

Nunamaker, R. J. (1971). Frequency control devices for mobile communications. *Proc. 25th Annu. Freq. Control Symp.*, p. 74.

Nyffeler, F. (1982). High-performance signal processing using SAW components. *Bull. Assoc. Suisse Electr.* **73**, 883–888. In German.

Ohnuki, A. (1977). Quartz crystal units for CB transceivers. *JEE J. Electron. Eng.* (121), 45–49.

Paige, E. G. S. (1971). Acoustic surface waves and their applications in electronics. *Proc. 7th International Congress on Acoustics* (*Hungary: Akademiai Kiado*), pp. 141–151.

Pajewski, W. (1971). Development in research and technology of piezoelectric elements. *Elektronika* (1), 25–34. In Polish.

Pajewski, W. (1973). Piezoelectronics and acoustoelectronics. *Elektronika* (1–2), 50–54. In Polish.

Redwood, M. (1980). Piezoelectric devices in electronics. *Phys. Educ.* **15**, 9–14.

Risley, A. S. (1974). The physical basis of atomic frequency standards. *In* "Time and Frequency: Theory and Fundamentals" (B. E. Blair, ed.), pp. 65–84. Natl. Bur. Stand. Monogr. 140.

Robrock, R. B. (1971). Quartz crystal applications in digital transmission. *Proc. 25th Annu. Freq. Control Symp.*, pp. 70–73.

Sabine, H., and Cole, P. H. (1971). Acoustic surface wave devices: a survey. *Proc. Inst. Radio Electron. Eng. Aust.* **32**, A12.

Sabine, H., and Cole, P. H. (1971). Acoustic surface wave devices: a survey. *Proc. Inst. Radio Electron. Eng. Aust.* **32**, 445–458.

Schmidt, L. (1970). The piezoelectric effect and its application to modern technology. *VOE Fachber.* **26**, 139–143.

Schmidt, L. (1970). The piezoelectric effect and its application in the modern technology. *Messen U. Prufen* **6**, 811–816. In German.

Shaw, H. J. (1971). An overview of surface-wave methods and devices. *81st Meeting of the Acoustical Society of America*, p. 29.

Shibayama, K. (1982). SAW materials and devices in Japan. *Ferroelectrics* **42**, 153–159.

Stevenson, S. A. (1969). Developments in the application of synthetic quartz. *Electronic Compon.* **10**, 1465–1466.

Stone, R. R., Jr., Phillips, D. H., and Berg, W. B. Jr. (1971). Technology forecasts: frequency and time. *Digest of Technical Papers of IEEE Region 2 Conference on Technology Forecasting and Assessment of Electrotechnology* (*New York: IEEE*), pp. 54–55.

Szlavy, A. (1980). Quartz crystals in electronics. II. *Finommech. Mikrotech.* **19**, 172–180. In Hungarian.

Tanaka, T. (1973). Recent developments and promising applications of piezo-resonators. *JEE J. Electron. Eng.* (80), 58–60, 62.

Tanaka, T. (1982). Piezoelectric devices in Japan. *Ferroelectrics* **40**, 167–187.

Tiesler, G. (1979). Quartz crystals for microprocessors. *Components Rep.* **14**, 91–93.

Warashina, N. (1978). Crystal oscillators and units improve frequencies for measuring instruments. JEE (144), 44–47.

White, R. M. (1970). Surface elastic waves. *Proc. IEEE* **58**, 1238–1276.

Wiefelsputz, F. G. (1978). Frequency control in radiocommunications. *Telecommun. J.* (*Engl. Ed.*) **45**, 395–402.

Williamson, R. C. (1978). Case studies of successful surface-acoustic-wave devices. *Ultrason. Symp. Proc.*, pp. 460–468.

Yakovkin, I., and Kohler, E. (1975). Components based on elastic surface waves. *Nachrichtentech. Elektron.* **25**, 186–189. In German.

Zelenka, J. (1980). The centennial of discovering piezoelectricity. *Slaboproudy Obz.* **41**, 237–244. In Czech.

CHAPTER BIBLIOGRAPHIES

Chapter 7

Adams, C., Kusters, J., and Benjaminson, A. (1968). Measurement techniques for quartz crystals. *Proc. 22nd Annu. Freq. Control Symp.*, pp. 248–258.

Akhtar, M. S. (1971). Piezoelectricity with special reference to piezoelectric analogous relationships, design and development of testing and measuring methods. *Nucleus* (*Karachi*) **8**, 53–58.

Allenstein, K. (1978). Measuring procedures for quartz crystal parameters. *Tech. Mess. ATM* **45**, 49–55.

Aubry, J. P., Gerard, E., and Lechopier, S. (1983). S.Y. parameters method for accurate measurement of bulk wave crystal resonators at frequencies up to 2 GHz. *Proc. 37th Annu. Freq. Control Symp.*, pp. 306–316.

Awender, H., and Sann, K. (1954). Classification of quartz oscillator circuits. *Funk Ton* **8**, 202–214, 253–265. In German.

Azovtsev, V. P., Golsnoi, O. V., Evitkhiev, N. N., Zakharov, V. P., Kukhtevich, V. I., Snezhko, Yu. A., and Chuiko, V. A. (1980). Use of a laser interferometer in the measurements of quartz resonator parameters. *Sov. J. Quantum. Electron.* **10**, 902–904.

Bahadur, H., and Parshad, R. (1977a). New method of detection of weak anharmonic modes of a quartz crystal and its applications for generating multicrystal resonance frequencies. *J. Appl. Phys.* **48**, 3141–3143.

Bahadur, H., and Parshad, R. (1977b). A new method for determination of the frequency spectrum of a quartz crystal and its applications for generation of a number of precise frequencies and time intervals. *Eur. Conf. Precise Electrical Measurement*, pp. 79–82.

Bahadur, H., and Parshad, R. (1978). A new method for determination of the frequency spectrum of a quartz crystal and its applications. *IEEE Trans. Sonics Ultrason.* **SU-25**, 24–29.

Ballato, A. (1970). Resonance in piezoelectric vibrators. *Proc. IEEE* **58**, 149–151.

Ballato, A. (1972). Transmission-line analogs for stacked piezoelectric crystal devices. *Proc. 26th Annu. Freq. Control. Symp.*, pp. 86–91.

Ballato, A. (1977). Doubly rotated thickness mode plate vibrators. *In* "Physical Acoustics," vol. XIII (W. P. Mason and R. N. Thurston, eds.), pp. 115–181. Academic Press, New York.

Ballato, A. (1978). Frequency–temperature–load capacitance behavior of resonators for TCXO application. *IEEE Trans. Sonics Ultrason.* **SU-25**, 185–191.

Ballato, A., and Oliva, G. R., Jr. (1970). Admittance bridge determination of quartz vibrator parameters using augmenting immittance elements. *IEEE Trans. Instrum. Meas.* **IM-19**, 127–134.

Ballato, A., and Tilton, R. (1977). Ovenless activity dip tester. *Proc. 31st Annu. Freq. Control Symp.*, pp. 102–107.

Ballato, A., and Tilton, R. (1978). Electronic activity dip measurement. *IEEE Trans. Instrum. Meas.* **IM-27**, 59–65.

Ballato, A., and Vig, J. R. (1978). Static and dynamic frequency–temperature behavior of singly and doubly rotated, oven-controlled quartz resonators. *Proc. 32nd Annu. Freq. Control Symp.*, pp. 180–188.

Barnes, J. A. (1970). Frequency measurement errors of passive resonators caused by frequency modulated exciting signals. *IEEE Trans. Instrum. Meas.* **IM-19**, 147–152.

Beaver, W. D., Van Loben Sels, W. E., and Wang, M. (1979). Quartz crystal measurements by a "phase–amplitude" method. *Proc. 33rd Annu. Freq. Control Symp.*, pp. 189–200.

Beetley, D. E., Blitch, B. R., and Snowden, T. M. (1981). The quartz resonator automatic aging measurement facility. *Proc. 35th Annu. Freq. Control Symp.*, pp. 263–270.

Beige, H., and Schmidt, G. (1982). Electromechanical resonances for investigating linear and nonlinear properties of dielectrics. *Ferroelectrics* **41**, 39–49.

Belostotskii, M. B., and Red'ko, Yu. P. (1977). Determination of the equivalent dynamic characteristics of a frequency measuring filter element. *Avtometriya* (4), 95–98. In Russian.

Bernstein, M. (1967). Increased crystal unit resistance at oscillator noise levels. *Proc. 21st Annu. Freq. Control Symp.*, 244–258.

Besson, R., and Decailliot, M. (1979). Application of sideband modulation oscillators for measurement of quartz resonators stability. *C.R. Hebd. Seances Acad. Sci., Ser. B.* **288**, 57–60. In French.

Bistline, G., and Pompeo, R. (1968). Temperature testing quartz crystals, equipment and methods. *Proc. 22nd Annu. Freq. Control Symp.*, p. 163.

Bloch, M. B., Meirs, M. P., and Strauss, A. (1978). Results of temperature slewing quartz crystals for anomalous responses. *Proc. 32nd Annu. Freq. Control Symp.*, pp. 344–353.

Boemmel, H. E., and Dransfeld, K. (1960). Excitation and attenuation of hypersonic waves in quartz. *Phys. Rev.* **117**, 1245–1252.

Bottom, V. E. (1982). "Introduction to Quartz Crystal Unit Design." Van Nostrand-Reinhold, New York.

Bryan, P. (1975). A rapid and simple in-process test method designed to improve quality of quartz resonators in current demand. *Proc. 29th Annu. Freq. Control Symp.*, pp. 237–239.

Butterworth, S. (1915). On electrically maintained vibrations. *Proc. Phys. Soc. London* **27**, 410–424.

Button, J. M. (1981). Measuring series resonance e.s.r. of a crystal. *Electron. Prod. Des. (GB)* **2**, 25.

Cady, W. G. (1964). "Piezoelectricity." Dover, New York.

Cole, R. H. (1983). Bridge sampling methods for admittance measurements from 500 kHz to 5 GHz. *IEEE Trans. Instrum. Meas.* **IM-32**, 42–47.

Darymov, V. I., Koshelev, F. P., Krivobokov, V. P., and Kurin, M. N. (1978). Method of determining the thickness of the broken layer on the surface of quartz. *Ind. Lab.* **44**, 355–356.

Essler, R. (1968a). On the dynamic measurement of equivalent circuit parameters of piezoelectric filter elements. *Nachrichtentechnik* **18**, 127–130. In German.

Essler, R. (1968b). Some problems of the dynamic measurement of equivalent circuit values of piezo-electric resonators. *Wiss. Z. Electrotech.* **11**, 1–15.

Euler, F., and Yannoni, N. F. (1981). Frequency retrace of quartz oscillators. *Proc. 35th Annu. Freq. Control Symp.*, pp. 492–500.

Feigen, I., Mackeen, D., and Fine, S. (1969). A method for detecting and measuring frequency of surface vibrations using a helium–neon laser. *Rev. Sci. Instrum.* **40**, 381–382.

Fiok, A. (1971). Measuring accuracy of the dynamic capacitance of quartz oscillators. *Elektronika* (3), 114–119. In Polish.

Fiok, A. (1979). Transmission method of quartz crystal units measurement by zero-phase techniques. *Pr. Inst. Tele. Radiotech.* (73), 13–24. In Polish.

Fiok, A. J. (1980). Method for automated measurement of HF quartz crystal unit frequency and resistance. *CPEM Dig. 1980*, pp. 336–342.

Fischer, H. (1977). Some results of frequency response measurements of 1 MHz precision quartzes. *Nachrichtentech. Elektron.* **27**, 154–155.

Fischer, R., and Schulzke, L. (1977). Extending the frequency range of the transmission line method for the measurement of quartz crystals up to 250 MHz. *Proc. 31st Annu. Freq. Control Symp.*, pp. 96–101.

Forster, H. J. (1977). Automatic recording of the frequency–temperature response of quartz crystals. *Frequenz* **31**, 375–381.

Franx, C. (1969). On precision measurements of frequency and resistance of quartz crystal units. *Proc. 23rd Annu. Freq. Control Symp.*, pp. 102–110.

Frerking, M. E. (1969). Vector voltmeter crystal measurement system. *Proc. 23rd Annu. Freq. Control Symp.*, pp. 93–101.

Fukada, E. (1972). An apparatus for piezo-electrical measurements. *JEE J. Electron. Eng.* (68), 24–30.

Gagnepain, J.-J. (1981). Nonlinear properties of quartz crystal resonators: a review. *Proc. 35th Annu. Freq. Control Symp.*, pp. 14–30.

Ganea, S. (1974). Quartz resonator parameters: measurement methods and equipment. *Autom. Electron. (Rumania)* **18**, 93–104.

Gerber, E. A., and Koerner, L. F. (1958). Methods of measurement of the parameters of piezoelectric vibrators. *Proc. IRE* **46**, 1731–1737.

Gerdes, R. J., and Wagner, C. E. (1971). Study of frequency control devices in the scanning electron microscope. *Proc. 25th Annu. Freq. Control Symp.*, p. 24.

Gibert, G., Broussou, S., and Morel, J. (1973). Quartz crystal units for space applications. *Proc. 27th Annu. Freq. Control Symp.*, pp. 39–41.

Godwin, P. F., Jr. (1977). Test techniques useful in identifying sources of discontinuous behavior in quartz crystal oscillators and crystal filters. *ATFA 1977 (IEEE)*, pp. 178–197.

Godwin, P. F., Jr., and Snider, G. L. (1977). Methods for production screening for anomalous responses in quartz crystals intended for high reliability applications. *Proc. 31st Annu. Freq. Control Symp.*, pp. 78–95.

Grachev, V. G., and Prozorov, V. A. (1976). A quartz filter spectrum analyzer. *Izv. Vyssh. Uchebn. Zaved., Radiofiz.* **19**, 1740–1744. In Russian.

Grenier, R. P. (1968). Technique for crystal resonance measurements based on phase detection in a transmission type measurement system. *Proc. 22nd Annu. Freq. Control Symp.*, pp. 259–268.

Grenier, R. P. (1970). Crystal resonance frequency measurement by phase detection. *W. Elec. Eng.* **14**, 15–19.

Grigor'ev, V. N. (1975). Instrument for measuring the parameters of quartz resonators. *Prib. Sist. Upr.* (9), 43–44. In Russian.

Grzeszykowski, M. (1978). Quartz resonator parameters wide band active meter. *Pr. Inst. Tele. Radiotech.* (77), 69–73. In Polish.

Guttwein, G. K., Ballato, A., and Lukaszek, T. J. (1968). Design considerations for oscillator crystals. *Proc. 22nd Annu. Freq. Control Symp.*, pp. 67–88.

Hafner, E. (1964). "Analysis and Design of Crystal Oscillators." Technical Report ECOM-2474, U.S. Army Electronics Research and Development Command, Fort Monmouth, New Jersey. Available from the National Technical Information Service, Springfield, Virginia, AD No. 611200.

Hafner, E. (1969). The piezoelectric crystal unit—definitions and methods of measurement. *Proc. IEEE* **57**, 179–201.

Hafner, E. (1974). Crystal resonators. *IEEE Trans. Sonics Ultrason.* **SU-21**, 220–237.

Hafner, E. (1978). Phase lock loop controlled offset local oscillator system. U.S. Patent No. 4,118,673.

Hafner, E., Ballato, A., and Blomster, P. (1970). Quartz crystal measurements. *Proc. 24th Annu. Freq. Control Symp.*, pp. 177–190.

Hafner, E., and Riley, W. J. (1976). Implementation of bridge measurement techniques for quartz crystal parameters. *Proc. 30th Annu. Freq. Control Symp.*, pp. 92–102.

Hammond, D. L., Adams, C. A., and Benjaminson, A. (1968). Hysteresis effects in quartz resonators. *Proc. 22nd Annu. Freq. Control Symp.*, pp. 55–66.

Hartemann, P., Rouvaen, J., Torguet, R., Bridoux, E., and Bruneel, C. (1976). Laser probing of a surface-acoustic-wave resonator. *Electron. Lett.* **12**, 176–177.

Healey, D. J., III, Hahn, H., and Powell, S. (1983). A measurement technique for determination of frequency vs acceleration characteristics of quartz crystal units. *Proc. 37th Annu. Freq. Control Symp.*, pp. 284–289.

Heising, R. A., ed. (1946). "Quartz Crystals for Electrical Circuits." D. Van Nostrand Co., Inc. (Reprinted in 1978 by the Electronic Industries Association, 2001 Eye Street, N. W., Washington, D.C.)

Hewlett-Packard (1976). Digital network and spectrum analysis primer. Hewlett-Packard Application Note No. 216, Palo Alto, California.

Hirose, Y., Tsuziki, Y., and Iijima, K. (1970). Measurement of contour vibrations of quartz plates by holographic technique. *Electron. Commun. Jpn.* **53**, 49–54.

Holland, R. (1967). Representation of dielectric, elastic, and piezoelectric losses by complex coefficients. *IEEE Trans. Sonics Ultrason.* **SU-14**, 18–20.

Holland, R., and EerNisse, E. P. (1969). Accurate method for measuring piezoelectric coefficients. *IEEE Trans. Sonics Ultrason.* **SU-16**, 21.

Horton, W. H., and Boor, S. B. (1965). Comparison of crystal measurement equipment. *Proc. 19th Annu. Freq. Control Symp.*, pp. 436–468.

Horton, W. H., and Smythe, R. C. (1983a). A new frequency for piezoelectric resonator measurement. *Proc. 37th Annu. Freq. Control Symp.*, pp. 297–299.

Horton, W. H., and Smythe, R. C. (1983b). A new frequency for piezoelectric resonator measurement. *Proc. IEEE* **71**, 280–282.

Horton, W. H., Payne, T. S., Smythe, R. C., and Symonds, D. A. (1981). Comparison of methods for measurement of quartz crystal resonators with load capacitance. *Proc. 35th Annu. Freq. Control Symp.*, pp. 271–279.

Howe, D. A. (1981). Properties of signal sources and measurement methods. *Proc. 35th Annu. Freq. Control Symp.*, pp. A1–A47.

Huchital, G. S., and Tomanic, J. P. (1980). Phase linearity of RF mixers. *IEEE Trans. Instrum. Meas.* **IM-29**, 477–479.

Hughes, S. J., Parfitt, R. W., and Hardy, J. S. (1978). The measurement of load resonance characteristics of quartz crystals using the zero phase pi-network. *Proc. 32nd Annu. Freq. Control Symp.*, pp. 337–343.

Ichino, T., Ohkawara, H., and Sugihara, N. (1980). Vector impedance analysis to 1000 MHz. *Hewlett-Packard J.* **31**, 22–32.

IEC (1962). "Guide to the Use of Quartz Oscillator Crystals." International Electrotechnical Commission Publication 122-2, Section 3, including Amendment 1 (1969), Geneva, Switzerland.

IEC (1973). "Basic Method for the Measurement of Resonance Frequency and Equivalent Series Resistance of Quartz Crystal Units by Zero Phase Technique in a Pi-Network." International Electrotechnical Commission Publication 444, 1st ed., Geneva, Switzerland.

IEEE (1966). "Standard Definitions and Methods of Measurement for Piezoelectric Vibrators." IEEE Standard No. 177, May 1966, IEEE, New York.

IEEE (1977). "IEEE Standard Dictionary of Electrical and Electronics Terms," 2nd ed. (F. Jay, ed.). ANSI/IEEE Standard 100-1977, IEEE, New York.

IEEE (1978). "Standard on Piezoelectricity." IEEE Standard No. 176, September 1978, IEEE, New York.

Iijima, K., Tsuzuki, Y., Hirose, Y., and Akiyama, M. (1976). Laser interferometric measurement of vibration displacements of a plano-convex AT-cut quartz crystal resonator. *Proc. 30th Annu. Freq. Control Symp.*, pp. 65–70.

Ikeda, T. (1974). Errors and corrections in the determinations of piezoelectric parameters by the resonance–antiresonance method. *J. Acoust. Soc. Jpn.* **30**, 5–13.

Knowles, J. E. (1975). On the origin of the second level of drive effect in quartz oscillators. *Proc. 29th Annu. Freq. Control Symp.*, pp. 230–236.

Koga, I. (1970). Precision measurement of crystal frequency by "center-line method". *Electron. Commun. Jpn.* **53**, 1–8.

Koga, I. (1974). Precision determination of parameters of V.H.F. crystals. *Proc. 28th Annu. Freq. Control Symp.*, pp. 49–56.

Koga, M., and Okamoto, Y. (1980). Latent vibration of quartz oscillation. *KDD Tech. J. (Japan)* (106), 397–402. In Japanese.

Kollmann, M. (1976). Measuring the parameters of piezocrystal units on a polyscope. *Sdelovaci Tech.* **24**, 83–85. In Czech.

Kraus, P., and Steffen, R. (1981). Measuring crystal equivalent-circuit parameters. *News Rohde & Schwarz (Germany)* **21**, 26–29.

Ksiazek, J., and Smolarski, A. (1971). Bridge circuit for measurement of parasitic resonances of crystal quartz. *Pr. Inst. Tele. Radiotech.* **15**, 71–76. In Polish.

Lamb, J., and Richter, J. (1966). Anisotropic acoustic attenuation with new measurements for quartz at room temperature. *Proc. Roy. Soc. London, Ser. A* **293**, 479–492.

Layden, O. P., Ballato, A., and Shibla, C. (1968). Newly developed crystal measurement instruments. *Proc. 22nd Annu. Freq. Control Symp.*, pp. 282–297.

Layden, O. P., Ballato, A. D., and Shibla, C. L. (1970). Crystal parameter measurement. *Instrum. Control Syst.* **43**, 67–71.

Linzer, M., and Stockelsberry, D. P. (1973). A frequency lock method for the measurement of Q factors of reflection and transmission resonators. *IEEE Trans. Instrum. Meas.* **IM-22**, 61–77.

Malinowski, G., and Hafner, E. (1978). Automatic microcircuit bridge for measurements on quartz crystal units. *Proc. 32nd Annu. Freq. Control Symp.*, pp. 354–364.

Malinowski, G., Snider, G. L., and Nyholm, C. (1981). Implementation of an automatic microcircuit bridge measuring system for quartz crystals. *Proc. 35th Annu. Freq. Control Symp.*, pp. 286–290.

Marshall, F. G. (1969). Equivalent circuit for the acoustoelectric oscillator. *Electron. Lett.* **5**, 581–582.

Martin, G. E. (1954). Determination of equivalent-circuit constants of piezoelectric resonators of moderately low Q by absolute admittance measurements. *J. Acoust. Soc. Am.* **26**, 413–420.

Masiani, G., and Zanardi, F. (1977). RC bridge transmission method for measurement of unwanted resonances in piezoelectric crystals. *Alta Freq.* **46**, 582–591. In Italian.

Mason, W. P. (1942). "Electromechanical Transducers and Wave Filters." Van Nostrand, New York.

Mason, W. P. (1950). "Piezoelectric Crystals and Their Application to Ultrasonics." D. Van Nostrand Co., Inc., New York.

McDermott, J. (1973). Focus on piezoelectric crystals and devices. *Electron. Des.* **21**, 44–54.

McKeown, D. (1958). Design parameters for VHF crystal units. *Proc. 12th Annu. Freq. Control Symp.*, pp. 317–333.

Meeker, T. R. (1972). Thickness mode piezoelectric transducers. *Ultrasonics* **10**, 26–36.

Meeker, T. R. (1979). A review of the new IEEE standard on piezoelectricity. *Proc. 33rd Annu. Freq. Control Symp.*, pp. 176–180.

Mel'kanovich, A. F., and Perlatov, V. G. (1978). Measuring the parameters of piezoelectric materials and cells. *Sov. J. Nondestr. Test. (Engl. Transl.)* **13**, 384–389.

Merigoux, H. (1974). Progress in checking quartz crystals. *Microtecnic* **28**, 31. In French.

Metcalf, W. S. (1973). Practical crystal measurements and standardisation. *Proc. 27th Annu. Freq. Control Symp.*, pp. 55–62.

Metcalf, W. S. (1975). Crystal measurement and standardisation. *Electron.* (68), 61–63.

Michaelis, M. (1977). Test equipment for quartz oscillators and filters. *Funkschau (Germany)* **49**, 810. In German.

Morse, P. M., and Feshbach, H. (1953). "Methods of Theoretical Physics." McGraw-Hill, New York.

Murashov, B. P., and Tsvetkov, Yu. P. (1976). Instrument for checking quartz-crystal oscillators with standard frequency signals in the long-wave and very-long-wave ranges. *Meas. Tech. (Engl. Transl.)* **19**, 1012–1015.

Nakajima, Y., and Nagata, T. (1977). Method for measuring frequency response of unplated piezoelectric ceramic plate and its application. *Trans. Inst. Electron. Commun. Eng. Jpn. [Part] E* **60**, 325.

Nakazawa, M., Lukaszek, T., and Ballato, A. (1981). Force- and acceleration-frequency effects in grooved and ring-supported resonators. *Proc. 35th Annu. Freq. Control Symp.*, pp. 71–91.

Nelson, D. W. (1969). Another look at specifying a crystal. *Proc. 23rd Annu. Freq. Control Symp.*, pp. 111–121.

Nelson, G. E. (1972). Calculator controlled testing of crystals and crystal filters. *Proc. 26th Annu. Freq. Control Symp.*, pp. 79–83.

Nelson, G. E., and Ricci, D. W. (1972). Faster gain–phase measurement with new automatic 50 Hz-to-13 MHz network analyzers. *Hewlett-Packard J.* **23**, 12–20.

Nier, E. (1976). Piezoelectric measuring equipment. *Meres Autom.* **24**, 210–217.

Oliva, G. R., Jr., and Ballato, A. (1969). "Quartz Vibrator Parameter Determination by Parallel Bridge Methods." Report ECOM 3121, Army Electronics Command, Ft. Monmouth, New Jersey, 55 pp. Available from the National Technical Information Service, Springfield, Virginia, AD No. 697110.

Orekhov, Yu. F., and Borovik-Romanov, A. A. (1979). Self-excited oscillator for examining a multimode piezoelectric resonator. *Instrum. Exp. Tech. (Engl. Transl.)* **22**, 1453–1454.

Pacuraru, I., and Toderean, G. (1977). Digital Q-meter for quartz. *Electroteh. Electron. Autom. Electroteh.* **25**, 281–284.

Panigati, R., and Stacchiotti, G. (1975). An automatic system for a quartz characterization both at fundamental and unwanted modes. *Alta Freq.* **44**, 405–411. In Italian.

Peach, R. C., Dyer, A. J., Byrne, A. J., and Doherty, S. P. (1982). New method for the measurement of quartz crystal resonator parameters. *Proc. 36th Annu. Freq. Control Symp.*, pp. 297–301.

Pegeot, C., and Gagnepain, J.-J. (1977). Quartz crystal parameters measurement system. *IEEE Trans. Instrum. Meas.* **IM-26**, 300–304.

Podgorski, A., Smolarski, A., and Wojcicki, M. (1979). Production measurements of temperature characteristics of quartz crystal resonators. [ATE]. *Pr. Inst. Tele. Radiotech.* (83), 15–25. In Polish.

Pompeo, R., and Wolf, F. (1969). Temperature run, MIL-C-3098, amendment I. *Proc. 23rd Annu. Freq. Control Symp.*, pp. 122–127.

Preobrazhenskii, N. S., and Il'in, V. K. (1976). Method of determining quality of piezoelectrics. *Ind. Lab.* **42**, 1421–1423.

Preobrazhenskii, N. S., and Il'in, V. K. (1977). Apparatus for determining axes of highest piezoelectric activity. *Ind. Lab.* **42**, 732–733.

Prichard, A. C., and Bernstein, M. (1954). Crystal impedance meters replace test sets. *Electronics* (May), 176–180.

Pustarfi, H. S., and Smith, W. L. (1973). An automatic crystal measurement system. *Proc. 27th Annu. Freq. Control Symp.*, pp. 63–72.

Ramadan, B., and Kos, J. F. (1978). "Crystal bridge" for measuring the equivalent electrical parameters of piezoelectric crystals. *Rev. Sci. Instrum.* **49**, 374–377.

Ridley, A. T. (1974). Measuring techniques in the production of quartz crystal components. *Radio Mentor Electron.* **40**, 359–361. In German.

Roberts, G. E. (1979). A four-frequency process for accurately measuring coupled-dual resonator crystals. *Proc. 33rd Annu. Freq. Control Symp.*, pp. 159–165.

Saul, R. P., and Bauer, C. L. (1967). Simplified bridge system for measurement of internal friction and fractional variations of Young's modulus at kilohertz frequencies. *Rev. Sci. Instrum.* **38**, 1449–1451.

Schade, R. W. (1968). Reliable and repeatable measurements of frequency and resistance changes of quartz crystals due to wide temperature variations. *Proc. 22nd Annu. Freq. Control Symp.*, pp. 164–167.

Schwarz, R. B. (1977). Simple system using one-crystal composite oscillator for internal friction and modulus measurements [in temperature range 1.7 to 300 K]. *Rev. Sci. Instrum.* **48**, 111–115.

Sedra, R. N., and Hanna, F. F. (1965). Various methods for the detection of harmonic vibrations of a quartz crystal. *Proc. Math. Phys. Soc. UAR* (29), 67–72.

Sherman, J. H., Jr. (1978). Comments on "a new method for determination of the frequency spectrum of a quartz crystal and its application." *IEEE Trans. Sonics Ultrason.* **SU-25**, 226.

Sherman, J. H., Jr. (1979). Trim sensitivity—a useful characterization of a resonator. *Proc. 33rd Annu. Freq. Control Symp.*, pp. 181–185.

Shevel'ko, M. M., and Yakovlev, L. A. (1977). Precision measurements of the elastic characteristics of synthetic piezoelectric quartz. *Sov. Phys.—Acoust. (Engl. Transl.)* **23**, 187–188.

Sinha, B. K., and Tiersten, H. F. (1980). Transient thermally induced frequency excursions in doubly-rotated quartz thickness-mode resonators. *Proc. 34th Annu. Freq. Control Symp.*, pp. 393–402.

Skripnik, Yu. A., Kuz'min, Yu. P., and Pavlov, V. K. (1975). Stabilising the power dissipated by quartz resonators during the measurement of their parameters. *Priborostroenie (Moscow)* (17), 35–41. In Russian.

Sladky, P. (1975). Apparatus for the measurements of internal friction by means of the composite oscillator technique. *Cesk. Cas. Fys. A.* **25**, 589–595.

Smolarski, A. J., and Wojcicki, M. S. (1977). Quartz crystal units measurement method with T-network. *Elektronika (Poland)* **18**, 281–285. In Polish.

Smolarski, A., and Wojcicki, M. (1978). Quartz resonators series resonance frequency direct measuring method. *Pr. Inst. Tele. Radiotech.* (77), 55–59. In Polish.

Smythe, R. C. (1981). An automated resonator measurement system using a reflection coefficient bridge. *Proc. 35th Annu. Freq. Control Symp.*, pp. 280–285.

Smythe, R. C., and Horton, W. H. (1983). Evaluation of crystal measurement systems. *Proc. 37th Annu. Freq. Control Symp.*, pp. 290–296.

Solc, I. (1971). The possibility of determining the resonant frequencies of piezoelectric crystal cuts by the method of double excitation. *Cesk. Cas. Fys. A.* **21**, 26–28. In Czech.

Spain, C. (1977). Measuring equivalent series resistance of crystals. *New Electron.* **10**, 42.

Srinivasan, P., and Chopra, O. K. (1969). Determination of resonant frequencies and mode shapes of vibrating plates by the use of solid CO_2 exciter. *Indian J. Pure Appl. Phys.* **7**, 256–258.

Stein, S., Glaze, D., Levine, J., Gray, J., Hilliard, D., and Howe, D. (1982). Performance of an automated high accuracy phase measurement system. *Proc. 36th Annu. Freq. Control Symp.*, pp. 314–320.

Stevenson, J. K., and Redwood, M. (1969). The motional reactance of a piezoelectric resonator—a more accurate and simpler representation for use in filter design. *IEEE Trans. Circuit Theory* **CT-16**, 568–572.

Stickland, W. J. (1968). Techniques for the measurement of quartz crystal parameters. *Marconi Instrum.* **11**, 2–5.

Stone, C. S., and Baltzer, O. J. (1982). A frequency domain reflectometer for quartz resonator investigations. *Proc. 36th Annu. Freq. Control Symp.*, pp. 321–326.

Swanson, T. W. (1978). Crystal filter AM–PM conversion measurements. *Proc. 32nd Annu. Freq. Control Symp.*, pp. 250–254.

Toki, M., and Tsuzuki, Y. (1976). Precise determination of equivalent circuit parameters of a quartz crystal unit. *Trans. Inst. Electron. Commun. Eng. Jpn. [Part] E* **59**, 24–25.

Toki, M., Tsuzuki, Y., and Kawano, O. (1979). Precise measurement of equivalent circuit parameters of ceramic resonators. *Trans. Inst. Electron. Commun. Eng. Jpn. [Part] E* **62**, 552–553.

Toki, M., Tsuzuki, Y., and Kawano, O. (1980). A new equivalent circuit for piezoelectric disc resonators. *Proc. 34th Annu. Freq. Control Symp.*, pp. 58–64.

Toki, M., Tsuzuki, Y., and Mitsuoka, T. (1983). Measuring method of equivalent series capacitance and negative resistance of quartz crystal oscillator circuits. *Proc. 37th Annu. Freq. Control Symp.*, pp. 300–305.

Tomikawa, Y. (1977). Finite element method and its application to analysis of equivalent circuit elements of piezo-tuning fork. *J. Inst. Telev. Eng. Jpn.* **31**, 457–466.

Tsuzuki, Y., and Toki, M. (1976). Precise determination of equivalent circuit parameters of quartz crystal resonators. *Proc. IEEE* **64**, 1149–1150.

Tsuzuki, Y., Hirose, Y., and Iijima, K. (1971). Measurement of vibrational modes of piezoelectric resonators by means of holography. *Proc. 25th Annu. Freq. Control Symp.*, pp. 113–117.

Tsuzuki, Y., Toki, M., Adachi, T., and Yanagi, H. (1979). Automatic measurement of parameters of VHF quartz crystal resonators. *Proc. 33rd Annu. Freq. Control Symp.*, pp. 201–205.

Uchino, K., and Cross, L. E. (1979). A high-sensitivity AC dilatometer for the direct measurement of piezoelectricity and electrostriction. *Proc. 33rd Annu. Freq. Control Symp.*, pp. 110–117.

Viles, R. S. (1972). Swept frequency techniques for accurate r.f. measurements. *Marconi Instrum.* **13**, 88–92.

Walls, F. L., and Wainwright, A. E. (1975). Measurement of the short-term stability of quartz crystal resonators and the implications for crystal design and applications. *IEEE Trans. Instrum. Meas.* **IM-24**, 15–20.

Watson, N. J. (1978). 110 MHz spectrum analyser, TF 2370. Crystal testing and measurements. *Marconi Instrum.* **16**, 35–36.

Weinert, F. (1966). The RF vector voltmeter—an important new instrument for amplitude and phase measurements from 1 MHz to 1000 MHz. *Hewlett-Packard J.* **17**, 2–12.

Weinert, F. K. (1980). An automatic precision IF-substitution vector ratio meter for the microwave frequency range. *IEEE Trans. Instrum. Meas.* **IM-29**, 471–477.

Wojcicki, M. (1973). Oscillating circuit for measurement of frequency and resistance change in quartz crystals. *Pr. Inst. Tele. Radiotech.* **17**, 71–76. In Polish.

Wojcicki, M. (1981). A new measurement method for the basic parameters of high frequency crystal resonators. *Pr. Inst. Tele. Radiotech.* (84), 19–33. In Polish.

Yamada, T., and Niizeki, N. (1970). Admittance of piezoelectric plates vibrating under the perpendicular field excitation. *Proc. IEEE* **58**, 941–942.

Yamaguchi, T., and Hamano, K. (1979). Interferometric method of measuring complex piezoelectric constants of crystals in a frequency range up to about 50 kHz. *Jpn. J. Appl. Phys.* **18**, 927–932.

Yamamoto, S., Sugawara, S., Tomikawa, Y., and Konno, M. (1978). A method for measuring equivalent circuit elements of a piezo-resonator. *J. Acoust. Soc. Jpn.* **34**, 455–461. In Japanese.

Yasuda, I., and Yamagata, S. (1976). Stress distribution measurement in oscillating quartz crystals with a laser probe. *Laser Electrooptical Systems*, p. 38.

Zakharov, V. P., Evtikhiev, N. N., Snezhko, Yu. A., and Tychinskii, V. P. (1976). Application of laser interferometry of the investigation of vibratory processes. *Sov. Phys.—Acoust. (Engl. Transl.)* **22**, 17–19.

Section 8.1

Allan, D. W., and Barnes, J. A. (1981). A modified "Allan variance" with increased oscillator characterization ability. *Proc. 35th Annu. Freq. Control Symp.*, pp. 470–475.

Allias, P. (1981). Quartz oscillators in ECL. *Toute Electron.* (468), 57–59. In French.

Al'tshuller, G. B. (1967). Temperature compensation for frequency-controlled quartz oscillators. *Telecommun. Radio Eng. (Engl. Transl.), Part 1* **21**, 49–51.

Al'tshuller, G. B. (1973). Variation of the center frequency of frequency-modulated quartz oscillators. *Telecommun. Radio Eng. (Engl. Transl.), Part 1* **27**, 47–50.

Al'tshuller, G. B., and Yelfimov, N. N. (1971). Transistor quartz oscillator frequency control. *Telecommun. Radio Eng. (Engl. Transl.), Part 1* **25**, 33–37.

Anonymous (1969). A voltage-controlled variable-frequency ultralinear quartz oscillator. *Electron. Microelectron. Ind.* (128), 674–675. In French.

Anonymous (1976). A universal quartz crystal oscillator. *Rev. Esp. Electron.* **23**, 35. In Spanish.

Anonymous (1978a). A voltage controlled quartz oscillator using a reactance diode. *Elektron. Entwickl.* **13**, 62. In German.

Anonymous (1978b). Practical oscillator calculations. VII. Quartz crystal oscillators. *Funk-Tech.* **33**, 270–274. In German.

Anonymous (1981). Quartz oscillators as building bricks. *Elektron. Entwickl.* **16**, 30–32. In German.

Apal'kov, V. K., Mitrofanov, V. P., and Shiyan, V. S. (1978). Frequency stability of oscillator with sapphire resonator. *Sov. Phys.—Dokl. (Engl. Transl.)* **23**, 671–672.

Arakelian, R., and Driscoll, M. M. (1977). Linear crystal controlled FM source for mobile radio application. *Proc. 31st Annu. Freq. Control Symp.*, pp. 400–406.

Arakelian, R., and Driscoll, M. M. (1978). Linear crystal controlled FM source for mobile radio application. *IEEE Trans. Veh. Technol.* **VT-27**, 43–50.

Arias, J. (1977). A calibrator with a crystal control oscillator. *Rev. Esp. Electron.* **24**, 50–52. In Spanish.

Arnoldt, M. (1978). Improved frequency stability circuit for 10 MHz quartz crystal. *Funk-Tech.* **33**, 380–381. In German.

Artym, A. D., and Zelenkov, A. A. (1967). Frequency stability of crystal oscillators. *Telecommun. Radio Eng. (Engl. Transl.), Part 2* **22**, 111–117.

Athey, R. J. (1979). LC network adapts PLL for crystal-overtone operation. *Electronics* **52**, 118.

Babitch, D., and Oliverio, J. (1974). Phase noise of various oscillators at very low Fourier frequencies. *Proc. 28th Annu. Freq. Control Symp.*, pp. 150–159.

Balaz, I. (1973). Frequency control of crystal oscillators. *Elektrotech. Cas.* **24**, 129–144. In Slovak.

Barnes, A. (1978). Sinewave of high purity from a crystal oscillator. *New Electron.* **11**, 18.
Barnes, J. A., Chi, A. R., Cutler, L. S., Healey, D. J., Leeson, D. B., McGunigal, T. E., Mullen J. A., Jr., Smith, W. L., Sydnor, R. L., Vessot, R. F. C., and Winkler, G. M. R. (1971). Characterization of frequency stability. *IEEE Trans. Instrum. Meas.* **IM-20**, 105–120.
Batdorf, H. A. (1969). Temperature-compensated crystal-controlled oscillators operating from 800 kHz to 1500 kHz. *Proc. 23rd Annu. Freq. Control Symp.*, pp. 192–197.
Beaussier, J. (1979). Research of an optimal configuration of high stability quartz oscillators on board aircraft and missiles. *Rech. Aerosp.* (6), 375–386. In French.
Beauvy, C. (1976). Stable frequency controlled oscillators. *Onde Electr.* **56**, 308–310. In French.
Beerbaum, R. H. (1976). Two inverters and a crystal assure oscillator start. *Electronics* **49**, 115.
Behnke, H. (1981). Frequency stabilization in the GHz region. *Radio Fernsehen Elektron.* **30**, 225–226. In German.
Belotsvetov, Yu. V., and Belousov, A. G. (1968). Circuit of a crystal controlled FM oscillator. *Telecommun. Radio Eng. (Engl. Transl.), Part 1*, **22**, 50–54.
Bernard, C. (1967). Quartz crystal oscillators with low drift. *Tech. Mitt. PTT* **45**, 603–609. In French.
Berry, A. H., and Sparkrite, E. D. A. (1982). Crystal oscillator adjuster. *Electron. Prod. Des.* **3**, 29.
Bertrand, A. (1976). Crystal oscillators. *Onde Electr.* **56**, 303–307. In French.
Besson, R. J., Emmons, D. A., Girardet, P. G., and Graf, E. P. (1980). Performances of new oscillators designed for "electrodeless" crystals. *Proc. 34th Annu. Freq. Control Symp.*, pp. 457–462.
Bezlud'ko, V. Ya., Zelenskii, A. A., and Solodovnik, V. F. (1978). Differential quartz oscillator with a wide relative tuning range. *Instrum. Exp. Tech. (Engl. Transl.)* **21**, 1004–1006.
Bidart, L., and Chauvin, J. (1981). Direct frequency crystal oscillator. *Proc. 35th Annu. Freq. Control Symp.*, pp. 356–375.
Blagovescenskii, M. V., and Balaz, I. (1973). Project optimization of voltage controlled crystal oscillators from the viewpoint of frequency control characteristic linearization. *Elektrotech. Cas.* **24**, 762–779. In Slovac.
Blankenburg, F. J., Drumheller, J. E., and Worsencroft, D. K. (1971). A transistorized 125 kHz crystal controlled oscillator for ESR field modulation. *Rev. Sci. Instrum.* **42**, 1377–1378.
Bloch, M. B., and Vulcan, A. I. (1976). The stability of precision oscillators in vibratory environments. *Proc. 30th Annu. Freq. Control Symp.*, pp. 284–291.
Bloch, M. B., Meirs, M. P., and Robinson, T. M. (1976). Stable oscillator for Pioneer Venus Programme. *Proc. 30th Annu. Freq. Control Symp.*, pp. 279–283.
Blood, B. (1978). Crystal VCO uses ECL line receiver. *Electron. Eng.* **50**, 23.
Bobkov, Yu. N., Mokrenko, P. V., and Necheporenko, V. I. (1971). Comparison of frequency control methods of quartz crystal generators. *Otbor Peredacha Inf.* (27), 64–68. In Russian.
Bolle, G., Coacci, R., and Marietti, P. (1982). Stable frequency and low power consumption quartz oscillator. *Alta Freq.* **51**, 43–48.
Borisenko, A. L. (1981). The effect of higher harmonic components of the frequency of a quartz oscillator with an *S*-type negatron. *Telecommun. Radio Eng. (Engl. Transl.), Part 2* **36**, 73–75.
Borisenko, A. L., and Sokolov, O. T. (1979). Crystal oscillator without inductance excited at the mechanical harmonics of the resonator. *Instrum. Exp. Tech. (Engl. Transl.)* **22**, 743–746.
Bowers, D. F., and Baker, E. F. D. (1980). A precision oscilloscope calibrator. *Elettron. Oggi* (1), 160–162. In Italian.
Bozic, S. M. (1968). Temperature compensation of frequency in crystal oscillators using varactor diodes. *Electron. Eng.* **40**, 670–672.
Brandenbenberger, H., Hadorn, F., Halford, D., and Shoaf, J. H. (1971). High quality quartz crystal oscillators: frequency domain and time domain stability. *Proc. 25th Annu. Freq. Control Symp.*, pp. 226–230.

Brendel, R., Groslambert, J., Marianneau, G., Olivier, M., and Uebersfeld, J. (1975a). Internal noise of a quartz crystal oscillator, influence of the parallel capacitance. *Proc. 29th Annu. Freq. Control Symp.*, pp. 311–315.
Brendel, R., Olivier, M., and Marianneau, G. (1975b). Analysis of the internal noise of quartz-crystal oscillators. *IEEE Trans. Instrum. Meas.* **IM-24**, 160–170.
Brown, D. E. (1967). Frequency measurement of quartz crystal oscillators. *Marconi Instrum.* **11**, 12–15.
Browning, T. I., and Lewis, M. F. (1977). A new class of quartz crystal oscillator controlled by surface-skimming bulk waves. *Proc. 31st Annu. Freq. Control Symp.*, pp. 258–265.
Buchanan, J. E. (1978). Crystal-oscillator design eliminates start-up problems. *EDN* **23**, 110.
Burgoon, R., and Wilson, R. L. (1979a). Design aspects of an oscillator using the SC cut crystal. *Proc. 33rd Annu. Freq. Control Symp.*, pp. 411–416.
Burgoon, R., and Wilson, R. L. (1979b). Performance results of an oscillator using the SC cut crystal. *Proc. 33rd Annu. Freq. Control Symp.*, pp. 406–410.
Burgoon, J. R., and Wilson, R. L. (1981). SC-cut quartz oscillator offers improved performance. *Hewlett-Packard J.* **32**, 20–21, 23–25, 28–29.
Buroker, G. E. (1972). "High Stability Temperature-Compensated Crystal Oscillator Study." Report ECOM-0136-1 on Contract DAAB-07-0136. Available from the National Technical Information Service, Springfield, Virginia, as Accession No. AD-738837.
Butcher, P. N., and Janus, H. M. (1972). The linear theory of acoustoelectronic oscillators with arbitrary static field distributions. *J. Phys. C* **5**, 567–581.
Cairns, P. (1972). Transistor crystal marker unit. *Radio Constructor* **25**, 458–462.
Capparelli, F., and Verrazzani, L. (1967a). Microminiature quartz crystal variable frequency oscillator for phase-lock receivers. *Elettrotecnica* **42**, B.2.6. In Italian.
Capparelli, F., and Verrazzani, L. (1967b). Comment on "variable frequency crystal oscillators." *Proc. IEEE* **55**, 1619–1621.
Carter, R. L., and Owens, J. M. (1983). The status of magnetostatic wave resonator stabilized oscillators. *Proc. 37th Annu. Freq. Control Symp.*, pp. 477–480.
Cartiann, G., and Marghescu, I. (1973). Electromechanical oscillators with capacitive transducer using an auxiliary i.f. carrier. *Posta Telecomunicatii* **3**, 232–236. In Rumanian.
Chiba, S. (1978). High stability reactance oscillator by zero input impedance amplifier. *Trans. Inst. Electron. Commun. Eng. Jpn.* [Part] E **61**, 575.
Chung, M. Y., Kim, Y. U., and Kim, B. S. (1971). Frequency modulated quartz oscillator using VVC diode. *J. Korean Inst. Electr. Eng.* **8**, 228–240. In Korean.
Chung, M. Y., Kim, Y. U., and Kim, B. S. (1973). The application of frequency modulated quartz oscillator using a V.V.C. diode. *J. Korean Inst. Electr. Eng.* **9**, 238–245. In Korean.
Collison, R. R., and Kmetovicz, R. E. (1976). Calibrated FM, crystal stability, and counter resolution for a low-cost signal generator. *Hewlett-Packard J.* **27**, 11–17.
Curtis, M. A. (1975). Crystal-derived 50 Hz for clocks. *Electron. Aust.* **37**, 79.
Cutler, L., and Searle, C. (1966). Some aspects of the theory and measurement of frequency fluctuations in frequency standards. *Proc. IEEE* **54**, 136–154.
Damljanovic, D. D. (1974). New quartz multivibrator. *Proc. IEEE* **62**, 640–641.
Dantard, F., and Payant, A. (1975). High stability frequency reference standard generator. *Cables Transm.* **29**, 123–126. In French.
Davies, T. (1977). CMOS crystal-controlled toneburst [oscillator]. *Radio Commun.* **53**, 603, 605.
Del Campo, J. (1982). Variable crystal oscillator. *Rev. Esp. Electron.* **29**, 20–23. In Spanish.
Dilworth, I. J. (1977). A channel scanning arrangement for quartz crystals. *Radio Commun.* **53**, 680–683.
Doktorov, A. A., and Morozov, V. A. (1975). Quartz oscillator with automatic frequency control. *Instrum. Exp. Tech. (Engl. Transl.)* **18**, 187–189.

Dowsett, J., and Smith, D. A. (1971). The trend towards packaged crystal oscillators. *Des. Electron.* **8**, 20–23.

Driscoll, M. M. (1972). Two stage self limiting series mode type quartz crystal oscillator exhibiting improved short-term frequency stability. *Proc. 26th Annu. Freq. Control Symp.*, pp. 43–49.

Driscoll, M. M. (1974). HF and VHF source stabilization technique incorporating Q-multiplied quartz crystal resonator. *IEEE Trans. Instrum. Meas.* **IM-23**, 131–140.

Driscoll, M. M. (1975). Low frequency noise quartz crystal oscillator. *IEEE Trans. Instrum. Meas.* **IM-24**, 21–26.

Driscoll, M. M., and Healey, D. J. (1971). Voltage-controlled crystal oscillators. *IEEE Trans. Electron Devices* **ED-18**, 528–535.

Dubey, G. C., and Singh, R. A. (1974). Thin film hybrid crystal oscillator. *J. Inst. Electron. Telecommun. Eng. (New Delhi)* **20**, 119–123.

Dwyer, D. F. J. (1977). Characteristics of quartz crystal oscillators. *Electron. Eng.* **49**, 24–25.

Dwyer, D. F. J., Roberts, J., and Haynes, G. (1969). Quartz crystal oscillator circuit without inductors. *Wireless World* **75**, 474–476.

Easton, R., Bartholomew, A., and Bloch, M. (1968). Crystal oscillator satellite experiment. *Proc. 22nd Annu. Freq. Control Symp.*, pp. 342–353.

Eaton, S. S. (1973). COS/MOS crystal oscillators advance timekeeping technology. *IEEE Int. Conv. Record* **VI**, 51.3/3.

Edson, W. A. (1953). "Vacuum Tube Oscillators." Wiley, New York.

Edwards, D. (1974). A crystal locked musical tone generator. *Electron. Aust.* **36**, 73–77, 115.

Embree, D. M., McClure, R. J., Paradysz, R. E., and Saari, V. R. (1980). Miniature packaged crystal. *Proc. 34th Annu. Freq. Control Symp.*, pp. 475–487.

Euler, F., and Yannoni, F. (1981). Frequency range of quartz oscillators. *Proc. 35th Annu. Freq. Control Symp.*, pp. 492–500.

Evans, B. (1978). Low cost crystal oscillator for the R6500. *Electron. Eng.* **50**, 17.

Farrell, B. F., Mattison, E. M., and Vessot, R. F. C. (1980). Application of modern time series analysis to high stability oscillators. *Proc. 34th Annu. Freq. Control Symp.*, pp. 228–232.

Felch, E. P., and Israel, J. O. (1955). A simple circuit for frequency standards employing overtone crystals. *Proc. IRE* **43**, 596–603.

Fiok, A. J. (1976). One-stage quartz oscillators with three reactance elements. *Rozpr. Elektrotech.* **22**, 913–924. In Polish.

Fischer, H. (1977). Linear calculation of the frequency response of quartz oscillators. *Nachrichtentech. Elektron.* **27**, 151–153. In German.

Flint, A. F., and Pustarfi, H. S. (1974). L5 system: 39A precision oscillator. *Bell Syst. Tech. J.* **53**, 2097–2107.

Fomin, N. N. (1967). Design of a tunnel diode oscillator with a quartz crystal in the capacitive arm of the tuned circuit. *Telecommun. Radio Eng. (Engl. Transl.), Part 2* **22**, 151–154.

Fomin, N. N. (1968). Nonlinear theory of tunnel-diode quartz oscillators. *Radiotekhnika (Moscow)* **23**, 23–30. In Russian.

Frank, R. (1974). Low frequency quartz and quartz oscillators. *Radio TV Electron* **34**, 771–774. In German.

Frank, R. (1975). Building instructions: a multiple quartz oscillator. *Radio TV Electron.* **35**, 146–148. In German.

Frensch, T. (1980a). Doubly-rotated crystals improve oscillators. *New Electron.* **13**, 58, 60.

Frensch, T. (1980b). Oscillator performance improved by crystal and oven design. *Aust. Electron Eng.* **13**, 75–79.

Frensch, T. (1980c). Quartz oscillators. *Elettron. Oggi* (10), 187–189, 192. In Italian.

Frerking, M. E. (1978). "Crystal Oscillator Design and Temperature Compensation." Van Nostrand-Reinhold, Princeton, New Jersey.

Gagnepain, J.-J. (1980). The effects of external factors of frequency instabilities and the sources of noise in crystal oscillators. *Pr. Inst. Tele. Radiotech.* (84), 35–49. In Polish.

Gagnepain, J.-J. and Besson, R. (1972). High level resonators and crystal oscillators. *Onde Electr.* **52**, 488–492. In French.

Gagnepain, J.-J., and Uebersfeld, J. (1976). From hertz to gigahertz: quartz oscillators. *Onde Electr.* **56**, 175–179.

Garner, P. J. (1978a). Voltage controlled crystal oscillators. *Conf. Radio Receivers and Associated Systems* (London, IERE), pp. 227–235.

Garner, P. J. (1978b). Voltage tunable crystal oscillators. *Philips Res. Lab. Annu. Rev.* 75.

Gauthier, N. (1978). Integrated quartz oscillator for TTL clock circuits. *Toute Electron.* (434), 53–55. In French.

Gavra, T. D., and Shabanov, Y. V. (1971). Transistor crystal-controlled VHF oscillator with improved operational frequency stability. *Telecommun. Radio Eng. (Engl. Transl.), Part 2* **26**, 95–98.

Gavra, T. D., Pruzhanskiy, M. M., and Shabanov, Y. V. (1967). Simple harmonic quartz transistorized meterwave oscillators. *Telecommun. Radio Eng. (Engl. Transl.), Part 2* **22**, 121–125.

Geesen, M., Brunet, M., Meirs, M., Strauss, A., and Rosenfeld, M. (1982). Argos and sargos quartz device performance and orbital data. *Proc. 36th Annu. Freq. Control Symp.*, pp. 499–506.

Gerber, E. A., and Sykes, R. A. (1966). State of the art—quartz crystal units and oscillators. *Proc. IEEE* **54**, 103–116.

Gersbach, J. E. (1979). Crystal oscillator. *IBM Tech. Disclosure Bull.* **21**, 3584–3585.

Gniewinska, B. (1978). Development trends of quartz crystal units and oscillators. *Elektronika* **19**, 309–314. In Polish.

Gniewinska, B. (1982). Development of piezoelectric frequency stabilization in Poland. *Przegl. Telekomun.* **55**, 44–46. In Polish.

Gniewinska, B., and Kwiatkowska, D. (1978). Analytical method for determination of modulation distortions in voltage controlled crystal oscillators. *Pr. Inst. Tele. Radiotech.* (79), 5–19. In Polish.

Gniewinska, B., and Kalinowska, B. (1980). Resonator dynamic thermal behaviour effects on thermostat controlled oscillator parameters. *Pr. Inst. Tele. Radiotech.* (85), 13–26. In Polish.

Goncharuk, N. M., Kotsarenko, N. Y., and Fedorchenko, A. M. (1974). The theory of an acoustic oscillator with a resonant electrical load. *Radio Eng. Electron. Phys. (Engl. Transl.)* **19**, 84–90.

Gray, J. E., and Allan, D. W. (1974). A method for estimating the frequency stability of an individual oscillator. *Proc. 28th Annu. Freq. Control Symp.*, pp. 243–246.

Greenhouse, H. M., McGill, R. L., and Clark, D. P. (1973). A fast warmup quartz crystal oscillator. *Proc. 27th Annu. Freq. Control Symp.*, pp. 199–217.

Greuter, A. (1969). Low power quartz crystal oscillator with a backward diode as the active elements. *Mitt. AGEN* (10), 92–97. In German.

Groslambert, J., Marianneau, G., Olivier, M., and Uebersfeld, J. (1974). The design and performance of a crystal oscillator exhibiting improved short term frequency stability. *Proc. 28th Annu. Freq. Control Symp.*, pp. 181–183.

Groslambert, J., Fest, D., Olivier, M., and Gagnepain, J.-J. (1981). Characterization of frequency fluctuations by crosscorrelations and by using three or more oscillators. *Proc. 35th Annu. Freq. Control Symp.*, pp. 458–463.

Hahn, H. (1969). Advice for the circuit design of quartz oscillators. I. *Bauelemente Elektrotech.* **4**, 40–50. In German.

Hajek, J. (1975). Crystal oscillators with TTL circuits. *Sdelovaci Tech.* **23**, 426–427. In Czech.

Hajek, J. (1976). A crystal oscillator controlled by a standard frequency transmitter. *Sdelovaci Tech.* **24**, 457–459. In Czech.

Hajek, J. (1979). Quartz oscillators of electronic chronometers. *Jenina Mech. Opt.* **24**, 165–171. In Czech.

Hajek, J. (1980). Crystal oscillators with transistors. *Sdelovaci Tech.* **28**, 343–344. In Czech.

Hall, T. M. (1982). Computer aided design and assembly of oscillators. *Proc. 36th Annu. Freq. Control Symp.*, pp. 507–512.

Hart, R. K., and Hicklin, W. H. (1972). "Tactical Miniature Crystal Oscillator." Report GIT-A-1344 ECOM-0301-1 (AD-749271), Georgia Institute of Technology, Atlanta, Georgia, 50 pp. Contract DAAB07-71-C-0301. Available from the National Technical Information Service, Springfield, Virginia.

Haynes, J. T., Salvo, H., and Moore, R. A. (1983). Low phase noise multiple frequency microwave source. *Proc. 37th Annu. Freq. Control Symp.*, pp. 87–90.

Healey, D. J. (1973). Low noise UHF crystal controlled source. *Proc. 27th Annu. Freq. Control Symp.*, pp. 170–179.

Healey, D. J., III, and Kwan, S. Y. (1981). SC cut quartz crystal units in low-noise oscillator application at VHF. *Proc. 35th Annu. Freq. Control Symp.*, pp. 440–454.

Helle, J. (1975). VCXO [voltage controlled crystal oscillator]—theory and practice. *Proc. 29th Annu. Freq. Control Symp.*, pp. 300–307.

Helle, J. (1976). Theory and practice of voltage controlled crystal oscillators. *Rev. Tech. Thomson—CSF* **8**, 607–637. In French.

Herrero, J. L. (1970). A new approach to provide a crystal accuracy frequency scale to microwave sweepers. *Singer Instrum. Rev.* **2**, 1–8.

Hinnah, H., and Newell, D. E. (1968). Automatic compensation equipment for TCSO's. *Proc. 22nd Annu. Freq. Control Symp.*, pp. 298–310.

Hirama, K., and Onoe, M. (1973). A temperature-compensated three-crystal oscillator. *Electron. Commun. Jpn.* **56**, 33–40.

Ho, J., and Bloch, M. (1977). A fast warmup oscillator for the GPS receiver. *Proc. 31st Annu. Freq. Control Symp.*, pp. 421–428.

Ho, J., and Nardin, R. (1974). Computer design and analysis for high precision oscillators. *Proc. 28th Annu. Freq. Control Symp.*, pp. 237–242.

Hobbs, A. G. (1980). Crystal controlled sinewave generator. *Elektor* **6–7**, 81–82.

Holmbeck, J. D. (1977). Frequency tolerance limitations with logic gate clock oscillators. *Proc. 31st Annu. Freq. Control Symp.*, pp. 390–395.

Honda, S., and Watahiki, T. (1975). On analysis of quartz crystal oscillator circuit for quartz watches. *J. Fac. Eng. Ibaraki Univ.* (23), 141–144. In Japanese.

Hopper, C. (1981a). The quartz crystal oscillator. *New Electron.* **14**, 88, 90–92.

Hopper, C. (1981b). The quartz crystal oscillator. II. *New Electron.* **14**, 59–60.

Horiba, Y., Nakao, Y., Komatsu, T., Tomisawa, O., and Ohkubo, T. (1978). Design for low power dissipation in CMOS quartz oscillator of watch use. *Trans. Inst. Electron. Commun. Eng. Jpn.* [Part] *E* **61**, 859–860.

Iizawa, N. (1982). Future bright for crystal clock oscillator. *JEE, J. Electron. Eng.* **19**, 64–67.

Iliev, S. G., Rajkov, K. G., and Durcev, N. H. (1974). Matrix analysis of a generator with quartz-type frequency stabilization. *Elektroprom. Priborostr.* **9**, 269–269. In Bulgarian.

Ivanchenko, Y. S., and Plonskii, A. F. (1973). A two-stage pulse-excited crystal-controlled self-running oscillator. *Izv. Vyssh. Uchebn. Zaved. Radioelektron.* **16**, 95–97. In Russian.

Ivanek, F. (1979). Frequency stabilisation. *Onde Electr.* **59**, 55–58. In French.

Jackson, H. W. (1980). Tactical miniature crystal oscillator. *Proc. 34th Annu. Freq. Control Symp.*, pp. 449–456.

Jackson, H. W. (1982). Update on the tactical miniature crystal oscillator program. *Proc. 36th Annu. Freq. Control Symp.*, pp. 492–498.

Jellicoe, R. (1982). Biasing arrangement for diode switched crystal oscillators. *Motorola Tech. Dev.* **2**, 16–17.

Karlinskii, S. I. (1974). Calculating the stability and excitation of one quartz oscillator circuit with a tunnel diode. *Otbor Peredacha Inf.* (41), 74–79. In Russian.

Katyl, R. H. (1977). Monolithic crystal oscillator. *IBM Tech. Disclosure Bull.* **20**, 970–972.

Kavun, E. P. (1978). High-power crystal oscillator. *Instrum. Exp. Tech. (Engl. Transl.)* **21**, 685–686.

Keller, T., Marvin, D., and Steele, R. (1980). Integrated circuit compensation of AT-cut crystal oscillators. *Proc. 34th Annu. Freq. Control Symp.*, pp. 498–503.

Kennedy, R. J., and Foster, I. M. (1978). A drive unit for a quartz composite oscillator. *J. Phys. E.* **11**, 889–891.

Kodama, S., and Sato, Y. (1979). An analysis of unwanted frequency oscillation in a crystal controlled oscillator. *Proc. 33rd Annu. Freq. Control Symp.*, pp. 417–424.

Komlik, V. V., and Uvarov, R. V. (1977). Control of the transmission coefficient at the resonant frequency in a four-terminal network with a paraelectric piezoresonator. *Izv. Vyssh. Uchebn. Zaved. Radioelektron.* **20**, 84–88. In Russian.

Korolev, V. S., and Matin, E. N. (1979). Low-frequency quartz oscillator designed from microcircuits. *Instrum. Exp. Tech. (Engl. Transl.)* **22**, 1349–1350.

Kukiekla, J. F., and Meyer, R. G. (1981). A high-frequency temperature-stable monolithic VCO. *IEEE J. Solid-State Circuits* **SC-16**, 639–647.

Kulagin, E. V., Pikhtelev, A. I., Sokolov, V. P., and Fateev, B. P. (1978a). Natural fluctuations in a quartz crystal oscillator with automatic gain control. *Radiophys. Quantum Electron. (Engl. Transl.)* **21**, 1125–1130.

Kulagin, E. V., Sokolov, V. P., Pikhtelev, A. I., and Fateev, B. P. (1978b). Technical fluctuations in a quartz crystal oscillator with automatic gain control. *Radiophys. Quantum Electron. (Engl. Transl.)* **21**, 1234–1238.

Kupka, K., and Thanhauser, G. (1970). Transistorised crystal oscillators in MHz frequencies for applications to carrier frequencies technique. *Frequenz* **34**, 357–363. In German.

Kupka, K., and Thanhauser, G. (1972). Phase-controlled crystal oscillators for integral frequency multiplication with applications in wide-band carrier frequency systems. *Frequenz* **26**, 14–18. In German.

Kuznetsov, A. A., and Baryshev, V. I. (1970). Crystal oscillator using field-effect transistors. *Instrum. Exp. Tech. (Engl. Transl.)* (2), 468–470.

Layden, O. P., Smith, W. L., Anderson, A. E., Bloch, M. E., Newell, D. E., and Sulzer, P. C. (1972). Crystal-controlled oscillators. *IEEE Trans. Instrum. Meas.* **IM-21**, 277–286.

Lean, G. D. (1975). A crystal-controlled solid-state source for 10 GHz. *Radio Commun.* **51**, 614–619.

Lega, M. C., and Frentzel, R. W. (1973). Crystal controlled frequency modulator. *Rev. Telegr. Electron. (Argentina)* **62**, 502–504. In Spanish.

Lesage, P., and Audoin, C. (1975). Frequency stability of oscillators: measurements in the frequency domain by a temporal method. *Onde Electr.* **55**, 82–89. In French.

Lipko, S. I., Negodenko, O. N., and Dzyuba, L. P. (1980). Microelectronic crystal oscillators using current limiters. *Izv. Vyssh. Uchebn. Zaved. Priborostr.* **23**, 66–70. In Russian.

Lipoff, S. J. (1976). Design of voltage controlled crystal oscillators. *Proc. 30th Annu. Freq. Control Symp.*, pp. 301–308.

Lipski, H. (1975). Adjustable digital function generator using a quartz oscillator. *Elektronik (Munich)* **24**, 77–78. In German.

Litvinenko, V. P., Novinskii, N. A., Undrevich, A. Y., and Kosogovski, V. V. (1976). Influence of quartz-crystal dynamical inductance on spurious amplitude modulation in frequency-modulated crystal-controlled oscillators. *Izv. Vyssh. Uchebn. Zaved. Radioelektron.* **19**, 99–101. In Russian.

Lue, J. T. (1976). A simple circuit of a crystal oscillator and its application to a high-resolution NMR spectrometer. *IEEE Trans. Instrum. Meas.* **IM-25**, 76–78.

Lukyavenko, Y. B., Ponomarev, M. F., and Fursa, E. A. (1975). A crystal-controlled sinusoidal transistor oscillator. *Izv. Vyssh. Uchebn. Zaved. Radioelektron.* **18**, 64–67. In Russian.

Luxmore, T., and Newell, D. E. (1977). The MXO-monolithic crystal oscillator. *Proc. 31st Annu. Freq. Control Symp.*, pp. 396–399.

Makarenko, B. I., Shmidt, V. V., Ovsyannikov, Y. V., Arkhipov, A. V., Bel'ko, A. A., and Bakhtin, V. D. (1976). Solid-state, three-frequency, quartz-crystal-stabilised, millimeter-range frequency source. *Radiotekhnika* (Kharkov) (39), 62–64. In Russian.

Malakhov, A. N. (1968). Natural fluctuations in quartz generator. *Izv. Vyssh. Uchebn. Zaved. Radiofiz.* (6), 850–865. In Russian.

Mallik, D. N. B., and Nag, B. R. (1967). Free and forced oscillations in a delay line oscillator. *Int. J. Electron.* **23**, 101–122.

Mancini, R. A. (1974). A low cost, crystal-controlled oscillator design. *Comput. Des.* **13**, 94–96.

Manukin, A. B., and Tikhonov, M. Y. (1970). The equivalent circuit of a capacitive mechanical oscillator. *Vestn. Mosk. Univ. Fiz. Astron.* (5), 584–585. In Russian.

Markus, N., and Rogner, R. (1976). The TN quartz pulse generator. *Nachr. Telefonbau Normalzeit* (77), 45–49. In German.

Marshall, F. G. (1969). Equivalent circuit for the acoustoelectric oscillator. *Electron. Lett.* **5**, 581–582.

Marshall, F. G. (1971). Vibration-mode patterns of acoustoelectric oscillators. *Electron. Lett.* **7**, 203–205.

Maslov, V. A. (1979). Improvement of the frequency control characteristics of a quartz oscillator. *Telecommun. Radio Eng. (Engl. Transl.), Part 2* **34**, 129–131.

Maslov, V. A., and Bashmakov, V. V. (1981). Calculation of the equivalent loss resistance of the oscillatory system of a controlled quartz oscillator. *Telecommun. Radio Eng. (Engl. Transl.), Part 2* **36**, 68–70.

Matthys, R. J. (1983). "Crystal Oscillator Circuits." Wiley, New York.

McVey, E. S., and Swanson, C. T. (1978). Capacitor temperature-compensated crystal oscillators. *IEEE Trans. Ind. Electron. Control Instrum.* **IECI-25**, 164–166.

Meek, P. (1981). HF oscillator for use with a quartz crystal monitor. *Vacuum* **31**, 377–378.

Meirs, M., Sherman, P., Bloch, M., and Ho, J. (1980). A fast warmup, high stability, crystal oscillator. *Proc. 34th Annu. Freq. Control Symp.*, pp. 463–470.

Mel'nikov, A. A., Ermolaev, N. A., Erasov, I. A., and Shesternin, A. N. (1981). Technological crystal oscillator of the type AMTS 1550. *Prib. Sist. Upr.* (9), 32. In Russian.

Meyer, R. G., and Soo, D. C.-F. (1980). MOS crystal oscillator design. *IEEE J. Solid-State Circuits* **SC-15**, 222–228.

Misra, R. K. (1973). A network that will keep a crystal oscillator operating at zero phase angle. *J. Inst. Electron. Telecommun. Eng. (New Delhi)* **19**, 555–557.

Miyajima, S., Asakura, T., and Oguchi, T. (1967). Frequency stabilization of a bridge oscillator. *J. Radio Res. Lab.* **14**, 27–56.

Mortley, W. S. (1972). Comments on "voltage-controlled crystal oscillators." *IEEE Trans. Electron. Devices* **ED-19**, 1065–1067.

Moses, J. (1976). NAVSTAR global positioning system oscillator requirements for the GPS manpack. *Proc. 30th Annu. Freq. Control Symp.*, pp. 390–400.

Mosuz, G., and Gagnepain, J.-J. (1976). Quartz crystal oscillator at very low temperature. *Cryogenics* **16**, 652–656.

Mroch, A. B., and Hykes, G. R. (1976). A miniature high stability TCXO using digital compensation. *Proc. 30th Annu. Freq. Control Symp.*, pp. 292–300.

Nadai, C. (1973). Piezo-electric tuning fork modules. *Electron. Microelectron. Ind.* (167), 39–48. In French.

Nardin, R., and Ho, J. (1974). Computer design and analysis for high precision oscillators. *Proc. 28th Annu. Freq. Control Symp.*, pp. 237–242.

Nedashkovskii, A. I. (1976). A crystal oscillator with frequency trimming. *Prib. Sist. Upr.* **12**, 47. In Russian.

Negodenko, O. N., and Ponomarev, M. F. (1972). A unijunction quartz-crystal transistor. *Izv. Vyssh. Uchebn. Zaved. Radioelekron.* **15**, 87–92. In Russian.

Neubig, B. (1979). Design of crystal oscillator circuits. *VHF Commun.*, Ed. 3 and 4.

Neubig, B. (1981). An extremely noiseless 96 MHz quartz oscillator for the UHF/VHF frequency control. *UKW Berichte* (1–2), 24–32, 91–100. In German.

Newell, D. E., and Hinnah, H. (1969). A report on TCXO's and segmented compensation. *Proc. 23rd Annu. Freq. Control Symp.*, pp. 187–191.

Noble, F. W. (1976). Need an adjustable crystal oscillator? *Electron. Des.* **24**, 88–90.

Noguchi, Y., Teramachi, Y., and Musha, T. (1981). $1/f$ frequency fluctuation of a quartz crystal oscillator. *Proc. 35th Annu. Freq. Control Symp.*, pp. 484–491.

Noguchi, Y., Teramachi, Y., and Musha, T. (1982a). $1/f$ frequency fluctuations of a quartz oscillator. *Appl. Phys. Lett.* **40**, 872–873.

Noguchi, Y., Teramachi, Y., and Musha, T. (1982b). Correlation between frequency fluctuations of a quartz oscillator and temperature fluctuations. *Jpn. J. Appl. Phys., Part I* **21**, 61–66.

Nonaka, S. (1974). Abnormal crystal oscillator frequency change with load capacitance and its elimination. *Proc. 28th Annu. Freq. Control Symp.*, pp. 203–210.

Norton, J. R. (1976). An ultrastable low power 5 MHz quartz oscillator qualified for space usage. *Proc. 30th Annu. Freq. Control Symp.*, pp. 275–278.

Novinskii, N. A. (1978). A crystal oscillator based on a field-effect transistor. *Izv. Vyssh. Uchebn. Zaved. Radioelektron.* **21**, 100–103. In Russian.

Novinskii, N. A., and Undrevich, A. Y. (1969). Design of quartz crystal self-running tunnel-diode oscillator. *Izv. Vyssh. Uchebn. Zaved. Radioelektron.* **12**, 543–547. In Russian.

Novinskii, N. A., Litvineneko, V. P., and Undrevich, A. Y. (1974). A double-frequency controlled quartz-crystal oscillator. *Izv. Vyssh. Uchebn. Zaved. Radioelektron.* **17**, 105–107. In Russian.

Nukiyama, D., and Miyazaki, N. (1967). A type of oscillator. *J. Res. Inst. Sci. Technol., Nihon Univ.* (34), 18–24. In Japanese.

Odess, L. (1973). Analysis of the frequency and sensitivity of crystal-controlled oscillators. *8th Conv. Electrical Electronics Engineers in Israel*, p. 66.

Odess, L. (1976). Analysis of the frequency and sensitivity of crystal-controlled oscillators. *Radio Electron. Eng.* **46**, 109–116.

Ohata, Y. (1974). New approach to the design of crystal oscillators. *Proc. 28th Annu. Freq. Control Symp.*, pp. 221–231.

Okano, S., and Ikeda, Y. (1978). Crystal oscillators facilitate future frequency control. *JEE, J. Electron. Eng.* (144), 40–43.

Okano, S., and Mitsuoka, T. (1980). Toyo's crystal oscillators for SBFM achieve high frequency stability. *JEE, J. Electron. Eng.* **17**, 48–52.

Okano, S., Mitsuoka, T., and Ohshima, T. (1980). Direct temperature compensated crystal oscillators for recent advanced UHF/UHF radio system. *Proc. 34th Annu. Freq. Control Symp.*, pp. 488–497.

Olivier, M., and Marianneau, G. (1976). High quality quartz oscillator. *Onde Electr.* **56**, 293–296. In French.

Omlin, L. (1977a). Analysis and component sizing of quartz oscillators. II. *Elektroniker (Switzerland)* **16**, EL8–14. In German.

Omlin, L. (1977b). Analysis and design of quartz oscillators. I. *Elektroniker (Switzerland)* **16**, EL30–36. In German.

Ormond, T. (1981). Components [crystal oscillators]. *EDN* **26**, 302, 304, 306, 313–314, 316.

Onoe, M., Yamagishi, I., and Nariai, H. (1978). Temperature compensation of crystal oscillator by microprocessor. *Proc. 32nd Annu. Freq. Control Symp.*, pp. 398–402.
Ostapenko, G. S., and Goncharov, A. Y. (1978). Low-frequency quartz-crystal generator using integrated circuits. *Meas. Tech. (Engl. Transl.)* **21**, 1403–1404.
Ovcharenko, V. V., and Ovcharenko, N. F. (1970). New tunnel-diode oscillators with quartz crystal in the capacitive arm of the circuit. *Radiotekhnika (Moscow)* **25**, 101–103. In Russian.
Paradysz, R. E., and Smith, W. L. (1975). Crystal controlled oscillators for radiation environments. *Radiat. Eff.* **26**, 213–218.
Parzen, B. (1980). Requirements and evaluation of the circuitry excluding the crystal, in crystal oscillators. *Proc. 34th Annu. Freq. Control Symp.*, pp. 471–474.
Parzen, B. (1982). Theoretical and practical effects of the resonator specifications and characteristics upon precision crystal oscillator design and performance. *Proc. 36th Annu. Freq. Control Symp.*, pp. 480–485.
Parzen, B. (1983). "Design of Crystal and Other Harmonic Oscillators." Wiley, New York.
Pashev, G. P. (1979). Mathematical description of flicker fluctuations in frequency using modified structure functions [quartz oscillators]. *Radiophys. Quantum Electron. (Engl. Transl.)* **22**, 1073–1074.
Paul, E. (1972). High-stability frequency generator. *Posta Telecomunicatii* **2**, 403–405. In Rumanian.
Pavlivec, J. (1981). Frequency detuning in quartz oscillators. *Slaboproudy Obz.* **42**, 378–384. In Czech.
Pichl, H. (1967). Crystal oscillator module for electronic control systems. *News from Rohde and Schwarz (Germany)* **7**, 9–12.
Pichler, H. (1975). Quartz oscillator with "SN 74" series TTL elements. *Radio Elektron. Schau* **51**, 209–210. In German.
Plonskiy, A. F., and Tearo, V. I. (1977). The frequency stability of a self-excited quartz oscillator with a line section. *Telecommun. Radio Eng. (Engl. Transl.), Part 2* **31**, 82–87.
Plonskii, A. F., and Samkov, E. Y. (1968). On the modulation characteristic of a piezoelectric oscillator stabilized by dipotassium tartrate and frequency modulated by means of a p–n junction capacitance. *Izv. Vyssh. Uchebn. Zaved. Radioelektron.* **11**, 299–307. In Russian.
Polikarpov, E. D., Undrevich, A. Y., and Khenkin, E. A. (1978). A nomographic design technique for a quartz-crystal oscillator with a double frequency control. *Izv. Vyssh. Uchebn. Zaved. Radioelektron.* **21**, 34–38. In Russian.
Polinski, S., and Vineis, D. (1980). Monolithic clock oscillator. *Motorola Tech. Disclosure Bull.* **1**, 8.
Pollard, G. B. (1982). A digitally compensated hybrid crystal oscillator. *Proc. 36th Annu. Freq. Control Symp.*, pp. 474–479.
Popov, G. Y., Dishkov, P. S., and Donchev, S. D. (1979). Hybrid integrated circuit of quartz generator. *Elektroprom. Priborostr.* **14**, 65–66. In Bulgarian.
Preston, B., and Rignall, M. W. (1967). Microelectronic crystal oscillators. *Proc. 2nd Int. Congress Microelectronics*, pp. 641–662.
Priestly, B. (1980). Simple crystal oscillator. *Electron. Prod. Des.* **1**, 22.
Pruzhanskii, M. M., and Gavra, T. D. (1967). Bridge circuits for transistorised harmonic quartz oscillators. *Radiotekhnika* **22**, 50–58. In Russian.
Przyjemski, J. M. (1978a). A compensation technique for acceleration-induced frequency changes in crystal oscillators. *Proc. IEEE Nat. Aerospace and Electronics Conf.*, pp. 55–60.
Przyjemski, J. M. (1978b). Improvement in system performance using a crystal oscillator compensated for acceleration sensitivity. *Proc. 32nd Annu. Freq. Control Symp.*, pp. 426–431.
Przyjemski, J. M., and Konop, P. L. (1977). Limitations on GPS receiver performance imposed by crystal-oscillator g-sensitivity. *Proc. IEEE Nat. Aerospace Electron. Conf.*, pp. 319–322.

Rapallini, R. E. (1976). A VXO oscillator exciter. *Rev. Telegr. Electron. (Argentina)* **64**, 25. In Spanish.
Remy, J. (1975). Direct measurement of the spectral purity of stable oscillators. *Onde Electr.* **55**, 90–94. In French.
Rippy, R. (1976). A new look at source stability. *Microwaves* **15**, 42–43, 46, 48.
Risley, A. S., and Shoaf, J. H. (1974). Frequency stabilization of X-band sources for use in frequency synthesis into the infrared. *IEEE Trans. Instrum. Meas.* **IM-23**, 187–195.
Rohde, U. L. (1975). Crystal oscillator provides low noise. *Electron. Des.* **23**, 98–99.
Rohde, U. L. (1978). Mathematical analysis and design of an ultra stable low noise 100 MHz crystal oscillator with differential limiter and its possibilities in frequency standards. *Proc. 32nd Annu. Freq. Control Symp.*, pp. 409–425.
Rossman, H., and Chino, J. J. (1977). Crystal oscillator vibration isolation for airborne radar applications. *IEEE Mech. Eng. in Radar Symp.*, pp. 72–74.
Roubicek, O. (1968). An electromechanical low-frequency control oscillator. *Automatizace* (9–10), 261–267. In Czech.
Rousseau, K. V., Yen, K. H., Lau, K. F., and Kong, A. M. (1983). High-frequency shallow bulk acoustic wave quartz frequency sources. *Proc. 37th Annu. Freq. Control Symp.*, pp. 428–433.
Rozwadowski, M. (1978). Application of crystal oscillators in modern telecommunication equipments. *Przegl. Telekomun.* **51**, 147. In Polish.
Rutman, J. (1970). Very short-term frequency instability (time domain) of an oscillator disturbed by additive internal thermal noise. *Proc. IEEE* **58**, 958–959.
Rutman, J. (1977). Oscillator specifications: a review of classical and new ideas. *Proc. 31st Annu. Freq. Control Symp.*, pp. 291–301.
Ryzhov, A. V., and Kremnev, Y. V. (1976). Short-term frequency stability of meter-wave quartz oscillators. *Telecommun. Radio Eng. (Engl. Transl.), Part 2* **31**, 82–85.
Sabatterie, R. (1973). Crystal controlled low-frequency oscillator. *IBM Tech. Disclosure Bull.* **15**, 3075–3077.
Saito, T., Ikeda, T., Katsuta, H., and Takahashi, I. (1967). A high power transistor crystal oscillator. *Mem. Def. Acad., Math., Phys., Chem. Eng. (Yokosuka, Jpn.)* **7**, 451–459.
Savage, E. (1978). How to build crystal oscillators. *Radio Electron.* **49**, 66–67.
Saxena, G. M., and Mathur, B. S. (1980). Stability measurements in time domain using dual mixer time difference system [crystal oscillators]. *Indian J. Pure Appl. Phys.* **18**, 220–223.
Schomezler, G., and Zwilling, H. (1967). Digital level oscillator 200 Hz to 2 MHz, a crystal-accurate level and sweep oscillator with programmable decade frequency control. *Entwicklungsber. Siemens Halske* **30**, 215–221. In German.
Scott, P. J. (1977). Design considerations for a digitally temperature compensated crystal oscillator. *Proc. 31st Annu. Freq. Control Symp.*, pp. 407–411.
Sharma, A. K., and Wilson, M. G. F. (1970). Linear theory of the acoustoelectric oscillator. *Proc. Inst. Electr. Eng.* **117**, 2216–2220.
Shevkoplyas, G. B. (1970). Matrix capacitor for the tuning of thick-film hybrid quartz crystal oscillators. *Izv. Vyssh. Uchebn. Zaved. Radioelektronika* **13**, 655–658. In Russian.
Shmidt, V. V., Sarafanov, V. F., and Bakhtin, V. O. (1977). Experimental investigation of fluctuations in UHF harmonic quartz oscillators. *Radiotekhnika* (Kharkov) (43), 119–121. In Russian.
Simpson, L. (1975). Quartz crystal drive for fluorescent readout clock. *Electron. Aust.* **37**, 74–75, 77.
Singh, D., and Garters, J. (1967). Crystal-controlled 164 MHz oscillator/quadrupler. *Electron. Eng.* **39**, 769–772.
Siukaev, A. V. (1975). Using a crystal oscillator. *Energetik* (4), 27. In Russian.
Slavik, M. (1981). A voltage controlled and temperature compensated gyrator crystal oscillator. *Tesla Electron.* **14**, 67–73.

Slavik, M., and Zelenka, J. (1976). Use of the integrated gyrator in a voltage controlled crystal oscillator. *Elektrotech. Cas.* **27**, 772–774.

Smagin, A. G. (1975a). A low-temperature oscillator with a frequency stability 4×10^{-14}. *Instrum. Exp. Tech. (Engl. Transl.)* **18**, 1853–1855.

Smagin, A. G. (1975b). Nonthermostated quartz generators with an instability of 10^{-8}. *Instrum. Exp. Tech. (Engl. Transl.)* **18**, 508–510.

Smagin, A. G. (1977). Very stable crystal oscillators aging less than 10^{-10} per month. *Instrum. Exp. Tech. (Engl. Transl.)* **20**, 188–189.

Smith, W. L. (1960). Miniature transistorized crystal-controlled precision oscillators. *IRE Trans. Instrum.* **9**, 141–148.

Smith, W. L., and Spencer, W. J. (1963). "Quartz Crystal Controlled Oscillators." Final report, Contract DA-66-039 SC-85373. Available from the National Technical Information Service, Springfield, Virginia.

Sokolo, V. P., Kulagin, E. V., Pikhtelev, A. I., and Fateev, B. P. (1978). An experimental study of technical fluctuations in a quartz crystal oscillator with automatic gain control. *Radiophys. Quantum Electron. (Engl. Transl.)* **21**, 1238–1243.

Solin, N. N. (1971a). Comparative analysis of fluctuations in various types of two-circuit quartz oscillators. *Radio Eng. Electron. Phys. (Engl. Transl.)* **16**, 272–276.

Solin, N. N. (1971b). Fluctuations of single-stage, crystal-controlled valve oscillators. *Izv. Vyssh. Uchebn. Zaved. Radioelektron.* **14**, 267–275. In Russian.

Solin, N. N. (1971c). The dynamics of two-circuit self-oscillator with nonlinear quartz resonator. *Izv. Vyssh. Uchebn. Zaved. Radiofiz.* **14**, 100–104. In Russian.

Solin, N. N. (1972). The limiting short-term frequency instability of self-excited quartz oscillators. *Radio Eng. Electron. Phys. (Engl. Transl.)* **17**, 69–72.

Solov'ev, I. I. (1972). Automatic adjustment of the amplitude of crystal oscillators with tunnel diodes. *Meas. Tech. (Engl. Transl.)* **15**, 599–601.

Stahl, A. (1983). Ultra-stable crystal oscillator for Beacons (program "SARSAT"). *Proc. 37th Annu. Freq. Control Symp.*, pp. 454–458.

Stein, S. R., Manney, C. M., Jr., Walls, F. L., Gray, J. E., and Besson, R. J. (1978). A systems approach to high performance oscillators. *Proc. 32nd Annu. Freq. Control Symp.*, pp. 527–530.

Steinmetz, J. H. (1980). Flexible circuitry improves crystal oscillator design. *Electron. Packag. Prod.* **20**, 123–126, 128, 130.

Steinmetz, J. H. (1981). Flexible circuit packaging of a crystal oscillator. *Hewlett-Packard J.* **32**, 26–28.

Stolarski, E., and Vojtasek, S. (1970). An approximate method for the solution of an oscillator with a piezotransistor. *Elektrotech. Cas.* **21**, 632–645. In Czech.

Suckling, C. W. (1976). A crystal-controlled frequency marker for 10 GHz. *Radio Commun.* **52**, 352–353.

Swanson, C. T., and McVey, E. S. (1979). A non-interative solution for a two-thermistor TCXO. *Proc. 33rd Annu. Freq. Control Symp.*, pp. 425–430.

Teramachi, Y., Horie, M., Kataoka, H., and Musha, T. (1979). Frequency response of a quartz oscillator to temperature fluctuations. *Proc. 33rd Annu. Freq. Control Symp.*, pp. 235–238.

Tesic, S., and Vasiljevic, D. (1976). Quartz-controlled complementary multivibrator. *Proc. Inst. Electr. Eng.* **123**, 851–854.

Tesic, S., and Vasiljevic, D. (1977). A quartz multivibrator using two regenerative switches. *Proc. IEEE* **65**, 166–167.

Theaker, M. E. (1976). CMOS crystal calibrator. *Pract. Wireless* **51**, 968–975.

Tourki, P. (1973). Quartz oscillator in complementary M.O.S. technology. *Electron. Lett.* **9**, 451–453.

Tuama, S. S. O. (1971). Crystallographic orientation dependence of electrical response of acoustoelectric oscillators. *Proc. Inst. Electr. Eng.* **118**, 746–749.

Tuama, S. S. O., and Richter, J. (1974). Frequency control and mode selectivity in the acoustoelectric oscillator. *J. Phys. D* **7**, 425–428.

Ueno, Y. (1981). Crystal oscillator: indispensable frequency source for diverse fields. *JEE, J. Electron. Eng.* **18**, 68–72.

Unkrich, M. A., and Meyer, R. G. (1982). Conditions for start-up in crystal oscillators. *IEEE J. Solid-State Circuits* **SC-17**, 87–90.

Valdois, M., Moreau, R., and Dupuy, A. (1976). Airborne quartz oscillators, applications. *Onde Electr.* **56**, 297–302. In French.

Van Der Windt, J., and Grassi, R. (1978). To specify a time-base oscillator, you'd better know your crystals. *Electron. Des.* **26**, 126–129.

Vasiljevic, D., and Tesic, S. (1977). An emitter-coupled quartz multivibrator. *Int. J. Electron.* **42**, 551–558.

Vinkler, E., Grebenyuk, V. M., and Zinov, V. G. (1978). Quartz-crystal stabilized 150-MHz oscillator. *Instrum. Exp. Tech. (Engl. Transl.)* **20**, 736–738.

Vovchenko, P. S. (1970). Flicker noise in quartz-crystal controlled oscillator. *Izv. Vyssh. Uchebn. Zaved. Radioelektron.* **13**, 754–758. In Russian.

Walker, D. A. S. (1972). "A Stable Crystal Oscillator Employing Digital Integrated Circuitry." Report AECL-4160, Atomic Energy Canada Ltd., 5 pp.

Walls, F. L., and Stein, S. R. (1978). A frequency-lock system for improved quartz crystal oscillator performance. *IEEE Trans. Instrum. Meas.* **IM-27**, 249–252.

Walls, F. L., and Wainwright, A. E. (1975). Measurement of the short-term stability of quartz crystal resonators and the implications for crystal oscillator design and applications. *IEEE Trans. Instrum. Meas.* **IM-24**, 15–20.

Watanabe, A. (1978). Quartz oscillator in Japan—mainly used for the wrist watch. *Bull. Jpn. Soc. Precis. Eng.* **12**, 61–66.

Watrobski, B. (1972). Possibilities of improving frequency stability in generating devices. *Pomiary, Autom., Kontrola* **18**, 498–499. In Polish.

Yamazaki, M., and Oomura, Y. (1980). A consideration of CMOS crystal oscillator. *Mem. Fac. Technol., Tokyo Metrop. Univ.* (30), 2897–2906.

Yamnyi, V. E. (1970). Study of low-frequency amplitude and phase fluctuations of quartz-crystal transistor oscillators. *Radio Electron. Commun. Syst. (Engl. Transl.)* **13**(5).

Yelfimov, N. N., and Al'tshuller, G. B. (1976). The amplitude relations in quartz oscillators. *Telecommun. Radio Eng. (Engl. Transl.), Part 1* **30**, 52–54.

Yoda, H., Ikeda, H., and Yamabe, H. (1972a). Low power crystal oscillator for electronic wrist watch. *JEE, J. Electron. Eng.* **62**, 24–30.

Yoda, H., Ikeda, H., and Yamabe, Y. (1972b). Low power crystal oscillator for electronic wrist watch. *Proc. 26th Annu. Freq. Control Symp.*, pp. 140–147.

Zamzow, D. (1968). Direct frequency modulation of transistorized quartz oscillators. *Tech. Mitt. RFZ* **12**, 125–130. In German.

Ziegler, R. R. (1976). Know your crystal oscillators. *Microwave J.* **19**, 44, 47.

Section 8.2

Allison, R., and Goldman, S. J. (1978). Vibration effects on close-in phase noise of a 300 MHz surface wave resonator oscillator. *Proc. 32nd Annu. Freq. Control Symp.*, pp. 66–73.

Anonymous. (1977). Surface-acoustive-wave oscillator tuned by magnetoelastic effect. *Electron. Lett.* **13**, 583–590.

Bale, R. A., Maines, J. D., and Palmer, K. J. (1975). Frequency hopping using SAW oscillators. *Ultrason. Symp. Proc.*, pp. 248–250.

Browning, L., and Lewis, M. F. (1978a). A new cut of quartz giving improved temperature stability to SAW oscillators. *Proc. 32nd Annu. Freq. Control Symp.*, pp. 87–94.

Browning, L., and Lewis, M. F. (1978b). A novel technique for improving the temperature stability of SAW SSBW devices. *Ultrason. Symp. Proc.*, pp. 474–477.

Browning, L., Crabb, J., and Lewis, M. F. (1975). A SAW frequency synthesizer. *Ultrason. Symp Proc.*, pp. 245–247.

Browning, L., and Lewis, M. F. (1976). Theory of multimoding in SAW oscillators. *Ultrason. Symp. Proc.*, pp. 256–259.

Campbell, C. K. (1980). Observations on the short term stability of a SAW delay line oscillator. *Ultrason. Symp. Proc.*, pp. 260–263.

Chen, C. L., and Field, M. E. (1977). Injection locking phenomena in SAW oscillators. *Ultrason. Symp. Proc.*, pp. 923–926.

Colvin, R. D. (1980a). UHF acoustic oscillators. *Microwave J.*, **23**, 22, 24, 26, 29–33.

Colvin, R. D. (1980b). Ultrahigh frequency (UHF) acoustic oscillators. *Proc. Soc. Photo-Opt. Instrum. Eng.*, pp. 183–192.

Crabb, J., Lewis, M. F., and Maines, J. D. (1973). Surface-acoustic wave oscillators: mode selection and frequency modulation. *Electron Lett.* 195–197.

Cullen, D. E., Gilden, M., and Montress, G. K. (1978). Design of stable SAW oscillators operating above 1 GHz. *Ultrason. Symp. Proc.*, pp. 433–437.

Davies, L. W., and Lawrence, M. W. (1971). Prospects for surface elastic wave crystal-controlled delay line oscillators. *Proc. Inst. Radio Electron. Eng. Aust.* **32**, 61–62.

Desormiere, B., and Hartemann, P. (1976). Acoustic surface-wave oscillators. *Onde Electr.* **56**, 186–188.

Dodson, D. J., Brunsman, M. D., and Kerr, R. W. (1980a). Injection locked SAW oscillators. *Ultrason. Symp. Proc.*, pp. 268–271.

Dodson, D. J., Lau, K. F., Huang, M. Y., and Lukaszek, T. J. (1980b). SAW stabilized 1680 MHz microwave oscillator. *Proc. 34th Annu. Freq. Control Symp.*, pp. 221–227.

Dolochycki, S. J., Staples, E. J., Wise, J., Schoenwald, J. S., and Lim, T. C. (1979). Hybrid SAW oscillator fabrication and packaging. *Proc. 33rd Annu. Freq. Control Symp.*, pp. 374–378.

Dragonetti, P. G., and Kosco, E. G. (1980). An 840 MHz SAW resonator stabilized radar system oscillator. *Proc. IEEE Int. Symp. Circuits and Systems*, pp. 718–722.

Dvornikov, A. A., Ogurtsov, V. I., and Utkin, G. M. (1979). On the theory of autonomous oscillators containing an acoustical surface wave delay line in the feedback loop. *Radio Eng. Electron. Phys. (Engl. Transl.)* **24**, 100–107.

Eschler, H., Sanchez-Hermosilla, L., Bulst, W. E., and Schucht, P. (1978). Design and construction of SAW oscillators for secondary radar systems. *Proc. 32nd Annu. Freq. Control Symp.*, pp. 58–65.

Gasior, B., Gregorkiewicz, W., and Kaliski, S. (1971). Experimental realization of a generator of spontaneous oscillations on a transverse surface wave. *Proc. Vib. Probl.* **12**, 273–284.

Gilden, M. (1977). Stabilized SAW comb spectrum generators. *Ultrason. Symp. Proc.*, pp. 927–931.

Gilden, M., Reeder, T. M., and DeMaria, A. J. (1975). The mode locked SAW oscillator. *Ultrason. Symp. Proc.*, pp. 251–254.

Gilden, M., Montress, G. J., Cullen, D. E., Wagner, R. A., and Reeder, T. M. (1978). Design of stable SAW oscillators operating above 1 GHz. *Ultrason. Symp. Proc.*, pp. 452–457.

Gilden, M., Montress, G. K., and Wagner, R. A. (1980). Long-term aging and mechanical stability of 1.4 GHz SAW oscillators. *Ultrason. Symp. Proc.*, pp. 184–187.

Grant, P. M., Hussain, K. M., Corner, R. C., and Collins, J. H. (1977). Mobile radio frequency synthesizers based on surface acoustic wave oscillators. *Radio Electron. Eng.* (GB), **47**, 209–216.

Gratze, S. C. (1975). Surface acoustic wave oscillators. *Electron. Ind.* **1**, 20–21, 23.

Gratze, S. C. (1977a). SAW oscillators —their current status. *Microwave J.* **20**, 45–48, 57.

Gratze, S. C. (1977b). The development of surface acoustic wave oscillators. *Electron. Eng.* **49**, 41–43.

Gulyaev, Yu. V., Kotelyansky, I. M., Medved, A. V., and Mishkinis, R. A. (1980). SAW monolithic acoustoelectronic oscillator. *Electron. Lett.* **16**, 114–115.

Gurevich, G. L., Koshurinov, E. I., Paskhin, V. M., and Sandler, M. S. (1978a). Oscillator with discrete frequency tuning and stabilized by surface-acoustic-wave resonator. *Radio Eng. Electron. Phys. (Engl. Transl.)* **23**, 152–155.

Gurevich, G. L., Sandler, M. S., and Sveshnikov, B. V. (1978b). One-frequency operating conditions and their stability in an oscillator employing an acoustic surface wave resonator. *Radio Eng. Electron. Phys. (Engl. Transl.)* **23**, 106–113.

Hartemann, P. (1975). Programmable acoustic-surface-wave oscillator. *Electron. Lett.* **11**, 119–120.

Hartemann, P. (1976). Oscillator temperature stability change induced by ion-implanation. *Ultrason. Symp. Proc.*, pp. 240–242.

Hauden, D., and Theobald, G. (1980). Dynamic thermal sensitivity of SAW quartz oscillators. *Ultrason. Symp. Proc.*, pp. 264–267.

Hauden, D., Michel, M., Bardeche, G., and Gagnepain, J.-J. (1977). Temperature effects on quartz-crystal surface-wave oscillators. *Appl. Phys. Lett.* **31**, 315–317.

Hauden, D., Rousseau, S., and Gagnepain, J.-J. (1980). Sensitivities of SAW oscillators to temperature, forces, and pressure: application to sensors. *Proc. 34th Annu. Freq. Control Symp.*, pp. 312–319.

Henaff, J. (1976). Elastic surface wave oscillators. *Onde Electr.* **56**, 189–196. In French.

Henaff, J. (1979a). Application of SAW oscillators to digital communications. *Ultrason. Symp. Proc.*, pp. 855–860.

Henaff, J. (1979b). Use of surface acoustic wave oscillators in telecommunications systems. *Onde Electr.* **59**, 95–101. In French.

Hohkawa, K., and Yoshikawa, S. (1979a). Surface acoustic wave oscillator with maximally flat temperature coefficient. *J. Acoust. Soc. Jpn.* **35**, 11–20. In Japanese.

Hohkawa, K., and Yoshikawa, S. (1979b). Temperature stable oscillators employing parallel-connected SAW resonators. *Ultrason. Symp. Proc.*, pp. 623–626.

Joseph, T. R. (1976). Phase locked SAW delay line and resonator oscillators. *Ultrason. Symp. Proc.*, pp. 234–239.

Joseph, T. R. (1977). SAW oscillators for phase locked applications. *Proc. 31st Annu. Freq. Control Symp.*, pp. 365–370.

Joshi, N. K. (1979). Surface acoustic waves. *Stud. J. Inst. Electron. Telecommun. Eng.* **20**, 76–83.

Karrer, H. E., and Dias, J. F. (1974). Surface acoustic wave oscillators. *Proc. 28th Annu. Freq. Control Symp.*, pp. 266–269.

Kinsman, R. G. (1978). Temperature compensation of crystals with parabolic temperature coefficients. *Proc. 32nd Annu. Freq. Control Symp.*, pp. 102–107.

Kurahatti, N. G., Dube, N. M., and Roy, M. K. (1978). A novel SAW oscillator. *Electro-Technology (Bangalore, India)* **22**, 73–77.

Kyuma, K., Hyakutake, J., Moriizumi, T., and Yasuda, T. (1977). Proposal and analysis of SAW oscillator using SAW amplifier with segmented structures. *Trans. Inst. Electron. Commun. Eng. Jpn., [Part] E.* **60**, 308–309.

Lantz, A., and Salset, J. (1979). Surface acoustic wave multimode oscillator. *Onde Electr.* **59**, 70–74.

Lao, B. Y., Schneier, N. J., Rowe, D. A., Dietterle, R. E., Schoenwald, J. S., Staples, E. J., and Wise, J. (1981a). Commercial satellite navigation using SAW oscillators. *Proc. 35th Annu. Freq. Control Symp.*, pp. 345–348.

Lao, B. Y., Schneier, N. J., Rowe, D. A., Dietterle, R. E., Schoenwald, J. S., Staples, E. J., and Wise, J. (1981b). SAW oscillators in UHF transit satellite links. *IEEE Trans. Microwave Theory Tech.* **MTT-29**, 1327–1333.

Lau, K. F., Yen, K. H., Kagiwada, R. S., and Kong, A. M. (1980a). A temperature stable 2 GHz SBAW delay line oscillator. *Proc. 34th Annu. Freq. Control Symp.*, pp. 237–242.

Lau, K. F., Yen, K. H., Kagiwada, R. S., and Kong, A. M. (1980b). High frequency temperature stable SBAW oscillators. *Ultrason. Symp. Proc.*, pp. 240–244.

Lawrence, M. W. (1973). Surface-elastic-wave delay-line oscillators. *AWA Tech. Rev.* **15**, 67–76.

Lawrence, M. W. (1976). Surface acoustic wave oscillator. *Wave Electron.* **2**, 199–218.

Lee, D. L. (1979). Design considerations for electronically compensated SAW delay line oscillators. *Ultrason. Symp. Proc.*, pp. 849–854.

Lee, D. L. (1980). *S*-band SSBW delay lines for oscillator applications. *Ultrason. Symp. Proc.*, pp. 245–250.

Lee, L. L., Hunsinger, B. J., and Cho, F. Y. (1975). A SAW-stabilized pulse generator. *IEEE Trans. Sonics Ultrason.* **SU-22**, 141–142.

Leeson, D. B. (1970). Short term stable microwave sources. *Microwave J.* **13**, 59–69.

Leja, I., and Parker, T. E. (1979). High-efficiency SAW oscillator using a dual-gate GaAs FET. *Ultrason. Symp. Proc.*, pp. 865–869.

Levesque, P., Valdois, M., Hauden, D., Gagnepain, J.-J., Hartemann, P., and Uebersfeld, J. (1979). Theoretical and experimental analysis of SAW quartz oscillator acceleration sensitivity. *Ultrason. Symp. Proc.*, pp. 896–899.

Lewis, M. F. (1973). The design, performance and limitations of SAW oscillators. *Int. Spec. Semin. Component Performance and Systems Appl. Surface Acoustic Wave Devices*, pp. 63–72.

Lewis, M. F. (1974a). The surface acoustic wave oscillator—a natural and timely development of the quartz crystal oscillator. *Proc. 28th Annu. Freq. Control Symp.*, pp. 304–314.

Lewis, M. F. (1974b). Surface acoustic wave devices and applications. **VI**. Oscillators—the next successful surface acoustic wave device? *Ultrasonics* **12**, 115–123.

Lewis, M. F. (1976). Oscillators and frequency synthesisers using SAW delay lines as control elements. *Proc. IEEE Int. Symp. Circuits and Systems*, pp. 702–705.

Lewis, M. F. (1979). Temperature compensation techniques for SAW devices. *Ultrason. Symp. Proc.*, pp. 612–622.

Lewis, M. F., and Thorp, T. L. (1978). Status of SAW and SSBW oscillators. *Proc. IEEE Int. Symp. Circuits and Systems*, pp. 553–557.

Maines, J. D., Paige, E. G. S., Saunders, A. F., and Young, A. S. (1969). Simple technique for the accurate determination of delay-time variations in acoustic-surface-wave structures. *Electron. Lett.* **5**, 678–680.

Mannucci, A., and Pantani, L. (1974). Mode selection and transducer design in surface-acoustic-wave oscillators. *Alta Freq.* **43**, 1036–1038.

Montress, G. K., Wagner, R. A., and Gilden, M. (1979). Stable microwave SAW oscillators for aging studies. *Ultrason. Symp. Proc.*, pp. 886–890.

Moriizumi, T., Kyuma, K., Hyakutake, J., and Yasuda, T. (1977). A monolithic surface-wave oscillator using a SAW amplifier and periodic gratings. *Ultrason. Symp. Proc.*, pp. 932–935.

Nandi, A. K., Costanza, S. T., and Wheatley, C. E., III (1974). Surface acoustic wave oscillator experiments. *Proc. 28th Annu. Freq. Control Symp.*, pp. 260–265.

Neylon, S. (1982). Hybrid SAW oscillators. *Microwave J.* **25**, 91–93.

Otto, O. W., and Weglein, R. D. (1976). High frequency periodic grating oscillator. *Ultrason. Symp. Proc.*, pp. 248–251.

Owashi, H., Matsumoto, K., Shiokawa, S., Moriizumi, T., and Yasuda, T. (1979). Experimental realization of SAW amplifier oscillation. *Ultrason. Symp. Proc.*, pp. 891–895.

Owashi, H., Matsumoto, K., Moriizumi, T., and Yasuda, T. (1980). A SAW oscillator using a SAW amplifier. *Trans. Inst. Electron. Commun. Eng. Jpn. [Part] E.* **63**, 768–769.

Parker, T. E. (1977a). Aging characteristics of SAW controlled oscillators. *Ultrason. Symp. Proc.*, 862–866.

Parker, T. E. (1977b). Current developments in SAW oscillator stability. *Proc. 31st Annu. Freq. Control Symp.*, pp. 359–364.

Parker, T. E. (1978). Frequency stability of surface wave controlled oscillators. *Proc. IEEE Int. Symp. Circuits and Systems*, pp. 558–562.

Parker, T. E. (1979a). 1/*f* phase noise in quartz SAW devices. *Electron. Lett.* **15**, 296–298.

Parker, T. E. (1979b). 1/*f* phase noise in quartz delay lines and resonators. *Ultrason. Symp. Proc.*, pp. 878–881.

Parker, T. E. (1980). Analysis of aging data on SAW oscillators. *Proc. 34th Annu. Freq. Control Symp.*, pp. 292–301.

Parker, T. E. (1982). Development of precision SAW oscillators for military applications. *Proc. 36th Annu. Freq. Control Symp.*, pp. 453–458.

Parker, T. E., and Callerame, J. (1981). Sensitivity of SAW delay lines and resonators to vibration. *Ultrason. Symp. Proc.*, pp. 129–134.

Parker, T. E., and Sage, J. P. (1976). A SAW oscillator using two acoustic paths. *Ultrason. Symp. Proc.*, pp. 243–247.

Parker, T. E., and Wichansky, H. (1979). Temperature compensated surface-acoustic-wave devices with SiO_2 film overlays. *J. Appl. Phys.* **50**, 1360–1369.

Pegeot, C., and Sauvage, G. (1980). UHF oscillator using SC-cut quartz crystal with low noise performances and high long term stability. *Proc. 34th Annu. Freq. Control Symp.*, pp. 233–236.

Penavaire, L., Seguignes, D., Lardat, C., Bonnier, J. J., Chevalier, J. Y., and Besson, Y. (1980). A 120 MHz SAW resonator stabilized oscillator with high spectral purity. *Ultrason. Symp. Proc.*, pp. 256–259.

Pookaiyaudom, S. (1975). Surface-acoustic wave delay-line controlled low-frequency oscillators. *Proc. IEEE* **63**, 1071–1072.

Pookaiyaudom, S., and Surawatpanya, C. (1978). Optimum short-term frequency stability improvement in multi-delay line surface-acoustic wave oscillators. *IEEE Trans. Instrum. Meas.* **IM-27**, 86–89.

Ragan, L. H. (1976). Voltage controlled surface wave resonator oscillators. *Ultrason. Symp. Proc.*, pp. 252–255.

Robbins, W. P., and Simpson, E. M. (1979). Tunable surface acoustic wave oscillators using magnetostrictive thin films. *Proc. IEEE* **67**, 1572–1573.

Rousseau, K. V., Yen, K. H., Lau, K. F., and Kong, A. M. (1982). High *Q*, single mode *S*-band SBAW oscillator. *Ultrason. Symp. Proc.*, pp. 279–283.

Ryzhkov, A. V. (1979). Oscillators using surface acoustic waves. *Telecommun. Radio Eng. (Engl. Transl.) Part 2*, **34**, 83–85.

Salmon, S. K. (1978). Surface acoustic wave oscillators at UHF. *Conf. Radio Receivers and Associated Systems*, pp. 101–106.

Salmon, S. K. (1979a). Practical aspects of surface acoustic wave oscillators. *IEEE MTT-S Int. Microwave Symp. Dig.*, pp. 165–167.

Salmon, S. K. (1979b). Practical aspects of surface-acoustic-wave oscillators. *IEEE Trans. Microwave Theory Tech.* **MTT-27**, 1012–1018.

Schaer, A., and Maloney, E. D. (1977). GHz fundamental acoustic-wave oscillators. *Microwave J.* **20**, 41–42.

Slobodnik, A. J., Jr., Colvin, R. D., Roberts, G. A., and Silva, J. H. (1981). A digitally compensated SAW oscillator. *Ultrason. Symp. Proc.*, pp. 135–138.

Staples, E. J., and Lim, T. C. (1977). 300 MHz oscillators using SAW resonators and delay lines. *Proc. 31st Annu. Freq. Control Symp.*, pp. 371–374.

Staples, E. J., Schoenwald, J. S., Dolochycki, S. J., Wise, J., and Lim, T. C. (1979). Application of SAW oscillators to low-noise communications systems. *IEEE MTT-S Microwave Symp. Dig.*, pp. 168–170.

Temmyo, J., and Yoshikawa, S. (1977). Photolithographic contact printing of 0.7 μm linewidth interdigital transducer and 1.1 GHz SAW oscillator. *J. Acoust. Soc. Jpn.* **33**, 549–556. In Japanese.

Temmyo, J., and Yoshikawa, S. (1979). Design and characteristics of a 2 GHz SAW delay line oscillator. *Trans. Inst. Electron. Commun. Eng. Jpn., [Part] E.* **61**, 885–890.

Thorpe, J. C., and Yen, K. H. (1979). 2.148 GHz surface acoustic wave oscillator. *Ultrason. Symp. Proc.*, pp. 882–885.

Urabe, S., Habuka, T., and Matsuura, T. (1982). SAW-resonator stabilized voltage-controlled-oscillator for PLL-FM modulator. *Trans. Inst. Electron. Commun. Eng. Jpn., [Part] E* **65**, 132.

Vaidois, M., Levesque, P., and Hartemann, P. (1977). Acceleration dependence of the surface acoustic wave oscillator frequency. *Ultrason. Symp. Proc.*, pp. 936–938.

Valdois, M., Levesque, P., and Hartemann, P. (1978). Influence of acceleration on surface acoustic wave oscillators. *Proc. AGARD Conf. No. 230. Impact Charge Coupled Devices and Surface Acoustic Wave Devices on Signal Processing and Imagery in Advanced Syst.*, Neuilly-sur-Seine, France, 2.5/1–6. In French.

Vasi'jevic, D. (1978). SAW oscillators. *Tehnika (Belgrade)* **33**, 1797–1799. In Serbo-Croatian.

Vollers, H. G., and Claiborne, L. T. (1974). RF oscillator control utilizing surface wave delay lines. *Proc. 28th Annu. Freq. Control Symp.*, pp. 256–259.

Volluet, G. (1978). Tunable magnetoelastic surface wave oscillators. *Proc. AGARD Conf. No. 230. Impact Charge Coupled Devices and Surface Acoustic Wave Devices on Signal Processing and Imagery in Advanced Syst.*, Neuilly-sur-Seine, France, 2.6/1–10.

Wearden, T. (1981). SAW devices. *Electron. Prod. Des.* **2**, 35–37.

Weglein, R. D. (1977). 1.2 GHz temperature-stable SAW oscillator. *Proc. 31st Annu. Freq. Control Symp.*, pp. 225–230.

Weglein, R. D., and Otto, O. W. (1976). The periodic grating oscillator (PGO). *Proc. 30th Annu. Freq. Control Symp.*, pp. 363–366.

Weglein, R. D., and Otto, O. W. (1977a). Effect of vibration on SAW-oscillator noise spectra. *Electron. Lett.* **13**, 103–104.

Weglein, R. D., and Otto, O. W. (1977b). Microwave SAW oscillators. *Ultrason. Symp. Proc.*, pp. 913–922.

Wilkinson, V. J. (1975). The design and development of a surface acoustic wave oscillator with a frequency modulation capability. *Marconi Rev.* **38**, 65–76.

Wilkinson, V. J., Farr, A. N., Gratze, S. C., and Salter, I. J. (1980). Some recent developments in surface acoustic wave oscillators. *Marconi Rev.* **43**, 96–115.

Williams, D. F., Cho, F. Y., and Sanchez, J. J. (1980). Temperature stable SAW devices using doubly rotated cuts of quartz. *Proc. IEEE Ultrason. Symp.*, pp. 429–433.

Wise, J., Dolochycki, S. J., and Staples, E. J. (1979). The design of SAW oscillators for low noise communications systems. *Proc. IEEE Ultrason. Symp.*, pp. 870–873.

Yamaguchi, M., Takahashi, Y., and Kogo, H. (1980). Discretely variable SAW oscillator. *Proc. IEEE Int. Symp. Circuits and Systems*, pp. 1043–1046.

Section 8.3

Akahane, Y. (1978). Highly precise standard signal circuit for timepiece. *Proc. 32nd Annu. Freq. Control Symp.*, pp. 403–408.

Aker, J. L. (1976). HP-25 calculator serves as clock. *Electronics* **49**, 116.

Aldridge, D., and Mouton, A. (1975). CMOS industrial clock/timer. *New Electron.* **8**, 45, 49.

Allan, D. W. (1966). Statistics of atomic frequency standards. *Proc. IEEE* **54**, 221–230.

Allan, D. W., and Hellwig, H. (1978). Time deviation and time prediction error for clock specification, characterization, and application. *IEEE Position Location and Navigation Symp.*, pp. 29–36.

Anonymous (1969). Radio frequency standards. *Bull. Radio Electr. Eng. Div., Nat. Res. Counc. Can.* **19**, 8.

Anonymous (1970a). A crystal controlled clock pulse generator. *ABU Tech. Rev.* (6), 10–15.

Anonymous (1970b). Review of frequency and time standards. *Instrum. Control-Syst.* **43**, 85.

Anonymous (1971). Characteristics of electromechanical resonators as frequency standards. *Eurocon Digest (IEEE)*, 2 pp.

Anonymous (1973). Development of a generator of standard frequencies. *Toute Electron.* (378), 51–53. In French.

Anonymous (1975). MOS-clock. II. *Elektor* **1**, 634–636.

Anonymous (1976). Crystal timebase for synchronous clocks. *Elektor* **2**, 721.

Anonymous (1977). Stable Pierce oscillator as TTL clock. *Electron. Aust.* **38**, 75.

Anonymous (1978). Economical crystal-controlled clock generator. *Electron. Eng.* **50**, 19.

Anonymous (1980). Long-wave clock with microcomputer. *Elekron. Prax.* **15**, 62, 64, 66. In German.

Arnoldt, M. (1974). 1 Hz quartz time base unit for digital watches. *Funk-Tech.* **24**, 873–874. In German.

Arnoldt, M. (1976). Integrated circuit quartz frequency reference. *Funk-Tech.* **31**, 476–478. In German.

Arnoldt, M. (1977). Quartz clock with six-digit liquid crystal display. *Funk-Tech.* **32**, 301–303, 306–307. In German.

Arnoldt, M. (1978). Universally applicable quartz time base. *Funk-Tech.* **33**, 289–290. In German.

Assmus, F. (1978). The influence of electronics on the development of clocks and watches. *Feinwerktech. Messtech.* **86**, 9–21. In German.

Babbitt, H. S., III (1977). Precision oscillators flown on the LES-8/9 spacecraft. *Proc. 31st Annu. Freq. Control Symp.*, pp. 412–420.

Babitch, D., Ho, J., and Bloch, M. (1972). The disciplined time/frequency standard: a new multi-function crystal oscillator. *Proc. 26th Annu. Freq. Control Symp.*, pp. 264–268.

Banner, G. H. (1967). The standard frequency and time signal installation at Rugby radio station: GPO equipment. *Colloquium Definition, Realisation and Use of Time and Frequency (IEE)*, pp. 6/1–6/10.

Barnes, J. A. (1969). Tables of bias functions B_1 and B_2 for variances based on finite samples of processes with power law spectral densities. *Tech. Note* 375, National Bureau of Standards, Boulder, Colorado.

Barnes, J. A., Chi, A. R., Cutler, L. S., Healey, D. J., Leeson, D. B., McGunigal, T. E., Mullen, J. A., Jr., Smith, W. L., Sydnor, R. L., Vessot, R. F. C., and Winkler, G. M. R. (1971). Characterization of frequency stability. *IEEE Trans. Instrum. Meas.* **IM-20**, 105–120.

Bartholomew, C. A. (1979). Clocks: evolution of frequency standards [Global Positioning System]. *In* "Principles and Operational Aspects of Precision Position Determination System," pp. 7/1–7/11. Report AGARD-AG-245, AGARD, Neuilly sur Seine, France.

Becker, G., and Rohbeck, L. (1975). A standard frequency quartz oscillator, controlled by the DCF 77 radio transmitter. *Elektronik (Munich)* **24**, 74–75. In German.

Begley, W. W., and Shipiro, A. H. (1970). Precision timing system. II. Stable clocks. *Instrum. Control Syst.* **43**, 90–94.

Bennett, C. (1983). SAW resonator stabilized oscillator. *Proc. 37th Annu. Freq. Control Symp.*, pp. 405–409.

Berger, T. V. (1978). Digital RPM-meter and digital quartz clock. *Radio–TV–Electron.* **38**, 42–44. In German.

Bergmann, G. (1978). A quartz crystal controlled clock generator using I^2L technique. *Elektroniker* **17**, 1–5. In German.

Besson, R. J. (1981). New advances in precision quartz oscillators and their impact on quantum standards. *J. Phys. Colloq. (Orsay, Fr.)* **42**, 199.

Besson, J. (1982). Frequency standards and their applications. *Onde Electr.* **62**, 71–79.

Besson, R. J., Emmons, D. A., Girardet, P. G., and Graf, E. P. (1980). Performances of new oscillators designed for "electrodes" crystals. *Proc. 34th Annu. Freq. Control Symp.*, pp. 457–462.

Bhat, C. L., Razdan, H., Sapru, M. L., and Kaul, I. K. (1978). An error monitoring and correction circuit for clocks. *J. Inst. Electron. Telecommun. Eng. (New Delhi)* **24**, 9–13.

Bloch, M. B., and Vulcan, A. I. (1976). The stability of precision oscillators in vibratory environments. *Proc. 30th Annu. Freq. Control Symp.*, pp. 284–291.

Bourgeois, C. (1971). Quartz crystals as frequency standards for wrist watches. *Eurocon Dig. (IEEE)*, 2 pp.

Bourke, B., and Penrod, B. (1983). An analysis of a microprocessor controlled disciplined frequency standard. *Proc. 37th Annu. Freq. Control Symp.*, pp. 485–491.

Breuer, R. (1977a). Circuit for the automatic regulation of digital clocks. Radio Fernsehen Elektron. (Germany), 26, p. 80. In German.

Breuer, R. (1977b). Radio-controlled digital clock. *Radio Fernsehen Elektron.* **26**, 734–736. In German.

Buhrer, C. F. (1976). Color-TV set calibrates standard oscillators. *Electronics* **49**, 114–115.

Bunn, W. (1978). National synchronisation reference clock. *Post Off. Electr. Eng. J.* **71**, 132–135.

Burckardt, G. (1975). Quartz time-piece with gearing mechanism. I. *Funkschau* **47**, 71–74. In German.

Cerzelka, G. (1975). High precision standard frequency spectrum for workshop and amateur. *Funk-Tech.* **30**, 131–135. In German.

Chi, A. R. (1975). Projection of timing capability and spacecraft clock calibration in 1980's. *Int. Telemetering Conf.*, Int. Found. Telemetering, Woodland Hills, California, p. 246.

Cierniewski, S., and Dominski, I. (1973). Quartz generator with $\pm 5.10^{-11}$ diurnal stability. *Postepy Astronaut.* **21**, 313–315. In Pollish.

Coelho, H. (1971). Quartz crystal clock. *Tecnica (Lisbon)* **33**, 519–522. In Portuguese.

Cometta, E. (1977). Electrical pulse clocks and watches. *Elettrificazione (Milan)* (9), 401–409. In Italian.

Cutler, L., and Searle, C. (1966). Some aspects of the theory and measurement of frequency fluctuations in frequency standards. *Proc. IEEE* **54**, 136–154.

Demchuk, M. I., Dmitriev, S. M., and Chernyavskii, A. F. (1977). Investigation of short-term fluctuations of the frequency in quartz shock-excitation generators. *Meas. Tech. (Engl. Transl.)* **20**, 721–725.

Dick, J. S. B. (1977). A perfect . . . [musical standard]. *Electron. Today Int.* p. 86.

Dowsett, J. (1967). Design of a 2.5 Mc/s standard of frequency. *Conf. Freq. Generation and Control Radio Syst. (IEE)*, pp. 58–63.

Dowsett, J. (1968). Design of a 2.5 MHz frequency standard. *Point to Point Telecommun.* **12**, 38–50.

Dunworth, J. V., and Dean, P. (1973). The National Physical Laboratory – aspects of work on the primary standards of measurement. *Proc. R. Soc. Edinburgh, Sect. A, Math. Phys. Sci.* **70**, 125–141.

Easton, R. L., Bartholomew, C. A., and Phillips, D. H. (1968). Crystal oscillator satellite experiment. *Proc. 22nd Annu. Freq. Control Symp.*, pp. 342–353.

Feichtinger, H. (1977). Standard frequency from DCF 77 [radio transmitter]. *Funkschau* **49**, 134–135. In German.

Filler, R. L. (1981). The effect of vibration on frequency standards and clocks. *Proc. 35th Annu. Freq. Control Symp.*, pp. 31–39.

Flanagan, T. M., Palkuti, L. J., Leadon, R. E., and Bloom, G. E. (1977). Hardening frequency standards for space applications. *IEEE Trans. Nucl. Sci.* **NS-24**, 2252–2258.

Gagnepain, J.-J., Ponçot, J.-C., and Pegeot, C. (1977). Amplitude–frequency behavior of doubly rotated quartz resonators. *Proc. 31st Annu. Freq. Control Symp.*, pp. 17–22.

Gerber, E. A., and Sykes, R. A. (1966). State of the art – Quartz crystal units and oscillators. *Proc. IEEE* **54**, 103–116.

Gerz, G., and Weissbacker, K. (1978). Electronic clock generator for the national STD services (EZTGN). *Fernmelde-Praxis* **55**, 177–190. In German.

Giarolli, G., and Perret, J. J. (1981). Standard clock for measuring frequency and time. *Toute Electron.* (468), 63–65. In French.

Gilabert, K., and Larcher, J. (1968). Modern frequency standards. *Onde Electr.* **48**, 382–392. In French.

Graf, E. P., and Walther, B. (1977). Generation of base-band frequencies for FDM and TDM telecommunications. *Proc. 31st Annu. Freq. Control Symp.*, pp. 484–488.

Haag, E. (1979). A radio controlled clock with a midnight detector. I. *Funkschau* **51**, 1527–1531. In German.

Hajek, J. (1975). The Chrometron Quartz crystal-controlled electronic clocks. *Jemna Mech. Opt.* **20**, 55–58. In Czech.

Hajek, J. (1979). Non-autonomous clocks. *Jemna Mech. Opt.* **24**, 17–21. In Czech.

Hegendorfer, M. (1975a). Quartz clock module supplies accurate time, programme number and tuning scale to TV set. *Funkschau* **47**, 51–53. In German.

Hegendorfer, M. (1975b). Quartz-clock module for screen display. *Radio Elektron. Schau* **51**, 562–564. In German.

Hellwig, H. (1972). Frequency standards and clocks. A tutorial introduction. *NBS Tech. Note (U.S.)* 616, 65 pp.

Hellwig, H. (1976). Design principles and characteristics of frequency and time standards. *IEEE Trans. Nucl. Sci.* **NS-23**, 1629–1635.

Hers, J. (1974). Improved portable electronic clock. *Mon. Not. Astron. Soc. S. Afr.* **33**, 118–120.

Hinnah, H. D. (1976). A new type of crystal controlled clock oscillator. *Proc. 26th Electron. Components Conf. (IEEE)*, pp. 203–212.

Holmbeck, J. D. (1971). Standards and the frequency control industry. *Proc. 25th Annu. Freq. Control Symp.*, pp. 34.

Il'nin, V. G., and Teverovskii, V. I. (1969). Design principles of a device for evaluating time and frequency sources. *Meas. Tech. (Engl. Transl.)* (4).

Janicke, J. M. (1979). A wide range frequency standard. *Rev. Telegr. Electron. (Argentina)* **67**, 749–750. In Spanish.

Jenness, C. A., and Morris, R. A. (1977). The television colour burst signal as a secondary frequency standard. *Radio Electron. Eng.* **47**, 567–570.

Kalliomaki, K., Wallin, P., and Vuorinen, J. (1979). National time and frequency standards of Finland. *Radio Sci.* **14**, 677–679.
Karstad, K., and Thurlow, L. (1979). A software-controlled real-time clock. *New Electron.* (12), 26, 28, 30, 32.
Kawasaki, R., Narita, Y., and Fujimori, Y. (1981). The short-term frequency stability measurement of TCXOs and crystal oscillators. *Trans. Inst. Electron. Commun. Eng. Jpn., [Part] E* **64**, 756.
Kogan, L. R. (1970). Oscillator stability requirements in radio interferometers. *Radiotekh. Elektron.* **15**, 1292–1294. In Russian.
Kraengel, W. D., Jr. (1979). Standby crystal time base backs up line-powered clock. *Electronics* **52**, 104–105.
Kramer, G. (1974). Noise in passive frequency standards. *Dig. Conf. Precision Electromagnetic Meas. (IEE)*, pp. 157–159.
Kulpinski, R. J. (1971). Application of crystal clocks for navigation and time-ordered communications. *Proc. 25th Annu. Freq. Control Symp.*, pp. 88–93.
Kusters, J. A., Fischer, M. C., and Leach, J. G. (1978). Dual mode operation of temperature and stress compensated crystals. *Proc. 32nd Annu. Freq. Control Symp.*, pp. 389–397.
LeFevre, E. N. (1969). Frequency standards for H.F. communications. *Proc. 23rd Annu. Freq. Control Symp.*, pp. 198–200.
Lender, R., and Szepan, R. (1978). Digital clock CADM extends R&S standard-frequency line. *News Rohde Schwarz* **18**, 4–7.
Luckau, H., Sellar, D., and Weil, G. (1976). Integrated quartz oscillator Q052. *Components Rep.* **11**, 162–166.
Malde, M. R., Shahasrabudhe, H. V., Kardile, Y. K., and Shah, S. G. (1972). Digital Clock. *J. Inst. Eng. (India), Part ET* **53**, 64–68.
McGuigan, D. F., and Douglass, D. H. (1977). Clocks based upon high mechanical Q single crystals. *Proc. 31st Annu. Freq. Control Symp.*, pp. 616–619.
Miller-Kirkpatrick, J. (1977). 24 hr digital clock with precision time switch. *Pract. Wireless* **53**, 204–209.
Mooser, L. (1967). Crystal frequency standards—applications and characteristics. *News Rohde Schwarz* **7**, 5–8.
Moynahan, C. F. (1972). An improved crystal calibrator using solid-state techniques. *CQ Radio Amat. J.* **28**, 18, 20.
Myers, L. (1978). Understanding precision crystal time bases. *Electronics* **51**, 114–118.
Nagata, M. (1981). Crystal clock oscillators are useful for most digital equipment. *JEE, J. Electron. Eng.* **18**, 54–55.
Nazarov, K. I. (1974). A transportable working frequency standard. *Meas. Tech. (Engl. Transl.)* **17**, 1460–1463.
Nehring, D. (1983). Modeling of TTL inverter amplifiers as applied to overtone crystal clock oscillators. *Proc. 37th Annu. Freq. Control Symp.*, pp. 459–472.
Nichols, S. (1973). A satellite frequency standard system with digital control. *Nat. Telecommun. Conf. (IEEE)* **1**, 19E/1–4.
Nolet, B. (1970). Patterns of electronic luminous clocks. *Electron. Ind.* (139), 775–784. In French.
Nonaka, K., Hanyuda, H., and Odagiri, H. (1981). Simulation for carrying accuracy of quartz watches and its application. *Bull. Ann. Soc. Suisse Chronom. Lab. Suisse Rech. Horlog.* **18**, 111–118.
Nowak, U., and Oszczak, S. (1977). Electronic corrector of the digital quartz clocks indications. *Postepy Astron.* **25**, 187–190. In Polish.
Oakes, J. B., and Mauck, R. A. (1967). A high stability crystal oscillator for the Geos spacecraft. *Conf. Frequency Generation Control Radio Syst. (IEE)*, pp. 53–57.

O'Shea, T., Sullivan, V., and Kindell, R. (1983). Precision L-Band SAW oscillator for satellite application. *Proc. 37th Annu. Freq. Control Symp.*, pp. 394–404.
Paradysz, R. E., and Smith, W. L. (1975). Crystal controlled oscillators for radiation environments. *Radiat. Eff.* **26**, 213–218.
Paulat, A. (1981). A quartz clock with synchronisation to the Omega navigation system, and with coded output signal. *Elektroniker* **20**, EL21–EL22. In German.
Payne, J. B. (1976). Measure and interpret short-term stability. *Microwaves* **15**, 34–35, 38, 41, 43–45.
Penfold, R. A. (1977). CMOS crystal calibrator. *Radio Electron. Constructor* **30**, 615–621.
Pocza, A. (1973). Frequency generators of high accuracy. *Hiradastechn. Ip. Kut. Intez. Kozl.* **24**, 55–60. In Hungarian.
Pogson, I. (1975). Frequency reference derived from VNG. *Electron. Aust.* **37**, 42–45, 47, 49.
Pogson, I. (1979a). Quartz crystal driver for Yaesu Musen clock. *Electron. Aust.* **40**, 44–46.
Pogson, I. (1979b). Quartz multiple frequency reference. *Electron. Aust.* **41**, 56–57, 59, 61, 63, 125.
Prat, M. (1974). Electronic clocks and watches. *Rev. Esp. Electron.* **21**, 48–50. In Spanish.
Prinz, D. (1975). A world time accessory for digital clocks. *Funkschau* **47**, 63–65. In German.
Prokysek, J. (1974). Electronic clocks and watches with crystal-controlled oscillator. *Jemna Mech. Opt.* **19**, 248–250. In Czech.
Prokysek, J. (1979). On the problems of setting the accuracy of crystal-controlled electronic clocks and watches. *Jemna Mech. Opt.* **24**, 23–26. In Czech.
Pustarfi, H. S. (1966). An improved 5 MHz reference oscillator for time and frequency standard applications. *IEEE Trans. Instrum. Meas.* **IM-15**, 196–202.
Rayer, F. G. (1974). 1 MHz crystal marker. *Radio Electron. Constructor* **28**, 22–24.
Reinhardt, V. S., and Costlow, R. J. (1983). Frequency (standard) combined selector. *Proc. 37th Annu. Freq. Control Symp.*, pp. 97–110.
Rhode, U. L. (1978). Mathematical analysis and design of an ultra stable low noise 100 MHz crystal oscillator with differential limiter and its possibilities in frequency standards. *Proc. 32nd Annu. Freq. Control Symp.*, pp. 409–425.
Rowe, J. (1977). Digital quartz clock module runs from 12 V. *Electron. Aust.* **39**, 50–51.
Rutman, J. (1978). Characterization of phase and frequency instabilities in precision frequency sources: fifteen years of progress. *Proc. IEEE* **66**, 1048–1075.
Saburi, Y. (1977). Precision of time standard and its applications. *Oyo Butsuri* **46**, 1203–1210. In Japanese.
Saxena, G. M., and Mathur, B. S. (1980). Stability measurements in time domain using dual-mixer time difference system. *Indian J. Pure Appl. Phys.* **18**, 220–223.
Schlenk, K. W. (1976). Electric clock installations in design and practice. *Elektromeister und Dtsch. Elektrohandwerk* **51**, 183–186, 199.
Schlenzig, K. (1977). Crystal-controlled clock with automatic time announcement. *Radio Fernsehen Elektron.* **26**, 168–171. In German.
Schlenzig, K. (1979). Extended application of quartz clocks. *Radio Fernsehen Elektron.* **28**, 55–57. In German.
Schreiber, H. (1977). Radio controlled digital clock with improved safety from disturbances. *Funk-Tech.* **32**, 358–936. In German.
Sen, A. K., and Saha, B. (1973). Worldwide standards of time and frequency. *J. Sci. Ind. Res.* **32**, 300–311.
Simpson, L. (1979). 4 to 6-digit quartz clock. *Electron. Aust.* **40**, 40–41, 43–44.
Spadoni, E. R. (1975). A versatile secondary frequency standard. *CQ Radio Amat. J.* **31**, 31–32.
Stadler, K. (1968). Low-noise frequency standard XSS. *News Rohde Schwarz* **8**, 22–25.
Stein, S. R., and Walls, F. L. (1978). Composite oscillator systems for meeting user needs for time and frequency. *IEEE Position Location Navigation Symp.*, pp. 22–28.

Steiner, C. (1970). From quartz clocks to electronic quartz wrist watches. *Jemna Mech. Opt.* **15**, 158–160. In Czech.

Suard, J. G. (1975). Industrial aspects of quartz clockmaking. *RGE, Rev. Gen. Electr.* **84**, 931–939. In French.

Takakuwa, S. (1981). Crystal clock oscillators are indispensable for digital equipment age. *JEE, J. Electron. Eng.* **18**, 73–76.

Taylor, J. H. (1983). Pulsars: Nature's most precise clocks. *Proc. 37th Annu. Freq. Control Symp.*, p. 6.

Uebersfeld, J., and Rutman, J. (1975). Stability characterization of frequency standards. *Colloq. Int. l'Electron. Mesure*, pp. 101–110. In French.

Veazey, R. L., and Nieman, T. A. (1977). Laboratory real time clock featuring computer, experiment, and manual interaction. *Anal. Chem.* **49**, 1466–1468.

Viehmann, H. H. (1979). Longwave clock with microcomputer SAB 8048 (8748). *Components Rep.* **14**, 204–208.

Viehmann, H. H. (1980). Time signal clock designed by Viehmann. *Radio Mentor Electron.* **46**, 32–33. In German.

Viney, K. (1977). Secondary standards [frequency]. *Radio Commun.* **53**, 862–863.

Voss, R. F. (1979). $1/f$ noise. *Proc. 33rd Annu. Freq. Control Symp.*, pp. 40–46.

Vovelle, P. (1975). Technical aspects of quartz clockwork. *RGE, Rev. Gen. Electr.* **84**, 919–930. In French.

Warner, A. W. (1960). Design and performance of ultraprecise 2.5 Mc quartz crystal units. *Bell Syst. Tech. J.* **39**, 1193–1217.

Wilhelmy, H. J. (1974). New quartz clocks. *Elektronik (Munich)* **23**, 261–262. In German.

Wilhelmy, H. J. (1976). Quartz crystal clocks and watches for the consumer. *Elektronik (Munich)* **25**, 67–72. In German.

Yasuda, Y. (1973). Accuracy of estimating clockface and rate of the frequency standards by normal regression theory. *Rev. Radio Res. Lab.* **19**, 21–30. In Japanese.

Zilio, G. (1981). Measurement of the short time stability of a frequency source. *Elettron. Oggi* (11), 115–118. In Italian.

Zima, V., Buzek, O., Hrdlicka, J., and Cermak, J. (1973). Secondary frequency standard controlled by radio signals in the range of long waves and very long waves. *EMISCON (Brno, Czechoslovakia: CSTV House of Technics)*, pp. 314–320. In Czech.

Chapter 9

Al'tshuller, G. B. (1967). Temperature compensation for frequency-controlled quartz oscillators. *Telecommun. Radio Eng. (Engl. Transl.)*, Part 1 (2), 49–51.

Ashida, T. (1970). Low temperature coefficient lithium niobate resonators by use of temperature sensitive capacitances. *Proc. IEEE* **58**, 146–147.

Ballato, A. (1977). Doubly rotated thickness mode plate vibrators. *In* "Physical Acoustics—Principles and Methods," Vol. 13 (W. P. Mason and R. N. Thurston, eds.), pp. 115–181. Academic Press, New York.

Ballato, A. (1978). Frequency-temperature-load capacitance behavior of resonators for TCXO application. *IEEE Trans. Sonics Ultrason.* **SU-25**, 185–191.

Batdorf, H. A. (1969). Temperature-compensated crystal-controlled oscillators operating from 800 kHz to 1500 kHz. *Proc. 23rd Annu. Freq. Control Symp.*, pp. 192–197.

Berry, B. S., and Pritchet, W. C. (1971). Temperature-compensation for constant-frequency electromechanical oscillators. *IBM Tech. Disclosure Bull.* **40**, 1237–1238.

Bozic, S. M. (1968). Temperature compensation of frequency in crystal oscillators using varactor diodes. *Electron. Eng.* **40**, 670–672.

Brekenfeld, H. (1975). Aspects of precision thermostats for quartz oscillators. *Feingeraetetechnik* **24**, 72–76.

Browning, L., and Lewis, M. (1978). A new cut of quartz giving improved temperature stability to SAW oscillators. *Proc. 32nd Annu. Freq. Control Symp.*, pp. 87–94.

Brunner, J. (1972). Wide-range temperature compensation by addition of two crystal-resonator frequencies: applications to quartz and $LiTaO_3$. *Electron. Lett.* **8**, 639–640.

Brunner, J. (1975). Wide-range temperature compensation by addition of two crystal-resonator frequencies: practical results with quartz and $LiTaO_3$. *Electron. Lett.* **11**, 304–305.

Burgoon, R., and Wilson, R. (1979). Design aspects of an oscillator using the SC cut crystal. *Proc. 33rd Annu. Freq. Control Symp.*, pp. 411–416.

Buroker, G. E. (1972). "High-Stability Temperature-Compensated Crystal Oscillator Study (HSTCXO). Report ECOM-0136-1 on Contract DAAB07-71-C-0136. Available as document AD-738837 from the National Technical Information Service, Springfield, Virginia.

Buroker, G. E., and Frerking, M. E. (1973). A digitally compensated TCXO. *Proc. 27th Annu. Freq. Control Symp.*, pp. 191–198.

Duckett, P., Pedito, R., and Chizak, G. (1970). Temperature compensated crystal oscillators. *Proc. 24th Annu. Freq. Control Symp.*, pp. 191–199.

Fewings, D. J., and Ince, C. R. S. (1967). A new form of temperature compensated crystal oscillator. *Conf. Freq. Generation Control Radio Syst.* IEE Conference Publication No. 31, pp. 38–41.

Fewings, D. J., and Ince, C. R. S. (1968). A self-compensating crystal oscillator. *Marconi Rev.* **31**, 57–78.

Forster, H. J. (1975). Temperature-compensated crystal oscillators for 2 MHz to 60 MHz. *Siemens Rev.* **42**, 545–549.

Frerking, M. E. (1978). "Crystal Oscillator Design and Temperature Compensation." Van Nostrand-Reinhold, Princeton, New Jersey.

Frerking, M. E. (1979). The application of microprocessors to communications equipment design. *Proc. 33rd Annu. Freq. Control Symp.*, pp. 431–435.

Frerking, M. E. (1982). Methods of temperature compensation. *Proc. 36th Annu. Freq. Control Symp.*, pp. 564–570.

Fujii, S., and Uchida, H. (1975). An analysis of frequency stability for TCXO (temperature compensated crystal oscillators). *Proc. 29th Annu. Freq. Control Symp.*, pp. 294–299.

Fujii, S., and Uchida, H. (1976). Improvement of frequency stability for TCXO. *NEC Res. Dev.* (43), 75–80.

Fujii, S., Kudo, T., Takodo, H., and Yamamoto, T. (1981). A new frequency temperature compensation method for TCXO [crystal oscillators]. *NEC Res. Dev.* (63), 74–82.

Gagnepain, J.-J., and Marianneau, G. (1980). Digital temperature control for ultrastable quartz oscillators. *Proc. 34th Annu. Freq. Control Symp.*, pp. 52–57.

Galla, W. D., and McVey, E. S. (1980). TCXO error due to aging adjustment. *Proc. 34th Annu. Freq. Control Symp.*, pp. 504–509.

Gerber, E. A., and Miles, M. H. (1961). Reduction of the frequency-temperature shift of piezoelectric resonators by mechanical stress. *Proc. IRE* **49**, 1650–1654.

Gniewinska, B., Kwiatkowska, D., and Rozwadowski, M. (1978). Temperature gradient free change of state [crystal oven]. *Elektronika* **19**, 511–512. In Polish.

Goodacre, J. B. (1968). Temperature control of a crystal-oscillator oven. *Control* **12**, 420–424.

Grabar, L. I., and Stebletsov, V. M. (1971). Thermal compensation of quartz-crystal oscillators. *Othor Peredacha Inf.* (30), 90–94. In Russian.

Greenhouse, H. M., McGill, R. J., and Clark, D. P. (1973). A fast warmup quartz crystal oscillator. *Proc. 27th Annu. Freq. Control Symp.*, pp. 199–217.

Grisdale, G. L., and Pipe, H. J. (1967). Miniature low-consumption crystal ovens. *Conf. Freq. Generation Control Radio Syst.* IEE Conference Publication No. 31, pp. 42–46.

Hajek, J. (1975). Temperature compensation of a crystal oscillator. *Sdelovaci Tech.* **23**, 151. In Czech.

Hamatsuki, T., Goto, T., and Uchida, H. (1973). High stability integrator-controlled oven for crystal oscillators. *Proc. 27th Annu. Freq. Control Symp.*, pp. 218–226.

Hardingham, C. (1967). Temperature-compensated crystal oscillators—a review of recent Australian developments. *Proc. IREE Aust.* **28**, 424–434.

Hart, R. K., and Hicklin, W. H. (1972). "Tactical Miniature Crystal Oscillator." Report ECOM-0301-1 on Contract DAABU7-71-C-0301. Available as document AD-74927 from the National Technical Information Service, Springfield, Virginia.

Hellé, J. (1975). VCXO—theory and practice. *Proc. 29th Annu. Freq. Control Symp.*, pp. 300–307.

Henaff, J., and Feldmann, M. (1978). A SAW temperature compensated oscillator using the difference between metallized and free delay temperature coefficients on $LiTaO_3$. *Ultrason. Symp. Proc.*, pp. 448–451.

Hinnah, H., and Newell, D. E. (1968). Automatic compensation equipment for TCXCs. *Proc. 22nd Annu. Freq. Control Symp.*, pp. 298–310.

Hirama, K. (1972). A temperature-compensated crystal oscillator utilizing three crystals. *Proc. 26th Annu. Freq. Control Symp.*, pp. 132–139.

Hirama, K. (1973). A temperature-compensated three-crystal oscillator. *Electron. Commun. Jpn.* **56**, 33–40.

Hirama, K., and Onoe, M. (1972). A temperature compensated crystal oscillator utilizing three crystals. *Proc. 26th Annu. Freq. Control Symp.*, pp. 132–139.

Ho, J., and Bloch, M. (1977). A fast warmup oscillator for the GPS receiver. *Proc. 31st Annu. Freq. Control Symp.*, pp. 421–428.

Hohkawa, K., and Yoshikawa, S. (1979a). Temperature compensated SAW oscillator employing multiple resonators with the same electrodes pattern. *Trans. Inst. Electron. Commun. Eng. Jpn. [Part] E* **62**, 689–690.

Hohkawa, K., and Yoshikawa, S. (1979b). Temperature-compensated SAW oscillator construction employing multiple resonators. *IEEE Trans. Sonics Ultrason.* **SU-26**, 348–353.

Hornung, F. (1968). A new circuit for equalizing the parabolic temperature performance of quartz oscillators. *Frequenz* **22**, 233–337. In German.

Hutton-Penman, P. R., and Billinshurst, F. M. (1967). Temperature control of a master oscillator by deep burial. *Conf. Freq. Generation Control Radio Syst.* IEE Conference Publication No. 31, pp. 64–71.

Hykes, G. R., and Newell, D. E. (1961). A temperature-compensated frequency standard. *Proc. 15th Annu. Freq. Control Symp.*, pp. 297–317.

Ikebe, T. (1975). Theory of controlling a small thermostatic oven (crystal oscillator frequency stability). *Anritsu Tech. Bull.* (33), 9–15. In Japanese.

Ivanchenko, Yu. S., and Medvedev, V. N. (1978). Computer-aided design of heat-compensated quartz-crystal oscillators. *Izv. Vyssh. Uchebn. Zaved. Radioelektron.* **21**, 139–142. In Russian.

Jeziorowski, M. (1972). Analysis of frequency variation of thermally compensated oscillators. *Pr. Inst. Tele. Radiotech.* **16**, 17–28. In Polish.

Jeziorowski, M. (1979). New designs of compensating circuits for temperature compensated crystal oscillators—TCXO. *Pr. Inst. Tele. Radiotech.* (71), 59–67. In Polish.

Kinsman, R. G. (1978). Temperature compensation of crystals with parabolic temperature coefficients. *Proc. 32nd Annu. Freq. Control Symp.*, pp. 102–107.

Kudo, T., Fujii, S., and Nanamatsu, S. (1983). A new frequency temperature compensation method for oscillators. *Proc. 37th Annu. Freq. Control Symp.*, pp. 448–453.

Kusters, J. A., Fischer, M. C., and Leach, J. G. (1978). Dual mode operation of temperature and stress compensated crystals. *Proc. 32nd Annu. Freq. Control Symp.*, pp. 389–397.

Kwiatkowska, D. K., and Rozwadowski, M. (1970). Thermostat for frequency standards. *Pomiary Autom. Kontrola* **16**, 256. In Polish.

Lewis, M. (1979). Temperature compensation techniques for SAW devices. *Ultrason. Symp. Proc.*, pp. 612–622.

Marianneau, G., and Gagnepain, J.-J. (1980). Digital temperature control for ultrastable quartz oscillators. *Proc. 34th Annu. Freq. Control Symp.*, pp. 52–57.

Maries, V. A. (1974). Synthesis and analysis of an electric circuit for the exact thermocompensation of quartz crystal oscillators for three temperatures. *Stud. Cercet. Energ. Electroteh.* **24**, 519–530. In Rumanian.

Maries, V. A. (1976). Analysis of an electric circuit for the thermocompensation of quartz crystal oscillators at four temperatures. *Rev. Roum. Sci. Tech. Ser. Electrotech Energ.* **21**, 75–84.

Mathieson, P. H. (1975). Economical crystal oven. *Electron. Aust.* **37**, 77.

McVey, E. S., and Swanson, C. T. (1978). Capacitor temperature-compensated crystal oscillators. *IEEE Trans. Ind. Electron. Control Instrum.* **IECI-25**, 164–166.

Michowski, K. (1976). Computer aided design of the temperature compensation of crystal oscillators. *Arch. Elektrotech. (Warsaw)* **25**, 255–269. In Polish.

Miguel, E. K. (1982). A temperature compensated SC cut quartz crystal oscillator. *Proc. 36th Annu. Freq. Control Symp.*, pp. 576–585.

Mroch, A. B., and Hykes, G. R. (1976). A miniature high stability TCXO using digital compensation. *Proc. 30th Annu. Freq. Control Symp.*, pp. 292–300.

Namekawa, H., and Honda, S. (1971). A design of temperature compensation network for quartz crystal oscillator by a successive approximation method. *J. Fac. Eng., Ibaraki Univ.*, pp. 95–102. In Japanese.

Nelson-Jones, L. (1970). Crystal oven and frequency standard. *Wireless World* **76**, 269–273.

Newell, D. E., and Hinnah, H. (1968). Automatic compensation equipment for TCXOs. *Proc. 22nd Annu. Freq. Control Symp.*, pp. 298–310.

Newell, D. E., and Hinnah, H. (1969). A Report on TCXOs and segmented compensation. *Proc. 23rd Annu. Freq. Control Symp.*, pp. 187–191.

O'Connell, R. M., and Carr, P. H. (1977). Temperature compensated cuts of berlinite and beta-eucryptite for SAW devices. *Proc. 31st Annu. Freq. Control Symp.*, pp. 182–186.

Okano, S., Mitsuoka, T., and Ohshima, T. (1980). Direct-temperature compensated crystal oscillator for recent advanced VHF/UHF radio communication system. *Proc. 34th Annu. Freq. Control Symp.*, pp. 488–497.

Onoe, M., Yamagishi, I., and Narai, H. (1978). Temperature compensation of crystal oscillator by microprocessor. *Proc. 32nd Annu. Freq. Control Symp.*, pp. 398–402.

Page, P. B. (1967). Temperature compensation of quartz crystal oscillators. *Conf. Freq. Generation Control Radio Syst.* IEE Conference Publication No. 31, pp. 33–37.

Page, P. B. (1972a). Wide range temperature compensation of miniature quartz crystal oscillators. I. *Electron. Components* **13**, 22, 24–26.

Page, P. B. (1972b). Wide range temperature compensation of miniature quartz crystal oscillators. II. *Electron. Components* **13**, 381–384.

Page, P. B. (1972c). Wide range temperature compensation of miniature quartz crystal oscillators. III. Compensating circuit synthesis. *Electron. Components.* **13**, 429–431.

Page, P. B. (1974). Wide range temperature compensation for miniature quartz oscillators. I. *Elektron. Anz.* **6**, 203–205.

Pavlovec, J. (1979). Rectification of the temperature dependence of the frequency generated by an oscillator using piezoelectric crystal units. *Slaboproudy Obz.* **40**, 463–468. In Czech.

Pichl, H. (1971). Design of high quality thermostats for crystal oscillators. *Int. Elektron. Rundsch.* **25**, 249–251. In German.

Podgorski, A., and Gniewinska, B. (1977). Automatic production of thermally compensated quartz generators. *Pol. Tech. Rev.* (7), 12–13.

Pogson, I. (1977). Temperature compensated crystal oscillator. *Electron. Aust.* **39**, 80–81, 83.
Pompei, J., and Kerforne, J. F. (1970). A temperature-compensated quartz oscillator. *Onde Electron.* **50**, 32–37. In French.
Prak, J. W. L., and Peduto, R. J. (1972). Digital IC's set temperature compensation for oscillators. *Electronics* **45**(17), 124–126.
Pupeza, D., and Maries, V. (1975). Thermal compensation of quartz oscillators. *Electroteh. Electron. Autom. Autom. Electron.* **19**, 170–174. In Rumanian.
Raghavan, R. S., Vetelino, J. F., and Jhunjhunwala, A. (1979). Temperature compensation with metallic overlay films on quartz. *Ultrason. Symp. Proc.*, pp. 606–611.
Renard, A. M., and Barnhill, K. (1981). Digital temperature compensation of crystal oscillators. *Proc. 35th Annu. Freq. Control Symp.*, pp. 455–457.
Roberts, E. A. (1968). Temperature compensation of AT cut crystals by thermally controlled non-linear reactances. *Proc. 22nd Annu. Freq. Control Symp.*, pp. 325–339.
Rosati, V., Schodowski, S., and Filler, R. (1983). Temperature compensated crystal oscillator survey and test results. *Proc. 37th Annu. Freq. Control Symp.*, pp. 501–505.
Rozwadowski, M. (1978). Application of crystal oscillators in modern telecommunication equipments. *Przegl. Telekomun.* **51**, 147. In Polish.
Ruback, R. (1982). Dual mode digitally temperature compensated crystal oscillator. *Proc. 36th Annu. Freq. Control Symp.*, pp. 571–575.
Sarkar, S. K. (1974). Explicit expressions for TCXO (temperature-compensated crystal oscillator) design. *Proc. 28th Annu. Freq. Control Symp.*, pp. 232–236.
Schodowski, S. (1966). Aging of temperature-compensated crystal oscillators. *Proc. IEEE* **54**, 808–809.
Schodowski, S. (1970). New approach to a high stability temperature compensated crystal oscillator. *Proc. 24th Annu. Freq. Control Symp.*, pp. 200–208.
Scott, P. J. (1977). Design considerations for a digitally temperature compensated crystal oscillator. *Proc. 31st Annu. Freq. Control Symp.*, pp. 407–411.
Slobodnik, A., Colvin, R., Roberts, G., and Silva, J. (1982). Reducing SAW oscillator temperature sensitivity with digital compensation. *Proc. 36th Annu. Freq. Control Symp.*, pp. 486–491.
Smirnov, V. I. (1970). Method of compensating the temperature instability of the frequency of a crystal-controlled oscillator. *Telecommun. Radio Eng. (Engl. Transl.)* **25**(10), 134–136.
Smith, D. A., and Holmes, P. A. (1971). Temperature compensated crystal oscillators. *Electron. Equipment News* **13**, 14–19.
Soluch, W. (1978). Piezoelectric crystals. *Elektronika* **19**, 8–12. In Polish.
Suzuki, F., Yoshida, M., and Morokawa, S. (1981). Integrated temperature compensation IC system for 32 kHz quartz wristwatch. *Bull. Ann. Soc. Suisse Chronom. Lab. Suisse Rech. Horlog.* **10**, 139–146.
Swanson, C. T., and McVey, E. S. (1979). A non-iterative solution for a two-thermistor TCXO. *Proc. 33rd Annu. Freq. Control Symp.*, pp. 425–430.
Teramachi, Y., Horie, M., Kataoka, H., and Musha, T. (1979). Frequency response of quartz oscillator to temperature fluctuation. *Proc. 33rd Annu. Freq. Control Symp.*, pp. 235–238.
Théobald, G., Marianneau, G., Prétot, R., and Gagnepain, J.-J. (1979). Dynamic thermal behavior of quartz resonators. *Proc. 33rd Annu. Freq. Control Symp.*, pp. 239–246.
Thomann, D. L. (1974). A microcircuit temperature compensated crystal oscillator (MCTCXO). *Proc. 28th Annu. Freq. Control Symp.*, pp. 214–220.
Tinta, F. G., Matistic, A. S., and Lagasse, G. A. (1970). The direct temperature control of quartz crystals in evacuated enclosures. *Proc. 24th Annu. Freq. Control Symp.*, pp. 157–167.
Turlington, I. R. (1979). Temperature controller for crystal resonators. *NASA Tech. Briefs* **4**(3), 320.

Uno, T., and Shimoda, Y. (1983). A new digital TCXO circuit using a capacitor-switch array. *Proc. 37th Annu. Freq. Control Symp.*, pp. 434–441.
Valentin, J. P. (1980). Internal heating and thermal regulation of bulk quartz resonators. *Proc. 34th Annu. Freq. Control Symp.*, pp. 194–201.
Vasil'yev, Yu. A., Il'ichev, V. A., and Chernobylkin, V. V. (1977). Optimizing the resistances of resistors in temperature-compensating networks for crystal oscillators. *Telecommun. Radio Eng. (Engl. Transl.) Part 2* **32**, 143–144.
Vovelle, P. G. (1968). Recent improvements to TCXO. *Proc. 22nd Annu. Freq. Control Symp.*, pp. 311–324.
Warwick, G. A., Gosling, W., and Prescott, A. J. (1978). A digital technique for temperature compensation of crystal oscillators. *Conf. Radio Receivers and Associated Syst. (IERE)*, pp. 207–216.
Whitten, S. V., Jr. (1971). A practical approach to the design of a temperature compensated crystal oscillator. *Nat. Telemetering Conf. Record (IEEE)*, pp. 54–59.
Wilson, J. S. (1983). An improved method of temperature compensation of crystal oscillators. *Proc. 37th Annu. Freq. Control Symp.*, pp. 442–447.
Zahariev, K. T. (1981). Method for compensating the temperature dependence of quartz generators by means of a controllable in-series capacitance. *Elektroprom. Proborostr.* **16**, 163–164. In Bulgarian.

Chapter 10

Abashev, Yu. G., Voronin, G. F., and Valitov, R. A. (1972). Velocity distribution in an atomic beam. *Meas. Tech. (Engl. Transl.)* **15**, 1679–1681.
Abashev, Yu. G., Voronin, G. F., and Kul'chatskii, N. A. (1976). Investigation of the angular distribution of cesium atoms diffusing from rectangular channels [time-frequency standard]. *Meas. Tech. (Engl. Transl.)* **19**, 1590–1594.
Alekseev, E. I., and Bazarov, E. N. (1970). Theory of a rubidium maser generator using optical pumping. *Radiotekh. Elektron.* **15**, 1044–1051. In Russian.
Alekseev, E. I., and Bazarov, E. N. (1975). Light-induced shifts of a quantum frequency standard with optical pulse pumping and optical display of a Ramsey line with suppressed side maxima [^{87}Rb]. *Sov. J. Quantum Electron. (Engl. Transl.)* **5**, 563–567.
Alekseev, E. I., Bazarov, Ye. N., and Grigor'ev, V. I. (1968). The effect of the filtering conditions of the light pump on the frequency of the O–O transition of the Rb^{87} atoms. *Radiotekh. Elektron.* **13**, 1041–1044. In Russian.
Alekseev, E. I., Bazarov, E. N., and Levshin, A. E. (1969). Frequency shifts due to the luminous pump in a passive frequency standard using Rb atoms. *Radiotekh. Elektron.* **14**, 2026–2035. In Russian.
Alekseev, E. I., Bazarov, E. N., and Levshin, A. E. (1974a). Theory of frequency standard with pulsed optical pumping. *Radio Eng. Electron. Phys. (Engl. Transl.)* **19**, 77–83.
Alekseev, E. I., Bazarov, E. N., and Telegin, G. I. (1974b). Frequency shifts in a standard with pulsed optical pumping and a continuous microwave field. *Radio Eng. Electron. Phys. (Engl. Transl.)* **19**, 87.
Alekseev, E. I., Bazarov, Ye. N., and Gubin, V. P. (1974c). Light shifts in a frequency standard with a rubidium cell in the presence of spatial separation of the optical pumping and interaction with the microwave field. *Radio Eng. Electron. Phys. (Engl. Transl.)* **19**, 58–63.
Alekseev, E. I., Bazarov, E. N., and Telegin, G. I. (1974d). Optical indication of the Ramsey structure of the line of the O–O transition of Rb^{87} atoms. *Radio Eng. Electron. Phys. (Engl. Transl.)* **19**, 88–91.

Alekseev, E. I., Bazarov, Ye. N., and Telegin, G. I. (1975a). Light shifts in a quantum frequency standard with pulsed optical pumping and optical indication of the Ramsey structure of the O–O transition line of Rb^{87} atoms. *Radio Eng. Electron. Phys. (Engl. Transl.)* **20**, 73–80.

Alekseev, E. I., Bazarov, Ye. N., and Telegin, G. I. (1975b). The change in the Ramsey structure of the O–O transition line of Rb^{87} atoms with an increase in the number of microwave pulses in the intervals between the optical pumping pulses. *Radio Eng. Electron. Phys. (Engl. Transl.)* **20**, 145–147.

Alekseev, E. I., Bazarov, Ye. N., Gubin, V. P., and Telegin, G. I. (1979). A study of the performance factor of a quantum frequency standard with pulsed optical pumping of Rb^{87} vapors. *Radio Eng. Electron. Phys. (Engl. Transl.)* **24**, 108–113.

Al-Jumaily, A.-R. M. (1979). "Double Beam Ammonia Maser Operated with an Open Resonator." Ph.D. Thesis, University of Keele, Staffs, England.

Allan, D. W., and Barnes, J. A. (1974). Modeling and optimum utilization of high performance clocks. *CPEM Dig.*, pp. 277–278.

Allan, D. W., Glaze, D. J., Machlan, H. E., Wainwright, A. E., Hellwig, H., Barnes, J. A., and Gray, J. E. (1973). Performance, modeling, and simulation of some cesium beam clocks. *Proc. 27th Annu. Freq. Control Symp.*, pp. 334–346.

Allan, D. W., Hellwig, H., Jarvis, S., Jr., Howe, D. A., and Garvey, R. M. (1977). Some causes and cures of frequency instabilities (drift and noise) in cesium beam frequency standards. *Proc. 31st Annu. Freq. Control Symp.*, pp. 555–561.

Andersen, S. G., Mortelmans, H. O., Wauters, P. J., and DePrins, J. (1968). Some experimental results of BaO applicable to a molecular beam frequency standard. *Proc. 22nd Annu. Freq. Control Symp.*, pp. 517–528.

Andresen, H. G. (1969). Atomic beam preparation for hydrogen maser operation with unpolarized atoms. *Z. Phys.* **223**, 71–102.

Andresen, H. G. (1970). Hydrogen maser atomic beam resonances. *Z. Phys.* **233**, 293–307.

Annabi, M., and Gillet, D. (1973). Adiabatic passage on the electric dipole transitions of a molecular beam traversing an inhomogeneous magnetic field. *C.R. Hebd. Seances Acad. Sci., Ser. B* **277**, 515–517. In French.

Anonymous (1969). Time studies with hydrogen maser. *Sci. Dimension (Canada)* **1**, 3–5. In English and French.

Anonymous (1971). Hydrogen frequency measured accurately. *Nat. Bur. Stand. (U.S.), Tech. News Bull.* **55**, 194–205.

Anonymous (1973). Frequency and time standard of the Dr. Neher Laboratory. *Data (The Netherlands)* **74**, 81–97. In Dutch.

Anonymous (1974). 2.2-pound rubidium standard for systems uses only 12 W. *Electron. Des.* **22**, 72.

Anonymous (1975). "Cesium-Atomic Beam Oscillator Technology for Navigation Satellites." Report by Frequency & Time Systems, Inc., under contract N00014-74-C-0061. Available from the National Technical Information Service, Springfield, Virginia.

Anonymous (1978). Construction of an improved cesium frequency standard (NRLM-II). *Jpn. J. Appl. Phys.* **17**, 749–750.

Arditi, M. (1981). Microwave Ramsey pattern in a laser pumped cesium beam. *J. Phys. Colloq. (Orsay, Fr.)* **42**, 261–269.

Arditi, M. (1982). A caesium beam atomic clock with laser optical pumping, as a potential frequency standard. *Metrologia* **18**, 59–66.

Arditi, M., and Cérez, P. (1972). Hyperfine structure separation of the ground state of ^{87}Rb measured with an optically pumped atomic beam. *IEEE Trans. Instrum. Meas.* **IM-21**, 391–395.

Arditi, M., and Picqué, J.-L. (1980a). Preliminary operation of a laser optically pumped caesium beam atomic clock. *C.R. Hebd. Seances Acad. Sci., Ser. B* **290**, 461–464. In French.

Arditi, M., and Picqué, J.-L. (1980b). A cesium beam atomic clock using laser optical pumping. Preliminary tests. *J. Phys. Lett. (Orsay, Fr.)* **41**, L379–L381.

Audoin, C. (1967). The hydrogen maser in a transient mode. *Rev. Phys. Appl.* **2**, 309ff. In French.

Audoin, C. (1973a). State of the art in the field of very stable frequency generators. *Onde Electr.* **53**, 39–45. In French.

Audoin, C. (1973b). Ultrastable atomic and molecular oscillators and their applications in navigation. *Navigation* **21**, 281–297. In French.

Audoin, C. (1981). Fast cavity auto-tuning systems for hydrogen masers. *Rev. Phys. Appl.* **16**, 125–130.

Audoin, C., and Jardino, M. (1978). Frequency offset due to spectral impurities in cesium beam frequency standards. *CPEM Dig.*, p. 4.

Audoin, C., and Schermann, J.-P. (1971). Physics of the hydrogen maser. *In* "Advances in Atomic and Molecular Physics," Vol. 7 (D. R. Bates and I. Esterman, eds.), pp. 1–45. Academic Press, New York.

Audoin, C., and Vanier, J. (1976). Atomic frequency standards and clocks. *J. Phys. E.* **9**, 697–720.

Audoin, C., Benoit, H., Desaintfuscien, M., Piejus, P., and Schermann, J.-P. (1968a). Triplet decomposition of the line $\Delta M = 0$ of a hydrogen maser under the influence of transitions between the Zeeman sub-levels. *C.R. Hebd. Seances Acad. Sci., Ser. B* **266**, 1521–1524. In French.

Audoin, C., Desaintfuscien, M., Petit, P., and Schermann, J.-P. (1968b). Design of a double focalisation in a hydrogen maser. *Conf. Precision Electromagn. Meas. (IEEE)*, pp. 49–50.

Audoin, C., Desaintfuscien, M., Schermann, J.-P., and Viennet, J. (1968c). Experimental study of a synchronised hydrogen maser. *C.R. Hebd. Seances Acad. Sci., Ser. B* **266**, 1264–1267. In French.

Audoin, C., Desaintfuscien, M., and Schermann, J.-P. (1968d). Application of the transient behavior to the study of the hydrogen maser. *Proc. 22nd Annu. Freq. Control Symp.*, pp. 493–516.

Audoin, C., Desaintfuscien, M., Petit, P., and Schermann, J.-P. (1969a). Efficiency of a single-hyperfine-state selector for hydrogen masers. *Electron. Lett.* **5**, 292–293.

Audoin, C., Desaintfuscien, M., Piejus, P., and Schermann, J.-P. (1969b). A new method for measurement of the population difference of hyperfine-levels of stored atoms. *Proc. 23rd Annu. Freq. Control Symp.*, pp. 288–296.

Audoin, C., Desaintfuscien, M., Piejus, P., and Schermann, J.-P. (1969c). Double-resonance method for the determination of level populations. *IEEE J. Quantum Electron.* **QE-5**, 431–434.

Audoin, C., Desaintfuscien, M., and Schermann, J.-P. (1969d). Dynamical time constants of the hydrogen maser and atomic relaxation times. *Phys. Lett. A* **30**, 321–322.

Audoin, C., Duchene, J.-L., and Schermann, J.-P. (1969e). Measurement of the populations of the atomic jet in a hydrogen maser. *C.R. Hebd. Seances Acad. Sci., Ser. B* **268**, 1757–1760. In French.

Audoin, C., Lesage, R., and Mungall, A. G. (1974a). Second order Doppler and cavity phase dependent frequency shifts in atomic beam frequency standards. *CPEM Dig.*, pp. 160–161.

Audoin, C., Lesage, P., and Mungall, A. G. (1974b). Second-order Doppler and cavity phase dependent frequency shifts in atomic beam frequency standards. *IEEE Trans. Instrum. Meas.* **IM-23**, 501–508.

Audoin, C., Jardino, M., Cutler, L. S., and Lacey, R. F. (1978a). Frequency offset due to spectral impurities in cesium-beam frequency standards. *IEEE Trans. Instrum. Meas.* **IM-27**, 325–329.

Audoin, C., Lesage, P., Viennet, J., and Barillet, R. (1978b). Analysis of H-maser autotuning systems. *Proc. 32nd Annu. Freq. Control Symp.*, pp. 531–541.

Audoin, C., Lesage, P., Viennet, J., and Barillet, R. (1980). Theory of hydrogen-maser autotuning systems based on the frequency or the phase method. *IEEE Trans. Instrum. Meas.* **IM-29**, 98–104.

Audoin, C., Viennet, J., and Lesage, P. (1981). Hydrogen maser: active or passive? *J. Phys. Colloq. (Orsay, Fr.)* **42**, 159–170.

Bahadur, H., and Parshad, R. (1974). Atomic frequency standards—a review. *J. Sci. Ind. Res.* **33**, 561–569.

Bahadur, H., and Parshad, R. (1976). Optical pumping for alkali gas cell frequency standard. *J. Opt. (India)* **5**, 59–67.

Bailey, R., Mungall, A. G., and Daams, H. (1967). The design, construction, and performance of a cesium-beam tube. *IEEE Trans. Instrum. Meas.* **IM-16**, 319–326.

Baker, M., Levine, M., Mueller, L., and Vessot, R. (1968). Progress in the development of hydrogen masers. *Proc. 22nd Annu. Freq. Control Symp.*, pp. 605–620.

Balogh, F. (1974). Frequency standards. *Meres Autom.* **22**, 417–421. In Hungarian.

Bangham, N. J., and Donaldson, R. W. (1971). Hydrogen maser work at the NPL. Report NPL-QU-17. National Physics Laboratory, Teddington, England, 14 pp.

Bardo, W. S. (1971). Oscillation transient in a molecular Q-switched ammonia maser. *J. Phys. D.* **4**, L42–L44.

Bardo, W. S., and Lainé, D. C. (1969). Induced spiking in an ammonia-maser oscillator. *Electron. Lett.* **5**, 688–689.

Bardo, W. S., and Lainé, D. C. (1971a). Ammonia maser operated without cryogenic pumping. *J. Phys E.* **48**, 595–597.

Bardo, W. S., and Lainé, D. C. (1971b). On detuning phenomena in cascaded cavity molecular beam masers. *J. Phys. B.* **4**, 1523–1535.

Barillet, R. (1976). Electronic circuits showing a level-independent phase shift for hydrogen-maser work applications. *IEEE Trans. Instrum. Meas.* **IM-25**, 465–468.

Barillet, R., and Audoin, C. (1976). Electronic circuits showing a level independent phase shift for hydrogen maser work applications. *Conf. Precision Electromagn. Meas. (IEEE)*, pp. 228–229.

Barnes, J. A. (1970). Frequency measurement errors of passive resonators caused by frequency-modulated exciting signals. *IEEE Trans. Instrum. Meas.* **IM-19**, 147–152.

Barnes, J. A., and Winkler, G. M. R. (1974). The standards of time and frequency in the USA. *NBS Tech. Note (U.S.)* 649, 86 pp.

Barnes, J. A., Chi, A. R., Cutler, L. S., Healey, D. J., Leeson, D. B., McGunigal, T. E., Mullen, J. A., Jr., Smith, W. L., Sydnor, R. L., Vessot, R. F. C., and Winkler, G. M. R. (1971). Characterization of frequency stability. *IEEE Trans. Instrum. Meas.* **IM-20**, 105–120.

Bashkin, A. S. (1971). Current status and development prospects of quantum frequency standards (review). *Krantovaya Elektron. (Kiev)* (5), 3–27. In Russian.

Basov, N. G., and Prokhorov, A. M. (1970). Possible methods of obtaining active molecules for a molecular oscillator. *In* "Maser, the Solid State," pp. 114–116. Pergamon, Oxford.

Basov, N. G., Borisenko, M. I., Vlasov, V. P., Dubonosov, S. P., Ivanov, N. E., Strakhovskii, G. M., Fedorenko, G. M., and Chikhakhev, B. M. (1967). Operating experience with a satellite-borne maser oscillator. *Cosmic Res. (Engl. Transl.)* **5**, 526–532.

Bava, E., Marchi, A. De. Rovera, G., Beverini, N., and Strumia, F. (1975). Measurements on optically pumped cesium vapor frequency standard. *Alta Freq.* **44**, 574–578.

Bazarov, Ye. N. (1969). Approximate theory of optically pumped rubidium vapor maser oscillator. *Radiotekh. Elektron.* **14**, 1035–1042. In Russian.

Bazarov, Ye. N., and Grigorev, V. I. (1969). Frequency shift of $S_{1/2}, F = 2, m = 0 \leftarrow S_{1/2}, F = 1, m_f = 0$ transition frequency of rubidium atoms using pulsed optical pumping. *Radiotekh. Elektron.* **14**, 1056–1064. In Russian.

Bazarov, Ye. N., and Gubin, V. P. (1969a). Experimental study of a fixed operating range of optically pumped rubidium vapour maser oscillator. *Radiotekh. Elektron.* **14**, 1043–1049. In Russian.

Bazarov, Ye. N., and Gubin, V. P. (1969b). Light frequency shift in a rubidium maser oscillator using modulated optical pumping. *Radiotekh. Elektron.* **14**, 1050–1055. In Russian.

Bazarov, Ye. N., and Gubin, V. P. (1970). Short-term frequency instability of an optically pumped rubidium maser. *Radio Eng. Electron. Phys. (Engl. Transl.)* **15**, 1860–1867.

Bazarov, Ye. N., Biketov, V. D., and Gubin, V. P. (1972a). Short-term instability of an optically pumped rubidium maser standard. *Radio Eng. Electron. Phys. (Engl. Transl.)* **17**, 697–699.

Bazarov, Ye. N., Biketov, V. D., Gubin, V. P., and Yukhvidin, Ya. A. (1972b). The effect of the buffer gas on the operation of an optically pumped Rb maser. *Radio Eng. Electron. Phys. (Engl. Transl.)* **17**, 432–439.

Bazarov, Ye. N., Gubin, V. P., and Telegin, G. I. (1973). Experimental study of shifts of the frequency of the $S = 1/2, F = 2, m = 0 \rightleftarrows S = 1/2, F = 1, m = 0$ transition of Rb^{87} atoms for pulsed optical pumping. *Radio Eng. Electron. Phys. (Engl. Transl.)* **18**, 1530–1535.

Becker, G. (1974). Time keeping at the Physikalisch-Technische Bundesanstalt and the primary time and frequency standard CS1 [caesium atomic beam standard]. *CPEM Dig.*, pp. 152–154.

Becker, G. (1976a). Recent progress in primary Cs beam frequency standards at the PTB. *IEEE Trans. Instrum. Meas.* **IM-25**, 458–465.

Becker, G. (1976b). Work on primary Cs beam frequency standards at the PTB. *Conf. Precision Electromagn. Meas. (IEEE)*, pp. 226–227.

Becker, G. (1977). Performance of the primary Cs-standard of the Physikalisch-Technische Bundesanstalt. *Metrologia* **13**, 99–104.

Becker, G. (1978a). Research on Cs beam frequency standards at the PTB: beam optics. Majorana transitions. *IEEE Trans. Instrum. Meas.* **IM-27**, 319–325.

Becker, G. (1978b). Research on primary Cs-beam time and frequency standard at the PTB. *CPEM Dig.*, pp. 1–2.

Becker, G. (1980a). Uncertainty of Cesium-beam time standards due to beam asymmetry. *IEEE Trans. Instrum. Meas.* **IM-29**, 297–300.

Becker, G. (1980b). Uncertainty of the primary Cs clock CS1 of the PTB. *CPEM Dig.*, p. 137.

Becker, G. (1982). "Exclusive flop-out" beam optics for the new primary-cesium clocks of the PTB. *Metrologia* **18**, 17–21.

Becker, G., Fischer, B., Kramer, G., and Muller, E. K. (1971). The primary time and frequency standard of the Physikalisch-Technische Bundesanstalt. *Eurocon Dig. (IEEE)*, 1 p.

Beehler, R. E. (1971). Cesium atomic beam frequency standards. *Proc. 25th Annu. Freq. Control Symp.*, pp. 297–308.

Beehler, R. E., and Glaze, D. J. (1966). Evaluation of a thallium atomic beam frequency standard at the National Bureau of Standards. *IEEE Trans. Instrum. Meas.* **IM-15**, 55–58.

Bell, C. M., and Babitch, D. (1968). A system analysis of the cesium beam atomic clock. *IEEE Trans. Instrum. Meas.* **IM-17**, 155–166.

Bender, P., and Cohen, V. W. (1970). New information on the physics of rubidium gas cells. *Proc. 24th Annu. Freq. Control Symp.*, p. 279.

Bennett, T. J., Hayes, R. E., Norton, G. T., and Zepler, M. M. (1971). A simplified rubidium atomic frequency source. *Syst. Technol.* (12), 7–11.

Ben-Reuven, A., and Kukolich, S. G. (1973). Relaxation rates in molecular beam maser experiments. *Chem. Phys. Lett.* **23**, 376–380.

Bernier, L. G., Brisson, A., Tetu, M., Savard, J. Y., and Vanier, J. (1980). Possible avenues of improvement of the short and long term stability of optically pumped passive rubidium frequency standards. *Proc. 34th Annu. Freq. Control Symp.*, pp. 376–383.

Bespalova, M. P., Mishakov, G. A., and Pikhtelev, A. I. (1973). Frequency shifts of the standard atomic transition in Rb^{87} appearing with optical pumping in a passive frequency standard. *Radio Eng. Electron. Phys. (Engl. Transl.)* **18**, 1707–1714.

Bespalova, M. P., Bogoslovskii, N. N., Kulagin, E. V., Kisel'nikova, S. I., Pikhtelev, A. I., and Ul'yanov, A. A. (1974). Some frequency characteristics of the Rb^{87} pair quantum frequency standard. *Izv. Vyssh. Uchebn. Zaved Radiofiz.* **17**, 767–770. In Russian.

Beverini, N., and Strumia, F. (1971). On the population inversion between the hyperfine sublevels of Cs. *Opt. Commun.* **4**, 56–57.

Beverini, N., and Vanier, J. (1979). Tuning of hydrogen maser cavity by means of a variable capacitance diode. *IEEE Trans. Instrum. Meas.* **IM-28**, 100–104.

Bogdan, D. A., and Demidov, N. A. (1971). Measurement of hydrogen atom temperature in the source of H-maser beam. *Izv. Vyssh. Uchebn. Zaved. Radiofiz.* **14**, 575–579. In Russian.

Bogdan, D. A., Demidov, N. A., Ezhov, E. M., Lavrov, A. I., Logachev, V. A., Sakharov, B. A., Chernov, G. M., Ul'yanov, A. A., Fateev, B. P., and Sharov, Yu. P. (1974). A hydrogen frequency standard. *Meas. Tech. (Engl. Transl.)* **17**, 1701–1704.

Bollinger, J. J., Itano, W. M., and Wineland, D. J. (1983). Laser cooled $^9Be^+$ accurate clock. *Proc. 37th Annu. Freq. Control Symp.*, pp. 37–41.

Bottcher, S., and Fruhauf, T. (1976). Rubidium oscillator XSRB. *News Rohde Schwarz* **16**, 22–23.

Brenner, D. (1970). Absolute frequency of the hydrogen maser using a flexible storage bulb. *J. Appl. Phys.* **41**, 2942–2950.

Brillet, A. (1981). Evaluation of the light shifts in an optically pumped cesium beam frequency standard. *Metrologia* **17**, 147–150.

Brousseau, R., and Vanier, J. (1971). Stimulated emission in a hydrogen maser. *Phys. Canada* **27**, 56. In French.

Brousseau, R., and Vanier, J. (1973). An electronic system for the tuning of maser. *IEEE Trans. Instrum. Meas.* **IM-22**, 367–375.

Brunet, M. (1978). Rubidium standards. *Mes. Regul. Autom.* **43**, 67–75. In French.

Busca, G., and Brandenberger, H. (1979). Passive H maser. *Proc. 33rd Annu. Freq. Control Symp.*, pp. 563–568.

Busca, G., Têtu, M., and Vanier, J. (1973a). Cavity tuning and light-shift in the Rb^{87} maser. *Proc. 27th Annu. Freq. Control Symp.*, pp. 400–403.

Busca, G., Têtu, M., and Vanier, J. (1973b). Light shift and light broadening in the Rb^{87} maser. *Can. J. Phys.* **51**, 1379–1387.

Busca, G., Têtu, M., and Vanier, J. (1973c). Light shift effects in the ^{87}Rb maser. *Appl. Phys. Lett.* **23**, 395–396.

Busca, G., Racine, J., and Vanier, J. (1974). A compact Rb^{87} maser. *Proc. 28th Annu. Freq. Control Symp.*, pp. 344–347.

Busca, G., Brousseau, R., and Vanier, J. (1975). Long-term frequency stability of the Rb^{87} maser. *IEEE Trans. Instrum. Meas.* **IM-24**, 291–296.

Busca, G., Savard, J.-Y., Rovea, S., Vanier, J., Petit, P., and Audoin, C. (1977). Zeeman effects on H and Rb masers. *Proc. 31st Annu. Freq. Control Symp.*, pp. 535–541.

Busca, G., Addor, F., Hadorn, F., Nicolas, G., Prost, L., Brandenberger, H., Thomann, P., and Johnson, L. (1982). Preliminary measurements on EFOS 1 H maser. *Proc. 36th Annu. Freq. Control Symp.*, pp. 260–264.

Cerez, P., and Bennett, S. J. (1978). New developments in iodine stabilized He-Ne lasers. *CPEM Dig.*, p. 72.

Cerez, P., and Hartmann, F. (1977). Theoretical analysis of the operation of an optically pumped rubidium atomic beam clock. *IEEE J. Quantum Electron.* **QE-13**, 344–351.

Chanchulski, A. (1975). Atomic frequency standards. *Pol. Tech. Rev.* (10), 2–3.

Checkrahamatoula (1968). A study of oscillation level saturation of the hydrogen maser as a function of the atomic flux entering the cavity. *Ann. Phys. (Paris)* **3**, 145–154. In French.

Cheng, Y. M., Hua, Y. L., Chen, C. B., Gao, J. H., and Shen, W. (1980). Hydrogen maser wall shift experiments and determination of the unperturbed hyperfine frequency of the ground state of the hydrogen atom. *IEEE Trans. Instrum. Meas.* **IM-29**, 316–319.

Chi, A. R., Roeder, J. H., Wardrip, S. C., and Kruger, B. (1968). Long-term frequency stability measurement of rubidium gas cell frequency standards. *Proc. 22nd Annu. Freq. Control Symp.*, pp. 592–605.

Chi, A. R., Major, F. G., and Lavery, J. E. (1970a). Frequency comparison of five commercial standards with a NASA experimental hydrogen maser. *Proc. 24th Annu. Freq. Control Symp.*, pp. 301–307.

Chi, A. R., Major, F. G., and Lavery, J. E. (1970b). Frequency comparison of five commercial cesium standards with a NASA experimental hydrogen maser. *Proc. IEEE* **58**, 142–143.

Chuang, C. H., and Jair, T. C. (1980). Atomic time and frequency standards development at Shanghai observatory, China. *IEEE Trans. Instrum. Meas.* **IM-29**, 158–163.

Citterio, R. (1979). Principles of the atomic clock. *RTE (Switzerland)* (12), 47, 49, 53. In German.

Clemence, G. M., and Szebehely, V. (1967). Annual variation of an atomic clock. *Astron. J.* **72**, 1355, 1324–1326.

Colson, C. (1982). Vibration compensation of the Seektalk rubidium oscillator. *Proc. 36th Annu. Freq. Control Symp.*, pp. 197–199.

Cordwell, C. R. (1968). "Frequency Standards," IEE. London. 14 pp.

Costain, C. C., Mungall, A. G., Daams, H., and Boulanger, J. S. (1981). A review of primary caesium clock development and satellite time comparison techniques at NRC. *J. Inst. Electron. Telecommun. Eng. (New Delhi)* **27**, 438–442.

Crampton, S. B. (1979). Improving maser frequency stability. *NASA Tech. Briefs* **4**, 357–358.

Crampton, S. B., and Wang, H. T. M. (1974). Density-dependent shifts of hydrogen maser standards. *Proc. 28th Annu. Freq. Control Symp.*, pp. 355–361.

Crampton, S. B., Fleri, E. C., and Wang, H. T. M. (1977). Effects of atomic resonance broadening mechanisms on atomic hydrogen maser long-term frequency stability. *Metrologia* **13**, 131–135.

Crampton, S. B., Krupczak, J. J., and Souza, S. P. (1981). Progress of the state-selected beam low temperature hydrogen maser. *J. Phys. Colloq. (Orsay, Fr.)* **42**, 181–184.

Cutler, L. S., and Vessot, R. F. C. (1968). Present status of clocks and frequency standards. *NEREM Record (IEEE)*, pp. 68–69.

Cutler, L. S., Giffard, R. P., and McGuire, M. D. (1983). Mercury-199 trapped ion frequency standard: recent theoretical progress and experimental results. *Proc. 37th Annu. Freq. Control Symp.*, pp. 32–36.

Daams, H. (1974a). Corrections for second order Doppler shift and cavity phase error in cesium atomic beam frequency standards. *CPEM Dig.*, pp. 162–163.

Daams, H. (1974b). Corrections for second-order Doppler shift and cavity phase error in cesium atomic beam frequency standards. *IEEE Trans. Instrum. Meas.* **IM-23**, 509–514.

Daams, H. (1976). Errors in cesium beam frequency standards due to small asymmetries in the beam excitation. *Conf. Precision Electromagn. Meas. (IEEE)*, pp. 235–236.

Daams, H. (1970). Cesium beam servo system using square wave frequency modulation. *Proc. 24th Annu. Freq. Control Symp.*, pp. 294–300.

Davidovits, P., and Novick, R. (1966). The optically pumped rubidium maser. *Proc. IEEE* **54**, 155–170.

Debely, P. (1970a). Hydrogen maser with deformable storage bulb. *Proc. 24th Annu. Freq. Control Symp.*, pp. 259–262.

Debely, P. E. (1970b). Hydrogen maser with deformable storage bulb. *Rev. Sci. Instrum.* **41**, 1290–1292.

Dehmelt, H. G. (1967). Radiofrequency spectroscopy of stored ions. *In* "Advances in Atomic and Molecular Physics," Vol. 3, pp. 109–154. Academic Press, New York.

DeLucia, F. (1969). Molecular-beam maser for the shorter-millimeter-wave region: spectral constraints of HCN and DCN. *Phys. Rev.* **187**, 58–65.

De Marchi, A. (1981). Improved performances in Cs standards with new-design resonators. *J. Phys. Colloq. (Orsay, Fr.)* **42**, 289–296.

De Marchi, A., and Bava, G. P. (1978). Stability limits for frequency standards using divergent beams. *Metrologia* **14**, 179–183.

De Marchi, A., Bava, E., Godone, A., and Giusfredi, G. (1982). Merits and limitations of sub-mm wavelength frequency standards based on a Mg(Ca) metastable beam. *CPEM Dig.*, p. M/3.

Demidov, N. A., Ezhov, E. M., Ul'yanov, A. A., and Fedorov, V. A. (1977). Frequency shifts of a hydrogen generator due to hydrogen atom collisions with storage flask walls. *Meas. Tech. (Engl. Transl.)* **20**, 1000–1002.

Desaintfuscien, M., and Audoin, C. (1974). Measurement of the time constant for filling the "storage flask" of a hydrogen maser. *C.R. Hebd. Seances Acad. Sci., Ser. B* **279**, 657–660. In French.

Desaintfuscien, M., Petit, P., Audoin, J. P., and Schermann, J.-P. (1970). Oscillation of a hydrogen maser for ambient temperatures between 77 and 293 K. *C.R. Hebd. Seances Acad. Sci., Ser. B* **270**, 906–908. In French.

Desaintfuscien, M., Audoin, C., and Petit, P. (1971). Method of measurement of relaxation times T_1 and T_2 of the hydrogen maser, for any value of atomic flux. *C.R. Hebd. Seances. Acad. Sci., Ser. B* **272**, 676–679. In French.

Desaintfuscien, M., Viennet, J., and Audoin, C. (1977). Discussion of temperature dependence of wall and spin exchange effects in the hydrogen maser. *Metrologia* **13**, 127–130.

Dicke, R. M. (1953). The effect of collisions upon the doppler width of spectral lines. *Phys. Rev.* **89**, 472–473.

Dittmann, H., and Kalau, M. (1978). The national time and frequency standard of the German Democratic Republic. *Radio Fernsehen Elektron.* **27**, 381–382. In German.

Dorenwendt, K. (1981). Development and performance of primary standards at the PTB. *J. Phys. Colloq. (Orsay, Fr.)* **42**, 229–231.

Dyubko, S. F., Efimenko, M. N., Svich, V. A., and Fesenko, L. D. (1976). Stimulated emission of radiation from optically pumped vinyl bromide molecules. *Sov. J. Quantum Electron. (Engl. Transl.)* **6**, 600–601.

Egorov, V. K., and Maslov, V. A. (1979). Optimum conditions for population inversion for the O–O transition in Cs^{133}. [Frequency standard]. *Sov. Tech. Phys. Lett. (Engl. Transl.)* **5**, 420–421.

Elkin, G. A. (1976a). Doppler frequency shift in atomic standards. *Meas. Tech. (Engl. Transl.)* **19**, 1594–1596.

Elkin, G. A. (1976b). Effect of output-signal-spectrum sidebands and resonator detuning on the frequency of an atomic standard. *Meas. Tech. (Engl. Transl.)* **19**, 1587–1588.

Elkin, G. A., and Zhestkova, N. D. (1979). Collision-dependent frequency shift in an atomic-hydrogen clock. *Meas. Tech. (Engl. Transl.)* **22**, 1076–1078.

Elkin, G. A., Zhestkova, N. D., and Kurnikov, G. P. (1973). Error reproduction of the frequency of undisturbed transition of the hydrogen atom. *Meas. Tech. (Engl. Transl.)* **16**, 394–397.

Elkin, G. A., Zhestkova, N. D., and Paramzin, V. A. (1977). Measuring wall-induced frequency shift in a hydrogen oscillator. *Meas. Tech. (Engl. Transl.)* **20**, 1453–1455.

Elkina, L. P., Elkin, G. A., and Strakhovskii, G. M. (1968). Measurement of the frequency drift of a hydrogen standard owing to atomic impacts on the flask wall. *Meas. Tech. (Engl. Transl.)* **6**, 841–842.

Emmons, D. A., and Rogers, P. J. (1979). New cesium beam tube utilizing hexapole state selection. *Proc. 33rd Annu. Freq. Control Symp.*, pp. 490–493.

English, T. C., and Jechart, E. (1981). Development of a sapphire lamp for use in satellite-borne atomic rubidium clocks. *Proc. 35th Annu. Freq. Control Symp.*, pp. 637–645.

Ermakov, V. I., Zemskov, E. M., and Sachkov, V. I. (1966). Certain errors in reproducing the frequency of a cesium reference standard, which are due to the electronic equipment. *Meas. Tech. (Engl. Transl.)* **9**, 1177–1181. In Russian.

Ernvein-Pecquenard, J. (1968). Atomic clock using sequential optical pumping. *Ann. Radioelectr.* **23**, 137–154. In French.

Ernvein-Pecquenard, J., and Mainar, L. (1969). Atomic clock with sequential optical pumping. *C.R. Hebd. Seances Acad. Sci., Ser. B* **268**, 817–820. In French.

Essen, L. (1971). Atomic standards of time. *Alta Freq.* **40**, 679–683.

Essen, L., and Parry, J. V. L. (1956). Atomic and astronomical time. *Nature* **177**, 744–745.

Essen, L., and Sutcliffe, D. S. (1969). Improvement to the National Physical Laboratory atomic clock. *Nature* **223**, 602–603.

Essen, L., Donaldson, R. W., Bangham, M. J., and Hope, E. G. (1971). Frequency of the hydrogen maser. *Nature* **229**, 110–111.

Essen, L., Donaldson, R. W., Hope, E. G., and Bangham, M. J. (1973). Hydrogen maser work at the National Physical Laboratory. *Metrologia* **9**, 128–137.

Farmer, D. J., and Long, J. D. (1967). Atomic frequency standards for special applications. *Conf. Freq. Generation and Control Radio Syst. (IEE)*, pp. 16–28.

Feldman, M., Bergquist, J. C., Lewis, L. L., and Walls, F. L. (1981). Preliminary investigation of a new optically pumped atomic rubidium standard. *Proc. 35th Annu. Freq. Control Symp.*, pp. 625–636.

Finnie, C., Sydnor, R., and Sward, A. (1971). Hydrogen maser frequency standard. *Proc. 25th Annu. Freq. Control Symp.*, pp. 348–351.

Fischer, M. C., and Heger, C. E. (1976). Measured performance and environmental sensitivities of a rugged cesium beam frequency standard. *Proc. 30th Annu. Freq. Control Symp.*, pp. 463–467.

Forman, P. (1982). Atomic clock: preview of an exhibit at the Smithsonian. *Proc. 36th Annu. Freq. Control Symp.*, pp. 220–222.

Frayne, P. G. (1969). Repetitive Q-modulated HCN gas maser. *J. Phys. B* **2**, 247–259.

Frerking, M. E. (1972). Ruggedized rubidium frequency standard. *Proc. IEEE* **60**, 628–629.

Frerking, M. E., and Johnson, D. E. (1972). Rubidium frequency and time standard for military environment. *Proc. 26th Annu. Freq. Control Symp.*, pp. 216–222.

Fruhauf, T. (1977). Improved rubidium frequency standard XSRM. *News Rohde Schwarz* **17**, 37.

Fruhauf, T., and Szepan, R. (1978). Crystal, rubidium, caesium: complete standard-frequency line. *News Rohde Schwarz* **18**, 4–9.

Fukuyo, H. (1975). Time and frequency standards. *J. Soc. Instrum. Control Eng. Jpn.* **14**, 521–528. In Japanese.

Fukuyo, H., Iga, K., Kuramochi, N., Matsuda, I., and Ishikawa, H. (1971). Fundamental characteristics and frequency stability in the early stage of a laboratory-made Rb atomic oscillator. *Bull. Tokyo Inst. Technol.* (107), 75–88.

Fuller, D. W. E., Hines, J., and Compton, B. (1969). Short-term frequency stability of the HCN maser. *Electron. Lett.* **5**, 448–449.

Gaigerov, B. A. (1973). Automatic stabilization of the magnetic field in a hydrogen generator. *Meas. Tech. (Engl. Transl.)* **16**, 464–465.

Gaigerov, B. A. (1979). Hydrogen masers with automatically tuned resonators. *Meas. Tech. (Engl. Transl.)* **22**, 1082–1086.

Gaigerov, B. A., and Elkin, G. A. (1968). Automatic tuning of the resonator of the hydrogen frequency standard. *Meas. Tech. (Engl. Transl.)* (6), 839–840.

Gaigerov, B. A., Elkin, G. A., Elkina, L. P., Zhestkova, N. D., Kurnikov, G. P., and Popov, B. P. (1972). Hydrogen maser as a quantum frequency standard. *Meas. Tech. (Engl. Transl.)* **15**, 1640–1643.

Ganter, W. A. (1973). Modeling of atomic clock performance and detection of abnormal clock behavior. *NBS Tech. Note (U.S.)* 636, 30 pp.

Garvey, R. M. (1981). Approaches to the realization of improved clock performance in cesium based devices. *J. Phys. Colloq. (Orsay, Fr.)* **42**, 185–188.

Garvey, R. M. (1982). A cesium beam frequency standard with microprocessor control. *Proc. 36th Annu. Freq. Control Symp.*, pp. 236–239.

Garvey, R. M., Hellwig, H. W., Jarvis, S., Jr., and Wineland, D. J. (1978). Two-frequency separated oscillating fields technique for atomic and molecular beam spectroscopy. *IEEE Trans. Instrum. Meas.* **IM-27**, 349–354.

George, J., and Vulcan, A. I. (1977). Development of a cesium beam clock for satellite application. *Proc. 31st Annu. Freq. Control Symp.*, pp. 542–550.

Gheorghiu, O. C., and Gheorghe, V. N. (1975). Characteristics of a UHF discharge used as atomic source for a maser. *Int. J. Electron.* **39**, 329–335.

Gheorghiu, O. C., and Giurgiu, L. C. (1975). The hydrogen maser of the Institute of Physics in Bucharest, Romania. *Rev. Roum. Phys.* **20**, 305–307.

Gheorghiu, O. C., and Mandache, C. M. (1979). On a hydrogen dissociator for maser. *Rev. Roum. Phys.* **24**, 317–323.

Gheorghiu, O., Viennet, T., Petit, P., and Audoin, C. (1974). Automatic tuning of the resonant cavity of hydrogen atomic clocks. *C.R. Hebd. Seances Acad. Sci., Ser. B* **278**, 109–161. In French.

Gheorghiu, O., Gheorghe, V., Giurgiu, L., Mandache, C., Bocaniciu, T., and Iordachescu, T. (1977). Hydrogen masers as frequency standards. *Metrol. Apl.* **24**, 75–77.

Glaze, D. J. (1970). Improvements in atomic cesium beam frequency standards at the National Bureau of Standards. *IEEE Trans. Instrum. Meas.* **IM-19**, 156–160.

Glaze, D. J., Hellwig, H., Jarvis, S., Jr., Wainwright, A. E., and Allan, D. W. (1973). Recent progress on the NBS primary frequency standard. *Proc. 27th Annu. Freq. Control Symp.*, pp. 347–356.

Glaze, D. J., Hellwig, H., Allan, D. W., Jarvis, S., Jr., Wainwright, A. E., and Bell, H. E. (1974a). Accuracy evaluation and stability of the NBS primary frequency standards. *CPEM Dig.*, pp. 155–156.

Glaze, D. J., Hellwig, H., Allan, D. W., Jarvis, S., Jr., and Wainwright, A. E. (1974b). Accuracy evaluation and stability of NBS primary frequency standards. *IEEE Trans. Instrum. Meas.* **IM-23**, 489–501.

Glaze, D. J., Hellwig, H., Allan, D. W., and Jarvis, S., Jr. (1977). NBS-4 and NBS-6: the NBS primary frequency standards. *Metrologia* **13**, 17–28.

Goldenberg, H., Kleppner, D., and Ramsey, N. (1960). Atomic beam resonance experiments with stored beams. *Phys. Rev.* **123**, 530–537.

Gordon, J. P., Zeiger, H. J., and Townes, C. H. (1955). The maser—new type of microwave amplifier, frequency standard, and spectrometer. *Phys. Rev.* **99**, 1264–1274.

Graf, E., Johnson, L. F., and Kern, R. H. (1975). A new compact cesium beam frequency standard. *Proc. 29th Annu. Freq. Control Symp.*, pp. 352–356.

Granveaud, M. (1976). TAI [temps atomique international] frequency. *Conf. Precision Electromagn. Meas. (IEEE)*, p. 230.

Granveaud, M., and Azoubib, J. (1976). TAI frequency. *IEEE Trans. Instrum. Meas.* **IM-25**, 469–472.

Gregory, T. K. (1977). New cesium beam frequency standards for flight and ground applications. *Proc. 31st Annu. Freq. Control Symp.*, pp. 551–554.

Gubkin, A. N., Novak, M. M., and Kholodova, G. K. (1972). Electric field of ring electrets and possible application for state selection in a maser. *Sov. Phys.–Tech. Phys. (Engl. Transl.)* **17**, 681–684.

Haefele, J. C., and Keating, R. E. (1972). Around the world atomic clocks: predicted and observed relativistic time gains. *Science* **177**, 166–170.

Hahn, S., Chachulski, A., and Kunski, R. (1967). Atomic caesium frequency standard. *Arch. Elektrotech. (Warsaw)* **16**, 841–855. In Polish.

Hahn, S. L., and Radecki, K. W. (1974). Design and preliminary experiments with a silver beam atomic clock. *CPEM Dig.*, pp. 166–168.

Hahn, S. L., and Radecki, K. W. (1978a). Features of a silver beam magnetic resonance apparatus as a frequency standard. *IEEE Trans. Instrum. Meas.* **IM-27**, 335–338.

Hahn, S. L., and Radecki, K. W. (1978b). Features of a silver beam magnetic resonance apparatus as a frequency standard. *CPEM Dig.*, pp. 13–15.

Hall, J. L. (1976). Problems of atomic frequency standards of extreme accuracy and a new atomic beam interaction goemtry. *Opt. Commun.* **18**, 62–63.

Hardin, J., and Uebersfeld, J. (1970). Radioelectric scheme equivalent to an ammoniacal maser. *C.R. Hebd. Seances Acad. Sci., Ser. B* **270**, 1617–1619. In French.

Hardin, J., and Uebersfeld, J. (1971). An ammonia maser used for electron paramagnetic resonance. *Rev. Phys. Appl.* **6**, 165–172. In French.

Hardy, W. N., and Morrow, M. (1981). Prospects for low temperature H masers using liquid helium coated walls. *J. Phys. Colloq. (Orsay, Fr.)* **42**, 171–179.

Hartmann, F. (1967). Maser amplification by an alkali vapour submitted to optical pumping application to the case of Rubidium 85. *Ann. Phys.* (Paris) **2**, 329–342. In French.

Hartmann, F. (1968). Frequency stability of the regenerative rubidium maser oscillator. *Phys. Lett. A* **28**, 193–194.

Hartmann, F. (1969). Resonance line shape and filling factor in an alkali vapor maser: influence of atomic motion. *IEEE J. Quantum Electron.* **QE-5**, 595–600.

Hashi, T., Chiba, K., and Takeuchi, C. (1981). A miniature, high-performance rubidium frequency standard. *Proc. 35th Annu. Freq. Control Symp.*, pp. 646–650.

Hayes, R. E., Bennett, T. J., Norton, G. T., and Zepler, M. M. (1970). Rubidium atomic frequency source having small size and fast warm up. *Electron. Lett.* **6**, 734–735.

Heger, C. E., Hyatt, R. C., and Seavey, G. A. (1976). A cesium beam frequency reference for severe environments. *Hewlett-Packard J.* **27**, 2–10.

Hellwig, H. (1970a). Areas of promise for the development of future primary frequency standards. *Metrologia* **6**, 118–126.

Hellwig, H. (1970b). Areas of promise for the development of future primary frequency standards. *Proc. 24th Annu. Freq. Control Symp.*, pp. 246–258.

Hellwig, H. (1970c). Hydrogen spin exchange frequency shifts. *NBS Tech. Note (U.S.)* 387 (PB-193701), 19 pp.

Hellwig, H. (1970d). The hydrogen storage beam tube, a proposal for a new frequency standard. *Metrologia* **6**, 56–60.

Hellwig, H. (1972). Frequency standards and clocks. Report NBS TN 616, National Bureau of Standards, Washington, D. C., 65 pp.

Hellwig, H. (1973). Status report on primary frequency standards. *NBS Tech. Note (U.S.)* 646, 12 pp.

Hellwig, H. (1974). Atomic frequency standards: a survey. *Proc. 28th Annu. Freq. Control Symp.*, pp. 315–339.

Hellwig, H. (1975). Atomic frequency standards: a survey. *Proc. IEEE* **63**, 212–229.

Hellwig, H. (1976). Design principles and characteristics of frequency and time standards. *IEEE Trans. Nucl. Sci.* **NS-23**, 1629–1635.

Hellwig, H. (1979). Microwave time and frequency standards. *Radio Sci.* **14**, 561–572.

Hellwig, H. (1981). Reliability, serviceability and performance of frequency standards. *J. Inst. Electron. Telecommun. Eng. (New Delhi)* **27**, 362–365.

Hellwig, H., and Bell, H. E. (1972a). Experimental results with atomic hydrogen storage beam systems. *Proc. 26th Annu. Freq. Control Symp.*, pp. 242–247.

Hellwig, H., and Bell, H. E. (1972b). Some experimental results with an atomic hydrogen storage beam frequency standard. *Metrologia* **8**, 96–98.

Hellwig, H., and Pannaci, E. (1967). Automatic tuning of hydrogen masers. *Proc. IEEE* **55**, 551–556.

Hellwig, H., and Pannaci, E. (1968). Maser oscillations with external gain. *J. Appl. Phys.* **39**, 5496–5498.

Hellwig, H., McKnight, R., Pannaci, E., and Wilson, G. (1968). Barium oxide beam tube frequency standard. *Proc. 22nd Annu. Freq. Control Symp.*, pp. 529–544.

Hellwig, H., Vessot, R. F. C., Levine, M. W., Zitzewitz, P. W., Allan, D. W., and Glaze, D. J. (1970). Measurement of the unperturbed hydrogen hyperfine frequency. *IEEE Trans. Instrum. Meas.* **IM-19**, 200–209.

Hellwig, H., Barnes, J. A., and Glaze, D. J. (1971). Frequency biases in a beam tube caused by Ramsey cavity phase differences. *Proc. 25th Annu. Freq. Control Symp.*, pp. 309–312.

Hellwig, H., Jarvis, S., Jr., Glaze, D. J., Halford, D., and Bell, H. E. (1973a). Time domain velocity selection modulation as a tool to evaluate cesium beam tubes. *Proc. 27th Annu. Freq. Control Symp.*, pp. 357–366.

Hellwig, H., Jarvis, S., Jr., Halford, D., and Bell, H. E. (1973b). Evaluation and operation of atomic beam tube frequency standards using time domain velocity selection modulation. *Metrologia* **9**, 107–112.

Hellwig, H., Evenson, K. M., and Wineland, D. J. (1978). Time, frequency and physical measurement. *Phys. Today* **31**, 23–30.

Helmcke, J., Zevgolis, D., and Yen, B. O. (1982). High resolution optical Ramsey resonances by means of four travelling wave interactions in a Cs atomic beam (frequency standard application). *CPEM Dig.*, pp. E/15–16.

Hernqvist, K. G. (1978). The hydrogen dissociator [H maser]. *IEEE Trans. Plasma Sci.* **PS-6**, 238–243.

Hibbard, L. U. (1967). The hydrogen maser as an Australian frequency standard. *Proc. Inst. Radio Electron. Eng. Aust.* **28**, 453–461.

Hibbard, L. U. (1981). Development of the CSIRO hydrogen maser. *J. Electr. Electron. Eng. Aust.* **1**, 243–250.

Holloway, J. H., and Lacey, R. F. (1964). Factors which limit the accuracy of cesium atomic beam frequency standards. *Proc. Int. Conf. Chronometry*, pp. 317–331.

Hope, S. (1978). "State Selection and Focusing of Molecular Beams." Ph.D. Thesis, University of Keele, Staffs, England.

Howe, D. A. (1976). Velocity distribution of cesium beam tubes. *Proc. 30th Annu. Freq. Control Symp.*, pp. 451–456.

Howe, D. A., and Salazar, H. F. (1975). A digital 5.00688 MHz synthesizer and squarewave FM servo system for cesium standards. *Proc. 29th Annu. Freq. Control Symp.*, pp. 387–393.

Howe, D. A., Bell, H. E., Hellwig, H., and DeMarchi, A. (1974). Preliminary research and development of the cesium tube accuracy evaluation system. *Proc. 28th Annu. Freq. Control Symp.*, pp. 362–372.

Howe, D. A., Walls, F. L., Bell, H. E., and Hellwig, H. (1979). A small, passively operated hydrogen maser. *Proc. 33rd Annu. Freq. Control Symp.*, pp. 554–562.

Hyatt, R., Throne, D., Cutler, L. S., Holloway, J. H., and Mueller, L. F. (1971). Performance of newly developed cesium beam tubes and frequency standards. *Proc. 25th Annu. Freq. Control Symp.*, pp. 313–324.

Hyatt, R. C., Mueller, L. F., and Osterdock, T. N. (1973). A high-performance beam tube for cesium beam frequency standards. *Hewlett-Packard J.* **25**, 14–23.

Iga, K., and Fukuyo, H. (1970). Optical pumping and optical detection mechanism in Rb atomic oscillator. *Electron. Commun. Jpn.* **53**, 54–59.

Iijima, S., Fujiwara, K., and Kato, T. (1976). An experiment on the effect of ambient temperature on the rate of cesium clocks. *Tokyo Astron. Bull.* (244), 2071–2075.

Iijima, S., Fujiwara, K., Kobayashi, H., and Kato, T. (1978). Effect of environmental conditions on the rate of a cesium clock. *Ann. Tokyo Astron. Obs.* **17**, 50–67.

Il'in, V. G., and Sazhin, V. V. (1977). New USSR state time and frequency standards. *Priroda (Moscow)* (8), 16–27. In Russian.

Il'in, V. G., Elkin, G. A., Abashev, Yu. G., and Purtov, V. I. (1976). The metrological cesium frequency standard MTs-1. *Meas. Tech. (Engl. Transl.)* **19**, 1450–1455.

Il'nin, V. G., Pushkin, S. B., Vavr, A., and Graf, E. (1979). Investigating the metrological characteristics of cesium clocks made by the Oscilloquartz Company. *Meas. Tech. (Engl. Transl.)* **22**, 1196–1197.

Ilyusnina, E. N., and Yukhvidin, Ya. A. (1976). Operating characteristics of atomic-beam tubes at the transition between the hyperfine structure levels in the absence of Zeeman splitting. *Radio Eng. Electron. Phys. (Engl. Transl.)* **21**, 140–141.

Imae, M. (1979). A technique of mean atomic time scale generation by cesium clocks. *Rev. Radio Res. Lab. Jpn.* **25**, 49–57. In Japanese.

Institute of Navigation (1980). "Global Positioning System." Institute of Navigation, Washington, D.C.

Itano, W. M., Lewis, L. L., and Wineland, D. J. (1981). Shift of $^2S_{1/2}$ hyperfine splittings due to blackbody radiation and its influence on frequency standards. *J. Phys. Colloq. (Orsay, Fr.)* **42**, 283–287.

Ivanov, N. I. (1975). Short-term frequency instability of the frequency synthesizer in an atomic clock. *Meas. Tech. (Engl. Transl.)* **18**, 248–251.

Ivanov, N. I., and Kravchenko, V. F. (1972). Fluctuations in a rubidium frequency standard. *Izv. Vyssh. Uchebn. Zaved. Radioelektron.* **15**, 890–894. In Russian.

Ivanov, N. I., Leikin, A. Ya., and Fertik, N. S. (1975). Fluctuations in atomic clocks. *Meas. Tech. (Engl. Transl.)* **18**, 389–390.

Ivanova, E. P., Ivanov, N. I., and Kravchenko, V. F. (1974). Shortlived fluctuations in the frequency of a Rb maser. *Radiotekhnika (Kharkov)* (31), 142–146. In Russian.

Jardino, M., Desaintfuscien, M., Barillet, R., Viennet, J., Petit, P., and Audoin, C. (1981a). Frequency stability of a mercury ion frequency standard. *Appl. Phys.* **24**, 107–112.

Jardino, M., Desaintfuscien, M., and Plumelle, F. (1981b). Prospects for a mercury ion frequency standard. *J. Phys. Colloq. (Orsay, Fr.)* **42**, 327–338.

Jarvis, S., Jr. (1974). Determined of velocity distributions in molecular beam frequency standards from measured resonance curves. *Metrologia* **10**, 87–88.

Jarvis, S., Jr., Wineland, D. J., and Hellwig, H. (1977). Two-frequency excitation for the Ramsey separated oscillatory field method. *J. Appl. Phys.* **48**, 5336–5337.

Jechart, E. (1973). A new miniature rubidium gas cell frequency standard. *Proc. 27th Annu. Freq. Control Symp.*, pp. 387–389.

Jechart, E. (1974). Miniaturized rubidium-gas-cell frequency standard. *Elektronik* **23**, 457–460. In German.

Jechart, E., and Hubner, G. (1968). XSR-primary frequency standard for atomic and universal time. *News Rohde Schwartz* **8**, 26–30.

Jelinek, F., and Vrba, J. (1968). Solid state microwave power source for an ammonia maser. *Proc. 3rd Colloq. Microwave Commun.*, Budapest, Hungary, pp. 693–701.

Jespersen, J., and Fitz-Randolph, J. (1977). "From Sundials to Atomic Clocks." National Bureau of Standards, Washington, D.C., 175 pp.

Johnson, A. C., and Osterdock, T. N. (1980). Longevity performance of cesium beam frequency standards. *Proc. 34th Annu. Freq. Control Symp.*, pp. 320–325.

Jones, H., and Eyer, A. (1973). Collisional transfer of energy in ammonia; some triple resonance experiments. *Z. Naturforsch. A* **28**, 1703–1706.

Jumonji, H., and Kihara, M. (1979). Analyses on the servo-control system of the cesium atomic beam frequency standard. *Trans. Inst. Electron. Commun. Eng. Jpn.* [*Part*] *E* **62**, 812–813.

Jumonji, H., and Kihara, M. (1979). Cesium frequency standard for network synchronization system [digital telephone system]. *Rev. Electr. Commun. Lab.* **27**, 830–840.

Jumonji, H., Tanaka, K., Toyama, J., Takaoka, H., Kariya, K., and Kawada, J. (1978). A new low voltage, maintenance-free, cesium beam tube for a frequency standard. *Proc. 32nd Annu. Freq. Control Symp.*, pp. 460–465.

Kapitanskii, V. R., Kolosov, A. S., Kostakov, A. V., Livshits, A. I., and Metter, I. M. (1968). Hydrogen atomic beam oscillator with a multichannel source output and a multichannel input into a storage box. *Zh. Tekh. Fiz.* **38**, 1366–1369. In Russian.

Kartaschoff, P. (1971). Power–linewidth relations in atomic beam tubes. *Eurocon Dig.* (*IEEE*), 2 pp.

Kartaschoff, P. (1978). "Frequency and Time." Academic Press, New York.

Kartaschoff, P., and Barnes, J. A. (1972). Standard time and frequency generation. *Proc. IEEE* **60**, 493–501.

Kbarchev, O. P. (1976). Rubidium cell frequency standard with pulse optical pumping. *Izv. Vyssh. Uchebn. Zaved. Priborostr.* **19**, 114–118. In Russian.

Khaplanov, G. M., Biketov, V. D., Volkova, N. I., Lukoshkova, G. I., Bazarov, Ye. N., Yukhvidin, Ya. A., and Gubin, V. P. (1968). Rb vapour maser. *Radiotekh. Elektron.* **13**, 165. In Russian.

Kirk, A. (1983). Performance of compact hydrogen masers. *Proc. 37th Annu. Freq. Control Symp.*, pp. 42–48.

Klemperer, W. K. (1972). Long-baseline radio interferometry with independent frequency standards. *Proc. IEEE* **60**, 602–609.

Kleppner, D., Berg, H. C., Crampton, S. B., Ramsey, N. F., Vessot, R. F. C., Peters, H. E., and Vanier, J. (1965). Hydrogen maser principles and techniques. *Phys. Rev. A* **138**, 972–983.

Kobayashi, M., Nakagiri, K., Urabe, S., Shibuki, M., and Saburi, Y. (1978a). Design of and preliminary results on a cesium-beam standard at the Radio Research Laboratories. *IEEE Trans. Instrum. Meas.* **IM-27**, 343–348.

Kobayashi, M., Nakagiri, K., Urabe, S., Shibuki, M., and Saburi, Y. (1978b). Design and preliminary result on a cesium beam standard at the RRL. *CPEM Dig.*, pp. 5–7.

Kocharovskaya, O. A., and Tsaregradskii, V. B. (1979). Mechanisms for broadening the spectral line of masers with a beam of inflying atoms. *Radiophys. Quantum Electron.* (*Engl. Transl.*) **22**, 997–1003.

Koga, Y., Nakadan, Y., and Yoda, J. (1976). A cesium beam frequency standard and its frequency stability. *Oyo Butsuri* **45**, 753–762. In Japanese.

Koga, Y., Nakadan, Y., and Yoda, J. (1981). The cesium beam frequency standard NRLM-II. *J. Phys. Colloq.* (*Orsay, Fr.*) **42**, 247–252.

Komiyama, B. (1978). View to the future VLBI. I. Improvement of frequency stability of local oscillators. *Rev. Radio Res. Lab. Jpn.* **24**, 531–534. In Japanese.

Korobov, V. K., Il'in, V. G., and Pushkin, S. B. (1976). New state standard of time and frequency, and methods of realizing its accuracy. *Meas. Tech.* (*Engl. Transl.*) **19**, 1444–1449.

Koshel'kov, V. A. (1975). On increasing the number of active molecules in a molecular oscillator. *Radio Eng. Electron. Phys.* (*Engl. Transl.*) **20**, 145–146.

Koshel'kov, V. A., and Krochik, G. M. (1972). The use of a four-pass winding as the sorting system for a molecular generator. *Radio Eng. Electron. Phys.* (*Engl. Transl.*) 854–857.

Koshurinov, Ye. I. (1969). Effect of the symmetry of potentials at the separating system and the resonator of a molecular oscillator. *Radiotekh. Elektron.* **14**, 1840–1842.

Kramer, G. (1974). Noise in passive frequency standards. *CPEM Dig.*, pp. 157–159.

Krause, W. H. U. (1968). Quantum-mechanical explanation of a detuning effect observed with two-cavity molecular beam masers. *Phys. Lett. A* **28**, 380–381.

Krause, W. H. U., and Lainé, D. C. (1973). Nuclear spin analogue of a molecular beam maser with cavities in series. *J. Phys. B* **6**, 1516–1530.

Kroupa, V. F., and Sojdr, L. (1980). Noise in standard frequency sources. *CPEM Dig.*, pp. 147–151.

Kroupnov, A. F., Skvortsov, V. A., and Sinegoubko, L. A. (1968). The study of operation regimes of two-resonator molecular generator with opposite beams. *Izv. Vyssh. Uchebn. Zaved. Radiofiz.* (2), 244–250. In Russian.

Kukolich, J. G. (1968). Measurements of the 3–2 inversion frequency and frequency stability of a two-cavity ammonia maser. *Proc. IEEE* **56**, 124–125.

Kupersmith, F., Thornburg, C., and Ho, J. (1970). New primary cesium beam frequency standard. *Proc. 24th Annu. Freq. Control Symp.*, pp. 308–314.

Kuramochi, N., Fukuyo, H., Matsuda, I., and Shiomi, N. (1976a). Spectral profiles of the ^{87}Rb pumping light source [for frequency standard]. *Jpn. J. Appl. Phys.* **15**, 949–954.

Kuramochi, N., Matsuda, I., Naruse, S., Iga, K., and Fukuyo, H. (1976b). Measurement of the frequency displacement of the ^{87}Rb pumping light passed through the ^{85}Rb filter cell. *Bull. Res. Lab. Precis. Mach. Electron.* (*Tokyo Inst. Technol.*) (38), 47–50.

Kwon, T. M., and Hahn, T. (1983). Improved vibration performance in passive atomic frequency standards by servo loop control. *Proc. 37th Annu. Freq. Control Symp.*, pp. 18–20.

Lacey, R. F. (1967). Thallium beam frequency standards. *Metrologia* **3**, 70–78.

Lacey, R. F. (1968). Phase shift in microwave Ramsey structures. *Proc. 22nd Annu. Freq. Control Symp.*, pp. 545–558.

Lacey, R. F., and Vessot, R. F. C. (1969). Improved state selection for hydrogen masers. *Proc. 23rd Annu. Freq. Control Symp.*, pp. 279–283.

Lacroix, M., and Malnar, L. (1968a). Rubidium vapour atomic clocks as atomic frequency standards. *Onde Electr.* **48**, 189–195. In French.

Lacroix, M., and Malnar, L. (1968b). The vapour rubidium atomic clocks among the atomic frequency standards. *Onde Electr.* **48**, 164–171. In French.

Lainé, D. C. (1967). Oscillation quenching in a molecular-beam maser. *Electron. Lett.* **3**, 454–455.

Lainé, D. C. (1973). Molecular beam masers. *Phys. Bull.* **24**, 79–84.

Lainé, D. C., and Al-Jumaily, A. M. (1979). Injection priming of a pulsed molecular-beam maser oscillator. *Electron. Lett.* **15**, 21–23.

Lainé, D. C., and Bardo, W. S. (1969). Transients in an ammonia-maser oscillator. *Electron. Lett.* **5**, 323–324.

Lainé, D. C., and Bardo, W. S. (1970). Comment on an anomalous saturation effect in an ammonia beam master. *J. Phys. B.* **3**, L23–24.

Lainé, D. C., and Bardo, W. S. (1971). Multiple population inversion in a beam maser. *J. Phys. B* **4**, 1738–1742.

Lainé, D. C., and Maroof, A. K. H. (1975). Oscillation pulsations in a two-cavity molecular beam maser. *Proc. 18th Ampere Cong. Magn. Res. Related Phenomena* **1**, 199–200. North-Holland Publ., Amsterdam.

Lainé, D. C., and Smart, G. D. S. (1971). Ammonia beam masers employing parallel plate and conical types of open resonator. *J. Phys. D* **4**, L23–25.

Lainé, D. C., and Smith, A. L. S. (1966). Modulation effects in an ammonia beam maser oscillator. *IEEE J. Quantum Electron.* **QE-2**, 399–408.

Lainé, D. C., and Sweeting, R. C. (1971a). Electret behaviour of solid ammonia observed in an ammonia beam maser. *Phys. Lett. A* **36**, 469–470.

Lainé, D. C., and Sweeting, R. C. (1971b). On the operation of molecular beam masers with electret focusers. *J. Phys D.* **4**, L44–46.

Lainé, D. C., and Sweeting, R. C. (1974). Operation of a molecular beam maser with an electret state separator. *J. Phys. D* **7**, 500–509.

Lainé, D. C., Truman, M. J., and Hope, S. (1980). Crystal video detection of stimulated emission and oscillation in a molecular beam maser. *Am. J. Phys.* **48**, 942–944.

Lainé, D. C., and Yassin, G. (1981). Bistability of elliptically polarized oscillation in a molecular beam maser operated with a disc resonator. *Phys. Lett. A* **87**, 33–36.

Lefrere, P. R. (1974). "Coupled Molecule-Radiation Field Effects in an Ammonia Beam Maser." Ph.D. Thesis, University of Keele, Staffs, England.

Lefrere, P. R., and Lainé, D. C. (1973a). Beat mode phase shifts in a molecular beam Zeeman maser oscillator operated with cavities in series. *Phys. Lett. A* **45**, 405–406.

Lefrere, P. R., and Lainé, D. C. (1973b). Molecular beam maser oscillator analogue of forced phase-locking in lasers. *J. Phys. D* **6**, L131–133.

Leikin, A. Ya., Linker, B. Yu., and Samoilovich, A. I. (1975). A combined gas cell for a passive quantum frequency standard based on rubidium vapor. *Meas. Tech. (Engl. Transl.)* **18**, 88–89.

Lender, R., and Szepan, R. (1978). Standard-frequency-controlled digital clock for high precision time measurements. *Nachr. Elektron.* **32**, 217–219. In German.

Lesage, P., and Audoin, C. (1979). Amplitude noise in actively and passively operated hydrogen masers. *Proc. 33rd Annu. Freq. Control Symp.*, pp. 515–535.

Lesage, P., and Audoin, C. (1981). Frequency stability of an oscillating maser: analysis of the effect of an external feedback loop. *IEEE Trans. Instrum. Meas.* **IM-30**, 182–186.

Lesage, P., Audoin, C., and Têtu, M. (1980). Measurement of the effect of thermal noise on the amplitude of oscillation of a maser oscillator. *IEEE Trans. Instrum. Meas.* **IM-29**, 311–315.

Leschiutta, S. (1968). Experiments with a commercial caesium resonator. *Alta Freq.* **37**, 916–922. In Italian.

Leschiutta, S. (1972). Atomic frequency standards. *Elettrotecnica* **59**, 333–338. In Italian.

Leschiutta, S., and Strumia, F. (1974a). Atomic frequency standards. *Alta Freq.* **43**, 844–848.

Leschiutta, S., and Strumia, F. (1974b). Optically pumped caesium cell frequency standards. *CPEM Dig.*, pp. 310–311.

Levine, M. W. (1981). Performance of the GPS cesium beam frequency standard in orbit. *Proc. 35th Annu. Freq. Control Symp.*, pp. 651–656.

Levine, M. W., and Vessot, R. F. C. (1970). Hydrogen-maser time and frequency standard at Agassiz Observatory. *Radio Sci.* **5**, 1287–1292.

Levine, M. W., Vessot, R., Mattison, E., Nystrom, G., Hoffman, T., and Blomberg, E. (1977). A new generation of SAO hydrogen masers. *Proc. 31st Annu. Freq. Control Symp.*, pp. 525–534.

Levine, M. W., Vessot, R. F., and Mattison, E. M. (1978). Performance evaluation of the SAO VLG-11 atomic hydrogen masers. *Proc. 32nd Annu. Freq. Control Symp.*, pp. 477–485.

Lewis, L. L., and Feldman, M. (1981). Optical pumping by lasers in atomic frequency standards. *Proc. 35th Annu. Freq. Control Symp.*, pp. 612–624.

Lewis, L. L., Howe, D. A., Stein, S. R., Manney, C., Mohler, M., Bergquist, J. C., Wineland, D. J., and Walls, F. L. (1980). Experiments to reduce cavity phase shift errors in the Cs beam tube. *CPEM Dig.*, pp. 129–133.

Lewis, L. L., Walls, F. L., and Glaze, D. J. (1981). Design considerations and performance of NBS-6, the NBS primary frequency standard. *J. Phys. Colloq. (Orsay, Fr.)* **42**, 241–246.

Lightfoot, H. W. (1975). "Construction and Investigation of an Atomic Hydrogen Beam Maser." Ph.D. Thesis, University of Keele, Staffs, England.

Lightfoot, H. W., and Lainé, D. C. (1976). Comments on oscillation amplitude settling transients in a hydrogen maser evoked by rapid frequency scanning. *J. Phys. D* **9**, L171–173.

Logachev, V. A., Morozov, V. N., Savva, V. A., and Strakhovskii, G. M. (1968). The properties of a molecular generator in magnetic field. *Radiotekh. Elektron* **13**, 2011–2018. In Russian.

Loutfy el Sayed, A. (1972). Frequency standard work in Egypt. *Proc. IEEE* **60**, 627–628.

Makarenko, B. I., Sultanov, A. S., Ivanov, M. A., Breslavets, V. P., and Shmidt, V. (1978). Selection of the optimal values of parameters of the phase automatic frequency control in frequency standards with a quantum oscillator. *Radiotekhnika (Kharkov)* (45), 57–62. In Russian.

Maleki, L., and Tucker, T. (1982). The development of a magnetically enhanced hydrogen gas dissociator. *Proc. 36th Annu. Freq. Control Symp.*, pp. 255–259.

Mandache, C. C. (1980). Wall shift in hydrogen maser. *Stud. Cercet. Fiz.* **32**, 649–659. In Rumanian.

Maroof, A. K. H. (1975). "Design, Construction and Investigation of an Ammonia Beam Maser Operated Under Conditions of Strong Oscillation." Ph.D. Thesis, University of Keele, Staffs, England.

Maroof, A. K. H., and Lainé, D. C. (1974). Operation of $J = 3$, $K = 2$, NH molecular beam maser oscillator without cryopumping or time limit. *J. Phys. E* **7**, 409–411.

Maroof, A. K. H., and Lainé, D. C. (1976). Molecular beam mass oscillation on the $J = K = 1$ inversion line of $^{14}NH_3$. *J. Phys. D* **9**, 697–700.

Matsuda, I., Sato, T., Kuramochi, N., and Fukuyo, H. (1975). Frequency stability of the Rb standard TTR-1. *Bull. Tokyo Inst. Technol.* (125), 9–15.

Matsuda, I., Shiomi, N., Kuramochi, N., and Fukuyo, H. (1978). ^{87}Rb resonant frequency change due to the spectral profile of the pumping light. *Bull. Res. Lab. Precis. Mach. Electron. (Tokyo Inst. Technol.)* (40), 7–16.

Mattison, E. M., Blomberg, E. L., Nystrom, G. N., and Vessot, R. F. C. (1979). Design and testing of a small passive hydrogen maser. *Proc. 33rd Annu. Freq. Control Symp.*, pp. 549–553.

McCaskill, T., White, J., Stebbins, S., and Buisson, J. (1978). NTS-2 cesium frequency stability results. *Proc. 32nd Annu. Freq. Control Symp.*, pp. 560–566.

McCoubrey, A., and Cutler, L. (1972). Holloway, J. H. (1929–1971)—Twenty years of progress in atomic frequency standards. *Proc. 26th Annu. Freq. Control Symp.*, pp. 202–210.

McGuire, M. D. (1977). The trapped mercury ion frequency standard. *Proc. 31st Annu. Freq. Control Symp.*, pp. 612–615.

Mehta, A. (1975). Maser. *J. Inst. Electron. Telecommun. Eng. (New Delhi)* **55**, 47–50.
Meirs, M., and Pascaru, I. (1980). Results of the development of the light weight cesium standard. *Proc. 34th Annu. Freq. Control Symp.*, pp. 370–375.
Meles, H. P. (1967). The atomic standard aspect. *Conf. Freq. Generation Control Radio Syst. (IEE)*, pp. 21–23.
Mengel, E. E., and Stover, D. W. (1983). Microprocessor for the NR series of hydrogen maser frequency standards. *Proc. 37th Annu. Freq. Control Symp.*, pp. 27–31.
Min, C. Y., Long, H. Y., Bar, C. C., Hong, G. J., and Wei, S. (1980). The experiments of the hydrogen maser wall shift and the determination of the unperturbated hyperfine frequency of the ground state of hydrogen atom. *CPEM Dig.*, pp. 157–160.
Missout, G., and Vanier, J. (1975a). Pressure and temperature coefficients of the more commonly used buffer gases in rubidium vapor frequency standards. *IEEE Trans. Instrum. Meas.* **IM-24**, 180–184.
Missout, G., and Vanier, J. (1975b). Some aspects of the theory of the passive rubidium frequency standards. *Can. J. Phys.* **53**, 1030–1043.
Missout, G., and Vanier, J. (1975c). Theoretical and experimental studies of some problems related to the passive rubidium gas cell frequency standard. *Proc. 29th Annu. Freq. Control Symp.*, p. 383.
Mockler, R. C. (1961). Atomic beam frequency standards. *In* "Advances in Electronics and Electon Physics," Vol. 15, pp. 1–71. Academic Press, New York.
Moore, R. B., Nichols, S. A., and White, J. D. (1973). Evaluation of a rubidium standard for satellite application. *Proc. 27th Annu. Freq. Control Symp.*, pp. 390–399.
Moreau, R. (1971). The use of atomic clocks in spacecraft location. *Eurocon Dig. (IEEE)*, 2 pp.
Morikawa, T. (1980). Hydrogen frequency standards [masers]. *Rev. Radio Res. Lab. Jpn.* **26**, 453–464. In Japanese.
Morris, D. (1971a). Hydrogen maser wall shift experiments at the National Research Council of Canada. *Proc. 25th Annu. Freq. Control Symp.*, pp. 343–347.
Morris, D. (1971b). Hydrogen maser wall shift experiments at the National Research Council of Canada. *Metrologia* **7**, 162–166.
Morris, D. (1978a). Time-dependent frequency shifts in the hydrogen maser. *IEEE Trans. Instrum. Meas.* **IM-27**, 339–343.
Morris, D. (1978b). Time-dependent frequency shifts in the hydrogen maser. *CPEM Dig.*, pp. 10–12.
Morris, D. (1982). Operation of a hydrogen maser with a state-mixed beam. *IEEE Trans. Instrum. Meas.* **IM-31**, 88–91.
Morris, D., and Nakagiri, K. (1976). The frequency stability of a pair of auto-tuned hydrogen masers. *Metrologia* **12**, 1–6.
Mukhamedgalieva, A. F., Oraevskii, A. N., and Strakhovskii, G. M. (1966). Investigation of a molecular oscillator with a molecular-ringing amplifier. *Izv. Vyssh. Uchebn. Zaved. Radiofiz.* **9**, 302–307. In Russian.
Mungall, A. G. (1971). The second order doppler shift in cesium beam atomic frequency standards. *Metrologia* **7**, 49–56.
Mungall, A. G. (1972). Cavity phase dependent frequency shifts in cesium beam frequency standards. *Metrologia* **8**, 28–32.
Mungall, A. G. (1976). The Millman effect in Cesium beam atomic frequency standards. *Metrologia* **12**, 151–158.
Mungall, A. G. (1977). Atomic time standards and time scales in Canada. *IEEE Conf. Exposition*, pp. 118–119.
Mungall, A. G. (1978). A new concept in atomic time keeping: the continuously operating long-beam primary cesium clock. *IEEE Trans. Instrum. Meas.* **IM-27**, 330–334.

Mungall, A. G., and Costain, C. C. (1977). NRC CsV primary clock performance. *Metrologia* **13**, 105–107.
Mungall, A. G., and Costain, C. C. (1982). Performance of the four NRC long beam primary cesium clocks, CsV, CsVIA, CsVIB and CsVIC. *CPEM Dig.*, p. N 3.
Mungall, A. G., and Daams, H. (1970). Cesium beam frequency standard cavity design. *Metrologia* **6**, 60–64.
Mungall, A. G., Bailey, R., Daams, H., and Morris, D. (1968a). A reevaluation of the NRC long cesium beam frequency standard. *Metrologia* **4**, 165–168.
Mungall, A. G., Morris, D., Daams, H., and Bailey, R. (1968b). Atomic hydrogen maser development at the National Research Council of Canada. *Metrologia* **4**, 87–94.
Mungall, A. G., Bailey, R., Daams, H., Morris, D., and Costain, C. C. (1973a). The new NRC 2.1 metre primary cesium beam frequency standard, Cs V. *Metrologia* **9**, 113–127.
Mungall, A. G., Bailey, R., Daams, H., Morris, D., and Costain, C. C. (1973b). A preliminary report on Cs V, the new NRC long beam primary frequency and time standard. *Proc. 27th Annu. Freq. Control Symp.*, pp. 317–333.
Mungall, A. G., Daams, M., Morris, D., and Costain, C. C. (1973c). The atomic second—to 13 significant figures. *Phys. Can.* **29**, 40.
Mungall, A. G., Daams, H., Morris, D., and Costain, C. C. (1976). Performance and operation of the NRC primary cesium clock, CsV. *Metrologia* **12**, 129–139.
Mungall, A. G., Daams, H., and Boulanger, J.-S. (1980a). Design and performance of the new 1 m NRC primary cesium clocks. *IEEE Trans. Instrum. Meas.* **IM-29**, 291–297.
Mungall, A. G., Daams, H., and Boulanger, J.-S. (1980b). Design and performance of the new 1-metre NRC primary cesium clocks. *CPEM Dig.*, pp. 134–136.
Mungall, A. G., Daams, H., and Boulanger, J.-S. (1981a). Design, construction, and performance of the NRC Cs VI primary cesium clocks. *Metrologia* **17**, 123–145.
Mungall, A. G., Daams, H., and Boulanger, J.-S. (1981b). Performance of the NRC primary times standards CsV, CsVI A, CsVI B, CsVI C. *J. Phys. Colloq. (Orsay, Fr.)* **42**, 233–240.
Nakadan, Y., and Koga, Y. (1982). A squarewave F.M. servo system with a digital signal processing for cesium frequency standards. *Proc. 36th Annu. Freq. Control Symp.*, pp. 223–229.
Nakagiri, K., Shibuki, M., Urabe, S., Hayashi, R., and Saburi, Y. (1981). Cesium beam frequency standard at the Radio Research Laboratories. *J. Phys. Colloq. (Orsay, Fr.)* **42**, 253–256.
Neuhauser, W., Hohenstatt, M., Toschek, P., and Dehmelt, H. (1978). Optical sideband cooling of visible atom cloud confined in parabolic well. *Phys. Rev. Lett.* **41**, 233–236.
Nichols, S. A., and White, J. (1974). Satellite application of a rubidium frequency standard. *Proc. 28th Annu. Freq. Control Symp.*, pp. 401–405.
Nichols, S. A., and Woodring, D. G. (1978). Applications of atomic frequency standards to SATCOM spread spectrum systems. *Proc. 32nd Annu. Freq. Control Symp.*, pp. 555–559.
Nichols, S. A., White, J. D., and Moore, R. B. (1973a). Evaluation of a rubidium standard for satellite application. *Proc. 27th Annu. Freq. Control Symp.*, pp. 390–399.
Nichols, S. A., White, J. D., and Moore, R. B. (1973b). Performance evaluation of a rubidium standard for space environment. *Nat. Telecommun. Conf.* **1**, 19A/1–6.
Nikilin, A. I., and Strakhovskii, G. M. (1969). The effect of contamination of the surface of a storage bulb on the operation of a hydrogen maser. *Izv. Vyssh. Uchebn. Zaved. Radiofiz.* **12**, 517–519. In Russian.
Nikitin, A. I., and Strakhovskii, G. M. (1967). Quantum generator using a beam of hydrogen atoms with a superinvar resonator. *Prib. Tekh. Eksp.* (1), 129–131.
Ohta, Y., Yoshimura, K., Shibuki, M., Nakagiri, K., Morikawa, T., Koybayashi, M., and Saburi, Y. (1974). On an automatic cavity tuner for hydrogen frequency standard. *Rev. Radio Res. Lab. Jpn.* **20**, 39–58. In Japanese.

Ojima, T., and Umezu, J. (1978). Domestic VLBI system. III. Receiver and local oscillator system in the VLBI experiment. *Rev. Radio Res. Lab. Jpn.* **24**, 471–474. In Japanese.

Olivier, M., and Plain, A. (1973). Extension of the theory of the frequency noise of maser oscillators. *C.R. Hebd. Seances Acad. Sci., Ser. B* **276**, 615–618. In French.

Olivier, M., and Pretot, R. (1967). Servo-system for frequency standard. *Rev. Phys. Appl.* **2**, 17–19. In French.

O'Neill, J. J., Phillips, D. H., and Stone, R. R. (1975). "Hydrogen Maser Frequency Translator." Report NRL-7858, Naval Research Laboratory, Washington, D.C., 10 pp.

Oraevskiy, A. N. (1968). Atomichron as an optical frequency standard. *Conf. Precision Electromagn. Meas. (IEEE)*, pp. 47–48.

Oyamada, H., Takahashi, K., Sato, Y., and Uchida, H. (1974). A consideration of rubidium lamp stability for rubidium frequency standard. *Proc. 28th Annu. Freq. Control Symp.*, pp. 340–343.

Oyamada, H., Takahashi, K., Sato, Y., and Uchida, H. (1976). Rubidium lamp stability and reliability for rubidium frequency standard. *NEC Res. Dev.* (43), 69–74.

Pankratov, V. A. (1974). Possible use of a rubidium maser as a combined frequency standard. *Sov. J. Quantum Electron. (Engl. Transl.)* **4**, 521–522.

Pascaru, I., and Meirs, M. (1979). Development of a light weight, military, cesium standard. *Proc. 33rd Annu. Freq. Control Symp.*, pp. 484–489.

Percival, D. B. (1976). A heuristic model of long-term atomic clock behaviour. *Proc. 30th Annu. Freq. Control Symp.*, pp. 414–419.

Percival, D. B. (1977). Prediction error analysis of atomic frequency standards. *Proc. 31st Annu. Freq. Control Symp.*, pp. 319–326.

Percival, D. B. (1978). Estimation of the spectrum of fractional frequency deviates. *Proc. 32nd Annu. Freq. Control Symp.*, pp. 542–548.

Peters, H. (1972). Hydrogen as an atomic standard. *Proc. 26th Annu. Freq. Control Symp.*, pp. 230–241.

Peters, H. E. (1975). The concertina hydrogen maser. *Proc. 29th Annu. Freq. Control Symp.*, pp. 362–370.

Peters, H. E. (1978). Small, very small, and extremely small hydrogen masers. *Proc. 32nd Annu. Freq. Control Symp.*, pp. 469–476.

Peters, H. E. (1980). New hydrogen maser designs. *Proc. 34th Annu. Freq. Control Symp.*, pp. 360–363.

Peters, H. E. (1981). Feasibility of extremely small hydrogen masers. *Proc. 35th Annu. Freq. Control Symp.*, pp. 662–666.

Peters, H. E. (1982). Experimental results of the light-weight hydrogen maser development program. *Proc. 36th Annu. Freq. Control Symp.*, pp. 240–248.

Peters, H. E., and Reinhardt, V. S. (1974). Atomic frequency standard relativistic Doppler shift experiment. *Proc. 28th Annu. Freq. Control Symp.*, pp. 247–255.

Peters, H. E., McGunigal, T. E., and Johnson, E. H. (1968). Hydrogen standard work at Goddard Space Flight Center. *Proc. 22nd Annu. Freq. Control Symp.*, pp. 464–492A.

Peters, H. E., Johnson, E. H., and McGunigal, T. E. (1969). Atomic hydrogen standards for NASA tracking stations. *Proc. 23rd Annu. Freq. Control Symp.*, pp. 297–304.

Peters, H. E., Hall, R. G., and Percival, D. B. (1972). Absolute frequency of an atomic hydrogen maser clock. *Proc. 26th Annu. Freq. Control Symp.*, pp. 319–322.

Petit, P., Viennet, J., Barillet, R., Desaintfuscien, M., and Audoin, C. (1973). Developments of hydrogen masers as frequency standards at Orsay. *Proc. 27th Annu. Freq. Control Symp.*, pp. 367–375.

Petit, P., Viennet, J., Barillet, R., Desaintfuscien, M., and Audoin, C. (1974). Development of hydrogen masers as frequency standards at the Laboratoire de l'Horloge Atomique. *Metrologia* **10**, 61–67.

Petit, R., Viennet, J., Barillet, R., Desaintfuscien, M., and Audoin, C. (1975). Atomic hydrogen frequency standards. *Colloq. Int. sur l'Electronique et la Mesure*, pp. 111–119. In French.

Petit, P., Desaintfuscien, M., and Audoin, C. (1977). Hydrogen maser with a double configuration bulb for wall shift measurements in the temperature range 25–120°C. *Proc. 31st Annu. Freq. Control Symp.*, pp. 520–524.

Petit, P., Desaintfuscien, M., and Audoin, C. (1980). Temperature dependence of the hydrogen maser wall shift in the temperature range 295–395 K. *Metrologia* **16**, 7–14.

Philibert, V. (1970). The cesium-beam atomic clock. *Electron. World* **83**, 40–41.

Picque, J. L. (1974). Hyperfine optical pumping of cesium with a CW GaAs laser. *IEEE J. Quantum Electron.* **QE-10**, 892–897.

Popa, A. E., Wang, H. T. M., Bridges, W. B., Chester, A. N., Etter, J. E., and Walsh, B. L. (1976). A study to identify hydrogen maser failure modes. *Proc. 30th Annu. Freq. Control Symp.*, pp. 489–492.

Pushkin, S. (1976). A new state time and frequency standard of the USSR. *Proc. 82nd Symp. Int. Astron. Union*, pp. 19–21.

Rabi, I. I. (1937). Space quantization in a gyrating magnetic field. *Phys. Rev.* **51**, 652–654.

Ramsey, N. F. (1956). "Molecular Beams." Clarendon, Oxford.

Ramsey, N. F. (1969). Atomic hydrogen hyperfine structure. *Proc. Arnold Sommerfeld Centennial Memorial Meeting*, pp. 218–234. North-Holland Publ., Amsterdam.

Ramsey, N. F. (1971a). History of atomic and molecular control of frequency and time. *Proc. 25th Annu. Freq. Control Symp.*, pp. 46–57.

Ramsey, N. F. (1971b). Hydrogen maser research. *Proc. Esfahan Symp. Fundamental Appl. Laser Phys.*, pp. 437–461.

Ramsey, N. F. (1972). History of atomic and molecular standards of frequency and time. *IEEE Trans. Instrum. Meas.* **IM-21**, 90–99.

Ramsey, N. F. (1983). History of atomic frequency standards. *Proc. 37th Annu. Freq. Control Symp.*, p. 5.

Reinhardt, V. S. (1980). Integral bulb and microwave cavity for masers. *NASA Tech. Briefs* **5**, 170.

Reinhardt, V. S., and Lavanceau, J. (1974). A comparison of the cesium and hydrogen hyperfine frequencies by means of Loran-C and portable clocks. *Proc. 28th Annu. Freq. Control Symp.*, pp. 379–383.

Reinhardt, V. S., and Peters, H. E. (1975). An improved method for measuring the magnetic inhomogeneity shift in hydrogen masers. *Proc. 29th Annu. Freq. Control Symp.*, pp. 357–361.

Reinhardt, V. S., Kaufmann, D. C., Adams, W. A., DeLuca, J. J., and Soucy, J. L. (1976). NASA atomic hydrogen standards program—an update. *Proc. 30th Annu. Freq. Control Symp.*, pp. 481–488.

Risley, A. (1971). The physical basis of atomic frequency standards. *NBS Tech. Note (U.S.)* 399, 54 pp.

Risley, A., and Busca, G. (1978). Effect of line inhomogeneity on the frequency of passive ^{87}Rb frequency standards. *Proc. 32nd Annu. Freq. Control Symp.*, pp. 506–513.

Risley, A., Jarvis, S., Jr., and Vanier, J. (1979). Study of the dependence of frequency upon microwave power of wall-coated and buffer-gas-filled passive ^{87}Rb frequency standards. *Proc. 33rd Annu. Freq. Control Symp.*, pp. 477–483.

Risley, A., Jarvis, S., Jr., and Vanier, J. (1980). The dependence of frequency upon microwave power of wall-coated and buffer-gas-filled gas cell Rb^{87} frequency standards. *J. Appl. Phys.* **51**, 4571–4576.

Ritz, V. H., Bermudez, V. M., and Folen, V. J. (1977). Characterization of degraded hydrogen dissociator envelopes by AES [w.r.t. atomic clocks]. *J. Appl. Phys.* **48**, 2096–2098.

Robinson, H. G., and Johnson, C. E. (1982). A new heart for Rb frequency standards: the evacuated, wall-coated, sealed cell. *CPEM Dig.*, pp. M/4–7.

Rovera, G., and Beverini, N. (1977). Frequency stability of the optically pumped passive cesium frequency standard. *European Conf. Precise Electr. Meas. (IEE)*, p. 83.

Rovera, G., De Marchi, A., and Vanier, J. (1976). The optically pumped passive cesium frequency standard: basic theory and experimental results on buffer gas frequency shifts. *IEEE Trans. Instrum. Meas.* **IM-25**, 203–216.

Rovera, G., Leschiutta, S., Busca, G., and Strumia, F. (1978). Parameters affecting the stability of an optically pumped cesium frequency standard. *Proc. 32nd Annu. Freq. Control Symp.*, pp. 466–468.

Rueger, L. J. (1981). Characteristics of the NASA research hydrogen maser. *J. Inst. Electron. Telecommun. Eng. (New Delhi)* **27**, 493–500.

Rueger, L. J., Bates, A., Stillman, L., Norton, J., Blackburn, C. M., and Reinhardt, V. A. (1978). NASA NR hydrogen maser. *Proc. 32nd Annu. Freq. Control Symp.*, pp. 486–491.

Sabisky, E. S., and Peters, H. E. (1977). Design of a spacecraft hydrogen maser. *Proc. 31st Annu. Freq. Control Symp.*, pp. 510–519.

Sabisky, E. S., and Weakliem, H. A. (1978). An operating development model spacecraft hydrogen maser. *Proc. 32nd Annu. Freq. Control Symp.*, pp. 499–505.

Sachkov, V. I. (1967). Phasing of resonators of a cesium frequency standard. *Meas. Tech. (Engl. Transl.)* (9), 1096–1099.

Sachkov, V. I. (1968). Application of U-shaped resonators in cesium frequency standards. *Meas. Tech. (Engl. Transl.)* (7), 997–998.

Sadvoskii, A. B., Pashev, G. P., Zuev, E. V., and Pikhtelev, A. I. (1975). Atomic clocks and the time errors of adjustable electronic clocks. *Meas. Tech. (Engl. Transl.)* **18**, 391–392.

Sato, Y., Kumamoto, H., Oyamada, H., and Uchida, H. (1972). Automatic frequency controlled rubidium frequency standard. *Proc. 26th Annu. Freq. Control Symp.*, pp. 211–215.

Savard, J.-Y., Busca, G., Rovea, S., Desaintfuscien, M., and Petit, P. (1979). Effects of coherently excited Zeeman transitions on a hydrogen maser hyperfine transition. *Can. J. Phys.* **57**, 904–916.

Schuessler, H. A. (1971). The ion storage tube, a proposal for a new atomic frequency standard. *Metrologia* **7**, 103–107.

Schulten, G. (1967). Simple molecular frequency standards for millimeter waves. *Microwave J.* **10**, 71–74.

Schutz, K. (1968). The efficiency of atomic frequency standards. *Frequenz* **22**, 225–229. In German.

Schutz, K. (1972). Measurements on hydrogen masers. I. *Frequenz* **26**, 338–343. In German.

Schutz, K. (1973). Performance of a hydrogen maser. II. *Frequenz* **27**, 12–17. In German.

Seances (1968). "Seances de la 13e Conference General des Poids et Mesures." Gauthier-Villars, Paris, France, October 1967.

Seavey, G. A., and Mueller, L. F. (1976). Performance of a dual beam high performance cesium beam tube [frequency standard]. *Proc. 30th Annu. Freq. Control Symp.*, pp. 457–462.

Shimoda, K. (1979). Invention of masers and lasers. *J. Inst. Electron. Commun. Eng. Jpn.* **62**, 113–117. In Japanese.

Siegmann, A. E. (1971). "An Introduction to Lasers and Masers." McGraw-Hill, New York.

Singh, G., DiLavore, P., and Alley, C. O. (1976). Comments on "Hyperfine optical pumping of cesium with a CW GaAs Laser." *IEEE J. Quantum Electron.* **QE-12**, 81–82.

Smart, G. D. S. (1973). "Construction and Characteristics of an Ammonia Beam Maser Employing a Fabry–Perot Cavity." Ph.D. Thesis, University of Keele, Staffs, England.

Smith, A. L. S., and Lainé, D. C. (1967). Fluctuations in the amplitude of oscillation of an ammonia beam maser. *Electron. Lett.* **3**, 90–91.

Smith, A. L. S., and Lainé, D. C. (1968). Further characteristics of a molecular beam maser oscillator operated with two cavities in series. *J. Phys. D* **1**, 727–732.

Smith, H. (1982). The steady march of atomic time. *New Sci.* **93**, 382–384.

Stadler, K. (1974). Rubidium frequency standard XSRM. *News Rohde Schwarz* **14**, 8–10.

Stadler, K. (1975). Calibrating crystal oscillators with frequency standard XSRM. *News Rohde Schwarz* **15**, 12–14.

Steiner, C. (1969). Atomic clocks. *Schweiz. Tech. Z.* **66**, 61–71. In French.

Stern, W. A., and Novick, R. (1969). An optically pumped ^{85}Rb maser frequency standard. *Proc. 23rd Annu. Freq. Control Symp.*, pp. 271–273.

Stern, W. A., and Novick, R. (1970). A field-independent optically pumped ^{85}Rb maser oscillator. *Appl. Phys. Lett.* **17**, 216–217.

Stern, W. A., and Novick, R. (1971). A field independent optically pumped ^{85}Rb maser frequency standard. *Proc. 25th Annu. Freq. Control Symp.*, pp. 325–330.

Stern, W. A., and Novick, R. (1972a). Further results on the rubidium-87 maser frequency standard. *Proc. 26th Annu. Freq. Control Symp.*, pp. 223–224.

Stern, W. A., and Novick, R. (1972b). Light and buffer-gas frequency shifts in the ^{85}Rb-maser frequency standard. *IEEE Trans. Instrum. Meas.* **IM-21**, 99–105.

Stern, W. A., Aulich, E., and Novick, R. (1973). Status of the development of the rubidium-87 maser frequency standard. *Proc. 27th Annu. Freq. Control Symp.*, pp. 404–405.

Straka, E. R. (1982). Performance characteristics of cesium beam tube electron multipliers. *Proc. 36th Annu. Freq. Control Symp.*, pp. 230–235.

Strumia, F. (1972). A proposal for a new absolute frequency standard, using a Mg or Ca atomic beam. *Metrologia* **8**, 85–90.

Strumia, F. (1978). Analysis of new microwave and optical frequency standards based on ions storage. *Proc. 32nd Annu. Freq. Control Symp.*, pp. 444–452.

Strumia, F., Minguzzi, P., Francesconi, M., and Benedetti, R. (1974). Mg frequency standard: optimization of the metastable atomic beam. *Proc. 28th Annu. Freq. Control Symp.*, pp. 350–354.

Strumia, F., Beverini, N., Moretti, A., and Rovera, G. (1976). Optimization of the buffer gas mixture for optically pumped Cs frequency standards. *Proc. 30th Annu. Freq. Control Symp.*, pp. 468–472.

Stuart, J. G., Larson, D. J., and Ramsey, N. F. (1980). Differential Stark shifts in the hydrogen maser. *Phys. Rev. A.* **22**, 2092–2097.

Sward, A., and Sydnor, R. (1968). Power density spectrum of the hydrogen maser. *Proc. IEEE* **56**, 1614–1616.

Tai-qian, D. (1980). The reduction of light shift in ^{87}Rb frequency standard using pulse sampling optical detection method. *CPEM Dig.*, pp. 161–162.

Tai-qian, D. (1981). Reduction of light shift in ^{87}Rb frequency standard using pulse sampling optical detection method. *Acta Phys. Sin.* **30**, 3–11. In Chinese.

Tang, H., and Happer, W. (1969). Light modulation at the Rb^{87} hyperfine frequency. *Proc. 23rd Annu. Freq. Control Symp.*, pp. 263–270.

Temple, R. E. (1971). "The Operation and Frequency Stability Measurement of a Hydrogen Cyanide Beam Type Maser at 88.6 GHz." Ph.D. Thesis, University of Colorado, Boulder, Colorado, 146 pp. Available from University Microfilms, Ann Arbor, Michigan, Order No. 71-25877.

Terrien, J. (1976). Standards of length and time. *Rep. Prog. Phys.* **39**, 1067–1108.

Tessier, M., and Vanier, J. (1971). Theory of the rubidium 87 maser. *Can. J. Phys.* **49**, 2680–2689. In French.

Têtu, M., and Tremblay, P. (1981). On the maximum of the spectral density of the amplitude fluctuations of a maser oscillator. *IEEE Trans. Instrum. Meas.* **IM-30**, 229–230.

Têtu, M., Busca, G., and Vanier, J. (1972). Short term stability of the Rb^{87} maser. *Proc. 26th Annu. Freq. Control Symp.*, pp. 225–229.

Têtu, M., Busca, G., and Vanier, J. (1973). Short-term frequency stability of the Rb^{87} maser. *IEEE Trans. Instrum. Meas.* **IM-22**, 250–257.

Têtu, M., Fortin, R., and Savard, J.-Y. (1976a). A new determination of the Rb^{85} unperturbed hyperfine transition frequency. *IEEE Trans. Instrum. Meas.* **IM-25**, 477–480.

Têtu, M., Fortin, R., and Savard, J.-Y. (1976b). A new determination of the Rb^{85} unperturbed hyperfine transition frequency. *Conf. Precision Electromagn. Meas. (IEEE)*, pp. 233–234.

Têtu, M., Audoin, C., and Lesage, P. (1980a). Measurement of the effect of thermal noise on the amplitude of oscillation of a maser oscillator. *CPEM Dig.*, pp. 143–146.

Têtu, M., Brousseau, R., and Vanier, J. (1980b). Frequency-domain measurement of the frequency stability of a maser oscillator. *IEEE Trans. Instrum. Meas.* **IM-29**, 94–97.

Têtu, M., Tremblay, P., Bonnier, D., and Vanier, J. (1982). Short-term frequency stability and systematic effects on the Rubidium 87 maser oscillator frequency. *Proc. 36th Annu. Freq. Control Symp.*, 340–347.

Thomann, P., and Busca, G. (1981). Modulation effects in passive Rb frequency standards. *J. Phys. Colloq. (Orsay, Fr.)* **42**, 189–197.

Thomsen, M. P. R., Stief, L. J., and Fallon, R. J. (1968). Study of phenomena affecting the composition of rubidium vapor cells. *Proc. 22nd Annu. Freq. Control Symp.*, pp. 559–572.

Throne, D. H. (1968). A rubidium-vapor frequency standard for systems requiring superior frequency stability. *Hewlett-Packard J.* **19**, 8–14.

Throne, D. H. (1969). A report of the performance characteristics of a new rubidium vapor frequency standard. *Proc. 23rd Annu. Freq. Control Symp.*, pp. 274–278.

Townes, C. H. (1978). Townes recalls the early days. *Laser Focus* **14**, 52–58.

Townes, C. H., and Schawlow, A. L. (1955). "Microwave Spectroscopy." McGraw-Hill, New York.

Truman, M. J., and Lainé, D. C. (1976). Anomalous behavior of an ammonia beam maser employing a ring focuser. *J. Phys. D.* **9**, L175–L178.

Urabe, S., Nakagiri, K., Ohta, Y., Kobayashi, M., and Saburi, Y. (1980a). Majorana effect on atomic frequency standards. *CPEM Dig.*, pp. 141–142.

Urabe, S., Nakagiri, K., Ohta, Y., Kobayashi, M., and Saburi, Y. (1980b). Majorana effect on atomic frequency standards. *IEEE Trans. Instrum. Meas.* **IM-29**, 304–310.

Uzgiris, E. E., and Ramsey, N. F. (1968a). Large storage box hydrogen maser. *IEEE J. Quantum Electron.* **QE-4**, 563–568.

Uzgiris, E. E., and Ramsey, N. F. (1968b). Large storage box hydrogen maser. *Proc. 22nd Annu. Freq. Control Symp.*, pp. 452–464.

Uzgiris, E. E., and Ramsey, N. F. (1970). Multiple-region hydrogen maser with reduced wall shift. *Phys. Rev. A* **1**, 429–446.

Uzgiris, E. E., and Zitzewitz, P. W. (1969). Recent results concerning the hydrogen maser wall shift problem. *Proc. 23rd Annu. Freq. Control Symp.*, pp. 284–287.

Vaillancourt, R., Missout, G., Têtu, M., and Vanier, J. (1970). Study of atomic clocks (and masers). *Abst. Pap. 38th ACFAS Congr.*, Quebec, Canada, p. 42. In French.

Valentin, M. (1978). Study of the behavior of a maser with eight ammonia jets using a Fabry Perot resonator. *Nuovo Cimento B* **44**, 205–227. In French.

Valentin, M. (1980). Spectral distribution of the output power of a molecular beam maser with a semi-confocal cavity. *J. Phys. D* **13**, 127–134.

Valentin, M., Hardin, J., and Mollier, J.-C. (1980). Absorption cell for passive standard of frequency. *Nuovo Cimento B* **59**, 241–246. In French.

Vanier, J., and Bernier, L. G. (1981). On the signal-to-noise ratio and short-term stability of passive rubidium frequency standards. *IEEE Trans. Instrum. Meas.* **IM-30**, 277–282.

Vanier, J., and Larouche, R. (1978). A comparison of the wall shift of TFE and FEP Teflon coatings in the hydrogen maser. *Metrologia* **14**, 31–37.

Vanier, J., and Strumia, F. (1976). Theory of the optically pumped cesium maser. *Can. J. Phys.* **54**, 2355–2366.

Vanier, J., and Vessot, R. F. C. (1970). H maser wall shift. *Metrologia* **6**, 52–53.

Vanier, J., Vaillancourt, R., Missout, G., and Têtu, M. (1970a). Progress report on the rubidium 85 maser. *Proc. 24th Annu. Freq. Control Symp.*, pp. 280–284.

Vanier, J., Vaillancourt, R., Missout, G., and Têtu, M. (1970b). Rubidium-85 maser-oscillator. *J. Appl. Phys.* **41**, 3188–3189.

Vanier, J., Brousseau, R., and Larouche, R. (1973). Stimulated emission in the hydrogen maser and the H spin-exchange cross section. *Can. J. Phys.* **51**, 1901–1909.

Vanier, J., Larouche, R., and Audoin, C. (1975). The hydrogen maser wall shift problem. *Proc. 29th Annu. Freq. Control Symp.*, pp. 371–382.

Vanier, J., Têtu, M., and Brousseau, R. (1977). Frequency and time domain stability of the Rb^{87} maser and related oscillators: a progress report. *Proc. 31st Annu. Freq. Control Symp.*, pp. 344–346.

Vanier, J., Têtu, M., and Bernier, L. G. (1978). Transfer of frequency stability from an atomic frequency reference to a quartz crystal oscillator. *Proc. 32nd Annu. Freq. Control Symp.*, pp. 520–526.

Vanier, J., Nguyen, D. H., Busca, G., and Têtu, M. (1979a). Study of the effect of light shifts and buffer gas shifts on the hyperfine transition of ^{87}Rb: influence of the long term frequency stability of the rubidium maser. *Can. J. Phys.* **57**, 1380–1387.

Vanier, J., Têtu, M., and Bernier, L. G. (1979b). Transfer of frequency stability from an atomic frequency reference to a quartz-crystal oscillator. *IEEE Trans. Instrum. Meas.* **IM-28**, 188–193.

Vanier, J., Kunski, R., Brisson, A., and Paulin, P. (1981). Progress and prospects in rubidium frequency standards. *J. Phys. Colloq. (Orsay, Fr.)* **42**, 139–150.

Vanier, J., Kunski, R., Cyr, N., Savard, J. Y., and Têtu, M. (1982a). On hyperfine frequency shifts caused by buffer gases. Application to the optically pumped passive rubidium frequency standard. *J. Appl. Phys.* **53**, 5387–5391.

Vanier, J., Kunski, R., Paulin, P., Savard, J. Y., Têtu, M., and Cyr, N. (1982b). On the lightshift and buffer gas shift in passive rubidium frequency standards. *Proc. 36th Annu. Freq. Control Symp.*, pp. 348–354.

Vessot, R. F. C., and Levine, M. W. (1968). "Atomic Hydrogen Maser for Space Vehicle Application, phase 1. Final report, 1 Mar. 1966–31 Mar. 1968. Report NASA-CR-94937, Hewlett-Packard Co., Frequency and Time Division, 58 pp. Contract NASW-1337. Available from CFSTI, Springfield, Virginia.

Vessot, R. F. C., and Levine, M. W. (1970a). A method for eliminating the wall shift in the atomic hydrogen maser. *Metrologia* **6**, 116–117.

Vessot, R. F. C., and Levine, M. W. (1970b). Studies of hydrogen maser wall shift for high molecular weight polytetra-fluorethylene. *Proc. 24th Annu. Freq. Control Symp.*, pp. 263–269.

Vessot, R. F. C., and Levine, M. W. (1974). Performance data of space and ground hydrogen masers and ionospheric studies for high-accuracy comparisons between space and ground clocks. *Proc. 28th Annu. Freq. Control Symp.*, pp. 408–414.

Vessot, R., Peters, H., Vanier, J., Beehler, R., Halford, D., Harrach, R., Allan, D., Glaze, D., Snider, C., Barnes, J., Cutler, L., and Bodily, L. (1966). An intercomparison of hydrogen and cesium frequency standards. *IEEE Trans. Instrum. Meas.* **IM-15**, 165–176.

Vessot, R., Levine, M., Cutler, L., Baker, M., and Mueller, M. (1968a). Progress in development of hydrogen masers. *Proc. 22nd Annu. Freq. Control Symp.*, pp. 605–620.

Vessot, R. F. C., Kleppner, D., and Ramsey, N. F. (1968b). Application of the hydrogen maser to experimental relativity. *IEEE J. Quantum Electron.* **QE-4**, 376.

Vessot, R. F. C., Mattison, E. M., and Blomberg, E. L. (1979). Experiments with a cryogenic hydrogen maser. *Proc. 33rd Annu. Freq. Control Symp.*, pp. 511–514.

Vessot, R. F. C., Levine, M. W., Mattison, E. M., Blomberg, E. L., Hoffman, T. E., Nystrom, G. U., Farrel, B. F., Decher, R., Eby, P. B., Baugher, C. R., Watts, J. W., Teuber, D. L., and Walls, F. D. (1980). Test of relativistic gravitation with a space-born hydrogen maser. *Phys. Rev. Lett.* **45**, 2081–2084.

Vessot, R. F. C., Mattison, E. M., and Imbier, E. (1983). Cold hydrogen maser research at SAO and related developments. *Proc. 37th Annu. Freq. Control Symp.*, pp. 49–54.

Viennet, J., Audoin, C., and Desaintfuscien, M. (1971). Discussion of cavity pulling in passive frequency standards. *Proc. 25th Annu. Freq. Control Symp.*, 337–342.

Viennet, J., Audoin, C., and Desaintfuscien, M. (1972). Cavity pulling in passive frequency standards. *IEEE Trans. Instrum. Meas.* **IM-21**, 204–209.

Vishina, A. V., and Gaigerov, B. A. (1976). Hydrogen time and frequency standards with redundancy. *Meas. Tech. (Engl. Transl.)* **19**, 1460–1461.

Wallard, A. J. (1972). Frequency stabilization of the helium–neon laser by saturated absorption in iodine vapour. *J. Phys. E.* **5**, 926–930.

Walls, F. L. (1982). Vibration and acceleration-induced timing errors with atomic clocks and clock systems. *Proc. 36th Annu. Freq. Control Symp.*, p. 371.

Walls, F. L., and Hellwig, H. (1976). A new kind of passively operating hydrogen frequency standard. *Proc. 30th Annu. Freq. Control Symp.*, pp. 473–480.

Walls, F. L., and Howe, D. A. (1978). A passive hydrogen maser frequency standard. *Proc. 32nd Annu. Freq. Control Symp.*, pp. 492–498.

Walls, F. L., and Howe, D. A. (1980). A passive hydrogen maser frequency standard. *CPEM Dig.*, pp. 152–156.

Walls, F. L., and Howe, D. A. (1981). Timekeeping potentials using passive hydrogen masers. *J. Phys. Colloq. (Orsay, Fr.)*, **42**, 151–158.

Walls, F. L., and Howe, D. A. (1982). Time keeping performance of a small passive hydrogen maser. *CPEM Dig.*, pp. M/20–21.

Walls, F. L., and Stein, S. R. (1976). "Servo Techniques in Oscillators and Measurement Systems." National Bureau of Standards Tech. Note 692, Boulder, Colorado.

Walls, F. L., Wineland, D. J., and Drullinger, R. E. (1978). New possibilities for frequency standards using laser cooling and detection of stored ions. *Proc. 32nd Annu. Freq. Control Symp.*, pp. 453–459.

Wang, H. T. M. (1979). Hydrogen frequency standard using free induction technique. *Proc. 33rd Annu. Freq. Control Symp.*, pp. 536–542.

Wang, H. T. M. (1980). An oscillating compact hydrogen maser. *Proc. 34th Annu. Freq. Control Symp.*, pp. 364–369.

Wang, H. T. M. (1982). Characteristics of oscillating compact hydrogen masers. *Proc. 36th Annu. Freq. Control Symp.*, pp. 249–254.

Wang, H. T. M. (1983). Application of metal hydrides for gas handling in hydrogen masers. *Proc. 37th Annu. Freq. Control Symp.*, pp. 7–11.

Wang, H. T. M., Lewis, J. B., and Crampton, S. B. (1979). Compact cavity for hydrogen frequency standard. *Proc. 33rd Annu. Freq. Control Symp.*, pp. 543–548.

White, J. (1983). Specifying performance for atomic standards. *Proc. 37th Annu. Freq. Control Symp.*, pp. 513–515.

White, J., and McDonald, K. (1981). Long term performance of VL-11 masers. *Proc. 35th Annu. Freq. Control Symp.*, pp. 657–661.

Williams, H. E., Kwon, T. M., and McClelland, T. (1983). Compact rectangular cavity for rubidium vapor cell frequency standards. *Proc. 37th Annu. Freq. Control Symp.*, pp. 12–17.

Wineland, D. J. (1977). The cesium beam frequency standard – prospects for the future. *Metrologia* **13**, 121–123.

Wineland, D. J., and Hellwig, H. (1977). Comment on "The Millman effect in cesium beam atomic frequency standards." *Metrologia* **13**, 173–174.

Wineland, D. J., and Ramsey, N. F. (1972). Atomic deuterium maser. *Phys. Rev. A* **5**, 821–837.

Wineland, D. J., Allan, D. W., Glaze, D. J., Hellwig, H., and Jarvis, S., Jr. (1976a). Results on limitations in primary cesium standard operation. *Conf. Precision Electromagn. Meas. (IEEE)*, p. 225.

Wineland, D. J., Allan, D. W., Glaze, D. J., Hellwig, H. W., and Jarvis, S., Jr. (1976b). Results on limitations in primary cesium standard operation. *IEEE Trans. Instrum. Meas.* **IM-25**, 453–458.

Wineland, D. J., Howe, D. A., and Mohler, M. B. (1977). Results with the special-purpose ammonia frequency standard. *Proc. 31st Annu. Freq. Control Symp.*, pp. 562–573.

Wineland, D. J., Drullinger, R. E., and Walls, F. L. (1978). Radiation-pressure cooling of bound resonant absorbers. *Phys. Rev. Lett.* **40**, 1639–1642.

Wineland, D. J., Howe, D. A., Mohler, M. B., and Hellwig, H. W. (1979). Special purpose ammonia frequency standard—a feasibility study. *IEEE Trans. Instrum. Meas.* **IM-28**, 122–132.

Wineland, D. J., Itano, W. M., Bergquist, J. C., and Walls, F. L. (1981). Proposed stored $^{201}Hg^{+}$ ion frequency standards. *Proc. 35th Annu. Freq. Control Symp.*, pp. 602–611.

Winkler, G. M. R., Hall, R. G., and Percival, D. B. (1970). The US Naval Observatory clock time reference and the performance of a sample of atomic clocks. *Metrologia* **6**, 126–134.

Xiaoren, Y. (1981). Works on Chinese primary frequency standards. *J. Phys. Colloq. (Orsay, Fr.)* **42**, 257–260.

Xue, C. (1980). Newly designed dipole-beam optics system for cesium-beam frequency standards. *IEEE Trans. Instrum. Meas.* **IM-29**, 301–304.

Xue, C. Y., and Yang, Y.-S. (1980). A newly designed dipole beam optic for cesium beam frequency standards. *CPEM Dig.*, pp. 138–140.

Yang, S. Q., and Zhong, X. B. (1980). Review of recent developments of the hydrogen atomic clock. *Wu Li* **9**, 342–349. In Chinese.

Yannoni, N. F. (1981). Clock requirements for navigation, communication and identification systems. *J. Phys. Colloq. (Orsay, Fr.)* **42**, 383–394.

Yassin, G. (1981). "Molecular Beam Maser Employing Quasi-Optical Resonators: Oscillation Behavior and Spectroscopic Applications." Ph.D. Thesis, University of Keele, Staffs, England.

Yassin, G., and Lainé, D. C. (1981). Elliptical oscillation in molecular beam maser with disk resonator. *Electron. Lett.* **17**, 156–157.

Yoda, J., and Koga, Y. (1982). Spatial profiles of a deflected cesium atomic beam. *Jpn. J. Appl. Phys., Part 1* **21**, 1244–1245.

Yoda, J., Nakadan, Y., and Koga, Y. (1978). Improvement of the frequency stability of the Cs frequency standard NRLM-I. *Jpn. J. Appl. Phys.* **17**, 1139–1140.

Yoshimura, K., and Kobayashi, M. (1973). Analysis of the servo system of the rubidium vapor frequency standard. *Rev. Radio Res. Lab. Jpn.* **19**, 117–127.

Yuuki, T., Uchida, H., Sato, Y., Kumamoto, H., Oyamada, H., Kawaji, H., and Kondo, K. (1974). Rubidium frequency standard. *NEC Res. Dev.* (31), 42–56.

Zepler, M. M. (1971). Miniaturized, rapid warm up rubidium frequency source. *Proc. 25th Annu. Freq. Control Symp.*, pp. 331–336.

Zhabotinskii, M. E., Karlov, N. V., and Shteinshleiger, V. B. (1967). Masers. *Radiotekh. Elektron* **12**, 2032–2051. In Russian.

Zhabotinskii, M. Ye. (1967). Quantum frequency standards. *Radiotekh. Elektron.* **12**, 2023–2031. In Russian.

Zhai, Z. C. (1981). Shanghai Observatory's hydrogen maser. *J. Inst. Electron. Telecommun. Eng. (New Delhi)* **27**, 510–513.

Zhai, Z. C., and Chuang, C. H. (1981). The developments of atomic time and frequency standards at Shanghai Observatory and some applications. *J. Inst. Electron. Telecommun. Eng. (New Delhi)* **27**, 500–503.

Zhestkova, N. D., and Elkin, G. A. (1979). Effect of nonuniform magnetic field on a hydrogen-maser frequency. *Meas. Tech. (Engl. Transl.)* **22**, 1079–1081.

Zhestkova, N. D., Elkin, G. A., and Zemskova, V. I. (1976). Hydrogen frequency standard and undisturbed frequency-transition evaluation. *Meas. Tech. (Engl. Transl.)* **19**, 1461–1463.

Zholnerov, V. S. (1977). Buffer mixtures for the gas cell of an optically pumped frequency standard. *Opt. Spectrosc. (Engl. Transl.)* **43**, 566–568.

Zholnerov, V. S., and Korniyenko, V. V. (1976). On optimizing the parameters of the static automatic frequency control system of a passive quantum frequency standard in terms of the accuracy characteristics. *Radio Eng. Electron. Phys. (Engl. Transl.)* **21**, 106–109.

Zitzewitz, P. W. (1970). Surface collision frequency shifts in the atomic hydrogen maser. *Proc. 24th Annu. Freq. Control Symp.*, pp. 263–269.

Zitzewitz, P. W., and Ramsey, N. F. (1971). Studies of the wall shift in the hydrogen maser. *Phys. Rev. A.* **3**, 51–61.

Zitzewitz, P. W., Uzgiris, E. E., and Ramsey, N. F. (1973). Wall shift of FEP Teflon in the hydrogen maser. *Rev. Sci. Instrum.* **41**, 81–86.

Chapter 11

Abate, J. A. (1976). Long-term frequency and intensity stabilization of a c.w. dye laser. *J. Appl. Phys.* **47**, 1464–1466.

Akimoto, Y., and Ohi, M. (1977). Frequency fluctuation analysis of CH_4 stabilized He–Ne lasers. *Jpn. J. Appl. Phys.* **16**, 385–386.

Akimoto, Y., and Ohi, M. (1978). Stability evaluation of frequency stabilized laser. *Oyo Butsuri* **47**, 425–431. In Japanese.

Akimoto, Y., and Tako, T. (1975). A double servo system for the CH_4 stabilized laser. *Oyo Butsuri* **44**, 635–640. In Japanese.

Alekseev, V. A., and Malyugin, A. V. (1977). Influence of the hyperfine structure on the frequency reproducibility of an He–Ne laser with a methane absorption cell. *Sov. J. Quantum Electron. (Engl. Transl.)* **7**, 1075–1081.

Ambartsumjan, R. V., Basov, N. G., and Letokhov, V. S. (1968a). Frequency stability of He–Xe laser with non-resonant feedback. *Conf. Precision Electromagn. Meas. (IEEE)*, p. 45.

Ambartsumjan, R. V., Basov, N. G., and Letokhov, V. S. (1968b). Investigation of the frequency characteristics of a Xe–He laser with a diffuse mirror. *Zh. Eksper. Teor. Fiz., Pis'ma Red.* **7**, 88–91. In Russian.

Andreev, P. S., Gusev, A. A., Kruzhalov, S. V., Pakhomov, L. N., and Petrun'kin, V. Yu. (1978). Stabilized single-frequency traveling-wave YAG:Nd^{3+} laser. *Sov. Tech. Phys. Lett. (Engl. Transl.)* **4**, 137–138.

Andronova, I. A., Mamaev, Yu. A., and Markelov, N. A. (1979). Operating characteristics of a frequency-stabilized ring laser with a methane cell. *Sov. J. Quantum Electron. (Engl. Transl.)* **9**, 543–547.

Anonymous (1977a). "Informative Meeting on Iodine Stabilised He–Ne Lasers." Phys.-Tech. Bundesanstalt, Braunschweig, Germany, p. 158.

Anonymous (1977b). Single frequency superstable gas laser. *Sov. J. Quantum Electron. (Engl. Transl.)* **7**, 1425–1426.

Anonymous (1981). He–Ne 0.633 μm laser frequency stabilised to the neon saturated absorption. *Laser J. (China)* **8**, 58–59. In Chinese.

Antropov, Ye. T., Kochetkov, Yu. A., Ostapets, V. N., Panov, Ye. I., Podobed, V. S., Silin-Bekchurin, I. A., Sobolev, N. N., and Taktarov, S. G. (1975). Automatic frequency control of a selective CO_2 laser by means of a piezoelectric device. *Radio Eng. Electron. Phys. (Engl. Transl.)* **19**, 59–62.

Arditi, M. (1975). Application of the light-shift effect to laser frequency stabilization with reference to a microwave frequency standard. *Opt. Commun.* **15**, 317–322.

Arzumanov, V. N., Zaitsev, G. F., Kruzhalov, S. V., Pakhomov, L. N., and Petrun'kin, V. Yu. (1977). Single-frequency YAG-Nd laser stabilised by a standard anisotropic resonator. *Avtometriya* (2), 125–127. In Russian.

Avtonomov, V. P., Alexandrescu, R., Dumitras, D., and Dutu, D. (1979). Possible stabilization of the frequency of a CO_2 laser using an external Stark cell containing 1-1 difluoroethane. *Sov. J. Quantum Electron. (Engl. Transl.)* **9**, 204–206.

Baer, T., Kowalski, F. V., and Hall, J. L. (1980). Frequency stabilization of a 0.633-μm He–Ne longitudinal Zeeman laser. *Appl. Opt.* **19**, 3173–3177.

Bagaev, S. N., Kolomnikov, Ju. D., Lisitsin, V. N., and Chebotaev, V. P. (1968a). Stabilization of reproducibility of frequencies of He–Ne lasers at 0.63 μ. *IEEE J. Quantum Electron.* **QE-4**, 868–870.

Bagaev, S. N., Kolomnikov, Yu. D., and Chebotaev, V. P. (1968b). Stabilization and reproducibility of a helium–neon laser frequency at $\lambda = 0.63$ μ. *Izmer. Tekh.* (8), 27–29. In Russian.

Bagaev, S. N., Vasilenko, L. S., and Chebotaev, V. P. (1970). An optical frequency standard with two absorption cells. *Opt. Spectrosk.* **29**, 156–159. In Russian.

Bagaev, S. N., Vasilenko, L. S., Matyugin, V. M., Klementev, V. M., Troshin, B. I., and Chebotaev, V. P. (1972). Some results of an investigation of the generation-frequency stability of gas lasers at 0.63 μm, 1.5 μm, 3.39 μm, and 9.6 μm. *Opt. Spectrosc.* **32**, 422–425.

Bagaev, S. N., Baklanov, E. V., Timov, E. A., and Chebotaev, V. B. (1974). Reproducibility of the frequency of a He–Ne laser with a methane absorption cell. *Zh. Eskp. Teor. Fiz., Pis'ma Red.* **20**, 292–296. In Russian.

Bagaev, S. N., and Chebotaev, V. P. (1975). Frequency stability and reproducibility of the 3.39 μm He–Ne laser stabilized on the methane line. *Appl. Phys.* **7**, 71–76.

Bagaev, S. N., Vasilenko, L. S., Gol'dort, V. G., Dmitriev, A. K., and Dychkov, A. S. (1977a). Helium–neon laser emitting $\lambda = 3.39\mu$ line of 7 Hz width. *Sov. J. Quantum Electron. (Engl. Transl.)* **7**, 665–666.

Bagaev, S. N., Chebotayev, V. P., and Vasilenko, L. S. (1977b). A narrow linewidth (10 Hz) frequency scannable 3.39 μm He–Ne laser and its application to frequency stabilization and high-resolution spectroscopy. *IEEE J. Quantum Electron.* **QE-13**, 33.

Bagaev, S. N., Dychkov, A. S., and Chebotaev, V. P. (1979). Stable gas laser with 0.4-Hz line width. *Sov. Tech. Phys. Lett. (Engl. Transl.)* **5**, 240–242.

Bagaev, S. N., Chebotayev, V. P., Dychkov, A. S., and Maltsev, S. V. (1981). Supernarrow resonances in methane on E-line of the P(7) transition of the ν_3 band and their application in optical frequency standards. *J. Phys. Colloq. (Orsay, Fr.)* **42**, 21–28.

Bagaev, S. N., Gol'dort, V. G., Dychkov, A. S., Klement'ev, V. M., Matyugin, Yu. A., Nikitin, M. V., Pecherskii, Yu. Ya., and Chebotaev, V. P. (1982). Joint time and length standard. *Sov. J. Quantum Electron.* (*Engl. Transl.*) **12**, 267.

Baird, K. M. (1969). Laser stabilization at N.R.C. (Canada). *Electron Technol.* **2**, 85–88.

Baird, K. M. (1983). Frequency measurement of optical radiation. *Phys. Today* **36**, 52–57.

Baird, K. M., and Hanes, G. R. (1974). Stabilization of wavelengths from gas lasers. *Rep. Prog. Phys.* **37**, 927–950.

Baird, K. M., Riccius, H. D., Siemsen, K. J., Hart, K. H., and Smith, D. S. (1971). Measurements of stabilized laser wavelengths. *Annu. Meeting Dig. Opt. Soc. Am.*, Washington, D.C., p. 25.

Bakumenko, V. M., and Valitov, R. A. (1970). Frequency stabilization and instability measurements of helium–neon lasers at a wavelength of 0.6328 μm. *Radiotekh. Elektron.* **15**, 2289–2293. In Russian.

Balhorn, R., Kunzmann, H., and Lebowsky, F. (1972). Frequency stabilization of internal-mirror helium–neon lasers. *Appl. Opt.* **11**, 742–744.

Balhorn, R., Lebowsky, F., and Ullrich, D. (1975). "Efficiency of the Frequency Stabilisation of He–Ne Lasers by the Two-Mode Comparison Method." Report PTB-Me-9, Phys.-Tech. Bundesanstalt, Braunschweig, Germany, 29 pp.

Baranov, V. Yu., Kazakov, S. A., Likhanskii, V. V., Mezhevov, V. S., Napartovich, A. P., Orlov, M. Yu., Pis'mennyi, V. D., and Starodubtsev, A. I. (1979). Stabilization of the frequency of a pulse-periodic TEA CO_2 laser by injection of a signal from a low-pressure CW laser. *Sov. J. Quantum Electron.* (*Engl. Transl.*) **9**, 1456–1458.

Barger, R. L., and Hall, J. L. (1969a). Pressure shift and broadening of methane line at 3.39 micron studied by laser-saturated molecular absorption. *Proc. 23rd Annu. Freq. Control Symp.*, p. 306.

Barger, R. L., and Hall, J. L. (1969b). Pressure shift and broadening of methane line at 3.39 μm studied by laser-saturated molecular absorption. *Phys. Rev. Lett.* **22**, 4–8.

Barger, R. L., and Hall, J. L. (1973). Wavelength of the 3.39 μm laser-saturated absorption line of methane. *Appl. Phys. Lett.* **22**, 196–199.

Barger, R. L., and West, J. B. (1975). Fast frequency stabilization of a CW dye laser. *Appl. Phys. Lett.* **27**, 31–33.

Barger, R. L., Sorem, M. S., and Hall, J. L. (1973). Frequency stabilization of a CW dye laser. *Appl. Phys. Lett.* **22**, 573–575.

Barger, R. L., English, T. C., and West, J. B. (1975). Frequency stabilization of a CW dye laser and laser saturation of atomic beams. *Proc. 29th Annu. Freq. Control Symp.*, pp. 316–320.

Basov, N. G., and Letokhov, V. S. (1968a). "Optical Frequency Standards," P. N. Lebedev Institute of Physics, Quantum Radiophys. Lab. (Moscow), Preprint No. 32.

Basov, N. G., and Letokhov, V. S. (1968b). Optical frequency standards. *Upspekhi Fiz. Nauk* **96**, 585–632. In Russian.

Basov, N. G., and Letokhov, V. S. (1969). Optical frequency standards. *Electron Technol.* **2**, 15–20.

Basov, N. G., Belenov, E. M., Danileiko, M. V., and Nikitin, V. V. (1971). Power resonances and frequency stabilization of a gas laser with a nonlinear-absorption cell. *Kvantovaya Elektron* (*Moscow*) (1), 42–52. In Russian.

Basov, N. G., Belenov, E. M., Vol'nov, M. I., Gubin, M. A., Nikitin, V. V., and Troshagin, V. N. (1972a). Stabilization of ring-laser frequency. *Zh. Eksp. Teor. Fiz., Pis'ma Red.* **15**, 659–661. In Russian.

Basov, N. G., Gubin, M. A., Nikitin, V. V., Protsenko, E. D., and Stepanov, V. A. (1972b). Frequency stabilization of a gas laser using mode-interaction effects. *Zh. Eksp. Teor. Fiz., Pis'ma Red.* **15**, 525–528. In Russian.

Basov, N. G., Belenov, E. M., Vol'nov, M. I., Gubin, M. A., Danileiko, M. V., and Nikitin, V. V. (1973). Frequency reproducibility of a stabilized ring laser. *Sov. Phys.—Dokl.* (*Engl. Transl.*) **18**, 316–317.

Batarchukova, N. R., Glozman, Ts. I., Kartashev, A. I., Irikova, L. A., and Ptitsyna, E. A. (1974). Certifying the wavelengths of He–Ne lasers stabilized by means of the Lamb dip. *Meas. Tech.* (*Engl. Transl.*) **17**, 1116–1117.

Bava, E., De Marchi, A., and Godone, A. (1978). Direct synthesis of the frequency of a long distance infrared source. *Alta Freq.* **47**, 851–858. In Italian.

Bayer-Helms, F. (1980). Frequency stabilized lasers with iodine measuring cell. *Jamna Mech. Opt.* **25**, 282–287. In Czech.

Bayer-Helms, F., Chartier, J.-M., Helmcke, J., and Wallard, A. (1977). Evaluation of the international intercomparison measurements (March 1976) with $^{127}I_2$-stabilised He–Ne-lasers: spacings of the hyperfine structure components. Informative Meeting on Iodine Stabilised He–Ne Lasers, Phys.-Tech. Bundesanstalt, Braunschweig, Germany, pp. 139–146.

Bazarov, E. N., Gerasimov, G. A., Gubin, V. P., and Posudin, Yu. I. (1977). Frequency stabilisation of CO_2-lasers using narrow resonances in OsO_4. *Izv. Vyssh. Uchebn. Zaved. Radioelektron.* **20**, 39–44. In Russian.

Bazarov, E. N., Gerasimov, G. A., Gubin, V. P., and Starostin, N. I. (1981a). CO_2 laser frequency stabilization according to narrow resonances in OsO_4. II. *Radio Electron. Commun. Syst.* (*Engl. Transl.*) **24**, 63–66.

Bazarov, E. N., Gerasimov, G. A., Gubin, V. P., Sazonov, A. I., Starostin, N. I., and Fomin, E. N. (1981b). Stabilization of the emission frequency of a high-pressure waveguide CO_2 laser with the aid of resonances of saturated absorption in OsO_4 molecules. *Kvantovaya Elektron.* (*Moscow*) **7**, 2646–2649.

Beehler, R. E. (1971). Cesium atomic beam frequency standards. *Proc. 25th Annu. Freq. Control Symp.*, pp. 297–308.

Belenov, E. M., Danileiko, M. V., Nedavnii, A. P., and Shpak, M. T. (1977). Frequency shifts in stabilized gas lasers. *Ukr. Fiz. Zh.* (*Russ. Ed.*) **22**, 1765–1779. In Russian.

Bennett, S. J., Ward, R. E., and Wilson, D. C. (1973). Comments on: frequency stabilization of internal mirror He–Ne lasers. *Appl. Opt.* **12**, 1406.

Bennett, S. J., Cerez, P., Hamon, J., and Chartier, A. (1979). Wavelength of a helium–neon laser stabilized by saturated absorption in iodine at 612 nm. *Metrologia* **15**, 125.

Bennett, W. R., Jr. (1972). Role of hole burning in the self-stabilization of gas laser frequencies. *Comments At. Mol. Phys.* **3**, 63–68.

Bergquist, J. C., and Wineland, D. J. (1979). Laser to microwave frequency division using synchroton radiation. *Proc. 33rd Annu. Freq. Control Symp.*, pp. 494–497.

Bergquist, J. C., Drullinger, R. E., Itano, W. M., Walls, F. L., and Wineland, D. J. (1981). Cooling atomic ions with lasers [time and frequency standards]. *Dimension* **65**, 23–24.

Bertinetto, F., and Rebaglia, B. I. (1977). Performances of IMGC He–Ne ($^{127}I_2$) lasers. *European Conf. Precise Electrical Meas.* (*IEE*), pp. 38–39.

Bertinetto, F., Rebaglia, B. I., Liverani, M., and Gualini, S. (1975). Present development of iodine stabilized He–Ne lasers at the Istituto di Metrologia Gustavo Colonnetti. *Alta Freq.* **44**, 569–573.

Bertrand, L., Monchalin, J.-P., Pitre, R., and Gagne, J. M. (1981). Frequency stability of a small scale HF CW laser. *J. Appl. Phys.* **52**, 6059–6063.

Bessmel'tsev, V. P., Vorob'ev, V. V., and Khanov, V. A. (1975). Stabilisation of the frequency difference in a two-frequency laser. *Avtometriya* (5), 94–96. In Russian.

Beterov, I. M., Klement'ev, V. M., and Chebotaev, V. P. (1969). Secondary frequency standard using mercury laser at microwaves. *Radiotekh. Elektron* **14**, 2066–2069. In Russian.

Beterov, I. M., Matyugin, Yu. A., Milushkin, G. A., Troshin, B. I., and Chebotaev, V. P. (1972a). High-stability gas laser based on non-linear absorption ($\lambda = 0.63\,\mu$). III. Optical system of a stabilised single frequency He–Ne laser at $\lambda = 0.63\,\mu$. *Avtometriya* (6), 55–63. In Russian.

Beterov, I. M., Matyugin, Yu. A., Milushkin, G. A., Troshin, B. I., and Chebotaev, V. P. (1972b). High stability gas-filled laser based on non-linear absorption ($\lambda = 0.63$ microns). I. Methods of frequency stabilisation for gas-filled power lasers. *Avtometriya* (5), 71–85. In Russian.

Beterov, I. M., Matyugin, Yu. A., Milushkin, G. A., Troshin, B. I., and Chebotaev, V. P. (1972c). High stability gas-filled laser based on non-linear absorption ($\lambda = 0.63$ microns). II. Selection of modes of oscillation in a He–Ne laser at $\lambda = 0.63$ microns. *Avtometriya* (5), 59–70. In Russian.

Beterov, I. M., Matyugin, Yu. A., Milushkin, G. A., Troshin, B. I., and Chebotaev, V. P. (1972d). High-stability gas laser based on non-linear absorption ($\lambda = 0.63\,\mu$). IV. Electronic automatic frequency stabilisation system. *Avtometriya* (6), 64–68. In Russian.

Beterov, I. M., Matyugin, Yu. A., Milushkin, G. A., Troshin, B. I., and Chebotaev, V. P. (1974). High-stability gas laser based on nonlinear absorption ($\lambda = 0.63$ micron). V. Experimental study of the dispersion characteristics of the optical discriminator and the stability and reproducibility of the laser emission frequency. *Avtometriya* (6), 53–54. In Russian.

Bikmukhametov, K. A., Klement'ev, V. M., and Chebotaev, V. P. (1972). Investigation of the stability of the oscillation frequency of a mercury laser emitting at $\lambda = 1.53\,\mu$. *Sov. J. Quantum Electron.* (*Engl. Transl.*) **2**, 254–256.

Bikmukhametov, K. A., Bobrik, V. I., Kolomnikov, Yu. D., and Mogil'nitskii, B. S. (1977). Helium–neon lasers as standard wavelength sources. *Meas. Tech.* (*Engl. Transl.*) **20**, 821–823.

Billings, B., ed. (1972). "American Institute of Physics Handbook." McGraw-Hill, New York.

Birnbaum, G. (1967). Frequency stabilization of gas lasers. *Proc. IEEE* **55**, 1015–1026.

Birnbaum, G. (1969). Frequency stabilized gas lasers. A summary. *Electron Technol.* **2**, 67–69.

Blabla, J. (1978). State of development of a He–Ne laser stabilised by saturated absorption in $^{127}I_2$. *Feingeraetetechnik* **27**, 111. In German.

Blanaru, C., Popescu, G. H., Chetroiu, A., Apostol, D., and Ionescu, A. (1982). Single-frequency stabilized He–Ne laser. *Rev. Roum. Phys.* **27**, 167–176.

Blaney, T. G., Bradley, C. C., Edwards, G. J., and Knight, D. J. E. (1973a). Absolute frequency measurement of a Lamb-dip stabilised water vapour laser oscillating at 10.7 THz (28 μm). *Phys. Lett. A* **43**, 471–472.

Blaney, T. G., Bradley, C. C., Edwards, G. J., Knight, D. J. E., Woods, P. T., and Jolliffe, B. W. (1973b). Absolute frequency measurement of the R(12) transition of CO_2 at 9.3 μm. *Nature* **244**, 504.

Blaney, T. G., Bradley, C. C., Edwards, G. J., Jolliffe, B. W., Knight, D. J. E., and Woods, P. T. (1975). Measurement of the frequency of the methane-stabilised laser at 3.39 μm and of the R(32) transition of CO_2 at 10.17 μm. *Nature* **254**, 584–585.

Blaney, T. G., Edwards, G. J., Jolliffe, B. W., Knight, D. J. E., and Woods, P. T. (1976). Absolute frequencies of the methane-stabilized HeNe laser (3.39 μm) and the CO_2, R(32) stabilized laser (10.17 μm). *J. Phys. D.* **9**, 1323–1330.

Blaney, T. G., Bradley, C. C., Edwards, G. J., Jolliffe, B. W., Knight, D. J. E., Rowley, W. R. C., Shotton, K. C., and Woods, P. T. (1977). Measurement of the speed of light. I. Introduction and frequency measurement of a carbon dioxide laser. *Proc. R. Soc. London, Ser. A* **355**, 61–88.

Bloom, A. L. (1971). Gas lasers and their application to precise length measurements. *In* "Progress in Optics," Vol. 9 (E. Wolf, ed.), pp. 3–30. North-Holland, Amsterdam.

Bloom, A. L., and Wright, D. L. (1966). Pressure shifts in a stabilized single wavelength helium–neon laser. *Appl. Opt.* **5**, 1528–1532.

Bobrik, V. I., Gol'dort, V. G., Kolomnikov, Yu. D., and Percherskii, Yu. Ya. (1974). Stabilization of laser frequencies. *Meas. Tech.* (*Engl. Transl.*) **17**, 1252–1253.

Bobrik, V. I., Kolomnikov, Yu. D., and Mogil'nitskii, B. S. (1975). Measuring the wavelength of a helium–neon laser. *Meas. Tech.* (*Engl. Transl.*) **18**, 1788–1789.

Bodlaj, V. (1969). Frequency stabilization of the He–Ne-laser with an external Ne absorption tube in the magnetic alternating field. *Frequenz* **23**, 92–94. In German.

Bodlaj, V. (1970a). Absolute frequency stabilization of a He–Ne laser by an external Ne-absorption cell in an alternating magnetic field. *8th Int. Conf. Microwave Opt. Generation Amplification*, Eindhoven, The Netherlands: MOGA70, 1 p.

Bodlaj, V. (1970b). Frequency stabilisation of the He–Ne laser with an external Ne-absorption tube in an alternating magnetic field. *Opto-electronics* (*London*) **2**, 221–226.

Bodlaj, V. (1971a). Frequency stabilization of a He–Ne laser with an external absorption tube in an alternating magnetic field. *Z. Angew. Phys.* **31**, 97–105. In German.

Bodlaj, V. (1971b). He–Ne laser wave as a secondary length standard. *Laser Angew. Strahlentech.* **3**, 21–28. In German.

Bodlaj, V. (1971c). Frequency stabilisation of a He–Ne laser in an alternating magnetic field. *Phys. Lett. A* **35**, 381–382.

Bodlaj, V. (1972). Ne absorption tube in an alternating magnetic field inside a laser cavity as a frequency standard. *Opt. Commun.* **6**, 12–14.

Bondarenko, A. N., and Irinitsyn, Yu. M. (1978). Frequency stabilisation in a He–Ne laser at $\lambda = 0.63\,\mu$ operating in competitive oscillation mode. *Avtometriya* (3), 115–119. In Russian.

Bondarenko, A. N., Vologdin, V. K., and Krinitsyn, Yu. M. (1978). Stabilized two-frequency He + Ne laser for 0.63 μ wavelength. *Instrum. Exp. Tech.* (*Engl. Transl.*) **21**, 1090–1092.

Bonsch, G. (1977). Wavelength intercomparison between methane- and iodine-stabilized He–Ne lasers: alignment and error estimations. Informative Meeting on Iodine Stabilised He–Ne Lasers. Phys.-Tech. Bundesanstalt, Braunschweig, Germany, pp. 151–158.

Borde, C., and Hall, J. (1973). Influence of hyperfine structure of methane stabilized He–Ne laser. *Proc. 27th Annu. Freq. Control Symp.*, p. 386.

Borde, C., and Henry, L. (1968). Study of the Lamb dip and of rotational competition in a carbon dioxide laser. Applications to the laser stabilization and to the measurement of absorption coefficients of gases. *IEEE J. Quantum Electron.* **QE-4**, 874–880.

Borde, C., Camy, G., Vialle, J. L., and Decomps, B. (1974). Frequency stabilization of an argon laser by saturated absorption or dispersion in iodine at 5145 Å. *CPEM Dig.*, p. 105.

Borisovskii, S. P., Vereikin, V. K., Vlasov, A. N., Ostapchenko, E. P., Teselkin, V. V., Chulyaeva, E. G., and Yakovlev, Yu. M. (1977). Measuring stability and reproducibility of gas-laser generation frequency. *Meas. Tech.* (*Engl. Transl.*) **20**, 1161–1165.

Bourdet, G., Orszag, A., and de Valence, Y. (1973). Utilization of the impedance variation of the plasma of a CO_2 laser for frequency stabilization on the "Lamb dip." *C. R. Hebd. Seances Acad. Sci., Ser. B* **277**, 207–209. In French.

Boyne, H. S. (1970). Laser frequency stabilization techniques and its applications. *Proc. 24th Annu. Freq. Control Symp.*, pp. 233–239.

Boyne, H. S. (1971). Laser frequency stabilization techniques and applications. *IEEE Trans. Instrum. Meas.* **IM-20**, 19–22.

Bradley, C. C., and Knight, D. J. E. (1971). Frequency locking an HCN laser to a molecular absorption line. *Electron. Lett.* **7**, 381–382.

Brillet, A., and Cerez, P. (1981). Laser frequency stabilization by saturated absorption. *J. Phys. Colloq.* (*Orsay, Fr.*) **42**, 73–82.

Brillet, A., Cerez, P., and Clergeot, H. (1974). Frequency stabilization of He–Ne lasers by saturated absorption. *IEEE J. Quantum Electron.* **QE-10**, 526–528.

Brown, N. (1981). Frequency stabilized lasers: optical feedback effects. *Appl. Opt.* **20**, 3711–3714.

Bruce, C. F. (1971). Stable single-frequency He–Ne laser. *Appl. Opt.* **10**, 880–883.
Bulygin, A. S., and Kapralov, V. P. (1977). Synchronization of laser radiation with a quantum frequency standard in the microwave region. *Opt. Spektrosk.* **42**, 154–160. In Russian.
Burmakin, V. A., Korolev, F. A., Lebedeva, V. V., Odintsov, A. I., Salimov, V. M., and Sinitsa, L. N. (1971). A method for absolute frequency stabilization of an argon-ion laser with a magnetic field. *Radiotekh. Elektron.* **16**, 1292–1296. In Russian.
Camy, G., Decomps, B., Gardissat, J.-L., and Borde, C. J. (1977). Frequency stabilization of argon lasers at 582.49 THz using saturated absorption in $^{127}I_2$. *Metrologia* **13**, 145–148.
Cerez, P. (1980). Lasers as stable frequency sources. *In* "Imaging Processes and Coherence in Physics," pp. 17–27. Springer-Verlag, Berlin and New York.
Cerez, P., and Audoin, C. (1978). Frequency stability of the helium–neon laser including an iodine cell with warm walls. *C. R. Hebd. Seances Acad. Sci., Ser. B* **286**, 53–56. In French.
Cerez, P., and Bennett, S. J. (1978). New developments in iodine-stabilized He–Ne lasers. *IEEE Trans. Instrum. Meas.* **IM-27**, 396–398.
Cerez, P., and Bennett, S. J. (1979). Helium–neon laser stabilized by saturated absorption in iodine at 612 nm. *Appl. Opt.* **18**, 1079–1083.
Cerez, P., and Brillet, A. (1977). Factors which limit the reproducibility of iodine stabilized He–Ne lasers. *Metrologia* **13**, 29–33.
Cerez, P., Brillet, A., Hajdukovic, S., and Man, N. (1977a). Iodine stabilized He–Ne laser with a hot wall iodine cell. *European Conf. Precise Electrical Meas. (IEE)*, p. 37.
Cerez, P., Brillet, A., Hajdukovic, S., and Man, N. (1977b). Iodine stabilised He–Ne laser with a hot wall iodine cell. Informative Meeting on Iodine Stabilised He–Ne Lasers. Phys.-Tech. Bundesanstalt, Braunschweig, Germany, pp. 71–84.
Cerez, P., Brillet, A., Hajdukovic, S., and Man, N. (1977c). Iodine stablized He–Ne laser with a hot wall iodine cell. *Opt. Commun.* **21**, 332–336.
Cerez, P., Brillet, A., and Man, C. (1979). Frequency stabilised He–Ne lasers. *Rev. Phys. Appl.* **14**, 347–351. In French.
Cerez, P., Brillet, A., Man-Pichot, C. N. (1980a). He–Ne lasers stabilized by saturated absorption in iodine at 612 nm. *IEEE Trans. Instrum. Meas.* **IM-29**, 352–354.
Cerez, P., Brillet, A., and Man, C. (1980b). He–Ne lasers stabilized by saturated absorption in iodine at 612 nm. *CPEM Dig.*, pp. 254–255.
Champagne, L. F. (1978). Electron beam controlled, neon stabilized XeF laser. *Proc. 4th Colloq. Electron. Transition Lasers.* Berlin, Germany (Springer-Verlag), pp. 32–36.
Chang, P. L., Chang, L. F., Yuan, S. S., and Han, S. F. (1978). Investigation of the frequency stabilization of a duel frequency laser. *J. Tsing Hua Univ.* (3), 21–31. In Chinese.
Chartier, J.-M. (1982). Results of international comparisons using methane stabilized He–Ne lasers at 3.39 μm and iodine stabilized He–Ne lasers at 633 nm. *CPEM Dig.*, pp. E18–21.
Chartier, J.-M., and Avrons, D. (1977a). International comparisons of iodine stabilized He–Ne lasers. Informative Meeting on Iodine Stabilised He–Ne Lasers, Phys.-Tech. Bundesanstalt, Braunschweig, Germany, pp. 133–138.
Chartier, J.-M., and Avrons, D. (1977b). Technological principles of iodine stabilized He–Ne lasers. Informative Meeting on Iodine Stabilised He–Ne Lasers, Phys.-Tech. Bundesanstalt. Braunschweig, Germany, pp. 13–31. In French.
Chartier, J.-M., Helmcke, J., and Wallard, A. J. (1976). International intercomparison of the wavelength of iodine-stabilized lasers. *IEEE Trans. Instrum. Meas.* **IM-25**, 450–453.
Chebotaev, V. P. (1978). Use of ultranarrow resonance in spectroscopy and for stabilizing gas laser frequencies. *Sov. J. Quantum Electron. (Engl. Transl.)* **8**, 1130–1135.
Chebotaev, V. P. (1979). Infrared and optical frequency standards. *Radio Sci.* **14**, 573–584.
Chiu, Y.-W. (1978). A survey of optical frequency standards. *Kexue Tongbao* **23**, 452–458. In Chinese.

Cho, Y., Tajime, T., and Matsuo, Y. (1968). Stabilization of a composite-cavity single-frequency laser. *IEEE J. Quantum Electron.* **QE-4**, 699–701.
Clairon, A., and Henry, L. (1974). Stabilisation of carbon dioxide gas lasers by saturated absorption. *C. R. Hebd. Seances Acad. Sci., Ser. B* **279**, 419–422. In French.
Clairon, A., Dahmani, B., and Rutman, J. (1980a). Accurate absolute frequency measurements on stabilized CO_2 and He–Ne infrared lasers. *IEEE Trans. Instrum. Meas.* **IM-29**, 268–272.
Clairon, A., Dahmani, B., and Rutman, J. (1980b). New measurements of the frequency of the stabilized $^{13}CO_2$ P(28), CO_2 R(30) and He–Ne(CH_4) lasers. *CPEM Dig.*, pp. 86–89.
Clairon, A., Van Lerberghe, A., Salomon, C., Ouhayoun, M., and Borde, C. J. (1980c). Towards a new absolute frequency reference grid in the 28 THz range. *Opt. Commun.* **35**, 368–372.
Clairon, A., Van Leberghe, A., Breant, Ch., Salomon, Ch., Camy, G., and Borde, Ch. J. (1981). A new absolute frequency reference grid in the 28 THz range. *J. Phys. Colloq. (Orsay, Fr.)* **42**, 127–135.
Clark, N. A. (1976). Laser frequency stabilization: combined integrating thermal-proportional servos. *Appl. Opt.* **15**, 1375.
Clarke, R. T., III. (1982). US Naval Observatory time scale at the operational level. *CPEM Dig.*, pp. M/18–19.
Cole, J. B. (1975). Laser frequency stabilization using a resonator containing a saturable absorber. *J. Phys. D.* **8**, 1392–1408.
Cole, J. B., and Bruce, C. F. (1975). Iodine stabilized laser with three internal mirrors. *Appl. Opt.* **14**, 1303–1310.
Corcoran, V. J. (1969). Frequency lock of the hydrogen cyanide laser to a microwave frequency standard. *IEEE J. Quantum Electronics* **QE-5**, 424–426.
Corcoran, V. J., Cupp, R. E., and Gallagher, J. J. (1969). Stability investigations of HCN laser. *Proc. 23rd Annu. Freq. Control Symp.*, pp. 307–311.
Corcoran, V. J., Cupp, R. E., Smith, W. T., and Gallagher, J. J. (1970a). Stabilization of a far-infrared molecular laser. *IEEE J. Quantum Electron.* **QE-6**, 184.
Corcoran, V. J., Cupp, R. E., and Gallagher, J. J. (1970b). Automatic frequency control and phaselocking of lasers. *Proc. 24th Annu. Freq. Control Symp.*, pp. 240–245.
Corcoran, V. J., Gallagher, J. J., and Cupp, R. E. (1970c). Stabilization of a submillimeter wavelength laser on a microwave frequency standard. *Symp. Submillimetre Waves* Polytechnic Press, New York, p. 2.
Cupp, R. E., Corcoran, V. J., and Gallagher, J. J. (1970). Phase lock of a far-infrared laser to an absolute frequency standard. *IEEE J. Quantum Electron.* **QE-6**, 160–162.
Dandwate, V. D., Puntambekar, P. N., and Sen, D. (1979). Iodine stabilised He–Ne laser. *Pramana* **12**, 465–474.
Danileiko, M. V., Nedavnii, A. P., Nikolaenko, A. N., Fedin, V. P., and Shpak, M. T. (1975). Use of self-excited lasing modes to increase the reproducibility of frequency-stabilised ring lasers. *Sov. Phys.—Dokl. (Engl. Transl.)* **20**, 625–626.
Dehmelt, H. (1981). Mono-ion oscillator as ultimate laser frequency standard. *Proc. 35th Annu. Freq. Control Symp.*, pp. 569–601.
Dehmelt, H. G. (1982). Mono-ion oscillator as potential ultimate laser frequency standard. *IEEE Trans. Instrum. Meas.* **IM-31**, 83–87.
Deki, K., Yamamoto, H., and Ohta, T. (1979). Frequency stabilization of a gas laser utilizing the magnetic field tuning dip. *Trans. Inst. Electron. Commun. Eng. Jpn. [Part] E* **62**, 56–57.
Dekker, H., and Lamberts, C. W. (1975). Stability measurements of a tunable single frequency He–Ne laser by means of self-locking phenomena. *Opt. Quantum Electron.* **7**, 239–245.
Domnin, Yu. S., Tatarenkov, V. M., and Shumyatskii, P. S. (1975). D_2O laser for absolute frequency measurements. *Sov. J. Quantum Electron. (Engl. Transl.)* **5**, 991–993.

Domnin, Yu. S., Tatarenkov, V. M., and Shumyatskii, P. S. (1976). Absolute frequency measurements of lasers in submillimeter and infrared ranges. *Meas. Tech. (Engl. Transl.)* **19**, 1475–1479.

Domnin, Yu. S., Tatarenkov, V. M., and Shumyatskii, P. S. (1977). Laser translator of standard frequency to submillimetre range. *Sov. J. Quantum Electron. (Engl. Transl.)* **7**, 661–662.

Domnin, Yu. S., Kardashova, L. M., Tatarenkov, V. M., and Shumyatskii, P. S. (1979a). Frequency stabilization of a CO_2 laser by fluorescence of the CO_2 gas. *Meas. Tech. (Engl. Transl.)* **22**, 1179–1181.

Domnin, Yu. S., Koshelyaevskii, N. B., Tatarenkov, V. M., and Shumyatskii, P. S. (1979b). Absolute measurement of IR laser frequencies. *Pis'ma Zh. Eksp. Teor. Fiz.* **30**, 273–275. In Russian.

Domnin, Yu. S., Koshelyaevskii, N. B., Tatarenkov, V. M., Shumyatskii, P. S., Kompanets, O. N., Kukudzhanov, A. R., Letokhov, V. S., and Mikhailov, E. L. (1979c). $CO_2/^{192}OsO_4$ laser: absolute light oscillation frequency and new possibilities. *Pis'ma Zh. Eksp. Teor. Fiz.* **30**, 269–272. In Russian.

Domnin, Yu. S., Tatarenkov, V. M., and Shumyatskii, P. S. (1980). Phase locking of a D_2O laser to a frequency standard. *Sov. J. Quantum Electron. (Engl. Transl.)* **10**, 116–117.

Dschao, K., Glaeser, M., and Helmcke, J. (1980). I_2 stablized He–Ne lasers at 612 nm. *IEEE Trans. Instrum. Meas.* **IM-29**, 354–357.

Dumitras, D. C., Dutu, D. C., Comaniciu, N., Draganescu, V., Alexandrescu, R., and Morjan, I. (1981). Frequency stabilized CO_2 laser design. *Rev. Roum. Phys.* **26**, 485–498.

Dutu, C. A. (1972). Frequency stabilization by phase control of a single frequency–single mode CO_2 laser. *Stud. Cercet. Fiz.* **24**, 535–544. In Rumanian.

Dutu, D. (1974). Investigation of an automatic frequency stabilized CO_2 laser. *Rev. Roum. Phys.* **19**, 3–15. In German.

Efremon, Yu. P., Kapralov, V. P., Krasnov, K. A., Krylov, P. S., Privalov, V. E., Tkachenko, L. P., and Fofanof, Ya. A. (1980). International comparisons of He–Ne lasers stabilized by saturated absorption in iodine. *Opt. Spectrosc. (Engl. Transl.)* **48**, 97–99.

Eliel, E. R., Hogervorst, W., Van Lecuwen, K. A. H., and Post, B. H. (1981). A frequency-doubled frequency-stabilized CW ring dye laser for spectroscopy. *Opt. Commun.* **36**, 366–368.

Eng, R. S., and Spears, D. L. (1975). Frequency stabilization and absolute frequency measurements of a CW HF/DF laser. *Appl. Phys. Lett.* **27**, 650–652.

Engelhard, E. J. G. (1969). The feasibility of establishing a new primary wavelength standard of length by a laser line. *Electron Technol.* **2**, 71–76.

Evenson, K. M., and Peterson, F. R. (1975). Stabilized lasers and applications. *In* "Laser Applications to Optics and Spectroscopy," Addison-Wesley, Reading, Massachusetts.

Evenson, K. M., Wells, J. S., and Matarrese, L. M. (1970). Absolute frequency measurement of the CO_2 CW laser. *Appl. Phys. Lett.* **16**, 251–253.

Evenson, K. M., Day, G. W., Wells, J. S., and Mullen, L. O. (1972a). Extension of absolute frequency measurements to the cw He–Ne laser at 88 THz (3.39 μ). *Appl. Phys. Lett.* **20**, 133–134.

Evenson, K. M., Wells, J. S., Petersen, F. R., Danielson, B. L., Day, G. W., Barger, R. L., and Hall, J. L. (1972b). "Laser Frequency and Wavelength Measurements and the Speed of Light." Optical Society of America, Washington, D.C., 22 pp.

Evenson, K. M., Jennings, D. A., Petersen, F. R., and Wells, J. S. (1977). Laser frequency measurements: a review, limitations, extension to 197 THz (1.5 μm). *In* "Laser Spectroscopy III," pp. 56–68. Springer-Verlag, Berlin and New York.

Ezekiel, S. (1968). A molecular beam reference for laser frequency stabilization. *IEEE J. Quantum Electron.* **QE-4**, 367.

Ezekiel, S. (1969). Laser frequency stabilization using a primary frequency reference. *Proc. 23rd Annu. Freq. Control Symp.*, p. 312.

Ezekiel, S., and Weiss, R. (1968). Laser-induced fluorescence in a molecular beam of iodine. *Phys. Rev. Lett.* **20**, 91–93.

Facklam, R. L. (1982). Ultra-stable laser clock. *Proc. 36th Annu. Freq. Control Symp.*, pp. 361–369.

Facklam, R. L. (1983). The second generation ring laser clock. *Proc. 37th Annu. Freq. Control Symp.*, pp. 21–26.

Ferguson, J. B., and Morris, R. H. (1978). Single-mode collapse in 6328-Å He–Ne lasers. *Appl. Opt.* **17**, 2924–2929.

Freed, C. (1968a). Design and short-term stability of single-frequency CO_2 lasers. Abstract in *IEEE J. Quantum Electron.* **QE-4**, 369.

Freed, C. (1968b). Design and short-term stability of single-frequency CO_2 lasers. *IEEE J. Quantum Electron.* **QE-4**, 404–408.

Freed, C. (1970). Advances in stable CO_2 laser design and performance. *Int. Electron Devices Meeting (IEEE)*, p. 92.

Freed, C. (1975). Frequency stabilization of CO_2 lasers. *Proc. 29th Annu. Freq. Control Symp.*, pp. 330–337.

Freed, C., and Javan, A. (1970). Standing-wave saturation resonances in the CO_2 10.6 μ transitions observed in a low-pressure room-temperature absorber gas. *Appl. Phys. Lett.* **17**, 53–56.

Freed, C., and O'Donnell, R. G. (1977). Advances in CO_2 laser stabilization using the 4.3 μm fluorescence technique. *Metrologia* **13**, 151–156.

Freed, C., O'Donnell, R. G., and Ross, A. H. M. (1976). Absolute frequency calibration of the CO_2 isotope laser transitions [using varactor diode]. *IEEE Trans. Instrum. Meas.* **IM-25**, 431–437.

Fukuyo, H., Iga, K., Ueno, A., and Sano, T. (1971). Pure Ne laser and its fundamental characteristics. *Bull. Tokyo Inst. Technol.* (107), 67–73.

Galkin, S. L., Kruzhalov, S. V., Nikolaev, V. M., Pakhomov, L. N., and Petrun'kin, V. Yu. (1977). A stabilised YAG:Nd^{3+} laser with synchronisation of longitudinal modes. *Pis'ma Zh. Tekh. Fiz.* **3**, 18–20. In Russian.

Gallagher, J. J. (1975). Limitations on miniature molecular frequency sources. *Proc. 29th Annu. Freq. Control Symp.*, pp. 344–351.

Galutin, V. Z., Zenkevich, S. S., Obukhov, I. V., and Skibarko, A. P. (1973). Frequency stability of a gas laser operating in a two-mode domain. *Izv. Vyssh. Uchebn. Zaved. Radioelektron.* **16**, 90–93. In Russian.

Galutva, G. V., and Ryazantsev, A. I. (1971). Gas-laser resonator stabilized by thermal compensation. *Kvantovaya Elektron. (Moscow)* (2), 32–39. In Russian.

Gelikonov, V. M., Zaitsev, Yu. I., and Malykin, G. B. (1979). Laser frequency self-stabilization effect in the presence of rapid perturbations. *Sov. J. Quantum Electron. (Engl. Transl.)* **9**, 227–229.

George, S. M., and Harris, C. B. (1981). Passively mode-locked Nd:glass laser oscillator optimized for TEM_{00} selectivity and reliability. *Rev. Sci. Instrum.* **52**, 852–857.

Gerhardt, H., and Tittel, F. K. (1976). A frequency stabilized, CW dye laser for high resolution spectroscopy. *Opt. Commun.* **16**, 307–309.

Gerhardt, H., Bodecker, V., and Welling, H. (1971). Frequency behavior of a frequency-stable YAG:Nd^{3+}-laser. *Z. Angew. Phys.* **31**, 11–15. In German.

Gerstenhauer, E. (1976). A stable CW HCN laser. *Laser Elektro-Opt.* **8**, 20–21. In German.

Giacomo, P. (1977). Length metrology and iodine stabilized lasers. Informative Meeting on Iodine Stabilised He–Ne Lasers. Phys.-Tech. Bundesanstalt, Braunschweig, Germany, pp. 9–11. In French.

Gill, P., and Bennett, S. J. (1979). Iodine saturation spectroscopy for multi-wavelength stabilization of an argon/krypton ion laser. *Metrologia* **15**, 117–125.

Gill, P., and Spieweck, F. (1979). NPL PTB intercomparison of iodine-stabilized ion lasers. Report NPL-MOM-42, National Physics Laboratory, Teddington, England, 19 pp.

Glaser, M. (1982a). Frequency shifts at low iodine pressure of $^{127}I_2$-stabilized He–Ne lasers at 633 nm wavelength. *Metrologia* **18**, 53–58.

Glaser, M. (1982b). Nonlinear frequency shifts at low iodine pressures of $^{127}I_2$ stabilized He–Ne lasers at 633 nm wavelength. *CPEM Dig.*, pp. E/6–8.

Gnatovskii, A. V., Belenov, E. M., Danileiko, M. V., Nikitin, V. V., Fedin, V. P., and Shpak, M. T. (1974). Reproducibility of the frequency of a laser stabilised according to the transition of the absorbing gas. *Pis'ma Zh. Eskp. Teor. Fiz.* **19**, 368–371. In Russian.

Godzinski, Z., Abramski, K. A., and Matras, E. (1981a). Ultrastable lasers based on saturable absorption effect. The He–Ne/CH_4 lasers. *Elektronika* **22**, 16–19. In Polish.

Godzinski, Z., Matras, E., and Abramski, K. (1981b). Ultrastable lasers frequency stabilized by the effect of saturated absorption. *Elektronika* **22**, 23–26. In Polish.

Goldberg, M. W. (1971). The inverted Lamb dip in spectroscopy and laser stabilization. Ph.D. Thesis, Case Western Reserve University, Cleveland, Ohio. Available from University Microfilms, Ann Arbor, Michigan, Order No. 72-41.

Goldberg, M. W., and Yusek, R. (1971). Doppler jitter stabilization of a CO_2 laser. *Appl. Phys. Lett.* **18**, 135–137.

Greenstein: H. (1972). Theory of a gas laser with internal absorption cell. *J. Appl. Phys.* **43**, 1732–1750.

Gronchi, M., and Sona, A. (1970). Frequency stabilized lasers as absolute standards. *Riv. Nuovo Cimento Soc. Ital. Fis.* **2**, 219–252.

Gubin, M. A., Nikitin, V. V., Petrovskii, V. N., Protsenko, E. D., Tyurikov, D. A., and Yatsenko, L. P. (1979). Investigation of the stability and frequency shifts of a two-mode He–Ne–CH_4 laser. *Sov. J. Quantum Electron.* (*Engl. Transl.*) **9**, 34–39.

Gudelev, V. G., and Yasinskii, V. M. (1980). Simple system for frequency stabilization of a gas laser. *Instrum. Exp. Tech.* (*Engl. Transl.*) **23**, 223–226.

Gusev, A. Yu. (1981). Evaluation of the frequency stability of lasers. *Avtometriya* (6), 102–104. In Russian.

Gusev, V. M., Kompanets, O. N., Kukudzhanov, A. R., Letokhov, V. S., and Makhailov, E. L. (1975). Stabilization of the emission frequency of a CO_2 laser to within 10^{-12} with the aid of narrow SF_6 and OsO_4 resonances. *Sov. J. Quantum Electron.* **4**, 1370–1372.

Hackel, L. A., Youmans, D. G., and Ezekiel, S. (1973). Molecular beam stabilized laser. *Proc. 27th Annu. Freq. Control Symp.*, pp. 382–385.

Hackel, L. A., Hackel, R. P., and Ezekiel, S. (1977). Molecular beam stabilized multiwatt argon lasers. *Metrologia* **13**, 141–143.

Halford, D., and Hellwig, H. (1972). Progress and feasibility for a unified standard for frequency, time, and length. *Proc. IEEE* **60**, 623–625.

Hall, D. R., Jenkins, R. M., and Gorton, E. K. (1978). A frequency-stabilised CW waveguide carbon dioxide laser. *J. Phys. D.* **11**, 859–869.

Hall, J. L. (1968). The laser absolute wavelength standard problem. *IEEE J. Quantum Electron.* **QE-4**, 638–641.

Hall, J. L. (1969). Laser frequency stabilization. *IEEE J. Quantum Electron.* **QE-5**, 324.

Hall, J. L. (1978). Stabilized lasers and precision measurements. *Science* **202**, 147–156.

Hall, J. L. (1981). Stable lasers and optical frequency standards for testing the postulates of physics. *Proc. 7th Int. Conf. Atomic Phys.* Plenum, New York, pp. 267–296.

Hall, J. L., and Borde, C. (1973a). Influence of hyperfine structure on methane-stabilized lasers. *Proc. 27th Annu. Freq. Control Symp.*, p. 386.

Hall, J. L., and Borde, C. (1973b). Measurement of methane hyperfine structure using laser saturated absorption. *Phys. Rev. Lett.* **30**, 1101–1104.

Hall, J. L., Hollberg, L., Long-sheng, M., and Robinson, H. G. (1981). Progress toward phase-stable optical frequency standards. *J. Phys. Colloq.* (*Orsay, Fr.*) **42**, 59–71.

Hanes, G. R. (1979). Doubly resonant intracavity generation of second harmonic of 1153-nm radiation with stabilization on hyperfine structure components of $^{127}I_2$. *Appl. Opt.* **18**, 3970–3974.

Hanes, G. R., and Dahlstrom, C. E. (1969). Iodine hyperfine structure observed in saturated absorption at 633 nm. *Appl. Phys. Lett.* **14**, 362–364.

Hanes, G. R., Baird, K. M., and DeRemigis, J. (1973). Stability, reproducibility, and absolute wavelength of a 633-nm He–Ne laser stabilized to an iodine hyperfine component. *Appl. Opt.* **12**, 1600–1605.

Hartmann, F. (1970). Optical frequency standards. *Ann. Phys.* (*Paris*) **5**, 281–290. In French.

Hellwig, H., Bell, H. E., Kartaschoff, P., and Bergquist, J. C. (1972). Frequency stability of methane-stabilized He–Ne lasers. *J. Appl. Phys.* **43**, 450–452.

Hellwig, H., Evenson, K. M., and Wineland, D. J. (1978). Time, frequency and physical measurement. *Phys. Today* **31**, 23–30.

Helmcke, J. (1973). Wavelength-stabilized He–Ne laser [for measurement]. Meeting on Length Measuring Techniques. Phys.-Tech. Bundesanstalt, Braunschweig, Germany, pp. 29–39. In German.

Helmcke, J., and Bayer-Helms, F. (1974a). He–Ne laser stabilized by saturated absorption in I_2. *IEEE Trans. Instrum. Meas.* **IM-23**, 529–531.

Helmcke, J., and Bayer-Helms, F. (1974b). He–Ne laser stabilized by saturated absorption in I_2. *CPEM Dig.*, p. 104.

Helmcke, J., and Bayer-Helms, F. (1974c). Stabilising ^3He–^{22}Ne lasers by saturated absorption in $^{129}I_2$. *Metrologia* **10**, 69–71. In German.

Helmcke, J., and Bayer-Helms, F. (1977). Estimation and investigation of instrumental frequency offsets of iodine stabilized He–Ne-lasers. Phys.-Tech. Bundesanstalt, Braunschweig, Germany, pp. 111–132.

Hochuli, U., and Haldemann, P. (1970). Relative frequency stability of stable He–Ne gas laser structures. *Int. Electron Devices Meeting* (*abstracts*) (*IEEE*), p. 92.

Hochuli, U., and Haldemann, P. (1971). Relative frequency stability of stable He–Ne gas laser structures. *IEEE J. Quantum Electron.* **QE-7**, 573–575.

Hochuli, U. E., Haldemann, P., and Li, H. A. (1974). Factors influencing the relative frequency stability of He–Ne laser structures. *Rev. Sci. Instrum.* **45**, 1378–1381.

Hohimer, J. P., Kelly, R. C., and Tittel, F. K. (1972). Frequency stabilization of a high power argon laser. *Appl. Opt.* **11**, 626–629.

Hull, J. L. (1978). Stabilized lasers and precision measurements. *Science* **202**, 147.

Iga, K., and Fukuyo, H. (1972). Frequency stabilization of pure neon laser. *Bull. Tokyo Inst. Technol.* (112), 43–47.

Ito, N., and Tanaka, K. (1978). Absolute wavelength measurements of the iodine 127 stabilized He–Ne laser of NRLM. *Metrologia* **14**, 47–51.

Ivanov, V. A., Leikin, A. Ya., Solov'ev, V. S., and Pavlov, V. G. (1973). Method for stabilisation of the output frequency of a carbon dioxide laser. *Sov. J. Quantum Electron.* (*Engl. Transl.*) **3**, 272–273.

Jardino, M., Desaintfuscien, M., Barillet, R., Viennet, J., Petit, P., and Audoin, C. (1980). Mercury ion frequency standard: preliminary results. *Proc. 34th Annu. Freq. Control Symp.*, pp. 353–359.

Javan, A. (1969). Frequency mixing and multiplication in the far infrared and infrared. *Proc. 23rd Annu. Freq. Control Symp.*, p. 305.

Jennings, D. A., Petersen, F. R., and Evenson, K. M. (1979a). Direct frequency measurement of the 260 THz (1.15 μm) ^{20}Ne laser: and beyond. *In* "Laser Spectroscopy," pp. 39–48. Springer-Verlag, Berlin and New York.

Jennings, D. A., Peterson, F. R., and Evenson, K. M. (1979b). Frequency measurement of the 260 THz He–Ne laser. *Opt. Lett.* **4**, 129.

Jimenez, J. J., and Petersen, F. R. (1977). Recent progress in laser frequency synthesis. *Infrared Phys.* **17**, 541–546.

Jolliffe, B. W., Kramer, G., and Chartier, M. (1976). Methane-stabilized He Ne laser intercomparisons 1976. *IEEE Trans. Instrum. Meas.* **IM-25**, 447–450.

Jolliffe, B. W., Rowley, W. R. C., Shotton, K. C., Wallard, A. J., and Woods, P. T. (1977). Recent studies on He–Ne lasers frequency-stabilized by reference to absorption transitions in iodine and methane, and the intercomparison of their wavelengths. *Conf. Precise Electr. Meas. (London, IEE)*, pp. 35–36.

Kapralov, V. P., Krylov, P. S., Mironov, A. V., Privalov, V. E., and Tkachenko, L. P. (1980a). Standard-460M He–Ne laser stabilized by saturated absorption in iodine 127. *Opt. Spectrosc. (Engl. Transl.)* **49**, 524–526.

Kapralov, V. P., Malyshev, G. M., Pavlov, P. A., Privalov, V. E., Fofanov, Ya. A., and Etsin, I. Sh. (1981). Measurement of the wavelength ratio of lasers stabilized by saturated absorption in iodine and methane. *Opt. Spectrosc. (Engl. Transl.)* **50**, 34–37.

Kapralov, V. P., Privalov, V. E., and Chulyaeva, E. G. (1980b). Investigation of the stability of the emission wavelength of a laser with an external neon absorption cell. *Kvantovaya Elektron. (Moscow)* **7**, 1837–1839. In Russian.

Kartaschoff, P., and Barnes, J. A. (1972). Standard time and frequency generation. *Proc. IEEE* **60**, 493–501.

Kasamatsu, M. (1968). Frequency stabilization of gas laser. *Bull. Electrotech. Lab. Jpn.* **32**, 48–65. In Japanese.

Kawamura, Y., Sakajiri, M., Matoba, M., Nakai, S., and Yamanaka, C. (1979). Stable subnanosecond modelock multiline TEA CO_2 laser controlled by a NaCl etalon. *Opt. Commun.* **31**, 178–179.

Kayak, L. K., Kalinin, N. A., and Kapralov, V. P. (1974). Research on frequency-stabilised gas lasers in the member nations of COMECON (Council for Economic Assistance). *Meas. Tech. (Engl. Transl.)* **17**, 829–831.

Kegung, D., Glaser, M., Reim, G., and Helmcke, J. (1980). I_2 stabilized HeNe laser at 611.8 nm. *CPEM Dig.*, pp. 256–258.

Kekung, C., Hsuch-ping, C., Chia-chi, C., and Cheng-hsian, L. (1978). Methane saturated absorption stabilized He–Ne laser. *Kexue Tongbao* **23**, 734–736. In Chinese.

Kelly, M. J., Thomas, J. E., Monchalin, J.-P., Kurnit, N. A., and Javan, A. (1975). Potential frequency accuracy of the CO_2 fluorescence saturation dip. *Proc. 29th Annu. Freq. Control Symp.*, pp. 338–343.

Kempf, R. A., Cupp, R. E., Smith, W. T., and Gallagher, J. J. (1968). Extension of frequency control techniques to the submillimeter wavelength region. *Proc. 22nd Annu. Freq. Control Symp.*, pp. 573–591.

Ketskemety, I., Bor, Zs., Racz, B., and Kozma, L. (1977). Improved line narrowing and wavelength stabilization technique of distributed feedback dye lasers. *Opt. Commun.* **22**, 275–277.

Khanov, V. A. (1979). A scheme for the automatic fine frequency tuning of the radiation from a helium–neon laser along the Lamb depression. *Instrum. Exp. Tech. (Engl. Transl.)* **22**, 811–812.

Kikuchi, K., and Okosi, T. (1981). Achievement of 1 MHz frequency stability of semiconductor lasers by double-loop AFC scheme. *Electron. Lett.* **17**, 515–516.

Kim, B. Y., and Choi, S. S. (1980). Frequency stabilization of 6328 Å internal mirror He–Ne lasers. *New Phys. (Seoul)* **20**, 119–124. In Korean.

Kleiman, A. S., Leikin, A. Ya., Pestovskii, V. I., and Fertik, N. S. (1969). Measurement of short-time instability of laser frequency at 3.3 $^{15}NH_3$ line. *Izv. Vyssh. Uchebn. Zaved. Radiofiz.* **12**, 1165–1168. In Russian.

Klement'ev, V. M., and Chebotarev, V. P. (1979). CO_2 laser with short-term stability of 10^{-14}. *Sov. Tech. Phys. Lett. (Engl. Transl.)* **5**, 427–428.

Knight, D. J. E., Edwards, G. J., and Blaney, T. G. (1977). Developments in laser frequency measurement towards realising the metre from a unified frequency and length standard. *European Conf. Precise Electr. Meas. (IEE)*, p. 40.

Knight, D. J. E., Edwards, G. J., Pearce, P. R., and Cross, N. R. (1980a). Frequency of the methane-stabilized He–Ne laser at 88 THz measured to ±3 parts in 10^{11} [for new metre definition]. *Nature* **285**, 388–390.

Knight, D. J. E., Edwards, G. J., Pearce, P. R., and Cross, N. R. (1980b). Measurement of the frequency of the 3.39 μm methane-stabilized laser to ±3 parts in 10^{11}. *IEEE Trans. Instrum. Meas.* **IM-29**, 257–264.

Knight, D. J. E., Edwards, G. J., Pearce, P. R., and Cross, N. R. (1980c). A measurement accurate to ±3 parts in 10^{11} of the frequency of the methane-stabilized, He–Ne laser at 88 THz. *CPEM Dig.*, pp. 81–84.

Knox, J. D., and Pao, Y.-H. (1970a). Laser wavelengths and frequency standards based on He–Ne lasers and $^{129}I_2$ vapor. *Int. Electron Devices Meetings (Abstracts) (IEEE)*, p. 90.

Knox, J. D., and Pao, Y. H. (1970b). "Stabilization of the ^{3}He ^{20}Ne Laser about Inverted Lamb-Dip Components in $^{129}I_2$ Vapor." Optical Society of America, Washington, D.C., p. 20.

Knox, J. D., and Pao, Y. H. (1970c). Absorption profiles and inverted Lamb dips of I_2 vapor at 633 nm as studied with a He–Ne laser. *Appl. Phys. Lett.* **16**, 129–131.

Koffend, J. B., Goldstein, S., Bacis, R., Field, R. W., and Ezekiel, S. (1978). Doppler-free stimulated-emission spectroscopy and secondary frequency standards using an optically pumped laser. *Phys. Rev. Lett.* **41**, 1040–1044.

Kompanets, O. N., and Mikhailov, E. L. (1979). Helium–neon 0.63 μ laser with a $^{129}I_2$ nonlinear absorption cell. *Sov. J. Quantum Electron. (Engl. Transl.)* **9**, 1020–1204.

Kompanets, O. N., Kukudzhanov, A. R., Letokhov, V. S., and Mikhailov, E. L. (1974). Stabilisation of the emission frequency of a carbon dioxide laser by an external nonlinearly absorbing SF_6 cell. *Sov. J. Quantum Electron. (Engl. Transl.)* **3**, 293–296.

Kompanets, O. N., Kukudzhanov, A. R., and Mikhailov, E. L. (1975). Highly stable CW CO_2 lasers obtained by automatic frequency control. *Instrum. Exp. Tech. (Engl. Transl.)* **18**, 296–297.

Kompanets, O. N., Kukudzhanov, A. R., and Mikhailov, E. L. (1977). Problem of reproducibility of the output frequency of a CO_2/OsO_4 laser. *Sov. J. Quantum Electron (Engl. Transl.)* **7**, 1150–1152.

Koning, J., and Schellekens, P. H. J. (1979). Wavelength stability of He–Ne lasers used in interferometry: limitations and traceability. *Ann. CIRP* **28**, 307–310.

Konovalov, I. P., and Protsenko, E. D. (1974). Frequency stabilization of a 3.39 μ He + Ne laser. *Instrum. Exp. Tech. (Engl. Transl.)* **17**, 1433–1436.

Koronkevich, V. P., and Khanov, V. A. (1975). Investigation of the spectral characteristics of helium–neon lasers with Lamb-dip stabilization. *Avtometriya* (5), 73–80. In Russian.

Koshelyaevskii, N. B., Mukhamedgalieva, A. F., Tatarenko, V. M., and Titov, A. N. (1970). Investigations and stabilization of the frequency of a helium–neon laser. *Izmer. Tekh.* **8**, 38–40. In Russian.

Koshelyaevskii, N. B., Tatarenkov, V. M., and Titov, A. N. (1972a). Frequency meters based on He–Ne lasers. *Meas. Tech. (Engl. Transl.)* **15**, 1644–1648.

Koshelyaevskii, N. B., Tatarenkov, V. M., and Titov, A. N. (1972b). Quantum frequency reference at 3.39 μ wavelength. *Zh. Eksp. Teor. Fiz., Pis'ma Red.* **15**, 461–464. In Russian.

Koshelyaevskii, N. B., Malyshev, Yu. M., Ovchinnikov, S. N., Rastorguev, Yu. G., Tatarenkov, V. M., and Titov, A. N. (1979). Quantum frequency standard utilizing the *E* component of methane. *Sov. J. Quantum Electron. (Engl. Transl.)* **9**, 200–202.

Koshelyaevski, N. B., Oboukhov, A., Tatarenkov, V. M., and Titov, A. N. (1981). International comparison of methane-stabilized He–Ne lasers. *Metrologia* **17**, 3–6.

Kramer, G., Weiss, C. O., and Helmcke, J. (1975). Laser frequency stabilization by means of saturation dispersion. *Z. Naturforsch. A.* **30**, 1128–1132.

Kuhn, H. (1976). Stabilised helium–neon-gas lasers (for length measurement). *Feingeraetetechnik* **25**, 259–261. In German.

Kurosawa, T., Kosaki, A., Sakurai, T., and Tanaka, K. (1977). Experiments of a CO_2 laser frequency stabilization. *Oyo Butsuri* **46**, 304–309. In Japanese.

Kuznetsov, V. M. (1970). Gas laser automatic frequency stabilization system. *Prib. Tekh. Eksp.* **1**, 189–191. In Russian.

Lachambre, J.-L., Otis, G., and Lavigne, P. (1978). Simultaneous frequency stabilization and injection in a TEA-CO_2 oscillator. *Appl. Opt.* **17**, 1015–1017.

Lamb, E. E., Jr. (1964). Theory of an optical maser. *Phys. Rev. A* **134**, A1429–A1450.

Layer, H. P. (1980a). A portable iodine stabilized helium–neon laser. *IEEE Trans. Instrum. Meas.* **IM-29**, 358–361.

Layer, H.P. (1980b). Recent developments in iodine stabilized helium–neon lasers. *CPEM Dig.*, pp. 259–260.

Layer, H. P. (1977). The iodine stabilized laser as a realization of the length unit. *Proc. Soc. Photo-Opt. Instrum. Eng.* **129**, 9–11.

Layer, H. P. (1981). National Physical Laboratory–National Bureau of Standards iodine-stabilized helium–neon laser intercomparison. *Opt. Lett.* **6**, 188–190.

Leclerc, M. C. (1974). Measurements of the wave-lengths emitted by laser tubes (type monomode 3He 20Ne) and their stability. *2nd European Electro-Opt. Conf.*, Mack-Brooks Exhibitions, St. Albans, Herts., England, 1p. In French.

Lee, P. H. (1972). Introduction to saturated optical absorption. *IEEE Trans. Instrum. Meas.* **IM-21**, 384–387.

Lee, P. H., and Skolnick, M. L. (1967). Saturated absorption inside a 6328-Å laser. *Appl. Phys. Lett.* **10**, 303–305.

Le Floch, A., Frere, P., and Brun, P. (1970). Frequency stabilization of a gas laser using the magnetic Lamb dip. *Appl. Phys. Lett.* **17**, 40–42.

Le Floch, A., Le Naour, R., Stephan, G., and Brun, P. (1976). Frequency stabilization and tunability of laser; use of mobile dips and peaks. *Appl. Opt.* **15**, 2673–2677.

Leiby, C. C., Jr., Picard, R. H., Thomas, J. E., Hemmer, P. R., and Ezekiel, S. (1982). A laser atomic beam standard. *Proc. 36th Annu. Freq. Control Symp.*, p. 370.

Leikin, A. Ya., and Solov'ev, V. S. (1967). Studying the stability of wavelengths radiated by a gas laser. *Izmer. Tekh.* (9), 29–32. In Russian.

Leikin, A. Ya., and Solov'ev, V. S. (1968). Stabilization of a laser radiation frequency. *Izmer. Tekh.* (8), 19–22. In Russian.

Leikin, A. J., and Solovjov, V. S. (1969). Determination of the emission wavelength stability of a gas laser. *Electron Technol.* **2**, 77–79.

Leikin, A. Ya., Solov'ev, V. S., and Moskienko, N. V. (1971). Stabilization of laser frequency by "extremum storage" automatic control systems. *Kvantovaya Elektron.* (4), 95–97. In Russian.

Leikin, A. Ya., Solov'ev, V. S., and Moskienko, N. V. (1972). Some problems in the calculation of frequency stabilization of lasers using the Lamb dip. *Radiotekhnika* (*Kharkov*) (22), 104–111. In Russian.

Leitkin, A. Ya., Solov'ev, V. S., and Fisher, A. M. (1973). Stabilizing the generation frequency of a helium–neon laser with a wavelength of 0.63 μ with respect to a generation frequency with a wavelength of 3.39 μ. *Meas. Tech.* (*Engl. Transl.*) **16**, 1321–1322.

Lemaire, J., Houriez, J., and Lapauw, J. M. (1972). Frequency stabilisation of CO_2 or N_2O laser by a rapid sampling method. *Rev. Phys. Appl.* **7**, 323–328. In French.

Le Naour, R., Le Floch, A., and Stephan, G. (1978). Comparative analysis of a laser stabilization method using a mobile and a fixed Lorentzian. *Opt. Quantum Electron.* **10**, 119–129.

Letokhov, V. S. (1967). Self-stabilization of laser optic-oscillation frequency by nonlinear absorption in gas. *Zh. Eksp. Teor. Fiz. Pis'ma, Red.* **6**, 597–600. In Russian.

Letokhov, V. S. (1971). Problems of laser frequency stabilization by nonlinear saturation of absorption resonance in gases. *Comments At. Mol. Phys.* **2**, 181–194.

Letokhov, V. S., and Chebotaev, V. P. (1974). Quantum optical frequency standards. *Sov. J. Quantum Electron.* (*Engl. Transl.*) **4**, 137–148.

Letokhov, V. S., and Minogin, V. G. (1981). Laser cooling of atoms and its application in frequency standards. *J. Phys. Colloq.* (*Orsay, Fr.*) **42**, 347–355.

Letokhov, V. S., and Pavlik, B. D. (1967). Production of coherent light by atomic or molecular beams. *Zh. Eksp. Teor. Fiz.* **53**, 1107–1115. In Russian.

Letokhov, V. S., and Pavlik, B. D. (1976). Method for establishing a quantum frequency standard in the visible range using atomic absorption lines and a CW dye laser. *Sov. J. Quantum Electron.* (*Engl. Transl.*) **6**, 32–38.

Letokhov, V. S., and Pavlik, B. D. (1970). The stability of the frequency of radiation of laser beams with coherent excitation. *Zh. Tekh. Fiz.* **40**, 1638–1648. In Russian.

Lewandowski, L. (1976). Methods of laser frequency stabilization. *Elektronika* **17**, 59–63. In Polish.

Lewis, L. L., Feldman, M., and Bergquist, J. C. (1981). Impact of lasers on primary frequency standards and precision spectroscopy. *J. Phys. Colloq.* (*Orsay, Fr.*) **42**, 271–281.

Likhanskii, V. V., and Napartovich, A. P. (1977). Stability of single-mode emission from a laser. *Sov. J. Quantum Electron* (*Engl. Transl.*) **7**, 763–765.

Lipchak, W. M. (1976). Improved frequency stability of the TEA CO_2 laser. *Opt. Commun.* **19**, 205–207.

Lisitsyn, V. H., and Chebotaev, V. P. (1969). On the use of the Zeeman effect for stabilisation of the frequency of a gas laser with nonlinear absorption. *Opt. Spektrosk.* **26**, 856–858. In Russian.

Lokhmatov, A. I., and Khanov, C. A. (1971). Frequency stabilising system of gas laser using Lamb depression effect. *Avtometriya* (1), 16–20. In Russian.

Lourtioz, J. M., and Adde, R. (1976). Design of a stable CW HCN laser for far infrared frequency synthesis. *Rev. Phys. Appl.* **11**, 533–540.

Lourtioz, J. M., Henaux, J. C., and Adde, R. (1976). Design of a stable and powerful oscillator at 891 GHz. *C. R. Hebd. Seances Acad. Sci., Ser. B* **282**, 161–164. In French.

Lund, M. W., Cogan, J. N., and Davis, J. A. (1979). Low-cost method for stabilization of a CO_2 laser for use in far infrared laser pumping. *Rev. Sci. Instrum.* **50**, 791–792.

Maischberger, K. (1970). "Long Term Frequency Stabilization of a Composite-Cavity Argon Laser Using a Reference Frequency Light Source." Report ESRIN-IN-117. European Space Res. Inst., Frascati, Italy, 27 pp. Available from the National Technical Information Service, Springfield, Virginia.

Maischberger, K. (1971). Long-term frequency stabilization of a composite-cavity argon laser. *IEEE J. Quantum Electron.* **QE-7**, 250–252.

Malyshev, Yu. M., Tatarenkov, V. M., and Titov, A. M. (1971). Optical frequency standard with a beam type absorbing cell. *Zh. Eksp. Teor. Fiz., Pis'ma Red.* **13**, 592–595. In Russian.

Malyshev, G. F., Troitskii, Yu. V., Khanov, V. A., and Khyuppenen, V. P. (1972). Stabilisation of a single-frequency helium–neon laser. *Avtometriya* (5), 86–93. In Russian.

Malyshev, Yu. M., Ovchinnikov, S. N., Rastorguev, Yu. G., Tatarenkov, V. M., and Titov, A. N. (1980). Reproducibility of the frequency of a quantum reference source stabilized by the E component of the methane molecule. *Sov. J. Quantum Electron.* (*Engl. Transl.*) **10**, 376–377.

Man, C. N., Cerez, O., and Brillet, A. (1977). A frequency stabilized CW dye laser for spectroscopic and metrological applications. *J. Phys. Lett.* (*Orsay, Fr.*) **38**, L287–L289.

Martinot-Lagarde, P., and Coumes, C. (1968). Argon ion laser in unique mode, stabilized. *Nachrichtentech. Fachber.* **35**, 695–702. In French.

Mathieu, P., and Izatt, J. R. (1978). Laser frequency control by spectrally depleted destructive two-beam interference. *Opt. Commun.* **26**, 86–90.

Matsumoto, H. (1981). Stabilized method of an infrared two-wavelength laser. *Appl. Phys.* **24**, 65–66.

Matyshev, G. F., and Troitskii, Yu. V. (1974). Frequency stabilisation of a single frequency He–Ne laser ($\lambda = 0.63$ micron) with a diffraction selector. *Avtometriya* (6), 71–76. In Russian.

Matyugin, Yu. A., Troshin, B. I., and Chebotaev, V. P. (1971). Method for stabilizing He–Ne laser frequency using the Lorentzian absorption profile in an external gas cell. *Opt. Spektrosk* **31**, 111–115. In Russian.

McDonald, D. G., Risley, A. S., Cupp, J. D., and Evenson, K. M. (1971). Harmonic mixing of microwave and far infrared laser radiation using a Josephson junction. *Appl. Phys. Lett.* **18**, 162–164.

Melnikov, N. A., Privalov, V. E., and Fofanov, Ya. A. (1977). Experimental investigation of He–Ne lasers stabilized by saturation absorption in iodine. *Opt. Spectrosc.* (*Engl. Transl.*) **42**, 425–428.

Mel'tsin, A. L. (1971). Experimental study of the system of frequency stabilisation of ring laser with an external absorption chamber. *Zh. Prikl. Spektrosk.* **15**, 214–218. In Russian.

Mel'tsin, A. L., and Shchegolev, V. V. (1975). Study of the stability of the standard frequency of an optical discriminator, based on an external gas discharge absorption cell. *Zh. Prikl. Spektrosk.* **22**, 985–990. In Russian.

Michalski, W., Nowicki, R., and Plinski, E. F. (1977). Noise, fluctuations and output power stabilization in a CO_2 laser. *Elektronika* **18**, 303–305. In Polish.

Mielenz, K. D. (1968). Length measurement and laser wavelength stability. *ISA Trans.* **6**, 293–297.

Mielenz, K. D., Nefflen, K. F., Rowley, W. R. C., Wilson, D. C., and Engelhard, E. (1968). Reproducibility of helium–neon laser wavelengths at 633 nm. *Appl. Opt.* **7**, 289–294.

Mikhal'tsova, I. A., Lenkova, G. A., and Lokhmatov, A. I. (1971). Single frequency stabilised helium–neon laser. *Avtometriya* (1), 10–15. In Russian.

Milovskii, N. D. (1973). Single-frequency laser stability. *Izv. Vyssh. Uchebn. Zaved. Radiofiz.* **16**, 537–544.

Minguzzi, P., and Tonelli, M. (1977). Simple frequency stabilization of CO_2 laser for far-infrared laser pumping. *J. Phys. E* **10**, 775–776.

Mocker, H. W. (1976). High stability CO_2 waveguide lasers. *EASCON'76 Record* (*IEEE*), pp. 151A/1–4.

Moffatt, S., and Smith, A. L. S. (1979). Optogalvanic laser stabilization. *Proc. 4th Natl. Quantum Electron. Conf.*, Edinburgh, Scotland, pp. 31–34.

Mogil'nitskii, B. S., Kolomnikov, Yu. D., Gol'dort, V. G., Gusev, A. Yu., and Om, A. E. (1981). The He–Ne/I_2 laser as a frequency standard in the visible spectrum. *Sov. Tech. Phys. Lett.* (*Engl. Transl.*) **7**, 111–112.

Mooradian, A., and Welford, D. (1982). Frequency stability and control characteristics of (GaAl)As semiconductor lasers. *Proc. 36th Annu. Freq. Control Symp.*, pp. 338–339.

Morinaga, A., and Tanaka, K. (1977). Stabilization of a complex resonator He–Ne laser by frequency offset lock. *Jpn. J. Appl. Phys.* **16**, 383–384.

Morinaga, A., and Tanaka, K. (1978). Stabilization of a complex resonator He–Ne laser. *Jpn. J. Appl. Phys.* **17**, 881–887.

Morris, R. H., Ferguson, J. B., and Warniak, J. S. (1975). Frequency stabilization of internal mirror He–Ne lasers in a transverse magnetic field. *Appl. Opt.* **14**, 2808.

Mukhamedgalieva, A. F., Tatarenkov, V. M., and Titov, A. N. (1969). Investigation of He–Ne laser with an absorbing cell. *Izv. Vyssh. Uchebn. Zaved. Radiofiz.* **12**, 1156–1158. In Russian.

Muller, F. H. (1981). Wavelength of an iodine-stabilized laser measured with a novel Michelson interferometer. *S. Afr. J. Phys.* **4**, 1–4.

Munch, J., Kolpin, M. A., and Levine, J. (1978). Frequency stability and stabilization of a chemical laser. *IEEE J. Quantum Electron.* **QE-14**, 17–22.

Nagai, H., and Taniguchi, I. (1973). A simple, single-frequency He–Ne laser for practical uses. *Jpn. J. Appl. Phys.* **12**, 434–438.

Nai-cheng, S., Chia-luan, A., Yao-hsiang, W., I-min, S., and Han-chien, S. (1978). Performance investigation of iodine saturated adsorption stabilized He–Ne lasers. *Kexue Tongbao* **23**, 730–733. In Chinese.

Nakazawa, M., and Musha, J. (1980a). Stability of FM-eliminated 3.39 μm He–Ne/CH_4 laser. *Jpn. J. Appl. Phys.* **19**, L237–329.

Nakazawa, M., and Musha, T. (1980b). Stability measurement of the 0.633 μm line in a CH_4-locked 3.39 μm He–Ne laser. *Jpn. J. Appl. Phys.* **19**, L315–L317.

Nakazawa, M., Musha, T., and Tako, T. (1979a). Frequency stabilization of a 3.39 μm He–Ne laser with no frequency modulation. *Trans. Inst. Electron. Commun. Eng. Jpn.*, [*Part*] *E* **62**, 51–52.

Nakazawa, M., Musha, T., and Tako, T. (1979b). Frequency stabilized 3.39-μm He–Ne laser with no frequency modulation. *J. Appl. Phys.* **50**, 2544–2547.

Nakazawa, M., Nakamura, J., and Musha, T. (1979c). Frequency stabilization of 0.633-μm line with the aid of 3.39-μm line locked to CH_4. *Appl. Phys. Lett.* **35**, 745–747.

Nakazawa, M., Nakamura, J., and Musha, T. (1980). FM eliminated CH_4 locked frequency stabilization of 3.39 μm He–Ne laser in dual feedback control. *IEEE J. Quantum Electron.* **QE-16**, 854–859.

Nussmeier, T. A., and Abrams, R. L. (1974). Stark cell stabilization of CO_2 laser. *Appl. Phys. Lett.* **25**, 615–617.

Ohi, M. (1979). Frequency stabilization of lasers. *Oyo Butsuri* **48**, 553–554. In Japanese.

Ohi, M., and Akimoto, Y. (1976a). Performance of methane-stabilized lasers with the method of saturated absorption. *Jpn. J. Appl. Phys.* **15**, 1177–1178.

Ohi, M., and Akimoto, Y. (1976b). Improvements in methane-stabilized lasers. *Jpn. J. Appl. Phys.* **15**, 1853–1854.

Ohi, M., and Akimoto, Y. (1977). Characteristics of low noise laser tubes for CH_4 stabilized lasers [3.39 μm He–Ne laser]. *Oyo Butsuri* **46**, 832–835. In Japanese.

Ohtsu, M., and Tako, T. (1978). Frequency stability of an H_2CO-stabilized He–Xe laser in an axial magnetic field. *Jpn. J. Appl. Phys.* **17**, 2169–2170.

Ohtsu, M., and Tako, T. (1982). Frequency stabilization of a He–^{22}Ne laser by intracavity polarization spectroscopy of CH_4. II. *Jpn. J. Appl. Phys., Part I* **21**, 722–724.

Ohtsu, M., Koyama, R., and Tako, T. (1979). Improvements in the long-term frequency stability of the He–Xe laser at 3.51 μm. *Jpn. J. Appl. Phys.* **18**, 1621–1622.

Ohtsu, M., Katsuragi, S., and Tako, T. (1981a). Performances of a frequency offset locked He–Xe laser system at 3.51 μm. *IEEE J. Quantum Electron.* **QE-17**, 1100–1105.

Ohtsu, M., Ohta, S., and Tako, T. (1981b). Frequency stabilization of a He–^{22}Ne laser by intracavity polarization spectroscopy of CH_4. *Jpn. J. Appl. Phys.* **20**, 1701–1707.

Ohtsu, M., Tsuchida, H., and Tako, T. (1982). Frequency stabilization of AlGaAs lasers. *Proc. 36th Annu. Freq. Control Symp.*, pp. 327–337.

Oraevskii, A. N. (1968). Beam laser as a frequency standard. *Izv. Vyssh. Uchebn. Zaved. Radiofiz.* **11**, 1554–1559. In Russian.

Oraevskii, A. N. (1978). Development of a highly stable optical frequency standard utilizing an atomic beam. *Sov. J. Quantum Electron* (*Engl. Transl.*) **8**, 1053–1055.

Ouhayoun, M., and Borde, C. J. (1977). Frequency stabilization of CO_2 lasers through saturated absorption in SF_6. *Metrologia* **13**, 149–150.

Pace, P., and Cruickshank, J. (1980a). Frequency-stabilized hybrid CO_2 laser. *Proc. Soc. Photo-Opt. Instrum. Eng.* **227**, 28–34.

Pace, P. W., and Cruickshank, J. M. (1980b). A frequency stabilized compact high repetition rate TEA-CO_2 laser. *IEEE J. Quantum Electron* **QE-16**, 937–944.

Pace, P., and Cruickshank, J. (1981). Frequency-stabilized multijoule TEA-CO_2 laser. *CLEO 81* (*IEEE*), p. 84.

Pak, P. E., Privalov, V. E., and Fofanov, Ya. A. (1981). Helium–neon laser (0.63 μm) stabilized without frequency deviation. *Opt. Spectrosc.* (*Engl. Transl.*) **51**, 5–6.

Pankratov, V. A. (1974). Rubidium laser with zero frequency shift caused by a buffer gas. *Sov. J. Quantum Electron.* (*Engl. Transl.*) **4**, 413.

Pao, Y. H., Knox, J. D., Yusek, R., and Goldberg, M. W. (1971). Frequency standards based on accurately stabilized lasers. *Proc. 3rd Biennial Cornell EE Conf. HF Gen. Ampl. devices* (*IEEE*), pp. 85–104.

Polanyi, T. G., and Tobias, I. (1968). The frequency stabilization of gas lasers. *In* "Laser Reviews" (A. K. Levine, ed.), Ch. V., pp. 374–423. Marcel Dekker, Paris.

Privalov, V. E., and Strokovskii, G. A. (1975). Improving the stability of the perimeter of a ring gas laser. *Izv. Vyssh. Uchebn. Zaved. Priborostr.* **18**, 111–115. In Russian.

Pucek, B. (1978). Circuits for stabilization of the laser radiation wavelength. *Cesk. Cas. Fys.* **28**, 241–244. In Czech.

Quinn, T. J. (1982). National Bureau of Standards, Boulder, Colorado, personal communication.

Rabinowitz, P., LaTourette, J. T., and Gould, G. (1967). Proposed ultrastable CO_2 oscillator. *Int. Electron Devices Meeting* (*IEEE*), p. 132.

Rabinowitz, P., Keller, R., and LaTourrette, J. T. (1970). Frequency stabilization of CO_2 lasers with respect to passive SF_6 and CO_2 line centers. *Proc. 24th Annu. Freq. Control Symp.*, pp. 275–278.

Ramsey, N. F. (1971). History of atomic and molecular control of frequency and time. *Proc. 25th Annu. Freq. Control Symp.*, pp. 46–51.

Rapier, J. L., Heimple, H. H., and Schawlow, A. L. (1967). Spontaneous emission from a helium–neon laser as a convenient wavelength standard. *Am. J. Phys.* **35**, 890–891.

Reynolds, R. S. (1968). "Stabilized Carbon Dioxide Gas Laser." Report NASA-CR-95055, 78 pp. Available from the National Technical Information Service, Springfield, Virginia.

Reynolds, R. S., and Sasnett, M. W. (1968). Active frequency stabilization of a 20-watt CO_2 laser with etalon wavelength selection. *Int. Electron Devices Meeting* (*IEEE*), p. 60.

Rowley, W. R. C. (1981a). "Frequency Dependence of a 633-nm He–He Laser Stabilized by $^{127}I_2$, upon Iodine Pressure, Modulation Amplitude, and Wall Temperature." Report NPL-MOM-54, National Physics Laboratory, Teddington, England, 13 pp.

Rowley, W. R. C. (1981b). "Power Shifts of a 633-nm $^{127}I_2$ Stabilized He–Ne Laser, for Various Mirror Curvatures." Report NPL-MOM-56, National Physical Laboratory, Teddington, England, 18 pp.

Rowley, W. R. C., and Wilson, D. C. (1972). Optical coupling effects in frequency stabilized lasers. *Appl. Opt.* **11**, 475–576.

Rutman, J. (1979). Standard frequency generators in the submillimeter infrared and visible light regions of the electromagnetic spectrum. *Onde Electr.* **59**, 91–96. In French.

Ryan, T. J., Youmans, D. G., Hackel, L. A., and Ezekiel, S. (1972). Molecular beam stabilized argon laser. *Appl. Phys. Lett.* **21**, 320–322.

Sakudrai, T., Tanaka, K., Kurosawa, T., Iwasaki, S., and Ito, N. (1978). The iodine stabilized He–Ne laser of NRLM. *Optica Hoy y Mañana, Proc. Congress Insituto de Optica ICO-11*, Madrid, Spain, pp. 459–462.

Sargent, M., III. (1973). Mode locking in quantum optics. *Appl. Phys.* **1**, 133–139.

Sasnett, M. W. (1969). "Frequency Stabilized Gas Laser [Final Report]." Report NASA-CR-102617, 81 pp. Available from the National Technical Information Service, Springfield, Virginia.

Sasnett, M. W., and Reynolds, R. S. (1969). Stabilized CO_2 laser source for 10.6 micron heterodyne communication system. *Int. Electron Devices Meeting* (*IEEE*), pp. 108–110.

Schellekens, P. (1977). Research on iodine stabilized lasers in the metrology laboratory of Eindhoven University of Technology. *Informative Meeting on Iodine Stabilized He–He Lasers*, Phys.-Tech. Bundesanstalt, Braunschweig, Germany, pp. 55–61.

Schiller, N., Grant, M., and Alfano, R. R. (1977). Ultrafast laser clocks. *Phys. Teach.* **15**, 396–404.

Schweitzer, W. G., Jr., Kessler, E. G., Deslattes, R. D., Layer, H. P., and Whetstone, J. R. (1973). Description, performance, and wavelengths of iodine stabilized lasers. *Appl. Opt.* **12**, 2927–2938.

Sen, D. (1981). Frequency-stabilized laser for measurement of length. *J. Inst. Electron. Telecommun. Eng.* (*New Delhi*) **27**, 596–600.

Shimoda, K. (1968). Absolute frequency stabilization of the 3.39 μm laser on a CH_4 line. *Conf. Precision Electromagn. Meas.* (*IEEE*), p. 46.

Shimoda, K. (1973a). Frequency shifts in methane-stabilized lasers. *Jpn. J. Appl. Phys.* **12**, 1393–1402.

Shimoda, K. (1973b). Ultimate stability of methane-stabilized lasers. *Jpn. J. Appl. Phys.* **12**, 1222–1226.

Shotton, K. C., and Rowley, W. R. C. (1976). "An Electronic Servocontrol System for Stabilized Lasers and Similar Application." Report NPL-QU-28, National Physics Laboratory, Teddington, England, 33 pp.

Shotton, K. C., Woods, P. T., and Rowley, W. R. C. (1976). Wavelength intercomparison of visible and infrared stabilised lasers. *Conf. Precision Electromagn. Meas.* (*IEEE*), pp. 186–187.

Siio, I., Ohtsu, M., and Tako, T. (1981a). The real-time measurement system for stability of laser frequency. *Bull. Res. Lab. Precis. Mach. Electron.* (*Tokyo Inst. Technol.*) (48), 47–52.

Siio, I., Ohtsu, M., and Tako, T. (1981b). Frequency stabilization of a He–Xe laser using a Stark spectrum in H_2CO. *Jpn. J. Appl. Phys.* **20**, L508–L510.

Simkin, G. S. (1968). Establishment of a single time and length standard. *Izmer. Tekh.* (10), 1308–1314. In Russian.

Skolnick, M. L. (1971). Frequency stabilized passively Q-switched CO_2 laser. *17th Int. Electron Devices Meeting* (*IEEE*), p. 86.

Smith, A. L. S., and Moffatt, S. (1980). High frequency opto-galvanic laser stabilisation. *33rd Ann. Gaseous Electron. Conf.*, University of Oklahoma), Norman, Oklahoma, p. 109.

Smith, D. S., Jones, L. H., and Baird, K. M. (1967). Temperature compensated gas laser. *Appl. Opt.* **6**, 2195.

Smith, P. W. (1966). On the stabilization of a high-power single-frequency laser. *IEEE J. Quantum Electron.* **QE-2**, 666–668.

Smith, P. W. (1968). Stabilized single-frequency output from a long ring laser. *IEEE J. Quantum Electron.* **QE-4**, 485–490.

Smith, P. W., and Maloney, P. J. (1973). A self-stabilized 3.5-μm waveguide He–Xe laser. *Appl. Phys. Lett.* **22**, 667–669.

Sorem, M. S., Barger, R. L., and Hall, J. L. (1973). Frequency stabilization of a CW dye laser. *IEEE/OSA Conf. Laser Eng. Appl. Dig. Tech. Papers*, p. 81.

Sośnowski, T. P., and Johnson, W. B. (1968). Frequency shifts of the Lamb dip minimum in the helium–neon laser. *IEEE J. Quantum Electron* **QE-4**, 370–371.

Souilhac, D., and Gundjian, A. (1982). Carbon dioxide laser stabilization by optoacoustic tracking of an SF_6 Lamb dip. *Appl. Opt.* **21**, 1478–1481.

Spieweck, F. (1967). Relating a laser frequency to the atomic frequency by means of sweeping. *Z. Naturforsch. A* **22**, 2067–2069. In German.

Spieweck, F. (1974). Wavelength stabilization of an Ar^+ laser with an external $^{129}I_2$ absorption cell. *Appl. Phys.* **3**, 429–430.

Spieweck, F. (1976). Wavelength stabilization of the green Ar II line using saturated absorption in an internal $^{129}I_2$ cell. *Metrologia* **12**, 43–46. In German.

Spieweck, F. (1977a). Classification of I_2 hyperfine components and their suitability for the stabilization of laser wavelengths. *Informative Meeting Iodine Stabilised He–Ne Lasers*, Phys.-Tech. Bundesantalt, Braunschweig, Germany, pp. 33–42.

Spieweck, F. (1977b). Development of wavelength stabilisers for the green Ar^+ laser line at $\lambda = 514.5$ nm for metrological applications. *Feinwerktech. Messtech.* **85**, 155–163. In German.

Spieweck, F. (1977c). Wavelength stabilization of the Ar^+ laser line at $\lambda = 515$ nm for length measurements of highest precision. *Laser 77 Opto-Electronics*, IPC Sci. Technol. Press, London, pp. 130–136.

Spieweck, F. (1978). Frequency stabilization of Ar^+ lasers by saturated absorption in external $^{127}I_2$ cells (at 582 THz). *IEEE Trans. Instrum. Meas.* **IM-27**, 398–400.

Spieweck, F. (1980a). Frequency stabilization of Ar^+ lasers at 582 THz using expanded beams in external $^{127}I_2$ cells. *IEEE Trans. Instrum. Meas.* **IM-29**, 361–363.

Spieweck, F. (1980b). Improvements on frequency stabilized Ar^+ lasers at 582 THz. *CPEM Dig.*, pp. 261–262.

Spieweck, F., Camy, G., and Gill, P. (1980). Beat frequency intercomparisons of $^{127}I_2$ stabilized ion lasers at 514.5 nm. *Appl. Phys.* **22**, 111–112.

Stein, S. R., and Van de Stadt, H. (1977). Electronic tuning and phase-lock techniques for optically pumped far infrared lasers. *Proc. 31st Annu. Freq. Control Symp.*, pp. 601–604.

Steiner, M., Walther, H., and Zygan, K. (1976). Highly stable dye lasers. *Opt. Commun.* **18**, 2.

Strakhovskii, G. M., Tatarenkov, V. M., and Titov, A. N. (1970). Frequency stabilization of a helium–neon laser having an internal absorptive cell, which operates at a wavelength of 0.63 μ. *Izmer. Tekh.* **12**, 25–28. In Russian.

Strumia, F. (1981). Frequency control and frequency modulation of far infrared laser by Stark effect. *J. Phys. Colloq. (Orsay, Fr.)* **42**, 105–114.

Takasaki, H., Umeda, N., and Tsukiji, M. (1980). Stabilized transverse Zeeman laser as a new light source for optical measurement. *Appl. Opt.* **19**, 435–441.

Tako, T., Ohi, M., Akimoto, Y., Sigiyama, A., and Shimoda, K. (1970). Frequency stabilization of the 3.39-μm laser on a CH_4 line. *Jpn. J. Appl. Phys.* **9**, 1535.

Tanaka, K. (1972). Method for stabilizing the frequency of an unmodulated laser output. *J. Opt. Soc. Am.* **62**, 24–29.

Tanaka, K., and Kurosawa, T. (1976). Optical feedback effect in iodine stabilised He–Ne laser with long path interferometer [Earth strain meter]. *Jpn. J. Appl. Phys.* **15**, 2271–2272.

Tanaka, K., and Morinaga, A. (1979). Preliminary experiment for stabilizing unmodulated He–Ne laser to an iodine hyperfine component. *J. Appl. Phys.* **50**, 38–40.

Tanaka, K., and Seino, S. (1974). Wavelength stabilization of He–Ne lasers and interferometric length measurements. *J. Jap. Soc. Precis. Eng.* **40**, 716–723. In Japanese.

Tanaka, K., Sakurai, T., and Kurosawa, T. (1974). Frequency stabilisation of the He–Ne laser by means of saturated absorption in iodine. *Trans. Soc. Instrum. Control Eng. Jpn.* **10**, 669–674. In Japanese.

Tanaka, K., Sakurai, T., and Kurosawa, T. (1977). Frequency stability and reproducibility of an iodine stabilized He–Ne laser. *Jpn. J. Appl. Phys.* **16**, 2071–2072.

Tanaka, K., Sakurai, T., and Kurosawa, T. (1978). Optical feedback effect in iodine stabilized laser with 25 m Michelson interferometer. *Optica Hoy y Mañana (Optics Present and Future). Proc. Congress ICO-11*, Instituto de Optica, Madrid, Spain, pp. 471–474.

Targ, R., French, J. M., and Yarborough, J. M. (1968). Frequency stabilization and noise suppression in the Argon FM laser. *IEEE J. Quantum Electron.* **QE-4**, 644–648.

Terrien, J. (1973). Wavelength standards, optical frequency standards, and the velocity of light. *Nouv. Rev. Opt.* **4**, 215–220. In French.

Thomas, J. E., Kelly, M. J., Monchalin, J. P., Kurnit, N. A., and Javan, A. (1980). Stable CO_2 and N_2O laser design. *Rev. Sci. Instrum.* **51**, 240–243.

Thomason, W. H., and Elbers, D. C. (1975). An inexpensive method to stabilize the frequency of a CO_2 laser. *Rev. Sci. Instrum.* **46**, 409–412.

Titov, E. A. (1976). Influence of transit effects on the frequency of a stabilized gas laser. *Sov. J. Quantum Electron. (Engl. Transl.)* **5**, 1207–1210.

Tomlinson, W. J., and Fork, R. L. (1969). Frequency stabilization of a gas laser. *Appl. Opt.* **8**, 121–129.

Topkov, A. N., Svich, V. A., and Pokormyakho, N. G. (1980). Stabilized HCN laser with HF pumping. *Instrum. Exp. Tech. (Engl. Transl.)* **23**, 1479–1481.

Tsao, J. Y., Sharp, R. C., and Yablonovitch, E. (1979). Digital feedback stabilization of a single-axial-mode CO_2 TEA laser. *Rev. Sci. Instrum.* **50**, 1023–1024.

Tschirnich, J., Sommer, M., and Bartl, B. (1981). Frequency stabilized He–Ne/I_2-lasers used for wavelength standards. *Feingeraetetechnik* **30**, 257–258. In German.

Tschudi, T., Blaser, P., and Wuthrich, M. (1971). Control system for the frequency stabilisation of a He–Ne laser. *Verh. Deut. Phys. Ges.* (10), 766. In German.

Tsdaka, A., Sela, A., Shamir, J., and Demner, Y. (1979). A system for frequency and power stabilization of a gas laser. *Proc. Electr. Electron. Eng. Israel (IEEE)*, pp. E1-6/1–5.

Tsetsegova, E. I. (1969). He–Ne laser frequency stabilization at the wavelength 3.39 μ. *Izv. Vyssh. Uchebn. Zaved. Radiofiz.* **12**, 1159–1164. In Russian.

Tuma, W., and Van der Hoeven, C. J. (1975). Helium–neon laser stabilized on iodine: design and performance. *Appl. Opt.* **14**, 1896–1897.

Umeda, N., Hirano, I., and Togawa, M. (1978a). Polarization mode and frequency stabilization of an internal mirror laser. *Oyo Butsuri* **47**, 42–49. In Japanese.

Umeda, N., Tuskiji, M., and Takaski, H. (1978b). Degeneration of longitudinal modes and frequency stabilization of an internal mirror He–Ne laser with a transverse magnetic field. *Oyo Butsuri* **47**, 432–436. In Japanese.

Umeda, N., Tsukiji, M., and Takasaki, H. (1980). Stabilized ^3He–^{20}Ne transverse Zeeman laser. *Appl. Opt.* **19**, 442–450.

Van Oorschot, B. P. J. (1977). Frequency shifts in iodine stabilized lasers. *J. Phys. D.* **10**, 1117–1124.

Van Oorschot, B. P. J., and Van der Hoeven, C. J. (1979). A recently developed iodine-stabilised laser. *J. Phys. E.* **12**, 51–55.

Vasilenko, L. S., Skvortsov, M. N., Chebotaev, V. P., Shershneva, G. I., and Shishaev, A. V. (1972). Frequency stabilization of a CO_2 laser. *Opt. Spectrosc. (Engl. Transl.)* **32**, 609–612.

Vergunov, V. B., Vol'nov, M. I., and Tyurikov, D. A. (1978). Electronic system for stabilizing the difference frequency of two lasers. *Instrum. Exp. Tech. (Engl. Transl.)* **21**, 765–766.

Vladimirskii, K. V., and Norvaishas, A. A. (1977). Stability of lasing on an asymmetrical inhomogeneously broadened line. II. *Sov. Phys.—Lebedev Inst. Rep. (Engl. Transl.)* **10**, 32–36.

Vlasov, A. N. (1978). Long-term instability and irreproducibility of a gas laser frequency and requirements to be satisfied by automatic frequency control systems. *Sov. J. Quantum Electron. (Engl. Transl.)* **8**, 866–869.

Voitovich, A. P., and Smirnov, A. Ya. (1974). The autostabilization of intermode pulse frequencies in a gas laser. *Zh. Prikl. Spektrosk.* **20**, 510–512. In Russian.

Vysotskii, V. G., Okunev, R. I., Nikolaev, V. M., and Petrun'kin, Yu. V. (1973). Longitudinal mode selection and frequency stabilization in the He–Ne ring laser. *Sov. Phys.—Tech. Phys. (Engl. Transl.)* **43**, 569–561.

Waksberg, A. L. (1968). Stabilization of a CO_2 laser using a three-mirror laser system. *IEEE J. Quantum Electron.* **QE-4**, 532–533.

Wallard, A. J. (1972). Frequency stabilization of the helium–neon laser by saturated absorption in iodine vapour. *J. Phys. E.* **5**, 926–930.

Wallard, A. J. (1973). Characteristic of the 633 nm He–Ne laser stabilized by saturated absorption in iodine vapour. *Proc. 27th Annu. Freq. Control Symp.*, pp. 376–381.

Wallard, A. J. (1974a). The reproducibility of 633 nm lasers stabilized by $^{127}I_2$. *CPEM Dig.*, pp. 106–107.

Wallard, A. J. (1974b). The reproducibility of 633-nm lasers stabilized by $^{127}I_2$. *IEEE Trans. Instrum. Meas.* **IM-23**, 532–535.

Wallard, A. J. (1977). Report on NPL activities. *Informative Meeting Iodine Stabilised He–Ne Lasers*, Phys.-Tech. Bundesanstalt, Braunschweig, Germany, pp. 43–53.

Wallard, A. J. (1979). "A Practical Approach to the Design and Construction of Iodine Stabilized Lasers." Report NPL-QU-51, National Physical Laboratory, Teddington, England, 79 pp.

Wallard, A. J., and Jolliffe, B. W. (1976). International comparison of the reproducibility of iodine and methane stabilized lasers. *Conf. Precision Electromagn. Meas. (IEEE)*, pp. 182–183.

Wallard, A. J., Chartier, J. M., and Hamon, J. (1975). Wavelength measurements of the iodine stabilized helium–neon laser. *Metrologia* **11**, 89–95.

Wang, C. P. (1976). Frequency stability of a CW HF chemical laser. *J. Appl. Phys.* **47**, 221–223.

Wang, C. P., and Varwig, R. L. (1979). Frequency stabilization of HF lasers by means of beat signals and anomalous dispersion. *J. Appl. Phys.* **50**, 3838–3840.

Wang, S. C. (1971). "Potential Methods of Frequency Stabilization for the Xenon 3.51 μ Laser Transition." Ph.D. Thesis, Stanford Univ., California, 75 pp. Available from University Microfilms, Ann Arbor, Michigan, USA Order No. 71-19774.

Wang, S. C., Byer, R. L., and Siegman, A. E. (1970). Observation of an enhanced Lamb dip with a pure Xe gain cell inside a 3.51 μ-He–Xe laser. *Appl. Phys. Lett.* **17**, 120–122.

Wellegehausen, B., and Guttner, A. (1973). Relative frequency stability measurements of single-mode lasers. *Z. Naturforsche. A.* **28**, 968–972. In German.

Welling, H., Schroder, H. W., Wellegehausen, B., and Nottbeck, N. (1973). Frequency-stable single-mode dye laser. *IEEE/OSA Conf. Laser Eng. Appl. Dig. Tech. Papers*, pp. 80–81.

Welling, H., Schroder, H. W., and Wellegehausen, B. (1975). Frequency stability and linewidth of single mode CW dye lasers. *Spectrosc. Lett.* **8**, 685–695.

Wells, J. S. (1972). A stabilized HCN laser for infrared frequency synthesis. *Proc. 26th Annu. Freq. Control Symp.*, pp. 250–256.

Wells, J. S. (1973). A stabilized HCN laser for infrared frequency synthesis. *IEEE Trans. Instrum. Meas.* **IM-22**, 113–118.

Wells, J. S., Evenson, K. M., Day, G. W., and Halford, D. (1972). Role of infrared frequency synthesis in metrology. *Proc. IEEE* **60**, 621–623.

Wenk, G. J. (1967). Frequency stabilisation of gas lasers. *Natl. Radio Electron. Eng. Conv.*, Sydney, Australia, pp. 170–171.

Wenk, G. J. (1969). Frequency stabilisation of gas lasers. *Proc. Inst. Radio Electron. Eng. Aust.* **30**, 250–259.

White, A. D. (1967). Gas laser frequency stabilization. *Microwaves* **6**, 51–61.

Whitford, B. G. (1979). Absolute frequencies of CO_2 laser transitions by multiplication of CO_2 laser difference frequencies. *Opt. Commun.* **31**, 363–366.

Whitford, B. G. (1980). Measurement of the absolute frequencies of CO_2 laser transitions by multiplication of CO_2 laser difference frequencies. *IEEE Trans. Instrum. Meas.* **IM-29**, 168–176.

Whitford, B. G., and Smith, D. S. (1977). Frequency of the methane-stabilized He–Ne laser at 3.39 μm measured relative to the 10.17 μm R(32) transition of the CO_2 laser [measurement standard]. *Opt. Commun.* **20**, 280–283.

Wineland, D. J. (1979). Laser-to-microwave frequency division using synchrotron radiation. *J. Appl. Phys.* **50**, 2528–2532.

Wineland, D. J., Bergquist, J. C., Drullinger, R. E., Hemmati, H., Itano, W. M., and Walls, F. L. (1981). Laser cooled, stored ion experiments at NBS and possible applications to microwave and optical frequency standards. *J. Phys. Colloq. (Orsay, Fr.)* **42**, 307–313.

Woods, P. T., and Jolliffe, B. W. (1976). Stable single-frequency carbon dioxide lasers. *J. Phys. E.* **9**, 395–402.

Wu, F. Y., and Ezekiel, S. (1977). Frequency stabilization of commercial CW dye lasers for ultrahigh resolution spectroscopy. *IEEE J. Quantum Electron.* **QE-13**, 30–31.

Wu, F. Y., Groves, R. E., and Ezekiel, S. (1974). CW dye laser for ultra-high-resolution spectroscopy. *Appl. Phys. Lett.* **25**, 73–75.

Yepifanov, V. P., Mazan'ko, I. P., and Yaroshenko, N. G. (1967). Study of build-up and stability of oscillations in a neon–helium laser. *Radiotekh. Elektron.* **12**, 1517–1518. In Russian.

Yoshino, T. (1980). Frequency stabilization of internal-mirror He–Ne ($\lambda = 633$ nm) lasers using the polarization properties. *Jpn. J. Appl. Phys.* **19**, 2181–2185.

Yusek, R. (1970). "CO_2 Laser Frequency Stabilization Using Resonant Absorbtion in SF_6." Ph.D. Thesis, Case Western Reserve University, Cleveland, Ohio, 129 pp. Available from University Microfilms, Ann Arbor, Michigan, Order No. 70-25930.

Zacharenko, Y., Kotkov, A., Melnikov, N., Chartier, J.-M., and Felder, R. (1981). International comparison of He–Ne lasers stabilized on the saturated absorption of 127 iodine at $\lambda = 633$ nm. *Metrologia* **17**, 81–82.

Zaitsev, Yu. I., and Khurtin, L. A. (1969). Frequency stabilization of a He–Ne laser by means of low-frequency oscillations of its intensity. *Prib. Tekh. Eksp.* (3), 177–179. In Russian.

Zakharenko, Yu. G., Mel'nikov, N. A., Privalov, V. E., and Fofanov, Ya. A. (1976). An He–Ne laser, stabilised by absorption saturation in vapours of iodine. *Pis'ma Zh. Tekh. Fiz.* **2**, 153–156. In Russian.

Chapter 12

Ablowich, D., Jr. (1966). Some observations concerning frequency and time standardization. *Proc. 21st Instrum. Soc. Am. Conf.* **21**, 20.

Akimochkin, I. K., Denisov, V. P., and Cherenkova, E. M. (1973). Long-term frequency comparator. *Meas. Tech (Engl. Transl.)* **16**, 83–85.

Aldridge, D. (1975). 5 MHz digital frequency meter. *Electron* (82), 61, 63–64, 66, 68.

Aldridge, D. (1978). 5 MHz digital frequency measuring instrument. *Elektron. Anz.* **10**, 15–18. In German.

Allan, D. W. (1966). Statistics of atomic frequency standards. *Proc. IEEE* **54**, 221–230.

Allan, D. (1975). "The Measurement of Frequency and Frequency Stability of Precision Oscillators." NBS Technical Note 669, National Bureau of Standards, Boulder, Colorado.

Allan, D. W., and Barnes, J. A. (1981). A modified "Allan variance" with increased oscillator characterization ability. *Proc. 35th Annu. Freq. Control Symp.*, pp. 470–473.

Allan, D. W., and Daams, H. (1975). Picosecond time difference measurement system. *Proc. 29th Annu. Freq. Control Symp.*, pp. 404–411.

Allan, D. W., and Hellwig, H. (1978). Time deviation and the prediction error for clock specification, characterization and application. *Proc. Position Location and Navigation Symp.*, pp. 29–36.

Allan, D. W., Gray, J. E., and Machlan, H. E. (1972). The National Bureau of Standards atomic time scales: generation, dissemination, stability, and accuracy. *IEEE Trans. Instrum. Meas.* **IM-21**, 388–391.

Allan, D. W., Gray, J. E., and Machlan, H. E. (1974). The National Bureau of Standards atomic time scales: generation, stability, accuracy and accessibility. *In* "Time and Frequency: Theory and Fundamentals" (B. E. Blair, ed.), *NBS Monogr. 140*, pp. 205–231.

Allan, D. W., Hellwig, H., and Glaze, D. J. (1975). An accuracy algorithm for an atomic time scale. *Metrologia* **11**, 133–138.

Andres, I. (1977). Straight talk on frequency counters. *Communications* **54**, 56–60.

Andriyanov, A. V., Glebovich, G. V., Krylov, V. V., Korsakov, S. Ya., and Ponomarev, D. M. (1980). Automated measurements in the time domain and a method of increasing their accuracy. *Izmer. Tekh.* **23**, 42–44. In Russian.

Anonymous (1967). Definition, realisation and use of time and frequency. *Colloq. Dig. IEE*, Paper no. 1/1-8/7.

Anonymous (1975a). Electromagnetic radiation in frequency measurements. *Electron. Aust.* **37**, 31, 33.

Anonymous (1975b). Analogue frequency meter (rev. counter). *Elektor (GB)* **1**, 737.

Anonymous (1975c). Universal frequency reference. *Elektor (GB)* **1**, 715.

Anonymous (1975d). A programmable counter type frequency meter. *Electron. Microelectron. Ind.* (213), 45–49. In French.

Anonymous (1976a). High accuracy timing devices. *Elektron. Elektrotech.* **31**, 9–11. In Dutch.

Anonymous (1976b). Time and frequency; two important quantities in modern measurements. *Tecnol. Elettr.* (12), 66–69. In Italian.

Anonymous (1977a). 50 MHz counter/timer. *CSIO Commun. (India)* **4**, 34.

Anonymous (1977b). A universal counting and time measuring device. *Elekron Int.* (5), 167–169. In German.

Anonymous (1977c). Precision timebase for frequency counter. *Elektor (GB)* **3**, 22–25.

Anonymous (1977d). Which counter? *Automation* **12**, 21, 23, 25.

Anonymous (1978a). Time measurement: where are we? *Mes. Regul. Autom.* **43**, 19–23. In French.

Anonymous (1978b). A universal counter on one chip. *Elektronikschau* **54**, 48. In German.

Anonymous (1978c). Yaesu Musen YC-500S frequency counter. *Electron. Aust.* **40**, 103.

Anonymous (1979a). A system of measurement and display of frequency for a AM/FM receiver. *Electron. Appl. Ind.* **271**, 55–56. In French.

Anonymous (1979b). A frequency counter for radio receivers. *Elektronikschau* **55**, 56–57. In German.

Anonymous (1979c). A special IC revolutionizes the design of universal counters. *Elekron. Prax.* **14**, 14–18. In German.

Anonymous (1979d). Microprocessor and LSI: two features of a universal 100 MHz counter. *Electron Appl. Ind.* **270**, 23–26. In French.

Anonymous (1979e). Time/frequency measurements in radar equipment—which technique? *Onde Electr.* **59**, 47–54. In French.

Antyufeev, V. I., Breslavets, V. P., Fedulov, V. M., and Fertik, N. S. (1980). Application of digital filtration for measuring instability. *Radiotekhnika (Kharkov)* **45**, 43–49. In Russian.

Arai, M. (1978a). Frequency counter trends: μ-processors facilitate improvements. *JEE, J. Electron. Eng.* **136**, 30–31.

Arai, M. (1978b). Universal counters are becoming intelligent. *JEE, J. Electron. Eng.* **136**, 32–34.

Arnoldt, M. (1974). A frequency counter with time-multiple indication. I. *Funk-Tech.* **20**, 721–724. In German.

Arnoldt, M. (1977). Frequency counter for ultra short wave radio receivers. *Funk-Tech.* **32**, 237–242, 244–245. In German.

Arnoldt, M. (1979). A frequency counter for VHF receivers with frequency control loops. *Fundschau* **51**, 1371–1374. In German.

Artyukh, Yu. N., Arnit, M. A., Gotlib, G. I., and Zagurskii, V. Ya. (1978). Instrument for measuring time intervals to an accuracy of 2 nsec. *Instrum. Exp. Tech. (Engl. Transl.)* **20**, 1039–1041.

Ashley, J. R., Searles, C. B., and Palka, F. M. (1968). The measurement of oscillator noise at microwave frequencies. *IEEE Trans. Microwave Theory Tech.* **MTT-16**, 753–760.

Auchterlonie, L. J., and Bryant, D. L. (1978). A direct method of measuring small frequency shifts using two open resonators at millimetre wavelengths. *Int. J. Electron.* **45**, 113–122.

Ausejo, R. (1976). Frequency and time meters. *Mundo Electron.* **50**, 59–66. In Spanish.

Azoubib, J., Granveaud, M., and Guinot, B. (1977). Estimation of the scale unit duration of time scales. *Metrologia* **13**, 87–93.

Baev, A. V., Rozkina, M. S., and Torbenkov, G. B. (1973). Capacitive method for measuring frequency. *Meas. Tech. (Engl. Transl.)* **16**, 1034–1036.

Bahadur, H., and Parshad, R. (1977). Measurement of time. *J. Inst. Electron Telecommun. Eng. (New Delhi)* **17**, 103–108.

Baidakov, I. G., Pushkin, S. B., and Titov, V. P. (1973). Securing unanimity of time and frequency measurement in the USSR at the highest section of the reference system. *Meas. Tech. (Engl. Transl.)* **16**, 60–63.

Baird, K. M., Hanes, G. R., Evenson, K. M., Jennings, D. A., and Petersen, F. R. (1979). Extension of absolute-frequency measurements to the visible: frequencies of ten hyperfine components of iodine. *Opt. Lett.* **4**, 263–264.

Balph, T. (1976). A 200 MHz autoranging frequency counter. *Electron. Equip. News*, April, p. 17.

Barber, R. E. (1971). Short-term frequency stability of precision oscillators and frequency generators. *Bell Syst. Tech. J.* **50**, 881–915.

Barnaba, J. F. (1972). USAF time and frequency calibration program. *Proc. 26th Annu. Freq. Control Symp.*, pp. 260–263.

Barnes, J. A. (1966). Atomic timekeeping and the statistics of precision signal generators. *Proc. IEEE* **54**, 207–219.

Barnes, J. A. (1969). Tables of bias functions B_1 and B_2 for variances based on finite samples of processes with power law spectral densities. *NBS Tech. Note (U.S.)* 375.

Barnes, J. A. (1972). Problems in the definition and measurement of frequency stability. *Proc. 26th Annu. Freq. Control Symp.*, p. 20.

Barnes, J. A. (1976a). A simulation of the fluctuations of International Atomic Time. *NBS Tech. Note (U.S.)* 609, 20 pp.

Barnes, J. A. (1976b). Models for the interpretation of frequency stability measurements. *NBS Tech. Note (U.S.)* 689, 39 pp.

Barnes, J. A., and Allan, D. W. (1966). A statistical model of flicker noise. *Proc. IEEE* **54**, 176–178.

Barnes, J. A., and Winkler, G. M. R. (1972). The standard of time and frequency in the USA. *Proc. 26th Annu. Freq. Control Symp.*, pp. 269–278.

Barnes, J. A., Chi, A. R., Cutler, L. S., Healey, D. J., Leeson, D. B., McGunigal, T. E., Mullen, J. A., Jr., Smith, W. L., Sydnor, R. L., Vessot, R. C. F., and Winkler, G. M. R. (1971). Characterization of frequency stability. *IEEE Trans. Instrum. Meas.* **IM-20**, 105–120.

Barrier, B., and Humbert, J.-P. (1973). Numerical frequency meters from A to Z. *Int. Electron.* **28**, 33–39. In French.

Bastelberger, J. (1968). Normal frequencies, their investigation and measurement. *Ingenieur* **22**, 23. In German.

Baugh, R. A. (1971). Frequency modulation analysis with the Hadamard variance. *Proc. 25th Annu. Freq. Control Symp.*, pp. 222–225.

Baugh, R. A. (1972). Low noise frequency multiplication. *Proc. 26th Annu. Freq. Control Symp.*, pp. 50–54.

Bava, E., De Marchi, A., and Godone, A. (1977). A narrow output linewidth multiplier chain for precision frequency measurements in the 1 THz region. *Proc. 31st Annu. Freq. Control Symp.*, pp. 578–582.

Bay, Z., and Luther, G. G. (1968). Locking a laser frequency to the time standard. *Appl. Phys. Lett.* **13**, 303–304.

Becker, G. (1976). The second as standard unit of time. *Umsch. Wiss. Tech.* **76**, 706–707. In German.

Becker, G., and Hubner, U. (1978). The generation of time scales. *Radio Sci.* **14**, 593–603.

Beckman, D. (1974). How accurate is your timer–counter? *Electron. Equip. News* **15**, 32–33.

Begley, W. W., and Shapiro, A. H. (1970). Precision timing systems. I. Standard scales. *Instrum. Control Syst.* **43**, 87–89.

Behnke, H. (1973). Standard frequency comparison by error multiplication. *Radio Fernsehen Elektron.* **22**, 642–643. In German.

Beisner, H. M. (1980). Clock error with a Wiener predictor and by numerical calculation. *IEEE Trans. Instrum. Meas.* **IM-29**, 105–113.

Belenov, E. M., and Uskov, A. V. (1979). Measurement of laser frequencies using superconducting point contacts. *Sov. J. Quantum Electron. (Engl. Transl.)* **9**, 1519–1522.

Belham, N. D. N. (1980). How accurate is a digital frequency meter? *Radio Commun.* **56**, 368–371.

Belomestnov, G. I., Dmitrienko, A. D., Emakov, A. S., and Korzh, V. F. (1976). Automatic system for acquiring, recording, and processing information by computer for secondary time-and-frequency standards. *Meas. Tech. (Engl. Transl.)* **19**, 1572–1574.

Belotserkovskii, D. Yu., Il'in, V. G., and Stepanova, I. V. (1976). International cooperation in the field of exact time and frequency measurements. *Meas. Tech. (Engl. Transl.)* **18**, 517–519.

Berger, F. (1975). Time metrology and quartz application. I. Time metrology. *Rev. Gen. Electr.* **84**, 907–918. In French.

Bezdrukov, S. M., and Preobrazhenskii, N. I. (1979). Increased accuracy in audio-frequency measurements with the S4-12 and S4-53 spectrum analyzers. *Instrum. Exp. Tech. (Engl. Transl.)* **21**, 714–716.

Bichler, H., and Fenk, J. (1981a). Simple universal 0 to 30 MHz frequency counter with SDA 5680A. *Siemens Components (Engl. Transl.)* **16**, 21–24.

Bichler, H., and Fenk, J. (1981b). The IC unit, SDA 5680A, universal frequency counter covering 100 kHz to 30 MHz. *Elektron Int.* **3–4**, 89–92. In German.

Blachman, N. M. (1976). The effect of noise upon polar-display instantaneous frequency measurement. *IEEE Trans. Instrum. Meas.* **IM-25**, 214–21.

Blair, B. E. (1974). Time and frequency: theory and fundamentals. *NBS Monogr. (U.S.) 140*, 460 pp.

Blaney, T. G., Cross, N. R., Knight, D. J. E., Edwards, G. J., and Pearce, P. R. (1980). Frequency measurement at 4.25 THz (70.5 μm) using Josephson harmonic mixer and phase-lock techniques. *J. Phys. D* **13**, 1365–1370.

Bodea, M., and Danila, T. (1979). Autoranging, digital time-interval meter. *Bull. Inst. Politeh. Gheorghe Gheorghiu-Dej Bucuresti Ser. Electroteh.* **40**, 57–63. In Rumanian.

Body, I., and Szemok, I. (1974). General problems of frequency measurement. *Meres Autom.* **22**, 422–428. In Hungarian.

Bologlu, A. (1975). Automatic 4.5-GHz counter provides 1-Hz resolution. *Hewlett-Packard J.* **27**, 14–18.

Bologlu, A. (1980). A new method of measuring the frequency of microwave signals, using microprocessors. *Nachr. Elektron.* **34**, 149–152. In German.

Bologlu, A., and Barber, V. A. (1978). Microprocessor-controlled harmonic heterodyne microwave counter also measures amplitudes. *Hewlett-Packard J.* **29**, 2–4, 6–7, 9–12, 14–16.

Bordt, A. (1973a). Universal digital counter for frequencies up to 12 MHz. I. *Radio Fernsehen Elektron.* **22**, 365–368. In German.

Bordt, A. (1973b). Universal digital counter for frequencies up to 12 MHz. II. *Radio Fernsehen Elektron.* **22**, 402–406. In German.

Borisochkin, V. V. (1972). Checking the frequency of highly stable generators. *Meas. Tech. (Engl. Transl.)* **15**, 460–463.

Bosnjakovic, P. (1976). A new solution of the precision line frequency measurement. *Automatika* **17**, 194–196. In Serbo-Croatian.

Bowman, J. A. (1973). Short and long term stability measurements using automatic data recording system. *Proc. 27th Annu. Freq. Control Symp.*, pp. 440–445.

Bowman, M. J., and Whitehead, D. G. (1977). A picosecond timing system. *IEEE Trans. Instrum. Meas.* **IM-26**, 153–157.

Brandenberger, H., Hadorn, F., Halford, D., and Shoaf, J. H. (1971). High quality quartz crystal oscillators: frequency domain and time domain stability. *Proc. 25th Annu. Freq. Control Symp.*, pp. 226–230.

Brown, D. E. (1957). Frequency measurement of quartz crystal oscillators. *Marconi Instrum.* **11**, 12–15.

Budreau, A. J., Slobodnik, A. J., Jr., and Carr, P. H. (1982). Fast frequency hopping achieved with SAW synthesizers. *Microwave J.* **25**, 71–73, 76–80.

Burgoon, R., and Fischer, M. C. (1978). Conversion between time and frequency domain of intersection points of slopes of various noise processes. *Proc. 32nd Annu. Freq. Control Symp.*, pp. 514–519.

Buchuev, F. I., and Ivakin, V. M. (1979). Electronic converter of the unit time dimension. *Meas. Tech. (Engl. Transl.)* **21**, 788–789.

Buxton, A. J. (1976). Digital frequency meter. *Pract. Electron.* **12**, 376–382.

Buzek, O., Cermak, J., Smid, J., and Medellin, H. (1980a). A time base controlled by the OMA 50 kHz transmitter. *Sdelovaci Tech.* **28**, 362–365. In Czech.

Buzek, O., Cermak, J., and Tolman, J. (1980b). Accurate time and frequency. *Slaboproudy Obz.* **41**, 263–266. In Czech.

Cantero, J. A., Pollan, T., and Barquillas, J. (1978). Digital frequency meter uses variable measuring and automatic scale conversion. *Mundo Electron.* **71**, 34–35. In Spanish.

Cardwell, W. T., Jr. (1978). Frequency counter in a probe. *Radio Electron Eng.* **49**, 67, 72–73, 100–101, 103.

Charriere, J.-J. (1977). A digital chronometer. I. *Rev. Polytech.* (6), 585, 587. In French.

Chebotayev, V. P., Goldort, V. G., Klementyev, V. M., Nikitin, M. V., Timchenko, B.A., and Zakharyash, V. F. (1982). Development of an optical time scale. *Appl. Phys. B* **29**, 63–65.

Coates, P. B. (1968). Fast measurement of short time intervals. *J. Sci. Instrum.* **1**, 1123–1127.

Cochran, W. T., Cooley, J. W., Favin, D. L., Helms, H. D., Kaenel, R. A., Lang, W. W., Maling, G. C., Jr., Nelson, D. E., Rader, C. M., and Welch, P. D. (1967). What is the fast Fourier transform? *IEEE Trans. Audio Electroacoust.* **AV-15**, 45–55.

Colburn, J., and Owen, B. (1979). 600 MHz portable frequency counter. *Radio Electron. Eng.* **50**, 39–43, 90.

Cole, H. M. (1975). Time domain measurements. *Electron. Electro-Optic Inf. Countermeas.* **1**, 38–42, 55.

Conway, A., and Urdaneta, N. (1978a). Considerations in selecting a frequency counter. *Communications* **15**, 22–23.

Conway, A., and Urdaneta, N. (1978b). Selecting a frequency counter. *Teleph. Eng. Management* **82**, 77–78.
Cordwell, C. R. (1968). "Frequency Measurements." Vacation school on electrical measurement practice. Institution of Electrical Engineers, London. 13 pp.
Cordwell, C. R. (1969). Frequency measurements. *Electron. Radio Tech.* **3**, 95–103.
Cosmelli, C., and Frasca, S. (1979). Fast new technique for measuring the resonance frequencies of high *Q* systems. *Rev. Sci. Instrum.* **50**, 1650–1651.
Cutler, L. S., and Searle, C. L. (1966). Some aspects of the theory and measurement of frequency fluctuations in frequency standards. *Proc. IEEE* **54**, 136–154.
Czarnecki, A. (1980). Test set for the comparison of standard frequencies, type FZ-530. *Pr. Inst. Tele-Radiotech.* (83), 27–32. In Polish.
Danilevich, V. V., Chernyavskii, A. F., and Yakushev, A. K. (1977a). Selectro-type time interval analyzer with a measurement range of 10^{-10} to 10^{-2} sec. *Instrum. Exp. Tech. (Engl. Transl.)* **20**, 326–327.
Danilevich, V. V., Kvachenok, V. G., Priimak, M. A., Chernyavskii, A. F., and Yakushev, A. K. (1977b). Signal generator for adjusting and calibrating time measurement systems. *Instrum. Exp. Tech. (Engl. Transl.)* **20**, 600.
Danzeisen, K. (1977). Remote frequency measurement using VHF–UHF receivers. *Funk-Tech.* **32**, 196–197. In German.
Davis, D. D. (1975). Calibrating crystal oscillators with TV color-reference signals. *Electronics* **48**, 107–112.
De Costanzo, L. (1979). Radio receiver frequency counter/clock. *Electron. Ind.* **5**, 16–17.
De Jong, G., and Kaarls, R. (1980). An automated time-keeping system. *IEEE Trans. Instrum. Meas.* **IM-29**, 230–233.
Denbnovetskii, S. V., and Kovtun, A. K. (1970). Time measurements. Digital time-interval meters. *Izmer. Tekh.* **10**, 29–31. In Russian.
Denbnovetskii, S. V., and Shkuro, A. N. (1975). Principles of eliminating ambiguity in digital time-interval meters (review). *Instrum. Exp. Tech. (Engl. Transl.)* **18**, 1659–1670.
De Prins, J. (1974). Timing systems. *In* "ELF–VLF Radio Wave Propagation Spatind, Norway," pp. 385–398. Reidel, Dordrecht, The Netherlands.
De Prins, J. (1977). Aspects of time and frequency measurement. *Rev. HF* **10**, 123–134. In French.
De Prins, J., and Cornelissen, G. (1974). Critique and discussion about frequency stability definitions with respect to various kinds of noises. *CPEM 74 Dig.*, pp. 54–56.
Dietzel, R. (1975). Passive resonators with noise feeding in frequency-analogue measuring systems. *Mess., Steuern. Regeln* **18**, 389–393. In German.
Dombrovskii, A. S., Zaitsev, V. N., and Pashev, G. P. (1974). Apparatus for time and frequency measurement. *Meas. Tech. (Engl. Transl.)* **17**, 919–921.
Domnin, Y. S., Kosheljaevsky, N. B., Tatarenkov, V. M., and Shumjatsky, P. S. (1980a). Precise frequency measurements in submillimeter and infrared region. *IEEE Trans. Instrum. Meas.* **IM-29**, 264–267.
Domnin, Yu. S., Kosheljaevsky, N. B., Tatarenkov, V. M., and Shumjatsky, P. S. (1980b). Precise frequency measurements in submillimeter and infrared region [lasers]. *CPEM Dig.*, p. 85.
Doring, F. W., and Hollenberg, K. (1981). Eight-channel time measurement system with 2 ns resolution. *J. Phys. E* **14**, 638–640.
Doronina, O. M., and Petukh, A. M. (1980). Interpolation method of increasing measurement accuracy for low frequencies. *Artometriya* (5), 89–92. In Russian.
Drake, J. M., and Rodriguez-Izquierdo, G. (1978). Analogue setup for fast-response frequency measurement. *Electron. Eng.* **50**, 41, 43.
Drake, J. M., Rodriguez-Izquierdo, G. (1980). Fast analogue measurement of low frequencies. *Rev. Telegr. Electron.* **69**, 1359–1360. In Spanish.

Egidi, C. (1969). Frequency/time metrology at the I.E.N.G.F. (Instituto Elettrotechnico Nazionale Galileo Ferraris). *RGE, Rer. Gen. Electr.* **78**, 275–282. In French.
Egidi, C., and Leschiutta, S. (1970). The true meaning of the word "time." *Alta Freq.* **39**, 689–693.
Egidi, C., and Leschiutta, S. (1971). The metrology of time. *Riv. Nuovo Cimento* **1**, 496–518. In Italian.
El-Ghoroury, H. S., and Gupta, S. C. (1976). Algorithmic measurement of digital instantaneous frequency. *IEEE Trans. Commun.* **COM-24**, 1115–1122.
Elkin, G. A., and Purtov, V. I. (1976). Automatic system for comparing the frequency of a [quantum] store with the transition frequency of cesium atoms. *Meas. Tech. (Engl. Transl.)* **19**, 1456–1460.
Ely, R. D. (1978). Frequency measurements by frequency meter or timer counter? *Electron. Power* **24**, 45–46.
Englert, R. (1978). Circuit for measuring very low frequencies. *Elektronik (Munich)* **27**, 67–68. In German.
Essen, L. (1967). Atomic units and scales of time. *IEE Colloq. Definition, Realisation and Use of Time and Frequency, Dig.*, Paper No. 1.
Essen, L. (1968). Time scales. *Metrologia* **4**, 161–165.
Essen, L. (1981). Leap seconds [transfer from astronomical to atomic time]. *Wireless World* **87**, 39–40.
Evenson, K. M., Wells, J. S., Petersen, F. R., Danielson, B. L., Day, G. W., Barger, R. L., and Hall, J. L. (1972). Laser frequency and wavelength measurement and the speed of light. *Abstr. Ann. Meeting Opt. Soc. Am.*, p. 22.
Faulkner, N. D., and Vilar, E. (1982). Sub-harmonic sampling for the accurate measurement of frequency stability of microwave oscillators. *CPEM Dig.*, pp. M/10–11.
Ferrari, H. I. (1976). Frequency meter and digital counter. *Rev. Telegr. Electron.* **64**, 234–238, 241–242. In Spanish.
Fichtenbaum, M. L. (1976). Counter inverts period to measure low frequency. *Electronics* **49**, 100–101.
Filin, N. A., and Trofimov, A. V. (1976). Time counter. *Instrum. Exp. Tech. (Engl. Transl.)* **19**, 1582.
Filous, L. (1979). Analogue measurement of frequency. *Sdeloraci Tech.* **27**, 325–328. In Czech.
Firth, G. F., and Pratt, D. M. (1976). A digital frequency counter and timer (direct read-out at 150 MHz). *Radio Commun.* **52**, 182–189.
Fischer, M. C. (1978). Frequency stability measurement procedures. *Onde Electr.* **58**, 291–299. In French.
Fischer, M. C. (1981). Methods for the measurement of the degree of stability in a frequency spectrum. *Nachr. Elektron.* **35**, 381–389. In German.
Fleys, M. (1978). Microwave frequency counters—which conversion technique to choose? *Mess. Regul. Autom.* **43**, 31–38. In French.
Freeman, R. L. (1977). The science of time and its inverse. *Telecommun. J. (Engl. Transl.)* **44**, 66–72.
Frenkel, L. (1969). Methods for the measurement of frequency and stability of laser generators of submillimeter oscillations. *Electron Technol.* **2**, 47–52.
Fukuyo, H. (1975). Time and frequency standards. *J. Soc. Instrum. Control Eng.* **14**, 521–528. In Japanese.
Fullagar, D. (1976). Frequency counter. *New Electron.* **9**, 28.
Gabry, A., Faucheron, G., Dubouis, B., and Petit, P. (1977). Distant comparison of stable frequency standards by means of the transmission of a beat note between the carrier of a TV broadcast signal and a frequency synthesized from the frequency standards. *Proc. 31st Annu. Freq. Control Symp.*, pp. 499–502.

Gardner, F. M. (1966). "Phaselock Techniques." Wiley, New York.

Godone, A., De Marchi, A., and Bava, E. (1979). An improved multiplier chain for precise frequency measurements up to 20 THz. *Proc. 33rd Annu. Freq. Control Symp.*, pp. 498–503.

Gonzalez, R. L., and Olivero, M. A. (1980). A digital frequency meter. *Rev. Telegr. Electron.* **68**, 67–72. In Spanish.

Granveaud, M. (1980). Contribution of the computation algorithm to the instability of atomic time scales. *CPEM Dig.*, pp. 7–8.

Granveaud, M., and Azoubib, J. (1974). The problem of ageing in the derivation of TAI [International Atomic Time]. *CPEM Dig.*, pp. 279–280.

Granveaud, M., and Guinot, B. (1978). The role of primary standards in establishing the International Atomic Time TAI. *CPEM Dig.*, pp. 39–41.

Grauling, C. H., Jr., and Healey, D. J., III (1966). Instrumentation for measurement of the short-term frequency stability of microwave sources. *Proc. IEEE* **54**, 249–257.

Gray, J. E. (1976). Clock synchronization and comparison: problems, techniques and hardware. *NBS Tech. Note (U.S.)* 691, 9 pp.

Greivulis, Ya. P., and Blumbergs, E. A. (1976). Frequency meter. *Izv. Vyssh. Vchebn. Zaved. Priborostr.* **19**, 13–15. In Russian.

Grenchik, T. J., and Fang, B. T. (1977). Time determination for spacecraft users of the Navstar Global Positioning System (GPS). *Proc. 31st Annu. Freq. Control Symp.*, pp. 1–3.

Groslambert, J. M. (1971). Automatic measurement system of oscillator frequency stability. *Eurocon Dig. (IEEE)*, p. 1.

Groslambert, J., Olivier, M., and Uebersfeld, J. (1972). Automatic plotting systems for frequency stability curves and discrete spectral density of frequency standards. *IEEE Trans. Instrum. Meas.* **IM-21**, 405–409.

Groslambert, J., Olivier, M., and Uebersfeld, J. (1974a). Spectral and short term stability measurements. *IEEE Trans. Instrum. Meas.* **IM-23**, 518–521.

Groslambert, J., Olivier, M., and Uebersfeld, J. (1974b). Spectral and short term stability measurements. *CPEM Dig.*, pp. 60–61.

Guignard, A., and Berney, J. C. (1967). A new series of electronic instruments for time measurements and standard-time distribution. *Mes., Regul., Autom.* **32**, 100. In French.

Guinot, B. (1967). Mean atomic time-scales. *Bull. Astron.* **2**, 449–464. In French.

Guinot, B. (1971). Characteristics of a scale of time. *Alta Freq.* **40**, 684–686.

Guinot, B. (1974). Long term stability and accuracy of time scales. *CPEM Dig.*, pp. 333–335.

Guinot, B. (1980). Problems of the generation, quality, and availability of the International Atomic Time Scale. *CPEM Dig.*, pp. 5–6.

Guinot, B., and Granveaud, M. (1972). Atomic time scales. *IEEE Trans. Instrum. Meas.* **IM-21**, 396–400.

Guinot, B., Granveaud, M., and Azoubib, J. (1981). Stability and accuracy of the international atomic time. *J. Inst. Electron. Telecommun. Eng. (New Delhi)* **27**, 524–527.

Gutnikov, V. S., Nedashkovskii, A. I., and Palkin, V. S. (1977). A specialised digital frequency meter used for operation with measuring frequency convertors. *Prib. Sist. Upr.* **5**, 22–24. In Russian.

Hafner, E. (1969). Frequency and time. *Proc. Conf. New Horizons in Measurements—Trends in Theory and Application (IEEE)*, pp. 58–68.

Halford, D., Wainwright, A. E., and Barnes, J. A. (1968). Flicker noise of phase in RF amplifiers and frequency multipliers: characterization, cause and cure. *Proc. 22nd Annu. Freq. Control Symp.*, pp. 340–341.

Halford, D., Shoaf, J. H., and Risley, A. S. (1973). Spectral density analysis: frequency domain measurements of frequency stability. *Proc. 27th Annu. Freq. Control Symp.*, pp. 421–431.

Hamanaka, A. (1978). New frequency counter series features high reliability. *JEE, J. Electron. Eng.* (142), 50–54.

Harry, E. (1978). Counter, scope team up for precise timing measurements. *Electronics* **51**, 126–127.

Healey, D. J., III (1972). Flicker of frequency and phase, and white frequency and phase fluctuations in frequency sources. *Proc. 26th Annu. Freq. Control Symp.*, pp. 29–42.

Healey, D. J., III (1974). $L(f)$ measurements on UHF sources comprising VHF crystal controlled oscillator followed by a frequency multiplier. *Proc. 28th Annu. Freq. Control Symp.*, pp. 190–202.

Hellwig, H. (1981). Reliability, serviceability and performance of frequency standards. *J. Inst. Electron. Telecommun. Eng. (New Delhi)* **27**, 362–365.

Hellwig, H., and Wineland, D. J. (1978). Time, frequency and physical measurement. *Phys. Today* **31**, 23–30.

Hocker, L. O., Small, J. G., and Javan, A. (1969). Extension of absolute frequency measurements to the 84 μ range. *Phys. Lett. A* **20**, 321–322.

Hodgkinson, G. (1977). Counters and timers, once lab luxuries, now everyday instruments. *Electron* **13**, 16, 19.

Hoene, J., and Holland-Nell, U. (1970). Time measuring equipment for the delayed representation of signals with high definition. *Nachrichtentechnik* **20**, 405–411. In German.

Hoffman, K. (1982). Time synchronisation via OTS-2. *CPEM Dig.*, pp. M/16–17.

Howe, D. A., Allan, D. W., and Barnes, J. A. (1981). Properties of signal sources and measurement methods. *Proc. 35th Annu. Freq. Control Symp.*, pp. A1–A47.

Hubner, U. (1977). Models and predictions for the realization of time scales. *Proc. 31st Annu. Freq. Control Symp.*, pp. 327–334.

Hudson, G. E., and Barnes, J. A. (1968). Clock error statistics as a renewal process. *Proc. 22nd Annu. Freq. Control Symp.*, pp. 384–418.

Hutchinson, F. (1976). Frequency measurement and timer-counters. *Electron. Equip. News* (March), 22–23.

IEEE (1975). "IEEE Standard Modular Instrumentation and Digital Interface System (CAMAC)—IEEE Standard 583-1975." IEEE, New York.

IEEE (1978). "IEEE Standard Digital Interface for Programmable Instrumentation—ANSI/IEEE Standard 488-1978." IEEE, New York.

Iijima, S., and Fujiwara, K. (1968). Precise measurement of radio time signals by means of pulsed oscillator. *Tokyo Astron. Obs. Rep.* **14**, 273–285.

Il'in, V. G., and Lukin, A. E. (1973). Phase fluctuations in a heterodyne multistage frequency multiplier [for standard frequency comparison]. *Meas. Tech. (Engl. Transl.)* **15**, 1659–1661.

Il'in, V. G., Sazhin, V. V., Bolotinikov, M. V., and Elkin, G. A. (1974). High-precision time and frequency measurements in the national economy and scientific investigations. *Meas. Tech. (Engl. Transl.)* **17**, 1033–1937.

Imshenetskii, V. V., and Martyniv, M. S. (1974). Extending the frequency limits of an electronic counting frequency meter. *Otbor Peredacha Inf.* **39**, 89–92. In Russian.

Ioannides, G. (1974). The 50 MHz universal counter UZ56/UZ56s. *Grundig Tech. Inf.* **21**, 307–310. In German.

Ivanov, N. I., and Kravshenko, V. F. (1973). Short-term frequency instability of an oscillator. *Izv. Vyssh. Uchebn. Zaved. Radioelektron.* **15**, 1391–1393. In Russian.

Ivanov, V. V., and Stepanov, B. M. (1971). Measurement of small duration intervals. *Izmer. Tekh.* **14**, 25–27. In Russian.

Izokh, V. V., and Tabachnik, E. I. (1977). Mean-square and information-theory estimates of time-interval measurement accuracy in the presence of noise. *Meas. Tech. (Engl. Transl.)* **20**, 343–347.

Jackisch, C., Schubert, H. J., and Hartmann, H. L. (1980). Measurement of time fluctuations in synchronous communication networks. *CPEM Dig.*, pp. 34–39.

Jayapal, R. (1977). Measure power frequency with a conventional counter. *Electron. Eng.* **49**, 17.

Jenkins, G. M., and Watts, D. G. (1968). "Spectral Analysis and Its Applications." Holden-Day, San Francisco.

Jennings, D. A., Petersen, F. R., and Evenson, K. M. (1975). Extension of absolute frequency measurements to 148 THz: frequencies of the 2.0 and 3.5 μm Xe laser. *Appl. Phys. Lett.* **26**, 510–511.

Jennings, D.A., Petersen, F. R., and Evenson, K. M. (1979). Frequency measurement of the 260-THz (1.15 μm) He–Ne laser. *Opt. Lett.* **4**, 129–130.

Jimenez, J. J., and Petersen, F. R. (1977). Recent progress in laser frequency synthesis. *Infrared Phys.* **17**, 541–546.

Job, A. (1969). Short term stability of sinusoidal generators. *Onde Electr.* **49**, 528–538. In French.

Jones, C. H. (1979). A test equipment for the measurement of phase and frequency instability in VHF and SHF sources. *Radio Electron. Eng.* **49**, 187–196.

Jutzi, K. H. (1973). Frequency measurement by signal sampling. *Frequenz* **27**, 309–311. In German.

Kahnt, D. (1977). ASMW time and frequency signals and their applications. *Radio Fernsehen Elektron.* **26**, 112–113. In German.

Kalau, M. (1980). The GDR atomic time scale. *CPEM Dig.*, pp. 11–14.

Kamas, G., and Howe, S. L. (1979). Time and frequency user's manual. *NBS Spec. Publ. (U.S.)* 559, 248 pp.

Kamyshan, V. V., and Valitov, R. A. (1969). Heterodyne method of frequency measurement in the millimeter range. *Instrum. Exp. Tech. (Engl. Transl.)* (4), 925–928.

Karpov, N. R. (1980). Vernier method of measuring time intervals. *Meas. Tech. (Engl. Transl.)* **23**, 817–822.

Kartaschoff, P. (1973). Terms and methods to describe frequency stability. *Tech. Mitt. PTT* **51**, 520–529. In German.

Kartaschoff, P. (1977). Frequency control and timing requirements for communications systems. *Proc. 31st Annu. Freq. Control Symp.*, pp. 478–483.

Kazi, A. M., and Perini, G. J. (1971). Program execution time measurement. *IBM Tech. Disclosure Bull.* **14**, 428.

Kendall, W. B., and Parsons, P. L. (1968). A precision frequency measurement technique for a moving signal with a low signal to noise ratio. *Conf. Precision Electromagn. Meas (IEEE)*, pp. 54–55.

Kesner, D. (1973). Take the guesswork out of phase-locked loop design. *EDN* **18**, 54.

Kiehne, F. (1967). FEGR-A multi-purpose 500 kHz counter. *News Rhode and Schwarz* **7**, 15–16.

Kimel'blat, V. I. (1978). Evaluation of measuring accuracy of middle frequency and bandwidth for radio-receiving apparatus. *Meas. Tech. (Engl. Transl.)* **21**, 541–543.

Kirchner, D. (1983). Precision timekeeping at the Observatory Lustbuehel, Graz, Austria. *Proc. 37th Annu. Freq. Control Symp.*, pp. 67–77.

Kirianaki, N. V., Kazantsev, E. M., and Mosievich, P. M. (1977). Multirange fast automatic digital frequency meter. *Izv. Vyssh. Uchebn. Zaved. Priborostr.* **20**, 9–14. In Russian.

Klimov, A. I., and Meleshko, E. A. (1977). Monitoring unit for time-interval analyzers of nanosecond range. *Instrum. Exp. Tech. (Engl. Transl.)* **20**, 1058–1060.

Knight, D. J. E., Edwards, G. J., and Blaney, T. G. (1977). Developments in laser frequency measurement towards realising the metre from a unified frequency and length standard. *European Conf. Precise Electr. Meas. (IEE)*, p. 40.

Kobayashi, M., Osawa, H., Morinaga, N., and Namekawa, T. (1973). Output signal-to-noise ratios in mean frequency measurement system. *Tech. Rep. Osaka Univ.* **23**, 515–526.

Kobayashi, M., Osawa, H., Morinaga, N., and Namekawa, T. (1976). Mean frequency and mean power measurement using correlation detection. *Trans. Soc. Instrum. Control Eng.* **12**, 613–618. In Japanese.

Kocaurek, R. (1968). Frequency comparison receiver EF 151 k. *News Rohde and Schwarz* **8**, 23–24.

Koch, E. (1979). An all-waveband receiver with a digital frequency display and a quartz clock. *Funkschau* **51**, 236–239. In German.

Koga, I. (1970). Precision measurement of crystal frequency by means of "center line method." *Proc. 24th Annu. Freq. Control Symp.*, pp. 168–171.

Kogan, L. R. (1970). Oscillator stability requirements in radio interferometers. *Radiotekh. Elektron.* **15**, 1292–1294. In Russian.

Kolbasin, A. I., and Pavlenko, Yu. F. (1978). Transfer of the dimension of a unit deviation of frequency from the special state standard to prototype means of measurement. *Meas. Tech. (Engl. Transl.)* **21**, 806–809.

Koppe, H. (1979). Frequency measurement using a microcomputer—a program and an instruction program. *Elektron. Prax.* **14**, 30, 35–36, 39. In German.

Kotel'nikov, A. V., Rubailo, G. T., and Uvarov, N. E. (1975). An instrument for measuring the ratio of time intervals. *Telecommun. Radio Eng. (Engl. Transl.), Part 1* **29**, 60–61.

Kourigin, E. I., Chernyshev, V. S., and Shumkin, Yu. V. (1979). High-speed device for time interval measurement. *Instrum. Exp. Tech. (Engl. Transl.)* **22**, 484–486.

Kramer, G. (1970). An electronic time intervalometer with high resolution. *Nachrichtentech. Z.* **23**, 433–436. In German.

Krause, W. H. U. (1968). Accurate time and frequency measurement. *Frequenz* **22**, 178–182. In German.

Kuchynka, K., and Preuss, A. (1981). Electronic counters facilitate time measurement. *Siemens Power Eng.* **3**, 179–182.

Kul'gavchuk, V. M. (1975). Frequency meters using devices with S-shaped volt-ampere characteristics. *Instrum. Exp. Tech. (Engl. Transl.)* **18**, 514–516.

Kuznetsov, V. P., and Reznikov, A. L. (1974). Adjacent time intervals measured by two frequency meters. *Meas. Tech. (Engl. Transl.)* **17**, 474–475.

Laker, K. R., and Slobodnik, A. J., Jr. (1975). "Impact of SAW Filters on RF. Pulse Frequency Measurement by Double Detection." Report AFCRL-PSRP-621, Air Force Cambridge Research Laboratories, Hanscom Air Force Base, Massachusetts, 194 pp. Available from the National Technical Information Service, Springfield, Virginia.

Lance, A. L., Seal, W. D., Mendoza, F. G., and Hudson, N. H. (1977). Automating phase noise measurements in the frequency domain. *Proc. 31st Annu. Freq. Control Symp.*, pp. 347–358.

Leah, P. (1977). Frequency counter/timer. *Pract. Electron.* **14**, 22–28.

Leikin, A. Ya., and Orlov, E. Z. (1973). Equipment for comparing frequencies of highly-stable generators. *Meas. Tech. (Engl. Transl.)* **16**, 1469–1470.

Leikin, A. Ya., Tomashenko, I. V., and Fertik, N. S. (1974). Application of a rubidium discriminator for the measurement of frequency fluctuations. *Izv. Vyssh. Uchebn. Zaved. Radiofiz.* **17**, 851–854. In Russian.

Lemesev, S. G., Rachev, B. T., Strugach, V. G., and Shub, S. M. (1975). Statistical method for measuring a recurrent time interval using a random pulse signal. *Izv. Vyssh. Uchebn. Zaved. Priborostr.* **18**, 16–21. In Russian.

Lesage, P. (1982). Characterization of frequency stability: bias due to the addition of time interval measurements. *CPEM Dig.*, pp. M/8–9.

Lesage, P. (1983). Characterization of frequency stability: bias due to the juxtaposition of time-interval measurements. *IEEE Trans. Instrum. Meas.* **IM-32**, 204–207.

Lesage, P., and Audoin, C. (1973). Characterization of frequency stability: uncertainty due to the finite number of measurements. *IEEE Trans. Instrum. Meas.* **IM-22**, 157–161, with corrections from *IEEE Trans. Instrum. Meas.* **IM-25**, 270.

Lesage, P., and Audoin, C. (1975a). A time domain method for measurement of the spectral density of frequency fluctuations at low Fourier frequencies. *Proc. 29th Annu. Freq. Control Symp.*, pp. 394–403.

Lesage, P., and Audoin, C. (1975b). Comments on "Characterization of frequency stability: uncertainty due to the finite number of measurements." *IEEE Trans. Instrum. Meas.* **IM-24**, 86.

Lesage, P., and Audoin, C. (1977). Estimation of the two-sample variance with a limited number of data [signal generator frequency stability]. *Proc. 31st Annu. Freq. Control Symp.*, pp. 311–318.

Lesage, P., and Audoin, C. (1979a). Characterization and measurement of time and frequency stability. *Radio Sci.* **14**, 521–539.

Lesage, P., and Audoin C. (1979b). Effect of dead time on the estimation of the two-sample variance. *IEEE Trans. Instrum. Meas.* **IM-28**, 6–10.

Lo Faso, G. (1968a). Digital frequency meter and chronometer in RTL micrologic. *Int. Elektron. Rundsch.* **22**, 63–66. In German.

Lo Faso, G. (1968b). RTL Micrologic in a digital frequency and time counter. *Int. Elektron. Rundsch.* **22**, 47–50. In German.

Lomas, G. (1974). Signal-frequency meter. *Wireless World* **80**, 429–434.

Loose, P. (1979). Modern electronic-based timing systems. *Electron. Eng.* **51**, 81, 83–84.

Lubentsov, V. F. (1973). The errors of the absolute method for measuring difference-signal frequency. *Telecommun. Radio Eng. (Engl. Transl.), Part 2* **28**, 96–99.

Lubentsov, V. F., and Ashitkov, I. N. (1968). Device for measuring the frequencies and errors of crystal oscillators. *Meas. Tech. (Engl. Transl.)* (7), 906–911.

Lukas, M. (1968). An intermediate frequency measuring equipment with an unusual frequency indication. *Slaboproudy Obz.* **29**, 323–326. In Czech.

MacLeod, K. J. (1973). A portable high-resolution counter for low-frequency measurements. *Hewlett-Packard J.* **25**, 10–15.

Maletz, W. (1974). 100 MHz universal counter FET 100. *News Rohde & Schwarz* **14**, 5–7.

Markowitz, W. (1968). Time and frequency measurement, atomic and astronomical. *Proc. 5th Annu. ISA Test Meas. Symp.*, Instrument Society of America, Pittsburgh, Pennsylvania, p. 6.

Martin, D. (1971). Frequency stability measurements by computing counter system. *Hewlett-Packard J.* **23**, 9–14.

Martin, D. (1974). Measure time interval precisely. *Electron. Des.* **22**, 162–167.

Martin, J. D. (1972). Digital methods of frequency measurements: a comparison. *Radio Electron. Eng.* **42**, 285–294.

Maton, G. W. (1978). Thoughts on frequency meters and counter–timers. *Electron* (134), 24, 27.

Maxwell, B. J. (1980). Perception of errors in instruments and applications. I. Time, our most accurate measurement. *Autom. Control (New Zealand)* **10**, 27–29.

McCarthy, E. P. (1979). A digital instantaneous frequency meter. *IEEE Trans. Instrum. Meas.* **IM-28**, 224–226.

McCaskill, T. B., and Buisson, J. A. (1975). NTS-1 (TIMATION III) [satellite] quartz and rubidium oscillator frequency stability results. *Proc. 29th Annu. Freq. Control Symp.*, pp. 425–428.

McCaskill, T., White, J., Stebbins, S., and Buisson, J. (1978). NTS-2 cesium frequency stability results. *Proc. 32nd Annu. Freq. Control Symp.*, pp. 560–566.

McClellan, G. (1978). Prescaler and LSI chip form 135-MHz counter. *Electronics* **51**, 97, 99.

Meer, P. (1977). Four function calculator can measure time. *Electron. Eng.* **49**, 35.

Melsa, J. L., and Schultz, D. G. (1969). "Linear Control Systems." McGraw-Hill, New York.

Mende, F. F., and Charkin, V. A. (1973). Superhigh frequency measurement with electronic-counter frequency meters. *Meas. Tech. (Engl. Transl.)* **16**, 1360–1362.

Millham, E. H. (1974). High-accuracy time meter. *IBM Tech. Disclosure Bull.* **17**, 1143–1144.

Mints, M. Ya., and Chinkov, V. N. (1980). Accuracy of time interval measurement by pulse counting. *Meas. Tech. (Engl. Transl.)* **23**, 603–606.

Mitsenko, I. D., and Borisov, S. K. (1975). Phase-pulse discriminator for measurement of nanosecond time intervals. *Instrum. Exp. Tech. (Engl. Transl.)* **18**, 144–145.

Mohos, Z. (1973). Time interval measurement by averaging. *Meres Autom.* **21**, 268–272. In Hungarian.

Mroz, T. J. (1977). Time-interval meter reads digitally to 99.9 ms on a DVM IC. *Electron. Des.* **25**, 108, 110.

Muchiauri, A. A. (1973). A digital method of frequency measurement for harmonic signals. *Meas. Tech. (Engl. Transl.)* **16**, 1710–1712.

Muhlenbroich, H. P. (1980). The mode of operation of time interval measurement. *Elektron. J.* **15**, 32–34. In German.

Mungall, A. G. (1971). Atomic time scales. *Metrologia* **7**, 146–153.

Murashov, B. P., and Tsvetkov, Yu. P. (1976). Instrument for checking quartz-crystal oscillators with standard frequency signals in the long-wave and very-long-wave ranges. *Meas. Tech. (Engl. Transl.)* **19**, 1012–1015.

Muzychuk, O. V., and Shepelevich, L. G. (1974). On the determination of short time signal frequency instability. *Izv. Vyssh. Uchebn. Zaved. Radiofiz.* **17**, 855–863. In Russian.

Nakadan, Y., and Koga, Y. (1977). Measurements of frequency stability of precision oscillators. *Oyo Butsuri* **46**, 572–579. In Japanese.

Navarro-Fernandez, A. (1974). Adapting a frequency meter into a digital clock. *Mundo Electron.* (34), 92. In Spanish.

Niki, S. (1975). Automatic frequency counter uses TRAHET technique to count to 32 GHz with −20 dBm sensitivity. *JEE, J. Electron. Eng.* (107), 20–23.

Offermann, R. W., Schultz, S. E., and Trimble, C. R. (1975). Active probes improve precision of time interval measurements. *Hewlett-Packard J.* **27**, 11–16.

Ohman, B. (1978). New task for the telecommunication authority—national measurement standards for time and frequency. *Tele* **84**, 14–24. In Swedish.

Orte, A. (1976). Comparison of various fundamental methods of defining time, with special reference to astronomical application. *Navigation* **24**, 72–84.

Osakabe, M., Sasao, K., and Kato, E. (1973). Field strength and frequency measuring instruments. *Anritsu Tech. Bull.* (29), 52–56. In Japanese.

Pacheu, Y. (1979). Analogue frequency meter. *Electron. Appl. Ind.* (262S), 15–16. In French.

Page, R. (1979). Time and frequency counting techniques. *Electron. Eng.* **51**, 47–48, 51, 53, 57–58.

Palamaryuk, G. O., and Kholkin, I. I. (1967). Digital smoothing frequency meter for variable-sign pulse signals. *Meas. Tech. (Engl. Transl.)* (7), 845–847.

Palii, G. N., and Pushkin, S. B. (1980). Improvement of time and frequency stabilization. *Meas. Tech. (Engl. Transl.)* **23**, 115–118.

Parkinson, B. A. R. (1970). Precise time and frequency measurement. II. *Electron. Equip. News* **12**, 60–65.

Pashev, G. P., and Parfenov, G. A. (1977). Analysis of the errors of statistical devices measuring repeated time intervals. *Meas. Tech. (Engl. Transl.)* **20**, 347–349.

Patankar, A. R., Nambiar, K. P. P., and Sitharaman, M. R. (1974). An automatic electronic frequency comparator. *J. Inst. Electron. Telecommun. Eng. (New Delhi)* **20**, 405–407.

Patykov, V. G., Podlesnyi, S. A., and Chmykh, M. K. (1976). Digital frequency meter with high noise immunity. *Instrum. Exp. Tech. (Engl. Transl.)* **19**, 1581.

Paul, F. (1973). Reciprocal frequency meters. *Electron. Microelectron. Ind.* (168), 55–59. In French.

Peltz, I. G. (1971). Highly stable audio generator for frequency measurements on clock crystals. *Elektronik (Munich)* **20**, 345–348. In German.

Percival, D. B. (1978a). The U.S. Naval Observatory clock time scales. *IEEE Trans. Instrum. Meas.* **IM-27**, 376–385.

Percival, D. B. (1978b). The U.S. Naval Observatory clock time scale. *CPEM Dig., Conf. Precision Electromagn. Meas.*, pp. 42–44.

Percival, D. B. (1982). Characterization of time and frequency instabilities: prediction error variance. *CPEM Dig.*, pp. N.7–9.

Percival, D. B., and Winkler, G. M. R. (1975). Timekeeping and the reliability problem. *Proc. 29th Annu. Freq. Control Symp.*, pp. 412–416.

Peres, A. (1980). Measurement of time by quantum clocks. *Am. J. Phys.* **48**, 552–557.

Perkinson, R. E. (1970). Time frequency technology in system development. *Proc. 24th Annu. Freq. Control Symp.*, pp. 315–321.

Petersen, A. P. (1980). A new apparatus for the precise determination of time and frequency on the LF band using transmitter DCF 77. *CPEM Dig.*, pp. 17–19.

Petrov, A. F., Zhukov, E. T., Kosharnovskii, G. V., Breslavets, V. P., and Fedulov, V. M. (1977). Frequency comparator based on a delay line. *Meas. Tech. (Engl. Transl.)* **20**, 1456–1458.

Pokorny, L. (1976). Modern frequency counters. *Radio Elektron. Schau (Austria)* **52**, 20–24. In German.

Pokorny, L. (1977). Hewlwtt-Packard 5328A universal counter with DVM options. *Elektroniskschau (Austria)* **53**, 56.

Potschke, H. (1976). Time measurement. *Nachr. Elektron.* **30**, 107–108. In German.

Powers, R. S., and Snyder, W. F. (1969). Radio-frequency measurements in the NBS Institute for Basic Standards *NBS Tech. Note (U.S.) 373*, pp. 37–42.

Pritchard, N. B. (1979). A frequency counter for a 144 MHz transmitter. *Radio Commun.* **55**, 410–415.

Prusakov, V. K., and Kilna, A. A. (1974). About digital harmonic signal frequency measuring accuracy. *Liet. TSR Mokslu Akad. Darb., Ser. B* (80), 141–148. In Russian.

Putkovich, K. (1972). Automated timekeeping. *IEEE Trans. Instrum. Meas.* **IM-21**, 401–405.

Ramamurthy, T. V., and Kumar, M. K. (1979). A measurement technique for low frequencies. *J. Phys. E.* **12**, 187–188.

Reeder, R. (1977). The not so simple counter. *Electron. Equip. News* (November), 9–10.

Reider, G. A. (1980). Standard deviation of averaged digital time interval measurement [error values]. *Rev. Sci. Instrum* **51**, 1423–1424.

Reid, J. H. (1972). The measurement of time. *J. R. Astron. Soc. Can.* **66**, 135–148.

Reinhardt, V., and Lavanceau, J. (1974). A comparison of the cesium and hydrogen hyperfine frequencies by means of Loran C and portable clocks. *Proc. 28th Annu. Freq. Control Symp.*, pp. 379–383.

Reussner, J., and Weiss, H.-J. (1973). Standard frequency receiver for calibrating frequency counters. *Radio Fernsehen Elektron.* **22**, 638–640. In German.

Ribenyi, A. (1967). Digital frequency measuring instruments. *Meres Automat.* **15**, 436–439. In Hungarian.

Rikhter, V., and Fogler, G. (1977). Influence of stresses due to discontinuous jamming on the accuracy of digital frequency measuring devices. *Prib. Sist. Upr.* (1), 21–23. In Russian.

Risley, A. S. (1976). The national measurement system for time and frequency. *NBS Spec. Publ. (U.S.)* 445–1, 64 pp.

Rivamonte, J. M. (1972). U.S. Army calibration program. *Proc. 26th Annu. Freq. Control Symp.*, pp. 258–259.

Roth, R. (1977). Alignment generator AS5 with quartz controlled frequency indicator. *Grundig Tech. Inf.* **24**, 209–216. In German.

Rozwadowski, M. (1971). Modern frequency stabilisation methods. *Przegl. Telekomun* **44**, 335–338. In Polish.

Ruderfer, M. (1979). One-way doppler effects in atomic timekeeping. *Speculations Sci. Technol.* **2**, 387–404.

Runyon, S. (1977). Focus on electronic counters. *Electron. Des.* **25**, 54–63.

Rusconi, L., and Sedmak, G. (1977). Estimates of the limiting standard deviation in the absolute timing of periodic sources. *Astrophys. Space Sci.* **46**, 301–308.

Rutman, J. (1972a). Comment on "Characterization of frequency stability." *IEEE Trans. Instrum. Meas.* **IM-21**, 85.

Rutman, J. (1972b). Short term frequency instability of signal generators. *Onde Electr.* **52**, 480–487. In French.

Rutman, J. (1974a). Characterization of frequency stability: a transfer function approach and its application to measurements via filtering of phase noise. *IEEE Trans. Instrum. Meas.* **IM-23**, 40–48.

Rutman, J. (1974b). Relations between spectral purity and frequency stability. *Proc. 28th Annu. Freq. Control Symp.*, pp. 160–165.

Rutman, J. (1977). Oscillator specifications: a review of classical and new ideas. *Proc. 31st Annu. Freq. Control Symp.*, pp. 291–301.

Rutman, J. (1978). Characterization of phase and frequency instabilities in precision frequency sources: fifteen years of progress. *Proc. IEEE* **66**, 1048–1075.

Rutman, J., and Sauvage, G. (1974a). Measurement of frequency stability in time and frequency domains via filtering of phase noise. *CPEM Dig.*, pp. 57–59.

Rutman, J., and Sauvage, G. (1974b). Measurement of frequency stability in time and frequency domains via filtering of phase noise. *IEEE Trans. Instrum. Meas.* **IM-23**, 515–518.

Rzewvski, M. (1976). Frequency deviation measurements by synchronized sampling method. *Przegl. Telekomun.* **49**, 7–9. In Polish.

Sakai, T. (1977). Frequency counters become sophisticated. *JEE, J. Electron. Eng.* (121), 20–23.

Saunders, W. K. (1972). Short term frequency stability in coherent radar applications. *Proc. 26th Annu. Freq. Control Symp.*, pp. 21–28.

Schneider, R. J. (1971). Time and frequency standardization. *Signal* **25**, 42–45.

Schommartz, G. (1979). On the measurement dynamics of digital frequency meters. *Mess., Steuern, Regeln* **22**, 261–267. In German.

Schreiber, H. (1978). Active test head for a frequency counter. *Funk-Tech.* **33**, 241–242. In German.

Secaze, G. (1975). Measurement of time-standards and their marketing. *Electron. Microelectron. Ind.* (208), 71–75. In French.

Senftleben, H. (1977). A digital universal counter. *Radio Fernsehen Elektron.* **26**, 441–445. In German.

Shoaf, J. H., Halford, D., and Risley, A. S. (1973). Frequency stability specification and measurement: high frequency and microwave signals. *NBS Tech. Note (U.S.) 632*, 65 pp.

Simpson, L. (1977). A low-cost 200 MHz digital frequency meter. *Electron. Aust.* **38**, 30–35, 37.

Simpson, L. (1978). Upgraded 200 MHz digital frequency meter. II. Construction details. *Electron. Aust.* **40**, 60–63.

Small, J. C., Monchalin, J. P., Kelly, M. J., Keilmann, F., Senchez, A., Singh, S. K., Kurnit, N. A., and Javan, A. (1972). Precision absolute frequency and wavelength measurements in the infrared: a review of activities at MIT. *Proc. 26th Annu. Freq. Control Symp.*, pp. 248–249.

Smith, H. M. (1967). Astronomical time scales. *Colloq. Definition, Realisation and Use of Time and Frequency, IEE Colloq. Dig.*, Paper No. 2.

Snyder, J. J. (1981). An ultra-high resolution frequency meter. *Proc. 35th Annu. Freq. Control Symp.*, pp. 464–469.

Sopel'nikov, M. D., and Fedorov, Yu. A. (1980). Investigation of errors in synchronizing time scales over wide-band communication channels. *Meas. Tech. (Engl. Transl.)* **23**, 118–120.

Sorden, J. L. (1974). A new generation in frequency and time measurements. *Hewlett-Packard J.* **25**, 2–8.

Spapens, W. (1972). Accurate time measurements with a counter and an oscilloscope. *Philips Test Meas. Not.* (2), 4–8.

Speake, B. (1979). The accurate setting of microwave frequencies. *Commun. Int.* **6**, 19, 21.

Stecher, R. (1973). Electronic time interval measurement with nanosecond resolution. *Nachrichtentech. Elektron.* **23**, 413–416. In German.

Steele, J. McA. (1967). Frequency measurement using standard frequency emissions. *Conf. Freq. Generation and Control Radio Syst.*, IEE Conference Publication No. 31.

Steer, G. (1973). A new UHF frequency measuring device. *Fernmelde-Praxis* **50**, 571–600. In German.

Stein, S., Glaze, D., Levine, J., Gray, J., Hilliard, D., Howe, D., and Erb, L. A. (1983). Automated high-accuracy phase measurement system. *IEEE Trans. Instrum. Meas.* **IM-32**, 227–231.

Steiner, C. I. (1969). Electronic methods of time measurement. *Elektroniker* **8**, 3–16. In German.

Stoyko, A. (1967). Ephemeris time according to the revised lunar theory of Brown. *Bull. Astron.* **2**, 411–416. In French.

Szata, R. (1968). New method of oscilloscopic frequency measurement. *Pomiary, Autom., Kontrola* **14**, 200–301. In Polish.

Szepan, R. (1978). Determining accuracy of receiver-controlled frequency standards. *News Rohde & Schwarz* **18**, 23–26.

Taylor, D. (1968). Time measurement. *Instrum. Rev.* **15**, 173–176.

Taylor, G. W. (1977). Time—a precious commodity. *Electron. Power* **23**, 61–64.

Tolman, J. (1970). Accurate frequency and time measurement at the Institute of Radio Engineering and Electronics. *Slaboproudy Obz.* **31**, 286–290. In Czech.

Tooley, M. (1979). In-line crystal calibrator. *Pract. Wireless* **55**, 49–50, 55.

Triplet, J. M. (1967). Ephemeris time determination by lunar photography. *Bull. Astron.* **2**, 465–527. In French.

Trkal, V. (1968). A new definition of the second on a quantum basis. *Cesk. Cas. Fyz. A.* **18**, 641–669. In Czechoslavakian.

Turrini, A. (1974). Heterodyne frequency meter No. 351C E.I.P. *Antenna* **46**, 62–68. In Italian.

Tyrsa, V. E., and Dyunyashev, V. V. (1981). Accuracy of frequency measurement based on the pulsed coincidence principle. *Meas. Tech. (Engl. Transl.)* **24**, 308–312.

Underhill, M. J., Sarhadi, M., and Aitchinson, C. S. (1978). Fast-sampling frequency meter. *Electron. Lett.* **14**, 366–367.

Upton, R. (1977). An objective comparison of analog and digital methods of realtime frequency analysis. *Bruel Kjaer Tech. Rev. (Denmark)* **1**, 18–26.

Vakman, D. Ye. (1979). The evaluation of frequency stability. *Telecommun. Radio Eng. (Engl. Transl.), Part 2* **34**, 49–53.

Vakman, D. Ye. (1979). Measuring the frequency of an analytical signal. *Radio Eng. Electron. Phys. (Engl. Transl.)* **24**, 63–69.

Valaskova, E. (1971). Measuring the frequency of damped oscillations. *Sdelovaci Tech.* **19**, 174–175. In Czech.

Valverde, R. M. (1968). A digital instantaneous frequency-meter. *Automaz. Strum.* **16**, 216–221. In Italian.

Van Blerkom, R., Freeman, D. G., and Crutchfield, R. C., Jr. (1968). Frequency measurement techniques. *IEEE Trans. Instrum. Meas.* **IM-17**, 133–145.

Van Den Brock, H. G. J. (1977). Two frequency counters for routine measurements. *Polytech. Tijdschr. Elektrotech. Elektron.* **32**, 517–518. In Dutch.

Van den Steen, L. (1979). A low frequency meter with instantaneous response. *IEEE Trans. Biomed. Eng.* **BME-26**, 137–140.

Van Straaten, J. (1979). A one-chip LSI frequency meter in the I^2L technology for FM and AM receivers. *IEEE Trans. Consum. Electron.* **CE-25**, 134–143.

Vessot, R., Mueller, L., and Vanier, J. (1966). The specification of oscillator characteristics from measurements made in the frequency domain. *Proc. IEEE* **54**, 199–206.

Viles, R. S. (1972). Swept frequency techniques for accurate r.f. measurements. *Marconi Instrum.* **13**, 88–92.

Voss, R. F. (1979). $1/f$ noise. *Proc. 33rd Annu. Freq. Control Symp.*, pp. 40–46.

Wainwright, A. E., Walls, F. L., and McCaa, W. D. (1974). Direct measurement of the inherent frequency stability of quartz crystal resonators. *Proc. 28th Annu. Freq. Control Symp.*, pp. 177–180.

Walls, F. L., and DeMarchi, A. (1975). RF spectrum of a signal after frequency multiplication; measurement and comparison with a simple calculation. *IEEE Trans. Instrum. Meas.* **IM-24**, 310–317.

Walls, F. L., and Stein, S. R. (1976). Servo techniques in oscillators and measurement systems. *NBS Tech. Note (U.S.) 692.*

Walls, F. L., Stein, S. R., Gray, J. A., and Glaze, D. J. (1976). Design considerations in state-of-the-art signal processing and phase noise measurement systems. *Proc. 30th Annu. Freq. Control Symp.*, pp. 269–274.

Ward, R. B. (1982). VHF/UHF frequency measurement using the surface acoustic wave delay difference device. *Appl. Phys. Lett.* **40**, 1010–1012.

Weiss, C. O., and Godone, A. (1982). Extension of frequency measurements with Schottky diodes to the 4 THz range. *Appl. Phys. B* **27**, 167–168.

Weiss, R. (1976). Time-signal and standard-frequency receiver for the DCF 77 with reserve. I. *Funkschau* **48**, 964–968. In German.

Wessel, R. (1973). A digital frequency meter. *Elektromeister Dtsch. Elektrohandwerk* **48**, 1066–1068. In German.

Westlund, R. C. (1978). Very short time interval measurements. *New Electron.* **11**, 13–14, 18.

Wheeler, K. G. (1976). An optimum solution for counting and timing. *New Electron.* **9**, 24, 28, 32.

Whittaker, A. E., and Westbury, P. R. (1976). Measuring low frequencies. *New Electron.* **9**, 36.

Wiley, R. G. (1977). A direct time-domain measure of frequency stability: the modified Allan variance. *IEEE Trans. Instrum. Meas.* **IM-26**, 38–41.

Woschni, E. G. (1975). Errors in high-precision frequency measurements due to interactive effects. *Wiss. Z. Tech. Hochsch. Karl-Marx-Stadt* **17**, 633–639. In German.

Woschni, E. G. (1976). On the optimum difference frequency in high accuracy frequency measurements of industrial parameters. *Mess., Steuern, Regeln Automatisierungsprax.* **19**, 334–335. In German.

Woschni, E. G. (1978). Application of microprocessors to the calculation of error correction for the synchronisation effect in highly accurate frequency measurements. *Wiss. Z. Tech. Hochsch. Karl-Marx-Stadt* **20**, 665–668. In German.

Wrzesien, M. (1976). Instantaneous frequency measuring circuit. *Pomiary, Autom., Kontrola* **22**, 90–91. In Polish.

Yasuda, Y. (1974). Accuracy of estimating clockface and mean rate of the frequency standard by normal regression theory. *J. Radio Res. Lab. (Japan)* **21**, 39–60.

Yoshimura, K. (1972). The generation of an accurate and uniform time scale with calibrations and prediction. *NBS Tech. Note (U.S.) 626*, 59 pp.

Yoshimura, K. (1978). Characterization of frequency stability: uncertainty due to the autocorrelation of the frequency fluctuations. *IEEE Trans. Instrum. Meas.* **IM-27**, 1–7.

Yoshimura, K. (1980). Calculation of unbiased clock-variances in uncalibrated atomic time scale algorithms. *Metrologia* **16**, 133–139.

Yoshimura, K., Harada, K., and Kobayashi, M. (1971). Measurement of short-term frequency stability of frequency standards. *Rev. Radio Res. Labs.* **17**, 437–443. In Japanese.

Yuval, I. (1982). Frequency comparator uses synchronous detection. *Electronics* **55**, 160.

Zander, H. (1977). Measurement of low frequencies with short duration. *Elektronik (Munich)* **26**, 63–64. In German.

Zelentosov, V. I., Sulakshin, A. S., and Fedorov, N. P. (1976). Meter for measuring the carrier frequency of single ultrahigh-frequency pulses. *Instrum. Exp. Tech. (Engl. Transl.)* **19**, 476–477.

Zhilin, N. S., and Subbotin, I. S. (1977). Devices for reproducing reference time intervals. *Meas. Tech. (Engl. Transl.)* **20**, 995–999.

Zhuk, A. V., Kazantsev, E. M., Kirianaki, N. K., and Mosievich, P. M. (1977). Computer investigation of the metrological characteristics of frequency meters with digital positive feedback and measures to improve them. *Otbor Peredacha Inf.* **50**, 110–115. In Russian.

Chapter 13

Akatsuka, K., Yasuda, Y., and Matsuura, T. (1977). International time and frequency comparison via Loran-C. *Rec. Radio Res. Lab.* **23**, 165–170. In Japanese.

Allan, D. W. (1972). Time transfer using near-synchronous reception of optical pulsar signals. *Proc. IEEE* **60**, 625–627.

Allan, D. W. (1981). Some methods of maintaining and/or generating time and frequency at arbitrary points on the surface of the Earth. *J. Inst. Electron. Telecommun. Eng. (New Delhi)* **27**, 383–388.

Allan, D. W. (1983). National and international time and frequency comparisons. *Proc. 37th Annu. Freq. Control Symp.*, pp. 55–60.

Allan, D. W., and Barnes, J. A. (1967). Some statistical properties of LF and VLF propagation. *In* "Phase and Frequency Instability in Electro-magnetic Propagation" (K. Davies, ed.). *Proc. 33rd AGARD Conf.*, pp. 219–230. Technivision Services, Slough, England.

Allan, D. W., and Barnes, J. A. (1982). Optimal time and frequency transfer using GPS signals. *Proc. 36th Annu. Freq. Control Symp.*, pp. 378–387.

Allan, D. W., and Weiss, M. A. (1980). Accurate time comparisons using a GPS satellite in common view. *Proc. 34th Annu. Freq. Control Symp.*, pp. 334–346.

Allan, D. W., Leschiutta, S., and Rovera, G. (1970a). TV frame pulses used for precision time synchronization and their noise distribution. *Alta Freq.* **34**, 180E.

Allan, D. W., Gray, J. E., and Machlan, H. E. (1970b). The NBS atomic time scale system: AT(NBS), SAT(NBS), and UTC(NBS). *Proc. 24th Annu. Freq. Control Symp.*, p. 361.

Allan, D. W., Blair, B. E., Davis, D. D., and Machlan, H. E. (1971). Precision and accuracy of remote synchronization via portable clocks, Loran C, and network television broadcasts. *Proc. 25th Annu. Freq. Control Symp.*, pp. 195–208.

Allan, D. W., Blair, B. E., Davis, D. D., and Machlan, H. E. (1972a). Precision and accuracy of remote synchronization via network television broadcasts. *Metrologia* **8**, 64–72.

Allan, D. W., Machlan, H. E., and Marshall, J. (1972b). Time transfer using nearly simultaneous reception times from a common transmitter. *Proc. 26th Annu. Freq. Control Symp.*, pp. 309–316.

Allan, D. W., Gray, J. E., and Machlan, H. E. (1972c). The National Bureau of Standards atomic time scales: generation, dissemination, stability, and accuracy. *IEEE Trans. Instrum. Meas.* **IM-21**, 388–391.

Allan, D. W., Shoaf, J. H., and Halford, D. (1974). "Statistics of Time and Frequency Data Analysis." National Bureau of Standards, Washington, D. C., 204 pp.

Allan, D. W., Hellwig, H., and Glaze, D. J. (1975). An accuracy algorithm for an atomic time scale. *Metrologia* **11**, 133–138.

Allan, D. W., Alley, C. O., Ashby, N., Decher, R., and Vessot, R. F. C. (1981). Ultra-accurate international time and frequency comparison via an orbiting hydrogen-maser clock. *J. Phys. Colloq. (Orsay, Fr.)* **42**, 395–413.

Allan, D. W., Alley, C. O., Decher, R., Vessot, R. F. C., and Winkler, G. (1982). Shuttle experiment to demonstrate high-accuracy global time and frequency transfer. *IEEE Trans. Geosci. Remote Sensing* **GE-20**, 321–325.

Allan, D. W., Davis, D. O., Weiss, M., Clements, A., Guinot, B., Granveaud, M., Dorenwendt, K., Fischer, B., Hetzel, P., Aoki, S., Fijimoto, M.-K., Charron, L., and Ashby, N. (1985). Accuracy of international time and frequency comparisons via global positioning system satellites in common-view. *IEEE Trans. Instrum. Meas.* **IM-34**, June.

Allen, R. T. (1982). The U.S. Navy's standardized precise time and time interval (PTTI) platform distribution system. (PDS). *Proc. 36th Annu. Freq. Control Symp.*, pp. 372–377.

Angelotti, E., and Leschiutta, S. (1980). Radio time signals and codes. *Elettrotecnica* **67**, 449–453. In Italian.

Anonymous (1969). NBS frequency and time broadcast services, Radio stations WWV, WWVH, WWVB, WWVL. *NBS Spec. Publ. (U.S.)*, 13 pp. Available from the Superintendent of Documents, U.S. Govt. Printing Office, Washington, D.C.

Anonymous (1970). Time dissemination and clock synchronization via television. *Natl. Bur. Stand. Tech. News Bull.* **54**, 125–126.

Anonymous (1971a). "NBS Frequency and Time Broadcast Services." Report Special Publication 236, National Bureau of Standards, Washington, D.C., 15 pp.

Anonymous (1971b). Standards and calibration. *Natl. Bur. Stand. Tech. News Bull.* **55**, 98–99.

Anonymous (1971c). UTC time scale to change in 1972. *Hewlett-Packard J.* **23**, 16.

Anonymous (1980). Time-signal clock from Viehmann. *Radio Mentor Electron.* **46**, 032–033. In German.

Arnoldt, M. (1982). Global time scale matching through transport of atomic clocks. *Nachr. Elektron.* **36**, 355–362. In German.

Ashby, N. (1975). An earth-based coordinate clock network. *NBS Tech. Note (U.S.)* 659.

Ashby, N., and Allan, D. W. (1979). Practical implications of relativity for a global coordinate time scale. *Radio Sci.* **14**, 649–669.

Barnerjee, P., Sood, P. C., Kumar, N., Suri, A. K., and Mathur, B. S. (1979). Time synchronization using standard time broadcast form ATA-NPL. *J. Inst. Electron. Telecommun. Eng. (New Delhi)* **25**, 358–360.

Barnes, J. A., and Winkler, G. M. R. (1974). The standards of time and frequency in the USA. Report NBS-TN-649, National Bureau of Standards, Washington, *NBS Tech. Note 649*, 86 pp.

Bastelberger, J. (1973). Transmission of the standard frequency of the German Federal Post Office. *Fernmelde-Ing.* **27**, 1–40. In German.

Becker, G., and Enslin, H. (1972). Exact time and frequency comparisons by means of television picture pulses. *Freqenz* **26**, 332–337. In German.

Becker, G., and Hubner, U. (1979). The generation of time scales. *Radio Sci.* **4**, 593–603.

Becker, G., and Kramer, G. (1969). Methods of international time and frequency comparison with v.l.f. *Frequenz* **23**, 256–261. In German.

Beehler, R. E. (1981). Time/frequency services of the US National Bureau of Standards and some alternatives for future improvements. *J. Inst. Electron Telecommun. Eng. (New Delhi)* **27**, 389–402.

Beehler, R. E., Davis, D. D., Cateora, J. V., Clements, A. J., Barnes, J. A., and Méndez-Quiñones, E. (1979). Time recovery measurements using operational GOES and TRANSIT satellites. *Proc. 11th Annu. Precise Time and Time Interval Appl. and Planning Meeting*, Conf. Pub. 2129, NASA, Greenbelt, Maryland, pp. 283–315.

Bel'kevich, D. A., Kurysheva, L. N., and Tel'pukhovskii, N. A. (1979). Accuracy in comparing the time scales of transportable clocks. *Meas. Tech.* (*Engl. Transl.*) **22**, 1190–1192.

Belomestnov, G. I., Dmitrienko, A. D., Emakov, A. S., and Korzh, V. F. (1976). Automatic system for acquiring, recording, and processing information by computer for secondary time-and-frequency standards. *Meas. Tech.* (*Engl. Transl.*) **19**, 1572–1574.

Belotserkovskii, D. Y., and Palii, G. N. (1971). New system for transmitting exact-time and standard-frequency radio signals. *Meas. Tech.* (*Engl. Transl.*) **14**, 1633.

Belotserkovskii, D. Y., Il'nin, V. G., and Stepanova, I. V. (1975). International cooperation in the field of exact time and frequency measurements. *Meas. Tech.* (*Engl. Transl.*) **18**, 517–519.

Belotserkovskii, D. Y., Il'in, V. G., Nazarov, K. I., Fedorov, Y. A., and Cherenkov, G. T. (1978). The USSR time and frequency state service. *Meas. Tech.* (*Engl. Transl.*) **21**, 1037–1040.

Benavente, J., Besson, J., and Parcelier, P. (1979). Clock comparison by laser in the nanosecond range. *Radio Sci.* **14**, 701–706.

Berger, U. (1978). DCF-77 clock with microprocessor. II. *Funkschau* **50**, 579–582. In German.

Berlin, P. (1981). World-space-time. *ESA Bull.* (27), 68–71.

Besson, J. (1970). Comparison of national time standards by simple overflight. *IEEE Trans. Instrum. Meas.* **IM-19**, 227–232.

Besson, J. (1974). Synchronisation of clocks to a precision of a few nanoseconds. *C. R. Hebd. Seances Acad. Sci., Ser. B* **279**, 147–150. In French.

Besson, J. (1975). Accurate synchronisation of ultra-stable clocks. *Colloq. Int. sur L'Electronique et la Mesure*, pp. 140–150. In French.

Besson, J., Brejaud, H., Moreau, J. P., Parcelier, P., and Benavente, J. (1978). Results of the laser synchronization by flyover between the observatories of Paris and San Fernando, Spain. *CPEM Dig.*, pp. 45–47. In French.

Bhat, C. L., and Razdan, H. (1978). A clock synchronization circuit using transmitted time-codes. *Def. Sci. J.* **28**, 153–156.

Bhat, C. L., Kaul, I. K., and Yadav, R. C. (1981). Time synchronization system in a two-station search for primordial blackholes. *J. Inst. Electron. Telecommun. Eng.* (*New Delhi*) **27**, 556–564.

Binelli, P., Detoma, E., D'Ottavio, A., Leschiutta, S., and Marconiccohio, F. (1978). Methods of transmission and applications of time and frequency signals, transmitted by SIRIO satellite. *25th Int. Scientific Congress on Electronics* (*Rome*), pp. 397–406. In Italian.

Blouet, J. (1975). International comparisons in high frequencies measurements. *Int. Conf. Electron. Meas.* (*Paris*), pp. 84–93. In French.

Bobra, A. D., Selvaraj, M., Alurkar, S. K., and Bhonsle, R. V. (1981). Time synchronization for a 3-site interplanetary scintillation (IPS) experiment using ATA time signal transmission. *J. Inst. Electron. Telecommun. Eng.* (*New Delhi*), **27**, 569–572.

Bocaniciu, T. (1978). Utilisation of standard television signal for distant testing of measuring apparatus for time and frequency. *Metrol. Apl.* **25**, 180–183. In Rumanian.

Bodily, L. N., and Hyatt, R. C. (1967). "Flying clock" comparisions extended to east Europe, Africa and Australia. *Hewlett-Packard J.* **19**, 12–16.

Bonanomi, J. (1981). Time and frequency dissemination system of moderate accuracy, sophistication and cost. *J. Inst. Electron. Telecommun. Eng.* (*New Delhi*) **27**, 443–449.

Borisochkin, V. V., and Fedorov, Y. A. (1981). Centralized synchronization of the Moscow TV center: a system for transmitting standard frequency and time signals. *Meas. Tech.* (*Engl. Transl.*) **24**, 110–112.

Borisov, Y. D., and Garf, L. M. (1980). Local chronometric system. *Meas. Tech.* (*Engl. Transl.*) **25**, 995–997.

Brokaw, A. P. (1974). Slave clock can run free at center frequency and lock in within one cycle. *Electron. Des.* **22**, 196–198.

Brunet, M. (1979). Synchronization of atomic clocks through the "Symphonie" satellite. *Radio Sci.* **14**, 721–730.

Buczkowski, T. (1980). International time comparisons by means of television signals. *CPEM Dig.*, pp. 31–33.

Buennagel, L. A., Spitzmesser, D. J., and Young, L. E. (1982). One nanosecond time synchronization using SERIES and GPS. *Proc. 14th Annu. Precise Time and Time Interval Appl. and Planning Meeting. Conf.* Publ. 2265, NASA, Greenbelt, Maryland, pp. 605–615.

Buisson, J. A. (1973). International time transfer using the Timation II satellite. *Proc. 27th Annu. Freq. Control Symp.*, pp. 277–285.

Buisson, J., McCaskill, T., and Smith, H. (1976). Precise worldwide station synchronization via the NAVSTAR GPS, Navigation Technology Satellite (NTS-1). *Proc. 8th Annu. Precise Time and Time Interval Appl. and Planning Meeting*, Washington, D. C., pp. 55–85.

Bureau International de l'Heure (1981). Annual Report. BIH, Paris, France.

Burgess, B., and Walker, D. (1970). Effects in Omega from propagation variations. *J. Inst. Nav.* **23**, 49–59.

Burns, A. A. (1971). Preliminary analysis of a proposed high-stability frequency standard distribution system. *IEEE Trans. Aerosp. Electron. Syst.* **AES-7**, 385–391.

Burtop, W. V., and Wilson, L. O. (1968). Precise frequency comparison using a frequency tracking technique. *Proc. 22nd Annu. Freq. Control Symp.*, pp. 441–451.

Bushuev, F. I., and Ivakin, V. M. (1980). Fitting for comparing time scales by Loran signals. *Meas. Tech.* (*Engl. Transl.*) **23**, 821–822.

Butterfield, F. F. (1976). Frequency control and time information in the NAVSTAR global positioning system. *Proc. 30th Annu. Freq. Control Symp.*, pp. 371–374.

Buzek, O., and Cermak, J. (1979). Precise time dissemination via OMA-50 kHz. *Radio Sci.* **14**, 681–684.

Calla, O. P. N., Hasija, M. L., Singh, G., and Barathy, S. (1981). Role of earth stations in clock synchronization via satellite. *J. Inst. Electron. Telecommun. Eng.* (*New Delhi*) **27**, 541–545.

Capitaine, N., and Gambis, D. (1981). A possibility of clock synchronization between two stations by the way of an artificial satellite. *Ann. Geophys.* **37**, 139–142.

Caprioli, G. (1973). Present-day requirement of astronomical and geodetic research [for clock synchronization]. *20th Int. Congr. Electron.*, TR-I-2, pp. 513–516. In Italian.

Cashion, R. E., and Hunt, G. A. (1979). Precise time recovery from Transit satellites. *Radio Sci.* **14**, 715–719.

Cashion, R. E., Klepczynski, W. J., and Putkovich, K. (1979). The use of Transit for time distribution. *Navigation* **26**, 63–69.

Cateora, J. V., Hanson, D. W. and Davis, D. D. (1978). Automatic path delay correction to GOES satellite time broadcasts. *NBS Tech. Note* (*U.S.*) 1003.

CCIR (1982). "Time/Frequency Dissemination and Coordination via Satellite." Rept. 518-3, XV Plenary Assembly, Vol. VII, International Radio Consultative Committee, International Telecommunication Union, Geneva, Switzerland.

Cermak, J., and Buzek, O. (1979). Time sharing in the OMA 50 kHz Czechoslovak station. *Slaboproudy Obz.* **40**, 53–56. In Czech.

Cherepukhin, M. A., and Polyak, A. G. (1976). Effect of the parameters of the propagation path on locking error when using signals from a Loran-S station. *Meas. Tech.* (*Engl. Transl.*) **19**, 1585–1586.

Chi, A. R. (1970). Diurnal phase of VLF signals near antipole of a transmitter. *Proc. 24th Annu. Freq. Control Symp.*, pp. 332–338.

Chi, A. R. (1975). Projection of timing capability and spacecraft clock calibration in 1980's. *Int. Telemetering Conf.*, p. 246.

Chi, A. R. (1979). Satellite time transfer via TDRSS and applications. *Proc. 11th Annu. Precise Time and Time Interval Appl. and Planning Meeting*, Conf. Pub. 2129, NASA, Greenbelt, Maryland, pp. 45–64.

Chi, A. R. and Fosque, H. S. (1972). A step in time changes in standard frequency and time signal broadcasts. *IEEE Spectrum* **9**, 82–86.

Chung, N. S., Kang, S. T., and Kim, J. O. (1981). Standard time and frequency in Korea and dissemination by AM FM broadcasting network. *J. Inst. Electron. Telecommun. Eng. (New Delhi)* **27**, 367–372.

Clark, T. A., Ryan, J. W., Counselman, C. C., III, Ford, P. G., Hanson, L. B., Hinteregger, H. F., Klepczynski, W. J., Knight, C. A., Robertson, D. S., Rogers, A. E. E., Shapiro, I. I., and Whitney, A. R. (1979). Synchronization of clocks by very-long-baseline interferometry. *IEEE Trans. Instrum. Meas.* **IM-28**, 184–187.

Clements, P. A. (1982). Intercontinental time and frequency transfer using a global positioning system timing receiver. *Proc. 14th Annu. Precise Time and Time Interval Appl. and Planning Meeting, Conf.* Pub. 2265, NASA, Greenbelt, Maryland, pp. 517–527.

Clifford, P. M. (1967). The use of standard frequency transmission in industry. *Colloq. Definition, Realisation and Use of Time and Freq.*, London, Paper No. 8/1–8/7.

Cooper, R. S., and Chi, A. R. (1979). A review of satellite time transfer technology: accomplishments and future applications. *Radio Sci.* **14**, 605–619.

Coralnick, P., and Stew, R. C. (1973). Active & passive relative synchronization of remote clocks in a time ordered system. *Proc. 27th Annu. Freq. control Symp.*, pp. 296–303.

Cordwell, C. R. (1967). N.P.L. standard frequency installation at rugby radio station. *Colloq. Definition, Realisation and Use of Time and Freq.*, London, Paper No. 5/1–5/8.

Costain, C. C. (1977). Time dissemination in Canada. *Int. Electr. Electron. Conf. and Exposition (IEEE)*, pp. 120–121.

Costain, C. C., Boulanger, J.-S., Daams, H., Hanson, D. W., Beehler, R. E., Clements, A. J., Davis, D. D., Klepczynski, W. J., Veenstra, L., Kaiser, J., Guinot, B., Azoubib, J., Parcelier, P., Fréon, G., and Brunet, M. (1979a). Two-way time transfer via geostationary satellites NRC/NBS, NRC/USNO and NBS/USNO via HERMES and NRC/LPTF (France) via SYMPHONIE. *Proc. 11th Annu. Precise Time and Time Interval Appl. Planning Meeting*, pp. 499–515.

Costain, C. C., Boulanger, J.-S., Daams, H., Miller, L. G., Guinot, B., Fréon, G., Parcelier, P., Brunet, M., and Azoubib, J. (1979b). Two-way time transfers between National Research Council (Ottawa) and Paris Observatory via the "Symphonie" satellite. *Proc. 33rd Annu. Freq. Control Symp.*, pp. 473–476.

Costain, C. C., Daams, H., and Boulanger, J.-S. (1983). Time dissemination from the National Research Council of Canada. *Proc. 37th Annu. Freq. Control Symp.*, pp. 78–80.

Counselmann, C. C., III, Shapiro, I. I., Rogers, A. E. E., Hinteregger, H. F., Knight, C. A., Whitney, A. R., and Clark, T. A. (1977). VLBI clock synchronization. *Proc. IEEE* **65**, 1622–1223.

Curtwright, J. B. (1969). Intra-DSCC microsecond timing using a communication microwave link. *JPL Space Programs Summary* **37–59**, (11), 154–157.

Danzeisen, K. (1977). Frequency measured remotely with VHF–UHF receivers ESU 2 and ESM 2. *News Rohde & Schwarz* **17**, 28–30.

Davis, D. D., Jespersen, J. L., and Kamas, G. (1970). The use of television signals for time and frequency dissemination. *Proc. IEEE* **58**, 931–933.

Davis, D. D., Weiss, M., Clements, A., and Allan, D. W. (1981). Construction and performance characteristics of a prototype NBS GPS receiver. *Proc. 35th Annu. Freq. Control Symp.*, pp. 546–552.

Decher, R., Allan, D. W., Alley, C. O., Baugher, C., Duncan, B. J., Vessot, R. F. C., and Winkler, G. M. R. (1982). High accuracy global time and frequency transfer with a space-borne hydrogen maser clock. *Proc. 14th Annu. Precise Time and Time Interval Appl. Planning Meeting*, Conf. Pub. 2265, NASA, Greenbelt, Maryland, pp. 205–220.

De Jong, G., and Kaarls, R. (1980). An automated time-keeping system. *IEEE Trans. Instrum. Meas.* **IM-29**, 230–233.

De Jong, G., and Kaarls, R. (1980). An automated time keeping system. *CPEM Dig.*, pp. 9–10.

Del Bello, R., Leschiutta, S., and Angeli, M. T. (1975). The main national time scales compared with the Italian UTC (IEN) time scales in the period 1970–1974. *Alta Freq.* **44**, 558–568.

Detoma, E. (1980). Synchronization technique via satellite. *Proc. 27th Int. Electron. Scientific Congr.*, pp. 173–184. In Italian.

Detoma, E., and Leschiutta, S. (1980). Two-way sequential time synchronization: preliminary results from the SIRIO-1 experiment. *Proc. 12th Annu. Precise Time and Time Interval Appl. Planning Meeting, Conf.* Pub. 2175, NASA, Greenbelt, Maryland, pp. 329–348.

Detoma, E., Leschiutta, S., and Pettiti, V. (1980). Initial results of the two-way time synchronization experiment via the SIRIO-1 satellite. *CPEM Dig.*, pp. 15–16.

Dittmann, H., and Kalau, M. (1978). The national time and frequency standard of the German Democratic Republic. *Radio Fernsehen Elektron.* **27**, 381–382. In German.

Dixit, P. S., and Mathur, B. S. (1981). Satellite laser ranging precise time transfer techniques: some comments on the possible Indian contribution. *J. Inst. Electron. Telecommun. Eng. (New Delhi)* **27**, 433–438.

Doherty, R. H., Hefley, G., and Linfield, R. F. (1961). Timing potentials of Loran-C. *Proc. IRE* **49**, 1659–1673.

Driegelinck, E., and Jodgne, J. C. (1979). Control of a quartz clock by coded radio signals from a DCF transmitter. *Publ. Inst. R. Meteorol. Belg., Ser. B* (103), 3–14. In French.

Dudnik, B. S., Kachcheev, B. L., Leikin, A. Ya., Smirnov, A. N., and Sopel'nikov, M. D. (1971). Use of meteoric reflection of radio waves to compare the clocks of time- and frequency-service stations. *Meas. Tech. (Engl. Transl.)* **14**, 1842–1847.

Dudnik, V. S., Leman, Yu. A., and Chernyr, V. I. (1974). Equipment for coordinating time standards using the meteoric propagation of radiowaves. *Radiotekhnika (Kharkov)* (28), 23–31. In Russian.

Dunne, J. F., Ive, J. G., and Wilkinson, J. H. (1976). Clock generation and distribution. *IBA Tech. Rev.* (8), 77–84.

Dworak, H. P. (1980). Time comparison at nanosecond-range laser synchronisation via geostationary satellites. *Nachr. Elektron.* **34**, 13–14. In German.

Dzhizhevskaya, L. A., Ivakin, V. M., and Til'k, E. M. (1981). Use of signals of the Loran-C navigation system for comparing time scales. *Meas. Tech. (Engl. Transl.)* **24**, 565–566.

Easton, R. L. (1972). The role of time/frequency in Navy navigation satellites. *Proc. IEEE* **60**, 557–563.

Easton, R. L., Bartholomew, C., and Bowman, J. (1970). A second satellite oscillator experiment. *Proc. 24th Annu. Freq. Control Symp.*, pp. 339–344.

Easton, R. L., Morgan, P., and Smith, H. M. (1974). Satellite time transfer from the U.S. Naval Observatory to the Royal Greenwich Observatory and to Australia. *CPEM Dig.*, pp. 281–283.

Easton, R. L., Fisher, L. C., Hanson, D. W., Hellwig, H. W., and Rueger, L. J. (1976). Dissemination of time and frequency by satellite. *Proc. IEEE* **64**, 1482–1493.

Egidi, C. (1972). The general adoption of the atomic unit of time. *Elettrotecnica* **59**, 430–433. In Italian.

Ehrlich, E. (1972). The role of time frequency in satellite position determination systems. *Proc. IEEE* **60**, 564–571.

Endsley, R. (1982). Private communication. Jet Propulsion Laboratory, Pasadena, California.

Essen, L. (1967a). A revolution in time-keeping. *Conf. Freq. Generation Control Radio Syst. (IEE)* (31), 11–15.

Essen, L. (1967b). Atomic units and scales of time. *Collog. on Definition, Realisation and Use of Time and Frequency (IEE)*, Paper No. 1/1–1/2.

Essen, L. (1978). Relativity and time signals. *Wireless World* **84**, 44–45.

Fedorov, Yu. A. (1971). Transmission of timing information by means of continuous harmonic oscillations. *Meas. Tech. (Engl. Transl.)* **14**, 41–44.

Fedorov, Yu. A., and Pushkin, S. B. (1979). Comparing the national standards of time and frequency of the USSR, Czechoslovakia, and East Germany. *Meas. Tech. (Engl. Transl.)* **22**, 1193–1195.

Fedorov, Yu. A., Nasidze, N. A., Bol'shakov, V. Ya., and Ermilov, N. I. (1977). Automatic system of synchronization of time scales on the channel of an All-Union television broadcasting station. *Meas. Tech. (Engl. Transl.)* **20**, 502–506.

Fedorov, Yu. A., and Bol'shakov, V. Ya. (1978). Comparing frequencies of highly stable oscillators by means of television signals. *Meas. (Engl. Transl.)* **21**, 786–788.

Fedorov, Yu. A., and Gonzales, Kh. (1981). Transmission of the dimensions of the units of time and frequency over the Cuban national television channels. *Meas. Tech. (Engl. Transl.)* **24**, 567–570.

Feichtinger, H. (1977). Standard frequency from DCF 77 [radio transmitter]. *Funkschau* **49**, 134–135. In German.

Fey, L. (1971). Time dissemination capabilities of the Omega system, *Proc. 25th Annu. Freq. Control Symp.*, pp. 167–170.

Fey, L., and Looney, C. H., Jr. (1966). A dual frequency V.L.F. timing system. *IEEE Trans. Instrum. Meas.* **IM-15**, 190–195.

Ficklin, B. P. (1967). Standard time-and-frequency accuracies obtainable with a stationary satellite. *Conf. Freq. Generation Control Radio Syst. (IEE)*, pp. 174–180.

Fisher, L. C., Hanson, D. W., Hellwig, H. W., and Rueger, L. J. (1976). Dissemination of time and frequency by satellite. *Proc. IEEE* **64**, 1482–1493.

Fleer, A. G., and Stepanov, V. A. (1972). Problems of experimental investigations of radiowave propagation for time service. *Meas. Tech. (Engl. Transl.)* **15**, 1671–1674.

Fleer, A. G., and Vorob'ev, L. Ya. (1976). Dynamics of seasonal variations in the transmission times of time signals and standard frequencies in the short- and very-long-wave ranges. *Meas. Tech. (Engl. Transl.)* **19**, 836–843.

Flynn, K. B. (1982a). A concept of a warship's master clock system. *J. Electr. Electron. Eng. Aust.* **2**, 40–42.

Flynn, K. B. (1982b). Requirements for frequency and time reference in communications. *J. Electr. Electron. Eng. Aust.* **2**, 36–39.

Friedberg, H., and Kral, W. A. (1978). Wireless time signals and wireless clocks: receiving of time signals for private and industrial use. *Nachr. Elektron.* **32**, 257–259. In German.

Fujiwara, K., Hara, T., and Sakai, T. (1972). Precise clock comparison by Loran-C signals. *Tokyo Astron. Obs. Rep.* **15**, 825–837. In Japanese.

Fujiwara, K., Kato, T., Hokugo, S., and Miyazaki, K. (1975). Precise clock comparison by means of TV signals (between Tokyo Astronomical Obs. and Kanozan Geodetic Obs.). *Tokyo Astron. Obs. Rep.* **17**, 261–283. In Japanese.

Gabry, A., Faucheron, G., Dubouis, B., and Petit, P. (1977). Distant comparison of stable frequency standards by means of the transmission of a beat note between the carrier of a TV broadcast signal and a frequency synthesized from the frequency standards. *Proc. 31st Annu. Freq. Control Symp.*, pp. 499–502.

Gatterer, L. F., Bottone, P. W., and Morgan, A. H. (1968). World-wide clock synchronization using a synchronous satellite. *Conf. Precision Electromagn. Meas. (IEEE)*, pp. 58–60.

Gerharz, R. (1975). Long-period time interval markers from Mercury transits. *J. Br. Astron. Assoc.* **85**, 252–254.

Giles, P. G., Hart, P. J., and Thomas, I. (1978). Radio clock for reception and display of MSF time-code transmission. *Mullard Tech. Commun.* **14**, 402–423.

Gill, P., and Spieweck, F. (1979). "NPL–PTB Intercomparison of Iodine-Stabilized Ion Lasers." Report NPL.MOM-42, National Physics Laboratory, Teddington, England, 19 pp.

Granveaud, M., and Guinot, B. (1978). The role of primary standards in establishing the International Atomic Time (TAI). *CPEM Dig.*, pp. 39–41.

Gray, J. E. (1976). Clock synchronization and comparison: Problems, techniques and hardware. *NBS Tech. Note (U.S.)* 691, 9 pp.

Grenchik, T. J., and Fang, B. T. (1977). Time determination for spacecraft users of the Navstar Global Positioning System (GPS). *Proc. 31st Annu. Freq. Control Symp.*, pp. 489–494.

Grimsley, S. W., and Miller, M. J. (1968). Phase comparison of frequency standards. *Proc. Inst. Radio Electron. Eng. Aust.* **29**, 14–17.

Guétrot, A., Allan, D. W., Higbie, L. S., and Lavancean, J. (1969). An application of statistical smoothing technique on VLF signals for comparison of time between USNO and NBS. *Proc. 23rd Annu. Freq. Control Symp.*, p. 248.

Guillaume, F., Lievin, J. C., and De Prins, J. (1977). Study of LF and VLF time signals by digital method. *Proc. 31st Annu. Freq. Control Symp.*, pp. 503–509.

Guinot, B. (1974). Long term stability and accuracy of time scales. *CPEM Dig.*, pp. 333–335.

Guinot, B. (1981). Status of the international atomic time TAI. *J. Phys. Colloq. (Orsay, Fr.)* **42**, 219–228.

Guinot, B., and Azoubib, J. (1980). Problems of the generation, quality, and availability of the International Atomic Time Scale. *IEEE Trans. Instrum. Meas. IM-29*, 226–229.

Guinot, B., and Granveaud, M. (1972). Atomic time scales. *IEEE Trans. Instrum. Meas.* **IM-21**, 396–400.

Gupta, A. S., Goel, G. K., and Mathur, B. S. (1981). Precise T & F intercomparison via VLF phase measurements. *J. Inst. Electron. Telecommun. Eng. (New Delhi)* **27**, 403–407.

Hafele, J. C., and Keating, R. E. (1972a). Around-the-world atomic clocks: predicted relativistic time gains. *Science* **177**, 166–168.

Hafele, J. C., and Keating, R. E. (1972b). Around-the-world atomic clock: observed relativistic time gains. *Science* **177**, 168–170.

Hall, D. L., and Putkovich, K. (1982). Test results of the STI GPS time transfer receiver. *Proc. 36th Annu. Freq. Control Symp.*, p. 388.

Hall, R. G., and Klepczynski, W. J. (1976). Time service. *Nav. Res. Rev.* **29**, 28–36.

Hanson, D. W., and Hamilton, W. F. (1971a). Clock synchronization from satellite tracking. *IEEE Trans. Aerosp. Electron. Syst.* **AES-7**, 895–899.

Hanson, D. W., and Hamilton, W. F. (1971b). One-way time synchronization via geostationary satellites at UHF. *IEEE Trans. Instrum. Meas.* **IM-20**, 147–153.

Hanson, D. W., and Hamilton, W. F. (1974). Time and frequency broadcast experiments from the ATS-3 satellite. *Tech. Note (U.S.) 645*, 107 pp.

Hanson, D. W., Davis, D. D., and Cateora, J. V. (1979). NBS time to the western hemisphere by satellite. *Radio Sci.* **14**, 731–740.

Hefley, G. (1972). The development of Loran-C navigation and timing. *NBS Monogr. (U.S.) 129*. 157 pp.

Hellwig, H. (1977). Clocks - time and frequency measurements. *Nachrichtentech Z.* **30**, 69. In German.

Hellwig, H. W. (1978). Worldwide timekeeping better than previously believed. *Dimensions* **61**, 23–25.

Hellwig, H., and Wainwright, A. E. (1975). Sub-microsecond time transport with a rubidium portable clock. *Proc. 29th Annu. Freq. Control Symp.*, pp. 384–385.

Hellwig, H., Allan, D. W., Stein, S. R., and Prichard, K. A. (1977). Transcontinental and intercontinental portable clock time comparison. *Proc. 31st Annu. Freq. Control Symp.*, pp. 495–498.

Hellwig, H. W., Allen, D. W., Stein, S. R., and Prichard, K. A. (1978). Transcontinental and intercontinental portable clock time comparison. *IEEE Trans. Instrum. Meas.* **IM-27**, 65–68.

Helsby, N. C. (1977). Atomic time receiver. *Pract. Wireless* **53**, 288–292.

Henderson, J. T. (1972). The foundation of time and frequency in various countries. *Proc. IEEE* **60**, 487–493.

Heron, M. L., and Rose, R. J. (1978). The accuracy of frequency standards disseminated by HF radio paths through the ionosphere. *Aust. J. Phys.* **31**, 333–345.

Herring, J. C., Abby, D. G., and Cook, J. A. (1970). "Time Synchronization of Primary Geodetic Sites through Use of Artificial Satellites." Report AFCRL-70-0333, 21 pp. Available from CFSTI, Springfield, Virginia.

Hietzke, W. (1979). Ramp time synchronization. *Radio Sci.* **14**, 695–699.

Higa, W. H. (1972). Time Synchronization via lunar radar. *Proc. IEEE* **60**, 552–557.

Hilberg, W. (1967). Radio-controlled clocks with digital standard-time indication. *Elektronik* **16**, 325–328. In German.

Hoffmann, K. (1982). Time synchronization via OTS-2. *CFEM Dig.*, pp. M16–M17.

Holmes, D. C. (1979). TEMPUS: a proposal for an international time transfer and precision tracking satellite. *J. Br. Interplanet. Soc.* **32**, 347–351.

Honma, S., and Kato, S. (1975). An automatic clock synchronizer using the 40 kHz standard frequency transmission. *Rev. Radio Res. Lab.* **21**, 165–176. In Japanese.

Hoult, N. S. (1979). A rugby MSF time-code clock. *Radio Commun.* **55**, 122–127.

Howe, D. A. (1972a). Nationwide precise time and frequency distribution utilizing an active code within network television broadcasts. *Proc. 26th Annu. Freq. Control Symp.*, pp. 292–308.

Howe, D. A. (1972b). Nationwide precise time and frequency distribution utilizing an active code within network television broadcasts. *IEEE Trans. Instrum. Meas.* **IM-21**, 263–266.

Howe, D. A. (1972c). Results of active line-1 TV timing. *Proc. IEEE* **60**, 634–637.

Howe, D. A. (1974). Precise frequency dissemination using the 19 kHz pilot tone on stereo FM radio stations. *IEEE Trans. Broadcast.* **BC-20**, 17–20.

Howe, S. L. (1976). NBS time and frequency dissemination services. *NBS Spec. Publ. (U.S.)*, 16 pp.

Hudson, G. E., Allan, D. W., Barnes, J. A., Hall, R. G., Lavanceau, J. D., and Winkler, G. M. R. (1969). A coordinate frequency and time system. *Proc. 23rd Annu. Freq. Control Symp.*, pp. 249–262.

Hundertmark, B., Kahnt, D., and Kalau, M. (1976). Standard frequency transmission by stabilised synchronising pulses of television in the DDR. *Radio Fernsehen Elektron* **25**, 277–279. In German.

Iijima, S. (1981). Time and frequency in Japan. *J. Inst. Electron. Telecommun. Eng. (New Delhi)* **27**, 327–378.

Il'nin, V. G., and Stepanova, I. V. (1977). Cooperation of the USSR time and frequency service with international organizations. *Meas. Tech. (Engl. Transl.)* **20**, 587–589.

Il'in, V. G., Palii, G. N., Tel'pukhovskii, N. A., Bel'kovich, D. A., Starodubtsev, N. A., and Ivanova, Yu. D. (1976). Comparison of secondary time-and-frequency standards, and determination of the time required for radio waves to travel over synchronization links. *Meas. Tech. (Engl. Transl.)* **19**, 1568–1572.

Il'in, V. G., Bushkin, S. B., and Stepanova, I. V. (1979). Prospects of establishing of common time and frequency service for the COMECON member countries. *Meas. Tech. (Engl. Transl.)* **22**, 28–31.

Imae, M., Okazawa, H., Sato, T., Urazuka, M., Yoshimura, K., and Yasuda, Y. (1982). Time comparison experiments with a small *K*-band antenna SSRA system via a domestic geostationary satellite. *CFEM Dig.*, pp. M5–M7.

Inouye, T., and Nara, M. (1975). The stability of time comparison by TV signal of common emission. *Trans. Soc. Instrum. Control Eng.* **11**, 269–274. In Japanese.

Iordachescu, T., and Matei, M. (1978). Comparison of the time and frequency standard with standard frequency signals type LORAN-C. *Metrol. Apl.* **25**, 184–190. In Rumanian.

Ishida, T., Soejima, S., and Ichidawa, Y. (1979). Present situation of Japanese satellite broadcasting for experimental purpose. *IEEE Trans. Broadcast.* **BC-25**, 105–112.

Ivanova, Yu. D., Palii, G. N., and Kozarenko, B. I. (1979). Estimate of the main error components in determining the time of signal passage over sateliite television channels. *Meas. Tech. (Engl. Transl.)* **22**, 1187–1189.

Jain, C. L., and Kumar, K. (1981). A direct reception system for time synchronization via INSAT-1. *J. Inst. Electron. Telecommun. Eng. (New Delhi)* **27**, 470–472.

Jain, C. L., Kumar, K., and Andharia, H. I. (1981). An NNSS satellite timing receiver. *J. Inst. Electron. Telecommun. Eng. (New Delhi)* **27**, 473–477.

Janes, H. B. (1970). Atmospheric errors in electromagnetic distance measurements: ESSA Hawaii experiments 1966–7. *AGARD Conf. Phase Freq. Instabilities in Electromagn. Wave Propagat. Proc.* **33**, 629–636. NASA, Langley Field, Virginia.

Jeansaume, G. (1975). The distribution of standard time. *Electron. Microelectron. Ind.* (208), 77–81. In French.

Jespersen, J. L. (1970). A survey of time & frequency dissemination techniques. *Proc. 24th Annu. Freq. Control Symp.*, pp. 322–324.

Jespersen, J. L., Kamas, G., Gatterer, L. E., and MacDoran, P. F. (1968). Satellite VHF transponder time synchronization. *Proc. IEEE* **56**, 1202–1206.

Jespersen, J. L., Blair, B. E., and Gatterer, L. E. (1972). Characterization and concepts of time–frequency dissemination. *Proc. IEEE* **60**, 502–521.

Joyner, K. H., and Butcher, L. C. (1977). The effects of the ionosphere on the phase of standard frequency transmissions. *Aust. Telecommun. Res.* **11**, 23–29.

Kamas, G., and Howe, S. (1979). Time and frequency user's manual. *NBS Spec. Publ. (U.S.) 559*.

Kamas, G., and Jespersen, J. L. (1983). A new frequency calibration service offered by the NBS. *Proc. 37th Annu. Freq. Control Symp.*, pp. 506–512.

Kartaschoff, P. (1977). Frequency control & timing requriements for communications systems. *Proc. 31st Annu. Freq. Control Symp.*, pp. 478–483.

Kirby, R. A. (1970). Evaluation of omega navigation system. *Geophysics* **35**, 344–356.

Klose, M. (1978). Frequency measurement in radio monitoring. *Commun. Int. (G.B.)* **5**, 38, 40, 44.

Kobayashi, S., Nakajima, M., and Sato, T. (1968). Accuracy of the domestic time synchronization by the reception of JJY signals at long distances. *Rev. Radio Res. Lab.* **14**, 373–377. In Japanese.

Kobayashi, S., Satoh, T., and Tanaka, M. (1978). Accuracy of time comparison by the reception of JJY signals propagating via the *E* region. *J. Radio Res. Lab.* **24**, 87–100.

Koide, F. K. (1966). Standard frequency transmission over telephone line. *Instrum. Control Syst.* **39**, 123–128.

Kovacevic, B. Z., Dimitrijevic, B. R., Arsic, M. Z., and Kovacevic, N. S. (1979). Precise real-time signal dissemination over the TV broadcasting satellite. *Radio Sci.* **14**, 685–694.

Kovacevic, B., Dimitrijevic, B., Arsic, M., and Golubobic, Lj. (1981). Precise International T/F Comparisons via ground and satellite TV systems. *J. Inst. Electron. Telecommun. Eng. (New Delhi)* **27**, 450–456.

Kuhnle, P. F., and Sydnor, R. L. (1981). Present and future frequency and timing capabilities of the Deep Space Network. *J. Phys. Colloq. (Orsay, Fr.)* **42**, 373–381.

Kulpinski, R. J. (1976). Minimum variance methods for synchronization of airborne clocks. *Proc. 30th Annu. Freq. Control Symp.*, pp. 401–413.

Laidet, L. M. (1972). Worldwide synchronization using the TRANSIT satellite system. *Proc. IEEE* **60**, 630–632.

Laios, S. C. (1972). Satellite time synchronization of a NASA network. *Proc. IEEE* **60**, 632–633.

Lake, R. (1981). Time and frequency transfer using SABCTV. *J. Inst. Electron. Telecommun. Eng. (New Delhi)* **27**, 456–459.

Lake, R., and Turner, R. (1979). The national and international role of the South African measuring standard for time. *Trans. S. Afr. Inst. Electr. Eng.* **70**, 254–259.

Leschiutta, S. (1973). Long-term accuracy of time comparisons via TV signal along radio relay links. *IEEE Trans. Instrum. Meas.* **IM-22**, 84–87.

Levine, J. (1977). Laser distance-measuring techniques. *Ann. Rev. Earth Planet. Sci.* **5**, 357–369.

Lobanova, Sh. P., Polyak, A. G., and Cherepukhin, M. A. (1976). Estimating the error in determining propagation times of short-wave signals. *Meas. Tech. (Engl. Transl.)* **19**, 1581–1588.

Lockwood, J. S. (1975). NBS frequency calibration service. *Communications* **8-12**, 15–16.

Lohrey, B. (1981). Time and frequency in New Zealand. *J. Inst. Electron. Telecommun. Eng. (New Delhi)* **27**, 357–361.

Luck, J. McK. (1979). Comparison and coordination of time scales. *Proc. Astron. Soc. Aust.* **3**, 357–363.

Lutes, G. (1981). Development of optical fiber frequency and time distribution systems. *Proc. 13th Annu. Precise Time and Time Interval Appl. Planning Meeting*, Conf. Pub. 2220, NASA, Greenbelt, Maryland, pp. 243–261.

Mac Doran, P. F. (1979). Satellite emission radio interferometric earth surveying series—GPS geodetic system. *Bull. Geod.* **53**, 117–138.

Maher, R. A. (1976). Oscillator and frequency management requirements for GPS user equipments. *Proc. 30th Annu. Freq. Control Symp.*, pp. 384–389.

Maiher, Y., and Ben-Nissim, Y. (1981). Centralized frequency-control system. *Proc. MELECON (IEEE)*, p. 5.1.5.1.

Markowitz, W., Lidback, C. A., Uyeda, H., and Muramatsu, K. (1966). Clock synchronization via RELAY II satellite. *IEEE Trans. Instrum. Meas.* **IM-15**, 177–184.

Markus, N. (1977). Centrally controlled electronic time service systems ranging from the quartz master clock to the time service central station. *Nachr. Telefonbau Normalzeit* (78), 44–51. In German.

Mathur, B. S. (1981). An overview of the frequency activities at National Physical Laboratory, New Delhi, India. *J. Inst. Electron. Telecommun. Eng. (New Delhi)* **27**, 350–354.

Mathur, B. S., and Saxena, G. M. (1980). Relativistic correction for the NPL (India)–PTB (West Germany) clock synchronization experiments. *Indian J. Pure Appl. Phys.* **18**, 601–603.

Mathur, B. S., Banerjee, P., Sood, P. C., Saxena, M., Kumar, N., and Suri, A. K. (1980). Precise time and frequency intercomparison between NPL, India, and PTB, Federal Republic of Germany via satellite SYMPHONIE-1. *Proc. 12th Annu. Precise Time and Time Interval Appl. Planning Meeting*, Conf. Pub. 2175, NASA, Greenbelt, Maryland, pp. 863–874.

Mathur, B. S., Banerjee, P., Sood, P. C., Saxena, M., Kumar, N., and Suri, A. K. (1981). Precise T & F intercomparison between NPL, India and PTB, Federal Republic of Germany via Satellite Symphonie-1. *J. Inst. Electron. Telecommun. Eng. (New Delhi)* **27**, 466–469.

Matindas, R. W. (1981). Present status of time and frequency in Indonesia. *J. Inst. Electron. Telecommun. Eng. (New Delhi)* **27**, 355–357.

Mazur, W. E., Jr. (1972). Dual transponder time synchronization at C band using ATS-3. *Proc. IEEE* **60**, 633–634.

Mazur, W. E., Jr. (1973). Time synchronization of NASA tracking stations via Loran C. *Proc. 27th Annu. Freq. control Symp.*, pp. 270–276.

Mercz, J. K. (1974). The public indication of time in the Netherlands. II. Conclusion. *Polytech. Tijdschr. Elektrotech. Elektron.* **29**, 862–867. In Dutch.

Miller, M. J. (1970). Synchronization of distant clocks by television pulse comparisons. *Proc. Astron. Soc. Aust.* **1**, 352.

Milliken, R. J., and Zoller, D. J. (1978). Principle of operation of NAVSTAR and system characteristics. *Navigation* **25**, 95–106.

Milton, J. B. (1969). Standard time and frequency. Its generation, control, & dissemination from the National Bureau of Standards time & frequency division. *NBS Tech. Note. (U.S.) 379*, 27 pp.

Milton, J. B. (1974). Standard time and frequency: its generation, control, and dissemination by the National Bureau of Standards. *NBS Tech. Note (U.S.) 656*, 18 pp.

Minullin, R. G., Palii, G. N., Sidorov, V. V., Sukhotskii, A. V., and Ivanova, Yu. D. (1971). Locking in to the state standard of time by using reflections from meteors. *Meas. Tech. (Engl. Transl.)* **14**, 33–35.

Montgomery, L. (1972). Standard frequency and time service using radio broadcasting facilities. *Proc. 26th Annu. Freq. Control Symp.*, pp. 317–318.

Moreau, J. P. (1977a). Measurement of time displacement between remote clocks. *Mes., regul., Autom.* **42**, 63–71. In French.

Moreau, J. P. (1977b). High resolution (100 ps) optical process of synchronization for remote atomic clocks, using injection laser diodes. *European Conf. Precise Electr. Meas. (IEE)*, pp. 84–86.

Mungall, A. G., Daams, H., Bailey, R., and Morris, D. (1969a). Mass-frequency effect on v.l.f. and portable clock comparisons of atomic frequency standards. *Metrologia* **5**, 31–32.

Mungall, A. G., Daams, H., and Bailey, R. (1969b). Note on atomic time keeping at the National Research Council. *Metrologia* **5**, 73–76.

Mungall, A. G., Costain, C. C., and Ekholm, W. A. (1981). Influence of temperature-correlated Loran C signal propagation delays on international time-scale comparisons. *Metrologia* **17**, 91–96.

Murray, J. A. (1983). Platform timing distribution system specifications. *Proc. 37th Annu. Freq. Control Symp.*, pp. 516–518.

Murray, J. A., Pritt, D. L., Blocker, L. W., Leavitt, W. E., Hooten, P. M., and Goring, W. D. (1971). Time transfer by defense communications satellite. *Proc. 25th Annu. Freq. Control Symp.*, pp. 186–193.

Nazarov, K. I., Unkovskii, K. V., and Melikhov, G. G. (1973). Device for receiving the reference frequency of 66.(6) kHz. *Meas. Tech. (Engl. Transl.)* **16**, 265–267.

Nezik, D. (1977). Atomic clock—exact time with the TN DCF 77 time signal regulating unit. *Nachr. Telefonbau Normalzeit* (78), 54–58. In German.

Nottarp, L., Schlueter, W., and Huebner, U. (1979). One way time transfer via METEOSAT capable of 30 ns accuracy. *Proc. 11th Annu. Precise Time and Time Interval Appl. Planning Meeting, Conf. Pub. 2129*, NASA, Greenbelt, Maryland, pp. 329–342.

Ochodo, G. N. (1981). The establishment of time and frequency services in Kenya. *J. Inst. Electron. Telecommun. Eng. (New Delhi)* **27**, 365–367.

Oganyan, N. A., and Savinova, V. S. (1971). Circuit for automatically synchronizing marine contact chronmeters with the state time scale. *Meas. Tech. (Engl. Transl.)* **14**, 149–150.

Okazaki, S., and Nasaka, M. (1969). Comparison among integrated atomic time systems. *Univ. Tokyo, Tokyo Astron. Obs. Rep.* **14**, 482–488. In Japanese.

Olsson, L. (1980). Loran-C reception in Lund, instrumentation and results. *CPEM Dig.*, pp. 23–26.

Pakos, P. E. (1969). Use of the Loran-C system for time and frequency dissemination. *Proc. 23rd Annu. Freq. Control Symp.*, pp. 236–247.

Palii, G. N., Luk'yanchenko, Ya. I., Fedorov, Yu. A., and Vnukov, E. M. (1972). Experimental high-precision system for transmitting time units and frequency over television channels. *Meas. Tech. (Engl. Transl.)* **15**, 54–59.

Palii, G. N., Ivanova, Yu. D., Malov, A. G., and Oksentyuk, A. R. (1976). Use of artificial Earth satellites to transmit exact time signals. *Meas. Tech. (Engl. Transl.)* **19**, 1480–1484.

Palmer, W. (1970). The Omega Navigation System as a source of frequency and time. *Proc. 24th Annu. Freq. Control Symp.*, pp. 345–360.

Parcellier, P. (1969). Frequencies comparison. *Rev. Gen. Electr.* **78**, 287–290. In French.

Parcelier, P. (1970). Time synchronization by television. *IEEE Trans. Instrum. Meas.* **IM-19**, 233–238.

Parkinson, C. E. (1977). Time frequency dissemination and clock synchronization. *Marconi Rev.* **40**, 225–235.

Percival, D. B. (1978). The U.S. Naval Observatory clock time scales. *IEEE Trans. Instrum. Meas.* **IM-27**, 376–385.

Phillips, D. H., Phillips, R. E., and O'Neill, J. J. (1970). Time & frequency transfer via microwave link. *Proc. 24th Annu. Freq. Control Symp.*, pp. 325–331.

Phillips, D. H., Phillips, R. E., Bowman, I. A., and O'Neil, J. J. (1971). Methods of local time and frequency transfer. *Proc. 25th Annu. Freq. Control Symp.*, pp. 209–216.

Pierce, J. A. (1957). Intercontinental frequency comparisons by very low frequency radio transmission. *Proc. IRE.* **45**, 794–803.

Pierce, J. A. (1965). Omega. *IEEE Trans. Aerosp. Electron. Syst.* **AES-1**, 206–215.

Pogson, I. (1977). Derived frequency reference from North West Cape. II. *Electron. Aust.* **38**, 56–61.

Polyak, A. G. (1976). Resolving ambiguity with multifrequency transmission of time signals. *Meas. Tech. (Engl. Trans.)* **19**, 1583–1585.

Potts, C. E., and Wieder, B. (1972). Precise time and frequency dissemination via the Loran-C system. *Proc. IEEE* **60**, 530–539.

Powers, R. F. (1974). Reference frequency transmission over Bell System radio and coaxial facilities. *Proc. 28th Annu. Freq. Control Symp.*, pp. 373–378.

Ptzcek, V. (1978). The long-term stability of time comparisons using the TV method. *Bull. Astron. Inst. Czech.* **29**, 372–375.

Pushkin, S. B. (1979). Improved accuracy in comparing time and frequency standards. *Meas. Tech. (Engl. Transl.)* **22**, 1072–1076.

Pushkin, S. B., Fedorov, Yu. A., Kalau, M., and Kant, D. (1976). Comparison of the national USSR and GDR time and frequency standards by means of transportable clocks and television signals. *Meas. Tech.* **19**, 1467–1471.

Putkovich, K. (1980). Initial test results of USNO GPS time transfer unit. *Proc. 34th Annu. Freq. Control Symp.*, pp. 326–333.

Putkovich, K. (1981). Time dissemination capabilities via navigation satellites. *J. Inst. Electron. Telecommun. Eng. (New Delhi)* **27**, 460–466.

Ramasastry, J., and Rosenbaum, B. (1973). Clock synchronization experiments performed via the ATS-1 and ATS-3 satellites. *IEEE Trans. Instrum. Meas.* **IM-22**, 9–12.

Rovera, G. (1972). On the accuracy of TV timing method. *Alta Freq.* **41**, 822–824.

Ruderfer, M. (1979). Detection of absolute motion from atomic timekeeping data: an experimental confirmation. *Speculations Sci. Technol. (Switzerland)* **2**, 405–420.

Rueger, L. J. (1971a). TRANSIT navigation system. *Proc. 2nd Annu. Precise Time and Time Interval Strategic Planning Meeting* **1**, 84–107.

Rueger, L. J. (1971b). One-way time dissemination from low altitudes satellites. *Proc. 25th Annu. Freq. Control Symp.*, pp. 179–185.

Rueger, L. J. (1976) The remote synchronization technology. *Proc. 30th Annu. Freq. Control Symp.*, pp. 444–450.

Rueger, L. J., and Bates, A. G. (1974). Frequency synthesizer for normalizing the frequency and time scales of crystal clocks on orbiting satellites. *Proc. 28th Annu. Freq. Control Symp.*, pp. 395–400.

Rueger, L. J., and Bates, A. G. (1979). Nova satellite time experiment. *Radio Sci.* **14**, 707–714.

Saburi, Y. (1977). Observed time discontinuity of clock synchronization in rotating frame of the Earth. *J. Radio Res. Lab.* **23**, 255–265.

Saburi, Y. (1981). Precision remote comparison of time and frequency. *J. Inst. Electron. Commun. Eng. Jpn.* **64**, 365–371. In Japanese.

Saburi, Y., Yamamoto, M., and Harada, K. (1976a). Precision inter-continental time comparison via geostationary satellite. *Conf. Precision Electromagn. Meas. (IEEE)*, pp. 231–232.

Saburi, Y., Yamamoto, M., and Harada, K. (1976b). High-precision time comparison via satellite and observed discrepancy of synchronization. *IEEE Trans. Instrum. Meas.* **IM-25**, 473–477.

Saburi, Y., Yasuda, Y., Kobayashi, S., and Sato, T. (1979). T & F comparisons via broadcasting satellite and navigation technology satellite. *Proc. 11th Annu. Precise Time and Time Interval Appl. and Planning Meeting. Conf.* Pub. 2129, NASA, Greenbelt, Maryland, pp. 315–328.

Saden, D. S., and Au, B. D. (1969). Daily variations of the frequency of a very accurate radio frequency. *Nature* **224**, 1291–1293.

Sain, M., Bhatnager, A. K., and Agrawal, H. O. (1981). Broadcasting and standard time and frequency disseminations. *J. Inst. Electron. Telecommun. Eng. (New Delhi)* **27**, 535–540.

Sare, A. (1978). Application of LORAN-C system in comparison of time and frequency. *Elektrotehnika (Zagreb)* (3-6), 164–166. In Serbo-Croatian.

Saull, V. A., Arcuri, J., and Lapierre, D. P. (1980). Use of standard broadcast signals to measure time intervals [seismic events]. *Rev. Sci. Instrum.* **51**, 997–998.

Saxena, G. M., and Mathur, B. S. (1977). Synchronization to microsecond accuracy of clocks in India through television transmission. *J. Inst. Electron. Telecommun. Eng. (New Delhi)* **23**, 78–80.

Schreiber, H. (1977a). Control of commerical clocks by time-signal [radio] transmitters. *Funkschau* **49**, 96–98. In German.

Schreiber, H. (1977b). Digital clock controlled by a signal-time station. *Mundo Electron.* (69), 63–72. In Spanish.

Schreiber, H. (1978). Control of electronic clocks by one-minute interval signals derived from standard frequency transmitter. *Funk-Tech.* **33**, 53–54, 59–62. In German.

Schumacher, P. (1979). The co-ordination of international time standards. *RTE (Switzerland)* (12), 54–55, 57, 59–60, 63. In German.

Schwartz, H. M. (1971). A new method of clock synchronization without light signals. *Am. J. Phys.* **39**, 1269–1270.

Semenov, S. F., Baidak, V. M., Dudnik, B. S., and Motora, A. A. (1974). Collation of dispersed time standards. *Radiotekhnika (Kharkov)* (29), 28–34. In Russian.

Sen, A. K. (1977). Precision of standard frequency radio signals in relation to ionospheric and trans-ionospheric propagation. *J. Inst. Electron. Telecommun. Eng. (New Delhi)* **23**, 365–369.

Sen, A. K., and Saha, B. (1973). Worldwide standards of time and frequency. *J. Sci. Ind. Res.* **32**, 300–311.

Sen, A. K., Saha, B., Saha, B., Saha, S. K., Trehan, S. K., Sehra, J. S., and Ghosh, R. N. (1978). Standardisation and calibration of various equipment by the use of standard frequency transmissions. *J. Inst. Electron. Telecommun. Eng. (New Delhi)* **24**, 320–323.

Serene, B. E. H. (1981). The Lasso experiment and its operational organization. *J. Inst. Electron. Telecommun. Eng. (New Delhi)* **27**, 422–432.

Serene, B., and Albertinoli, P. (1979). The LASSO experiment. *Proc. 11th Annu. Precise Time and Time Interval Appl. and Planning Meeting*, Conf. Pub. 2129, NASA, Greenbelt, Maryland, pp. 145–170.

Shapiro, L. D. (1968). Time synchronization from Loran-C. *IEEE Spectrum* **5**, 46–55.

Slabon, R. W. (1977). Results of investigations for the clock frequency control and distribution system in the digital telephony and data networks of the Deutsche Bundespost and future plans. *Proc. 31st Annu. Freq. Control Symp.*, pp. 455–462.

Smith, C. (1978). Time: who needs it? [Time signals from satellites]. *Dimensions* **62**, 16–19.

Smith, H. (1969). International coordination of radio time signal emissions. *Proc. 23rd Annu. Freq. Control Symp.*, pp. 18–20.

Smith, H. M. (1972). International time and frequency coordination. *Proc. IEEE* **60**, 479–487.

Smith, H. M. (1981). The evolution of TAI and UTC [precision time-keeping]. *J. Inst. Electron. Telecommun. Eng. (New Delhi)* **27**, 407–414.

Smith, H. M., Easton, R. L., Buisson, J. A., and McCaskill, T. B. (1977). Sub-microsecond intercontinental time comparisons by satellite. *European Conf. Precise Electr. Meas. (IEE)*, pp. 87–89.

Somayajulu, Y. V., Mathor, B. S., Banerjee, P., Garg, S. C., Singh, L., Sood, P. C., Tyagi, T. R., Jain, C. L., and Kumar, K. (1979). Clock synchronization experiment in India using Symphonic satellite. *J. Inst. Electron. Telecommun. Eng. (New Delhi)* **25**, 481–487.

Sood, P. C., Taneja, P. N., Banerjee, P., and Mathur, B. S. (1980). Portable clock for precise time transfer. *J. Inst. Electron. Telecommun. Eng. (New Delhi)* **26**, 599–602.

Sopel'nikov, M. D., and Fedorov, Yu. A. (1980). Investigation of errors in synchronizing time scales over wide-band communication channels. *Meas. Tech. (Engl. Transl.)* **23**, 118–120.

Souček, A. (1969). Travel time stability on TV relay links. *Radio Televirion (Oirt Publication)* (5), 29–31.

Spellman, M. L., Cain, J. B., and Bradley, D. B. (1977). Frequency control and digital network synchronization. *Proc. 31st Annu. Freq. Control Symp.*, pp. 436–477.

Sperry Gyroscope Co. (1967). "Study of Methods for Synchronizing Remotely-Located Clocks." Sperry Gyroscope Co., Rep. NASA CR-738, 206 pp.

Stadler, K. (1968). Standard frequency receiver XKD for monitoring secondary frequency standards. *News Rohde and Schwarz* **8**, 20–22.

Stansell, T. A., Jr. (1971). TRANSIT, the Navy navigation satellite system. *Navigation* **18**, 93–109.

Starker, S., Nau, H., Hammesfahr, J., and Tschiesche, H. (1982). NAVEX – a space shuttle experiment with atomic clocks. *Proc. 14th Annu. Precise Time and Time Interval Appl. and Planning Meeting*, Conf. Pub. 2265, NASA, Greenbelt, Maryland, pp. 181–201.

Stecher, R. (1967). Precision reading comparison of time standards at long distance from each other. *Nachrichtentechnik* **17**, 404–408. In German.

Steele, J. M. (1967). Past and future development of standard frequency emissions. *IEE Colloqu. Dig.*, paper no. 4/1–4/5.

Steele, J. M., Markowitz, W., and Lidback, C. A. (1964). Telstar time synchronization. *IEEE Trans. Instrum. Meas.* **IM-13**, 164–170.

Stone, R. R., Gattis, T. H., Petit, R. C., and Lieberman, T. N. (1971). Time control of frequency shift keyed transmission at VLF. *Proc. 25th Annu. Freq. control Symp.*, pp. 152–158.

Stow, R. C., and Coralnick, P. (1973). Active and passive relative synchronization of remote clocks in a time ordered system. *Proc. 27th Annu. Freq. Control Symp.*, pp. 296–303.

Strohbehn, K., and Brown, R. G. (1978). Filtering precision time signals. *Proc. 21st Midwest Symp. Circuits and Systems*, pp. 476–480.

Swanson, E. R., and Kugel, C. P. (1971). Omega VLF Timing. *Proc. 25th Annu. Freq. Control Symp.*, pp. 159–166.

Swanson, E. R., and Kugel, C. P. (1972). VLF timing: conventional and modern techniques including Omega. *Proc. IEEE* **60**, 540–451.

Szepan, R. (1978). Determining accuracy of receiver-controlled frequency standards. *News Rohde & Schwarz* **18**, 23–26.

Takahashi, F. (1976a). Proposal of accurate time-dissemination method using a broadcasting satellite. *Rev. Radio Res. Lab.* **22**, 135–142. In Japanese.

Takahashi, F. (1976b). A proposal of accurate time dissemination using TV signals from a broadcasting satellite. *J. Radio Res. Lab. (Japan)* **23**, 267–283.

Taylor, R. J. (1974). Satellite to ground timing experiments. *Proc. 28th Annu. Freq. Control Symp.*, pp. 384–388.

Tennant, D. M. (1981). NAVSTAR global positioning system (GPS) clock program: present and future. *Proc. 35th Annu. Freq. Control Symp.*, pp. 532–536.

Tolman, J., Ptáček, V., Souček, A., and Stecher, R. (1967). Micro-second clock comparison by means of TV synchronizing pulses. *IEEE Trans. Instrum. Meas.* **IM-16**, 247–254.

Van Dierendonck, A. J. (1979). GPS time. *In* "Principle and Operational Aspects of Precision Position Determination Systems," pp. 8/1–10. Report AGARD-AG-245, AGARD, 463 pp.

Vasin, L. D., Kiritsev, E. S., and Kireev, B. M. (1972). Apparatus for frequency collation using the signals of super-long wave radio stations. *Meas. Tech. (Engl. Transl.)* **15**, 1656–1658.

Vessot, R. F. C. (1981). Development and use of high stability clocks in space. *J. Inst. Electron. Telecommun. Eng. (New Delhi)* **27**, 481–492.

Vessot, R. F. C., and Levine, M. W. (1974). Performance data of space and ground hydrogen masers and ionospheric studies for high accuracy comparison between space and ground clocks. *Proc. 28th Annu. Freq. Control Symp.*, pp. 408–414.

Vulcan, A., and Bloch, M. (1981). The NATO III 5 MHz distribution system. *Proc. 35th Annu. Freq. Control Symp.*, pp. 553–564.

Ward, K. (1976). Precision worldwide time transfer using the GPS. *Natl. Telecommun. (IEEE)*, p. 41.2/1.

Wardrip, C., Buisson, J., Oaks, O., Lister, M., Stebbins, S., Guinot, B., Granveaud, M., Schulter, W., Nottarp, K., Reinhardt, V., Kruger R., Dachel, P., Detoma, E., Ingold, J., Roloff, R., and Stalder, T. (1983). An international time transfer experiment. *Proc. 37th Annu. Freq. Control Symp.*, pp. 61–66.

Weiss, R. (1976a). Time-signal and standard-frequency receiver for the DCF 77 with reserve. I. *Funkschau* **48**, 964–968. In German.

Weiss, R. (1976b). Standard time and frequency receiver for DCF 77 with auxiliary channel. *Funkschau* **48**, 1122–1125. In German.

Weiss, R. (1976c). Time-signal and standard frequency receiver for DCF 77 with reserve. III. *Funkschau* **48**, 1086–1088. In German.

Wieder, B. (1971). Use of Loran-C over land. *Proc. 25th Annu. Freq. Control Symp.*, pp. 171–178.

Winkler, G. M. R. (1968). Recent improvements in the US Naval Observatory timekeeping and time distribution operations. *Proc. 22nd Annu. Freq. Control Symp.*, p. 383.

Winkler, G. M. R. (1971). International coordinated clock time and the coming improvements in the system "UTC." *Proc. 25th Annu. Freq. Control Symp.*, pp. 217–221.

Winkler, G. M. R. (1972). Path delay, its variations, and some implications for the field use of precise frequency standards. *Proc. IEEE* **60**, 522–529.

Wright, J. G. (1979). A system to provide and utilize stable time references from satellites. *Can. Aeronaut. Space J.* **25**, 344–340.

Wu, G. C., and Zhang, H. (1981). The atomic time scale TA (CSAO). *J. Inst. Electron. Telecommun. Eng. (New Delhi)* **27**, 530–532.

Xiao, C. (1981). Clock synchronization experiment via SYMPHONIE satellite. *IEEE Trans Instrum. Meas.* **IM-30**, 273–277.

Yakos, M. D., and Hirt, E. H. (1981). Time dissemination using NAVSTAR global positioning system (GPS) phase II B user equipment. *Proc. 35th Annu. Freq. Control Symp.*, pp. 537–545.

Yamamoto, M., Harada, K., and Saburi, Y. (1976). A time comparison experiment performed by SSRA system via ATS-1. *J. Radio Res. Lab. (Japan)* **23**, 85–103.

Yannoni, N. F. (1980). Frequency standards, clocks and IFF [identification friend or foe systems]. *EASCON Record (IEEE)*, pp. 445–457.

Yasuda, Y., and Saburi, Y. (1981). Recent activities on time and frequency at the Radio Research Laboratories. *J. Inst. Electron. Telecommun. Eng. (New Delhi)* **27**, 345–350.

Chapter 14

Anan'ev, L. L., Gerasimova, T. M., Gerasimov, N. P., Golubkov, V. P., Krasnoperov, E. P., and Reinov, N. M. (1969). Superconducting oscillating circuit with lumped parameters. *Prib. Tekh. Eksp.* **6**, 130–131.

Anan'ev, L. L., Gerasimov, N. P., Reinov, N. M., and Terent'eva, N. M. (1972). Temperature dependence of the resonance frequency of a superconducting lumped-parameter circuit. *Zh. Tekh. Fiz.* **42**, 222–224. In Russian.

Arams, F. R., Fradkin, J., Kornfeld, D., Sard, E. W., and Siegel, K. (1967). Superconducting ultrahigh Q tunable RF preselector. *IEEE Trans. Electromagn. Compat.* **EMC-9**, 110–123.

Arnoldt, M. (1980). Competition by quartz resonators. *Antenna* **52**, 427–428. In Italian.

Arnoldt, M. (1982). The superconduction stabilised oscillator as a frequency standard. *Elektronik (Munich)* **31**, 62–64. In German.

Bindal, V. N., and Singhal, S. K. (1976). A piezoelectric miniaturized tuning fork. *Indian J. Pure Appl. Phys.* **14**, 378–381.

Bischoff, M., Plattner, A., Rembold, B., and Sicking F. (1981). Possibilities of stabilising the frequency of Gunn millimetre wave oscillators. *Wiss. Ber. AEG-Telefunken* **54**, 197–202. In German.

Bjorkholm, J. E., and Danielmeyer, H. G. (1970). Frequency control of a pulsed optical parametric oscillator by radiation injection. *IEEE J. Quantum Electron.* **QE-6**, 7.

Bloomfield, D. L. H., and Pointon, A. J. (1973). Short-term frequency stability of an L band oscillator with a superconducting cavity. *Electron. Lett.* **9**, 461–462.

Bobryshev, V. D., Verkin, B. I., Dmitriev, V. M., and Prentslu, N. N. (1978). Cryogenic high-frequency stable systems with mode-conversion cavities. *Cryogenics* **18**, 601–606.

Bobryshev, V. D., Verkin, B. I., Dmitriev, V. M., and Prentslau, N. N., Yatsenko, V. A. (1980). Stabilized cryogenic UHF oscillator. *Instrum. Exp. Tech. (Engl. Transl.)* **22**, 1683.

Bushy, P. W. (1975). Electronic tuning fork. *Pract. Electron.* **11**, 882–888.

Campisi, I. E., and Hamilton, W. O. (1981). Use of superconducting cavities in the stabilization of tunnel diode oscillators. *Physica B, C* **108B,C**, 1363–1364.

Chuang, S. S. (1981). Quartz tuning fork crystal using overtone flexure modes. *Proc. 35th Annu. Freq. Control Symp.*, pp. 130–143.

Cutler, L. S., and Searle, C. L. (1966). Some aspects of the theory and measurement of frequency fluctuations in frequency standards. *Proc. IEEE* **54**, 136–154.

Davidheiser, R. (1980). Frequency stable sources using superconducting microstrip resonators. *Proc. 34th Annu. Freq. Control Symp.*, pp. 252–254.

Debeau, J., and Minet, R. (1973). Superconductor high frequency filters. *Echo Rech.* (72), 14–21. In French.

Dick, G. J., and Strayer, D. M. (1983). The superconducting cavity stabilized ruby maser oscillator. *Proc. 15th Precise Time and Time Interval Applications and Planning Meeting*, pp. 723–737. NASA GSFC, Greenbelt, Maryland 20771.

Diepers, H., Schmidt, O., Martens, H., and Sun, F. S. (1971). A new method of electropolishing niobium. *Phys. Lett. A.* **37**, 139–140.

Dydyk, M. (1977). Dielectric resonators add Q to MIC filters. *Microwaves* **16**, 150–151, 154–156.

Engdahl, J., and Matthey, H. (1975). 32 kHz quartz crystal unit for high precision wrist watch. *Proc. 29th Annu. Freq. Control Symp.*, pp. 187–194.

Forrer, M. P. (1969). A flexure mode quartz for an electronic wrist watch. *Proc. 23rd Annu. Freq. Control Symp.*, pp. 157–162.

Hellwig, H. (1979). Microwave time and frequency standards. *Radio Sci.* **14**, 561–572.

Hirai, K., Okikawa, T., and Aiba, N. (1978). New types of frequency-stabilized Gunn oscillator. *Toshiba Rev. (Int. Ed.)* (115), 37–41.

Jimenez, J. J., and Septier, A. (1973). S- and X-band superconducting cavity stabilized oscillators. *Proc. 27th Annu. Freq. Control Symp.*, pp. 406–413.

Jimenez, J. J., Viet, N. T., Bernard, J., and Septier, A. (1973). Frequency standards of cavity superconductors. *Electron. Fis. Apl.* **16**, 79–84. In French.

Kanbayashi, S., Okano, S., Hirama, K., Kudama, T., Konno, M., and Tomikawa, Y. (1976). Analysis of tuning fork crystal units and application into electronic wrist watches. *Proc. 30th Annu. Freq. Control Symp.*, pp. 167–174.

Kee, P. Y. (1977). Simple tuning fork. *Pract. Electron.* **13**, 221.

Kochubei, A. D., and Mitrofanov, V. D. (1978). Electric-oscillation generator stabilized by a mechanical sapphire resonator at a temperature 4.2 K. *Instrum. Exp. Tech. (Engl. Transl.)* **21**, 1316–1318.

Koga, I. (1928). Tuning fork made of quartz crystal. *J. Inst. Electr. Eng. Jpn.* **48**, 100–101.

Komatsu, Y., Murakami, Y., Yamaguchi, T., Otobe, T., and Hirabayashi, M. (1981). A frequency-stabilized MIC oscillator using a newly-developed dielectric resonator. *IEEE MTT Symp. Dig.*, pp. 313–315.

Komiyama, B., and Yasuda, Y. (1980). Superconducting cavity stabilized oscillators by self-injection locking. *Trans. Inst. Electron. Commun. Eng. Jpn., Sect. E.* **63**, 291–292.

Kukushkin, A. V., and Nasonov, V. S. (1969). Phase fluctuations of the signal of a generator with a traveling-wave tube using a superconducting resonator. *Instrum. Exper. Tech. (Engl. Transl.)* (6), 1514–1516.

Kusters, J. A., Adams, C. A., Karrer, H. E., and Ward, R. W. (1976). Analytical and experimental investigations of 32 kHz quartz tuning forks. *Proc. 30th Annu. Freq. Control Symp.*, pp. 175–183.

McGuigan, D. F., and Douglass, D. H. (1977). Clocks based upon high mechanical Q single crystals. *Proc. 31st Annu. Freq. Control Symp.*, pp. 616–619.

Michael, J. (1980). Quartz resonator for the watch. *Proc. Journess d'Electonique et de Mecrotechnique on the Subject Limits to Miniaturization*, Lausanne, Switzerland, Swiss Federal Inst. Technol., pp. 173–180. In French.

Minakova, I. I., Minina, G. P., Nazarov, V. I., Panov, V. I., and Papel'nyuk, V. D. (1976). Stabilizing the frequency of an oscillator for high Q-factors of the stabilizing resonator. *Vestn. Mosk. Univ. Fiz., Astron.* **17**, 722–727. In Russian.

Minakova, I. I., Minina, G. P., Panov, V. I., and Petnikov, V. G. (1976). A free-running oscillator, stabilised by a three-cavity system with a superconducting resonator. *Izv. Vyssh. Uchebn. Zaved. Radioelektron.* **19**, 16–23. In Russian.

Minakova, I. I., Nazarov, V. I., Panov, V. I., and Popel'nyuk, V. D. (1978). Frequency stabilization of a solid-state oscillator with a superconducting sapphire resonator. *Sov. Tech. Phys. Lett. (Engl. Transl.)* **4**, 71–72.

Momosaki, S., Kogure, S., Inoue, M., and Sonoda, T. (1979). New quartz tuning fork with very low temperature coefficient. *Proc. 33rd Annu. Freq. Control Symp.*, pp. 247–255.

Musa, F. H., and Daniels, R. G. (1971). The Crystal controlled electronic watch system. *Proc. 25th Annu. Freq. Control Symp.*, pp. 75–81.

Nukiyama, D., and Miyazaki, N. (1967). A type of oscillator. *J. Res. Inst. Technol., Nihon. Univ.* (34), 18 et seq. In Japanese.

Ota, M. Nagase, T., Oyanagi, T., and Kenmotsu, N. (1971). Micro tuning fork. *Hitachi Hyoron* **53**, 37–42. In Japanese.

Panov, V. I. (1980). Method of stabilizing the frequency of klystron microwave oscillators. *Prib. Tekh. Eksp.* **23**, 124–126.

Pierce, J. M. (1974). Superconducting microwave resonators. *In* "Methods of Experimental Physics," Vol. II. (R. V. Coleman, ed.), pp. 541–594. Academic Press, New York.

Plourde, J. K., Linn, D. F., Tatsuguchi, I., and Swan, C. B. (1977). A dielectric resonator oscillator with 5 ppm long term frequency stability at 4 GHz. *Int. Microwave Symp. Dig. (IEEE)*, pp. 273–276.

Pudalov, V. M. (1980). Superconducting SHF resonators and their use in metrology. *Meas. Tech. (Engl. Transl.)* **23**, 600–601.

Richtmeyer, R. D. (1939). Dielectric resonator. *J. Appl. Phys.* **10**, 391–395.

Rose, B. E. (1978). 10 GHz cavity stabilized FET oscillator. *Proc. 32nd Annu. Freq. Control Symp.*, pp. 385–388.

Saito, T., Arai, Y., Komizo, H., Itoh, Y., and Nishikawa, T. (1979). A 6 GHz highly stabilized GaAs FET oscillator using a dielectric resonator. *Int. Microwave Symp. Dig. (IEEE)*, pp. 197–199.

Sanchez-Miranda, T. (1981). New tuning fork resonators. *Rev. Esp. Electron.* **28**, 54–56. In Spanish.

Schwarz, H. R. (1972). Eigenfrequencies of tuning-forks. *Comput. Methods Appl. Mech. Eng.* **1**, 159–172.

Staudte, J. H. (1973). Subminiature quartz tuning fork resonator. *Proc. 27th Annu. Freq. Control Symp.*, pp. 50–54.

Stein, S. R. (1974a). "The Superconducting-Cavity Stabilized Oscillator and an Experiment to Detect Time Variation of the Fundamental Constants." Report HEPL-741, Stanford University, Stanford, California, 111 pp. Available from The National Technical Information Service, Springfield, Virginia.

Stein, S. R. (1974b). "The Superconducting-Cavity Stabilized Oscillator and an Experiment to Detect Time Variation of the Fundamental Constants." Ph.D. Thesis, Stanford University, Stanford, California, 111 pp. Available from University microfilms, Ann Arbor, Michigan, Order No. 75-6932.

Stein, S. R. (1975). Application of superconductivity to precision oscillators. *Proc. 29th Annu. Freq. Control Symp.*, pp. 321–327.

Stein, S. R., and Turneaure, J. P. (1972). A superconducting cavity stabilized oscillator. *Proc. 26th Annu. Freq. Control Symp.*, p. 257.

Stein, S. R., and Turneaure, J. P. (1973). The development of the superconducting cavity stabilized oscillator. *Proc. 27th Annu. Freq. Control Symp.*, pp. 414–420.

Stein, S. R., and Turneaure, J. P. (1975). Superconducting-cavity stabilized oscillators with improved frequency stability. *Proc. IEEE* **63**, 992–993.

Stein, S. R., and Turneaure, J. P. (1978). Superconducting resonators: high stability oscillators and applications to fundamental physics and metrology. *AIP Conf. Proc.* (44), 192–213.

Stiglitz, M. R. (1981). Dielectric resonators past, present, and future. *Microwave J.* **24**, 19–36.

Stone, J. L., and Hartwig, W. H. (1967). Oscillators utilizing superconducting resonators. *Southwestern Conf. Rec. Techn. Program, (IEEE)*, pp. 931–938.

Tomikawa, Y. (1980). Second-mode tuning forks for high frequencies: finite element analysis and experiments. *IEEE Trans. Sonics Ultrason.* **SU-27**, 253–257.

Tomikawa, Y., Miura, H., and Dong, S. B. (1978). Analysis of electrical equivalent circuit elements of piezo-tuning forks by the finite element method. *IEEE Trans. Sonics Ultrason.* **SU-25**, 206–212.

Tomikawa, Y., Sugawara, S., and Konno, M. (1980). Characteristics of a quartz crystal tuning fork by finite element analysis. *Trans. Inst. Electron. Commun. Eng. Jpn.*, [Part] *E* **63**, 177–183.

Tomikawa, Y., Oyama, S., and Konno, M. (1982). A quartz crystal tuning fork with modified basewidth for a high quality factor: finite element analysis and experiments. *IEEE Trans. Sonics Ultrason.* **SU-29**, 217–223.

Turneaure, J. P., and Weissman, I. (1968). Microwave surface resistance of superconducting niobium. *J. Appl. Phys.* **39**, 4417–4427.

Van Degrift, C. T. (1975). Tunnel diode oscillator for 0.001 ppm measurements at low temperature. *Rev. Sci. Instrum.* **46**, 599–607.

Vig, J. R., and Gikow, E. (1972). A superconductive tunable filter with broad tuning range. *Proc. 26th Annu. Freq. Control Symp.*, pp. 193–201.

Wakimo, K., Nishikawa, T., Tamura, S., and Tamura, H. (1983). An *X*-band GaAs FET oscillator using a dielectric resonator. *Proc. 37th Annu. Freq. Control Symp.*, pp. 481–484.

Wineland, D. J., Howe, D. A., and Mohler, M. B. (1977). Results with the special purpose ammonia frequency standard. *Proc. 31st Annu. Freq. Control Symp.*, pp. 562–573.

Withers, R. S., Wright, P. V., Green, J. B., Anderson, A. C., and Reible, S. A. (1983). Superconductive tapped delay line for low insertion loss wide band analog signal processing filters. *Proc. 37th Annu. Freq. Control Symp.*, pp. 81–86.

Yoda, H., Ikeda, H., and Yamabe, Y. (1972). Low power crystal oscillation for electric wrist watch. *Proc. 26th Annu. Freq. Control Symp.*, pp. 140–147.

Chapter 15

Abe, H., Takayama, Y., Higashisaka, A., and Takamizawa, H. (1978). A highly stabilized low-noise GaAs FET integrated oscillator with a dielectric resonator in the *C* band. *IEEE Trans. Microwave Theory Tech.* **MTT-26**, 156–160.

Akahane, Y. (1979). New twin quartz system revolutionizes timekeeping accuracy [digital watches]. *JEE, J. Electron. Eng.* **16**, 24–27.

Anonymous. (1972). Quartz timepiece components. *Microtecnic* **26**, 157–162.

Anonymous. (1975). The ULTRA-QUARTZ electronic quartz wafer. *Jemna Mech. Opt.* **20**, 86. In Czech.

Anomymous. (1976). The quartz era. *Elettrificazione (Milan)* (11), 524–525. In Italian.

Anonymous. (1978). Trends in quartz wristwatches. *Funkschau* **50**, 1278–1279. In German.

Anonymous. (1979). Some problems with the change over to electronic clocks. *Sdeloraci Tech.* **27**, 62. In Czech.

Assmus, F. (1978). Development of the clock and watch industry in the electronic age. *Polytech. Tijdschr. Elektrotech. Elektron.* **33**, 733–747. In Dutch.

Baker, M. A. (1969). Vacuum applications of the quartz crystal microbalance. *Vacuum* **19**, 327–330.

Ballato, A. (1960). Effects of initial stress on quartz plates vibrating in thickness modes. *Proc. 14th Annu. Freq. Control Symp.*, pp. 89–114.

Ballato, A., and Vig, J. R. (1978). Static and dynamic frequency–temperature behavior of singly and doubly rotated, oven-controlled quartz resonators. *Proc. 32nd Annu. Freq. Control Symp.*, pp. 180–188.

Battison, A. H. (1971). Ionized light emitter using piezoelectric crystal. *IBM Tech. Disclosure Bull.* **14**, 555–557.

Bechmann, R., Ballato, A. D., and Lukaszek, T. J. (1962). Frequency temperature characteristics of quartz resonators derived from the temperature behavior of the elastic constants. *Proc. 16th Annu. Freq. Control Symp.*, pp. 77–109.

Behrndt, K. H. (1971). Long-term operation of crystal oscillators in thin-film deposition. *J. Vac. Sci. Technol.* **8**, 622–626.

Benndorf, C., Keller, G., Seidel, H., and Thieme, F. (1977). High-resolution quartz oscillator microbalance and its application to the initial oxidation of aluminium. *J. Vac. Sci. Technol.* **14**, 819–821.

Berenshtein, B. Sh., and Bobrikov, V. S. (1973). The restoration of quartz resonators that are used to measure the thickness and rate of vacuum deposition of thin films. *Instrum. Exp. Tech. (Engl. Transl.)* **16**, 1518.

Besson, R. J. (1976). A new piezoelectric resonator design. *Proc. 30th Annu. Freq. Control Symp.*, pp. 77–83.

Besson, R. J. (1977). A new electrodeless resonator design. *Proc. 31st Annu. Freq. Control Symp.*, pp. 147–152.

Bourgeois, C. (1971). Quartz crystals as frequency standards for wrist watches. *Eurocon Dig. (IEEE)*, 2 pp.

Bryant, A., Lee, D. L., and Vetelino, J. F. (1981). A surface acoustic wave gas detector. *Proc. IEEE Ultrason. Symp.*, pp. 171–174.

Bryant, A., Poirier, M., Lee, D. L., and Vetelino, J. F. (1982). A surface acoustic wave gas detector. *Proc. 36th Annu. Freq. Control Symp.*, pp. 276–283.

Bucur, R. V., Pascalau, M., and Mecea, V. (1972). A piezoelectrical quartz crystal micro-balance for hydrogen–metal interaction studies. *Rev. Roum. Phys.* **17**, 887–891.

Chuang, S. S. (1983). Force sensor using double-ended tuning fork quartz crystals. *Proc. 37th Annu. Freq. Control Symp.*, pp. 248–254.

Corlet, J. (1977). A small quartz watch with automatic digital frequency regulation. *Bull. Ann. Soc. Suisse Chronom. Lab. Suisse Rech. Horlog.* **7**, 341–342. In French.

Daniels, R. G., and Musa, F. H. (1971). The crystal-controlled electronic wrist-watch system: a Si-gate CMOS-MSI approach. *Proc. 25th Annu. Freq. Control Symp.*, pp. 75–81.

Dauwalter, C. (1972). The temperature dependence of the force sensitivity of AT-cut quartz crystals. *Proc. 26th Annu. Freq. Control Symp.*, pp. 108–112.

Dias, J., and Karrer, E. (1974). Stress effects in acoustic surface wave circuits and applications to pressure and force transducers. *Int. Solid-State circuits Conf. Dig. Tech. Papers (IEEE)* **17**, 166–167.

Dinger, R. J. (1982). The torsional quartz tuning fork as a temperature sensor. *Proc. 36th Annu. Freq. Control Symp.*, pp. 265–269.

Dorogov, V. N., and Shavaiko, S. N. (1978). Inductive gauge with quartz resonator. *Sov. J. Nondestr. Test. (Engl. Transl.)* **14**, 672–673.

Dror, S., and Cannel, D. S. (1974). A ± 15 microdegree temperature controller. *Rev. Sci. Instrum.* **45**, 1082–1088.

EerNisse, E. P. (1972). Simultaneous thin-film stress and mass-change measurements using quartz resonators. *J. Appl. Phys.* **43**, 1330–1337.

EerNisse, E. P. (1975a). Vacuum applications of quartz resonators. *J. Vac. Sci. Technol.* **12**, 564–577.

EerNisse, E. P. (1975b). Quartz resonator frequency shifts arising from electrode stress. *Proc. 29th Annu. Freq. Control Symp.*, pp. 1–4.

EerNisse, E. P. (1976). Calculations on the stress compensated (SC-cut) quartz resonator. *Proc. 30th Annu. Freq. control Symp.*, pp. 8–11.

EerNisse, E. P. (1978). Rotated X-cut quartz resonators for high temperature application. *Proc. 32nd Annu. Freq. Control Symp.*, pp. 255–259.

EerNisse, E. P. (1979). Temperature dependence of the force–frequency effect for the rotated X-cut. *Proc. 33rd Annu. Freq. Control Symp.*, pp. 300–305.

EerNisse, E. P., Lukaszek, T. J., and Ballato, A. (1978). Variational calculation of force-frequency constants of doubly rotated quartz resonators. *IEEE Trans. Sonics Ultrason.* **SU-25**, 132–138.

Florio, J. V. (1968). Quartz-crystal microbalance technique for the preparation of alkali-antimonide photocathodes. *J. Appl. Phys.* **39**, 3121–3128.

Fonjallaz, C., and Vittoz, E. (1970). The crystal electronic wrist-watch. III. Electronic circuits for crystal wrist-watches. *Schweiz. Tech. Z.* **67**, 458–461. In French.

Forrer, M. (1970). The crystal electronic wrist-watch. I. Synopsis. *Schweiz. Tech. Z.* **67**, 454–455. In French.

Genis, A., and Newell, D. E. (1977). Using the X–Y flexure watch crystal as a pressure-force transducer. *Proc. 31st Annu. Freq. Control Symp.*, pp. 71–77.

Gerber, E., and Ahlstrom, E. R. (1969). Solid-state laser with vibrating reflector. *IEEE J. Quantum Electron.* **QE-5**, 403–409.

Gerber, E., and Miles, M. (1961a). Reduction of the frequency–temperature shift of piezoelectric resonators by mechanical stress. *Proc. IRE* **49**, 1650–1654.

Gerber, E. A., and Miles, M. H. (1961b). Temperature compensation of piezoelectric resonators by mechanical stress. *Proc. 15th Annu. Freq. Control Symp.*, pp. 49–65.

Gniewinska, B., Czarnecki, A., and Rozwadowski, M. (1977). Digital quartz thermometer. *Pol. Tech. Rev.* (4–5), 23–24.

Gorini, I., and Sartori, S. (1962). Quartz thermometer. *Rev. Sci. Instrum.* **33**, 883–884.

Grandjean, R. (1980). Miniaturisation of the quartz watch. *Proc. Journees d'Electronique et de Microtechnique on the Subject Limits to Miniaturization*, Lausanne, Switzerland, Swiss Federal Inst, Technol., pp. 285–295. In French.

Greuter, A. (1971). Some remarks concerning flexural type quartz vibrators for wristwatches. *Eurocon Dig. (IEEE)*, 1 p.

Gubser, D. U., and Mapother, D. E. (1969). Remotely controlled piezoelectric vibrator for low temperature applications. *Rev. Sci. Instrum.* **40**, 843–845.

Guilbault, G. G., Tomita, Y., and Kolesar, E. S., Jr. (1981). A coated piezoelectric crystal to detect organophosphorous compounds and pesticides. *Sens. Actuators* **2**, 43–57.

Guye, R., Chauvy, D., and Hubner, K. (1970). The crystal electronic wrist-watch. IV. Integrated circuits of a crystal wrist-watch. *Schweiz. Tech. Z.* **67**, 461–464. In French.

Hajek, J. (1979). The EMES-SOLARQUARTZ electronic alarm clock with solar batteries. *Jemna Mech. Opt.* **24**, 355–356. In Czech.

Hama, T. (1977). Electronic watches using quartz crystal oscillators. *Jpn. J. Appl. Phys.* **16**, 185–189.

Hammer, D., Benes, E., and Pulker, H. K. (1976). A digital quartz deposition monitor using a microprocessor. *Thin Solid Films* **32**, 47–50.

Hammer, M. W. (1977). A small quartz watch with automatic digital frequency regulation. *Bull. Ann. Soc. Suisse Chronom. Lab. Suisse Rech. Horlog.* **7**, 337–340. In French.

Hammond, D. L., and Benjaminson, A. (1969). The crystal resonator—a digital transducer. *IEEE Spectrum* **6**, 53–58.

Hammond, D. L., Adams, C. A., and Schmidt, P. (1965). A linear quartz crystal temperature-sensing element. *Trans. Instrum. Soc. Am.* **4**, 349–354.

Hartemann, P., and Meunier, P. L. (1981). Surface acoustic wave accelerometer. *Proc. IEEE Ultrason. Symp.*, pp. 152–154.

Hauden, D., Rousseau, S., and Gagnepain, J.-J. (1980). Sensitivities of SAW oscillators to temperature, forces, and pressure: applications to sensors. *Proc. 34th Annu. Freq. Control Symp.*, pp. 312–319.

Hauden, D., Jaillet, G., and Coquerel, R. (1981). Temperature sensor using SAW delay line. *Proc. IEEE Ultrason. Symp.*, pp. 148–151.

Hauden, D., Rousseau, S., Jaillet, G., and Coquerel, R. (1982). Pressure and temperature measurements with SAW sensors. *Proc. 36th Annu. Freq. Control Symp.*, pp. 284–289.

Hermann, J., Forrer, M., and Omlin L. (1970). The crystal electronic wrist-watch. II. Wrist-watch crystal resonator. *Schweiz. Tech. Z.* **67**, 456–458. In French.

Hillecke, D., and Mayer, H. (1970). UHV microbalance and quartz oscillator at low temperatures in progress in vacuum. *Microbalance Tech.* **7**, 135–143.

Holland, R. (1974). Nonuniformally heated anisotropic plates: I. Mechanical distortion and relaxation. *IEEE Trans. Sonics Ultrason.* **SU-21**, 171–178.

Hordejuk, J. (1971). Application of low-frequency electromechanical filters to seismological investigations. *Acta Geophys. Pol.* **19**, 351–364.

Iglsias, G., and Bertini, E. (1981). A piezoelectric accelerometer. *Rev. Telegr. Electron.* (823), 958–961. In Spanish.

Ishitani, J., Ito, S., and Yamashita, A. (1979). Quartz crystal units enhance quartz watch designs. *JEE. J. Electron. Eng.* **16**, 66–68.

Ishitani, J., Hashimoto, H., and Tateyama, M. (1980). Miniaturization and constant mass-productivity: these are keywords for crystal units for watches. *JEE, J. Electron, Eng.* **17**, 58–61.

Ivanov, G. A. (1972). Microweighing with piezoelectric quartz crystals. *Ind. Lab.* **38**, 884–890.

Ivanov, G. A., Pekar', I. K. I., Roitbert, M. B., and Guglya, V. G. (1971). Expanding the temperature range of a piezoelectric quartz microbalance. *Zavod. Lab.* **37**, 798–800. In Russian.

Ivanov, G. A., Ivanov, L. A., and Zhukhovitskii, A. A. (1973). Possible use of quartz resonators in laboratory practice. *Zavod. Lab.* **39**, 436–438. In Russian.

Iwakura, R., Morokawa, S., Sekiya, F., Nakayama, T., and Hishida, H. (1981). Low-power IC for 4.2 MHz analogue wristwatch. *Bull. Ann. Soc. Suisse Chronom. Lab. Suisse Rech. Horlog.* **10**, 133–137.

Janghorbani, M., and Freund, H. (1973). Application of a piezoelectric quartz crystal as a partition detector. Development of a digital sensor. *Anal. Chem.* **45**, 325–332.

Janiaud, D., Nissim, I., and Gagnepain, J.-J. (1978). Analytical calculation of initial stress effects on isotropic crystals: application to quartz resonators. *Proc. 32nd Annu. Freq. Control Symp.*, pp. 169–179.

Kanbayashi, S., Okano, S., Hirama, K., and Kudama, T. (1976). Analysis of tuning fork crystal units and application into electronic wrist watches. *Proc. 30th Annu. Freq. Control Symp.*, pp. 167–174.

Karrer, E., and Ward, R. (1977). A low-range quartz resonator pressure transducer. *ISA Trans.* **16**, 90–98.

Kertzman, J. (1971). Piezoelectric sensors for use as pollution detectors, meterorology monitors and research instruments. *Proc. 25th Annu. Freq. Control Symp.*, pp. 102–103.

Keyes, R., and Blair, F. (1967). Stress dependence of the frequency of quartz plates. *Proc. IEEE* **55**, 565–566.

King, W. H., Jr. (1971). The present state of the art in piezoelectric sensors. *Proc. 25th Annu. Freq. Control Symp.*, pp. 104–108.

Kornstein, E., Kikuyama, A., and Horiuchi, A. (1975). The quartz analog watch still lives. *WESCON Tech. Papers*, N. Hollywood, California, Western Periodicals, **19**, 5 pp.

Kusters, J. A., Adams, C. A., and Yoshido, H. (1977). TTC's—further developmental results. *Proc. 31st Annu. Freq. Control Symp.*, pp. 3–8.

Kusters, J., Fischer, M., and Leach, J. (1978). Dual mode operation of temperature and stress compensated crystals. *Proc. 32nd Annu. Freq. Control Symp.*, pp. 389–397.

Laan, C. J., and Frankena, H. J. (1977). Monitoring of optical thin films using a quartz crystal monitor. *Vacuum* **27**, 391–397.

Lao, B. (1980). Gyroscopic effect in surface acoustic waves. *Proc. IEEE Ultrason. Symp.*, pp. 687–691.

Lee, P., Wang, Y., and Markenscoff, X. (1976). Nonlinear effects of initial bending forces on the vibrations of crystal plates. *J. Acoust. Soc. Am.* **59**, 90–96.

Levchuk, E. A., Chudnovskii, A. F., and Samuilova, S. I. (1971). Maximum sensitivity of humidity transducers with crystal plates. *Meas. Tech. (Engl. Transl.)* **14**, 1608–1609.

Lewis, O., and Lu, C. S. (1975). Relationship of resonant frequency of quartz crystal to mass loading. *Proc. 29th Annu. Freq. Control Symp.*, pp. 5–9.

Lostis, P. (1971). Control of thin films by piezoelectric quartz. *Vide* **26**, 159–163. In French.

Lu, C. S. (1972). Investigation of film-thickness determination by oscillating quartz resonators with large mass load. *J. Appl. Phys.* **43**, 4385–4390.

Lu, C. S. (1975). Mass determination with piezoelectric quartz crystal resonators. *J. Vac. Sci. Technol.* **12**, 578–583.

Luscher, J., and Rusznyak, A. (1982). A 4.2-MHz quartz oscillator for watch applications. *Bull. Assoc. Suisse Electr.* **73**, 108–112.

Marianneau, G., and Gagnepain, J.-J. (1980). Digital temperature control for ultrastable quartz oscillators. *Proc. 34th Annu. Freq. Control Symp.*, pp. 52–57.

Matsuzawa, H., Kamiryo, K., and Kano, T. (1973). Temperature control of quartz crystals for deposited thin-film thickness monitors. *Rec. Electr. Commun. Eng. Conversazione Tohoku Univ.* **42**, 211–214. In Japanese.

Mecea, V., and Bucur, R. V. (1974). The use of RF voltage in quartz crystal microbalance measurements: application to nonmetallic films. *J. Phys. E* **7**, 348–349.

Momosaki, E., and Kogure, S. (1982). The application of piezoelectricity to watches. *Ferroelectrics* **40**, 203–216.

Mueller, R. M, and White, W. (1968). Direct gravimetric calibration of quartz crystal microbalance. *Rev. Sci. Instrum.* **39**, 291–295.

Nagy, G. (1967). Piezoelectric crystal-type thickness measuring instrument for vacuum evaporated films. *Meres Autom.* **15**, 433–435. In Hungarian.

Nishiguchi, Y., and Nosaka, S. (1978). Quartz crystal units allow smaller, thinner watches. *JEE, J. Electron. Eng.* (144), 48–51.

Noiray, J. C., Lanteri, H., Bindi, R., Borgnino, J., and Martin, F. (1975). Study and development of an oscillating quartz-crystal microbalance-comparison with optical and mechanical measurement methods. *Thin Solid Films* **26**, 293–303. In French.

Nuvolone, R., and Boiziau, C. (1972a). A very sensitive vibrating quartz balance working in ultra-high vacuum and at very low temperatures. *Rev. Phys. Appl.* **7**, 55–60. In French.

Nuvolone, R., and Boiziau, C. (1972b). Realization of a very sensitive quartz balance. *Vide* **27**, 10–16. In French.

Oguey, H. (1971). A resonant motor for quartz watches. *Rev. Polytech. Suisse* (1287), 249–263. In French.

Oguey, H., and Droz, J. C. (1970). The crystal electronic wrist-watch. V. Display micromotor in the crystal wrist-watch. Theory. *Schweiz. Tech. Z.* **67**, 464–467. In French.

Onoe, M., Furusawa, K., Ishigami, S., Sase, T., and Sato, M. (1977). Quartz crystal accelerometer insensitive to temperature variation. *Proc. 31st Annu. Freq. Control Symp.*, pp. 62–70.

Orlov, Yu. G. (1981). Application of surface acoustic waves (SAW) in sorption gas analyzers. *Ind. Lab.* **47**, 268–271.

Pekar', I. K. I., and Yaroslavskii, M. I. (1971). Quartz resonators for temperature measurements. *Zavod. Lab.* **37**, 986–987. In Russian.

Porter, W. A., and Anderson, S. W. (1972). The effects of temperature on the accuracy of crystal oscillator thickness monitors. *J. Vac. Sci. Technol.* **9**, 1472–1474.

Pulker, H. K. (1971). Experiments on the realizable precision in continuous film thickness measurement with a quartz oscillator. *Vide* **26**, 150–158. In French.

Pulker, H. K., Benes, E., Hammer, D., and Sollner, E. (1976). Progress in monitoring thin film thickness with quartz crystal resonators. *Thin Solid films* **32**, 27–33.

Raabe, M. (1973). Integrated CMOS circuit with low power consumption for quartz-crystal wristwatches. *Elektronik (Munich)* **22**, 424–426. In German.

Ramadan, B., Piyakis, K., and Kos, J. F. (1979). High accuracy quartz crystal thin film monitor. *Rev. Sci. Instrum.* **50**, 867–871.

Ratajski, J. (1966). The force-sensitivity of AT-cut quartz crystal. *Proc. 20th Annu. Freq. Control Symp.*, pp. 33–34.

Ratajski, J. (1968). Force-frequency coefficient of singly-rotated vibrating quartz crystals. *IBM J. Res. Dev.* **12**, 92–99.

Reeder, T. M., and Cullen, D. E. (1976). Surface acoustic wave pressure and temperature sensors. *Proc. IEEE* **64**, 754–756.

Riddle, J. L., Furakawa, G. T., and Plumb, H. H. (1973). Platinum resistance thermometry. *NBS Monogr. (U.S.)* 126.

Rozwadowski, M., and Czarnecki, A. (1975). Quartz crystal resonator with linear dependence of frequency upon temperature. *Pr. Inst. Tele-Radiotech.* **19**, 85–90. In Polish.

Rozwadowski, M., Czarnecki, A., Szulc, W., and Zynca, A. (1978). A quartz thermometer with temperature resolution of 10^{-4} C. *Elektronika* **19**, 431. In Polish.

Sauerbrey, G. (1959). Use of oscillator quartz crystals for weighing thin layers and microweighing. *Z. Phys.* **155**, 206–222.

Schilling, H., and Pechhold, W. (1970). Two quartz resonator methods for the investigation of the complex shear modulus of polymers. *Acustica* **22**, 244–253. In German.

Schooley, J. F., ed. (1982). "Temperature: Its Measurement and Control in Science and Industry." American Institute of Physics, New York.

Scialdone, J. J. (1974). Molecular fluxes from a spacecraft measured with quartz microbalances. *J. Vac. Sci. Technol.* **12**, 569–572.

Seed, A. (1971). Quartz Crystals for timepieces. *Eurocon Dig. (IEEE)*, 2 pp.

Shiojiri, M., Hasegawa, Y., Mupata, Y., and Matsumura, S. (1969). Quartz crystal microbalance techniques applicable to the studies of sulphuration and oxidation of thin metal films. *Jpn. J. Appl. Phys.* **8**, 783–791.

Smagin, A. G., and Mil'shtein, B. G. (1970). Quartz frequency thermometer. *Instrum. Exp. Tech. (Engl. Transl.)* (3), 932–934.

Smith, W. L., and Spencer, W. J. (1963). Quartz crystal thermometer for measuring temperature deviations in the 10^{-3} to 10^{-6} range. *Rev. Sci. Instrum.* **34**, 268–270.

Sollner, E., Benes, E., Biedermann, A., and Hammer, D. (1977). Properties of heavily preloaded quartz crystals for thin film thickness monitors. *Vacuum* **27**, 367–371.

Stanley, J. M., Wasshausen, H., and Schodowski, S. (1972). Frequency control devices for high stability remote sensor transmitters. *Proc. 26th Annu. Freq. Control Symp.*, pp. 120–131.

Staples, E. J., Wise, J., and DeWames, R. E. (1981). Pressure and acceleration sensitivity of a SAW interferometer. *Proc. IEEE Ultrason. Symp.*, pp. 155–158.

Staples, E. J., Wise, J., and Andrews, A. P. (1982). Inertial guidance and underwater sound detection using SAW sensors. *Proc. 36th Annu. Freq. Control Symp.*, pp. 270–275.

Staudte, J. H. (1975). "Quartz Crystals for Watches." WESCON Technical Papers. Western Periodicals, N. Hollywood, California. **19**, 6 pp.

Stein, S. R., Manney, C. M., Walls, F. L., and Gray, J. E. (1978). A systems approach to high performance oscillators. *Proc. 32nd Annu. Freq. Control Symp.*, pp. 527–530.

Stockbridge, C. D. (1963). Effects of gas pressure on quartz crystal microbalances. *Vac. Microbalance Tech.* **3**, 147–178.

Stockbridge, C. D. (1966). Effect of hydrostatic pressure on rotated Y-cut quartz crystal resonators. *Vac. Microbalance Tech.* **5**, 179–191.

Strekalov, P. V., and Mikhailovsii, Yu.N. (1971). Quartz resonator method for studying atmospheric corrosion processes. *Zashch. Met.* **7**, 148–153. In Russian.

Swinbank, E., Heeks, T. R., and Shelly, J. H. (1974). Quartz-crystal watches. *Electron. Power* **20**, 887–891.

Theobald, G., Marianneau, G., Pretot, P., and Gagnepain, J.-J. (1979). Dynamic thermal behavior of quartz resonators. *Proc. 33rd Annu. Freq. Control Symp.*, pp. 239–246.

Thommen, W., and Ruegg, H. (1971). Bipolar micropower circuits for crystal controlled watches. *Eurocon Dig. (IEEE)*, 2 pp.

Tiersten, H. F. (1981). Circulating flexural wave rotation rate sensor. *Proc. IEEE Ultrason. Symp.*, pp. 163–166.

Tiersten, H. F., Stevens, D., and Das, P. (1980). Acoustic surface wave acceleration and rotation rate sensor. *Proc. IEEE Ultrason. Symp.*, pp. 692–695.

Valdois, M., Besson, J., and Gagnepain, J.-J. (1974). Influence of environment conditions of a quartz resonator. *Proc. 28th Annu. Freq. Control Symp.*, pp. 19–32.

Van Ballegooijen, E. C., Boersma, F., and Van der Steen, C. (1978). Application of a quartz crystal with electrode-tab configuration for simultaneous mass and temperature determination. *J. Acoust. Soc. Am.* **63**, 806–814.

Van Empel, F. J., Van Ballegooyen, E. C., Boersma, F., Poulis, J. A., and Massen, C. H. (1972a). Application of resonating quartz crystals in thermogravimetry. *Proc. 3rd Int. Conf. Therm. Anal.* **1**, 583–589.

Van Empel, F. J., Van Ballegooyen, E. C., Boersma, F., Poulis, J. A., and Massen, C. H. (1972b). Influence of temperature on weighing with quartz oscillators and its compensation. *Thermochim. Acta* **5**, 129–132.

Von Willisen, F. K. (1979). The quartz watch: its life and times. *IEEE Spectrum* **16**, 18–23.

V'yukhin, V. N., Vanyushev, B. V., and Chernyshov, A. I. (1978). High-speed two-channel generator of a grid of quartz-controlled frequencies [for control of acoustooptical deflector]. *Instrum. Exp. Tech. (Engl. Transl.)* **21**, 1001–1003.

Wallace, D. A. (1972). Use of the quartz crystal microbalance for outgasssing and optical contamination measurements. *J. Vac. Sci. Technol.* **9**, 462–466.

Warashina, N. (1978). Crystal oscillators and units improve frequencies for measuring instruments. *JEE, J. Electron. Eng.* **144**, 44–47.

Warner, A. W., and Stockbridge, C. D. (1963). Mass measurement with resonating crystalline quartz. *Vac. Microbalance Tech.* **3**, 55–73.
Warner, A. W., Fraser, D. B., and Stockbridge, C. D. (1965). Fundamental studies of aging in quartz resonators. *IEEE Trans. Sonics Ultrason.* **SU-12**, 52–59.
Wellinger, R. P. (1971). Electronic watchmaking, present and future. *Eurocon Dig. (IEEE)*, 2 pp.
Wood, S. D., Mangum, B. W., Filliven, J. J., and Tillett, S. B. (1978). An investigation of the stability of thermistors. *J. Res. Nat. Bur. Stand.* **83**, 247–263.
Yamazaki, S. (1977). Quartz thermometers achieve high accuracy. *JEE, J. Electron. Eng.* **131**, 59–61.
Yoda, H. (1974a). Crystal oscillators growing influence in watch field. *JEE, J. Electron. Eng.* **87**, 37–42.
Yoda, H. (1974b). Crystal watches herald new dimension in timepiece field. II. *JEE, J. Electron. Eng.* **88**, 44–48.
Yoda, H. (1975). A view of general trends in electronic watches and new developments in watch oscillators. *JEE, J. Electron. Eng.* **101**, 12–14.
Yoda, H. (1977). Quartz Crystal units for electronic watches become standardized. *JEE, J. Electron, Eng.* **121**, 42–45.
Yoda, H., and Horie, N. (1974). Technical aspects of crystal wrist watches. I. *Proc. 28th Annu. Freq. Control Symp.*, pp. 57–66.

Chapter 16

Anonymous. (1980). Quartz crystals for accuracy. *Telonde (France)* (1), 38–41.
Filler, R. L. (1983). Modernization of the military specification for quartz crystal units. *Proc. 37th Annu. Freq. Control Symp.*, pp. 519–523.
Holmbeck, J. D. (1971). Standards and the frequency control industry. *Proc. 25th Annu. Freq. Control Symp.*, pp. 148–151.
IEEE (1966). Definitions and methods of measurement for piezoelectric vibrators. *IEEE Standard*, pp. 177–1966.
IEEE (1978). Piezoelectricity. *IEEE Standard*, pp. 176–1978.
Mariani, E. A. (1983). Review of new military specification on surface acoustic wave devices. *Proc. 37th Annu. Freq. Control Symp.*, pp. 525–526.
Meeker, T. R. (1979). A review of the new IEEE standard on piezoelectricity. *Proc. 33rd Annu. Freq. Control Symp.*, pp. 176–180.
Nelson, D. W. (1969). Another look at specifying a crystal. *Proc. 23rd Annu. Freq. Control Symp.*, pp. 111–121.
Rosati, V., and Schodowski, S. (1983). Revision of the military specification for quartz crystal oscillators (MIL-0-55310). *Proc. 37th Annu. Freq. Control Symp.*, p. 524.
Szlavy, A. (1980). Quartz crystals in electronics. II. *Finommech.-Mikrotech.* **19**, 172–180. In Hungarian.

Index to Volumes 1 and 2

Bold faced numerals indicate the volume in which the following pages appear. For subjects that appear on two or more consecutive pages, only the first page in that range is listed.

A

Absorber, nonlinear, **2:** 188
Absorption
  cell, **2:** 188
  dip, **2:** 183
  of gases, **1:** 275
Acceleration, due to gravity, **2:** 269
  sensitivity, **1:** 182
  transducer, **2:** 292
Accuracy, **2:** 126
  atomic standards, **1:** 126
Acoustic loss, **1:** 148, 150
Acoustic relaxation, **1:** 150, 154
Acoustic properties, modification, **1:** 280
Acoustic transmission, line, **1:** 249
Acoustical coupling, **1:** 199
Active hydrogen maser, **2:** 162
Additive noise, **2:** 275, 278
Admittance. *See also* Immittance
  acoustic, **1:** 233
  crystal, **2:** 50, 51
  transducer, **1:** 251
AGC, **2:** 59
Aging, **1:** 271
  causes of, **1:** 273
  influence of mounting and adhesives, **1:** 282
  influence of operating power, **1:** 282
  isolation of causes, **1:** 277
  as one-rate process, **1:** 277
  SAW delay lines, **1:** 283
  of surface-wave (SAW) devices, **1:** 279
  of SAW resonators with etched groove arrays, **1:** 281
  tuning fork, **1:** 273
Aging processes, **1:** 273
Aging rate
  for low-frequency crystal, **1:** 272
  of thickness-shear resonators, **1:** 273
Air-abrasive unit, **1:** 169
Airgap electrodes, **1:** 277
Allan variance, **2:** 201
Alpha-quartz. *See also* Quartz
  Al-hole center, **1:** 43
  aluminum concentration, **1:** 44
  conductivity, **1:** 44
  determination of Q, **1:** 41
  dielectric loss, **1:** 44
  electrical conductivity, **1:** 43
  electron spin resonance, **1:** 43
  infrared absorption, **1:** 41, 44
  interstitial ions, **1:** 42
  radiation hardness, **1:** 44
  resonator resistance, **1:** 44
  specific heat, **1:** 40
  sweeping effectiveness, **1:** 42
  thermal conductivity, **1:** 40
  thermal diffusivity, **1:** 40

Aluminum phosphate (berlinite), **1:** 20
Admittance circle, **2:** 9
Ammonia, **2:** 149
Ammonia maser, **2:** 115, 169
Amplifier
  sustaining, **2:** 55
  phase errors, **2:** 60
Amplitude
  measurements, **2:** 32
  of oscillation, **2:** 289
  transmission factor, **1:** 134
Analysis, statistical, **2:** 197
Anelastic absorption, **1:** 157
Anelastic loss, **1:** 157
Anelastic process, **1:** 150
Anelasticity, **1:** 36
Angle, crystallographic, **1:** 71. *See also* Cut
Anisotropy. *See* Crystal
Annealing, **1:** 153
Annealing process, **1:** 154
Anodization, **1:** 174
Antiresonance, **2:** 15
Antisymmetric modes, **1:** 201
Apodization, **1:** 263
Apodization weighting, **1:** 264
Application in science of atomic standards, **2:** 174
  gravitational potential, **2:** 174
  gravitational red shift, **2:** 174
  relativity, **2:** 174
Application in technology of atomic standards, **2:** 175
  communication, **2:** 175
  navigation, **2:** 175
Approximation. *See also* Simulation; Theory
  Mindlin, **1:** 60
  quasi-static, **1:** 52
  thin plate, **1:** 56, 60
    power series, **1:** 90, 93
    trigonometric, **1:** 93
Array, reflective, **1:** 126
Array grooves, **1:** 122, 127
AT cut, **1:** 182, 213
Atmospheric effects, **2:** 251
Atom detector, **2:** 142
Atomic clock, **2:** 115
Atomic hydrogen maser, **2:** 161
  frequency stability, **2:** 163
Atomic clock, **2:** 116
  accuracy, **2:** 116
  long-term measurement, **2:** 219
  primary standards, **2:** 116
  time-keeping potential, **2:** 125
Atomic resonator, **2:** 122
Atomic standard, passive, **2:** 126
Atomic time, international (TAI), **2:** 268
Atomic transition, **2:** 177
Autoclave, **1:** 26
Axis. *See* Coordinate

B

B mode, **2:** 295
Balanced bridge, **2:** 25, 27, 30, 40
Balanced-bridge measurement, **2:** 36
Bandpass shaping, **1:** 238
Bandstop filters, SAW, **1:** 266
Bandwidth
  hardware, **2:** 205
  software, **2:** 205
  transition, **1:** 269
Bar, thin, narrow, **1:** 78, 80
Barium oxide, **2:** 148
Baseband, **1:** 258
Baseline interferometry, **2:** 263
BAW oscillator, **2:** 47
Beam optics, **2:** 139
Beam trajectories, **2:** 139
Berlinite ($AlPO_4$), **1:** 219
Bidirectional loss, **1:** 243
Bimorph, **1:** 83, 87
Bismuth germanium oxide, **1:** 19
Boundary condition, **1:** 52, 67, 79, 86, 93, 104
Bragg diffraction, **1:** 165
Breit–Rabi equation, **2:** 116
Bridge attenuation, **2:** 29
Bridge unbalance, **2:** 29
Broadening
  homogeneous, **2:** 182
  inhomogeneous, **2:** 182
BT cut, **1:** 182
Buffer gas, **2:** 151
Bulk-wave model, **1:** 232, 241, 245, 257
  advanced, **1:** 249
Bulk-acoustic-wave oscillator. *See* BAW oscillator
BVA_2 technology, **2:** 296

C

C mode, **2:** 295
Cadmium sulfide, **1:** 213
Capacitance
  clamped, high-frequency, **1:** 80
  free, low-frequency, **1:** 80
  interdigital transducer, **1:** 236
  motional, **1:** 106
  ratio, **1:** 71
  shunt, **1:** 106
Capacitive weighting, **1:** 263
Carrier frequency, **1:** 232, 259
Cavity
  design, **1:** 132
  dielectrically loaded, **2:** 281, 284
  Fabry–Perot, **1:** 122, 129
  lead and niobium, **2:** 281
  lead–ceramic, **2:** 284
  niobium, frequency stability, **2:** 282
  phase shift, **2:** 147, 149
  pulling, **2:** 141, 161
  sapphire sphere, **2:** 284
  spacing, **1:** 126
  stabilization, **2:** 162
  superconducting, environmental sensitivity, **2:** 283
  superconductive, **2:** 281
Center frequency
  grating-reflection band, **1:** 133
  stopband, **1:** 128
Centrosymmetric crystal, **1:** 3
Ceramic filters, **1:** 187
Cesium frequency standard, **2:** 186
Cesium maser, **2:** 166
Cesium resonator, **2:** 236
Cesium standards, accuracy, **2:** 236
Cesium-beam standard, **2:** 143
C field, **2:** 117
Characteristic frequencies, **2:** 11
Characteristic parameters, **2:** 11
Charge compensator, **1:** 148
Chebyshev polynominals, **1:** 254
Chemical etching, **1:** 213
Chemical polishing, **1:** 32
Chi-squared distribution, **2:** 211
Christoffel, **1:** 58, 65, 74
CI meter. *See* Crystal impedance meter
Circuit. *See* Network
Cissoidal impedance plot, **2:** 10
Cleaning technology, **1:** 170
Clear-access signal, **2:** 261
Clock flyover mode, **2:** 261
Clock transition, **2:** 117
Clocks, portable, **2:** 251
Coaxial techniques, **2:** 253
Coefficient, temperature, **1:** 110. *See also* Constant
Coefficients as function of angle, **2:** 101
Coherence, **2:** 179
Coherent observation time, **2:** 122
Collimation, **2:** 137
Collimator, **2:** 159
Collisions, **2:** 151
Coloration of quartz, **1:** 155
Common-view approach, **2:** 262
Common-view technique, **2:** 236
Communication satellite, **2:** 260
Comparison of frequency standards with regard to volume, weight, power demand, and selling price, **2:** 174
  cesium beam, **2:** 174
  crystal oscillator, **2:** 174
  hydrogen maser, **2:** 174
  rubidium gas cell, **2:** 174
Compensation, in dual-mode oscillator, **2:** 289
Compliance tensor, **1:** 9
Confinement, of the atom, **2:** 122
Constant
  elastic
    fourth-order, **1:** 57
    stiffened, **1:** 59
    third-order, **1:** 56, 58
  material, higher order, **1:** 55
  quartz, piezoelectric, **1:** 107
Constitutive equations, **1:** 8, 246
Constitutive relations, **1:** 120
Contaminant, **1:** 170
Convention, sign, **1:** 54
Conversion method, multiple, **2:** 227
Cooling, of atoms or ions, **2:** 170
Coordinate
  laboratory, **1:** 64
  material, **1:** 54
  normal. *See* Mode, normal; Eigenvector
  rotation, **1:** 55
  time, **2:** 269
Coriolis acceleration, sensitivity, **2:** 292
Cost-effectiveness, of clock transports, **2:** 252
Coupled-mode analysis, **1:** 133

Coupled-mode formalism, **1:** 128
Coupled-resonator device, **1:** 199
Coupled strip resonator, **1:** 206
Coupling, elastic, **1:** 51, 82, 90
Coupling coefficient, **1:** 120; **2:** 6
  electromechanical (piezoelectric), **1:** 69, 71, 75, 80, 83, 85, 100
  piezoelectric, **1:** 213
Coupling factor, effective, **1:** 253
Coupling-of-modes technique, **1:** 127
Crossed-field bulk-wave model, **1:** 245
Crossed-field model, **1:** 247, 250
Cryogenic-oscillator transmission filter, **2:** 283
Crystal
  doubly rotated, **2:** 102
  drive level, **2:** 55
  motional resistance, **2:** 55
  overtone mode, **2:** 60
  of rhomboid geometry, **1:** 277
  semiconducting, **1:** 52. *See also* Resonator; Cut; Constant
Crystal-controlled oscillator, **2:** 47
Crystal filter, **1:** 187
  acoustically coupled, **1:** 191
  bandpass, **1:** 189
  discrete-resonator, **1:** 192
  monolithic, **1:** 187
  two-pole, narrow-band, **1:** 196
  wide-band, symmetrical lattice, **1:** 196
Crystal header, **1:** 175
Crystal holder, **1:** 175
Crystal impedance meter, **2:** 3, 19
Crystal oscillator, **2:** 51
  frequency stability, **2:** 100
  packaged, **2:** 51, 52
  temperature compensated, **2:** 51
  temperature controlled, **2:** 52
  voltage controlled, **2:** 51
Crystal resonator, **2:** 2
  in electrical circuits, **2:** 4
  electrodeless, **2:** 80
Crystal systems, **1:** 3
Crystal unit, **2:** 7
Crystallographic axis, **1:** 4
Customer–vendor relationship, **2:** 298
Current
  drive, **1:** 56
  resonator, **1:** 75, 79, 86, 89
Cutting crystals, **1:** 163
Cutoff frequency, **1:** 203, 207
Cut, doubly rotated, **1:** 167
Cut, quartz. *See also* Resonator; Mode
  AT, BT, **1:** 111
  CT, DT, **1:** 77
  GT, **1:** 50
  IT, **1:** 111
  LC, **1:** 111
  RT, **1:** 111
  SC, **1:** 69, 111
  X, Y, **1:** 111
Cyclotron orbit, of electron, **2:** 189
Czochralski technique, **1:** 15, 19

D

Deep-space experiments, **2:** 268
Defect center, substitutional Al^{3+}, **1:** 148
Deformation. *See also* Displacement
  elastic, **1:** 79
  finite, **1:** 57
Degree of freedom, **2:** 213
Delay
  differential, **2:** 236
  temperature coefficient, **1:** 120
Delay line, **1:** 267
  frequency response, **1:** 134
  (YZ) $LiNbO_3$, **1:** 253
Delay-line filter, **1:** 121
Delay-line system, **2:** 222
Density
  α-quartz, **1:** 12
  aluminum phosphate, **1:** 21
  bismuth germanium oxide, **1:** 20
  lithium niobate, **1:** 14
  lithium tantalate, **1:** 14
Desorption of gases, **1:** 275
Dewar flask, **2:** 105
Detector, atomic beam device, **2:** 137
Deuterium maser, **2:** 166
Dicke regime, **2:** 121
Dielectric cavity, **2:** 166
Dielectric constants, **1:** 5
Differential propagation, **2:** 263
Diffraction, SAW, **1:** 262
Digital computation methods, **2:** 63
Digital measurement, **2:** 217
Digital signal processing, **2:** 198
Dipole, **2:** 138
  double, **2:** 138
  multiple, **2:** 138

Dipole movement, **2:** 138
  electric, **2:** 138
  magnetic, **2:** 138
Dipole optics, **2:** 139
Diode, step-recovery, **2:** 135
Discriminator, **2:** 222
Disc resonator, **1:** 222
Dislocations, **1:** 29
Dispersion relations, **1:** 51, 60, 82, 94, 247
Displacement. *See also* Deformation
  elastic, **1:** 79, 90, 92
  electric, **1:** 52, 78, 234
Displacement effects, **1:** 152
Dissemination techniques, **2:** 271
Dissociation, of H_2, **2:** 160
Distortion, in FM, **2:** 131
Diurnal variations, **2:** 237
Doppler broadening, **2:** 182
Doppler effect, **2:** 120
  first-order, **2:** 120
  second-order, **2:** 120
Doppler frequency, **2:** 183
Doppler velocity, **2:** 183
Doppler width, **2:** 183
Double-heterodyne system, **2:** 135
Drift rate, **2:** 80
Drive. *See* Current
Drive level, **2:** 35
Dual-beam device, **2:** 144
Dual-mixer technique, **2:** 229
Dynamic frequency–temperature effect, **2:** 37

E

E^1 center. *See* Oxygen vacancy
Effects
  temperature, **1:** 110
  thermal. *See* Effects, temperature
  magnetic, **1:** 61
Eigenvalue, **1:** 64, 67, 74
Eigenvector, **1:** 65, 67, 74
Eight-pole filter, **1:** 209
Elastic compliance, **1:** 7
Elastic constant, **1:** 6
  changes, **1:** 153
  compliance, **1:** 12
    α-quartz, **1:** 12
    lithium niobate, **1:** 14
    lithium tantalate, **1:** 16
  nonlinear, **1:** 218
  stiffness, **1:** 12
    α-quartz, **1:** 12
    aluminum phosphate, **1:** 21
    bismuth germanium oxide, **1:** 20
    lithium niobate, **1:** 14
    lithium tantalate, **1:** 16
Elastic nonlinearity, **1:** 218
Elastic stiffness, **1:** 7
Electric displacement, **1:** 5
Electric field, **1:** 5
Electric polarization, **1:** 5, 8
Electric susceptibility, **1:** 5
Electric-dipole transition, **2:** 169
Electrical analog, of a mechanically vibrating system, **2:** 4
Electrical measurements, on crystal resonators, **2:** 16
Electrical noise, **2:** 51
Electrode, **1:** 87
  interdigital (IDT), **1:** 120
  mass loading, **1:** 100
Electrode positioning, **1:** 260
Electrode withdrawal, **1:** 263
Electromechanical coupling constant, **1:** 241, 255
Electron bombardment, **1:** 174
Electron–hole pair, **1:** 148
Electron multiplier, internal, **2:** 145
Electron spin resonance, **1:** 33, 155
Elliptic integral, **1:** 236
Emissivity factor, **2:** 106
Enantiomorphous form, **1:** 3
Enclosure, **1:** 175
  alumina ceramic, **1:** 274
Energy trapping, **1:** 93, 99. *See also* Resonator
Environmental effects, **1:** 182; **2:** 173
  cesium beam, **2:** 173
  crystal oscillator, **2:** 173
  hydrogen maser, **2:** 173
  rubidium gas cell, **2:** 173
Equation
  constitutive, **1:** 52, 60, 66, 73, 78, 81, 92, 104
  differential, **1:** 53, 92, 104
  frequency, **1:** 51, 68
  graphical solution, **1:** 69
Equivalent circuit, SAW IDTs, **1:** 250
Equivalent electrical circuit, **2:** 2, 4, 6, 43
  elements, **2:** 14

Equivalent motional inductance, **2:** 49
Error-correcting routines, **2:** 31
Etch, **1:** 167
Etched grooves, **1:** 126
Etch tunnels, quartz, **1:** 30, 32
Etching, **1:** 32
Evaporation, **1:** 174
Excitation
  lateral, of plates, **1:** 64, 73
  parallel-field. *See* Excitation, lateral
  parallel to length, in bars, **1:** 78
  perpendicular to length in bars, **1:** 80, 87
  thickness, of plates, **1:** 63, 81, 83
Extension, of frequency measurements, **2:** 186
Extrapolation, of shorter tests, **1:** 281
Extraterrestrial time and frequency comparison, **2:** 253

F

Fabrication, SAW devices, **1:** 178
Fabrication facility, crystals, **1:** 176
Feedback, **2:** 54
  positive, **2:** 47
Field electric, **1:** 52, 78, 92
Figure, of merit, **2:** 14
Filter
  asymmetric-amplitude, **1:** 263
  bulk-acoustic-wave (BAW), **1:** 187, 230
  discrete-resonator, **1:** 191
  disk–wire, **1:** 225
  dispersive, **1:** 262
  electromechanical, **1:** 187, 221
  extensional-mode, **1:** 224
  half-lattice, **1:** 193
  hermitian-baseband, **1:** 263
  lattice, **1:** 193
  mechanical, **1:** 188
  monolithic crystal, **1:** 93, 102
  nondispersive, **1:** 262
  SAW resonator, **1:** 230
  surface-acoustic wave (SAW), **1:** 187
  tapped delay-line. *See* Filter, transversal
  television IF. *See* Television IF filter
  three-phase, **1:** 263
  torsional mode, **1:** 226
  transversal, **1:** 187
  tuning fork, **1:** 224
  two-phase, **1:** 263
  (YZ)$LiNbO_3$, response curve, **1:** 256
Filter measurements, **2:** 19
Filter synthesis, impulse response, **1:** 263
Filter transfer formation, **2:** 194
Flexure-mode bars and plates, **1:** 223
Flicker
  of frequency floor, **2:** 168
  of phase noise, **2:** 124
Flicker floor, **2:** 123
Flop-in, flop-out system, **2:** 143
Flow
  generalized, **1:** 64
  heat, **1:** 61
  power, **1:** 60
Fluorescence, **2:** 150
Forbidden transitions, **2:** 189
Force. *See also* Stress
  generalized, **1:** 64
  static, **1:** 58
Fourier frequency, **2:** 193
Fourier transform, **1:** 121, 239, 250, 256, 258; **2:** 199
Fractional frequency accuracy, **2:** 173
  cesium beam, **2:** 173
  crystal oscillator, **2:** 173
  hydrogen maser, **2:** 173
  rubidium gas cell, **2:** 173
Fractional frequency stability, **2:** 172, 242
  cesium beam, **2:** 172
  crystal oscillator, **2:** 172
  hydrogen maser, **2:** 172
  rubidium gas cell, **2:** 172
Fractional linewidth, **2:** 121, 178
Frequency
  antiresonance, **1:** 66, 69, 102, 106
  cutoff, **1:** 95
  fractional, **2:** 195
  inharmonic, **1:** 98, 100
  instantaneous, **2:** 196
  mean, **2:** 207
  of oscillation, **2:** 48
  resonance, **1:** 66, 69, 98, 102, 106
  torsional, **1:** 76
Frequency accuracy, **2:** 47
Frequency adjustment, varactor diode, **2:** 86
Frequency anomalies, **1:** 217
Frequency change, **1:** 149
  short-term, **1:** 271
Frequency deviation, fractional, **2:** 200
Frequency division, one-step, **2:** 189
Frequency domain, **2:** 203

Frequency drift, **2:** 207
  aging, **2:** 124
Frequency–drive-level effect, **2:** 35
Frequency fluctuations, random, **1:** 284
Frequency instability, sources, **2:** 48
Frequency-lock servo, **2:** 128
  frequency modulation, **2:** 129
  integrator, **2:** 130
  phase modulator, **2:** 130
Frequency measurement, **2:** 219
  interpretation, **2:** 93
  long-term drift, **2:** 93
  short-term measurement, **2:** 93
  optical regime, **2:** 186
Frequency multiplication, **2:** 231
Frequency reproducibility, **2:** 182
Frequency response, hermitian, **1:** 261
Frequency stability, **1:** 180; **2:** 47, 182, 193, 195
  long-term, **2:** 57
  measurement, **2:** 89
    beat-frequency method, **2:** 90
    dual-mixer technique, **2:** 90
  short-term, **2:** 93
    definition, **2:** 93, 94
    power spectral density function, **2:** 95
    time domain representation, **2:** 95
Frequency–temperature
  and aging measurements, **2:** 37
  rate of change, **2:** 103
Frequency–temperature dependence, of a quartz crystal resonator, **2:** 17
Frequency synthesis, **2:** 227
  stabilized-laser, **2:** 187
Frequency syntonization accuracy, **2:** 271
Frequency transfer, **2:** 252
Frequency transients, stress induced, **2:** 294

G

Gain curve, laser, **2:** 181
Gas cell, **2:** 150
Generalized motional arm reactances, **2:** 41
Generic sources, of measurement errors, **2:** 3
Getter, **2:** 144
Global high-precision comparison, of clocks, **2:** 264
Global positioning system (GPS), **2:** 260
Geostationary meteorological satellite, **2:** 266
Geostationary operational environmental satellite (GOES), **2:** 253
Geostationary satellite, **2:** 270
GOES satellite time code, **2:** 257
Goniometer, **1:** 167
Gradients, thermal, **1:** 55, 60
Graphite-coated surface, **2:** 144
Grating positioning, **1:** 132
Grating reflector, **1:** 123, 126
Green's function, **1:** 249
Groove depth, **1:** 131
Ground-wave accuracy, **2:** 248
Ground-wave propagation, **2:** 248
Group delay, **1:** 265
Growth
  berlinite ($AlPO_4$), **1:** 22
  $LiNbO_3$, **1:** 15
  $LiTaO_3$, **1:** 17

H

Heater location, **2:** 104
Heisenberg's uncertainty relationship, **2:** 122
Heterodyne technique, **2:** 220
Hexapoles, **2:** 138
High-polymer coating, **2:** 158
High-Q LC circuits, **2:** 275
Hilbert transform, **1:** 236, 251
Holder
  cold-welded metal, **1:** 275
  glass, **1:** 275
Holder design, **1:** 274
Hole, **1:** 148
Hole burning, **2:** 182
Hole-compensated Al center, **1:** 151
Hole-compensated centers, **1:** 156
Homodyne technique, **2:** 221
Hydrogen anneal, **1:** 278
Hydrogen effects, **1:** 154
Hydrogen maser, **2:** 159
Hydrogen storage beam tube, **2:** 168
Hydrothermal growth, **1:** 25, 29
Hyperfine energy level, **2:** 118
Hysteresis, **2:** 38, 111

I

Iconoscope, **1:** 165

IDT
acoustic reflection, **1:** 257
admittance, **1:** 130, 273
aperture, **1:** 243
apodization, **1:** 132
bandwidth, **1:** 242
double electrode, **1:** 236
electrical Q, **1:** 242
frequency response, **1:** 134
frequency specification, **1:** 259
impedance element, **1:** 268
impulse response, **1:** 121
maximum coupling, **1:** 242
perturbation, **1:** 263
self-resonant, **1:** 268
series resistance, **1:** 131
simple electrode, **1:** 236
size, **1:** 131
spurious resonator modes, **1:** 131
synchronous frequency, **1:** 133
three-phase, **1:** 265
transverse modes, **1:** 132
unapodized, **1:** 130
unwanted modes, **1:** 132
IF substitution method, **2:** 32
Imaging technique, **1:** 262
Immittance
elastic wave, **1:** 65
matrix, **1:** 64
normalized, **1:** 70
resonator, **1:** 62, 75, 79, 82, 102
Immittance diagram, **2:** 2
Immittance plot, **2:** 36
Impedance. *See also* Immittance
characteristic, **1:** 248
crystal, **2:** 51
mechanical, **1:** 246
Impedance analyzer, **2:** 33
Impedance circle, **2:** 9
Impulse model, **1:** 233, 239
delta-function, **1:** 257
sine-wave, **1:** 257
Impulse response
baseband, **1:** 259
finite, **1:** 258
real, **1:** 260, 261
Impurity content, **1:** 148
Impurity defects, model, **1:** 148
Impurities, effect of, **1:** 278
Inductance, motional, **1:** 106, 112
Inductorless bandwidth, **1:** 211
Inductorless limit, **1:** 211
Inelasticity, **1:** 217
Inflection point, **2:** 61
Infrared absorption, **1:** 148
Initial aging, **1:** 273
Initial stabilization period, **1:** 273, 278
In-line model, **1:** 247
Insertion loss, **1:** 232, 242; **2,** 69
SAW delay line, **2:** 69
SAW resonator, **2:** 71
Insulation, foam, **2:** 105
Interaction region, **2:** 139, 145
Interdigital transducer, **1:** 230. *See also* IDT
Interferometry, very-long-baseline (VLBI), **2:** 268
Intermediate-band design, **1:** 198
Intermodulation, **1:** 216
International atomic time (TAI), **2:** 234
International symbols, **1:** 4
Interstitial impurities, **1:** 154
Inversion transition, **2:** 169
Inverter, admittance, **1:** 251
Ion
individual, **2:** 189
in Penning trap, **2:** 189
Ion-etch process, **1:** 138
Ion implantation, **1:** 126
Ion milling, **1:** 179, 213
Ion mobility, **1:** 183
Ion pump, **2:** 144
Ion storage, **2:** 169
Ion trap, radio-frequency, **2:** 170
Ionic current, **1:** 157
Ionization potential, **2:** 148
Ionizing radiation, **1:** 39, 147, 183
Ionosphere, **2:** 237, 242
Ionosphere propagation errors, **2:** 262
IR studies, **1:** 155
Isolation amplifier, **2:** 21, 30
Isotopic overlap, **2:** 157

J

Jaumann network. *See* Filter, half-lattice

K

Kirchhoff, **1:** 90
Krypton light source, **2:** 179

L

Lamb dip, **2:** 183
Lapping saw, **1:** 164
Laser
CO_2, **2:** 187
color-center, **2:** 188
diode, **2:** 149
dye, **2:** 149, 188
F-center, **2:** 189
fine and coarse tunable, **2:** 189
HCN, **2:** 186
He–Ne, **2:** 180, 186
with CO_2 cell, **2:** 185
with I_2 cell, **2:** 185
with Methane cell, **2:** 185
with Ne cell, **2:** 184
H_2O, **2:** 187
millimeter-wave, **2:** 188
potential role, **2:** 179
saturation-absorption stabilized, **2:** 186
tunable, **2:** 188
Laser–methane cell combination, **2:** 182
Laser signals, pulsed, **2:** 264
Laser stabilization, **2:** 182
Laser synchronization, **2:** 263
Lateral field resonator, **1:** 276
Lateral field excitation, **1:** 220
LC-cut, **1:** 182
Legendre polynominal, **1:** 236
Length standard, **2:** 178
Length and time standard, combined, **2:** 178
Level control, automatic (ALC), **2:** 54, 56, 84
LF (low frequency) broadcast, **2:** 242
Lifetime, resonator-limited, **2:** 173
cesium beam, **2:** 173
crystal oscillator, **2:** 173
hydrogen maser, **2:** 173
rubidium gas cell, **2:** 173
Lift-off process, **1:** 138
Light shift, **2:** 158
Line shape, Lorentzian, **2:** 128
Line width, **2:** 121
natural, **2:** 121
Lithium niobate, **1:** 11, 219, 241
YZ-cut, **1:** 241, 243, 248
128° Y-cut, **1:** 266
Lithium tantalate, **1:** 11, 213, 220
doubly rotated cuts, **1:** 220
rotated-Y-cut monolithic filters, **1:** 220
rotated-Y-cut resonators, **1:** 220
X-cut, **1:** 220
Z-cut, **1:** 220
Load capacitor, **2:** 12, 24, 35
Long-term aging, **1:** 179. *See also* Aging
Long-term drift, **2:** 48. *See also* Aging
Long-term stability, **2:** 125
atomic standards, **2:** 125
Loop filter, **2:** 225
Loop gain vector, **2:** 48
Loop-phase conditions, **2:** 57
Loop-phase error, **2:** 20
Loran-C, **2:** 235, 248
Lorentzian line shape, **2:** 194
Loss–bandwidth relation, **1:** 243
Loss–fractional bandwidth, **1:** 244
Lumped-element-equivalent electrical circuit, **2:** 41
Lumped-mass spring system, **2:** 5

M

Magnetic dipole moment, **2:** 119
Magnetic dipole transition, **2:** 117
Magnetic field dependency, **2:** 118
Magnetic field environment, **2:** 252
Magnetic field inhomogeneities, **2:** 146
Magnetic hyperfine splitting, **2:** 119
Magnetic hyperfine transition, **2:** 116
Magentic shielding, **2:** 117
Magnetostrictive ferrites, **1:** 221
Magnetostrictive transducer, **1:** 222
Majorana transition, **2:** 147
Maser, oscillating threshold, **2:** 161
Maser oscillator, **2:** 135
active, **2:** 126
Mass changes, **2:** 17
Mass loading, **1:** 204, 274
crystal resonator, **2:** 288
Mass spectrometer, **2:** 145
Material. *See also* Crystal
Material changes, **1:** 274
Material quality, **1:** 157
Matrix, **1:** 9, 54, 61, 65, 78, 81, 83, 85, 88. *See also* Tensor; Immittance
Maximum admittance, **2:** 16
Maxwell distribution, **2:** 121, 138
Measurement hierarchy, **2:** 197
Memory, **2:** 110
Mercury resonances, **2:** 170

Metallization, **1:** 181
Meteorological monitor, **2:** 289
Meteorological satellite system, **2:** 257
Methane cell, **2:** 181
Metrology, **2:** 171
  astronomical time, **2:** 171
  atomic time, **2:** 171
  coordinated universal time, **2:** 171
  international atomic time, **2:** 171
  radio astronomy, **2:** 171
  timekeeping, **2:** 171
  very-long-baseline interferometry, **2:** 171
Microcircuit bridge, **2:** 29
Microcircuit chip resistor, **2:** 24
Microwave cavity, **2:** 141
Microwave interrogation, **2:** 139
Mindlin, **1:** 60, 90
Minimum impedance, **2:** 16
Mirror, equivalent, **1:** 129
Mixer efficiency, **2:** 128
Mobility analogy, **1:** 221
Mode
  A,B,C, thickness, **1:** 68, 71
  contour, **1:** 77
    flexure, **1:** 51, 77
  coupled, **1:** 51, 82, 90
  dilatation, **1:** 52
  extension, **1:** 77, 80, 93
  face-shear, **1:** 81, 90, 93
  flexure, **1:** 83, 87, 90, 93
  normal, **1:** 62, 64, 74
  resonance, **1:** 50
  shear, fast, slow, **1:** 68
  single, **1:** 65
  spectrum, **1:** 56; **2:** 33
  thickness, **1:** 63, 73
  thickness shear, **1:** 51, 72, 93
  thickness twist, **1:** 93
  torsion, **1:** 51, 75
Mode coupling, nonlinear, **1:** 216
Mode spacing, **1:** 207
Modified crystal resonator, **2:** 7
Modulation, square-wave, **2:** 132
Molecular flow, **2:** 137
Molecular hydrogen, **2:** 159
Monolithic crystal filter, **1:** 199
Mössbauer effect, **2:** 121
Motional arm, **2:** 5, 38
Motional-arm resonance, **2:** 14
Motional energy, **1:** 157
Motional resistance, **2:** 49
Mounting, **1:** 175
Mounting structure, **2:** 7
Mounting system, **1:** 272
Mount, type of, **1:** 180
Multistrip coupler, **1:** 265

N

Na defect, **1:** 150
Narrow-band (NB) design, **1:** 198
Natural linewidth, **2:** 122
NAVSTAR. *See* Global Positioning System
Navy navigational satellite system (NNSS), **2:** 258
Network
  distributed, **1:** 104
  equivalent electric, **1:** 87, 103
  lumped element, **1:** 103
  multiport, **1:** 65
Network analyzer, **2:** 23, 30, 36
Noise, **2:** 204, 206
  amplitude, **2:** 195
  flicker frequency, **2:** 204
  flicker phase, **2:** 204
  in oscillators, **2:** 193
  perturbing the phase, **2:** 276
  phase, **2:** 195
  phase-fluctuation, **2:** 84
  pseudo-random (PRN), **2:** 265
  in SAW oscillators, **2:** 72
    flicker noise, **2:** 74
    phase noise, **2:** 72
  random-walk frequency, **2:** 204
  white frequency, **2:** 204
  white phase, **2:** 204
  wideband, **2:** 54
Noise bandwidth, **2:** 194
Noise floor, **1:** 124
Noise processes, **2:** 94
  frequency-scintillation noise, **2:** 94, 96
  frequency white noise, **2:** 94, 96
Noise model, **2:** 196
Noise modulation, **2:** 195
Noise pedestal, **2:** 195
Noise processes, **2:** 94
  phase-scintillation noise, **2:** 94, 96
  phase white noise, **2:** 94, 96
  random-walk-frequency noise, **2:** 94, 96
Nonlinear effects, **1:** 216, 227

Normal-mode analysis, **1:** 234
Normal-mode model, **1:** 233
Normal-mode theory, **1:** 239, 255
Notch filter, **1:** 266
  interferometer, **1:** 267
  (YZ) $LiNbO_3$, **1:** 267
N-sample variance, **2:** 201
Nuclear spin, **2:** 119
Nyquist frequency, **2:** 200

O

Offset methods, **2:** 35
Omega navigation system, **2:** 248
Omega transmitters, **2:** 250
Operational-satellite techniques, **2:** 253
Optical absorption, **1:** 153
Optical detection, **2:** 150
Optical fibers, **2:** 253
Optical frequencies, measurement, **2:** 185
Optical pumping, **2:** 115, 149, 152
Optical transition, **2:** 121
Oriascope, **1:** 165
Oscillating magnetic field, **2:** 121
Oscillator
  all-cryogenic, parametric, **2:** 283
  conditions for SAW oscillation, **2:** 68
  feedback, **2:** 66
  gain control, **2:** 85
  mechanical effects, **2:** 88
    acceleration, **2:** 88
  miniature, **2:** 60
  miniature integrated circuit, **2:** 64
  modified Pierce, **2:** 82
  multifrequency SAW, **2:** 76
  precision quartz crystals, **2:** 79
  temperature-compensated (TCXO), **2:** 108
    analog compensation, **2:** 109
    digital compensation, **2:** 10
    electrical compensation, **2:** 108
    microprocessor compensation, **2:** 111
    thermal loss, **2:** 105
    thermistor-network configurations, **2:** 109
    varactor, **2:** 108
  temperature compensation, of SAW, **2:** 75
  temperature-controlled, **2:** 101
    amplifier as heater, **2:** 105
    crystal oven control circuit, **2:** 102
    double oven, **2:** 102
    dual mode oscillator, **2:** 105
    location, of heater and thermistor, **2:** 104
    rate, of frequency change, **2:** 103
    single oven, **2:** 102
    stabilization time, **2:** 107
    time required to heat crystal, **2:** 107
    uniformity of temperature, **2:** 104
Oscillator circuits, **2:** 53
  bridge, **2:** 54
  Butler, **2:** 60
  common base, **2:** 59
  common collector, **2:** 58
  emitter coupled, **2:** 60
  modified piece, **2:** 56
Oven, **2:** 87
  single-stage, **2:** 87
  temperature control, **2:** 101
  two-chamber, **2:** 137
Oxygen vacancy, **1:** 153

P

Palladium leak, **2:** 160
Parallel field. *See* Lateral field
Parallel resonance, **2:** 15
Paramagnetic center, **1:** 151
Parasitic inductance, **2:** 20
Parseval's theorem, **2:** 194
Passive hydrogen maser, **2:** 162
Path delay, **2:** 254, 257, 266
  variation, **2:** 256
Path-delay correction, **2:** 264
Pattern definition process, **1:** 179
Pattern generator, **1:** 261
Penning trap, **2:** 170
Period measurement, **2:** 219
Performance, of crystal resonators, **2:** 16
Performance model, **2:** 197
Permittivity, **1:** 5
Permittivity constant
  α-quartz, **1:** 12
  aluminum phosphate, **1:** 21
  bismuth germanium oxide, **1:** 20
  lithium niobate, **2:** 14
  lithium tantalate, **1:** 16
Perturbations, acoustic, **1:** 126
Phase
  linearity, **1:** 264
  transfer, **2:** 82
Phase angle, **2:** 18
Phase condition, loop, **2:** 82

Phase detector, **2:** 222
Phase-difference measurement, **2:** 218
Phase error, **1:** 232; **2:** 18, 23
Phase fluctuation, **2:** 51
Phase-lock servo, **2:** 128
Phase-locked loop, **2:** 128, 223
Phase measurement, **2:** 32
Phase multiplier, **2:** 231
Phase noise, **1:** 135
  excess, **1:** 216
  white, **2:** 124
Phase shift
  per collision, **2:** 165
  in crystal network, **2:** 49
  SAW oscillators, **2:** 68
Phase shifter, **2:** 222
Phase slope, **2:** 57, 82
Phase spectrum, **2:** 195
Phase stability, **2:** 48, 60
Photolithography, **1:** 138, 180
Photon recoil, **2:** 121
Photon transformer, **2:** 150
Photoresist, **1:** 138, 178
Piezoelectric ceramics, **1:** 221
Piezoelectric ceramic transducers, **1:** 223
Piezoelectric constants, **1:** 7
Piezoelectric crystal resonator, **2:** 38
Piezoelectric devices, as circuit elements, **2:** 2
Piezoelectric loading, **1:** 204
Piezoelectric matrix. *See also* Tensor; Matrix
  α-quartz, **1:** 9
  bismuth germanium oxide, **1:** 10
  lithium niobate, **1:** 9
Piezoelectric strain coefficients, **1:** 8
Piezoelectric strain constant, **1:** 13
  α-quartz, **1:** 13
  aluminum phosphate, **1:** 21
  lithium niobate, **1:** 15
  lithium tantalate, **1:** 17
Piezoelectric stress coefficients, **1:** 8
Piezoelectric stress constant, **1:** 13
  α-quartz, **1:** 13
  aluminum phosphate, **1:** 21
  bismuth germanium oxide, **1:** 20
  lithium niobate, **1:** 15
  lithium tantalate, **1:** 17
Piezoelectric tensor, **1:** 9. *See also* Tensor; Matrix
Piezoelectrically stiffened resonator, **2:** 41
Piezoelectrically unstiffened resonator, **2:** 41
Pi-network, **2:** 21, 31, 40
Planck's equation, **2:** 122
Planetary lap, **1:** 168
Plasma etching, **1:** 179
Plate, piezoelectric, **1:** 63, 73, 81, 83
Point-contact diodes, **2:** 186
Point groups, **1:** 3
Polariscope, **1:** 165
Polarization, **1:** 2; **2:** 157
Polishing, **1:** 168
  chemical, **1:** 168, 180
Population difference, **2:** 123
Portable clock, **2:** 269
Port
  electrical, **1:** 247
  mechanical, **1:** 247
Position-location system, **2:** 261
Potential
  electric, **1:** 52, 92
  electrostatic, **1:** 237, 239
  Rayleigh wave, **1:** 232
  transducer, **1:** 236
Power flow, acoustic, **1:** 240
Power-law model, **2:** 203
Power spectral density, one-sided, **2:** 231
Power spectrum, **2:** 194
Poynting theorem, **1:** 235
Poynting vector. *See* Flow, power
Pressure changes, **1:** 274
Pressure sensitivity, **1:** 183
Primary frequency standard, **2:** 235
Primary loop, **2:** 135
Processing techniques, SAW, **1:** 138
Propagation delay, **2:** 237, 266
Propagation loss, **1:** 120
Pulling factor, **2:** 168
Pump
  cryogenic, **1:** 172
  diffusion, **1:** 171
  ionization, **1:** 171
  roughing, **1:** 173
  turbo, **1:** 171

Q

Q, **2:** 142. *See also* Quality factor
  cavity, **2:** 142
  electrical, **1:** 237, 242
  line, **2:** 142
  material, **1:** 163

Quadrupoles, **2:** 138
Quality assurance, **2:** 299
Quality factor, **1:** 50, 102; **2:** 14, 38
  atomic frequency standard, **2:** 121
  SAWR, **1:** 124
Quantum transition, **2:** 178
Quartz, **1:** 2, 11. *See also* α-quartz
  acoustic loss, **1:** 28, 33, 36, 38
  $Al-Li^+$ center, **1:** 38
  $Al-Na^+$ center, **1:** 37
  aluminum-related centers, **1:** 33
  anelastic loss, **1:** 36
  Al-hole center, **1:** 33
  charge compensation, **1:** 33
  conductivity, **1:** 156
  coordinate system, **1:** 24
  cultured, **1:** 162, 166
  defects, **1:** 25, 28
  dielectric loss, **1:** 33, 36, 38
  dielectric relaxation, **1:** 156
  dislocations, **1:** 29
  electrical conductivity, **1:** 39
  electrodiffusion, **1:** 35
  electrolytically swept cultured, **1:** 149
  fault surfaces, **1:** 29
  growth, **1:** 25, 27
  high-*Q*, **1:** 149
  high-*Q* cultured, **1:** 28
  infrared absorptions, **1:** 27, 33
  internal friction, **1:** 36
  interstitial impurities, **1:** 32
  lithium-doped, **1:** 149
  mobility of interstitials, **1:** 39
  natural, **1:** 149, 165
  neutron-irradiated, **1:** 153
  oxygen vacancy center, **1:** 35
  phase transition, **1:** 25
  point defects, **1:** 32, 35
  quality factor *Q*, **1:** 36
  radiation response mechanism, **1:** 38
  relaxation time, **1:** 37
  ST-cut, **1:** 241, 248; **2:** 75
  structure, **1:** 23
  thermal properties, **1:** 39
  trimming, **1:** 25
Quartz crystal oscillator, **2:** 126
Quartz crystal units, **2:** 3
Quartz resonator, **2:** 80
  AT-cut, **2:** 60, 80
  double-rotated cuts, **2:** 81
  GT-cut, **2:** 80
  overtone mode, **2:** 61, 81
  SC-cut, **2:** 62, 80
  X-cut, 80
Quartz thermometer, **2:** 294

R

Rabi cavity, **2:** 139
Rabi pedestal, **2:** 140, 146
Radar filters, **1:** 230
Radiation, influence on aging, **1:** 279
Radiation conductance, **1:** 238, 252, 255
Radiation effect, **1:** 147
Radiation loss, **2:** 106
Radio broadcast services, **2:** 242
Radio interference, **2:** 273
Radioactive lifetime, **2:** 151
Ramsey cavity, **2:** 140
Ramsey pattern, **2:** 145
Rayleigh wave, **1:** 119, 232, 234, 246, 252
  amplitude, **1:** 234
  potential, **1:** 240
Reactance, acoustic, **1:** 268
Recoil shift, **2:** 120
Recovery time, **1:** 278
Reference channel, **2:** 23
Reference oscillator, **2:** 126
Reflection
  acoustic, **1:** 249, 257, 264
  bandwidth, **1:** 128
  magnitude, **1:** 128
  phase, **1:** 129
Reflection coefficient, **2:** 16, 23, 25
  grating, **1:** 129
Rejection, out-of-band, **1:** 264
Relation. *See* Equation; Condition
Relativistic corrections, **2:** 268
Relaxation, exponential, **2:** 163
Relaxation time, **2:** 151
Remote frequency calibration, **2:** 250
Remote synchronization, **2:** 268
Replication technique, **1:** 261
Requirements, for oscillation, **2:** 48
Resistance
  anomalous, **1:** 216
  motional, **1:** 113
Resistance anomalies, **1:** 217

Resolution, of balanced-bridge measurements, **2:** 29
Resonance, **2:** 15
  nonlinear, **1:** 216
  with load capacitor, **1:** 15
Resonance curve, **2:** 38
Resonance line
  homogeneous, **2:** 158
  inhomogeneous, **2:** 157
Resonance range, **2:** 9
Resonance spectrum, atomic, **2:** 140
Resonator. *See also* Cut; Mode
  AT, **1:** 94, 111
  BT, **1:** 94, 111
  bulk acoustic wave (BAW), **2:** 3
  contoured, **1:** 100
  CT, **1:** 77, 94
  doubly rotated, **1:** 71, 111
  DT, **1:** 77, 94
  E, F, **1:** 94, 111
  electrodeless, **1:** 182
  extensional mode, **1:** 272
  face-shear mode, **1:** 272
  flexure-type, **1:** 272
  GT, **1:** 50, 94, 111
  IT, **1:** 111
  LC, **1:** 111; **2:** 294
  mass loaded, **1:** 100
  RT, **1:** 111
  SC, **1:** 69, 111; **2:** 295
  sensitivity to temperature gradients, **2:** 102
  surface acoustic wave (SAW), **2:** 3
  trapped energy, **1:** 93, 99
  tuning fork, **1:** 94
  width-shear, **1:** 272
  X, **1:** 111
  Y, **1:** 111
Resonator environment, **2:** 39
Resonator immittance, **2:** 39
Resonator measurement, **2:** 2
Response time, **2:** 296
Rochelle salt, **1:** 2
Rubidium isotope, **2:** 153
Rubidium maser, **2:** 165
Rubidium standard, **2:** 261
  filter cell, **2:** 156
  integrated gas cell, **2:** 156
  photocell, **2:** 156
  pressure shift, **2:** 154
  temperature coefficient, **2:** 154

S

Sample Allan variance, **2:** 214
Sample variance, **2:** 200
Sawing, **1:** 163
SAW, harmonic responses, **1:** 256
SAW bandpass filters, **1:** 257
SAW bandstop filter, **1:** 257. *See also* Bandstop filters, SAW
SAW delay line
  effective Q, **1:** 142
  maximum unloaded Q, **1:** 140
  SAW delay-line filter, **1:** 122
  SAW delay line oscillator, **2:** 68
  SAW filter
    bandwidth, **1:** 243
    insertion loss, **1:** 242, 244
SAW IDT
  dispersive, **1:** 253
  impulse response model, **1:** 232, 239, 254
  in-line model, **1:** 245
  $LiNbO_3$ substrate, **1:** 269
  ST-cut quartz, **1:** 269
  synthesis, **1:** 252
SAW (Surface acoustic wave) oscillator, **2:** 66
SAW reflection, **1:** 254
SAW regeneration, **1:** 254
SAW resonator (SAWR), **1:** 122
  acceleration sensitivity, **1:** 144
  advantages, **1:** 144
  and BAWR, comparison, **1:** 123
  cavity losses, **1:** 135
  fabrication method, **1:** 137
  loss
    conversion of energy, **1:** 137
    coupled to atmosphere, **1:** 137
    diffraction, **1:** 136
    geometrical nonuniformities, **1:** 137
    ohmic, **1:** 135
    material, **1:** 135
    radiation, **1:** 136
    scattering, from imperfections, **1:** 137
    scattering, into bulk waves, **1:** 136
  maximum unloaded Q, **1:** 140
  minimum series resistance, **1:** 142
  one-port, **1:** 125
  performance specification, **1:** 133
  Q, unloaded, **1:** 144
  stability, long-term, **1:** 144

SAW resonator *(continued)*
  temperature stability, **1:** 144
  two-port, **1:** 125
SAW resonator (SAWR) oscillator, **2:** 70
  aging rate, **1:** 143
  force sensitivity, **1:** 143
  new cuts and materials, **1:** 142
  stability, short-term, **1:** 143
  ST quartz, **1:** 142
  temperature stability, **1:** 142
SAW transduction, **1:** 232, 252
SAW trimming, **1:** 138
SAWR model, **1:** 133
Satellite ephemeris error, **2:** 263
Satellite techniques, **2:** 258, 273
Saturated absorption, **2:** 181
Saturated gain, **2:** 183
Scattering-parameter measurements, **2:** 31
SC-cut, **1:** 159, 182, 276
Schering bridge, **2:** 27
Scaling, **1:** 175
Second definition, **2:** 115, 268
Secondary loop, **2:** 135
Sensitivity, to mass changes, **2:** 289
Sensors, **2:** 289
  acceleration, **2:** 291
  chemical, **2:** 289
  environmental, **2:** 289
  force, **2:** 290
  gas, **2:** 289
  hydrostatic pressure, **2:** 291
  temperature, **2:** 293
Separated-oscillatory-field technique, **2:** 140
Series resonance frequency, **2:** 49
Servo electronics, **2:** 127
Servo loop, **2:** 127
Short-term stability, **2:** 124
  atomic standards, **2:** 124
Shot noise, **2:** 124
Sidelobe, time-domain, **1:** 262
Sidelobe ratio, **1:** 232
Signal-to-noise consideration, **2:** 186
Signal-to-noise ratio, **2:** 125
  atomic standards, **2:** 125
  optimum, **2:** 135
Simulation. *See also* Approximation; Theory
  computer, **1:** 56
  finite element, **1:** 56
  Green's function, **1:** 56
  variational, **1:** 56
Sky-wave accuracy, **2:** 248
Slave oscillator, **2:** 127
Source, for atoms or molecules, **2:** 137
Spacelab experiment, **2:** 264
Spatial averaging, **2:** 158
Specification, **2:** 297
  basic, **2:** 299
  military, **2:** 300
Spectral density, **2:** 193, 199
  one-sided, **2:** 198
Spectrum, two-sided, **2:** 193
Speed, of light, **2:** 180
Spin-exchange cavity tuning, **2:** 162
Spin-exchange collisions, **2:** 154, 162
Spurious modes, **2:** 17, 25, 33
Sputter etching, **1:** 179
Sputtering, **1:** 174
Stability
  averaged, **2:** 186
  long term
    BAWR and SAWR, **1:** 124
    SAW, **1:** 138
  of oscillators, **2:** 72
    influence of temperature, **2:** 75
    long-term, **2:** 76
    short-term, **2:** 72
  short-term, **2:** 80, 186
Standard, for frequency, time, and length, unified, **2:** 180
Standard frequency- and time-signal broadcasts, **2:** 238
Standards, **2:** 299
State selection
  optical, **2:** 152
  spatial, **2:** 138
State selector, **2:** 137, 142
Static capacitance C_0, **2:** 38
Static charge, **1:** 183
Static frequency–temperature effect, **2:** 37
Stern and Gerlach experiment, **2:** 119
Stiffness tensor, **1:** 9
Storage bulb, **2:** 159
Storage vessel, **2:** 150
Stored-ion technique, **2:** 170
Strain, elastic, **1:** 52, 92
Strain changes, **1:** 274
Strain tensor, **1:** 7, 9
Stress
  compressional, **1:** 6
  elastic, **1:** 52, 78, 92. *See also* Force

Stress *(continued)*
mechanical, **1:** 2
shear, **1:** 6
tensile, **1:** 6
Stress relaxation, **1:** 150; **2:** 17
Stress tensor, **1:** 7, 9
Stripline oscillator, **2:** 279
Structural defects, **1:** 18
Sub-Doppler observation, **2:** 181
Substitution elements, **2:** 20
Substitution measurement, **2:** 27
Substitution technique, **2:** 39
Substitutional Al^{3+} defect, **1:** 150
Substrate, **1:** 180
Surface-acoustic-wave oscillator. *See* SAW oscillator
Surface-acoustic-wave resonator. *See* SAWR
Surface contouring, **1:** 169
Surface ionization, **2:** 148
Surface layer, **2:** 151
Surface wave, backward-traveling, **1:** 126
Sweep rate, **2:** 33
Sweeping process, **1:** 148, 156
Sweeping technique, **1:** 35
Symmetric modes, **1:** 201
Symmetry, **1:** 54
Synchronization error, **2:** 207
Synchronous detectors, **2:** 32
Synthesis, SAW bandpass filter, **1:** 257
Synthetic quartz, Z-growth, **1:** 151
Syntonization, **2:** 273

T

Tandem lattice configuration, **1:** 196
Tandem two-pole configuration, **1:** 209
TDRS (tracking and data relay satellite), **2:** 265
Television IF filter, **1:** 265
zinc oxide on glass, **1:** 265
$LiNbO_3$ cuts, **1:** 265
Television filters, **1:** 230, 265
Television signals, precise T/F comparison methods, **2:** 250
Temperature coefficient
elastic compliance, **1:** 12
α-quartz, **1:** 12
lithium niobate, **1:** 14
lithium tantalate, **1:** 16
elastic stiffness, **1:** 12
α-quartz, **1:** 12
aluminum phosphate, **1:** 21
lithium niobate, **1:** 14
lithium tantalate, **1:** 16
permittivity, **1:** 12
α-quartz, **1:** 12
lithium niobate, **1:** 14
lithium tantalate, **1:** 16
piezoelectric strain constant, **1:** 13
α-quartz, **1:** 13
lithium niobate, **1:** 15
lithium tantalate, **1:** 17
piezoelectric stress constant, **1:** 13
α-quartz, **1:** 13
aluminum phosphate, **1:** 21
lithium niobate, **1:** 15
lithium tantalate, **1:** 17
Temperature-compensated dielectric-resonator material, **2:** 284
Temperature control
and compensation. *See* Oscillator
of oscillators, **2:** 86
Temperature-control circuit, **2:** 87
Temperature control techniques, **2:** 61
Temperature gradients, **1:** 159
Temperature influence, on aging, **1:** 279
Temperature measurements, **2:** 293
Temperature resolution, **2:** 295
Temperature sensitivity, SAW filters, **1:** 232, 267
Temperature stability requirements, **2:** 61
Temperature stabilization rate, **2:** 53
Temperature transients, **2:** 107, 111
Tensor, **1:** 55. *See also* Matrix
fourth-rank, **1:** 7
second-rank, **1:** 7
Tensor notation, **1:** 9
Terrestrial-based T/F services, **2:** 259
Terrestrial methods, **2:** 237
Terrestrial time comparison, **2:** 266
Test channel, **2:** 23
Test network, **2:** 31
Test oscillator, **2:** 19
T/F dissemination experiments, **2:** 266
Thallium, **2:** 148
Theory. *See also* Approximation; Simulation
linear, **1:** 53
nonlinear, **1:** 56
Thermal conductivity, **1:** 19; **2:** 106

Thermal effects, **1:** 158
Thermal expansion
α-quartz, **1:** 12
aluminum phosphate, **1:** 21
lithium niobate, **1:** 14
lithium tantalate, **1:** 16
Thermal gradient effect, **1:** 276
Thermal isolation, **2:** 86
Thermal noise, **2:** 275
Thermal resistance, **2:** 107
Thermistor location, **2:** 104
Thickness-shear vibration, **1:** 202
Thickness-shear (TS) wave, **1:** 204
Thickness-twist (TT) wave, **1:** 204
Thin-film measurement, **2:** 288
Time
and frequency comparison, **2:** 272
and frequency standard, **2:** 178
between resynchronization, **2:** 172
cesium beam, **2:** 172
crystal oscillator, **2:** 172
hydrogen maser, **2:** 172
rubidium gas cell, **2:** 172
Time code, **2:** 254
Time comparison, point-to-point, **2:** 260
Time-comparison experiments, **2:** 264
Time delay, **1:** 258
Time-difference measurement, **2:** 218
Time domain, **2:** 203
Time domain characterization, **2:** 123
Time domain envelope, **1:** 259
Time-interval counter, **2:** 230
Time-interval measurement, **2:** 217
Time stability, **2:** 193, 272
Time synchronization, **2:** 237
Time transfer, **2:** 251
Time-transfer accuracy, **2:** 265, 271
Tolerance, **2:** 297
Tomography, light scattering, **1:** 32
Tool-made sample, **2:** 298
Transducer, **1:** 221, 234
apodized, **1:** 253, 258
Transducer admittance, **1:** 235
Transducer impedance, **1:** 233
Transducer metallization, source of relaxation, **1:** 284
Transducer potential, **1:** 238, 240
Transfer oscillator, **2:** 229
Transfer phase, **2:** 60
Transfer standard, **2:** 26, 236
Transformation, similarity, **1:** 64
Transient effects, **1:** 154
Transient frequency change, **1:** 154
Transient thermal effects, **1:** 154
Transit or Nova satellite system, **2:** 258, 264
Transit time, **2:** 140
Transition temperature, **2:** 282
Translation technique, **2:** 203
Transmission, **2:** 237
HF- and medium-frequency, **2:** 237
low- and very-low-frequency, **2:** 237
Transmission bridge, **2:** 25, 30
Transmission line, **2:** 25, 30
Transmission-line form, **1:** 246
Transmission-line model, **1:** 126
Transmission network, **2:** 4, 40
Transmission test set, **2:** 22
Transponder channel, **2:** 260
Trap characterization, **1:** 156
Trapped-energy analysis, **1:** 202
Trapped ion, **2:** 169
Trimming, final frequency, **1:** 174
Trim-to-frequency, **1:** 169, 179, 181
Triple transit, **1:** 249, 264
TTC-cut, **1:** 159
Tuning forks, **2:** 275
flexural vibrations, **2:** 277
length-extensional vibrations, **2:** 277
quartz, **2:** 276
temperature sensitivity, **2:** 278
Tunnel-diode oscillator, **2:** 279
Turning point, **2:** 101
Turnover temperature, **2:** 61, 81, 86
TV frame synchronization, **2:** 250
TV methods, **2:** 250
TV time sychronization, **2:** 266
Twinning, **1:** 165
Two-sample (Allan) variance, **2:** 123
Types, of attributes, **2:** 298

U

Ultraviolet laser **2:** 167
Unit variations, **2:** 298
Unity gain point, **2:** 136
Universal coordinate time (UTC), **2:** 234
Unperturbed radiation state, **2:** 122
UV-ozone cleaning, **1:** 180
Unwanted modes, suppression, **1:** 209

V

Vacuum deposition, **1:** 170
Vacuum system, **1:** 173
Varactor, **2:** 27
Vector-ratio meter, **2:** 21, 31, 40
Velocity
  elastic particle, **1:** 52
  wave, **1:** 79
Velocity distribution, **2:** 141
Velocity perturbation, **1:** 242
Very-low-frequency (VLF) broadcast, **2:** 242
Very-narrow-band (VNB) design, **1:** 198
Vibration, modes of. *See* Modes
Vibrational transition, **2:** 169
Voltage, mean-square, **2:** 193
Voltage spectrum, **2:** 194
Voltage-controlled (crystal) oscillator (VCO or VCXO), **2:** 127

W

Wafer processing, **1:** 137
Wall coating, **2:** 158
Wall collisions, **2:** 165
Wall shift, **2:** 165
Wave
  elastic, nonlinear, **1:** 56
  longitudinal, **1:** 120
  plane, **1:** 66
  transverse (shear), **1:** 120
  velocity, **1:** 79, 128
Wavelength standard, **2:** 179
Wavenumber, lateral, **1:** 93. *See also* Dispersion relations
Weak coupling approximation, **1:** 233, 237, 240
Wide-band design, **1:** 198
Window function, **2:** 199

X

X-ray diffraction, **1:** 166
X-ray topography, **1:** 18, 30, 32

Z

Zeeman level, **2:** 163
Zeeman transition, **2:** 118
Zero crossing, **2:** 252
Zero-field transition, **2:** 119
Zero-phase condition, **2:** 22
Zero-phase π network, **2:** 22, 35
Zero-phase technique, **2:** 34
Zero reactance, **2:** 39
ZnO film, **2:** 214